

**THE ROLE OF OCCLUDIN TIGHT JUNCTION PROTEIN
IN FRESHWATER TELEOST FISH OSMOREGULATION**

Helen Chasiotis

A DISSERTATION SUBMITTED TO THE FACULTY OF GRADUATE STUDIES
IN PARTIAL FULFILMENT OF THE REQUIREMENTS FOR THE DEGREE OF
DOCTOR OF PHILOSOPHY

GRADUATE PROGRAM IN BIOLOGY
YORK UNIVERSITY,
TORONTO, ONTARIO, CANADA

OCTOBER 2011



Library and Archives
Canada

Published Heritage
Branch

395 Wellington Street
Ottawa ON K1A 0N4
Canada

Bibliothèque et
Archives Canada

Direction du
Patrimoine de l'édition

395, rue Wellington
Ottawa ON K1A 0N4
Canada

Your file Votre référence

ISBN: 978-0-494-88659-5

Our file Notre référence

ISBN: 978-0-494-88659-5

NOTICE:

The author has granted a non-exclusive license allowing Library and Archives Canada to reproduce, publish, archive, preserve, conserve, communicate to the public by telecommunication or on the Internet, loan, distribute and sell theses worldwide, for commercial or non-commercial purposes, in microform, paper, electronic and/or any other formats.

The author retains copyright ownership and moral rights in this thesis. Neither the thesis nor substantial extracts from it may be printed or otherwise reproduced without the author's permission.

AVIS:

L'auteur a accordé une licence non exclusive permettant à la Bibliothèque et Archives Canada de reproduire, publier, archiver, sauvegarder, conserver, transmettre au public par télécommunication ou par l'Internet, prêter, distribuer et vendre des thèses partout dans le monde, à des fins commerciales ou autres, sur support microforme, papier, électronique et/ou autres formats.

L'auteur conserve la propriété du droit d'auteur et des droits moraux qui protègent cette thèse. Ni la thèse ni des extraits substantiels de celle-ci ne doivent être imprimés ou autrement reproduits sans son autorisation.

In compliance with the Canadian Privacy Act some supporting forms may have been removed from this thesis.

While these forms may be included in the document page count, their removal does not represent any loss of content from the thesis.

Conformément à la loi canadienne sur la protection de la vie privée, quelques formulaires secondaires ont été enlevés de cette thèse.

Bien que ces formulaires aient inclus dans la pagination, il n'y aura aucun contenu manquant.

Canada

ABSTRACT

The tetraspan transmembrane protein occludin is an integral component of the tight junction (TJ) complex in vertebrate epithelia. In mammalian epithelia, occludin has been shown to contribute significantly to the TJ barrier by limiting the paracellular movement of solutes between epithelial cells. However, nothing is known about occludin in fishes. In the present set of studies, freshwater (FW) stenohaline goldfish (*Carassius auratus*) and euryhaline rainbow trout (*Oncorhynchus mykiss*) were used to examine a role for occludin in the maintenance of salt and water balance in fishes. Occludin exhibited broad expression in fish tissues, but was predominantly abundant in the gill where it was found to be associated with pavement cells (PVCs) and mitochondria-rich cells (MRCs) of the gill epithelium. When salt and water balance were perturbed in goldfish either by: i) food deprivation; ii) ion-poor water (IPW) acclimation; or iii) elevated systemic cortisol levels using exogenous cortisol administration, results indicated that occludin may contribute to gill epithelial “tightening” in order to reduce passive salt loss in a hypo-osmotic environment. This idea was supported by studies using a primary cultured “reconstructed” rainbow trout gill epithelium, which was found to exhibit a significant increase in occludin abundance in association with reduced paracellular permeability. However, in a newly developed primary cultured goldfish gill model (a flat polarized epithelium composed of gill PVCs only), little changes in occludin levels were observed. This discrepancy is attributed to species-specific differences in the response to cortisol, which was used to reduce the permeability of the cultured gill preparations.

Supplementation of the cultured goldfish gill model with serum collected from IPW-acclimated goldfish however, increased occludin abundance and supported the “tightening” effect suggested by *in vivo* observations. Furthermore, when small interfering RNAs (siRNA) were used to reduce occludin abundance in the cultured goldfish gill model, permeability to a paracellular marker was increased. Collectively, this research provides significant insight into the physiology and function of occludin in teleost fishes, as well as a greater fundamental understanding of the regulation and role of TJ proteins in FW fish osmoregulation.

ACKNOWLEDGMENTS

First and foremost, I would like to extend my sincerest thanks to my supervisor and friend Dr. Scott Kelly. Thank you for providing me with every possible opportunity to help me grow as a student, scientist and individual. I truly could not have imagined a more inspirational mentor. I greatly appreciate that your door was always open whenever I needed advice and that you were always willing to lend a helping hand at the bench. Thank you for your genuine kindness and patience, great taste in music and cheesy sense of humour.

To the past and present members of the Kelly lab, I would like to thank you for making my life as a graduate student a really interesting and fun experience. I would especially like to thank my partners-in-crime, Mazdak Bagherie-Lachidan, Phuong Bui, Eric Clelland, Lucy Fernandez, Eli Javasky and Dennis Kolosov for their friendship and support in the lab.

A special thanks goes out to fellow graduate students, post-docs and faculty members who generously offered me their time, expertise and equipment over the years, including Guodong Fu, Edyta Marcon, Dr. Peter Moens, Dr. Spencer Mukai, Sadia Munir, Jonathan Labonne, Lubna Nadeem and Karen Rethoret. Thank you to my committee members Dr. Barry Loughton and Dr. Chun Peng for their valuable advice, motivation and immense support.

Last but certainly not least, I would like to thank my family. To Mom, Dad, Faye, Mike, Michael and Nathan, it would have been impossible for me to complete this work without your constant encouragement, patience, understanding, love and support. Thank you!

TABLE OF CONTENTS

Copyright Page	ii
Certificate Page	iii
Abstract	iv
Acknowledgments	vi
Table of Contents	vii
List of Tables	x
List of Figures	xi
List of Abbreviations	xv
Statement of Contribution	xvii
Chapter One: Overview	1
1.1 Transport pathways across epithelia	2
1.2 The tight junction complex	2
1.2.1 What is the tight junction complex?	2
1.2.2 Tight junction proteins	6
1.2.2.1 Occludin	6
1.2.2.2 Claudins	9
1.2.2.3 Zonula occludens-1	11
1.3 Salt and water regulation in teleost fishes	12
1.3.1 General osmoregulatory strategies	12
1.3.2 Ionic regulation by the teleost gill epithelium	15
1.3.3 Primary cultured gill epithelial models	18
1.4 Research objectives	21
1.5 References	25
Chapter Two: Occludin immunolocalization and protein expression in goldfish ...	39
2.1 Abstract	40
2.2 Introduction	41
2.3 Materials and Methods	44
2.4 Results	52
2.5 Discussion	66
2.6 References	75
Chapter Three: Occludin expression in goldfish held in ion-poor water	85
3.1 Abstract	86
3.2 Introduction	87
3.3 Materials and Methods	91
3.4 Results	96
3.5 Discussion	107
3.6 References	115

Chapter Four: Cortisol reduces paracellular permeability and increases occludin abundance in cultured trout gill epithelia	120
4.1 Abstract	121
4.2 Introduction	122
4.3 Materials and methods	125
4.4 Results	133
4.5 Discussion	141
4.6 References	146
Chapter Five: Permeability properties and occludin expression in a primary cultured model gill epithelium from the stenohaline freshwater goldfish	150
5.1 Abstract	151
5.2 Introduction	152
5.3 Materials and Methods.....	155
5.4 Results	164
5.5 Discussion	175
5.6 References	185
Chapter Six: Effect of cortisol on permeability and tight junction protein transcript abundance in primary cultured gill epithelia from stenohaline goldfish and euryhaline trout	190
6.1 Abstract	191
6.2. Introduction	192
6.3. Materials and Methods	195
6.4 Results	206
6.5 Discussion	219
6.6 References	230
Chapter Seven: Effects of elevated circulating cortisol levels on hydromineral status and gill tight junction protein abundance in stenohaline goldfish	238
7.1 Abstract	239
7.2 Introduction	240
7.3 Materials and Methods	244
7.4 Results	249
7.5 Discussion	259
7.6 References	265
Chapter Eight: Permeability properties of the goldfish gill epithelium under ion-poor conditions	276
8.1 Abstract	277
8.2 Introduction	278
8.3 Materials and Methods	281

8.4 Results	288
8.5 Discussion	297
8.6 References	306
Chapter Nine: siRNA-mediated reductions in occludin expression increases permeability across cultured goldfish gill epithelia.....	312
9.1 Rationale and methodology.....	311
9.2 Results and discussion.....	315
9.3 References.....	318
Chapter Ten: Summary and future directions	319
10.1 Summary	320
10.1.1 Occludin is a component of the tight junction complex in fish tissues	320
10.1.2 A role for occludin in freshwater teleost osmoregulation	321
10.1.3 Primary cultured gill model from the stenohaline freshwater goldfish	323
10.1.4 Occludin is a barrier-forming tight junction protein in the teleost gill	324
10.2 Future directions	327
10.3 References	329
Appendix A: Supplementary Data	333
A.1 Primary cultured goldfish gill cells form polarized epithelia	334
A.2 Validation of a commercial cortisol EIA kit for measuring cortisol titres in goldfish serum	339
A.3 References	341
Appendix B: Publications	342

LIST OF TABLES

Chapter Three

Table 3-1: Summary of statistics for abrupt exposure of goldfish (from freshwater to ion-poor water) generated by two-way ANOVAs of 0 – 120 h time course data	99
Table 3-2: Serum glucose levels (mg/100 ml) in goldfish abruptly exposed to ion-poor water or acclimated to ion-poor water for 14 and 28 day periods	100

Chapter Six

Table 6-1: Primer sequences and corresponding fish orthologs for goldfish corticosteroid receptors	200
Table 6-2: Primer sequences and corresponding fish orthologs for goldfish claudins and ZO-1	201
Table 6-3: Primer sequences and corresponding fish orthologs for trout claudins.....	203

Chapter Seven

Table 7-1: Effects of elevated circulating cortisol levels on corticosteroid receptor mRNA abundance in goldfish gills	255
--	-----

LIST OF FIGURES

Chapter One

Figure 1-1: Transepithelial solute movement can occur via transcellular or paracellular pathways	3
Figure 1-2: Generalized model of the tight junction complex between epithelial cells	8
Figure 1-3: Summary of osmoregulation and salt and water movement in freshwater and seawater teleost fishes	14
Figure 1-4: Generalized models of Na^+ and Cl^- uptake and extrusion by the freshwater and seawater teleost gill epithelium respectively	17
Figure 1-5: Primary cultured gill epithelial model	20

Chapter Two

Figure 2-1: Immunofluorescent staining of Na^+ - K^+ -ATPase and occludin in longitudinal sections of a goldfish gill filament	53
Figure 2-2: Immunofluorescent staining of Na^+ - K^+ -ATPase and occludin in cross-sections of goldfish intestine	54
Figure 2-3: Schematic illustration of a goldfish nephron, and cross-section of goldfish kidney immunostained for Na^+ - K^+ -ATPase and occludin	56
Figure 2-4: Immunofluorescent staining of Na^+ - K^+ -ATPase and occludin in cross-sections of the proximal tubule, distal tubule and collecting duct of the goldfish nephron	57
Figure 2-5: Western blot analysis of occludin expression in goldfish gill, intestine and kidney	59
Figure 2-6: Effects of 1, 2 and 4 weeks feeding and food deprivation on relative weight gain/loss in goldfish	60
Figure 2-7: Effects of 1, 2 and 4 weeks feeding and food deprivation on serum osmolality, Na^+ and Cl^- , and muscle water content in goldfish	61
Figure 2-8: Effects of 1, 2 and 4 weeks feeding and food deprivation on gill Na^+ - K^+ -ATPase activity and normalized gill occludin expression in goldfish	63
Figure 2-9: Effects of 1, 2 and 4 weeks feeding and food deprivation on intestine Na^+ - K^+ -ATPase activity and normalized intestine occludin expression in goldfish.....	64
Figure 2-10: Effects of 1, 2 and 4 weeks feeding and food deprivation on kidney Na^+ - K^+ -ATPase activity and normalized kidney occludin expression in goldfish.....	65

Chapter Three

Figure 3-1: Effect of abrupt exposure to ion-poor water on serum osmolality, Na^+ and Cl^- , and muscle moisture content of goldfish	97
Figure 3-2: Effect of abrupt exposure to ion-poor water on gill Na^+ - K^+ -ATPase activity and occludin protein expression	98
Figure 3-3: Effect of 14 and 28 days acclimation to ion-poor water on serum osmolality, Na^+ and Cl^- , and muscle moisture content in goldfish	102

Figure 3-4: Effect of 14 and 28 days acclimation to ion-poor water on gill Na ⁺ -K ⁺ -ATPase activity and occludin protein expression	103
Figure 3-5: Effect of 14 and 28 days acclimation to ion-poor water on kidney Na ⁺ -K ⁺ -ATPase activity and occludin protein expression	105
Figure 3-6: Effect of 14 and 28 days acclimation to ion-poor water on intestine Na ⁺ -K ⁺ -ATPase activity and occludin protein expression	106

Chapter Four

Figure 4-1: Effect of cortisol on transepithelial resistance, [³ H]PEG-4000 permeability And net Na ⁺ flux rates across cultured rainbow trout gill epithelia	134
Figure 4-2: Quantitative real-time PCR generated occludin mRNA expression profile for discrete rainbow trout tissues	136
Figure 4-3: Immunolocalization of occludin and representative western blot of occludin protein in cultured trout gill epithelia	137
Figure 4-4: Occludin mRNA abundance in cultured trout gill epithelia in response to 12 h apical freshwater exposure, and cortisol treatment under symmetrical and asymmetrical culture conditions	138
Figure 4-5: Effect of cortisol (500 ng/ml) on occludin mRNA and protein abundance in flask-cultured rainbow trout pavement cell epithelia	140

Chapter Five

Figure 5-1: Phase contrast, scanning electron and transmission electron micrographs of cultured goldfish gill cells in flasks and culture inserts under symmetrical culture conditions	165
Figure 5-2: Immunolocalization of occludin and Na ⁺ -K ⁺ -ATPase in a cultured goldfish gill epithelium at 48 h post-seeding in a culture insert under symmetrical culture conditions	167
Figure 5-3: Changes in transepithelial resistance (TER) of cultured goldfish gill epithelia post-seeding in culture inserts under symmetrical culture conditions, and the effect of short-term (3 h) asymmetrical culture conditions and subsequent recovery under symmetrical conditions on the TER of cultured goldfish gill epithelia	168
Figure 5-4: Occludin mRNA expression profile for discrete goldfish tissues as generated by quantitative real-time PCR	170
Figure 5-5: Effect of long-term (24 h) asymmetrical culture conditions on transepithelial resistance and [³ H]PEG-4000 permeability across goldfish gill epithelia cultured in inserts	171
Figure 5-6: Effect of long-term asymmetrical culture conditions on transepithelial resistance, and occludin mRNA and protein abundance in primary cultured goldfish gill epithelia	173

Chapter Six

Figure 6-1: Corticosteroid receptor mRNA expression in goldfish gill tissue and cultured goldfish gill cells by reverse transcriptase-PCR and gel electrophoresis, and dose-dependent effects of 24 h cortisol treatment on transepithelial resistance and [³ H]PEG-4000 flux across cultured goldfish gill epithelia	207
Figure 6-2: Goldfish occludin, claudin and ZO-1 mRNA abundance in cultured gill cells and gill tissue by quantitative real-time PCR analysis	209
Figure 6-3: Dose-dependent effects of 24 h cortisol treatment on occludin, claudin b, c, d, e, h, 7, 8d and 12, and ZO-1 mRNA abundance in cultured goldfish gill epithelia	211
Figure 6-4: Time-course effects of 48 and 96 h cortisol treatment on transepithelial resistance, and occludin, claudin c, h and 12, and ZO-1 mRNA abundance in cultured goldfish gill epithelia	213
Figure 6-5: Comparative effects of cortisol on transepithelial resistance, [³ H]PEG-4000 flux and tight junction protein mRNA abundance in cultured goldfish and rainbow trout gill epithelia	217

Chapter Seven

Figure 7-1: Dose-dependent effects of cortisol implants on goldfish serum cortisol levels	250
Figure 7-2: Effect of elevated circulating cortisol levels on goldfish serum osmolality, Na ⁺ , Cl ⁻ and glucose, muscle water content and gill Na ⁺ -K ⁺ -ATPase activity.....	251
Figure 7-3: Quantitative real-time PCR generated mRNA expression profiles for claudin b, c, d, e, h, 7, 8d and 12, and ZO-1 in discrete goldfish tissues	253
Figure 7-4: Effect of elevated circulating cortisol levels on tight junction protein mRNA abundance in goldfish gills	257
Figure 7-5: Effect of elevated circulating cortisol levels on occludin protein abundance in goldfish gills	258

Chapter Eight

Figure 8-1: Effect of ion-poor water acclimation on tight junction protein mRNA abundance in goldfish gills	289
Figure 8-2: Transmission electron micrographs of tight junctions (TJs) and measurements of TJ depth between pavement cells in the gills of goldfish acclimated to freshwater and ion-poor water	290
Figure 8-3: Effect of ion-poor water acclimation on tight junction protein mRNA abundance in pavement cells isolated from goldfish gills	292
Figure 8-4: Effect of fetal bovine serum or goldfish serum derived from fish acclimated to freshwater or ion-poor water on transepithelial resistance and [³ H]PEG-4000 flux across primary cultured goldfish gill epithelia	293

Figure 8-5: Effect of fetal bovine serum or goldfish serum derived from fish acclimated to freshwater or ion-poor water on tight junction protein mRNA abundance in primary cultured goldfish gill epithelia	294
Figure 8-6: Effect of fetal bovine serum or goldfish serum derived from fish acclimated to freshwater or ion-poor water on transepithelial resistance and [³ H]PEG-4000 flux across primary cultured goldfish gill epithelia following exposure to asymmetrical culture conditions	296

Chapter Nine

Figure 9-1: Effect of goldfish occludin siRNA transfection on occludin mRNA and protein abundance in cultured goldfish gill epithelia.....	316
Figure 9-2: Effect of goldfish occludin siRNA transfection on transepithelial resistance and [³ H]PEG-4000 flux across cultured goldfish gill epithelia	317

Appendix A

Figure A-1: Effect of abrupt apical freshwater (FW) exposure or basolateral FW exposure, and subsequent recovery under symmetrical culture conditions on cultured goldfish gill epithelial cell morphology	337
Figure A-2: Effect of abrupt apical freshwater (FW) exposure or basolateral FW exposure, and subsequent recovery under symmetrical culture conditions on the transepithelial resistance of cultured goldfish gill epithelia	338
Figure A-3: Validation of a commercial cortisol EIA kit for measuring cortisol titres in goldfish serum with parallelism curves	340

LIST OF ABBREVIATIONS

AC – accessory cell
ADB – antibody dilution buffer
ADB/PBS – 10% ADB in PBS
aGI – anterior gastrointestinal tract
ANOVA – analysis of variance
BLAST – Basic Local Alignment Search Tool
BSA – bovine serum albumin
CA – carbonic anhydrase
cDNA – complementary deoxyribonucleic acid
CDS – coding sequence
CFTR – cystic fibrosis transmembrane regulator
CVS – central venous sinus
DAPI – 4',6-diamidino-2-phenylindole
DNA – deoxyribonucleic acid
dNTP – deoxynucleotide triphosphate
DTT – dithiothreitol
EDTA – ethylenediaminetetraacetic acid
EF1 α – elongation factor 1-alpha
EIA – enzyme immunoassay
ENaC – epithelial Na⁺ channel
EST – expressed sequence tag
FBS – fetal bovine serum
FITC – fluorescein isothiocyanate
FW – freshwater
FW/L15 – apical freshwater/basolateral L15
GFS – goldfish serum
GI – gastrointestinal
GR1 – glucocorticoid receptor 1
GR2 – glucocorticoid receptor 2
HIER – heat-induced epitope retrieval
HMW – high molecular weight
HRP – horseradish peroxidase
IL – interlamellar
IPW – ion-poor water
JAM – junctional adhesion molecule
L15 – Leibovitz's L-15 culture medium with 2 mM glutamine
L15/FW – apical L15/basolateral FW
L15/L15 – apical L15/basolateral L15
LMW – low molecular weight
MDCK – Madin-Darby canine kidney

mGI – middle gastrointestinal tract
MR – mineralocorticoid receptor
mRNA – messenger RNA
MRC – mitochondria-rich cell
MS-222 – tricaine methanesulfonate
ND – not detected
NKA – Na⁺-K⁺-ATPase
NKCC – Na⁺-K⁺-2Cl⁻ co-transporter
occludin-ir – occludin immunoreactivity
PBS – phosphate-buffered saline
PCR – polymerase chain reaction
PEG-4000 – polyethylene glycol-4000
PET – polyethylene terephthalate filter
PF/dH₂O – 0.4% Kodak Photo-Flo 200 in distilled water
PF/PBS – 0.4% Kodak Photo-Flo 200 in PBS
pGI – posterior gastrointestinal tract
pK_i – isoelectric point
PMSF – phenylmethylsulfonyl fluoride
PVC – pavement cell
PVDF – polyvinylidene difluoride
qRT-PCR – quantitative real-time PCR
RACE – rapid amplification of cDNA ends
RNA – ribonucleic acid
RT – room temperature
RT-PCR – reverse transcriptase PCR
SDS-PAGE - sodium dodecyl sulfate polyacrylamide gel electrophoresis
SEI – homogenization buffer containing sucrose, EDTA and imidazole
SEID – SEI with sodium deoxycholate
s.e.m. – standard error of the mean
SEM – scanning electron microscopy
siRNA – small interfering RNA
SW – seawater
TBS – Tris-buffered saline
TBS-T – TBS with Tween-20
TEM – transmission electron microscopy
TER – transepithelial resistance
TJ – tight junction
TJPI – tight junction protein-1
TPA – Third Party Annotation
TRITC – tetramethyl rhodamine isothiocyanate
TX/PBS – 0.05% Triton X-100 in PBS
ZO-1 – zonula occludens-1
ZONAB – ZO-1-associated nucleic acid binding protein

STATEMENT OF CONTRIBUTION

Chapter Two

This chapter was written by H. Chasiotis with valuable guidance from Dr. S.P. Kelly. Goldfish food deprivation experiments, immunohistochemistry, western blots and all hydromineral endpoint analyses were conducted by H. Chasiotis.

Chapter Three

This chapter was co-written by H. Chasiotis and Dr. S.P. Kelly. Goldfish ion-poor water exposure experiments and hydromineral endpoint analyses (i.e. serum osmolality, Na⁺, Cl⁻, muscle moisture content, tissue Na⁺-K⁺-ATPase activity) were conducted by J.C. Effendi as part of her undergraduate honours thesis project under the co-supervision of H. Chasiotis. All occludin western blot analyses were conducted by H. Chasiotis.

Chapter Four

This chapter was co-written by H. Chasiotis and Dr. S.P. Kelly. Rainbow trout gill epithelia were cultured and cortisol experiments were conducted jointly by H. Chasiotis and Dr. S.P. Kelly. Occludin gene cloning and characterization, immunocytochemistry, western blotting and real-time PCR analyses were conducted by H. Chasiotis. Na⁺ flux rate measurements were conducted by Dr. S.P. Kelly during his postdoctoral fellowship with Dr. C.M. Wood at McMaster University in Hamilton, Ontario, Canada.

Chapter Five

This chapter was written by H. Chasiotis with valuable guidance from Dr. S.P. Kelly. The development and characterization of the *in vitro* goldfish gill model, microscopy, immunocytochemistry, goldfish occludin gene cloning, western blots and all other experiments and analyses were conducted by H. Chasiotis. Valuable technical assistance with the electron microscopy was provided by K. Rethoret.

Chapter Six

This chapter was written by H. Chasiotis with valuable guidance from Dr. S.P. Kelly. Goldfish gill epithelia were cultured and goldfish cortisol experiments were conducted by H. Chasiotis. Rainbow trout gill epithelia were cultured and trout cortisol experiments were conducted jointly by H. Chasiotis and Dr. S.P. Kelly. Goldfish and rainbow trout tight junction protein genes and goldfish corticosteroid receptor genes described in this chapter were cloned and characterized by H. Chasiotis. Real-time PCR analyses were conducted by H. Chasiotis.

Chapter Seven

This chapter was written by H. Chasiotis with valuable guidance from Dr. S.P. Kelly. Goldfish cortisol implantation experiments, cortisol and hydromineral endpoint analyses, real-time PCR and western blotting were conducted by H. Chasiotis.

Chapter Eight

This chapter was co-written by H. Chasiotis and Dr. S.P. Kelly with valuable discussion with D. Kolosov. Goldfish gill epithelia were cultured and goldfish serum experiments were conducted by H. Chasiotis with assistance by Dr. S.P. Kelly. Real-time PCR analyses in cultured gill tissue were conducted by H. Chasiotis. Goldfish ion-poor water exposure experiments, pavement cell separation procedures, and transmission electron microscopy and real-time PCR analyses in whole gill tissue and isolated pavement cells were conducted by D. Kolosov as part of his undergraduate honours thesis project under the co-supervision of H. Chasiotis.

Chapter Nine

This chapter was written by H. Chasiotis with valuable discussion with Dr. S.P. Kelly. Goldfish gill epithelia were cultured and siRNA experiments were conducted by H. Chasiotis. Real-time PCR, western blotting and all other analyses were also conducted by H. Chasiotis.

Appendix A

All supplementary experiments and analyses described in this section were conducted by H. Chasiotis.

Helen Chasiotis (PhD Candidate)

Dr. Scott P. Kelly (PhD Supervisor)

CHAPTER 1:

OVERVIEW

1.1 Transport pathways across epithelia

In metazoans, epithelia comprise contiguous sheets of specialized cells that cover internal and external body surfaces. As such, epithelia serve as barriers which separate compositionally distinct fluid compartments of the body from one another, as well as from the external environment. In order to maintain optimal internal composition and gradients necessary for the proper functioning of tissues, epithelia also selectively regulate the exchange of biological solutes (e.g. nutrients, ions, wastes) between compartmental body fluids and the outside milieu. This regulation of solute movement can occur via inter-dependent transcellular and paracellular pathways across epithelia (Anderson, 2001). In the transcellular pathway, solutes are transported across the membranes of epithelial cells (Fig. 1-1). Movement along this route is energy-dependent and tightly controlled by a well-defined suite of selective membrane-bound pumps, transporters and channels (Anderson, 2001). In the paracellular pathway on the other hand, solutes do not enter epithelial cells, but rather move between them along the intercellular space (Fig. 1-1). Although this type of movement is completely passive, relying on existing gradients (e.g. osmotic, concentration or electrical) across epithelia, in vertebrate organisms, the permeability of the paracellular route is strictly controlled by the tight junction complex (Fig. 1-1; Anderson, 2001).

1.2 The tight junction complex

1.2.1 What is the tight junction complex?

As the apical-most component of the cell–cell junctional complex of vertebrate epithelia and endothelia, the tight junction (TJ) acts as a “gate” to the paracellular pathway by

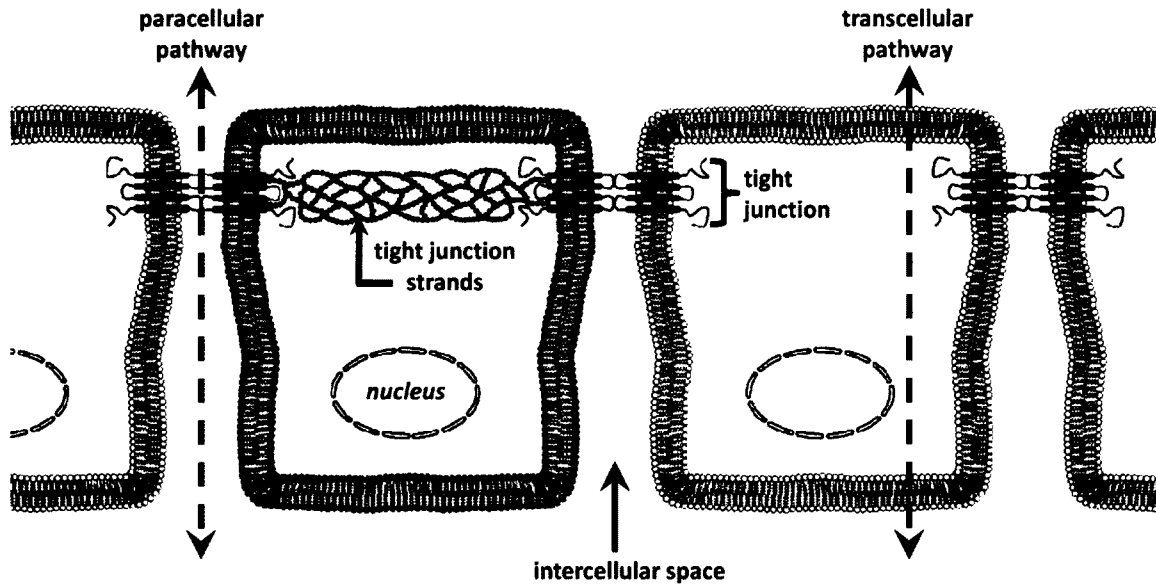


Figure 1-1: Transepithelial solute movement can occur via transcellular or paracellular pathways. In the transcellular route, solutes are actively transported across membranes of epithelial cells via membrane-bound pumps, transporters and channels. In the paracellular pathway, solutes passively move between epithelial cells along the intercellular space by diffusion. The tight junction (green) appears as a belt-like network of anastomosing strands. These act as a “gate” to the paracellular pathway by “sealing” the intercellular space and selectively regulating the passage of solutes between epithelial cells. The tight junction also forms a “fence” that prevents membrane-bound molecules on the apical side of epithelia (red) from intermixing with those on the basolateral side (blue).

“sealing” the intercellular space between adjacent epithelial cells (Fig. 1-1; González-Mariscal et al., 2003). TJ proteins, the molecular constituents of the TJ complex, organize into fibrils at sites of cell-cell contact, and by freeze-fracture electron microscopy, appear as networks of anastomosing strands (Fig. 1-1), which interact between adjacent cells to close the intercellular space (Claude and Goodenough, 1973; González-Mariscal et al., 2003). Because these belt-like networks continuously encircle entire cells at their apical ends, TJs also maintain epithelial cell polarity by forming a “fence” that prevents the intermixing of apical and basolateral membrane-bound molecules (Fig. 1-1; González-Mariscal et al., 2003).

Despite what its name implies however, the TJ is not always “tight,” but in fact semi-permeable. The TJ barrier can dynamically alter between a “tight” seal that impedes the passage of select solutes and a “leaky” seal that selectively facilitates solute movement. Alternatively, the TJ barrier can also be “tight” with respect to the paracellular diffusion of certain solutes whilst simultaneously “leaky” to others. Transepithelial resistance (TER) is an electrophysiological measurement commonly used to assess overall epithelial integrity or “tightness” (Harhaj and Antonetti, 2004). Although changes in TER are generally accepted to be a consequence of altered paracellular transport, it actually represents a measurement of resistance to the movement of ions across both transcellular and paracellular pathways (Harhaj and Antonetti, 2004). As such, a change in TER may not always necessarily reflect a change in the TJ barrier, but rather altered transcellular transport across membrane-bound channels or pumps. Moreover, TER measurements do not account for alterations in the paracellular

movement of non-charged solutes. As a result, TER is often used in conjunction with measurements of flux to radioactive or fluorescently-labeled paracellular tracer molecules (e.g. polyethylene glycol, inulin, mannitol, dextran) (Harhaj and Antonetti, 2004). These can traverse epithelia only through the intercellular space and thus can be used to specifically assess TJ integrity or “tightness”.

The permeability characteristics of the TJ barrier depend on two general factors: ultrastructural TJ organization, and to a greater degree, the molecular composition of the TJ complex. Electrophysiological TER measurements together with freeze-fracture studies in epithelia have underscored a general correlation between epithelial “tightness” and junctional organization, whereby “leaky” epithelia possess simple TJs composed of one to two strands (e.g. proximal tubules of *Necturus* kidney), and “tighter” epithelia exhibit complex networks of several TJ strands (e.g. frog urinary bladder) (Claude and Goodenough, 1973). However, two Madin-Darby canine kidney cell lines (MDCK I and MDCK II; classical epithelial models for TJ studies) were reported to show no discernable difference in TJ strand number and complexity despite a striking difference in TER measurements between the two strains (i.e. TER across MDCK I is ~30-fold higher than MDCK II) (Stevenson, 1988). This observation led to the suggestion that other factors, aside from ultrastructural TJ organization, may govern the permeability of the TJ barrier. Indeed, with the discovery of TJ proteins during the mid 1980s to late 1990s, it became clear that the TER disparity between MDCK I and MDCK II cells, and the TJ barrier properties of all epithelia in general, had less to do with specific TJ ultrastructure,

and more to do with variations in the molecular components comprising the TJ (Stevenson et al., 1989; Furuse et al., 2001; González-Mariscal et al., 2003).

1.2.2 Tight junction proteins

Since the discovery of the first TJ protein over 20 years ago (Stevenson et al., 1986), more than 40 TJ-associated transmembrane and cytoplasmic proteins have been identified in vertebrate epithelia and endothelia (González-Mariscal et al., 2003). These molecular TJ constituents are believed to be responsible for the magnitude of the TJ barrier as well as TJ permselectivity (i.e. the ability to impede or facilitate paracellular solute movement based on size and charge). Not all identified TJ proteins however contribute to the TJ “gate” function as described above. Numerous TJ proteins have been recognized that act either directly or indirectly with other TJ proteins to fulfill a wide range of other functions, such as TJ assembly (e.g. ZO-1, Par-3; Chen and Macara, 2005; Fanning, 2006), monocyte migration across endothelia (e.g. JAM; Martín-Padura et al., 1998), and the regulation of gene expression (e.g. ZO-1, ZONAB; Balda and Matter, 2000), cell differentiation (e.g. symplekin; Buchert et al., 2009) and cell proliferation (e.g. cingulin, ZONAB; Balda et al., 2003; Guillemot and Citi, 2006). With respect to the formation of the TJ barrier however, the transmembrane TJ proteins occludin and claudins, which directly bridge the intercellular space to form the regulated TJ seal, and the cytosolic TJ protein zonula occludens-1 have received the most attention and will therefore be discussed in greater detail below.

1.2.2.1 Occludin

Occludin was the first transmembrane TJ protein identified and isolated from vertebrate

epithelia (Furuse et al., 1993). Comprising cytoplasmic amino- and carboxyl-termini, and two distinctive extracellular loops (Fig. 1-2; Furuse et al., 1993), this tetraspan protein was found to localize exclusively to TJ fibrils at sites of cell-cell contact in a wide variety of epithelial and endothelial tissues (Furuse et al., 1993; Fujimoto, 1995; Saitou et al., 1997). Multiple lines of evidence support a role for occludin in the formation of the TJ barrier and thus the regulation of paracellular permeability. For example, over-expression of occludin in MDCK cells significantly elevated TER and correspondingly increased the number and complexity of TJ strands within epithelial cells (McCarthy et al., 1996). Furthermore, anti-sense oligonucleotide-mediated reductions in occludin protein abundance in human arterial and venous endothelia resulted in a significant increase in permeability to a paracellular tracer molecule (Kevil et al., 1998). In the mammalian nephron, occludin protein expression and immunostaining correlate with renal epithelial “tightness”, such that “tighter” distal tubules express higher levels of occludin protein and exhibit stronger occludin immunostaining than “leakier” proximal segments (Kwon et al., 1998; González-Mariscal et al., 2000). Moreover, several gastroenterological diseases associated with impaired intestinal barrier function, such as irritable bowel syndrome, Crohn’s disease and ulcerative colitis, have been characterized by significant reductions in occludin within intestinal tissues (e.g. Gassler et al., 2001; Zeissig et al., 2007; Coëffier et al., 2010). Additional studies have demonstrated that occludin mediates the formation of the TJ seal via associations of occludin extracellular loops between adjacent cells (Fig. 1-2). For example, the administration of synthetic peptides designed to disrupt occludin extracellular loop interactions in *Xenopus* kidney A6 epithelia and

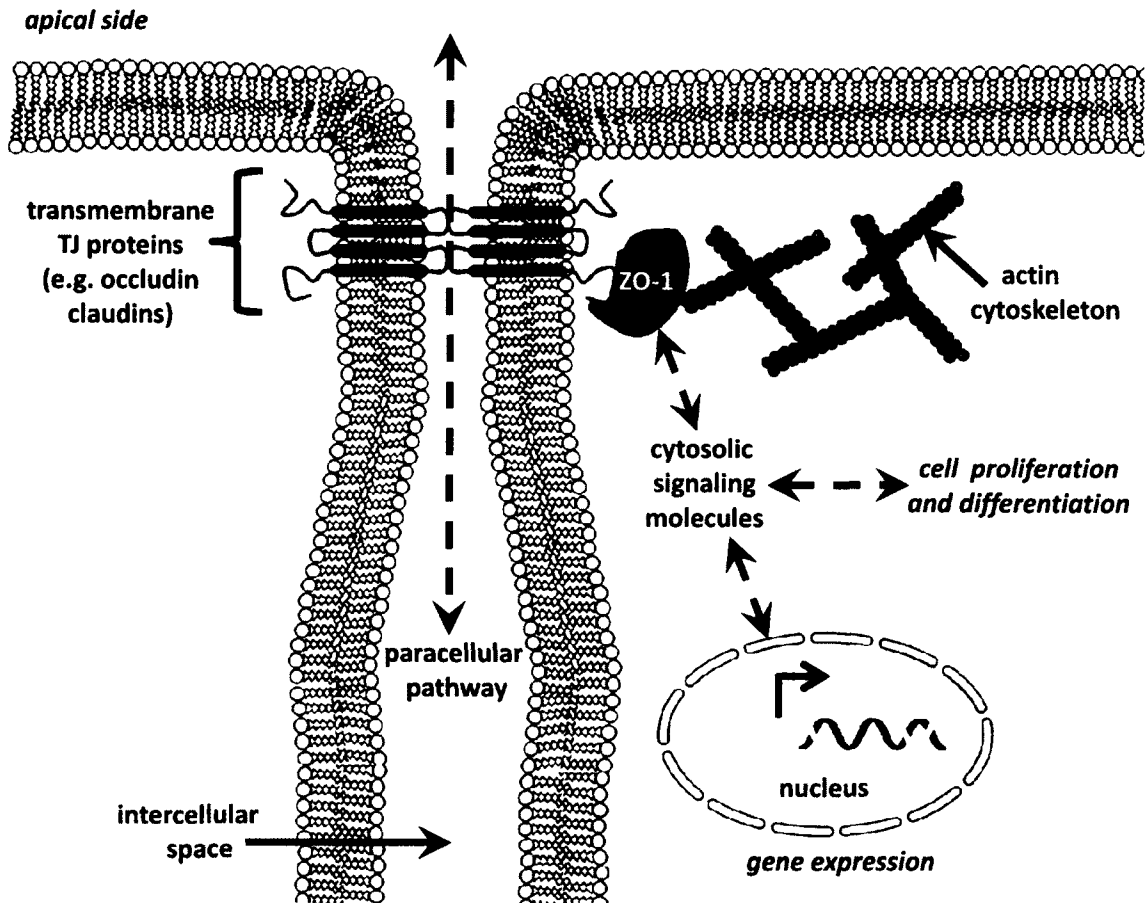


Figure 1-2: Generalized model of the tight junction (TJ) complex between epithelial cells. The tetraspan transmembrane TJ proteins (e.g. occludin and claudins; shown in green) directly regulate the permselectivity characteristics of the TJ by bridging the intercellular space to form the TJ barrier. Zonula occludens-1 (ZO-1; shown in blue) provides structural support to TJs by linking the transmembrane TJ proteins to the actin cytoskeleton, and transduces signals between the inside of the cell and the outside environment to influence TJ permeability. ZO-1 also participates in intracellular signaling pathways related to gene expression, cell proliferation and differentiation by interacting with cytosolic signaling molecules.

primary cultured Sertoli cells from rat testes significantly reduced TER in a dose-dependent and reversible manner, and increased permeability to paracellular markers (Wong and Gumbiner, 1997; Lacaz-Vieira et al., 1999; Chung et al., 2001).

Although evidence clearly implicates a role for occludin in the formation of the paracellular barrier, controversy still persists as to the degree of its contribution. For example, when occludin was transfected into L-fibroblasts which lack TJs, only a small numbers of short and straight TJ-like strands were formed at sites of cell-cell contact, in stark contrast to the large anastomosing networks of TJ fibrils normally observed in epithelia (Furuse et al., 1998). Furthermore, an occludin knock-out embryonic stem cell line could still differentiate into polarized epithelia and exhibited well-developed networks of TJ strands that were identical to wild-type cells (Saitou et al., 1998). Along the same lines, occludin-null mice possessed intestinal epithelia that maintained an effective intestinal epithelial barrier, as determined by electrophysiological measurements, and structurally-intact TJs that were morphologically indistinguishable from those of wild-type mice (Saitou et al., 2000). These observations, when taken together, suggested the existence of other molecular components that could form TJ fibrils and maintain the paracellular barrier in the absence of occludin. This ultimately led to the search for and discovery of the claudins.

1.2.2.2 Claudins

The claudins form a large multi-gene family of transmembrane tetraspan TJ proteins that can polymerize into extensive networks of TJ fibrils when transfected into TJ-deficient L-fibroblasts (Furuse et al., 1998). Similar to occludin, claudins also possess cytoplasmic

amino- and carboxyl-termini, and two extracellular loops (Fig. 1-2), however claudins share no sequence homology with occludin (Furuse et al., 1998; González-Mariscal et al., 2003; Hua et al., 2003). Multiple claudin species are generally expressed at TJs of most epithelial and endothelial cells in a tissue-specific manner, and can interact in either a homotypic fashion with the same claudins or heterotypically with different claudins between TJ fibrils of adjacent cells in order to “seal” the intercellular space (Furuse et al., 1999; Daugherty et al., 2007; Krause et al., 2008). Claudin interactions occur mainly via their highly variable first extracellular loops, which are believed to dictate the unique permselectivity properties observed amongst the different members of the claudin family (Colegio et al., 2003; Krause et al., 2008). In fact, while the tyrosine and glycine-rich extracellular loops of occludin bear no net charge (Furuse et al., 1993), the extracellular domains of claudin members have isoelectric points (pK_i) ranging from 4.05 to 10.5 (Schneeberger and Lynch, 2004), suggesting that at physiological pH (e.g. 7.3 to 7.4), different claudins can carry a net positive or net negative charge and thus may facilitate the paracellular movement of charged solutes. This is consistent with a large body of research implicating claudins in the formation of charge-selective channels or pores within the TJ complex (reviewed by Krause et al., 2008). For example, claudin-15 reversed paracellular charge selectivity from Na^+ to Cl^- when negatively charged amino acids on its first extracellular loop were substituted for positive charges (Colegio et al., 2002). Furthermore, over-expression and knockdown of claudin-2 in MDCK cell lines increased and decreased Na^+ permeability respectively (Amasheh et al., 2002; Van Itallie et al., 2003; Hou et al., 2006). Conversely, over-expression of claudin-3 in MDCK cells

increased TER and correspondingly increased the paracellular barrier to ions as well as charged and uncharged molecules (Milatz et al., 2010). Over-expression of claudin-8 in MDCK cells similarly reduced the paracellular permeation of cations (Yu et al., 2003). The various members of the claudin family, therefore, can be generally classified as either “tightening” barrier-building claudins that hinder paracellular solute movement or “leaky” pore-forming claudins that augment the paracellular permeation of solutes, particularly charged molecules. Given the sheer number of members within the claudin superfamily (at least 24 proteins identified in mammals and 56 genes encoding for claudins found in the Japanese puffer fish, *Takifugu rubripes*), the possible combinations of claudin associations within and between TJ fibrils (e.g. homo- and heterotypic) and the diversity of their permselectivity properties, claudins are believed to bestow the wide-ranging and distinct barrier properties exhibited within and between different types of epithelial and endothelial tissues (Loh et al., 2004; reviewed by Krause et al., 2008). This notion is particularly highlighted by the mammalian kidney and gut, where multiple claudins have been shown to exhibit differential expression patterns along the proximal-to-distal axes of the nephron and intestine respectively that correlate with segment-specific permeability and function (e.g. Rahner et al., 2001; Kiuchi-Saishin et al., 2002; Holmes et al., 2006; Fujita et al., 2006; Markov et al., 2010; reviewed by Amasheh et al., 2011).

1.2.2.2 Zonula occludens-1

Zonula occludens-1 (ZO-1) was the first TJ protein discovered (Stevenson et al., 1986) and is arguably one of the most versatile TJ components identified. Frequently described

as a TJ “scaffolding” or “adaptor” protein, ZO-1 is found on the inner cytosolic surface of TJs and has several binding domains which target other TJ proteins (e.g. occludin and claudins), cytosolic signaling molecules (e.g. transcription factors) and F-actin of the cytoskeleton (Fig. 1-2; Fanning et al., 1998; Itoh et al., 1999; Wittchen et al., 1999; reviewed by Bauer et al., 2010). Based on its multiple and various binding partners, it is believed that ZO-1 plays a dual role: 1) to provide indispensable structural support to TJs by linking occludin and claudins to the actin cytoskeleton; and 2) to transduce signals relating to TJ permeability, as well as gene expression, cell proliferation and differentiation, between the outside environment and the inside of the cell via interactions with intracellular signaling pathways (Fig. 1-2; Stevenson and Begg, 1994; Van Itallie et al., 2009; Bauer et al., 2010).

1.3 Salt and water regulation in teleost fishes

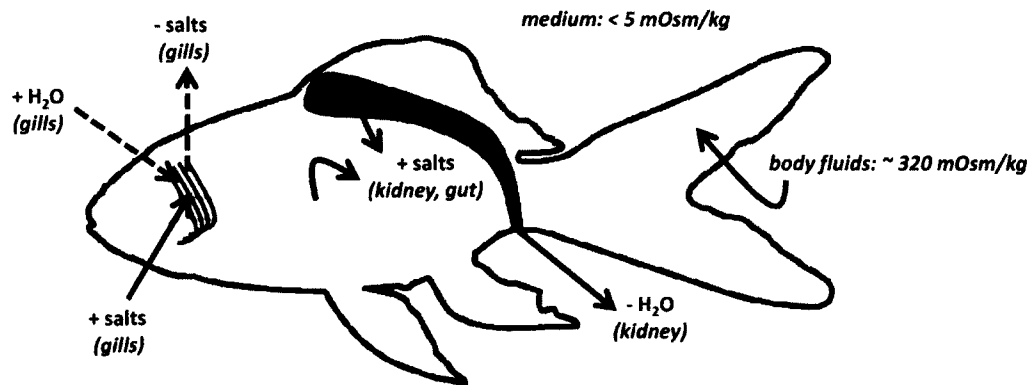
1.3.1 General osmoregulatory strategies

Teleost (bony) fishes constitute at least half of all extant animals within the vertebrate taxon (Barton, 2007). Measured in terms of species diversity and abundance, and their invasion of just about every kind of aquatic environment, teleosts also represent the most successful group of aquatic vertebrates (Bone and Marshall, 1982). With respect to their habitat versatility, teleostean success is due in part to their astounding capacity to osmoregulate, that is, control and maintain internal salt and water balance within a narrow range, despite the osmotic challenges imposed by the outside environment (Barton, 2007). Since aquatic habitats can range from extremes such as nearly pure water to hypersaline pools, as well as fluctuating estuarine waters, it is crucial for teleosts to be

able to make the necessary internal salt and water adjustments needed in order to maintain the proper internal concentrations necessary for optimal tissue functioning. Few teleosts (~5%) however are euryhaline and have the broad capacity to osmoregulate in both dilute and concentrated environments (McCormick, 2001). The majority of teleost species (~95%), are in fact stenohaline and thus remain permanent residents of either freshwater (FW) or seawater (SW) due to their limited capacity to regulate their internal ionic concentrations outside of a certain range (McCormick, 2001). Since FW and SW environments however have considerably lower and higher salt concentrations respectively than the internal concentration of fishes, stenohaline teleosts still need to osmoregulate, and do so in order maintain their internal body concentrations higher than their FW surroundings (hyper-osmoregulation) or conversely lower than their SW surroundings (hypo-osmoregulation) (Barton, 2007).

The osmoregulatory capacity of a teleost fish is defined by the barrier and transport properties of its epithelial tissues, particularly the gill, gut and kidney, which work together to modify body fluids internally and regulate water and salt exchange between internal compartments and the outside aqueous environment. Since FW is an extremely dilute medium with salt concentrations far below that of fish blood, water tends to enter the bodies of FW fishes osmotically, risking lethal dilution of their internal fluids (Fig. 1-3A). Small ions, such as Na^+ and Cl^- , are furthermore continually lost by passive diffusion across permeable body surfaces, such as the gills, which are in direct contact with the surroundings (Fig. 1-3A). In order to compensate for this obligatory influx of water and loss of body salts, ions are actively taken up from the water by the

(A) Freshwater



(B) Seawater

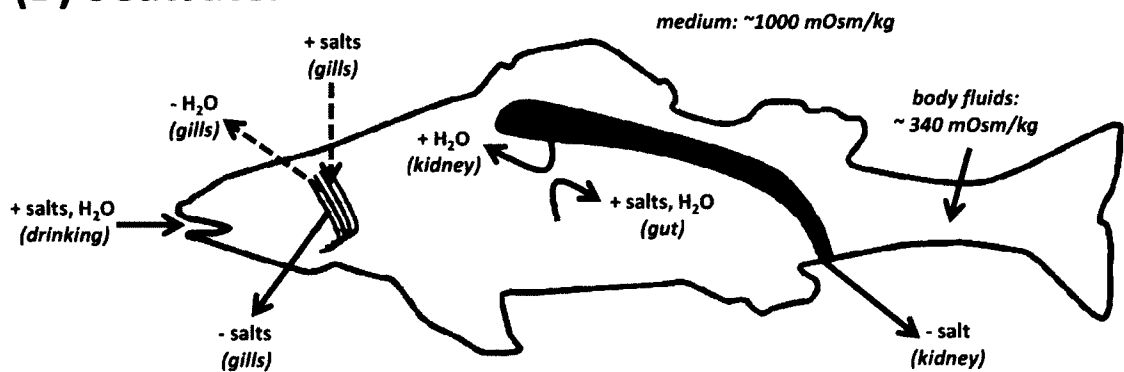


Figure 1-3: Summary of osmoregulation and salt and water movement in (A) freshwater and (B) seawater teleost fishes. (A) The body fluids of freshwater (FW) teleosts have a higher salt concentration than their external medium. FW teleosts are therefore subject to passive salt loss as well as passive water gain across the gills which are in direct contact with the environment. Salt loss is compensated for by active salt uptake at the gills, salt absorption by the gut from food sources and salt re-absorption at the kidneys. Excess water is excreted as large amounts of dilute urine. (B) Seawater (SW) teleosts, on the other hand, have body fluids that are more dilute than SW and are therefore subject to passive salt gain and passive water loss across the gills. To prevent dehydration, marine teleosts drink SW and the gut actively takes up salts in order to facilitate water absorption. The resulting excess salt load (obtained both passively and actively) is excreted by the gills. The kidneys conserve water by producing small amounts of concentrated urine. Active transport is indicated by the solid blue arrows. Passive movement is indicated by the broken green arrows. + and - indicate gain and loss respectively. (Models based on Marshall and Grosell, 2005).

gills and salt is conserved by re-absorption at the kidneys (Fig. 1-3A; reviewed by Marshall and Grosell, 2005). Some ions are additionally regained by the gut from dietary sources and excess water is excreted by the kidney as large amounts of dilute urine (Fig. 1-3A; Marshall and Grosell, 2005). SW, on the other hand, has salt concentrations much greater than that of fish blood (Fig. 1-3B), and therefore water is osmotically lost from the bodies of SW fishes and excess salts are passively gained across the permeable gills (Fig. 1-3B). To prevent dehydration, marine teleosts drink SW and the gut actively takes up salts in order to facilitate water absorption (Fig. 1-3B; Marshall and Grosell, 2005). The resulting excess salt load (obtained both passively and by active drinking) is excreted by the gills, and the kidneys conserve water by producing small amounts of concentrated urine (Fig. 1-3B; Marshall and Grosell, 2005).

1.3.2 Ionic regulation by the teleost gill epithelium

The teleost fish gill is a multifunctional organ consisting of a thin and permeable epithelium overlying a highly complex vasculature (Evans et al., 2005). As the direct interface between body fluids (i.e. blood) and surrounding water (on the apical side), the gill epithelium is the primary site for the active and passive exchange of water and salts during fish osmoregulation, in addition to the transport and movement of other molecules relating to acid-base balance, the elimination of nitrogenous wastes and gas exchange (Evans et al., 2005). Although the teleost gill epithelium is multicellular, it consists primarily of two cell types, mitochondria-rich cells (MRCs) and pavement cells (PVCs) (Evans et al., 2005; Marshall and Grosell, 2005). The MRCs cover less than 10% of the gill epithelial surface area, but are considered to be the main site of ionic regulation in the

gill (Evans et al., 2005). As their name suggests, MRCs possess numerous mitochondria, but are also rich in $\text{Na}^+\text{-K}^+\text{-ATPase}$ (NKA), a basolateral enzyme presumed to be one of the major driving forces behind salt uptake by the FW gill and salt extrusion by the SW gill (Wilson and Laurent, 2002). Although the PVCs, on the other hand, cover the vast majority (over 90%) of the gill epithelial surface area, their role in ionic regulation is considered for the most part to be passive (Wilson and Laurent, 2002; Evans et al., 2005). Recent studies have suggested that PVCs may contribute to active ion uptake by the FW gill, but it is presumed that this role is likely to be minor, as PVCs express relatively little ionomotive NKA (Marshall and Grosell, 2005).

Based on pharmacological studies utilizing specific inhibitors and blockers, immunolocalization analyses, as well as the use of molecular techniques for gene cloning and assessing gene expression, numerous membrane-bound pumps, exchangers and channels involved in ionic regulation by the gill epithelium have been identified (reviewed by Marshall and Grosell, 2005). Together with observations of TJ ultrastructure, generalized models for transcellular and paracellular pathways involved in salt uptake and extrusion by the FW and SW teleost gill epithelium respectively have been proposed. In one current model for salt uptake by the FW gill (Evans et al., 2005; Marshall and Grosell, 2005), Na^+ enters MRCs via apical epithelial Na^+ channels (ENaC) as a result of an electric gradient generated by apical V-type $\text{H}^+\text{-ATPases}$ which actively extrude protons out of the MRCs (Fig. 1-4A). Na^+ is then pumped into the blood by basolateral NKAs. Intracellular CO_2 hydration via carbonic anhydrase (CA) maintains the proton supply, but also produces HCO_3^- , which exits MRCs through an apical $\text{Cl}^-/\text{HCO}_3^-$

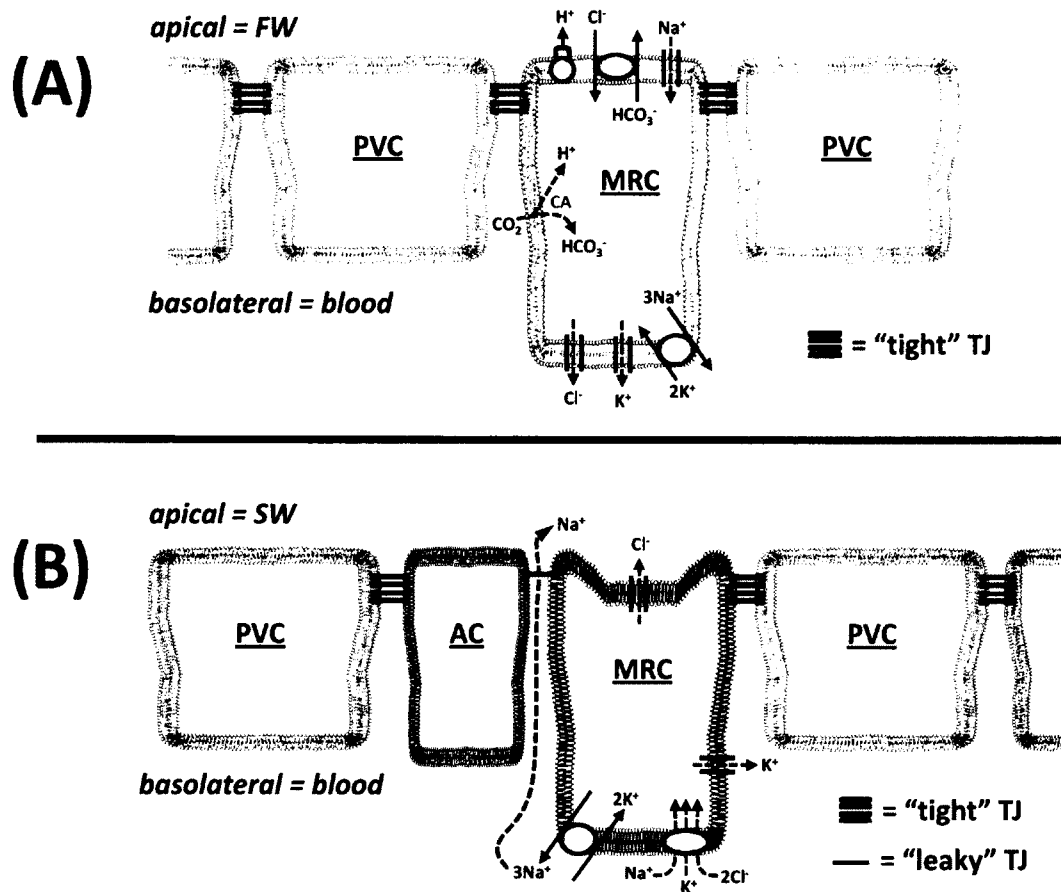


Figure 1-4: Generalized models of Na^+ and Cl^- uptake and extrusion by the freshwater (FW) and seawater (SW) teleost gill epithelium respectively. (A) In the FW gill, Na^+ uptake by the mitochondria-rich cell (MRC) is electrically coupled to an apical V-type H^+ -ATPase. Na^+ enters the cells via an apical epithelial Na^+ channel (ENaC) and exits into the blood via a basolateral Na^+ - K^+ -ATPase (NKA). Cl^- enters the MRC through an apical $\text{Cl}^-/\text{HCO}_3^-$ exchanger and diffuses into the blood via a basolateral Cl^- channel. H^+ and HCO_3^- gradients are maintained via intracellular hydration of CO_2 by carbonic anhydrase (CA), and K^+ is recycled via basolateral K^+ channels. Tight junctions (TJs) between pavement cells (PVCs) and the MRC are "tight". (B) In the SW gill, ion transport is dependent upon a Na^+ gradient generated by a basolateral NKA. This gradient facilitates the transport of Cl^- into the cell from the blood via a basolateral Na^+ - K^+ - 2Cl^- co-transporter (NKCC). Cl^- passively diffuses into the water via an apical cystic fibrosis transmembrane regulator (CFTR) Cl^- channel. Na^+ passively moves into the water via "leaky" TJs between the MRC and an adjacent accessory cell (AC). Active transport is indicated by the solid arrows. Passive movement is indicated by the broken arrows. (Models based on Evans et al., 2005; Marshall and Grosell, 2005).

exchanger and thus transports Cl^- into the MRCs. Cl^- accumulates intracellularly and then diffuses into the blood via basolateral Cl^- channels. Multi-stranded and “deep” TJ networks found between PVC-PVC and PVC-MRC contacts in the FW gill epithelium are presumed to be “tight” in order to reduce passive salt loss to the dilute FW environment (Fig. 1-4A; Sardet et al., 1979).

In a current SW gill model (reviewed by Evans et al., 2005), on the other hand, salt extrusion is dependent upon a Na^+ gradient generated by basolateral NKAs. This gradient facilitates the transport of Cl^- into MRCs from the blood via basolateral $\text{Na}^+ - \text{K}^+ - 2\text{Cl}^-$ (NKCC) co-transporters (Fig. 1-4B). Cl^- then moves down its electrochemical gradient into the water via apical cystic fibrosis transmembrane regulator (CFTR) Cl^- channels. Cl^- extrusion on the apical side generates a positive transepithelial potential on the basolateral blood side. As a result, Na^+ diffuses from the blood into the water via the paracellular pathway between MRCs and adjacent accessory cells (ACs) (Fig. 1-4B). ACs are found juxtaposed and interwoven with MRCs in the SW gill epithelium only. It is believed that TJs found between MRC-AC contacts, which are “shallow” and exhibit fewer TJ strands than those between PVC-MRC and PVC-PVC contacts (Sardet et al., 1979; Kawahara et al., 1982), are “leaky” and thus facilitate Na^+ extrusion in the SW environment (Fig. 1-4B).

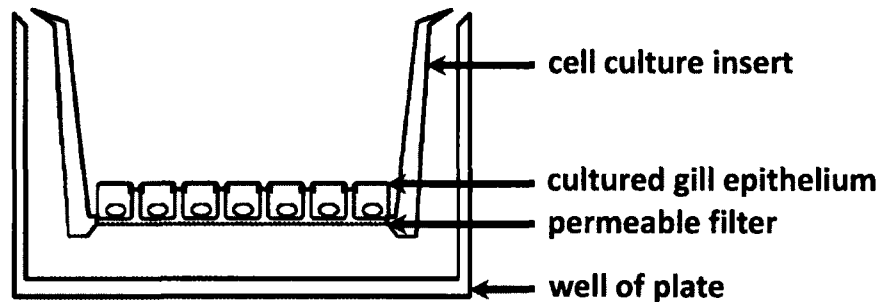
1.3.3 Primary cultured gill epithelial models

Although ultrastructural analysis of TJs between different gill epithelial cells types has provided valuable insight into a possible role for TJs in gill permeability and thus teleost osmoregulation, *in vivo* limitations have made actual measurements of gill permeability

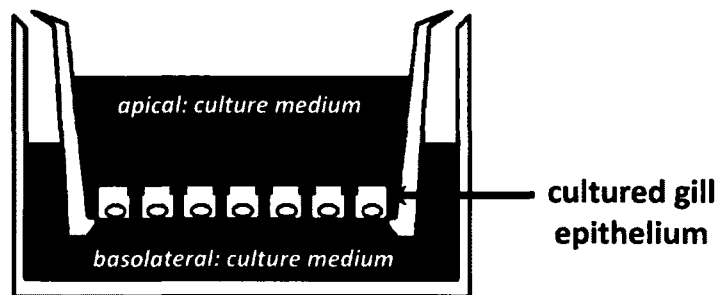
by traditional methods challenging. For example, the complex and intricate three-dimensional architecture of the intact gill physically hinders the *in vivo* application of electrophysiological techniques for measurements of TER. Furthermore, measurements of systemically administered paracellular permeability tracers across the gill epithelium of fishes are complicated by the movement of tracer molecules across other epithelial tissues, such as the gut, kidney or skin. Along the same lines, the gill itself is a heterogeneous tissue composed of several cell types including an underlying vasculature, therefore making it difficult to delineate between which TJs and what cell types the tracers are moving across.

Recently developed techniques for the primary culture of fish gill epithelia have presented simplified “reconstructed” gill models that can overcome some of these *in vivo* limitations and allow gill permeability measurements to be easily made (Wood et al., 2002). In these models, isolated primary gill cells are cultured on the upper surface of a highly permeable filter (Fig. 1-5A). When grown in this manner, cells form a flat and polarized epithelium separating an apical and basolateral compartment. Initially, the gill epithelium is cultured under symmetrical conditions, that is, with culture medium bathing both apical and basolateral surfaces (Fig. 1-5B). However, by subsequently culturing the gill preparation under asymmetrical conditions, that is, with culture medium (which simulates blood) bathing the basolateral surface and water of varying composition bathing the apical surface, conditions experienced by the *in vivo* gill can be “reconstructed” in the *in vitro* model (Fig. 1-5C; Wood et al., 2002). Because this model allows access to both apical and basolateral surfaces of the gill epithelium, these cultured

(A) Cultured gill model



(B) Symmetrical



(C) Asymmetrical

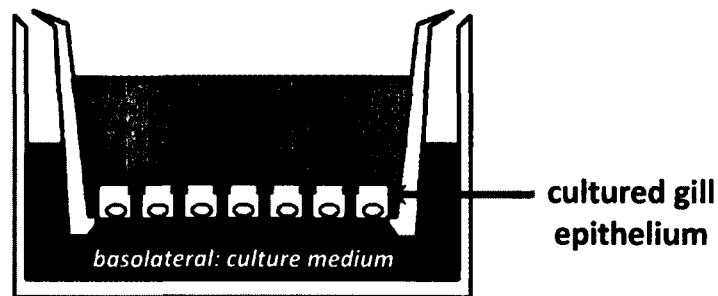


Figure 1-5: Primary cultured gill epithelial model. (A) Isolated primary gill cells form a polarized and electrically “tight” epithelium when cultured on the upper surface of a highly permeable filter. The filter is supported by a plastic cell culture insert that is housed in a well of a cell culture plate. (B) The gill epithelium is initially cultured under symmetrical conditions, i.e. with culture medium bathing both apical and basolateral surfaces. (C) To mimic conditions experienced by the gill *in vivo*, the gill epithelium can be subsequently cultured under asymmetrical conditions, i.e. with culture medium (which simulates blood) bathing the basolateral surface and water of varying composition bathing the apical surface. This set-up essentially “reconstructs” the gill epithelium *in vitro*.

preparations permit the easy measurement of TER as well as the determination of permeability to paracellular tracer molecules. In fact, these models have been shown to closely mimic the electrophysiological and passive transport characteristics of the FW gill epithelium *in vivo* (Wood et al., 1998; Wood et al., 2002). Depending on the methodology utilized, these epithelia can also be composed purely of PVCs or both PVCs and MRCs, and are always devoid of endothelial tissue from the gill vasculature (Wood and Pärt, 1997; Fletcher et al., 2000; Kelly et al., 2000). Furthermore, a number of studies have demonstrated that these cultured epithelia are responsive to physiologically relevant doses of endocrine factors as well as supplementation with homologous fish serum (e.g. Kelly and Wood, 2001; Kelly and Wood, 2002a, 2002b). These treatments have also been shown to alter the paracellular permeability characteristics of cultured gill preparations (Kelly and Wood, 2001; Kelly and Wood, 2002a), and thus may provide promising tools for manipulating TJ physiology and studying TJ function within gill epithelia. Currently however, procedures for “reconstructed” gill models have only been developed for euryhaline teleosts such as the sea bass (Avella and Ehrenfeld, 1997), rainbow trout (Wood and Pärt, 1997; Fletcher et al., 2000; Kelly et al., 2000) and tilapia (Kelly and Wood, 2002).

1.4 Research objectives

Although both transcellular and paracellular pathways have been included in current models of ionic regulation by the teleost gill epithelium (reviewed in Section 1.3.2), studies examining the molecular and mechanistic details of the paracellular route have substantially lagged behind those examining the transcellular elements. At the beginning

of the current studies in fact, nothing was known about TJs or TJ proteins with respect to epithelial permeability and fish osmoregulation beyond the ultrastructural observations made by electron microscopy which led to the “tight” vs. “leaky” TJ paradigm in FW vs. SW gill epithelia respectively (as discussed in Section 1.3.2). Considering the undeniably important and dynamic role that TJ proteins play in regulating the permeability and permselectivity properties of the paracellular pathway, a more detailed and mechanistic understanding of these molecular TJ components within fish osmoregulatory tissues was clearly required. The initial objectives of these studies, therefore, were to identify and characterize TJ proteins in FW fishes (both stenohaline and euryhaline) and establish whether TJ proteins play a role in teleost osmoregulation by investigating their contribution to the barrier properties of osmoregulatory tissues.

The FW goldfish (*Carassius auratus*) was selected as the stenohaline teleost model. The goldfish has served as a popular model organism for multiple disciplines (including osmoregulation, feeding, reproduction, vision, behavior and the stress response), and is readily available and easily maintained in a laboratory setting (e.g. Bernier, 2006; Kelly and Peter, 2006; Mora-Ferrer and Neumeyer, 2009; Marlatt et al., 2010; Kang et al., 2011; Mennigen et al., 2011). As a member of the Cyprinidae family of fishes, the goldfish is also related to the zebrafish (*Danio rerio*), an important genetic model. The zebrafish itself however was not selected for these studies, as its small size would yield insufficient amounts of tissues required for the proposed experiments, particularly for the development of a cultured stenohaline fish gill model (see below). The FW rainbow trout (*Oncorhynchus mykiss*) on the other hand was chosen as the

euryhaline teleost model. The rainbow trout was selected based on the well-established methodology for the preparation of cultured gill epithelia derived from this fish (Wood and Pärt, 1997; Fletcher et al., 2000).

As reviewed in Section 1.2.2.1, the transmembrane TJ protein occludin has been shown to contribute significantly to the TJ barrier. In fact, since its expression has a well-defined correlation with measurements of paracellular permeability in a wide variety of mammalian epithelial models, both *in vivo* and *in vitro*, occludin has been rendered a very valuable and reliable marker of overall epithelial “tightness” in these systems. The initial objectives of these studies, therefore, became more specifically focused on the identification and characterization of occludin in teleost fishes, and the investigation of a role for occludin in FW fish osmoregulation by examining its contribution to the barrier properties of osmoregulatory tissues. Based on mammalian studies, the working hypothesis was that occludin in fish osmoregulatory epithelia, particularly the gill, would alter in response to changes in hydromineral status, and that these occludin alterations would correlate with changes in epithelial permeability such that occludin functions as barrier-forming TJ protein. The principal aims of this research were as follows:

- 1) Identify occludin as a component of the TJ complex in goldfish and rainbow trout osmoregulatory tissues.
- 2) Establish a potential role for occludin in the regulation of salt and water balance in FW teleost fishes.
- 3) Develop and characterize a primary cultured model gill epithelium from the stenohaline FW goldfish.

- 4) Determine the contribution of occludin to the barrier properties of FW stenohaline and euryhaline fish gill epithelia.

1.5 References

Anderson JM. 2001. Molecular structure of tight junctions and their role in epithelial transport. *News Physiol Sci* 16:126-130.

Amasheh S, Fromm M, Günzel D. 2011. Claudins of intestine and nephron - a correlation of molecular tight junction and barrier function. *Acta Physiol (Oxf)* 201:133-140.

Amasheh S, Meiri N, Gitter AH, Schöneberg T, Mankertz J, Schulzke JD, Fromm M. 2002. Claudin-2 expression induces cation-selective channels in tight junctions of epithelial cells. *J Cell Sci* 115:4969-4976.

Avella M, Ehrenfeld J. 1997. Fish gill respiratory cells in culture: a new model for Cl⁻ secreting epithelia. *J Membr Biol* 156:87-97.

Balda MS, Matter K. 2000. The tight junction protein ZO-1 and an interacting transcription factor regulate ErbB-2 expression. *EMBO J* 19:2024-2033.

Balda MS, Garrett MD, Matter K. 2003. The ZO-1-associated Y-box factor ZONAB regulates epithelial cell proliferation and cell density. *J Cell Biol* 160:423-432.

Barton M. 2007. Origin of fishes. In: *Bond's biology of fishes*, 3rd edition (ed. M Barton), pp 19-30. Belmont:Thomson Brooks.

Bauer H, Zweimueller-Mayer J, Steinbacher P, Lametschwandtner A, Bauer HC. 2010. The dual role of zonula occludens (ZO) proteins. *J Biomed Biotechnol* 2010:402593.

Bernier NJ. 2006. The corticotrophin-releasing factor system as a mediator of the appetite-suppressing effects of stress in fish. *Gen Comp Endocrinol* 146:45-55.

Bone Q, Marshall NB. 1982. The abundance and diversity of fishes. In: *Biology of fishes* (ed. Q Bone, NB Marshall), pp 1-19. New York:Chapman and Hall.

Buchert M, Darido C, Lagerqvist E, Sedello A, Cazevieille C, Buchholz F, Bourgaux JF, Pannequin J, Joubert D, Hollande F. 2009. The symplekin/ZONAB complex inhibits intestinal cell differentiation by the repression of AML1/Runx1. *Gastroenterology* 137:156-164.

Chen X, Macara IG. 2005. Par-3 controls tight junction assembly through the Rac exchange factor Tiam1. *Nat Cell Biol* 7:262-269.

Chung NP, Mruk D, Mo MY, Lee WM, Cheng CY. 2001. A 22-amino acid synthetic peptide corresponding to the second extracellular loop of rat occludin perturbs the blood-testis barrier and disrupts spermatogenesis reversibly in vivo. *Biol Reprod* 65:1340-1351.

Claude P, Goodenough DA. 1973. Fracture faces of zonulae occludentes from "tight" and "leaky" epithelia. *J Cell Biol* 58:390-400.

Coëffier M, Gloro R, Boukhattala N, Aziz M, Lecleire S, Vandaele N, Antonietti M, Savove G, Bôle-Feysot C, Déchelotte P, Reimund JM, Ducrotté P. 2010. Increased proteasome-mediated degradation of occludin in irritable bowel syndrome. *Am J Gastroenterol* 105:1181-1188.

Colegio OR, Van Itallie CM, McCrea HJ, Rahner C, Anderson JM. 2002. Claudins create charge-selective channels in the paracellular pathway between epithelial cells. *Am J Physiol Cell Physiol* 283:C142-147.

Colegio OR, Van Itallie C, Rahner C, Anderson JM. 2003. Claudin extracellular domains determine paracellular charge selectivity and resistance but not tight junction fibril architecture. *Am J Physiol Cell Physiol* 284:C1346-1354.

Daugherty BL, Ward C, Smith T, Ritzenthaler JD, Koval M. 2007. Regulation of heterotypic claudin compatibility. *J Biol Chem* 282:30005-30013.

Evans DH, Piermarini PM, Choe KP. 2005. The multifunctional fish gill: dominant site of gas exchange, osmoregulation, acid-base regulation, and excretion of nitrogenous waste. *Physiol Rev* 85: 97-177.

Fanning AS, Jameson BJ, Jesaitis LA, Anderson JM. 1998. The tight junction protein ZO-1 establishes a link between the transmembrane protein occludin and the actin cytoskeleton. *J Biol Chem* 273:29745-29753

Fanning AS. 2006. ZO proteins and tight junction assembly. In: *Tight junctions* (ed. L. González-Mariscal), pp 64-75. New York:Springer Science.

Fletcher M, Kelly SP, Pärt P, O'Donnell MJ, Wood CM. 2000. Transport properties of cultured branchial epithelia from freshwater rainbow trout: a novel preparation with mitochondria-rich cells. *J Exp Biol* 203:1523-1537.

Fujimoto K. 1995. Freeze-fracture replica electron microscopy combined with SDS digestion for cytochemical labeling of integral membrane proteins. Application to the immunogold labeling of intercellular junctional complexes. *J Cell Sci* 108:3443-3449.

Fujita H, Chiba H, Yokozaki H, Sakai N, Sugimoto K, Wada T, Kojima T, Yamashita T, Sawada N. 2006. Differential expression and subcellular localization of claudin-7, -8, -12, -13, and -15 along the mouse intestine. *J Histochem Cytochem* 54:933-944.

Furuse M, Hirase T, Itoh M, Nagafuchi A, Yonemura S, Tsukita S, Tsukita S. 1993. Occludin: a novel integral membrane protein localizing at tight junctions. *J Cell Biol* 123:1777-1788.

Furuse M, Fujita K, Hiiiragi T, Fujimoto K, Tsukita S. 1998. Claudin-1 and -2: novel integral membrane proteins localizing at tight junctions with no sequence similarity to occludin. *J Cell Biol* 141:1539-1550.

Furuse M, Sasaki H, Tsukita S. 1999. Manner of interaction of heterogenous claudin species within and between tight junction strands. *J Cell Biol* 147:891-903.

Furuse M, Furuse K, Sasaki H, Tsukita S. 2001. Conversion of zonulae occludentes from tight to leaky strand type by introducing claudin-2 into Madin-Darby Canine Kidney I cells. *J Cell Biol* 153:263-272.

Gassler N, Rohr C, Schneider A, Kartenbeck J, Bach A, Obermüller N, Otto HF, Autschbach F. 2001. Inflammatory bowel disease is associated with changes of enterocytic junctions. *Am J Physiol Gastrointest Liver Physiol* 281:G216-G228.

González-Mariscal L, Namorado MC, Martin D, Luna J, Alarcon L, Islas S, Valencia L, Muriel P, Ponce L, Reyes JL. 2000. Tight junction proteins ZO-1, ZO-2, and occludin along isolated renal tubules. *Kidney Int* 57:2386-2402.

González-Mariscal L, Betanzos A, Nava P, Jaramillo BE. 2003. Tight junction proteins. *Prog Biophys Mol Biol* 81:1-44.

Guillemot L, Citi S. 2006. Cingulin regulates claudin-2 expression and cell proliferation through the small GTPase RhoA. *Mol Biol Cell* 17:3569-3577.

Harhaj NS, Antonetti DA. 2004. Regulation of tight junctions and loss of barrier function in pathophysiology. *Int J Biochem Cell Biol* 36:1206-1237.

Holmes JL, Van Itallie CM, Rasmussen JE, Anderson JM. 2006. Claudin profiling in the mouse during postnatal intestinal development and along the gastrointestinal tract reveals complex expression patterns. *Gene Expr Patterns* 6:581-588.

Hou J, Gomes AS, Paul DL, Goodenough DA. 2006. Study of claudin function by RNA interference. *J Biol Chem* 281:36117-36123.

Hua VB, Chang AB, Tchieu JH, Kumar NM, Nielsen PA, Saier Jr MH. 2003. Sequence and phylogenetic analyses of 4 TMS junctional proteins of animals: connexins, innexins, claudins and occludins. *J Membr Biol* 194:59-76.

Itoh M, Furuse M, Morita K, Kubota K, Saitou M, Tsukita S. 1999. Direct binding of three tight junction associated MAGUKs, ZO-1, ZO-2 and ZO-3, with the COOH termini of claudins. *J Cell Biol* 147:1351-1363.

Kang KS, Yahashi S, Matsuda K. 2011. The effects of ghrelin on energy balance and psychomotor activity in a goldfish model: an overview. *Int J Pept* 2011:171034.

Kawahara T, Sasaki T, Higashi S. 1982. Intercellular junctions in chloride and pavement cells of *Opkgnethus fasciatus*. *J Electron Microsc* 31:162-170.

Kelly SP, Fletcher M, Pärt P, Wood CM. 2000. Procedures for the preparation and culture of “reconstructed” rainbow trout branchial epithelia. *Methods Cell Sci* 22:153-163.

Kelly SP, Wood CM. 2001. Effect of cortisol on the physiology of cultured pavement cell epithelia from freshwater trout gills. *Am J Physiol* 281:R811-R820.

Kelly SP, Wood CM. 2002a. Cultured gill epithelia from freshwater tilapia (*Oreochromis niloticus*): Effect of cortisol and homologous serum supplements from stressed and unstressed fish. *J Membr Biol* 190: 29-42.

Kelly SP, Wood CM. 2002b. Prolactin effects on cultured pavement cell epithelia and pavement cell plus mitochondria-rich cell epithelia from freshwater rainbow trout gills. *Gen Comp Endocrinol* 128:44-56.

Kelly SP, Peter RE. 2006. Prolactin-releasing peptide, food intake, and hydromineral balance in goldfish. *Am J Physiol Regul Integr Comp Physiol* 291:R1474-R1481.

Kevil CG, Okayama N, Trocha SD, Kalogeris TJ, Coe LL, Specian RD, Davis CP, Alexander JS. 1998. Expression of zonula occludens and adherens junctional proteins in human venous and arterial endothelial cells: role of occludin in endothelial solute barriers. *Microcirculation* 5:197-210.

Kiuchi-Saishin Y, Gotoh S, Furuse M, Takasuga A, Tano Y, Tsukita S. 2002. Differential expression patterns of claudins, tight junction membrane proteins, in mouse nephron segments. *J Am Soc Nephrol* 13:875-886.

Krause G, Winkler L, Mueller SL, Haseloff RF, Piontek J, Blasig IE. 2008. Structure and function of claudins. *Biochim Biophys Acta* 1778:631-645.

Kwon O, Myers BD, Sibley R, Dafoe D, Alfrey E, Nelson WJ. 1998. Distribution of cell membrane-associated proteins along the human nephron. *J Histochem Cytochem* 46:1423-1434.

Lacaz-Vieira F, Jaeger MM, Farshori P, Kachar B. 1999. Small synthetic peptides homologous to segments of the first external loop of occludin impair tight junction resealing. *J Membr Biol* 168:289-297.

Loh YH, Christoffels A, Brenner S, Hunziker W, Venkatesh B. 2004. Extensive expansion of the claudin gene family in the teleost fish, *Fugu rubripes*. *Genome Res* 14:1248-1257.

Markov AG, Veshnyakova A, Fromm M, Amasheh M, Amasheh S. 2010. Segmental expression of claudin proteins correlates with tight junction barrier properties in rat intestine. *J Comp Physiol B* 180:591-598.

Marlatt VL, Lakoff J, Crump K, Martyniuk CJ, Watt J, Jewell L, Atkinson S, Blais JM, Sherry J, Moon TW, Trudeau VL. 2010. Sex- and tissue-specific effects of waterborne estrogen on estrogen receptor subtypes and E₂-mediated gene expression in the reproductive axis of goldfish. *Comp Biochem Physiol A Mol Integr Physiol* 156:92-101.

Martín-Padura I, Lostaglio S, Schneemann M, Williams L, Romano M, Fruscella P, Panzeri C, Stoppacciaro A, Rucó L, Villa A, Simmons D, Dejana E. 1998. Junctional adhesion molecule, a novel member of the immunoglobulin superfamily that distributes at the intercellular junctions and modulates monocyte transmigration. *J Cell Biol* 142:117-127.

Marshall WS, Grosell M. 2005. Ion transport, osmoregulation and acid-base balance. In: *The Physiology of Fishes*, 3rd edition (ed. DH Evans, JB Claiborne), pp 177-230. New York: CRC Press.

McCarthy KM, Skare IB, Stankewich MC, Furuse M, Tsukita S, Rogers RA, Lynch RD, Schneeberger EE. 1996. Occludin is a functional component of the tight junction. *J Cell Sci* 109:2287-2298.

McCormick SD. 2001. Endocrine control of osmoregulation in teleost fish. *Amer Zool* 41:781-794.

Mennigen JA, Stroud P, Zamore JM, Moon TW, Trudeau VL. 2011. Pharmaceuticals as neuroendocrine disruptors: lessons learned from fish on Prozac. *J Toxicol Environ Health B Crit Rev* 14:387-412.

Milatz S, Krug SM, Rosenthal R, Günzel D, Müller D, Schulzke JD, Amasheh S, Fromm M. 2010. Claudin-3 acts as a sealing component of the tight junction for ions of either charge and uncharged solutes. *Biochim Biophys Acta* 1798:2048–2057.

Mora-Ferrer C, Neumeyer C. 2009. Neuropharmacology of vision in goldfish: review. *Vision Res* 49:960-969.

Rahner C, Mitic LL, Anderson JM. 2001 Heterogeneity in expression and subcellular localization of claudins 2, 3, 4, and 5 in the rat liver, pancreas, and gut. *Gastroenterology* 120:411-422.

Saitou M, Ando-Akatsuka Y, Itoh M, Furuse M, Inazawa J, Fujimoto K, Tsukita S. 1997. Mammalian occludin in epithelial cells: its expression and subcellular distribution. *Eur J Cell Biol* 73:222-231.

Saitou M, Fujimoto K, Doi Y, Itoh M, Fujimoto T, Furuse M, Takano H, Noda T, Tsukita S. 1998. Occludin-deficient embryonic stem cells can differentiate into polarized epithelial cells bearing tight junctions. *J Cell Biol* 141:397-408.

Saitou M, Furuse M, Sasaki H, Schulzke JD, Fromm M, Takano H, Noda T, Tsukita S. 2000. Complex phenotype of mice lacking occludin, a component of tight junction strands. *Mol Biol Cell* 11:4131-4142.

Sardet C, Pisam M, Maetz J. 1979. The surface epithelium of teleostean fish gills. *J Cell Biol* 80:96-117.

Schneeberger EE, Lynch RD. 2004. The tight junction: a multifunctional complex. *Am J Physiol Cell Physiol* 286:C1213-1228.

Stevenson BR, Siliciano JD, Mooseker MS, Goodenough DA. 1986. Identification of ZO-1: a high molecular weight polypeptide associated with the tight junction (zonula occludens) in a variety of epithelia. *J Cell Biol* 103:755-766.

Stevenson BR, Anderson JM, Goodenough DA, Mooseker MS. 1988. Tight junction structure and ZO-1 content are identical in two strains of Madin-Darby canine kidney cells which differ in transepithelial resistance. *J Cell Biol* 107:2401-2408.

Stevenson BR, Anderson JM, Braun ID, Mooseker MS. 1989. Phosphorylation of the tight junction protein ZO-1 in two strains of Madin-Darby canine kidney cells which differ in transepithelial resistance. *Biochem J* 263:597-599.

Stevenson BR, Begg DA. 1994. Concentration-dependent effects of cytochalasin D on tight junctions and actin filaments in MDCK epithelial cells. *J Cell Sci* 107:367-375.

Van Itallie CM, Fanning JM, Anderson JM. 2003. Reversal of charge selectivity in cation or anion-selective epithelial lines by expression of different claudins. *Am J Physiol Renal Physiol* 285:1078-1084.

Van Itallie CM, Fanning AS, Bridges A, Anderson JM. 2009. ZO-1 stabilizes the tight junction solute barrier through coupling to the perijunctional cytoskeleton. *Mol Biol Cell* 20:3930-3940.

Wilson JM, Laurent P. 2002. Fish gill morphology: inside out. *J Exp Zool* 293:192-213.

Wittchen ES, Haskins J, Stevenson BR. 1999. Protein interactions at the tight junction. Actin has multiple binding partners, and ZO-1 forms independent complexes with ZO-2 and ZO-3. *J Biol Chem* 274:35179-35185.

Wong V, Gumbiner BM. 1997. A synthetic peptide corresponding to the extracellular domain of occludin perturbs the tight junction permeability barrier. *J Cell Biol* 136:399-409.

Wood C, Pärt P. 1997. Cultured branchial epithelia from freshwater fish gills. *J Exp Biol* 200:1047-1059.

Wood CM, Gilmour KM, Pärt P. 1998. Passive and active transport properties of a gill model, the cultured branchial epithelium of the freshwater rainbow trout (*Oncorhynchus mykiss*). *Comp Biochem Physiol A* 119:87-96.

Wood CM, Kelly SP, Zhou B, Fletcher M, O'Donnell MJ, Eletti B, Pärt, P. 2002. Cultured gill epithelia as models for the freshwater fish gill. *Biochim Biophys Acta* 1566:72-83.

Yu AS, Enck AH, Lencer WI, Schneeberger EE. 2003. Claudin-8 expression in Madin-Darby canine kidney cells augments the paracellular barrier to cation permeation. *J Biol Chem* 278:17350–17359.

Zeissig S, Bürgel N, Günzel D, Richter J, Mankerz J, Wahnschaffer U, Kroesen AJ, Zeitz M, Fromm M, Schulzke JD. 2007. Changes in expression and distribution of claudin 2, 5 and 8 lead to discontinuous tight junctions and barrier dysfunction in active Crohn's disease. *Gut* 56:61-72.

CHAPTER 2:
**OCCLUDIN IMMUNOLOCALIZATION AND
PROTEIN EXPRESSION IN GOLDFISH**

Helen Chasiotis and Scott P. Kelly

Department of Biology, York University, Toronto, Ontario, Canada M3J 1P3

This chapter has been published and reproduced with permission:

Chasiotis H, Kelly SP. 2008. Occludin immunolocalization and protein expression in goldfish. *J Exp Biol* 211:1524-1534.

2.1 Abstract

Tight junctions (TJs) are an integral component of models illustrating ion transport mechanisms across fish epithelia, however little is known about TJ proteins in fishes. Using immunohistochemical methods and Western blot analysis, we examined the localization and expression of occludin, a transmembrane TJ protein, in goldfish tissues. In goldfish gills, discontinuous occludin immunostaining was detected along the edges of secondary gill lamellae and within parts of the interlamellar region that line the lateral walls of the central venous sinus. In the goldfish intestine, occludin immunolocalized in a TJ-specific distribution pattern to apical regions of columnar epithelial cells lining the intestinal lumen. In the goldfish kidney, occludin was differentially expressed in discrete regions of the nephron. Occludin immunostaining was strongest in the distal segment of the nephron, moderate in the collecting duct and absent in the proximal segment. To investigate a potential role for occludin in the maintenance of hydromineral balance of fishes, we subjected goldfish to 1, 2 and 4 weeks of food deprivation, and then examined endpoints of hydromineral status, $\text{Na}^+\text{-K}^+\text{-ATPase}$ activity and occludin protein expression in the gills, intestine and kidney. Occludin expression altered in response to hydromineral imbalance in a tissue-specific manner suggesting a dynamic role for this TJ protein in the regulation of epithelial permeability in fishes.

2.2 Introduction

Hydromineral balance in freshwater (FW) fishes is regulated by strategies of ion retention and ion acquisition across ionoregulatory epithelia. While ion retention mechanisms limit outwardly directed solute movement across epithelia, ion acquisition compensates for obligatory losses to the environment (e.g. ion loss to FW due to epithelial permeability). Studies examining the role of ionoregulatory epithelia in the maintenance of hydromineral status in fishes have generally focused on transcellular mechanisms/routes of ion movement, through which actively driven ion transport takes place. In contrast, far less emphasis has been placed on mechanisms that enhance ion retention, i.e. those that limit paracellular ion loss. As a result, while transcellular pathways are well characterized and are known to incorporate a multifaceted suite of pumps, exchangers and channels which associate with either apical or basolateral cell membranes (Loretz, 1995; Marshall, 2002; Evans et al., 2005), the paracellular pathway, which is controlled by the tight junction complex, remains poorly understood in aquatic vertebrates.

Tight junctions (TJs) are composed of transmembrane and cytosolic protein complexes that form strands around the apical domain of an epithelial cell. TJ proteins of adjacent epithelial cells associate with one another to form a semi-permeable paracellular seal that restricts solute movement between cells (Cereijido and Anderson, 2001). In addition to regulating paracellular permeability and limiting solute movement, TJs also demarcate apicobasal polarity and establish cell-cell contacts which aid in the regulation of cellular processes such as transcription and proliferation (reviewed by Schneeberger and Lynch, 2004). To date, over 40 TJ and TJ-associated proteins have been identified at

the epithelial TJ complex (González-Mariscal et al., 2003). Isolated from chick liver, occludin was the first transmembrane TJ protein identified (Furuse et al., 1993). The presence of this tetraspan protein within TJ fibrils (Fujimoto, 1995) and its capacity to form TJ-like strands when transfected into cells lacking TJs (Furuse et al., 1998) quickly underscored a structural role for occludin within TJ complexes. Several other lines of evidence, however, also suggested a vital functional role for occludin in TJ sealing and the regulation of solute movement through the paracellular pathway. For example, the over-expression of chick occludin in Madin-Darby canine kidney (MDCK) epithelial cells led to an increase in transepithelial resistance (TER) (Balda et al., 1996; McCarthy et al., 1996). In contrast, treatment of *Xenopus* A6 epithelial cells with a synthetic peptide designed to disrupt occludin associations between adjacent cells led to a significant decrease in TER and an increase in permeability to paracellular markers (e.g. [³H]mannitol, [¹⁴C]inulin and dextrans) (Wong and Gumbiner, 1997). Moreover, microinjection of mRNA encoding COOH-terminally truncated occludin into *Xenopus* embryos resulted in TJs exhibiting a “leaky” phenotype (Chen et al., 1997). This “leaky” phenotype could be rescued by co-injection with full-length occludin mRNA (Chen et al., 1997).

While various TJ forms (e.g. “leaky” versus “tight”) are widely accepted to play critical roles in the way fish epithelia function (for reviews see Loretz, 1995; Marshall, 2002; Evans et al., 2005), little is known about TJ proteins in fishes. Given its role in regulating TJ barrier function and its use as an indicator of changes in paracellular permeability, we conducted studies on the integral TJ protein occludin in goldfish to

investigate a potential role for occludin in the maintenance of hydromineral balance of fishes. Using Western blot analysis and immunohistochemistry, we first examined occludin protein expression and localization in select goldfish epithelial tissues (i.e. gill, intestine and kidney). We then hypothesized that occludin protein expression would alter in response to hydromineral imbalance. To test this hypothesis we subjected goldfish to varying periods of food deprivation, working on the assumption that the restricted nutritional state would disrupt normal, energy-dependent mechanisms of ion acquisition in a time-dependent manner. Using endpoint measurements of hydromineral status and $\text{Na}^+\text{-K}^+\text{-ATPase}$ activity, we characterized the response of goldfish to negative energy status in conjunction with measurements of occludin protein expression.

2.3 Materials and Methods

2.3.1 Experimental animals: Goldfish (*Carassius auratus*) were obtained from a local supplier and held at 18-19°C under simulated natural photoperiod (12 h light:12h dark) in aerated 200-liter opaque polyethylene tanks at a density of 10-12 fish per tank. Each tank was supplied with flow through dechlorinated FW (~ composition in mM: [Na⁺] = 0.59, [Cl⁻] = 0.92, [Ca²⁺] = 0.76 and [K⁺] = 0.43) at a rate of ~ 250 – 300 ml/min. Fish were held for at least 4 weeks prior to experimentation and during this period were fed *ad libitum* once daily with commercial koi and goldfish pellets (Martin Profishent, Elmira, ON, Canada).

2.3.2 Immunohistochemistry and Western blot analysis

2.3.2.1 Tissue collection: Fish were randomly selected and anaesthetized using 1 g/L tricaine methanesulfonate (MS-222; Syndel Laboratories Ltd., Qualicum Beach, BC, Canada). For immunohistochemistry, gill and kidney tissues were carefully isolated and fixed in Bouin's solution for 3-4 hours. A standardized region of the intestine (i.e. a section approximately one third from the anterior most region, relative to the full gastrointestinal tract length), was also isolated and gently flushed of any gut contents with Bouin's solution. The tissue was then immersed in Bouin's solution and fixed for 3-4 hours. Following fixation, all tissues were rinsed twice with 70% ethanol and stored in 70% ethanol at 4°C until further processing. For Western blot analysis, samples of goldfish blood cells, gill, kidney and intestine were collected. Blood was sampled from anesthetized fish via caudal puncture using a 25 gauge needle, following which fish were killed by spinal transection. Blood was allowed to clot at 4°C for 1 hour and was then

centrifuged at 10 600 g for 5 minutes at 4°C. Resulting serum was discarded and the pellet of packed blood cells was quick-frozen in liquid nitrogen and stored at -85°C until further processing. The intestinal segment collected for Western blot analysis was the same as that described above, however, any residual gut contents were gently flushed out with 0.7% NaCl (i.e. not flushed with Bouin's solution). Rat kidney tissue was donated by G. Sweeney (York University, Toronto, ON, Canada). After collection, all tissues were quick frozen in liquid nitrogen and stored at -85°C until further analysis.

2.3.2.2 Immunohistochemistry: Fixed tissues were dehydrated through an ascending series of ethanol rinses (70 – 100%), cleared with xylene and infiltrated and embedded in Paraplast Plus Tissue Embedding Medium (Oxford Worldwide, LLC., Memphis, TN, USA). Sections (3 µm thick) were cut using a Leica RM 2125RT manual rotary microtome (Leica Microsystems Inc., Richmond Hill, ON, Canada), collected on 2% bovine-serum albumin (BSA; BioShop Canada Inc., Burlington, ON, Canada) coated glass slides and incubated overnight at 45°C. Sections were deparaffinized with xylene, rehydrated to water via a descending series of ethanol rinses (100 – 50%), and subjected to heat-induced epitope retrieval (HIER). HIER was accomplished by immersing slides in a sodium citrate buffer (10 mM, pH 6.0) and heating both solution and slides in a microwave oven for 4 minutes. The solution was allowed to cool for 20 minutes, reheated for 2 minutes, and cooled for a further 15 minutes. Slides were then washed three times with phosphate-buffered saline (PBS, pH 7.4) and quenched for 30 minutes in 3% H₂O₂ in PBS. Following quenching, slides were then successively washed with 0.4% Kodak Photo-Flo 200 in PBS (PF/PBS, 10 minutes), 0.05% Triton X-100 in PBS (TX/PBS, 10

minutes), and 10% Antibody Dilution Buffer (ADB; 10% goat serum, 3% BSA and 0.05% Triton X-100 in PBS) in PBS (ADB/PBS, 10 minutes). Slides were incubated overnight at room temperature with rabbit polyclonal anti-occludin antibody (1:100 dilution in ADB; Zymed Laboratories, Inc., South San Francisco, CA, USA) and mouse monoclonal anti-Na⁺-K⁺-ATPase α -subunit antibody (α 5; 1:10 in ADB; Developmental Studies Hybridoma Bank, Iowa City, IA, USA). The anti-occludin antibody is epitope-affinity purified and directed against the C-terminal region of the human occludin protein. As negative controls, two set of slides were also incubated overnight with ADB alone or with normal rabbit serum. Normal rabbit serum was donated by P. Moens (York University). Following overnight incubation, sections were successively washed with PF/PBS, TX/PBS and ADB/PBS (10 minutes each) as previously described, and incubated with tetramethyl rhodamine isothiocyanate (TRITC)-labeled goat anti-rabbit antibody (1:500 in ADB; Jackson ImmunoResearch Laboratories, Inc., West Grove, PA, USA) and fluorescein-isothiocyanate (FITC)-labeled goat anti-mouse antibody (1:500 in ADB; Jackson ImmunoResearch Laboratories, Inc.) for 1 hour at 37°C. Slides were then successively washed with PF/PBS, TX/PBS, PF/PBS (10 minutes each) and rinsed 3 times with 0.4% Kodak Photo-Flo 200 in distilled water (PF/dH₂O, 1 minute each). Slides were air-dried for 1 hour and mounted with Molecular Probes ProLong Antifade (Invitrogen Canada Inc., Burlington, ON, Canada) containing 5 μ g/ml 4',6-diamidino-2-phenylindole (DAPI; Sigma-Aldrich Canada Ltd., Oakville, ON, Canada). Fluorescent images were captured using a Reichert Polyvar microscope (Reichert Microscope Services, Depew, NY, USA) and Olympus DP70 camera (Olympus Canada Inc.,

Markham, ON, Canada), and merged using Adobe Photoshop CS2 software (Adobe Systems Canada, Toronto, ON, Canada).

2.3.2.3 Western blotting: Goldfish tissues (blood pellet, gills, intestine, kidney) and rat kidney were thawed and homogenized on ice in chilled homogenization buffer (200 mM sucrose, 1 mM EDTA, 1 mM PMSF, 1 mM DTT in 0.7% NaCl) containing 1:200 protease inhibitor cocktail (Sigma-Aldrich Canada Ltd.). Tissues were homogenized at a 1:3 w:v tissue to homogenization buffer ratio using a PRO250 homogenizer (PRO Scientific Inc., Oxford, CT, USA). Homogenates were centrifuged at 3200g for 20 minutes at 4°C and supernatants were collected after centrifugation. Protein content was quantified using the Bradford assay (Sigma-Aldrich Canada Ltd.) according to the manufacturer's guidelines with BSA as a standard. Samples were prepared for SDS-PAGE by boiling at 100°C with 6X sample buffer (360 mM Tris-HCl, 30% Glycerol, 12% SDS, 600 mM DTT, 0.03% bromophenol blue). 20 µg of rat kidney and 75 µg of goldfish blood pellet, gill, intestine and kidney were electrophoretically separated by SDS-PAGE in 12% acrylamide gels at 150V. After electrophoresis, protein was transferred to a Hybond-P polyvinylidene difluoride (PVDF) membrane (GE Healthcare Bio-Sciences Inc., Baie d'Urfé, QC, Canada) over a 2 hour period using a TE 70 Semi-Dry Transfer unit (GE Healthcare Bio-Sciences Inc.). Following transfer, the membrane was washed in Tris-buffered saline with Tween-20 [TBS-T; TBS (10 mM Tris, 150 mM NaCl, pH 7.4) with 0.05% Tween-20], and blocked for 1 hour in 5% non-fat dry skim milk powder in TBS-T (5% skim milk TBS-T). The membrane was then incubated for ~16 hours at 4°C with rabbit polyclonal anti-occludin antibody (1:1000 dilution in 5%

skim milk TBS-T; Zymed Laboratories, Inc.). Following incubation with primary antibody, the membrane was washed with TBS-T and incubated at room temperature with horseradish peroxidase (HRP)-conjugated goat anti-rabbit antibody (1:5000 in 5% skim milk TBS-T; Bio-Rad Laboratories, Inc., Mississauga, ON, Canada) for 1 hour, and then washed with TBS-T and TBS respectively. Protein bands were visualized using Enhanced Chemiluminescence Plus Western Blotting Detection System (GE Healthcare Bio-Sciences Inc.).

2.3.3 Food deprivation experiments

2.3.3.1 Experimental animals and tissue sampling: Goldfish (mean weight = 19.2 ± 0.7 g, $n = 60$), were acclimated to conditions as outlined above (see Section 2.3.1) and randomly assigned to one of six experimental groups. Fish were food deprived for either 1, 2 or 4 weeks and for each unfed group, a corresponding fed control group was run. Fed control fish were provided pellets at a ration of 1.5% their body weight once daily. Control fish were not fed 24 hours prior to sampling. Goldfish were weighed immediately prior to commencing experiments and at the end of each experimental period (i.e. at the time of tissue sampling) enabling calculation of body weight change. Individual fish were identified by unique markings. At 1, 2 and 4 weeks, fed and unfed fish were anaesthetized using 1 g/L MS-222 and blood was rapidly sampled (within ~ 2 minutes) via caudal puncture using a 25 gauge needle. Blood was processed as described previously and serum was collected, quick-frozen in liquid nitrogen and stored at -85°C until further analysis. For analysis of muscle moisture content, a standardized region of epaxial white muscle was removed. Gill, kidney and intestinal tissues for enzyme and

Western blot analyses were removed, frozen in liquid nitrogen and stored at -85°C until further processing.

2.3.3.2 Muscle moisture content and serum analysis: Pre-weighed muscle tissue was placed in an oven and dried to a constant weight at 60°C . Muscle moisture content was subsequently determined gravimetrically. Serum osmolality was measured using a Model 5500 Vapor Pressure Osmometer (Wescor, Inc., Logan, UT, USA). Serum Na^+ concentration was determined by atomic absorption spectroscopy using an AAnalyst 200 spectrometer (PerkinElmer Life and Analytical Sciences, Woodbridge, ON, Canada). Serum Cl^- concentration was determined using the colorimetric assay as described by Zall et al. (1956) and measured using a Multiskan Spectrum microplate reader (Thermo Fisher Scientific, Nepean, ON, Canada).

2.3.3.3 Na^+ - K^+ -ATPase enzyme activity: The activity of Na^+ - K^+ -ATPase was examined using methods previously outlined by McCormick (1993), with some minor modifications. Briefly, gill, kidney or intestinal tissues were homogenized at 4°C in a 1:10 w:v pre-chilled SEI (150 mM sucrose, 10 mM EDTA, 50 mM imidazole, pH 7.3):SEID (0.5 g sodium deoxycholate/100 mL SEI) buffer mixture (4:1 mixture of SEI:SEID) using a PRO250 homogenizer. Homogenates were centrifuged at $3200g$ for 10 minutes at 4°C and supernatants were collected, quick-frozen in liquid nitrogen and stored at -85°C until enzyme analysis. For analysis, supernatants were thawed on ice and assayed for Na^+ - K^+ -ATPase activity using solutions that couple ATP hydrolysis to ADP with the oxidation of NADH. The sensitivity of goldfish Na^+ - K^+ -ATPase activity to ouabain inhibition varies from tissue to tissue (see Busacker and Chavin, 1981).

Therefore, to distinguish Na⁺-K⁺-ATPase from total ATPase activity, samples were run in assay solutions either with or without K⁺ present, under the assumption that K⁺-dependent ATPase activity is almost exclusively Na⁺-K⁺-ATPase activity. The use of K⁺-free assay solutions yielded equivalent results to using 0.5 mM and 10 mM ouabain for kidney and gill/intestine tissues respectively. This corresponds with the observations of Busacker and Chavin (1981) who reported that maximal inhibition of gill and kidney Na⁺-K⁺-ATPase activity occurred at an ouabain concentration of 10 mM, but that gill activity was less sensitive to higher ouabain concentrations than kidney tissue. Na⁺-K⁺-ATPase activity was standardized to ADP release and was expressed as μmol ADP mg protein⁻¹ h⁻¹. The protein content of supernatants used for analysis was measured using a Bradford assay with BSA as a standard, as previously described.

2.3.3.4 Western blot analysis: Western blots for occludin were carried out as outlined above (see Section 2.3.2.3) using equal amounts of protein from each tissue sampled. As a loading control, membranes were subsequently stripped with stripping buffer (100 mM glycine, 30 mM KCl, 20 mM sodium acetate, pH 2.2), washed with TBS-T, blocked with 5% skim milk TBS-T and incubated for ~16 hours at 4°C with mouse monoclonal anti-α-tubulin (12G10; 1:10,000 in 5% skim milk TBS-T; Developmental Studies Hybridoma Bank). Membranes were then washed with TBS-T and incubated at room temperature with HRP-conjugated goat anti-mouse antibody (1:5000 in 5% skim milk TBS-T; Bio-Rad Laboratories, Inc.) for 1 hour, washed with TBS-T and TBS respectively, and then visualized as described above. Occludin and α-tubulin protein expression were quantified using Labworks Image Acquisition and Analysis software (UVP BioImaging Systems

and Analysis Systems, Upland, CA, USA), and α -tubulin was used for normalization of occludin expression.

2.3.4 Statistical analyses: All data are presented as mean values \pm s.e.m (n) where n equals the number of fish in a treatment group. A one-way ANOVA was used to examine for significant differences between control groups at 1, 2 or 4 weeks. In all cases no significant differences were found. Therefore, data were subsequently analyzed using a Student's t -test to examine for significant differences ($P < 0.05$) between control (fed) and experimental (unfed) groups within a time point. A one-way ANOVA was also used to examine for significant differences between experimental (unfed) groups at 1, 2 or 4 weeks. All statistical analyses were run using GraphPad InStat Software Version 3.00 (GraphPad Software, Inc., San Diego, CA, USA).

2.4 Results

2.4.1 Immunohistochemistry

2.4.1.1 *Occludin and Na⁺-K⁺-ATPase immunolocalization in the gill:* Na⁺-K⁺-ATPase immunolocalized to select cells within the interlamellar (IL) region of primary filaments and at the base of the secondary gill lamellae of goldfish gills (Fig. 2-1A). Immunofluorescence microscopy revealed pronounced and discontinuous occludin immunostaining along the edges of secondary lamellae and medial parts of lamellae that are embedded within the body of the primary filament (Fig. 2-1B,C,E). In addition, occludin immunostaining appeared to be associated with cells of the secondary lamellae that also express Na⁺-K⁺-ATPase (Fig. 2-1C,D). Furthermore, occludin immunofluorescence was also prominent in parts of the IL region that line the lateral walls of the central venous sinus (CVS) (Fig. 2-1B). While there appeared to be no difference in staining for occludin between the afferent and efferent edges of gill filaments, Na⁺-K⁺-ATPase immunostaining was generally prominent along the trailing edge of primary gill filaments (cross-sections not shown). No co-localization of occludin or Na⁺-K⁺-ATPase was found, and no TRITC or FITC fluorescence was observed in control sections which had been probed with secondary antibody only (Fig. 2-1F) or with normal rabbit serum (not shown).

2.4.1.2 *Occludin and Na⁺-K⁺-ATPase immunolocalization in the intestine:* Immunohistochemical analysis of goldfish intestine revealed prominent basolateral Na⁺-K⁺-ATPase immunostaining and distinct apical occludin immunostaining in columnar epithelial cells lining the intestinal lumen (Fig. 2-2A,B,C). While basolateral Na⁺-K⁺-

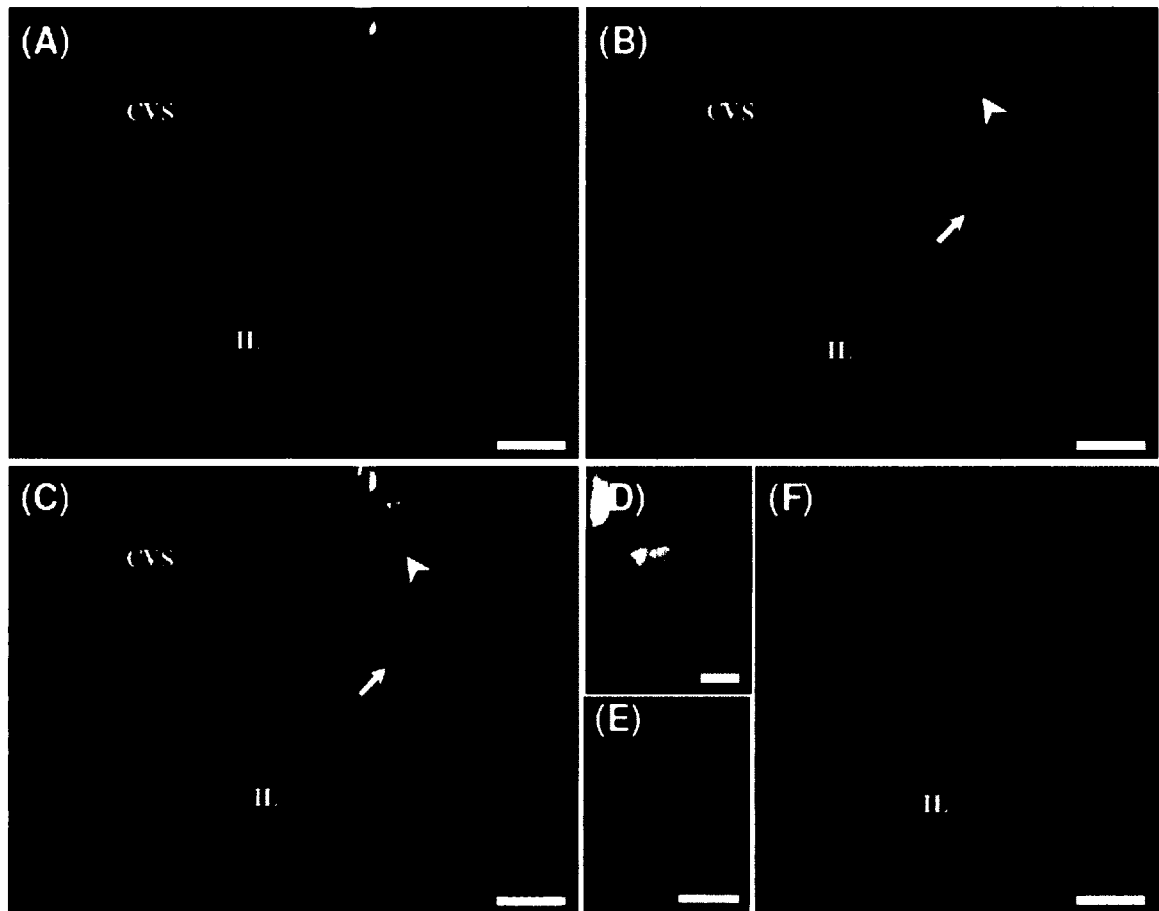


Figure 2-1: Immunofluorescent staining of (A) $\text{Na}^+\text{-K}^+\text{-ATPase}$ (green) and (B) occludin (red) in longitudinal sections of a goldfish gill filament. Nuclei are stained with DAPI (blue) in (A,F). (C) is a merged image of (A) and (B). In (A), $\text{Na}^+\text{-K}^+\text{-ATPase}$ immunolocalizes to select cells within the interlamellar (IL) region of the primary filament and at the base of secondary gill lamellae. In (B), discontinuous occludin immunostaining is concentrated along the edges of secondary gill lamellae (white arrow), including medial parts of lamellae that are embedded within the body of the primary filament, and is associated with cells that also stain for $\text{Na}^+\text{-K}^+\text{-ATPase}$ (white arrowhead). Occludin immunostaining is also prominent in parts of the IL region that line the lateral walls of the central venous sinus (CVS). (D) and (E) show, at higher magnification, areas from (C) that are indicated by the white arrowhead and white arrow respectively. Control sections probed with secondary antibody only show DAPI fluorescence (F). Scale bars in (A,B,C,F) = 20 μm . Scale bars in (D,E) = 5 μm .

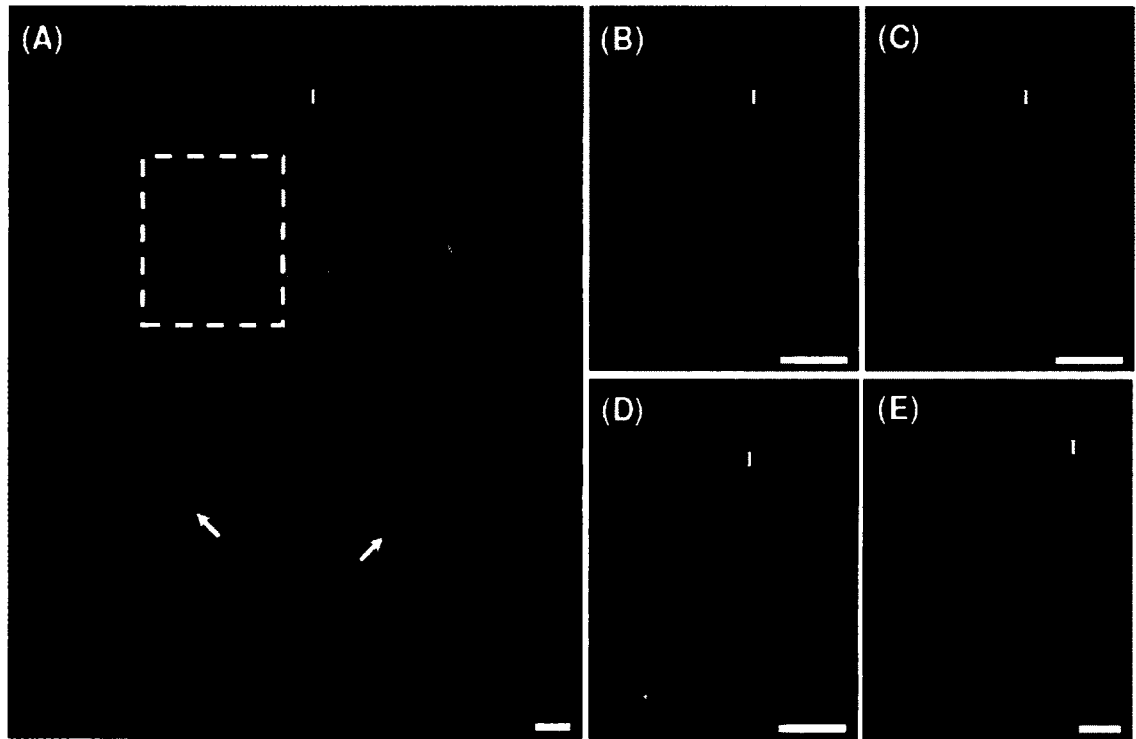


Figure 2-2: Immunofluorescent staining of (A,B) $\text{Na}^+\text{-K}^+\text{-ATPase}$ (green) and (A,C) occludin (red) in cross-sections of goldfish intestine. (D) is a merged image of (B) and (C). In (A), immunostaining for $\text{Na}^+\text{-K}^+\text{-ATPase}$ is concentrated to basolateral regions and occludin immunostaining is apparent in apical regions of epithelia lining the intestinal lumen (L). Occludin immunostaining appears less prominent in epithelial cells at the base of the intestinal villi (see white arrows in A). At higher magnification (see dashed box in A which outlines area magnified in C,D), occludin immunostaining appears as a typical honeycomb-like TJ pattern. Nuclei are stained with DAPI (blue), and only DAPI staining is observed in sections probed with secondary antibody alone (E). All scale bars = 20 μm .

ATPase immunostaining also extended to epithelial cells lining the base of intestinal villi, apical occludin immunostaining appeared less prominent in this region (Fig. 2-2A). Observation of intestinal villi and occludin immunostaining at higher magnification revealed a honeycomb-like TJ protein apical distribution pattern facing the intestinal lumen (Fig. 2-2C). No TRITC or FITC fluorescence was observed in control sections probed with secondary antibody only (Fig. 2-2E) or with normal rabbit serum (not shown).

2.4.1.3 Occludin and Na⁺-K⁺-ATPase immunolocalization in the kidney:

Immunofluorescence microscopy of the goldfish kidney revealed differential immunostaining patterns in discrete regions of the nephron for both occludin and Na⁺-K⁺-ATPase (Fig. 2-3B). No TRITC or FITC fluorescence was observed in control sections probed with secondary antibody only (Fig. 2-3C) or with normal rabbit serum (not shown). Within the proximal region of the nephron, immunostaining for Na⁺-K⁺-ATPase appeared to be restricted primarily to basal regions of the plasma membrane of renal epithelial cells (Figs. 2-3B, 2-4A). In contrast, Na⁺-K⁺-ATPase immunostaining in renal epithelial cells of the distal tubule and collecting duct exhibited patterns consistent with localization in basolateral regions of the plasma membrane (Figs. 2-3B, 2-4B,C). An observable difference in Na⁺-K⁺-ATPase immunostaining between the distal tubule and collecting duct was the intensity of immunoreactivity, where basolateral Na⁺-K⁺-ATPase immunostaining was consistently weaker in the collecting duct (Figs. 2-3B, 2-4C) than in the distal tubule (Figs. 2-3B, 2-4B). While no occludin immunostaining could be observed in proximal segments of the goldfish nephron (Figs. 2-3B, 2-4D), strong and

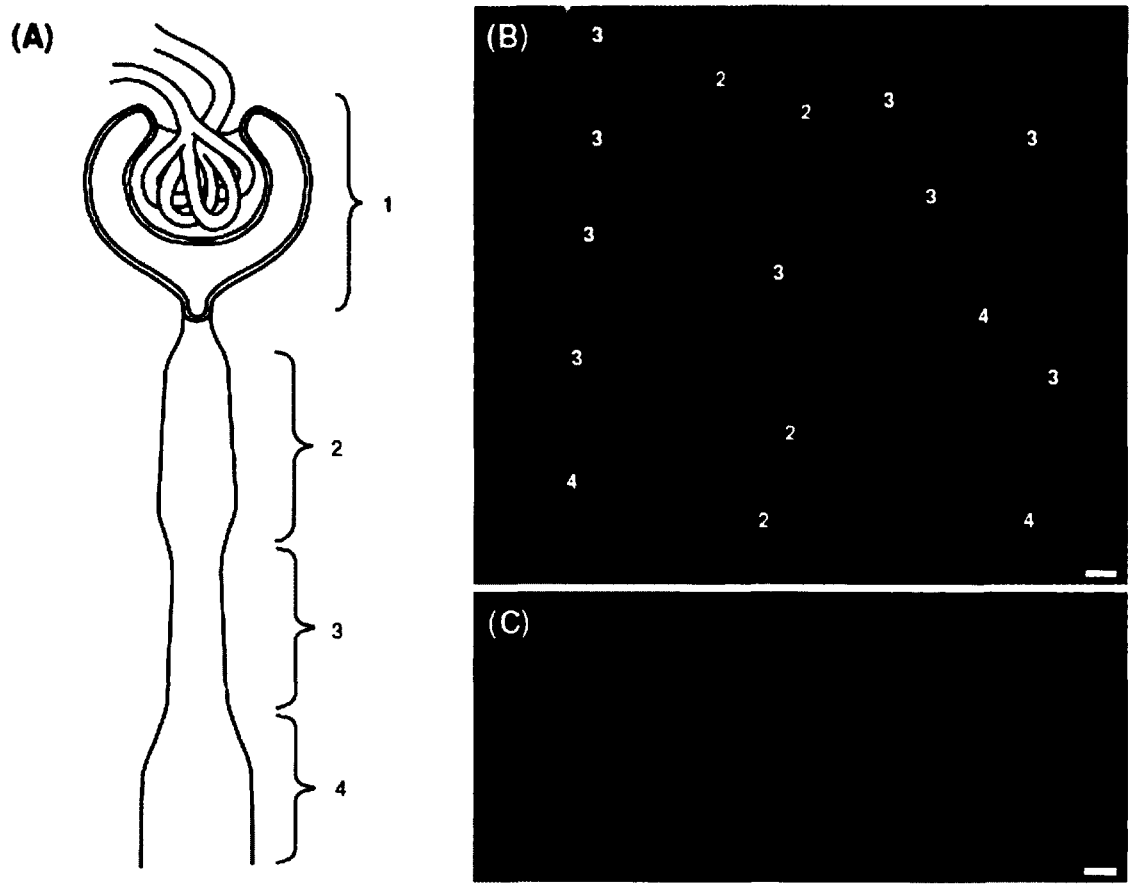


Figure 2-3: (A) Schematic illustration of a goldfish nephron based on morphological criteria outlined by Sakai (1985). The goldfish nephron can be divided into the following regions: 1. renal corpuscle (Bowman's capsule and glomerulus); 2. proximal tubule; 3. distal tubule; and 4. collecting duct. (B) Cross-section of goldfish kidney immunostained for occludin (red) and Na⁺-K⁺-ATPase (green). Occludin and Na⁺-K⁺-ATPase show region specific immunostaining along the nephron. Numbered labels indicate regions of the nephron as defined in (A). No occludin or Na⁺-K⁺-ATPase immunostaining was found in the renal corpuscle. A control section can be seen in (C), (i.e. DAPI fluorescence only). All scale bars = 20 μm.

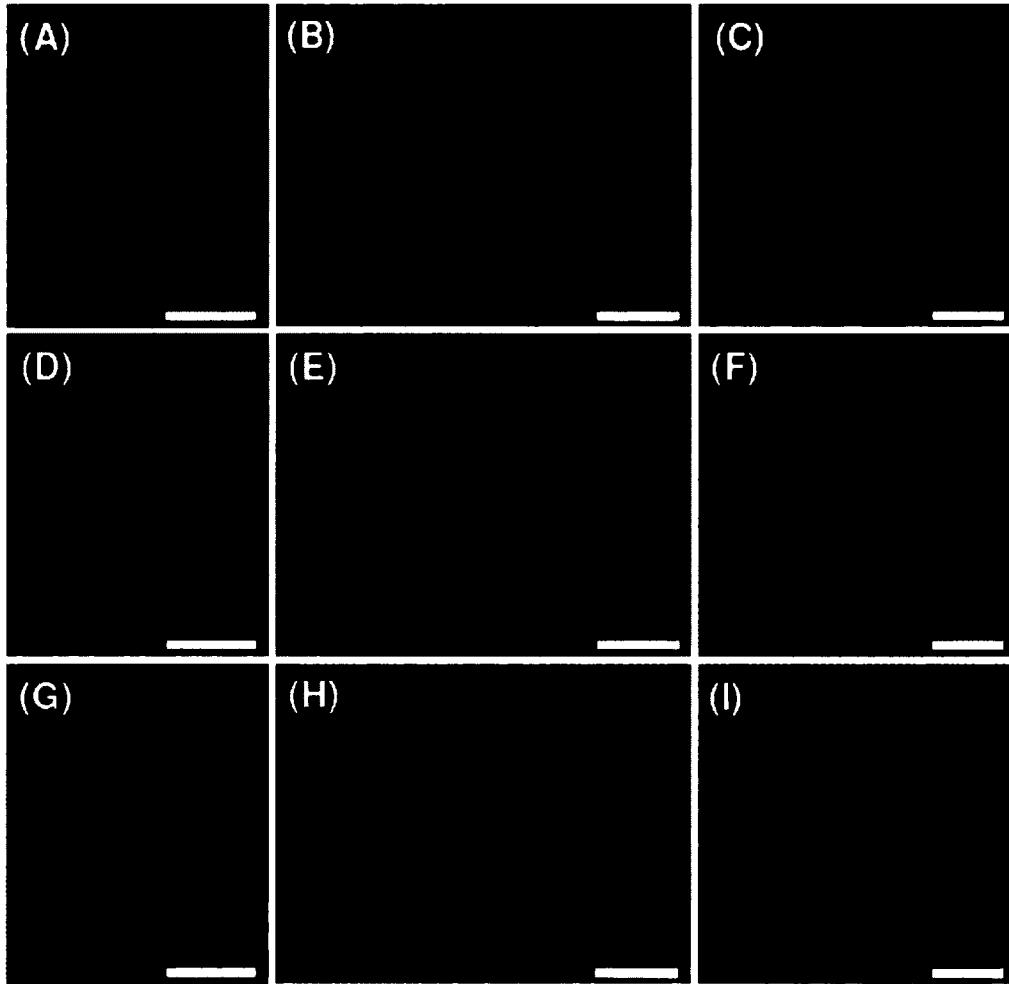


Figure 2-4: Immunofluorescent staining of (A-C) $\text{Na}^+\text{-K}^+\text{-ATPase}$ (green) and (D-F) occludin (red) in cross-sections of goldfish (A,D,G) proximal tubule, (B,E,H) distal tubule and (C,F,I) collecting duct. Nuclei are stained with DAPI (blue) in (A-C). (G), (H) and (I) are merged images of (A,D), (B,E) and (C,F) respectively. Immunostaining for $\text{Na}^+\text{-K}^+\text{-ATPase}$ is restricted primarily to the basal membrane of renal epithelial cells in the proximal region of the nephron (A) and to the basolateral membrane of renal epithelial cells in distal and collecting segments (B,C). No occludin immunostaining is observed in proximal segments of the nephron (D). Strong and moderate occludin immunostaining is concentrated to the apical membrane of renal epithelial cells lining the lumen of the distal tubule and collecting duct respectively (E,F). All scale bars = 20 μm .

moderate occludin immunostaining was concentrated to the apical membrane of renal epithelial cells lining the lumen of the distal tubule and collecting duct respectively (Figs. 2-3B, 2-4E,F). There appeared to be no occludin or Na⁺-K⁺-ATPase immunostaining at the goldfish renal corpuscle (not shown).

2.4.2 Western blot analysis: Western blot analysis of protein isolated from goldfish gill, intestine and kidney revealed single occludin immunoreactive bands at ~68 kDa, however no immunoreactive bands were detected from protein isolated from goldfish blood cells (Fig. 2-5). A single occludin immunoreactive band from protein isolated from rat kidney resolved at ~65 kDa (Fig. 2-5).

2.4.3 Food deprivation experiments

2.4.3.1 Body weight changes: The effects of 1, 2 and 4 weeks of food deprivation on goldfish body weight are shown in Fig. 2-6. Control fish, fed 1.5% their initial body weight, gained an average (\pm s.e.m.) of $4.5 \pm 0.6\%$, $13.5 \pm 1.7\%$ and $26.6 \pm 1.6\%$ their initial body weight during the 1-, 2- and 4-week experimental periods respectively. In contrast, food deprived fish lost an average of $8.6 \pm 0.6\%$ (1 week), $12 \pm 1\%$ (2 weeks) and $17.5 \pm 1.1\%$ (4 weeks) of their initial body weight.

2.4.3.2 Serum osmolality, electrolytes and muscle moisture content: After 1 week of food deprivation, no significant ($P > 0.05$) alterations in serum osmolality, Na⁺ or Cl⁻ levels were observed (Fig. 2-7A,B,C). Similarly, 1 week of food deprivation had no significant ($P > 0.05$) effect on muscle moisture content (Fig. 2-7D). In contrast, following 2 and 4 weeks of food deprivation, serum osmolality, Na⁺ and Cl⁻ levels significantly ($P < 0.05$) decreased, while muscle water content significantly ($P < 0.05$) increased (Fig. 2-7).

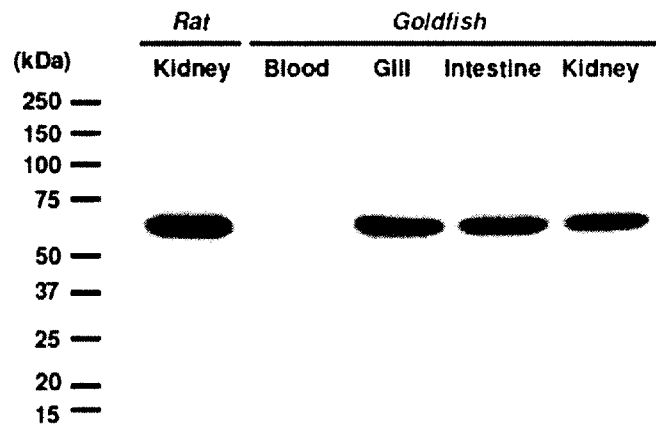


Figure 2-5: Western blot analysis of occludin expression in goldfish gill, intestine and kidney. Single occludin immunoreactive bands (at ~68 kDa) always appeared for goldfish epithelial tissue. A non-epithelial negative control tissue (goldfish blood cells) was not immunoreactive. A positive tissue control (rat kidney) was found to resolve at ~65 kDa.

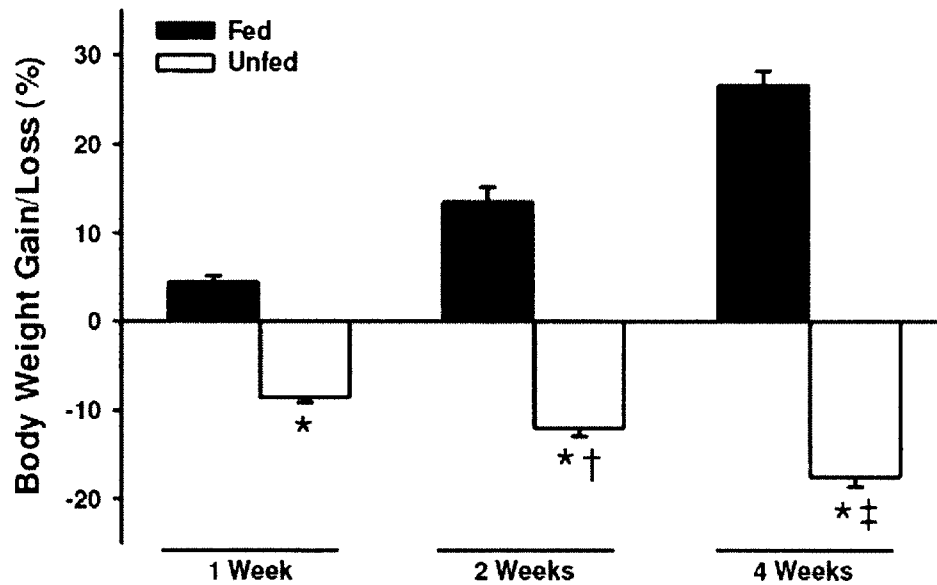


Figure 2-6: Effects of 1, 2 and 4 weeks feeding and food deprivation on relative weight gain/loss in goldfish. Data are expressed as mean values \pm s.e.m. ($n = 10$). * Significant difference ($P < 0.05$) between fed and unfed groups at the same time point. † Significant difference ($P < 0.05$) from 1 week unfed group. ‡ Significant difference ($P < 0.05$) from 2 weeks unfed group.

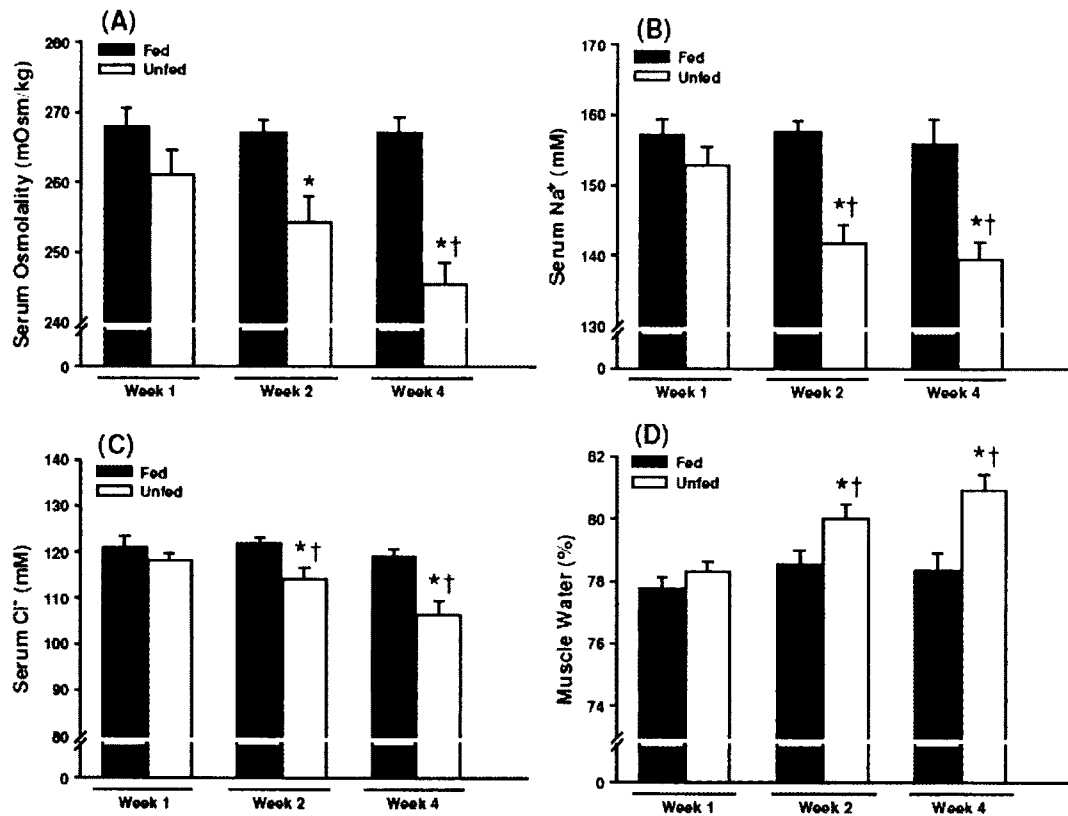


Figure 2-7: Effects of 1, 2 and 4 weeks feeding and food deprivation on (A) serum osmolality, (B) serum Na⁺, (C) serum Cl⁻ and (D) muscle water content in goldfish. Data are expressed as mean values ± s.e.m. (*n* = 10). * Significant difference (*P* < 0.05) between fed and unfed groups at the same time point. † Significant difference (*P* < 0.05) from 1 week unfed group.

2.4.3.3 *Na⁺-K⁺-ATPase enzyme activity and occludin protein expression*: When compared to fed fish groups, goldfish gill Na⁺-K⁺-ATPase activity significantly ($P < 0.05$) decreased (~16%) following 1 week of food deprivation, increased (~11%, $P > 0.05$) following 2 weeks of food deprivation and significantly ($P < 0.05$) increased (~13%) following 4 weeks of food deprivation (Fig. 2-8A). Gill occludin protein expression in food deprived goldfish was significantly ($P < 0.05$) lower than control groups by ~41%, ~58% and ~31% following 1, 2 and 4 weeks of food deprivation respectively (Fig. 2-8B). Intestinal Na⁺-K⁺-ATPase activity in goldfish following 1, 2 and 4 weeks of food deprivation significantly ($P < 0.05$) decreased by ~46%, ~66% and ~44% respectively when compared to fed fish (Fig. 2-9A). Intestinal occludin protein expression did not significantly ($P > 0.05$) alter in goldfish following 1 and 2 weeks of food deprivation when compared to control groups, however, intestinal occludin protein expression significantly ($P < 0.05$) decreased by ~34% following 4 weeks of food deprivation when compared to fed fish (Fig. 2-9B). Food deprivation did not significantly ($P > 0.05$) alter goldfish kidney Na⁺-K⁺-ATPase activity at any point during the experiment (Fig. 2-10A), however goldfish kidney occludin protein expression significantly ($P < 0.05$) increased by ~640% and ~160% following 1 and 2 weeks of food deprivation respectively and significantly ($P < 0.05$) decreased by ~60% following 4 weeks food deprivation when compared to fed groups (Fig. 2-10B). The loading control, α -tubulin, was detected at ~52 kDa and its expression did not change following 1, 2 and 4 weeks of food deprivation (not shown).

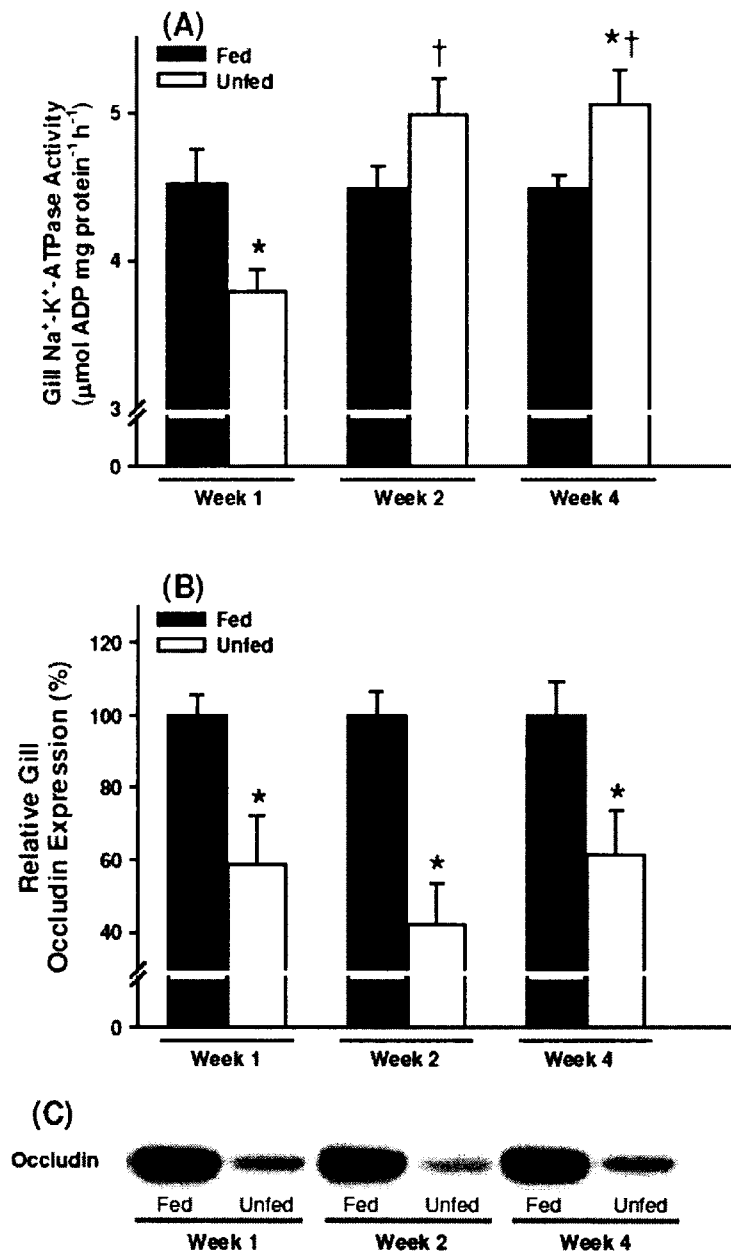


Figure 2-8: Effects of 1, 2 and 4 weeks feeding and food deprivation on (A) gill Na⁺-K⁺-ATPase activity and (B) normalized gill occludin expression in goldfish as determined by Western blot analyses. (C) Representative Western blot of gill occludin protein expression in fed and unfed goldfish. Data are expressed as mean values ± s.e.m. (*n* = 8-10). * Significant difference (*P* < 0.05) between fed and unfed groups at the same time point. † Significant difference (*P* < 0.05) from 1 week unfed group.

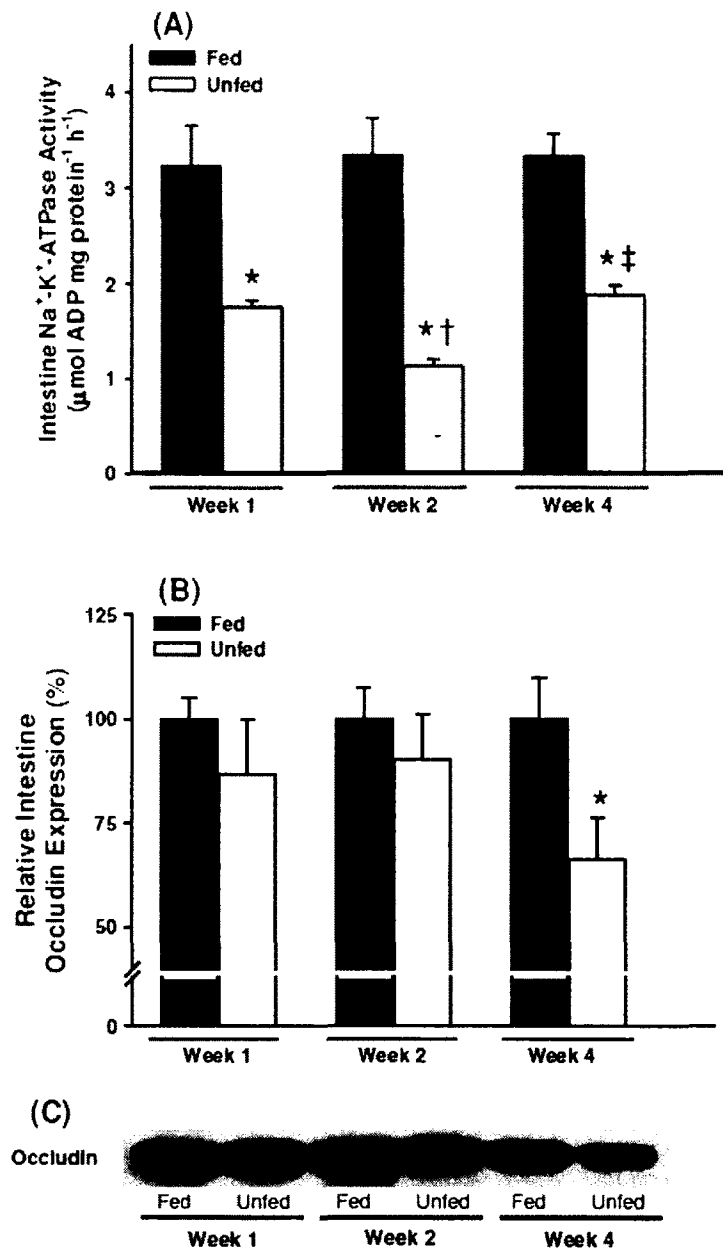


Figure 2-9: Effects of 1, 2 and 4 weeks feeding and food deprivation on (A) intestine $\text{Na}^+\text{-K}^+\text{-ATPase}$ activity and (B) normalized intestine occludin expression in goldfish as determined by Western blot analyses. (C) Representative Western blot of intestine occludin protein expression in fed and unfed goldfish. Data are expressed as mean values \pm s.e.m. ($n = 8-10$). * Significant difference ($P < 0.05$) between fed and unfed groups at the same time point. † Significant difference ($P < 0.05$) from 1 week unfed group. ‡ Significant difference ($P < 0.05$) from 2 weeks unfed group.

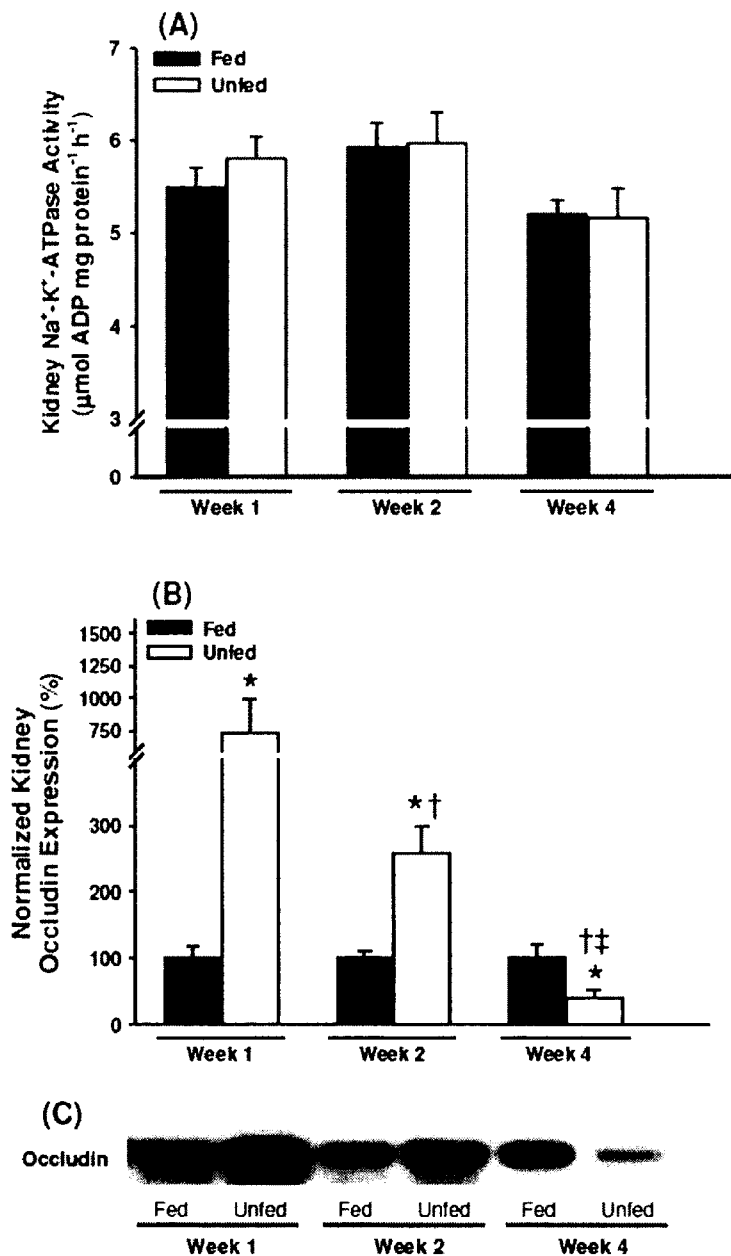


Figure 2-10: Effects of 1, 2 and 4 weeks feeding and food deprivation on (A) kidney Na⁺-K⁺-ATPase activity and (B) normalized kidney occludin expression in goldfish as determined by Western blot analyses. (C) Representative Western blot of kidney occludin protein expression in fed and unfed goldfish. Data are expressed as mean values ± s.e.m. (*n* = 8-10). * Significant difference (*P* < 0.05) between fed and unfed groups at the same time point. † Significant difference (*P* < 0.05) from 1 week unfed group. ‡ Significant difference (*P* < 0.05) from 2 weeks unfed group.

2.5 Discussion

2.5.1 Overview: Despite the universal inclusion of TJs in illustrative models of ion transport across fish epithelia, studies specifically investigating TJs in fishes have largely been limited to morphological analyses by electron microscopy (Sardet et al., 1979; Bartels and Potter, 1991; Freda et al., 1991; McDonald et al., 1991). To the best of our knowledge, no studies have examined the immunohistochemical localization and protein expression of any integral TJ protein in fish gill, intestine or renal epithelial tissue, although recently Kato et al. (2007) described the localization of zonula occludens-1 (ZO-1, a cytosolic TJ-related protein) in puffer fish gills. Furthermore, no studies have examined if or how TJ protein expression may adjust in response to altered hydromineral status in aquatic vertebrates. We examined the localization and expression of the integral transmembrane TJ protein occludin in fish tissues for the first time. Our observations suggest a role for occludin in the maintenance of hydromineral balance and that its regulation of epithelial “tightness” may be tissue specific. Furthermore, within tissue composed of heterogeneous regions of physiological function, such as the nephron, the role of occludin is likely to vary between discrete zones. Overall, alterations in occludin protein expression in response to hydromineral imbalance suggest that occludin may play a dynamic role in the regulation of epithelial permeability in fish.

2.5.2 Immunolocalization and Western blot analysis of occludin: Na⁺-K⁺-ATPase immunolocalization to cells within the IL region of goldfish primary filaments and at the base of the secondary gill filaments (particularly along the trailing edge of primary gill filaments) (Fig. 2-1A) corresponds with the location of mitochondria-rich cells (MRCs)

in goldfish gills (Kikuchi, 1977) and FW fish gills in general (Perry, 1997; Wilson et al., 2000). Pronounced and discontinuous occludin immunostaining along the edges of goldfish gill secondary lamellae, (Fig. 2-1B,E), and along the edges of gill epithelial cells that immunostain for Na⁺-K⁺-ATPase (and are thus presumed to be MRCs) (Fig. 2-1D), suggests that occludin may be associated with TJs between cells of the lamellar epithelium (e.g. pavement cells or MRCs) and/or with TJs between pillar cells that surround and form the lamellar blood spaces. This generally agrees with previous reports where freeze fracture and electron microscopy observations of fish gill epithelia have shown that pavement cells (PVCs), MRCs and pillar cells all form TJ complexes with adjacent cells - i.e. PVCs with adjacent PVCs, PVCs with MRCs, or pillar cells with adjacent pillar cells (Hughes and Grimstone, 1965; Sardet et al., 1979; Bartels and Potter, 1991; Kudo et al., 2007). Furthermore, a recent study has immunolocalized ZO-1, which is believed to associate with the COOH-terminal region of occludin (Furuse et al., 1994), to pillar cells within the gills of marine puffer fish (Kato et al., 2007). When taken together, the results of our study combined with the observations of Kato et al. (2007) indicate that the close association between ZO-1 and occludin that has been observed in mammals is likely to exist in fishes as well. While our data suggest a potential role for occludin in the regulation of gill permeability, future studies using higher resolution microscopy techniques will be beneficial to ascertain the exact nature of occludin expression and interaction between gill cells (e.g. PVCs, MRCs and/or pillar cells) within branchial lamellae.

Similar to immunohistochemical studies in other fish species (Giffard-Mena et al., 2006), $\text{Na}^+\text{-K}^+\text{-ATPase}$ immunostaining in the goldfish intestine was concentrated along the basolateral membrane of columnar epithelial cells lining the intestinal lumen (Fig. 2-2A,B). In contrast, occludin immunostaining was most prominent in apical regions of intestinal epithelial cells (Fig. 2-2A,C). When observed more closely, occludin immunostaining along the apical membrane of intestinal epithelial cells appeared to be distributed in a honeycomb-like arrangement (Fig. 2-2C), a typical TJ protein distribution pattern that has been observed along the gastrointestinal tract of other vertebrates (Inoue et al., 2006; Ridyard et al., 2007).

The goldfish kidney revealed differential immunostaining patterns in discrete regions of the nephron for both $\text{Na}^+\text{-K}^+\text{-ATPase}$ and occludin (Fig. 2-3B). Similar differential $\text{Na}^+\text{-K}^+\text{-ATPase}$ staining patterns have been observed in other fish species, and basolateral localization of $\text{Na}^+\text{-K}^+\text{-ATPase}$ concurs with models illustrating region specific ion transport mechanisms in fish renal epithelia (Nebel et al., 2005; Beyenbach, 2004). Furthermore, specific patterns of $\text{Na}^+\text{-K}^+\text{-ATPase}$ distribution along the nephron have also been reported for several other vertebrate groups (Piepenhagen et al., 1995; Kwon et al., 1998; Sabolić et al., 1999; Sturla et al., 2003). The differential occludin expression patterns observed in the goldfish nephron were similar to those observed in the mammalian kidney (Kwon et al., 1998; González-Mariscal et al., 2000). In mammals, differential occludin immunostaining patterns correlate with renal epithelial “tightness”, such that “tighter” nephron segments (as determined by TER measurements) express higher levels of occludin protein than “leakier” nephron regions. In human and rabbit

renal tubules, occludin immunostaining was weakest in “leaky” proximal tubules and strongest in “tight” distal tubules (Kwon et al., 1998; González-Mariscal et al., 2000). Furthermore, Western blot analysis of microdissected rabbit renal tubules revealed low occludin protein expression in “leaky” proximal tubules and significantly higher occludin protein expression in “tight” distal and collecting segments (González-Mariscal et al., 2000). The proximal tubule of the FW fish nephron is characterized as a relatively water permeable and “leaky” epithelium that reabsorbs a small percentage of Na⁺ and Cl⁻ ions, as well as glucose and other organic solutes, from glomerular filtrate (Logan et al., 1980; Dantzler, 2003). The distal tubule and collecting duct of the FW teleost nephron, on the other hand, reabsorb the majority of salts from glomerular filtrate and are characterized as “tight” epithelia (Nishimura et al., 1983; Dantzler, 2003). In the goldfish nephron, no occludin immunostaining was observed in “leaky” proximal regions (Fig. 2-4D), however, strong apical occludin immunoreactivity was detected in the “tighter” distal regions and moderate expression was observed in the collecting segments (Fig. 2-4E,F). These observations suggest that occludin may regulate goldfish renal epithelial “tightness” in a manner similar to mammals, and may thus influence the re-absorptive capacity of the different segments of the nephron.

Western blot analysis of occludin protein expression in homogenized rat kidney revealed a single immunoreactive band at ~65 kDa, while single immunoreactive bands at ~68 kDa were detected for homogenized goldfish gills, intestine and kidney (Fig. 2-5). No occludin immunoreactivity was detected for goldfish blood cells, a non-epithelial tissue (Fig. 2-5). Although predominantly detected as a 65 kDa protein in mammals,

many reports have identified several occludin immunoreactive bands between ~62 and 82 kDa (Sakakibara et al., 1997; Wong, 1997), therefore the occludin immunoreactive band found for goldfish epithelial tissue is consistent with the molecular weight range found in other vertebrates.

2.5.3 Hydromineral balance and occludin expression in food deprived goldfish: Food deprivation in goldfish resulted in negative energy balance (negative changes in fish weights) at all time periods examined in the current study (Fig. 2-6). However, only fish that were food deprived for 2 weeks or longer exhibited alterations in endpoints associated with salt and water balance. The observed reductions in serum osmolality, Na^+ and Cl^- levels and a concomitant increase in muscle hydration (Fig. 2-7) indicate that food deprivation can elicit changes in the hydromineral status of goldfish. These observations are in line with other studies that have described the reorganization of ionoregulatory machinery in response to restricted dietary regimes or food deprivation (Kültz and Jürss, 1991; Vijayan et al. 1996; Kelly et al. 1999).

Short-term food deprivation (1 week) in goldfish resulted in a significant reduction in gill $\text{Na}^+\text{-K}^+\text{-ATPase}$ activity while a longer period without feeding (e.g. 4 weeks) resulted in a significant increase in gill $\text{Na}^+\text{-K}^+\text{-ATPase}$ activity (Fig. 2-8A), suggesting an initial (temporary) down-regulation of active ion transport across the gills followed by a significant up-regulation. An up-regulation of gill $\text{Na}^+\text{-K}^+\text{-ATPase}$ activity after 4 weeks of food deprivation was unexpected. Kültz and Jürss (1991) have reported that food deprivation (albeit 6 weeks) in FW tilapia caused a reduction in gill $\text{Na}^+\text{-K}^+\text{-ATPase}$ activity. However, results may be time or species specific as Vijayan et al.

(1996) reported no change in gill $\text{Na}^+\text{-K}^+\text{-ATPase}$ activity after 2 weeks food deprivation in the same species. In contrast to $\text{Na}^+\text{-K}^+\text{-ATPase}$ activity, occludin protein expression decreased in response to food deprivation after 1 week and remained consistently low after 2 and 4 weeks (Fig. 2-8B). Although these results allow us to accept our original hypothesis, that occludin protein expression would alter in response to hydromineral imbalance, it is difficult to rationalize a reduction in occludin protein expression, as opposed to an increase that might be expected to occur in association with gill epithelial tightening and reduced passive ion loss. There are several possible explanations: (1) gill epithelia may become “leakier” in food deprived goldfish, however this would seem maladaptive (furthermore, Nance et al. (1987) have reported reductions in gill epithelial permeability in response to food deprivation in a FW fish); (2) the role of occludin in regulating gill epithelial permeability during periods of food deprivation may be overshadowed by other TJ proteins such as claudins, a family of transmembrane TJ proteins that also significantly contribute to the TJ barrier function (for recent review see Koval, 2006); or (3) the use of whole gill homogenates and the heterogeneous nature of the gill epithelium may mask specific changes in occludin expression between specific gill cell types. For example, Kültz and Jürss (1991) reported a significant reduction in MRC numbers in response to food deprivation in a FW fish. A reduction in MRC number, and thus a reduction in MRC/PVC TJ interactions, could potentially result in an overall reduction in gill occludin expression with little to no change in gill permeability, since PVC/PVC TJs would presumably remain intact. Regardless, the exact reason(s) for a reduction in gill occludin expression in food deprived goldfish requires further study.

Absorption of dietary Na^+ and Cl^- by intestinal epithelial cells of FW fishes is dependent upon an electrochemical gradient generated by Na^+ - K^+ -ATPase (Loretz, 1995). Food deprivation at all time points resulted in a significant reduction in goldfish intestinal Na^+ - K^+ -ATPase activity (Fig. 2-9A) suggesting a diminished capacity for active dietary salt and nutrient absorption by starved fish. Reduced intestinal Na^+ - K^+ -ATPase activity as a result of food deprivation has also been reported by Kültz and Jürss (1991) in FW tilapia and may be indicative of a depletion of the intestinal absorptive mucosa, a starvation-associated condition observed in other fish species (Bogé et al., 1981; Avella et al., 1992). Intestinal occludin expression significantly decreased following 4 weeks of food deprivation only (Fig. 2-9B), suggesting that over longer periods of dietary restriction, occludin may become involved in modifications of the barrier function of the goldfish intestine. Collie (1985) reported significant reductions in intestine epithelial TER and increased Na^+ -independent intestinal influx of proline in FW-adapted coho salmon following 2 weeks of food deprivation, indicating impairment of barrier function in response to starvation in a FW fish. In other vertebrates, occludin down-regulation occurs in association with decreased intestine epithelial resistance, TJ protein re-distribution and intestinal barrier dysfunction (Zeissig et al., 2007; Musch et al., 2006). These areas require further attention.

The FW fish kidney actively reabsorbs salts from glomerular filtrate producing dilute urine. Solute reabsorption across proximal and distal tubules of the nephron is driven by an electrochemical gradient of Na^+ generated by Na^+ - K^+ -ATPase (Dantzler, 2003). Although in the current study, negative energy balance appeared to have no

overall effect on kidney $\text{Na}^+\text{-K}^+\text{-ATPase}$ activity (Fig. 2-10A), it is possible that food deprivation may have resulted in nephron specific alterations in $\text{Na}^+\text{-K}^+\text{-ATPase}$ activity such that there was no observable alteration in “total” activity. For example in humans, dietary restriction and food deprivation is associated with reduced Na^+ reabsorption across the proximal tubule of the nephron and a concomitant increase in Na^+ reabsorption by distal segments to counterbalance natriuresis, presumably both of which are associated with opposing alterations in ionomotive enzyme activity (Satta et al., 1984). Occludin protein expression in the goldfish kidney, however, exhibited an apparent biphasic pattern in food deprived fish, markedly increasing after 1 week and significantly decreasing after 4 weeks (Fig. 2-10B), suggesting that food deprivation provokes a biphasic effect on renal function in the goldfish. A starvation induced biphasic response in renal function has previously been documented in both humans and rats (Boulter et al., 1973; Boim et al., 1992; Wilke et al., 2005), where short-term starvation can result in natriuresis and polyuria that are eventually corrected and compensated for over longer experimental periods (Boulter et al., 1973; Wilke et al., 2005). Assuming the observed biphasic alterations in kidney occludin expression in food deprived goldfish lead to adaptive function, one can rationalize that resulting regional changes in nephron permeability would enhance ion reabsorption and augment water elimination. In this regard, it is noteworthy that the highest and lowest renal expression of occludin in food deprived goldfish occurs in association with reduced and elevated gill $\text{Na}^+\text{-K}^+\text{-ATPase}$ activity respectively, indicating an interplay of strategies worthy of further investigation.

2.5.4 Conclusion: To summarize, we have immunolocalized occludin in goldfish ionoregulatory epithelia and demonstrated that occludin protein expression levels alter in response to hydromineral imbalance. The changes that occur in occludin protein abundance in response to starvation-induced hydromineral imbalance are tissue specific and, based on morphological evidence, are likely to be regionally different within specific tissues. The current study suggests that occludin should be expected to play an important role in the regulation of paracellular solute movement in aquatic vertebrates. While the response of occludin to hydromineral imbalance in goldfish often fits with its currently accepted role as an integral transmembrane TJ protein involved in regulating epithelial permeability, alterations in gill tissue are less easily explained. This underscores the paucity of information in the area of TJ physiology and the role these proteins play in the homeostatic control of hydromineral balance in aquatic vertebrates. This alone is an impetus for further study.

2.6 References

Avella M, Blaise O, Berhaut J. 1992. Effects of starvation on valine and alanine transport across the intestinal mucosal border in sea bass, *Dicentrarchus labrax*. *J Comp Physiol B* 162:430-435.

Balda MS, Whitney JA, Flores C, González S, Cereijido M, Matter K. 1996. Functional dissociation of paracellular permeability and transepithelial electrical resistance and disruption of the apical-basolateral intramembrane diffusion barrier by expression of a mutant tight junction membrane protein. *J Cell Biol* 134:1031-1049.

Bartels H, Potter IC. 1991. Structural changes in the zonulae occludentes of the chloride cells of young adult lampreys following acclimation to seawater. *Cell Tissue Res* 265:447-457.

Beyenbach KW. 2004. Kidney sans glomeruli. *Am J Physiol Renal Physiol* 286:F811-F827.

Bogé G, Rigal A, Pérès G. 1981. A study of in vivo glycine absorption by fed and fasted rainbow trout (*Salmo gairdneri*). *J Exp Biol* 91:285-292.

Boim MA, Ajzen H, Ramos OL, Schor N. 1992. Glomerular hemodynamics and hormonal evaluation during starvation in rats. *Kidney Int* 42:567-572.

Boulter PR, Hoffman RS, Arky RA. 1973. Pattern of sodium excretion accompanying starvation. *Metabolism* 22:675-683.

Busacker GP, Chavin W. 1981. Characterization of $\text{Na}^+ + \text{K}^+$ -ATPases and Mg^{2+} -ATPases from the gill and the kidney of the goldfish (*Carassius auratus* L). *Comp Biochem Physiol B* 69:249-256.

Cerejido M, Anderson JM. 2001. Introduction: Evolution of ideas on the tight junction. In: Cerejido M and Anderson JM (eds) *Tight Junctions*. CRC Press, Boca Raton, pp. 1-18.

Chen Y, Merzdorf C, Paul DL. 1997. COOH terminus of occludin is required for tight junction barrier function in early *Xenopus* embryos. *J Cell Biol* 138:891-899.

Collie NL. 1985. Intestinal nutrient transport in coho salmon (*Oncorhynchus kisutch*) and the effects of development, starvation, and seawater adaptation. *J Comp Physiol B* 156:163-174.

Dantzler WH. 2003. Regulation of renal proximal and distal tubule transport: sodium, chloride and organic anions. *Comp Biochem Physiol A* 136:453-478.

Evans DH, Piermarini PM, Choe KP. 2005. The multifunctional fish gill: dominate site of gas exchange, osmoregulation, acid-base regulation, and excretion of nitrogenous waste. *Physiol Rev* 85:97-177.

Freda J, Sanchez DA, Bergman HL. 1991. Shortening of branchial tight junctions in acid-exposed rainbow trout (*Oncorhynchus mykiss*). *Can J Fish Aquat Sci* 48:2028-2033.

Fujimoto K. 1995. Freeze-fracture replica electron microscopy combined with SDS digestion for cytochemical labeling of integral membrane proteins. Application to the immunogold labeling of intercellular junctional complexes. *J Cell Sci* 108:3443-3449.

Furuse M, Hirase T, Itoh M, Nagafuchi A, Yonemura S, Tsukita S, Tsukita S. 1993. Occludin: a novel integral membrane protein localizing at tight junctions. *J Cell Biol* 123:1777-1788.

Furuse M, Itoh M, Hirase T, Nagafuchi A, Yonemura S, Tsukita S, Tsukita S. 1994. Direct association of occludin with ZO-1 and its possible involvement in the localization of occludin at tight junctions. *J Cell Biol* 127:1617-1625.

Furuse M, Sasaki H, Fujimoto K, Tsukita S. 1998. A single gene product, claudin-1 or -2, reconstitutes tight junction strands and recruits occludin in fibroblasts. *J Cell Biol* 143:391-401.

Giffard-Mena I, Charmantier G, Grousset E, Aujoulat F, Castille R. 2006. Digestive tract ontogeny of *Dicentrarchus labrax*: implication in osmoregulation. *Develop Growth Differ* 48:139-151.

González-Mariscal L, Namorado MC, Martin D, Luna J, Alarcon L, Islas S, Valencia L, Muriel P, Ponce L, Reyes JL. 2000. Tight junction proteins ZO-1, ZO-2, and occludin along isolated renal tubules. *Kidney Int* 57:2386-2402.

González-Mariscal L, Betanzos A, Nava P, Jaramillo BE. 2003. Tight junction proteins. *Prog Biophys Mol Biol* 81:1-44.

Hughes GM, Grimstone AV. 1965. The fine structure of the secondary lamellae of the gills of *Gadus pollachius*. *Quart J Micr Sci* 106:343-353.

Inoue K, Oyamada M, Mitsufuji S, Okanou T, Takamatsu T. 2006. Different changes in the expression of multiple kinds of tight-junction proteins during ischemia-reperfusion injury of the rat ileum. *Acta Histochem Cytochem* 39:35-45.

Kato A, Nakamura K, Kudo H, Tran YH, Yamamoto Y, Doi H, Hirose S. 2007. Characterization of the column and autocellular junctions that define the vasculature of gill lamellae. *J Histochem Cytochem* 55:941-953.

Kelly SP, Chow INK, Woo NYS. 1999. Alterations in Na⁺-K⁺-ATPase activity and gill chloride cell morphometrics of juvenile black sea bream (*Mylio macrocephalus*) in response to salinity and ration size. *Aquaculture* 172:351-367.

Kikuchi S. 1977. Mitochondria-rich (chloride) cells in the gill epithelia from four species of stenohaline fresh water teleosts. *Cell Tiss Res* 180:87-98.

Koval M. 2006. Claudins – key pieces in the tight junction puzzle. *Cell Commun Adhes* 13:127-138.

Kudo H, Kato A, Hirose S. 2007. Fluorescence visualization of branchial collagen columns embraced by pillar cells. *J Histochem Cytochem* 55:57-62.

Kültz D, Jürss K. 1991. Acclimation of chloride cells and Na/K-ATPase to energy deficiency in tilapia (*Oreochromis mossambicus*). *Zool Jb Physiol* 95:39-50.

Kwon O, Myers BD, Sibley R, Dafoe D, Alfrey E, Nelson WJ. 1998. Distribution of cell membrane-associated proteins along the human nephron. *J Histochem Cytochem* 46:1423-1434.

Logan AG, Moriarty RJ, Rankin JC. 1980. A micropuncture study of kidney function in the river lamprey, *Lampetra fluviatilis*, adapted to fresh water. *J Exp Biol* 85:137-147.

Loretz CA. 1995. Electrophysiology of ion transport in teleost intestinal cells. In: Wood CM and Shuttleworth TJ (eds) *Fish Physiology, Volume 14, Cellular and Molecular Approaches to Fish Ionic Regulation*. Academic Press, San Diego, pp.25-56.

Marshall WS. 2002. Na⁺, Cl⁻, Ca²⁺ and Zn²⁺ transport by fish gills: retrospective review and prospective synthesis. *J Exp Zool* 293:264-283.

McCarthy KM, Skare IB, Stankewich MC, Furuse M, Tsukita S, Rogers RA, Lynch RD, Schneeberger EE. 1996. Occludin is a functional component of the tight junction. *J Cell Sci* 109:2287-2298.

McCormick SD. 1993. Methods for nonlethal gill biopsy and measurement of Na⁺, K⁺-ATPase activity. *Can J Fish Aquat Sci* 50:656-658.

McDonald DG, Freda J, Cavdek V, Gonzalez R, Zia S. 1991. Interspecific differences in gill morphology of freshwater fish in relation to tolerance of low-pH environments. *Physiol Zool* 64:124-144.

Musch MW, Walsh-Reitz MM, Chang EB. 2006. Roles of ZO-1, occludin, and actin in oxidant-induced barrier disruption. *Am J Physiol* 290:G222-G231.

Nance JM, Mason A, Sola F, Bornancin M. 1987. The effects of starvation and sexual maturation on Na⁺ transbranchial fluxes following direct transfer from fresh water to sea-water in rainbow trout (*Salmo gairdneri*). *Comp Biochem Physiol A* 87:613-622.

Nebel C, Romestand B, Nègre-Sadargues G, Grousset E, Aujoulat F, Bacal J, Bonhomme F, Charmantier G. 2005. Differential freshwater adaptation in juvenile sea-bass *Dicentrarchus labrax*: involvement of gills and urinary system. *J Exp Biol* 208:3859-3871.

Nishimura H, Imai M, Ogawa M. 1983. Sodium chloride and water transport in the renal distal tubule of the rainbow trout. *Am J Physiol* 244:F247-F254.

Perry SF. 1997. The chloride cell: structure and function in the gills of freshwater fishes. *Annu Rev Physiol* 59:325-347.

Piepenhagen PA, Peters LL, Lux SE, Nelson WJ. 1995. Differential expression of Na⁺-K⁺-ATPase, ankyrin, fodrin, and E-cadherin along the kidney nephron. *Am J Physiol* 269:C1417-C1432.

Ridyard AE, Brown JK, Rhind SM, Else RW, Simpson JW, Miller HRP. 2007. Apical junction complex protein expression in the canine colon: differential expression of claudin-2 in the colonic mucosa in dogs with idiopathic colitis. *J Histochem Cytochem* 55:1049-1058.

Sabolić I, Herak-Kramberger CM, Breton S, Brown D. 1999. Na/K-ATPase in intercalated cells along the rat nephron revealed by antigen retrieval. *J Am Soc Nephrol* 10:913-922.

Sakai T. 1985. The structure of the kidney from the freshwater teleost *Carassius auratus*. *Anat Embryol* 171:31-39.

Sakakibara A, Furuse M, Saitou M, Ando-Akatsuka Y, Tsukita S. 1997. Possible involvement of phosphorylation of occludin in tight junction formation. *J Cell Biol* 137:1393-1401.

Sardet C, Pisam M, Maetz J. 1979. The surface epithelium of teleostean fish gills. Cellular and junctional adaptations of the chloride cell in relation to salt adaptation. *J Cell Biol* 80:96-117.

Satta A, Faedda R, Olmeo NA, Soggia G, Branca GF, Bartoli E. 1984. Studies on the nephron segment with reduced sodium reabsorption during starvation natriuresis. *Ren Physiol* 7:283-292.

Schneeberger EE, Lynch RD. 2004. The tight junction: a multifunctional complex. *Am J Physiol Cell Physiol* 286:1213-1228.

Sturla M, Prato P, Masini MA, Uva BM. 2003. Ion transport proteins and aquaporin water channels in the kidney of amphibians from different habitats. *Comp Biochem Physiol C Toxicol Pharmacol* 136:1-7.

Vijayan MM, Morgan JD, Sakamoto T, Grau EG, Iwama GK. 1996. Food-deprivation affects seawater acclimation in tilapia: hormonal and metabolic changes. *J Exp Biol* 199:2467-2475.

Wilke C, Sheriff S, Soleimani M, Amlal H. 2005. Vasopressin-independent regulation of collecting duct aquaporin-2 in food deprivation. *Kidney Int* 67:201-216.

Wilson JM, Laurent P, Tufts BL, Benos DJ, Donowitz M, Vogl W, Randall DJ. 2000. NaCl uptake by the branchial epithelium in freshwater teleost fish: an immunological approach to ion-transport protein localization. *J Exp Biol* 203:2279-2296.

Wong V. 1997. Phosphorylation of occludin correlates with occludin localization and function at the tight junction. *Am J Physiol* 273:C1859-C1867.

Wong V, Gumbiner BM. 1997. A synthetic peptide corresponding to the extracellular domain of occludin perturbs the tight junction permeability barrier. *J Cell Biol* 136:399-409.

Zall DM, Fisher D, Garner MD. 1956. Photometric determination of chlorides in water. *Anal Chem* 28:1665-1678.

Zeissig S, Bürgel N, Günzel D, Richter J, Mankertz J, Wahnschaffe U, Kroesen AJ, Zeitz M, Fromm M, Schulzke JD. 2007. Changes in expression and distribution of claudin-2, -5 and -8 lead to discontinuous tight junctions and barrier dysfunction in active Crohn's disease. *Gut* 56:61-72.

CHAPTER 3:

OCCLUDIN EXPRESSION IN GOLDFISH HELD IN ION-POOR WATER

Helen Chasiotis, Jennifer C. Effendi and Scott P. Kelly

Department of Biology, York University, Toronto, Ontario, Canada M3J 1P3

This chapter has been published and reproduced with permission:

Chasiotis H, Effendi JC, Kelly SP. 2009. Occludin expression in goldfish held in ion-poor water. *J Comp Physiol B* 179:149-154.

3.1 Abstract

With an emphasis on the tight junction protein occludin, the response of goldfish following abrupt exposure (0 – 120h) as well as long-term acclimation (14 and 28 days) to ion-poor water (IPW) was examined. Both abrupt and long-term exposure to IPW lowered serum osmolality, $[Na^+]$ and $[Cl^-]$, and elevated serum glucose. After abrupt exposure to IPW, gill tissue exhibited a prompt and sustained decrease in Na^+-K^+ -ATPase activity, and a transient increase in occludin expression that returned to control levels by 6 h. Following 14 and 28 days in IPW, gill occludin expression was markedly elevated while Na^+-K^+ -ATPase activity was only significantly different (elevated) at day 14. Kidney tissue exhibited an elevation in both Na^+-K^+ -ATPase activity and occludin expression after 28 days, however in the intestine, occludin expression declined at day 14 but did not differ from FW fish at day 28. These studies demonstrate that goldfish can tolerate abrupt as well as sustained exposure to ion-poor surroundings. Data also suggest that occludin may play an adaptive role in fishes acclimated to ion-poor conditions by contributing to the modulation of epithelial barrier properties in ionoregulatory tissues.

3.2 Introduction

Fishes are often found in environments that vary greatly in ionic composition. In order to maintain internal homeostasis, these organisms have evolved a complex suite of ionoregulatory mechanisms that control water and solute movement across epithelial surfaces. The passage of water and dissolved solutes across epithelia can occur through the transcellular and/or paracellular pathways. The permeability of the paracellular route is regulated by the tight junction (TJ) complex. Comprising integral transmembrane as well as cytoplasmic scaffolding TJ proteins, the TJ complex forms a semi-permeable paracellular “seal” between epithelial cells (González-Mariscal et al., 2003). The passive movement of solutes between compartments of the body is dictated by the permeability properties of the TJ complex and in aquatic vertebrates, the permeability characteristics of epithelia that come into direct contact with surrounding water (e.g. gills) play an important role in regulating solute movement between the internal and external environments (see Chapter 2; Kelly and Wood, 2001, 2002a, 2002b, 2008; Bagherie-Lachidan et al., 2008; Chasiotis and Kelly, 2009).

Occludin was the first integral TJ protein to be isolated and identified from vertebrate epithelia (Furuse et al., 1993). It is a tetraspan protein with three cytoplasmic domains ranging from 10 – 254 aa in length, and two extracellular loops of equal size (i.e. 44 and 45 aa) (González-Mariscal et al., 2003). Studies examining the physiological role of occludin in the TJ complex indicate that it contributes significantly to epithelial integrity and substantial evidence suggests that occludin is a major determinant in the regulation of barrier properties in vertebrate epithelia (for review see Feldman et al.,

2005). For example, the over-expression or disruption of occludin in epithelial cell lines (such as MDCK or A6 kidney cells) has been demonstrated to cause elevations or reductions in transepithelial resistance (TER) (Balda et al., 1996; McCarthy et al., 1996; Wong and Gumbiner, 1997). Furthermore, where occludin disruption causes a reduction in TER, increased permeability to paracellular marker molecules (e.g. [¹⁴C]inulin, [³H]mannitol etc.) also occurs (Wong and Gumbiner, 1997).

The effect of environmental salinity on the permeability of ionoregulatory epithelia is well documented in fishes (for review see Marshall and Grosell, 2005). Most notable are the changes that occur when euryhaline fishes move from freshwater (FW) to seawater (SW). Gill and intestinal epithelia generally become “leakier” in order to assist salt and water movement into the body (i.e. across the intestinal epithelium) and subsequent ion elimination from the body (i.e. across the gill). In the kidney, discrete regions of the nephron also alter in response to SW acclimation, where “electrically tight” diluting segments that are designed to retain ions and eliminate water in hypo-osmotic surroundings exhibit varying levels of structural or functional degeneration in SW (Nishimura and Fan, 2003). Therefore, alterations in epithelial permeability upon SW entry contribute to an overall net water gain and thus prevent dehydration. Goldfish are not capable of acclimating to a SW environment but are capable of gradually acclimating from FW to ion-poor FW (Cuthbert and Maetz, 1972; Kelly and Peter, 2006). In this regard, alterations that occur in the endocrine system (e.g. elevated pituitary prolactin expression) and extracellular fluids (e.g. lowered serum osmolality) of goldfish

acclimated from regular FW to IPW are analogous to the physiological changes that take place when euryhaline fishes move from SW to FW (Kelly and Peter, 2006).

In a recent study, we examined the localization of occludin in the osmoregulatory tissues of goldfish (see Chapter 2). Occludin was found in the gill epithelium, intestine and discrete regions of the goldfish nephron (i.e. distal tubule and collecting duct) (see Chapter 2). Furthermore, when we subjected goldfish to varying periods of food deprivation in order to perturb the active and passive transport properties of osmoregulatory epithelia, occludin expression altered in a tissue-specific manner and in association with time dependent variations in hydromineral status (also see Chapter 2). These observations point to a potential role for occludin in the regulation of salt and water balance in fishes. However, by altering the hydromineral status of fishes through limiting (or withdrawing) access to food, the consequences of negative energy status may have also directly affected the function of TJ proteins. Therefore, it would be of further interest to examine the response of occludin to environmental change directly and in particular, alterations in environmental ion levels.

In the current studies, we hypothesized that goldfish would tolerate abrupt exposure to ion-poor water (IPW). Under the assumption that goldfish would tolerate abrupt exposure to IPW, our objectives were to investigate systemic endpoints of hydromineral balance and gill occludin expression during the time-course of exposure. We hypothesized that occludin expression would alter in an adaptive manner in response to ion-poor conditions. In order to further investigate our contention that occludin would be involved in the acclimation of goldfish to IPW, we examined alterations in

hydromineral endpoints as well as occludin expression in gill, renal and intestinal tissues in goldfish acclimated to IPW for longer time periods (i.e. up to 4 weeks). To the best of our knowledge, these are the first experiments to investigate the response of TJ proteins to ion-poor conditions in an aquatic vertebrate.

3.3 Materials and Methods

3.3.1 Experimental animals and culture conditions: Common variety goldfish (*Carassius auratus*, 6 – 11g) were purchased from a local supplier and held in 600 L opaque plastic aquaria supplied with regular flow-through dechlorinated FW. The composition of dechlorinated FW (in μM) was as follows: $[\text{Na}^+]$, 590; $[\text{Cl}^-]$, 920; $[\text{Ca}^{2+}]$, 760; $[\text{K}^+]$, 43; pH 7.35). Water temperature was maintained at 15–16°C and photoperiod was 12 h L:12 h D. Fish were held in these conditions for at least two weeks. During this settling period, fish were fed *ad libitum* once daily with commercial koi and goldfish pellets (Martin Profishent, Elmira, ON, Canada).

3.3.2 Abrupt exposure of goldfish to IPW: Two weeks prior to experimentation, goldfish were transferred into 65 liter opaque glass aquaria ($n = 15$ per tank) supplied with flow-through dechlorinated FW and maintained under culture conditions as described above (see Section 3.3.1). Feeding was terminated 48 h prior to the introduction of IPW and goldfish remained unfed throughout the duration of the experiment, (i.e. for 120 h post-IPW introduction). The composition of IPW (in μM) was as follows: $[\text{Na}^+]$, 20; $[\text{Cl}^-]$, 40; $[\text{Ca}^{2+}]$, 2; $[\text{K}^+]$, 0.4; pH 6.5. Without disturbing the fish, IPW was introduced into experimental tanks via inlet pipes and was allowed to overflow until ion-poor conditions were achieved (approx. 30 mins). At this point, timing began and fish were held in IPW for 1, 3, 6, 12, 24 and 120 h. At each designated time point, samples were collected from up to 10 fish held in each tank (for details see Section 3.3.4 below). To confirm that none of the aforementioned treatments were “lethal,” fish remaining in each tank were then re-acclimated to regular FW (by switching inlet pipe water back to dechlorinated FW).

Identical control experiments were run simultaneously, with control fish being sampled at the same time points. For control experiments, regular dechlorinated FW was used instead of IPW.

3.3.3 Long-term acclimation of goldfish to IPW: Stock goldfish were transferred into 200 liter opaque plastic aquaria and held in culture conditions identical to those described above (see Section 3.3.1). After a two-week settling period, goldfish were introduced to IPW abruptly as previously described (see Section 3.3.2), however this time fish were fed throughout the acclimation process and daily thereafter. Goldfish were held in these conditions for 14 and 28 days prior to sampling.

3.3.4 Blood and tissue sampling: Fish were rapidly net captured and anaesthetized in 0.5 g/L tricaine methanesulfonate (MS-222; Syndel Laboratories Ltd., Canada). Blood was drawn from caudal vessels using a 1 mL syringe/25 gauge needle by multiple individuals to reduce sampling time. Blood was allowed to clot at 4°C for 30 min and was centrifuged at 10 000 rpm for 10 minutes to collect serum. Following blood collection, fish were killed by spinal transection and select tissues were collected for further analysis. For initial studies conducted on fish rapidly exposed to IPW (and monitored for up to 120 h), gill tissue was collected from either side of the head for measurement of enzyme activity and occludin protein expression respectively. A full flank of epaxial white muscle (i.e. dorsal to the lateral line) was also collected. Tissues collected for experiments that examined the long-term response of fish to ion-poor conditions (i.e. 14 and 28 days) were as follows: gill and white muscle as already described, as well as kidney and a standardized region of the gastrointestinal tract (see Chapter 2). All tissues

were quick frozen in liquid nitrogen immediately upon collection and stored at -80°C until further analysis.

3.3.5 Serum analysis, muscle moisture content and Na⁺-K⁺-ATPase activity: Serum osmolality was determined using a Model 5500 Wescor vapour pressure osmometer (Wescor Inc., Logan, UT, USA). Serum Na⁺ was measured, after appropriate dilution, by atomic absorption spectrometry using an AAAnalyst PerkinElmer spectrometer (PerkinElmer Life and Analytical Sciences, ON, Canada). Serum Cl⁻ was determined using the colorimetric assay described by Zall et al. (1956) and serum glucose was measured using PGO Enzymes according to the manufacturer's instructions (Sigma-Aldrich Canada Ltd., Oakville, ON, Canada). Gill, kidney and intestinal Na⁺-K⁺-ATPase activity was determined using the methodology of McCormick (1993) with modifications as described in Chapter 2.

3.3.6 Western blot analysis: Occludin protein expression was examined by western blot analysis according to methodology previously reported in Chapter 2. Briefly, tissues were homogenized in ice-cold homogenization buffer (200 mM sucrose, 1 mM EDTA, 1 mM PMSF, 1 mM DTT in 0.7% NaCl) containing protease inhibitor cocktail (1:200; Sigma-Aldrich Canada Ltd) using a PRO250 homogenizer (PRO Scientific Inc., Oxford, CT, USA). Homogenates were centrifuged (3200 g at 4°C) and supernatants were collected. In preparation for SDS-PAGE, samples (75 µg of protein each) were boiled at 100°C in 6X sample buffer (360 mM Tris-HCl, 30% glycerol, 12% SDS, 600 mM DTT, 0.03% bromophenol blue) and separated along 12% acrylamide gels. Following electrophoresis, resolved protein was transferred onto Hybond-P polyvinylidene difluoride (PVDF)

membrane using a TE semi-dry transfer unit (GE Healthcare Bio-Sciences Inc., Baie d'Urfé, QC, Canada). Membranes were washed, blocked for 1 hour in 5% non-fat dry skim milk powder in TBS-T (5% skim milk, 10 mM Tris, 150 mM NaCl, 0.05% Tween-20, pH7.4), incubated overnight at 4°C with rabbit polyclonal anti-occludin antibody (Zymed Laboratories Inc.), and then washed again prior to incubation with horseradish peroxidase (HRP)-conjugated goat anti-rabbit antibody (Bio-Rad Laboratories Inc., Mississauga, ON, Canada) for 1 hour at room temperature. The rabbit polyclonal anti-occludin antibody is directed against the C-terminal region of the human occludin protein, and its use in goldfish has previously been validated (see Chapter 2). Protein bands were visualized using an Enhanced Chemiluminescence Plus Western blotting system (GE Healthcare Bio-Sciences Inc., Baie d'Urfé, QC, Canada). After examining occludin expression, membranes were stripped and re-probed with mouse monoclonal anti- β -actin antibody (Sigma-Aldrich Canada Ltd.) and HRP-conjugated goat anti-mouse antibody (Bio-Rad Laboratories Inc.) respectively as an internal loading control. Occludin and β -actin expression was quantified using Labworks Image Acquisition and Analysis software (UVP BioImaging Systems and Analysis Systems, Upland, CA, USA). Occludin is expressed as a normalized value relative to β -actin as an internal control.

3.3.7 Statistical analysis: All data are expressed as mean values \pm s.e.m (n) where n equals the number of fish in a treatment group. To examine for significant differences between treatments, a two-way analysis of variance (ANOVA) was run followed by a Student-Newman-Keuls multiple comparison test. For clarity, only significant differences between FW and IPW groups are shown on 0 – 120 h graphics (see Table 3-1 for

additional information). A fiducial limit of $P < 0.05$ was used throughout. All statistical analyses were performed using SigmaStat 3.1 (Systat Software Inc., USA).

3.4 Results

3.4.1 Abrupt exposure to IPW: No experimental goldfish died over the 120 h period following abrupt IPW introduction. After sampling at each time point, a subset of fish that were abruptly exposed to IPW were reintroduced to regular FW to confirm that the abrupt IPW exposure had no deleterious effect on the continued survival of fish. In these animals, no mortality or abnormal behaviour was observed for up to two weeks following the experiments.

Goldfish abruptly introduced to IPW exhibited a rapid and sustained reduction in serum osmolality (Fig. 3-1A). Serum $[Na^+]$ initially appeared to increase (i.e. at 1 h) but then reduced over the first 24 h of exposure to IPW (Fig. 3-1B). Serum $[Cl^-]$ did not significantly alter until 24 h after introducing fish to IPW (Fig. 3-1C, Table 3-1). After 120 h in IPW, serum osmolality, $[Na^+]$ and $[Cl^-]$ exhibited further reductions relative to control fish as well as to fish exposed to IPW for up to 24 h (Fig. 3-1A-C, Table 3-1). Blood glucose levels elevated in goldfish approximately 3 h after abrupt exposure to IPW (Table 3-2). For the remainder of the 120 h experiment, blood glucose levels were higher in fish exposed to IPW. Muscle moisture was stable over the duration of the experiment but did significantly differ between groups after 120 h exposure to IPW (Fig. 3-1D).

In the gills of goldfish abruptly exposed to IPW, Na^+K^+ -ATPase activity appeared to rapidly decline and, with the exception of the activity measured at 6 h, remained lower than the activity recorded for fish held in regular FW for the entire 120 h duration of the experiment (Fig. 3-2A). In contrast, gill occludin expression significantly increased 1 h after introduction of fish to IPW (Fig. 3-2B). Thereafter, gill occludin

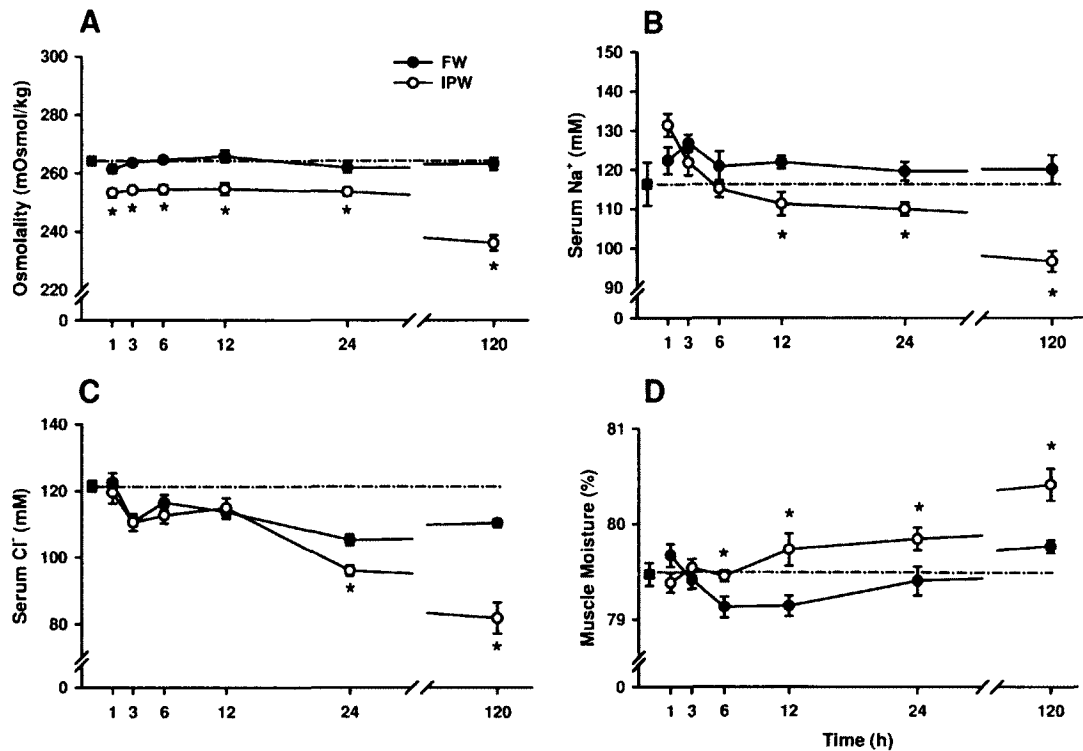


Figure 3-1: Effect of abrupt exposure to ion-poor water (IPW) on (A) serum osmolality, (B) serum Na⁺, (C) serum Cl⁻ and (D) muscle moisture content of goldfish. Data are expressed as mean values \pm s.e.m ($n = 10$). Control fish were exposed to regular freshwater (FW). * Significant difference ($P < 0.05$) between mean values from FW and IPW fish at the same time point. Further statistical details can be seen in Table 3-1.

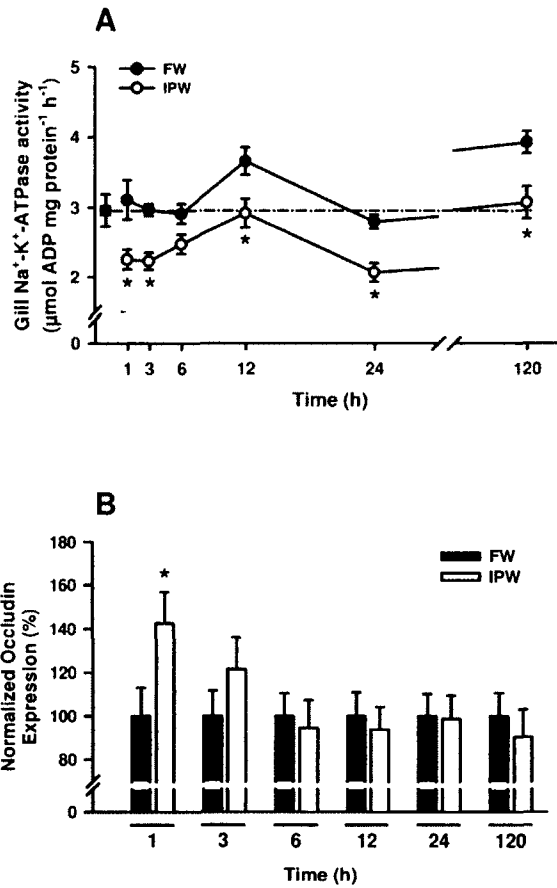


Figure 3-2: Effect of abrupt exposure to ion-poor water (IPW) on gill (A) Na⁺-K⁺-ATPase activity and (B) occludin expression. Data are expressed as mean values ± s.e.m. (*n* = 10). Control fish were exposed to regular freshwater (FW). * Significant difference (*P* < 0.05) between FW and IPW at the same time point. For Na⁺-K⁺-ATPase activity, further statistical details can be seen in Table 3-1. At each time point in IPW, gill occludin is expressed relative to control fish in FW.

Table 3-1: Summary of statistics for abrupt exposure of goldfish (from FW to IPW) generated by Two-Way ANOVAs of 0 – 120 h time course data.

Variable	Parameter Measured					
	[†] Osmolality	[†] Na ⁺	[†] Cl ⁻	[‡] Glucose	[†] Muscle Moisture	*Na ⁺ -K ⁺ -ATPase activity
Water	P<0.001	P<0.001	P<0.001	P<0.001	P<0.01	P<0.001
Time	P<0.001	P<0.001	P<0.001	P<0.001	NS	P<0.001
Water x Time	P<0.001	P<0.001	P<0.001	P<0.001	P<0.001	NS

[†]: Data from **Figure 3-1**

[‡]: Data from **Table 3-2**

*: Gill Na⁺-K⁺-ATPase activity, see **Figure 3-2**

Table 3-2: Serum glucose levels (mg/100 ml) in goldfish abruptly exposed to IPW or acclimated to IPW for 14 and 28 day periods.

	Time (hours)						Time (days)	
	1	3	6	12	24	120	14	28
FW	38.4 ± 4.0	44.1 ± 6.6	38.7 ± 5.2	52.4 ± 6.4	44.3 ± 5.4	40.6 ± 2.6	34.9 ± 3.2	39.5 ± 2.6
IPW	47.5 ± 2.5	79.3 ± 8.2*	60.4 ± 6.6*	68.3 ± 7.0	70.9 ± 3.2*	135.1 ± 5.6*	77.0 ± 8.1*	101.0 ± 9.7*†

All data are expressed as mean values ± SE (n = 7-10/group).

Control fish were held in regular FW.

An asterisk denotes significant difference ($P \leq 0.05$) between FW and IPW at a specific time period.

A † denotes significant difference ($P \leq 0.05$) between IPW groups held for 14 and 28 days.

expression returned to levels that did not significantly differ from control fish for the remainder of the 120 h experimental period (Fig. 3-2B).

3.4.2 Long-term acclimation of goldfish to IPW: Goldfish were able to acclimate to IPW for up to 28 days without mortality or exhibiting any signs of abnormal behaviour.

3.4.3 Serum endpoints and muscle moisture content: Serum osmolality, $[\text{Na}^+]$ and $[\text{Cl}^-]$ were all significantly lower after 14 days acclimation to IPW (Fig. 3-3A-C). After 28 days, serum osmolality remained lower in IPW fish than in FW fish (Fig. 3-3A) and serum $[\text{Cl}^-]$ declined further relative to levels measured in fish acclimated to IPW for 14 days (Fig. 3-3C). In contrast, serum $[\text{Na}^+]$ in fish acclimated to IPW for 28 days was not found to be significantly different from fish held in regular FW (Fig. 3-3B). Serum glucose levels were elevated in fish acclimated to IPW after both 14 and 28 days, and glucose levels in IPW fish after 28 days were significantly higher than those measured in fish acclimated to IPW for 14 days (Table 3-2). Muscle moisture did not significantly differ between any fish groups after longer periods of acclimation to IPW (Fig. 3-3D).

3.4.4 Gill, kidney and intestine Na^+/K^+ -ATPase activity and occludin expression: Gill Na^+/K^+ -ATPase activity was significantly elevated in goldfish acclimated to IPW for 14 days. However, after 28 days in IPW, gill Na^+/K^+ -ATPase activity declined to levels that were not significantly different from those found in control fish (Fig. 3-4A). During the same time period, gill occludin expression in the gills of fish acclimated to IPW was markedly elevated relative to occludin expression found in fish held in regular FW (Fig. 3-4B).

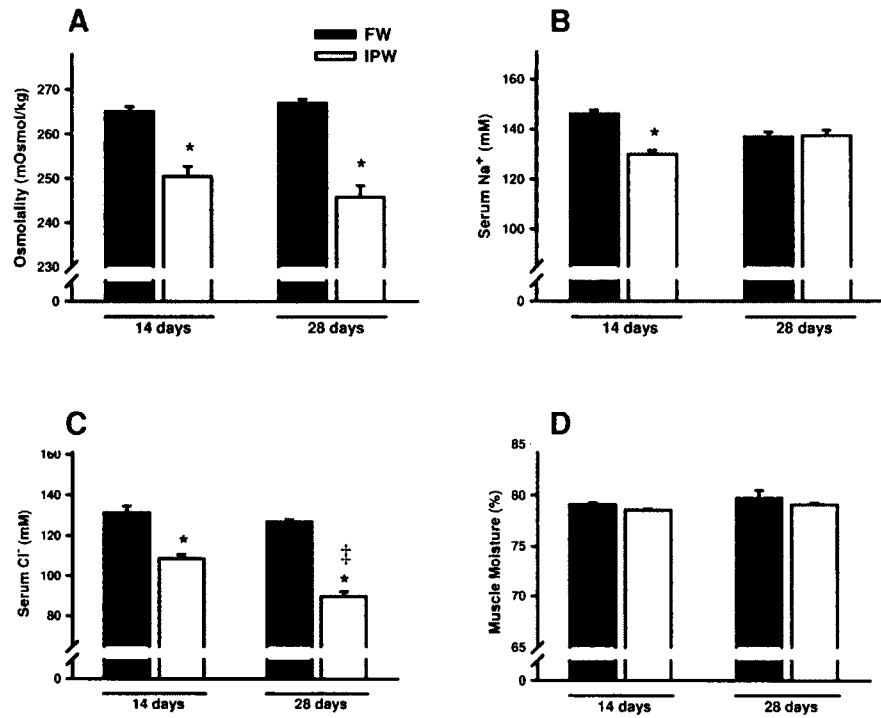


Figure 3-3: The effect of 14 and 28 days acclimation to ion-poor water (IPW) on (A) serum osmolality, (B) serum Na⁺, (C) serum Cl⁻ and (D) muscle moisture content in goldfish. Data are expressed as mean values ± s.e.m. (*n* = 7). * Significant difference (*P* < 0.05) between FW and IPW at the same time point. † Significant difference (*P* < 0.05) between 14 and 28 days acclimation within an environment.

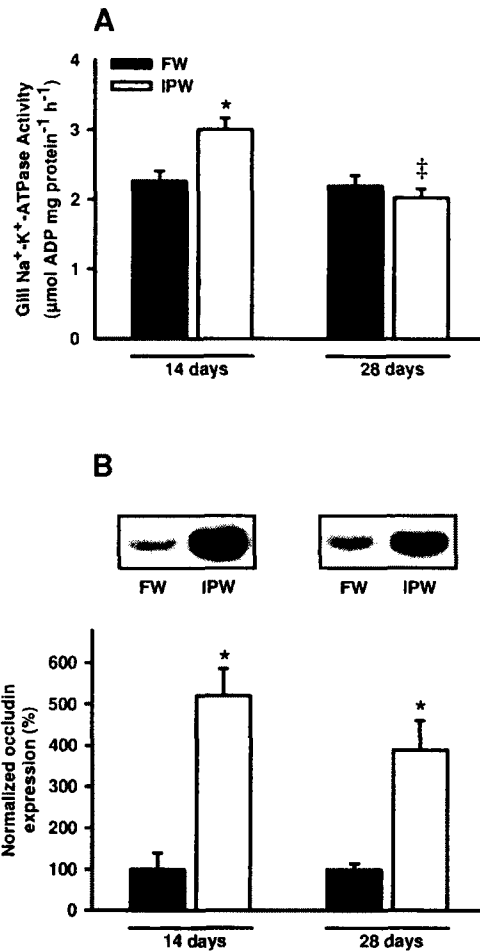


Figure 3-4: The effect of 14 and 28 days acclimation to ion-poor water (IPW) on gill (A) Na⁺-K⁺-ATPase activity and (B) occludin expression. Insets show representative western blot analyses. Data are expressed as mean values ± s.e.m. (*n* = 7). Control fish were held in regular freshwater (FW). * Significant difference (*P* < 0.05) between FW and IPW at the same time point. ‡ Significant difference (*P* < 0.05) between 14 and 28 days acclimation within an environment.

In the kidney of fish acclimated to IPW, Na⁺-K⁺-ATPase activity was elevated relative to fish held in FW at both time points examined but only significant at 28 days (Fig. 3-5A). After 28 days in IPW surroundings, kidney Na⁺-K⁺-ATPase activity was significantly greater than after 14 days. Similarly, kidney occludin expression was elevated after 28 days acclimation to IPW conditions (Fig. 3-5B). However when fish were held in IPW for 14 days, no significant difference was observed in renal occludin expression relative to fish held in FW (Fig. 3-5B).

In the intestine of goldfish, Na⁺-K⁺-ATPase activity was elevated after 28 days in IPW but not after 14 days (Fig. 3-6A). In contrast, intestinal occludin expression was significantly lower in fish held in IPW for 14 days relative to fish held in FW, and after 28 days no significant difference in intestinal occludin expression was observed between groups (Fig. 3-6B).

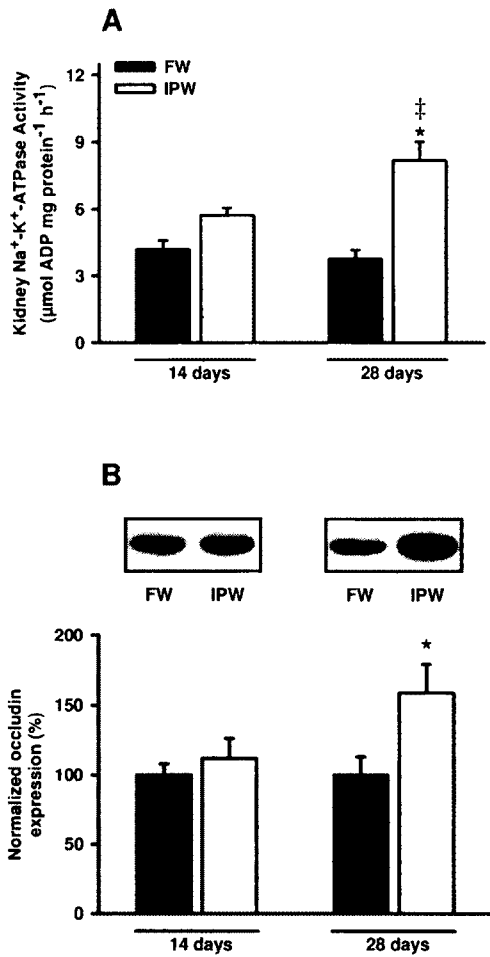


Figure 3-5: The effect of 14 and 28 days acclimation to ion-poor water (IPW) on kidney (A) Na⁺-K⁺-ATPase activity and (B) occludin expression. Insets show representative western blot analyses. Data are expressed as mean values \pm s.e.m. ($n = 7$). Control fish were held in regular freshwater (FW). * Significant difference ($P < 0.05$) between FW and IPW at the same time point. ‡ Significant difference ($P < 0.05$) between 14 and 28 days acclimation within an environment.

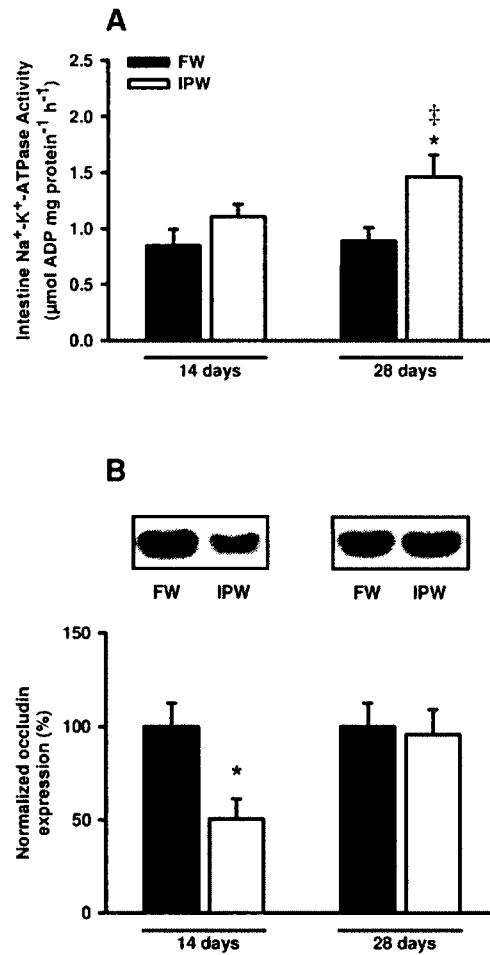


Figure 3-6: The effect of 14 and 28 days acclimation to ion-poor water (IPW) on intestine (A) Na⁺-K⁺-ATPase activity and (B) occludin expression. Insets show representative western blot analyses. Data are expressed as mean values ± s.e.m. (*n* = 7). Control fish were held in regular freshwater (FW). * Significant difference (*P* < 0.05) between FW and IPW at the same time point. ‡ Significant difference (*P* < 0.05) between 14 and 28 days acclimation within an environment

3.5 Discussion

3.5.1 Overview: In the current study, the abrupt exposure of goldfish to ion-poor surroundings did not result in any mortality. We can therefore accept our first hypothesis, that goldfish are capable of tolerating abrupt exposure to IPW. Over the course of the 120 h experiment, goldfish generally exhibited either a transient response or relatively rapid and sustained alteration in circulating electrolytes and glucose, ionomotive enzyme activity and TJ protein abundance upon exposure to IPW. Most notably, branchial occludin expression quickly altered following exposure to IPW. Furthermore, robust, tissue specific alterations in occludin expression were observed in goldfish acclimated to IPW for 14 and 28 days. It is our contention that these alterations are adaptive and fit with current models of ion transport across the osmoregulatory epithelia of FW fishes. Therefore we can also accept our second hypothesis, that occludin expression will alter in an adaptive manner in response to ion-poor conditions.

3.5.2 Abrupt exposure of goldfish to IPW: The ability of fishes to tolerate rapid alterations in the ionic composition of their surroundings is well documented (e.g. Leray et al., 1981; Jacob and Taylor, 1983; Usher et al., 1991; Mancera et al., 1993; Kelly and Woo, 1999). However, the majority of studies that examine this phenomenon transfer fishes between FW and SW (or vice versa). In the current study, we abruptly exposed FW fish to IPW and observed physiological responses that generally appeared to mirror those exhibited by euryhaline fishes during challenges of a more typical nature i.e. – lowered serum osmolality and circulating ion levels as well as increased substrate mobilization in the form of elevated glucose levels following transfer from a hyper-osmotic (e.g. SW) to a

hypo-osmotic (e.g. FW) environment. However, it should be emphasized that in the current study, goldfish are being abruptly exposed to an environment that will amplify the external to internal osmotic/ionic gradient (i.e. FW to more “dilute” FW), and not reverse it as would be the case if SW fish were exposed to FW. This, taken together with the “stenohaline” nature of goldfish, may explain some of the differences that appear to occur in the physiological response of this species when compared to the response of other typical euryhaline fishes. For example, despite a rapid reduction in serum osmolality in response to IPW exposure, there does not appear to be a time-dependent post-exposure recovery in this parameter (see Fig. 3-1A). A similar phenomenon occurs for serum glucose levels (see Table 3-2). Therefore, the prominent acute and recovery phase typically found in the hydromineral endpoints of euryhaline fishes after rapid exposure from one salinity to another (e.g. Kelly and Woo, 1999) does not appear to manifest in the serum endpoints measured in this species under these conditions. While it could be argued that goldfish were not given enough time to recover, data from fish acclimated to IPW for 14 and 28 days would seem to suggest otherwise. In fact, the only variable measured in the abrupt exposure experiment that altered transiently and appeared to “recover” was gill occludin expression (see Fig. 3-2B). In the branchial epithelium, occludin expression increased sharply in response to IPW exposure and then eventually decreased back to control levels for the remainder of the 120 h experiment. These observations suggest that occludin may aid in the immediate modulation of gill epithelial barrier properties in response to an abrupt change in environmental ion concentrations, however further studies will be required to decipher which TJ proteins play a prominent

role after this immediate response. Regardless, the role of occludin appears to be a biphasic one as a substantial elevation in expression is once again observed after longer periods of acclimation to IPW (see Fig. 3-4B and discussion below).

3.5.3 Long-term acclimation of goldfish to IPW: Following exposure to IPW for longer time periods (i.e. 14 and 28 days), goldfish continued to exhibit lowered serum osmolality, $[Cl^-]$ and $[Na^+]$ (the latter at 14 days at least) (see Fig. 3-3A-C), as well as elevated glucose (see Table 3-2) with no fish mortality or observable abnormal behaviour. Furthermore, muscle moisture content, a general index of hydration status, was not significantly different between fish held in FW and IPW at either 14 or 28 days (see Fig. 3-3D). Combined, these data indicate that goldfish can establish new steady state conditions in IPW that are not deleterious to fish health. However, elevated glucose levels point to a potential increase in the energetic expenditure of maintaining salt and water balance in IPW. Since elevated glucose levels may also reflect an increase in circulating stress hormones (e.g. glucocorticoids such as cortisol), it seems possible that continuous culture in IPW could eventually result in the manifestation of pathophysiological problems normally associated with chronic stress (e.g. poor growth) (Mommsen et al., 1999).

3.5.4 Tissue occludin and Na^+-K^+ -ATPase activity after 14 days in IPW: In gill tissue, Na^+-K^+ -ATPase activity and occludin expression were both elevated after 14 days in IPW (see Fig. 3-4). An increase in both of these variables would suggest that ion transport across the transcellular route (presumably in the inward direction) is increased while solute movement through the paracellular route (i.e. in the outward direction) is reduced.

In a tissue that comes into direct contact with the surrounding environment, such as the gill, this would make adaptive sense as it would enhance ion acquisition from the surroundings whilst limiting obligatory ion loss. In a previous study where goldfish were acclimated to deionized water for 21 days, Na^+ influx was seen to double relative to control FW fish while Na^+ efflux exhibited a more than 6-fold decrease (Cuthbert and Maetz, 1972). Our data are consistent with these observations and would suggest that alterations in ionomotive enzyme activity (e.g. $\text{Na}^+-\text{K}^+-\text{ATPase}$) as well as TJ protein expression (e.g. occludin) seem likely to contribute to this strategy of maintaining salt and water balance. In addition, recent *in vitro* studies have demonstrated that the TER measured across FW gill epithelia “externally” exposed to IPW is significantly greater than the TER across epithelia bathed with regular FW on the apical surface (Kelly and Wood, 2008). Combined, these observations strongly suggest that in IPW, TJ proteins reduce the paracellular permeability of the gill epithelium, and this would be adaptive in minimizing obligatory ion loss to the surroundings.

In contrast to the response of goldfish gill tissue following 14 days of IPW acclimation, alterations in $\text{Na}^+-\text{K}^+-\text{ATPase}$ activity and occludin expression in renal tissue were less obvious (see Fig. 3-5). Although this may initially seem to suggest that the renal system does not play an “enhanced” role when goldfish are acclimated to IPW, such a conclusion can be rejected based on the alterations that occur in the renal system after 28 days in IPW (see discussion below). Therefore it appears that in goldfish, the development of an “enhanced” role for the kidney is likely governed by time spent in

IPW, and that after 14 days, goldfish may not be fully acclimated to IPW surroundings (i.e. further changes have yet to occur).

The physiological consequences of alterations in occludin expression in the goldfish intestine after 14 days acclimation to IPW are not clear (see Fig. 3-6). This is due to a paucity of information on the regulation of TJ proteins in the intestinal epithelia of aquatic vertebrates as well as (to the best of our knowledge) an absence of studies that have examined the role of this tissue in ionoregulatory homeostasis of fishes acclimated to IPW conditions. Nevertheless, it seems likely that a limited ability to acquire ions from the surrounding water will result in salts derived from dietary sources playing an increasingly important role in replenishing the supply of ions to IPW fish (for review see Marshall and Grosell, 2005), and a decrease in intestinal permeability would likely facilitate ion absorption from the chyme of feeding goldfish. Indeed, it has been recently suggested by Scott et al. (2006), that ion absorption from chyme is critical to ionoregulatory homeostasis of euryhaline killifish transferred from brackish water to FW. Furthermore, Scott et al. (2006) observed that alterations in ion movement (uptake) across the gut were generally not coupled with alterations in transcellular transport mechanisms, leading to the suggestion that alternate mechanisms are likely responsible for enhanced ion uptake. Modulated epithelial permeability may contribute to these alternate mechanisms. Indeed, the interesting parallel between killifish held in FW and goldfish held in IPW relates to the observations of Wood and Laurent (2003) which indicate that feeding is essential in order to maintain killifish health in FW environments. Correspondingly, we also observed that goldfish exposed to IPW and deprived of access

to food began to exhibit abnormal behaviour (e.g. disequilibrium) after ~ 10 – 12 days exposure (Effendi and Kelly, unpublished observations).

3.5.5 Tissue occludin and Na⁺-K⁺-ATPase activity after 28 days in IPW: The status of both gill and kidney tissue in goldfish acclimated to IPW for 28 days alters relative to observations made after 14 days. In the branchial epithelium, occludin expression remained markedly elevated relative to fish held in regular FW, most likely continuing to function by enhancing gill barrier properties. In contrast, Na⁺-K⁺-ATPase activity in the gill declined at 28 days and was no longer found to significantly differ from the activity recorded in FW fish (see Fig. 3-4A). To compensate for this potential reduction in ion acquisition by the gill, the kidney appeared to be reorganized for a more central role in ion reabsorption after 28 days in IPW (i.e. kidney Na⁺-K⁺-ATPase activity increased almost 3-fold, see Fig. 3-5A). In goldfish kidney, Na⁺-K⁺-ATPase is particularly abundant in the distal tubule and (to a lesser extent) the collecting duct of the nephron (see Chapter 2). Within these segments (in particular the early distal tubule), Na⁺-K⁺-ATPase generates a Na⁺ gradient that permits the operation of luminal facing Na⁺-K⁺-2Cl⁻ co-transporters and Na⁺-H⁺ exchangers, resulting in Na⁺ and Cl⁻ uptake from luminal filtrate (Dantzler, 2003; Nishimura and Fan, 2003). In association with abundant Na⁺-K⁺-ATPase, the distal tubules and collecting ducts are the only regions of the goldfish nephron that appear to express occludin (see Chapter 2), which in FW fishes in general, are the electrically “tight” and relatively water-impermeable diluting segments of the kidney (Dantzler, 2003; Nishimura and Fan, 2003). Therefore, the observed increase in kidney occludin expression that occurs in conjunction with an elevation in kidney Na⁺-

K^+ -ATPase activity after 28 days in IPW (see Fig. 3-5) would likely decrease the permeability of the diluting segments of the nephron to enhance ion reabsorption and retention with little water accompaniment. These observations are consistent with the differences found in renal TJ protein expression between euryhaline fish acclimated to either FW or SW (Bagherie-Lachidan et al. 2008).

Following 28 days in IPW, occludin expression in the goldfish intestine was no longer significantly different between FW and IPW fish, however, Na^+ - K^+ -ATPase activity was now elevated in fish held in IPW relative to those held in FW (see Fig. 3-6). These data suggest that, as opposed to strategies suggested previously (see above discussion), goldfish may eventually begin to rely more on the active transport of ions across the intestinal epithelium from dietary sources rather than the facilitation of passive movement. Clearly this area will require further study.

3.5.6 Perspectives: The current studies demonstrate the plasticity of goldfish within the context of an extreme FW environment (i.e. ion-poor FW). In this regard, goldfish appear to be a suitable model species for studying rapid as well as long-term alterations in the physiological processes associated with maintaining salt and water balance in ion-poor surroundings. In the gill epithelium, the integral TJ protein occludin exhibited rapid transient alterations as well as robust long term changes, while alterations in the primary ionomotive enzyme of fish gills, Na^+ - K^+ -ATPase, seemed relatively moderate by comparison. In future studies, it will be interesting to examine the response of other TJ proteins (e.g. claudins), particularly right after IPW exposure when occludin expression declines. Recent studies have shown that gill claudin mRNA expression (e.g. claudin 30)

alters at least 24 h after SW to FW transfer in euryhaline tilapia (Tipsmark et al., 2008). Furthermore, it is well established from *in vitro* studies that gill epithelial permeability responds rapidly to changes in the ionic concentration of surrounding water as well as to endocrine factors (e.g. cortisol, prolactin etc.) that mediate biochemical reorganization of ionoregulatory epithelia in response to salinity change (e.g. Perry and Laurent, 1989; Kelly and Wood, 2001; Kelly and Wood, 2002a, 2002b). These same endocrine factors have also been demonstrated to improve epithelial integrity in normal FW as well as IPW (Kelly and Wood, 2001, 2002a, 2008). It will be interesting to further examine the interplay of these endocrine factors with the molecular components that regulate the permeability of the TJ complex.

3.6 References

Bagherie-Lachidan M, Wright SI, Kelly SP. 2008. Claudin-3 tight junction proteins in *Tetraodon nigroviridis*: cloning, tissue specific expression and a role in hydromineral balance. *Am J Physiol Regul Integr Comp Physiol* 294: 1638-R1647.

Balda MS, Whitney JA, Flores C, González S, Cerejido M, Matter K. 1996. Functional dissociation of paracellular permeability and transepithelial electrical resistance and disruption of the apical-basolateral intramembrane diffusion barrier by expression of a mutant tight junction membrane protein. *J Cell Biol* 134:1031-1049.

Chasiotis H, Kelly SP. 2009. Occludin and hydromineral balance in *Xenopus laevis*. *J Exp Biol* 212: 287-296.

Cuthbert AW, Maetz J. 1972. The effects of calcium and magnesium on sodium fluxes through gills of *Carassius auratus*, L. *J Physiol* 221:633-643.

Dantzler WH. 2003. Regulation of renal proximal and distal tubule transport: sodium, chloride and organic anions. *Comp Biochem Physiol A* 136:453-478.

Feldman GJ, Mullin JM, Ryan MP. 2005. Occludin: Structure, function and regulation. *Adv Drug Deliv Rev* 57:883-917.

Furuse M, Hirase T, Itoh M, Nagafuchi A, Yonemura S, Tsukita S, Tsukita S. 1993. Occludin: a novel integral membrane protein localizing at tight junctions. *J Cell Biol* 123:1777-1788.

González-Mariscal L, Betanzos A, Nava P, Jaramillo BE. 2003. Tight junction proteins. *Prog Biophys Mol Biol* 81:1-44.

Jacob WF, Taylor MH. 1983 The time course of seawater acclimation in *Fundulus heteroclitus* L. *J Exp Zool* 228:33-39.

Kelly SP, Peter RE. 2006. Prolactin-releasing peptide, food intake and hydromineral balance in goldfish. *Am J Physiol Regul Integr Comp Physiol* 291:R1474-R1481.

Kelly SP, Woo NYS. 1999. The response of seabream following abrupt hyposmotic exposure. *J Fish Biol* 55:732-750.

Kelly SP, Wood CM. 2001. Effect of cortisol on the physiology of cultured pavement cell epithelia from freshwater trout gills. *Am J Physiol Regul Integr Comp Physiol* 281:R811-R820.

Kelly SP, Wood CM. 2002a. Cultured gill epithelia from freshwater tilapia (*Oreochromis niloticus*): Effect of cortisol and homologous serum supplements from stressed and unstressed fish. *J Membr Biol* 190:29-42.

Kelly SP, Wood CM. 2002b. Prolactin effects on cultured pavement cell epithelia and pavement cell plus mitochondria-rich cell epithelia from freshwater rainbow trout gills. *Gen Comp Endocrinol* 128:44-56.

Kelly SP, Wood CM. 2008. Cortisol stimulates calcium transport across cultured gill epithelia from freshwater rainbow trout. *In Vitro Cell Dev Biol – Animal* 44:96-104.

Leray C, Colin DA, Florentz A. 1981. Time course of osmotic adaptation and gill energetics of rainbow trout (*Salmo gairdneri* R.) following abrupt changes in external salinity. *J Comp Physiol* 144:175-181.

Mancera JM, Perez-Figares JM, Fernandez-Llebrez P. 1993. Osmoregulatory responses to abrupt salinity changes in the euryhaline gilthead sea bream (*Sparus aurata* L.). *Comp Biochem Physiol* 106A:245–250.

Marshall WS, Grosell M. 2005. Ion transport, osmoregulation and acid-base balance. In: *The Physiology of Fishes*, 3rd edition (ed. DH Evans, JB Claiborne), pp 177-230. New York: CRC Press.

McCarthy KM, Skare IB, Stankewich MC, Furuse M, Tsukita S, Rogers RA, Lynch RD, Schneeberger EE. 1996. Occludin is a functional component of the tight junction. *J Cell Sci* 109:2287-2298.

McCormick SD. 1993. Methods for nonlethal gill biopsy and measurement of Na⁺, K⁺-ATPase activity. *Can J Fish Aquat Sci* 50:656-658.

Mommsen TP, Vijayan MM, Moon TW. 1999. Cortisol in teleosts: dynamics, mechanisms of action, and metabolic regulation. *Rev Fish Biol Fisher* 9:211-268.

Nishimura H, Fan Z. 2003. Regulation of water movement across vertebrate renal tubules. *Comp Biochem Physiol* 136A:479-498.

Perry SF, Laurent P. 1989. Adaptational responses of rainbow trout to lowered external NaCl concentration – contribution of the branchial chloride cell. *J Exp Biol* 147:147–168.

Scott GR, Schulte PM, Wood CM. 2006. Plasticity of osmoregulatory function in the killifish intestine: drinking rates, salt and water transport, and gene expression after freshwater transfer. *J Exp Biol* 209:4040-4050.

Tipsmark CK, Baltzegar DA, Ozden O, Grubb BJ, Borski RJ. 2008. Salinity regulates claudin mRNA and protein expression in the teleost gill. *Am J Physiol Regul Integr Comp Physiol* 294:R1004–R1014.

Usher ML, Talbot C, Eddy FB. 1991. Effects of transfer to seawater on growth and feeding in Atlantic salmon smolts (*Salmo salar* L). *Aquaculture* 94:309-326.

Wong V, Gumbiner BM. 1997. A synthetic peptide corresponding to the extracellular domain of occludin perturbs the tight junction permeability barrier. *J Cell Biol* 136:399-409.

Wood CM, Laurent P. 2003. Na⁺ versus Cl⁻ transport in the intact killifish after rapid salinity transfer. *Biochim Biophys Acta* 1618:106-119.

Zall DM, Fisher D and Garner MD (1956) Photometric determination of chlorides in water. *Anal Chem* 28:1665-1678.

CHAPTER 4:

**CORTISOL REDUCES PARACELLULAR PERMEABILITY
AND INCREASES OCCLUDIN ABUNDANCE IN CULTURED TROUT
GILL EPITHELIA**

Helen Chasiotis^a, Chris M. Wood^b and Scott P. Kelly^a

^aDepartment of Biology, York University, Toronto, Ontario, Canada M3J 1P3

^bDepartment of Biology, McMaster University, Hamilton, Ontario, Canada, L8S 4K1

This chapter has been published and reproduced with permission:

Chasiotis H, Wood CM, Kelly SP. 2010. Cortisol reduces paracellular permeability and increases occludin abundance in cultured trout gill epithelia. *Mol Cell Endocrinol* 323:232-238.

4.1 Abstract

A role for the tight junction (TJ) protein occludin in the regulation of gill paracellular permeability was investigated using primary cultured “reconstructed” freshwater (FW) rainbow trout gill epithelia composed solely of pavement cells. Cortisol treatment reduced epithelial permeability characteristics, measured as changes in transepithelial resistance (TER) and paracellular [³H]PEG-4000 flux. Cortisol also reduced net Na⁺ flux rates when epithelia were exposed to apical FW. cDNA encoding for the TJ protein occludin was cloned from rainbow trout and found to be particularly abundant in gill tissue. In cultured gill preparations, occludin immunolocalized to the TJ complex and transcript abundance dose-dependently increased in response to cortisol treatment and in association with reduced paracellular permeability. Occludin protein abundance also increased in response to cortisol treatment. However, occludin mRNA levels did not change in response to apical FW exposure, and [³H]PEG-4000 permeability did not decrease. These data support a role for occludin in the endocrine regulation of paracellular permeability across gill epithelia of fishes.

4.2 Introduction

The tight junction (TJ) complex plays an important role in the regulation of epithelial permeability in vertebrates. It is composed of a number of transmembrane and cortical proteins and the presence, as well as abundance, of different TJ proteins appears to be a key element in TJ heterogeneity between and within tissues. Occludin is a tetraspan transmembrane TJ protein that is broadly expressed in vertebrate epithelia (Feldman et al., 2005). Since the initial discovery of occludin (Furuse et al., 1993), numerous studies have suggested an important role for this TJ protein in the regulation of epithelial permeability (Feldman et al., 2005). More specifically, an increase in occludin abundance is most often associated with reductions in paracellular permeability across diverse epithelia and endothelia (Feldman et al., 2005). However, the majority of work conducted on the physiological function of occludin in vertebrate epithelia has been accomplished using mammalian models. Recently it has been proposed that occludin may contribute to the regulation of epithelial permeability in aquatic vertebrates under conditions of altered hydromineral status (see Chapters 2 and 3; Chasiotis and Kelly, 2009). In this regard, occludin has been found to be abundant in epithelia that regulate salt and water balance in fishes, such as the gill, kidney and gastrointestinal (GI) tract (see Chapters 2 and 3). In the freshwater (FW) goldfish kidney, a spatially distinct distribution pattern of occludin can be observed along the nephron (see Chapter 2). The “tight” distal tubules and collecting ducts of the nephron exhibit robust occludin immunoreactivity (occludin-ir), while the “leakier” proximal regions of the nephron exhibit little or no occludin-ir. Furthermore, in the gill tissue of goldfish, occludin protein abundance significantly

increased when fish were acclimated to ion-poor water (see Chapter 3). This has been proposed to contribute to a reduction in the permeability of the paracellular pathway across the gill and is consistent with the observations of Cuthbert and Maetz (1972) who reported that the gill epithelium of goldfish exposed to ion-poor conditions exhibits a considerable reduction in outwardly directed ion movement. This presumably results in a beneficial reduction in passive ion loss in an environment where limitations are set on active ion acquisition.

Despite the above observations, and to the best of our knowledge, there are no studies that have related alterations in the specific machinery of the TJ complex in fishes with measured changes in epithelial permeability. Primary cultured gill epithelial models that allow for the “reconstruction” of FW gill epithelia *in vitro* present an appropriate tool for such studies (see Wood and Pärt, 1997; Fletcher et al., 2000; Kelly et al., 2000; Kelly and Wood, 2002). These models exhibit passive transport and permeability characteristics that closely mimic the *in vivo* characteristics of the FW gill epithelium (Wood and Pärt, 1997; Fletcher et al., 2000; Kelly et al., 2000; Kelly and Wood, 2002). Furthermore, corticosteroid (cortisol) treatment of cultured gill epithelia results in a distinct epithelial “tightening” effect which is driven at least in part by reduced paracellular permeability properties (Kelly and Wood, 2001, 2002). This sensitivity to cortisol provides a simple means by which to manipulate transepithelial as well as paracellular permeability characteristics, and these observations in fishes are in accord with the tightening effects of corticosteroids on other vertebrate epithelia and endothelia (Zettl et al., 1992; Stelwagen et al., 1999; Antonetti et al., 2002; Förster et al., 2005).

Based on this knowledge, the objectives of the current study were to examine cortisol-induced alterations in the permeability characteristics of a cultured gill epithelium prepared from FW rainbow trout and relate alterations in paracellular permeability to modifications in occludin abundance. We hypothesized that if occludin is involved in regulating the barrier properties of gill epithelia in fishes, occludin abundance should increase in association with reductions in paracellular permeability.

4.3 Materials and methods

4.3.1 Cultured rainbow trout gill epithelia: The preparation and culture of gill epithelia from FW rainbow trout was carried out in order to produce preparations composed of gill pavement cells only. Methods have been detailed by Kelly et al. (2000) and were originally developed by Wood and Pärt (1997). Briefly, cultured epithelia were prepared using stock rainbow trout (200-450 g) held in flow-through dechlorinated tap water (approximate composition in mM: $[\text{Na}^+] = 0.55\text{--}0.59$, $[\text{Cl}^-] = 0.70\text{--}0.92$, $[\text{Ca}^{2+}] = 0.76\text{--}0.90$, $[\text{K}^+] = 0.04\text{--}0.05$, pH range 7.4–8.0) at 10–12°C. Cells were initially cultured in 25cm² flasks in Leibovitz's L-15 medium supplemented with 2 mM glutamine and 6% fetal bovine serum (L15). At confluence (~4–5 days), cells were harvested and seeded into cell culture inserts (0.9cm² growth area, 0.4µm pore size, 1.6×10⁶ pores/cm² pore density; Falcon BD, Mississauga, ON, Canada). Culture inserts were housed in companion cell culture plates (Falcon BD) and after cell seeding (at a density of 700,000 cells/culture insert), epithelia were allowed to develop a stable transepithelial resistance (TER) (over ~5 days) with L15 culture media present on both apical and basolateral surfaces of the preparation (i.e. symmetrical culture conditions). The treatment of epithelia with cortisol was conducted according to methods previously outlined by Kelly and Wood (2001). Two physiologically relevant doses of cortisol were selected (50 and 500 ng/ml) based on the aforementioned study as well as observations made by Kelly and Wood (2002). Cortisol was added to culture media in flasks 24 h after first seeding and when epithelia were cultured in inserts, cortisol was added to the basolateral media only. Therefore, epithelia cultured in flasks and subsequently in inserts were exposed to

cortisol for a total of 9–10 days. In a separate set of experiments which were conducted in order to determine whether alterations in occludin transcript abundance translated into alterations in occludin protein abundance, only flask-cultured epithelia were used to harvest tissue. The rationale for this was that inserts did not provide enough protein for western blot analysis after conducting the extraction protocol used in these studies (see Section 4.3.6). Therefore, in these experiments cultured epithelial cells were exposed to a single dose of cortisol (500 ng/ml) for 5 days. This period of time and dose of cortisol is sufficient to elicit a significant increase in TER and accompanying decrease in [³H]PEG-4000 permeability (see Section 4.3.2) in cultured epithelia (data not shown). Finally, in experiments where FW was added to the apical side of cultured preparations (i.e. asymmetrical culture conditions), temperature-equilibrated sterile dechlorinated FW (composition as detailed above) was used.

4.3.2 Electrophysiological, [³H]PEG-4000 and net Na⁺ flux measurements: Measurements of TER were conducted using chopstick electrodes (STX-2) fitted to a custom-modified voltohmmeter (World Precision Instruments, Sarasota, FL, USA). TER was recorded every 24 h after seeding cells onto culture inserts to monitor epithelial development. Under asymmetrical conditions, TER was monitored at 3 h intervals. All measurements of TER are reported as background-corrected values taking into account the resistance measured across a “vacant” culture insert containing appropriate solutions. Paracellular permeability across cultured epithelia was examined using the paracellular permeability marker, [³H]polyethylene glycol (molecular mass 4000 Da; ‘PEG-4000’; NEN-Dupont, Mississauga, ON, Canada) according to previously detailed methods and

calculations (Kelly and Wood, 2001). [³H]PEG-4000 (1 µCi) was added to the basolateral compartment of culture preparations and its appearance in the apical compartment was monitored as a function of time and epithelial surface area. Net Na⁺ flux rates from basolateral to apical compartments under asymmetrical culture conditions were measured and calculated according to methods detailed by Kelly and Wood (2001).

4.3.3 Cloning and qRT-PCR analysis of rainbow trout occludin cDNA: Total RNA was isolated from trout gill tissue using TRIZOL[®] Reagent (Invitrogen Canada Inc., Burlington, ON, Canada), according to manufacturer's instructions. Gill RNA was then treated with DNase I (Amplification Grade; Invitrogen Canada Inc.) and first-strand cDNA was synthesized using SuperScript[™] III Reverse Transcriptase and Oligo(dT)₁₂₋₁₈ primers (Invitrogen Canada Inc.). Using a ClustalX multiple sequence alignment of occludin coding sequences from 9 different species (human [NM 002538]; mouse [NM 008756]; rat [NM 031329]; cow [NM 001082433]; dog [NM 001003195]; platypus [XM 001510548]; opossum [XM 001380557]; frog [NM 001088474]; zebrafish [NM 212832]), degenerate primers were designed based on highly conserved regions. A partial rainbow trout cDNA fragment was amplified by reverse transcriptase PCR (RT-PCR) using occludin degenerate primers under the following reaction conditions: 1 cycle of denaturation (95°C, 4min), 40 cycles of denaturation (95°C, 30 s), annealing (53°C, 30 s) and extension (72°C, 30 s), respectively, final single extension cycle (72°C, 5 min) (0.2 µM dNTP, 2 µM forward and reverse primers, 1× Taq DNA polymerase buffer, 1.5 mM MgCl₂ and 1U Taq DNA polymerase) (Invitrogen Canada Inc.). Gel electrophoresis (1% agarose for ~90 min at 5 V/cm) verified a PCR product at the predicted amplicon size of

~796 bp. The DNA fragment was excised from the gel and purified using a QIAquick Gel Extraction Kit (QIAGEN Inc., Mississauga, ON, Canada). The purified amplicon was sequenced in the York University Core Molecular Biology and DNA Sequencing Facility (Department of Biology, York University, Toronto, ON, Canada). A partial coding sequence (CDS) of trout occludin was confirmed using a Basic Local Alignment Search Tool (BLAST) search. To obtain the complete rainbow trout occludin CDS, both 5'- and 3'-rapid amplification of cDNA ends (RACE) PCR was performed using a SMART™ RACE cDNA Amplification Kit (Clontech Laboratories Inc., Mountain View, CA, USA) as per manufacturer's instructions. RACE-PCR products were resolved by electrophoresis, purified and sequenced as described above in order to complete the trout occludin CDS, GenBank accession number GQ476574.

4.3.4 Occludin expression profile and qRT-PCR analysis of occludin mRNA abundance in rainbow trout tissues: Quantitative real-time PCR (qRT-PCR) was used to examine occludin mRNA distribution and abundance in discrete rainbow trout tissues, as well as occludin transcript abundance in cultured epithelia from flasks and cell culture inserts. For expression profile studies, total RNA was extracted from the following tissues: brain, eye, gill, bulbus arteriosus, atrium, ventricle, esophagus, anterior and posterior stomach, pyloric ceca, anterior intestine, middle intestine and posterior intestine, liver, gallbladder, spleen, swimbladder, kidney, muscle, adipose tissue and blood. The extraction of RNA and synthesis of cDNA from all tissues was conducted as outlined in the previous section. Primers for trout occludin (forward: 5' CAGCCCAGTTCCTCCAGTAG 3' and reverse: 5' GTCATCCAGCTCTCTGTCC 3', predicted amplicon size ~340 bp) were designed

using the CDS generated by 5'- and 3'-RACE-PCR described above. β -actin was used as an internal control (forward: 5' GGACTTTGAGCAGGAGATGG 3' and reverse: 5' GACGGAGTATTTACGCTCTGG 3', predicted amplicon size ~354 bp). β -actin primers were designed based on GenBank accession number AF157514. qRT-PCR analysis of occludin and β -actin was conducted using SYBR Green I Supermix (Bio-Rad Laboratories Ltd., Mississauga, ON, Canada) and a Chromo4™ Detection System (CFB-3240, Bio-Rad Laboratories Canada Ltd.) under the following conditions: 1 cycle denaturation (95°C, 4min) followed by 40 cycles of denaturation (95°C, 30 s), annealing (58°C, 30 s) and extension (72°C, 30 s), respectively. To ensure that no primer-dimers or other non-specific products were synthesized during reactions, a melting curve analysis was carried out after each qRT-PCR run.

4.3.5 Immunolocalization of rainbow trout occludin: Trout gill epithelia cultured in inserts were allowed to develop a stable TER under symmetrical culture conditions. Epithelia were briefly rinsed with phosphate buffered saline (PBS, pH 7.7) and fixed for 20 min at room temperature (RT) with 3% paraformaldehyde. Fixed epithelia were then permeabilized with ice-cold methanol for 5 min at -20°C, washed with 0.01% Triton X-100 in PBS for 10 min and blocked for 1 h at RT with antibody dilution buffer (ADB; 10% goat serum, 3% BSA and 0.05% Triton X-100 in PBS). Epithelia were incubated overnight at RT with a custom-synthesized polyclonal antibody raised in rabbit against a synthetic peptide (CHIKKMVG DYDRRA) corresponding to a 14-amino acid region of rainbow trout occludin (1:100 dilution in ADB; New England Peptide, LLC, Gardner, MA, USA). For a negative control, epithelia were also incubated overnight with ADB

lacking primary antibody. Epithelia were then washed with PBS and incubated for 1 h at RT with TRITC-labeled goat anti-rabbit antibody (1:500 in ADB; Jackson ImmunoResearch Laboratories Inc., West Grove, PA, USA). After a final wash with PBS, epithelia were excised from the insert housings using a scalpel and mounted on glass microscopy slides with Molecular Probes ProLong Antifade (Invitrogen Canada Inc.) containing 5 µg/ml DAPI (Sigma–Aldrich Canada Ltd., Oakville, ON, Canada). Fluorescence images were captured using a Reichert Polyvar microscope (Reichert Microscope Services, Depew, NY, USA) and an Olympus DP70 camera (Olympus Canada, Markham, ON, Canada). Adobe Photoshop CS2 software was used for contrast and brightness adjustment of entire images (Adobe Systems Canada, Toronto, ON, Canada).

4.3.6 Western blotting and protein quantification of rainbow trout occludin: Trout gill epithelia cultured in flasks were briefly rinsed with ice-cold PBS, scraped using a plastic cell scraper into a lysis buffer (10 mM Tris–HCl, pH 7.5, 1 mM EDTA, 0.1 mM NaCl, 1 mM PMSF) containing 1:200 protease inhibitor cocktail (Sigma–Aldrich Canada Ltd.) and then homogenized by repeatedly passing through a 26G needle. Homogenates were centrifuged at 20,000 g for 25 min at 4°C to remove cell debris and the resultant supernatant was collected. To separate cytosolic and membrane protein fractions, supernatant was further centrifuged at 54,000 g for 90 min at 4°C and the remaining pellet (membrane fraction) was resuspended in a solubilizing buffer (50 mM Tris–HCl, pH 7.5, 1 mM EDTA, 1% Triton-X-100, 0.5% SDS, 1 mM PMSF) containing 1:200 protease inhibitor cocktail. Pellet protein concentrations were determined using the

Bradford assay (Sigma–Aldrich Canada Ltd.) according to the manufacturer’s guidelines. Samples (2 µg) were boiled at 100°C in 6X sample buffer (360 mM Tris–HCl, 30% glycerol, 12% SDS, 600 mM DTT, 0.03% Bromophenol Blue) and subjected to SDS-PAGE on 12% acrylamide gels followed by semi-dry transfer to polyvinylidene difluoride (PVDF) membranes for 2 h. Membranes were blocked for 1 h at RT in blocking solution [Tris-buffered saline (TBS-T; 10 mM Tris, 150 mM NaCl, 0.05% Tween-20, pH 7.4) containing 5% nonfat dry skim milk powder], incubated overnight at 4°C with the custom rabbit polyclonal anti-trout occludin antibody described above (1:1000 dilution in blocking solution), washed with TBS-T, incubated for 1 h at RT with horseradish peroxidase (HRP)-conjugated goat anti-rabbit antibody (Bio-Rad Laboratories Canada Ltd.; 1:5000 in blocking solution), and then washed once more prior to antigen reactivity detection using an Enhanced Chemiluminescence Plus Western blotting system (GE Healthcare BioSciences Inc., Baie d’Urfé, QC, Canada). After occludin detection, membranes were stripped and incubated with mouse monoclonal anti-actin antibody (JLA20; Developmental Studies Hybridoma Bank, Iowa City, IA, USA; 1:500 in blocking solution) and HRP-conjugated goat anti-mouse antibody (Bio-Rad Laboratories Canada Ltd.; 1:5000 in blocking solution), respectively as an internal loading control. The abundance of occludin and actin was quantified using a Molecular Imager Gel Doc XR+ System and Quantity One 1D analysis software (Bio-Rad Laboratories Canada Ltd.). Occludin is expressed as a normalized value relative to actin.

4.3.7 Statistical analysis: All data are expressed as mean values \pm s.e.m. (n), where n represents the number of filter inserts, except in Fig. 4-2, where n represents the number

of fish sampled, and Fig. 4-5 where n represents the number of cell culture flasks. Significant differences ($P < 0.05$) between groups were determined using either a two-way or one-way analysis of variance (ANOVA) as appropriate followed by a Student–Newman–Keuls test (Sigmastat Software; Systat Software Inc., San Jose, CA, USA).

4.4 Results

4.4.1 Cultured gill epithelia and effects of cortisol on TER, [³H]PEG-4000 and net Na⁺ flux: Under symmetrical culture conditions (L15 apical/L15 basolateral), untreated cultured trout gill epithelial preparations (i.e. 0 ng/ml cortisol added) exhibited a mean TER of ~ 2,900 Ωcm² (Fig. 4-1A). The addition of cortisol to culture media (50 or 500 ng/ml) dose-dependently elevated TER (Fig. 4-1A). In accord with cortisol-induced elevations in TER, cortisol treatment of cultured gill preparations dose-dependently reduced the movement (efflux) of the paracellular permeability marker [³H]PEG-4000 (Fig. 4-1B).

When exposed to asymmetrical culture conditions (FW apical/L15 basolateral), dose dependent effects of cortisol on TER and [³H]PEG-4000 permeability were also observed (Fig. 4-1A,B). However, FW addition to the apical side of preparations significantly elevated TER in both the control and 50 ng/ml treated preparations relative to measurements under symmetrical conditions (Fig. 4-1A). In 500 ng/ml treated preparations, no additional significant increase in TER was observed (Fig 4-1A). In association with changes in TER, [³H]PEG-4000 flux significantly increased in control and 50 ng/ml cortisol-treated epithelia under asymmetrical culture conditions (Fig 4-1B) but no significant increase in [³H]PEG-4000 flux was observed in epithelia treated with 500 ng/ml cortisol. Under asymmetrical culture conditions, cortisol dose-dependently reduced the efflux rates (basolateral to apical movement) of Na⁺ (Fig 4-1C).

4.4.2 Cloning of trout occludin cDNA, tissue expression profile and immunolocalization: Sequencing and analysis of the 1500-bp CDS of rainbow trout occludin revealed an open

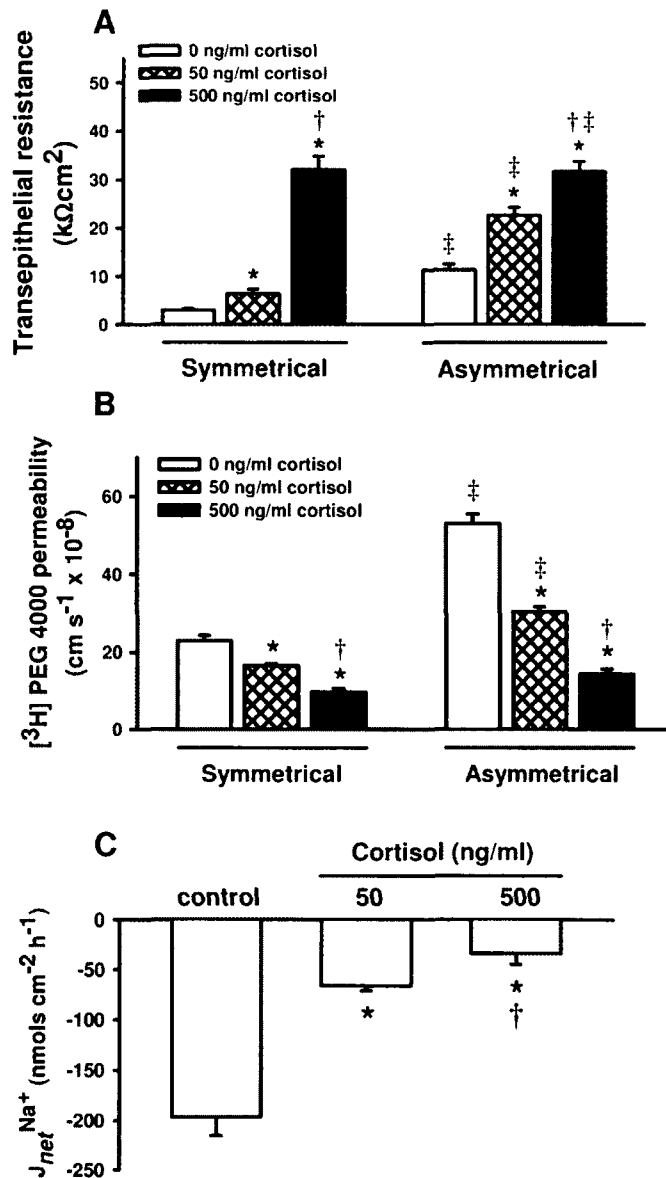


Figure 4-1: Effect of cortisol on (A) transepithelial resistance (TER), (B) [³H]PEG-4000 permeability and (C) net Na⁺ flux rates across cultured rainbow trout gill epithelia. TER and [³H]PEG-4000 permeability were measured under both symmetrical (L15 apical/L15 basolateral) and asymmetrical (FW apical/L15 basolateral) culture conditions while net Na⁺ flux rates were measured under asymmetrical culture conditions only. Data are expressed as mean values ± s.e.m. (*n* = 4-6). * Significant difference (*P* < 0.05) from control treatment (0 ng/ml cortisol). † Significant difference (*P* < 0.05) between cortisol doses (50 versus 500 ng/ml cortisol). ‡ Significant difference (*P* < 0.05) between symmetrical and asymmetrical culture conditions.

reading frame for a 499-amino acid protein that exhibited 46 - 48% amino acid sequence identity with mammalian occludin (i.e. human, mouse, rat, cow, dog, platypus and opossum), ~ 50% identity with frog occludin and ~ 63% identity with zebrafish occludin. Using qRT-PCR analysis, occludin transcript was found to be broadly distributed in rainbow trout tissues (Fig. 4-2). Occludin mRNA was particularly abundant in gill tissue as well as some other tissues involved either directly or indirectly in the regulation of salt and water balance (e.g. skin and GI tract). Occludin was absent in red blood cells (a non-epithelial tissue). Immunocytochemical analysis of cultured preparations revealed occludin-ir along the cultured pavement cell periphery at the location of the TJ (Fig. 4-3A). A negative control exhibited no occludin-ir (Fig. 4-3B). Western blot analysis of cultured gill tissues using the custom-synthesized rainbow trout occludin antibody revealed a single immunoreactive band that resolved at ~ 70 kDa (Fig. 4-3C).

4.4.3 Effects of culture conditions and cortisol on occludin abundance: In epithelia cultured on inserts, no significant differences in occludin mRNA abundance were observed between preparations held under symmetrical or asymmetrical culture conditions (Fig. 4-4A). In contrast, cortisol treatment significantly elevated occludin mRNA abundance in both 50 and 500 ng/ml treated epithelia in cell culture inserts under symmetrical conditions (Fig. 4-4B) and in 500 ng/ml treated preparations under asymmetrical culture conditions (Fig. 4-4C). No alterations in β -actin abundance were seen in any of these treatments (symmetrical versus asymmetrical, $P = 0.78$; control versus cortisol-treated inserts under symmetrical conditions, $P = 0.13$; control versus cortisol-treated inserts under asymmetrical conditions, $P = 0.18$).

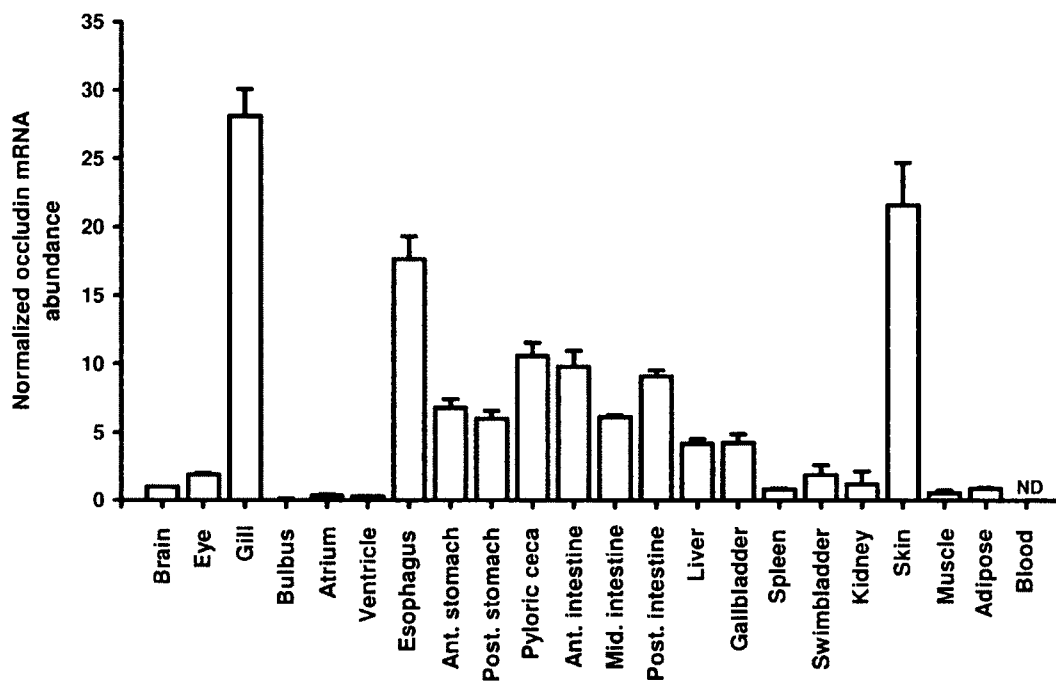


Figure 4-2: qRT-PCR generated occludin mRNA expression profile for discrete rainbow trout tissues. Occludin mRNA abundance was normalized with β -actin and the abundance of occludin in each tissue was expressed relative to the brain assigned a value of 1.0. Data are expressed as mean values \pm s.e.m. ($n = 4$). Amplicon size was 340 bp and 354 bp for occludin and β -actin respectively. ND = not detected.

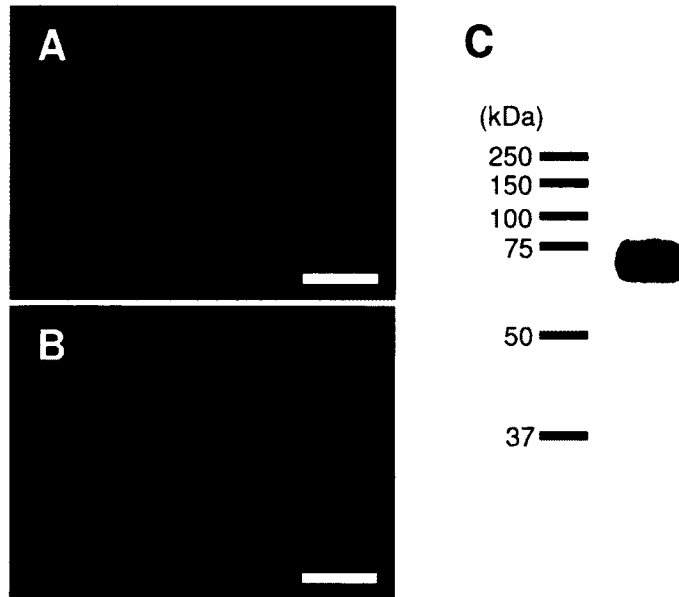


Figure 4-3: (A) Immunolocalization of occludin (red) in cultured trout gill epithelia under symmetrical (L15 apical/L15 basolateral) culture conditions using a custom synthesized rabbit polyclonal antibody raised against a synthetic region of trout occludin. Negative control (primary antibody omitted) is shown in (B). Panel (C) presents a representative western blot using the same custom synthesized occludin antibody used for immunolocalization. A single occludin-immunoreactive band resolved at ~70 kDa. In panels (A) and (B), nuclei were stained with DAPI (blue) and each scale bar = 20 μ m.

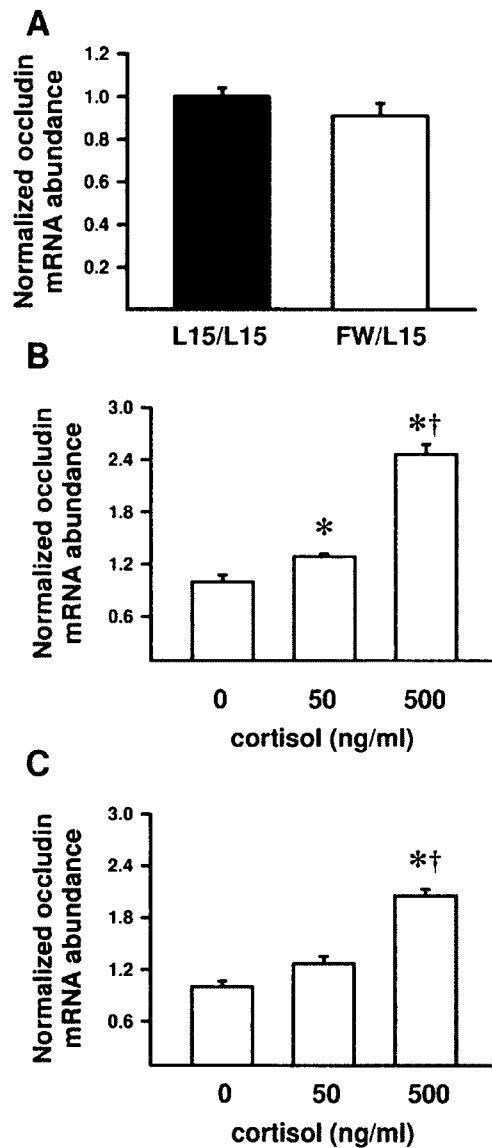


Figure 4-4: Occludin mRNA abundance in response to (A) 12 h apical FW exposure and cortisol addition to media under (B) symmetrical (L15 apical/L15 basolateral) and (C) asymmetrical (FW apical/L15 basolateral) culture conditions. Data are expressed as mean values \pm s.e.m. ($n = 4-6$). In (A), β -actin normalized occludin mRNA abundance for epithelia exposed to apical FW (asymmetrical) is expressed relative to symmetrical culture conditions assigned a value of 1.0. In panels (B) and (C), β -actin normalized occludin mRNA abundance for cortisol-treated epithelia are expressed relative to untreated (0 ng/ml cortisol) epithelia assigned a value of 1.0. * Significant difference ($P < 0.05$) from control treatment (0 ng/ml cortisol). † Significant difference ($P < 0.05$) between cortisol doses (50 versus 500 ng/ml cortisol).

In flask-cultured epithelia exposed to 500 ng/ml cortisol for 5 days and subsequently harvested for either mRNA or protein analysis, cortisol significantly elevated both transcript and protein abundance (Fig. 4-5). For these studies, actin was also used to normalize both mRNA and protein abundance. Again, no significant alterations in actin levels were observed as a result of cortisol treatment (mRNA, cortisol versus control $P = 0.19$; protein, cortisol versus control $P = 0.76$).

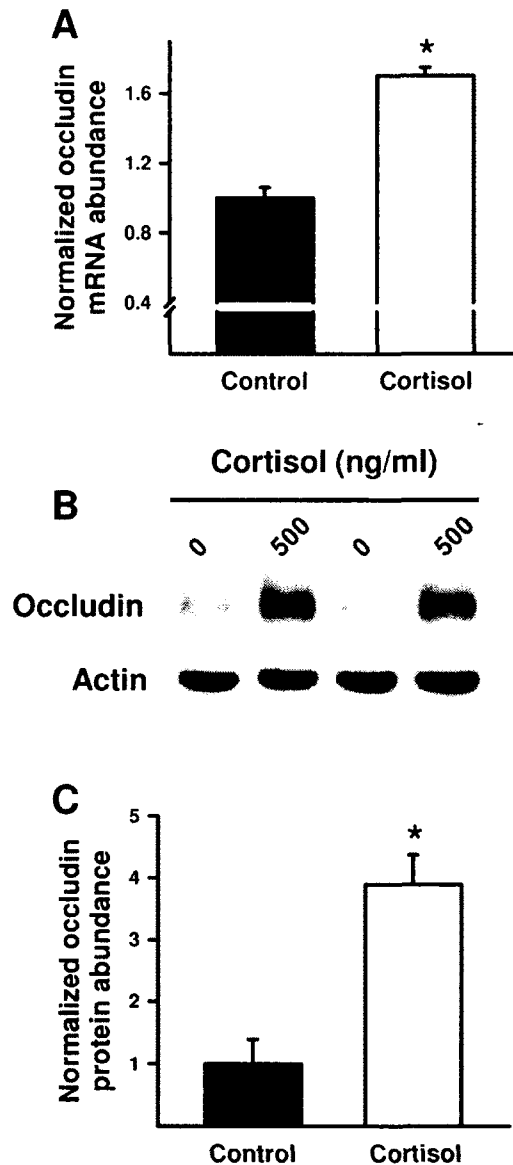


Figure 4-5: Effect of cortisol (500 ng/ml) on occludin abundance in flask-cultured rainbow trout pavement cell epithelia. Alterations in occludin (A) mRNA and (B) and (C) protein abundance are shown. In (A) occludin mRNA abundance in cortisol-treated epithelia is normalized with β -actin and expressed relative to untreated (0 ng/ml cortisol) epithelia assigned a value of 1.0. (B) shows a representative western blot where both occludin and actin immunoreactivity can be observed. (C) presents occludin protein abundance normalized to actin and expressed relative to untreated (0 ng/ml cortisol) epithelia assigned a value of 1.0. In panels (A) and (C), data are expressed as mean values \pm s.e.m. ($n = 4-6$). * Significant difference ($P < 0.05$) from untreated controls.

4.5 Discussion

4.5.1 Cultured gill epithelia and effects of cortisol on TER, [³H]PEG-4000 and net Na⁺ flux: The electrophysiological and permeability characteristics of untreated (0 ng/ml cortisol added) cultured trout pavement cell epithelia in symmetrical culture conditions were typical for these preparations (see Fig. 4-1; Kelly et al., 2000), and cortisol treatment dose-dependently elevated TER in accord with previous reports (see Kelly and Wood, 2001). Since TER is a function of both transcellular and paracellular permeability, dose-dependent reductions in the efflux rates of the paracellular permeability marker PEG-4000 in cortisol-treated epithelia (see Fig. 4-1B) demonstrated that elevated TER measurements were driven at least in part by reductions in the permeability of the paracellular pathway. Under asymmetrical culture conditions, epithelia exhibited a qualitatively similar response to cortisol treatment (Fig. 4-1A,B). However, exposure of epithelia to apical FW caused a significant elevation in TER across control and 50 ng/ml treated preparations. In epithelia cultured in the presence of a high cortisol dose (i.e. 500 ng/ml), no further increase in TER was observed. In control epithelia and epithelia treated with 50 ng/ml cortisol, elevated TER in response to apical FW addition occurs in conjunction with a paradoxical increase in paracellular permeability. This is usual for cultured trout gill epithelia and suggests that elevated TER under asymmetrical conditions in these preparations predominantly reflects decreased transcellular permeability, while paracellular permeability may actually increase upon acute FW exposure (Wood et al., 1998). Treatment with higher doses of cortisol appears to dampen this phenomenon, most likely by causing a reduction in both transcellular and

paracellular conductance prior to FW exposure. When epithelia are exposed to apical FW, cortisol caused a dose-dependent reduction in the efflux rates (basolateral to apical movement) of Na⁺. This has previously been hypothesized to reflect a beneficial reduction in passive ion loss across the gill surface of FW fishes under “stressed” conditions where cortisol would be naturally elevated in the circulatory system of a FW fish (see Kelly and Wood, 2001).

4.5.2 Cloning of trout occludin cDNA, tissue expression profile and immunolocalization: qRT-PCR analysis of occludin in discrete tissues of rainbow trout revealed a broad expression pattern (Fig. 4-2). This is in accord with widespread distribution of occludin in other vertebrates (e.g. Furuse et al., 1993; Saitou et al., 1997; Feldman et al., 2005; Chasiotis and Kelly, 2009). In epithelia that are directly exposed to the external environment (such as the gill and skin), as well as other tissues involved in the regulation of salt and water balance in fishes, occludin was particularly abundant. Similar observations have been reported regarding occludin expression patterns in the goldfish (see Chapter 2). Occludin was also observed to immunolocalize to the periphery of cultured trout pavement cells, where TJs maintain epithelial integrity and contribute to the regulated separation of fluid compartments (Fig. 4-3A). This observation is in line with reports of occludin immunolocalization in numerous other vertebrate epithelia (e.g. see Chapter 2; Saitou et al., 1997; González-Mariscal et al., 2000; Ridyard et al., 2007; Chasiotis and Kelly 2009). In goldfish gills, occludin has been reported to immunolocalize between epithelial cells in a similar manner. However, occludin has also been found to immunolocalize to the capillary endothelium (see Chapter 2). Since the

cultured preparations are composed entirely of gill epithelial pavement cells, this model allows us to evaluate the effects of cortisol on paracellular permeability properties and TJ protein mRNA abundance in gill epithelial cells only and negates any contribution from capillary endothelia.

4.5.3 Effects of culture conditions and cortisol on occludin mRNA abundance: In the absence of cortisol, exposure of cultured gill epithelia to asymmetrical culture conditions (i.e. apical FW) resulted in a significant increase in TER. However, occludin mRNA abundance did not significantly alter in response to asymmetrical culture conditions (see Fig. 4-4A). In this regard, elevated TER is not driven by a reduction in the permeability of the paracellular pathway as [³H]PEG-4000 flux did not decrease in conjunction with an increase in TER (see Fig. 4-1 and discussion above). Therefore it is not unexpected that occludin mRNA levels did not increase. In contrast, it is noteworthy that occludin mRNA levels did not significantly decrease in association with an increase in PEG-4000 flux across cultured preparations. Despite these observations, cortisol treatment did significantly elevate occludin mRNA and protein abundance in association with both an increase in TER and decrease in PEG-4000 flux. This would suggest that the endocrine system, and more specifically corticosteroids, play an important role in regulating occludin abundance in the fish gill epithelium. In line with these observations, corticosteroid treatment of mouse mammary epithelia has been reported to result in both a decrease in paracellular permeability and increase in occludin abundance (Stelwagen et al., 1999). Furthermore, capillary endothelia of the blood-brain-barrier as well as the blood-retinal barrier also exhibit a similar response (Antonetti et al., 2002; Förster et al.,

2005). Correspondingly, it was recently shown that glucocorticoids directly up-regulate occludin expression via activated glucocorticoid receptor binding to a glucocorticoid response element within the human occludin gene promoter (Harke et al., 2008). Given that cortisol-induced alterations in the paracellular permeability of gill epithelial preparations can be almost entirely blocked using the glucocorticoid receptor antagonist RU486 (Kelly and Wood, 2002) it is plausible that a similar mechanism may also be in place in the gill epithelial tissue of fishes.

4.4 Conclusion: The response of the gill epithelium to corticosteroid treatment is qualitatively similar to corticosteroid-induced occludin up-regulation in the epithelium and endothelium reported in other vertebrates. Therefore this report highlights a conservation of fundamental alterations in the molecular machinery of the TJ complex in response to hormone treatment across vertebrate groups. While the current study strongly supports a role for occludin in regulating the barrier properties of osmoregulatory tissue such as the gill, within the confines of this study the endocrine regulation of this process appears to surpass any response to environmental change alone (i.e. no alteration in occludin mRNA abundance after switching apical culture conditions from L15 to FW). However, under natural conditions, a fish rapidly transitioning from saline conditions to FW would typically respond by elevating circulating cortisol levels (e.g. Scott et al., 2006). A key question to address in future studies with respect to the endocrine regulation of occludin and the role that this TJ protein plays in regulating epithelial permeability in tissues such as the gill will be to determine how alterations such as those described in the current study fit into the broader scheme of endocrine-mediated alterations in the

molecular machinery of the TJ complex. For example, using a primary culture system similar to the cultured trout gill preparations used in this study, Bui et al. (2010) have recently demonstrated that mRNAs encoding for 9 of 12 salinity-responsive claudin TJ proteins in puffer fish (*Tetraodon nigroviridis*) are found in cultured pavement cell epithelia and differentially respond to physiologically relevant doses of cortisol *in vitro*. Furthermore, Tipsmark et al. (2009) have also reported alterations in claudin mRNA abundance in cortisol-treated gill explants from salmon, albeit at doses higher than used here. These observations, together with the present findings, provide momentum for further study.

4.6 References

Antonetti DA, Wolpert EB, DeMaio L, Harhaj NS, Scaduto RC Jr. 2002. Hydrocortisone decreases retinal endothelial cell water and solute flux coincident with increased content and decreased phosphorylation of occludin. *J Neurochem* 80: 667-677.

Bui P, Bagherie-Lachidan M, Kelly SP. 2010. Cortisol differentially alters claudin isoform mRNA abundance in a cultured gill epithelium from puffer fish (*Tetraodon nigroviridis*). *Mol Cell Endocrinol* 317:120-126.

Chasiotis H, Kelly SP. 2009. Occludin and hydromineral balance in *Xenopus laevis*. *J Exp Biol* 212:287-296.

Feldman GJ, Mullin JM, Ryan MP. 2005. Occludin: structure, function and regulation. *Adv Drug Deliv Rev* 57:883-917.

Fletcher M, Kelly SP, Pärt P, O'Donnell M, Wood CM. 2000. Transport properties of cultured branchial epithelia from freshwater rainbow trout: A novel preparation with mitochondria-rich cells. *J Exp Biol* 203:1523-1537.

Förster C, Silwedel C, Golenhofen N, Burek M, Kietz S, Mankertz J, Drenckhahn D. 2005. Occludin as direct target for glucocorticoid-induced improvement of blood-brain barrier properties in a murine *in vitro* system. *J Physiol* 565:475-486.

Furuse M, Hirase T, Itoh M, Nagafuchi A, Yonemura S, Tsukita S. 1993. Occludin: a novel integral membrane protein localizing at tight junctions. *J Cell Biol* 123:1777-1788.

González-Mariscal L, Namorado MC, Martin D, Luna J, Alarcon L, Islas S, Valencia L, Muriel P, Ponce L, Reyes JL. 2000. Tight junction proteins ZO-1, ZO-2, and occludin along isolated renal tubules. *Kidney Int* 57:2386-2402.

Harke H, Leers J, Kietz S, Drenckhahn D, Förster C. 2008. Glucocorticoids regulate the human occludin gene through a single imperfect palindromic glucocorticoid response element. *Mol Cell Endocrinol* 295:39-47.

Kelly SP, Fletcher M, Pärt P, Wood CM. 2000. Procedures for the preparation and culture of “reconstructed” rainbow trout branchial epithelia. *Methods Cell Sci* 22:153-163.

Kelly SP, Wood CM. 2001. Effect of cortisol on the physiology of cultured pavement cell epithelia from freshwater trout gills. *Am J Physiol Regul Integr Comp Physiol* 281:R811-R820.

Kelly SP, Wood CM. 2002. Cultured gill epithelia from freshwater tilapia (*Oreochromis niloticus*): Effect of cortisol and homologous serum supplements from stressed and unstressed fish. *J Membrane Biol* 190:29-42.

Ridyard AE, Brown JK, Rhind SM, Else RW, Simpson JW, Miller HRP. 2007. Apical junction complex protein expression in the canine colon: differential expression of claudin-2 in the colonic mucosa in dogs with idiopathic colitis. *J Histochem Cytochem* 55:1049-1058.

Saitou M, Ando-Akatsuka Y, Itoh M, Furuse M, Inazawa J, Fujimoto K, Tsukita S. 1997. Mammalian occludin in epithelial cells: its expression and subcellular distribution. *Eur J Cell Biol* 73:222-231.

Scott GR, Schulte PM, Wood CM. 2006. Plasticity of osmoregulatory function in the killifish intestine: drinking rates, salt and water transport, and gene expression after freshwater transfer. *J Exp Biol* 209:4040-4050.

Stelwagen K, McFadden HA, Demmer J. 1999. Prolactin, alone or in combination with glucocorticoids, enhances tight junction formation and expression of the tight junction protein occludin in mammary cells. *Mol Cell Endocrinol* 156:55-61.

Tipsmark CK, Jorgensen C, Brande-Lavridsen N, Engelund M, Olesen JH, Madsen SS. 2009. Effects of cortisol, growth hormone and prolactin on gill claudin expression in Atlantic salmon. *Gen Comp Endocrinol* 163:270-277.

Wood CM, Pärt P. 1997. Cultured branchial epithelia from freshwater fish gills. *J Exp Biol* 200:1047-1059.

Wood CM, Gilmour KM, Pärt P. 1998. Passive and active transport properties of a gill model, the cultured branchial epithelium of the freshwater rainbow trout (*Oncorhynchus mykiss*). *Comp Biochem Physiol A* 119:87-96.

Zettl KS, Sjaastad MD, Riskin PM, Parry G, Machen TE, Firestone GL. 1992. Glucocorticoid formation of tight junctions in mouse mammary epithelial cells *in vitro*. *Proc Natl Acad Sci USA* 89:9069-9073.

CHAPTER 5:

PERMEABILITY PROPERTIES AND OCCLUDIN EXPRESSION IN A PRIMARY CULTURED MODEL GILL EPITHELIUM FROM THE STENOHALINE FRESHWATER GOLDFISH

Helen Chasiotis and Scott P. Kelly

Department of Biology, York University, Toronto, Ontario, Canada M3J 1P3

This chapter has been published and reproduced with permission:

Chasiotis H, Kelly SP. 2011. Permeability properties and occludin expression in a primary cultured model gill epithelium from the stenohaline freshwater goldfish. *J Comp Physiol B* 181:487-500.

5.1 Abstract

Techniques for the primary culture of fish gill epithelia on permeable supports have provided “reconstructed” gill models appropriate for the study of gill permeability characteristics *in vitro*. Models developed thus far have been derived from euryhaline fish species that can tolerate a wide range of environmental salinity. This study reports on procedures for the primary culture of a model gill epithelium derived from goldfish, a stenohaline freshwater (FW) fish that cannot tolerate high environmental salt concentrations. The reconstructed goldfish gill epithelium was cultured on permeable filter inserts and using electron microscopy and immunocytochemical techniques, was determined to be composed exclusively of gill pavement cells. When cultured under symmetrical conditions (i.e. with culture medium bathing both apical and basolateral surfaces), epithelial preparations generated appreciable transepithelial resistance (TER) (e.g. $1150 \pm 46 \Omega\text{cm}^2$) within 36 – 42 h post-seeding in inserts. When apical medium was replaced with FW (asymmetrical conditions to mimic conditions that occur *in vivo*), epithelia exhibited increased TER and elevated paracellular permeability. Changes in permeability occurred in association with altered occludin-immunoreactive band position by western blot and no change in occludin mRNA abundance. We contend that the goldfish gill model will provide a useful *in vitro* tool for examining the molecular components of a stenohaline fish gill epithelium that participate in the regulation of gill permeability. The model will allow molecular observations to be made together with assessment of changing physiological properties that relate to permeability. Together, this will allow further insight into mechanisms that regulate gill permeability in fishes.

5.2 Introduction

The fish gill is a complex multifunctional tissue (reviewed by Evans et al., 2005). As a consequence, determining the permeability characteristics of the fish gill epithelium *in vivo* is technically challenging. Typically, the permeability properties of an epithelium can be established using electrophysiological endpoints such as transepithelial resistance (TER). In addition, epithelial paracellular permeability can be examined by quantifying the movement of radiolabelled paracellular permeability markers (e.g. [³H]PEG-4000, [³H]mannitol, [³H]inulin) across an epithelium. The complex architecture of the fish gill, however, hinders the use of electrophysiological techniques *in vivo* and systemically administered paracellular permeability tracers can move across other epithelial tissues such as the skin or kidney. Moreover, the gill epithelium is heterogeneous and overlays an extensive vasculature. Therefore, alterations in the molecular components of the fish gill epithelium that contribute to changes in permeability can be experimentally difficult to isolate.

Techniques for the “reconstruction” of gill epithelia on permeable filter supports have allowed for some of the abovementioned challenges to be addressed (reviewed by Wood et al., 2002). A “reconstructed” model gill epithelium is formed by isolated gill epithelial cells that are cultured on permeable filters at the base of culture inserts (see Kelly et al., 2000; Wood et al., 2002). These primary cultured gill epithelia are not architecturally complex. Composed of a simple flat epithelium separating an apical and basolateral compartment, reconstructed gill preparations permit the electrophysiological measurement of transepithelial permeability (i.e. TER) as well as the determination of

paracellular permeability using radiotracers. Additionally, primary cultured gill epithelia have been shown to exhibit permeability characteristics that faithfully mimic those observed *in vivo* (see Wood et al., 2002). Furthermore, depending on the techniques used to generate a primary cultured gill preparation, these epithelia can be composed of gill pavement cells (PVCs) only or both PVCs and mitochondria-rich cells (MRCs; see Wood and Part, 1997; Fletcher et al., 2000; Kelly et al., 2000). In this regard, cultured gill preparations not only provide a useful model for the physiological examination of gill permeability, but also a practical tool for (1) the investigation of molecular components in the fish gill epithelium that contribute to the regulation of gill permeability (see Chapter 4) and (2) the examination of cell specific alterations in these components (see Bui et al., 2010).

To date, methods have been developed and described for the primary culture of gill epithelia from sea bass (Avella and Ehrenfeld, 1997), rainbow trout (Wood and Pärt, 1997; Fletcher et al., 2000), tilapia (Kelly and Wood, 2002) and puffer fish (Bui et al., 2010). Although recent studies have started to utilize cultured gill preparations for the examination of factors that regulate gill permeability (see Chapter 4; Bui et al., 2010), all cultured preparations developed thus far are derived from euryhaline fish species (i.e. species that can tolerate a wide range of environmental salinity). To the best of our knowledge, there are currently no primary cultured model gill epithelia derived from a stenohaline species of fish (i.e. species that can tolerate only a narrow range of environmental salinity). We contend that to gain broader insight into the importance of factors that regulate epithelial permeability in fishes, it will not only be beneficial to

examine euryhaline species, but also stenohaline fishes. In this regard, we have recently reported that when hydromineral status is challenged in the stenohaline goldfish, the abundance of occludin, a key tight junction (TJ) protein in vertebrate epithelia, significantly alters in tissues such as the gill (see Chapters 2 and 3). Therefore in the present study, our objectives were to: (1) develop a method for the primary culture of a model gill epithelium from goldfish, a stenohaline freshwater (FW) fish that cannot tolerate high environmental salt concentrations; and (2) utilize the *in vitro* model to expand our understanding of molecular mechanisms (e.g. alterations in occludin) that may contribute to changes in the permeability of the goldfish gill epithelium.

5.3 Materials and Methods

5.3.1 Animals: Goldfish (*Carassius auratus*, 20 - 40 g) were obtained from a local supplier (Aleongs International, Mississauga, ON, Canada) and held at $25 \pm 1^\circ\text{C}$ in 200-L opaque polyethylene tanks supplied with flow-through dechlorinated FW (approximate composition in mM: $[\text{Na}^+]$ 0.59, $[\text{Cl}^-]$ 0.92, $[\text{Ca}^{2+}]$ 0.76, $[\text{K}^+]$ 0.43, pH 7.35. Fish were fed *ad libitum* once daily with commercial koi and goldfish pellets (Martin Profishent, Elmira, ON, Canada) and held in these conditions for at least 3 weeks prior to use.

5.3.2 Preparation of a primary cultured goldfish gill epithelium: Methods for gill cell isolation and culture were conducted in a laminar flow hood using sterile techniques and were based on procedures developed by Wood and Pärt (1997) for trout gill epithelia as described in detail by Kelly et al. (2000). However, procedures for the isolation and culture of gill cells from goldfish, as outlined in the following section, involve modifications in gill tissue trypsination time, cell seeding density, the use of collagen to enhance cell attachment in flasks, culture time in flasks as well as an increase in cell culture incubation temperature. More specifically, goldfish gill arches were collected and rinsed with phosphate-buffered saline (PBS, pH 7.7) at room temperature (RT). Branchial tissue was carefully removed from gill cartilage, cut into smaller pieces and washed (3 x 10 min) in ice-cold PBS containing 200 IU/mL penicillin, 200 $\mu\text{g}/\text{mL}$ streptomycin, 275 $\mu\text{g}/\text{mL}$ gentamicin and 2.5 $\mu\text{g}/\text{mL}$ fungizone. Gill cells were then isolated from gill filaments using three consecutive cycles of tryptic digestion (10 min each at 4°C ; 0.05% trypsin in PBS with 5.5 mM EDTA). At the end of each 10 min tryptic digestion, gill tissue was mechanically agitated by repetitively drawing the trypsin solution plus tissue

up and down with a sterile plastic transfer pipette. Following mechanical agitation, the tissue slurry was placed on a 100 µm cell strainer so that isolated cells could filter through into ice-cold PBS containing 10% fetal bovine serum (FBS). The resulting gill cell suspension was subsequently centrifuged (10 min at 500 x g, 4°C) to form a pellet which was resuspended in ice-cold PBS containing 2.5% FBS. The resuspended cells were then centrifuged again (10 min at 500 x g, 4°C) and gently resuspended in Leibovitz's L-15 culture medium supplemented with 2 mM L-glutamine and 6% FBS (L15, pH 7.6 - 7.65). At this stage, antibiotics (100 IU/mL penicillin, 100 µg/mL streptomycin and 50 µg/mL gentamicin) were also present in the L15 media. Gill cells were counted using a haemocytometer and seeded into culture flasks (BD Falcon™; BD Biosciences, Mississauga, ON, Canada) at a density of 0.24 - 0.28 x 10⁶ cells/cm². To enhance cell attachment, culture flasks were pre-coated with collagen (10 µg/cm² type I, rat tail; Sigma-Aldrich Canada Ltd., Oakville, ON, Canada). After 24 h incubation at 27°C in an air atmosphere, medium was aspirated from flasks to remove non-adherent material, and temperature-equilibrated L15 plus antibiotics was added. After a further 24 h in culture, flasks were gently rinsed with ice-cold PBS and subjected to four consecutive rounds of tryptic digestion (1 min each at RT). After each 1 min trypsination, ice-cold PBS was added to flasks which were then gently agitated to facilitate cell detachment. The resulting suspensions were poured into PBS containing FBS (10%). Cells were pelleted by centrifugation (8 min at 500 x g, 4°C), gently resuspended in L15 (minus antibiotics) and seeded onto permeable polyethylene terephthalate (PET) filters (0.9 cm² growth area; 0.4 µm pore size; 1.6 x 10⁶ pore/cm² pore density) at the base of

culture inserts (BD Falcon™) at a density of 0.7×10^6 cells/insert. Inserts were held in 12-well companion plates (BD Falcon™). Initially, inserts (apical side) and companion wells (basolateral side) contained 1 mL of L15 each. After incubation for a further 20 - 22 h, medium was carefully aspirated from inserts and wells, and 1.5 mL and 2 mL of temperature-equilibrated L15 was added to apical and basolateral sides respectively (symmetrical conditions; L15/L15). Epithelia were held under symmetrical culture conditions until a stable transepithelial resistance (TER; see Section 5.3.4 below) developed. When the effects of asymmetrical (FW/L15) conditions were tested, temperature-equilibrated sterile dechlorinated FW was added to the apical side of the insert after several careful rinses to ensure removal of residual medium. The FW was sterilized by passing through a 0.2 µm filter (VWR International, Mississauga, ON, Canada) and was the same composition as the original holding water detailed previously.

5.3.3 Microscopy

5.3.3.1 Phase contrast microscopy: Gill epithelia cultured in flasks and inserts were routinely examined by phase contrast microscopy using a Leica inverted microscope. Phase contrast images were captured using a Leica DFC 420 camera and Leica Imaging Suite software (Leica Microsystems Inc., Richmond Hill, ON, Canada). Adobe Photoshop CS2 software was used for contrast and brightness adjustment of entire images (Adobe Systems Canada, Toronto, ON, Canada).

5.3.3.2 Scanning and transmission electron microscopy: Goldfish gill arches and inserts containing cultured goldfish gill epithelia were briefly rinsed with PBS and fixed in 2.5 - 3.5% glutaraldehyde in phosphate buffer (0.1 M, pH 7.2) at 4°C for 4 h. Following

fixation, tissues were washed with phosphate buffer (2 x 10 min, RT) and post-fixed with 1% osmium tetroxide in phosphate buffer (2 h at RT). For scanning electron microscopy (SEM) studies, filaments and epithelia were dehydrated in a graded acetone series (30 - 100%), dried with tetramethylsilane and mounted on aluminum stubs using double-sided non-conductive tape. Mounted tissues were then sputter coated (Hummer VI Au/Pd 40/60; Anatech USA, Orange, MA, USA) and examined using a Hitachi S-520 scanning electron microscope (Hitachi High-Technologies Canada, Inc., Toronto, ON, Canada). SEM images were captured using a Quartz PCI Version 6 image capture system (Quartz Imaging Corporation, Vancouver, BC, Canada).

For transmission electron microscopy (TEM) studies, epithelia were dehydrated in a graded ethanol series (50 - 100%) and embedded in Spurr's resin. Thin sections (50 nm) were cut using an ultramicrotome, mounted on copper grids, stained with 2% uranyl acetate (20 min at 60°C) and Reynold's lead citrate (at RT) respectively, and examined using a Philips EM 201 transmission electron microscope (Philips, Eindhoven, NB, Netherlands). For both SEM and TEM images, Adobe Photoshop CS2 software was used for contrast and brightness adjustment of entire images (Adobe Systems Canada).

5.3.3.3 Immunocytochemistry and immunohistochemistry: Goldfish gill epithelia cultured in inserts were briefly rinsed with PBS and fixed with 3% paraformaldehyde (20 min at RT). To examine for the presence of MRCs, several randomly selected inserts were pre-stained with the mitochondria specific dye, Mitotracker[®] Deep Red FM (100 nM in L15 for 45 min, 27°C; Invitrogen Canada Inc., Burlington, ON, Canada) prior to fixation. Fixed epithelia were then permeabilized with ice-cold methanol (5 min at -20°C), washed

with 0.01% Triton X-100 in PBS (10 min at RT) and blocked with antibody dilution buffer (ADB; 10% goat serum, 3% BSA and 0.05% Triton X-100 in PBS; 1 h at RT). Epithelia were subsequently incubated overnight at RT with a rabbit polyclonal anti-occludin antibody (1:100 dilution in ADB; Zymed Laboratories, Inc., South San Francisco, CA, USA) and mouse monoclonal anti-Na⁺-K⁺-ATPase α -subunit (NKA) antibody (α 5, 1:10 in ADB; Developmental Studies Hybridoma Bank, Iowa City, IA, USA). As negative controls, several inserts were also incubated overnight with ADB alone (primary antibodies omitted). After washing with PBS (3 x 5 min at RT), epithelia were incubated (1h at RT) with TRITC-labeled goat anti-rabbit and FITC-labeled goat anti-mouse antibodies (1:500 in ADB each; Jackson ImmunoResearch Laboratories Inc., West Grove, PA, USA). Epithelia were washed with PBS once more (3 x 5 min at RT) and then filters were excised from insert housings and mounted on slides with Molecular Probes ProLong Antifade (Invitrogen Canada Inc.) containing 5 μ g/mL DAPI. Mitotracker[®] staining was examined using a Nikon Eclipse Ti inverted microscope (Nikon Instruments Inc., Melville, NY, USA). Occludin and NKA immunolocalization was examined using a Reichert Polyvar microscope (Reichert Microscope Services, Depew, NY, USA) and an Olympus DP70 camera (Olympus Canada, Markham, ON, Canada). Immunohistochemical analysis of NKA in goldfish gill tissue was conducted according to procedures outlined in Chapter 2. Adobe Photoshop CS2 software was used for contrast and brightness adjustment of entire images (Adobe Systems Canada).

5.3.4 Transepithelial resistance (TER) and [³H]PEG-4000 flux measurements: TER was measured using chopstick electrodes (STX-2) connected to an EVOM epithelial

voltohmmeter (World Precision Instruments, Sarasota, FL, USA). All TER measurements are expressed as Ωcm^2 and background-corrected for TER measured across blank inserts bathed in appropriate solutions. Paracellular permeability across cultured epithelia was determined using the paracellular marker, [^3H] polyethylene glycol (molecular mass 4000 Da; PEG-4000; PerkinElmer, Woodbridge, ON, Canada) according to methods and calculations previously outlined by Wood et al. (1998). Briefly, [^3H]PEG-4000 flux from the basolateral to apical compartment was monitored at appropriate time intervals after the addition of 1 μCi of [^3H]PEG-4000 to basolateral culture medium. All flux measurements are expressed as a function of time and epithelial surface area.

5.3.5 Cloning of goldfish occludin cDNA: Total RNA was isolated from goldfish gill tissue using TRIzol[®] Reagent (Invitrogen Canada Inc.) according to manufacturer's instructions. Gill RNA was then treated with DNase I (Amplification Grade; Invitrogen Canada Inc.) and first-strand cDNA was synthesized using SuperScript[™] III Reverse Transcriptase and Oligo(dT)₁₂₋₁₈ primers (Invitrogen Canada Inc.). Based on highly conserved regions of zebrafish (NM 212832) and rainbow trout (NM 001190446) occludin coding sequences (as determined by a ClustalX multiple sequence alignment), degenerate primers were designed and used to amplify a partial goldfish occludin cDNA fragment by reverse transcriptase PCR (RT-PCR). The following reaction conditions were utilized: 1 cycle of denaturation (95°C, 4 min), 40 cycles of denaturation (95°C, 30 sec), annealing (53°C, 30 sec) and extension (72°C, 30 sec) respectively, final single extension cycle (72°C, 5 min) (0.2 μM dNTP, 2 μM forward and reverse primers, 1x Taq DNA polymerase buffer, 1.5 mM MgCl_2 and 1 IU *Taq* DNA polymerase) (Invitrogen

Canada Inc.). Gel electrophoresis (1% agarose) verified a PCR product at the predicted amplicon size. The putative occludin fragment was then excised, purified using a QIAquick Gel Extraction Kit (QIAGEN Inc., Mississauga, ON, Canada) and sequenced in the York University Core Molecular Biology and DNA Sequencing Facility (Department of Biology, York University, ON, Canada). A partial coding sequence (CDS) of goldfish occludin was confirmed using a Basic Local Alignment Search Tool (BLAST) search. To obtain the complete goldfish occludin CDS, both 5'- and 3'-rapid amplification of cDNA ends (RACE) PCR was subsequently performed using a SMART™ RACE cDNA Amplification Kit (Clontech Laboratories Inc., Mountain View, CA, USA) according to manufacturer's instructions. The GenBank accession number for goldfish occludin is HQ110086.

5.3.6 Quantitative real-time PCR analysis: Quantitative real-time PCR (qRT-PCR) was used to examine occludin mRNA distribution and abundance in discrete goldfish tissues, as well as occludin mRNA transcript abundance in cultured goldfish gill epithelia. For expression profile studies, total RNA was extracted from the following goldfish tissues: brain, eye, heart, gill, gastrointestinal (GI) tract, liver, gallbladder, spleen, swimbladder, kidney, skin, muscle, fat and blood. Because the goldfish GI tract is not separated into morphologically distinct regions, the total length of the GI tract was measured and then dissected into eight equal segments. These segments were numbered as GI 1 – GI 8 (anterior-most segment to posterior-most segment). RNA extraction and cDNA synthesis from all goldfish tissues and cultured gill epithelia was conducted as outlined above (see Section 5.3.5). Primers for goldfish occludin (forward: 5'

CAACAGCACAAACTACGACAAACC 3' and reverse: 5' CCACTTCAGCCAGACGCTTG 3', amplicon size ~ 356 bp) were designed based on the complete goldfish CDS. β -Actin was used as an internal control and β -actin primers (forward: 5' CTACGAGGGTTATGCTCTTC 3' and reverse: 5' ATTGAGTTGAAGGTGGTCTC 3', amplicon size ~ 351 bp) were designed based on GenBank accession number AB039726. qRT-PCR analysis of occludin and β -actin was conducted using SYBR[®] Green I Supermix (Bio-Rad Laboratories Canada Ltd., Mississauga, ON, Canada) and a Chromo4[™] Detection System (CFB-3240; Bio-Rad Laboratories Canada Ltd.) under the following conditions: 1 cycle denaturation (95°C, 4 min) followed by 40 cycles of denaturation (95°C, 30 sec), annealing (60°C for occludin or 51°C for β -actin, 30 sec) and extension (72°C, 30 sec) respectively. Samples were run in duplicate, and to ensure that a single PCR product was synthesized during reactions, a melting curve was carried out after each qRT-PCR run. For all qRT-PCR analyses, occludin mRNA abundance was normalized to β -actin abundance. For the occludin expression profile, occludin mRNA abundance in goldfish tissues was expressed relative to GI 1 which was assigned a value of 100. For epithelia exposed to asymmetrical culture conditions (12 and 24 h) as well as epithelia held under symmetrical control conditions at 24 h, occludin mRNA data are expressed relative to occludin abundance in symmetrical culture conditions at 12 h which was assigned a value of 100.

5.3.7 Western blotting: Cultured goldfish gill epithelia were processed in ice-cold lysis buffer (50mM Tris-HCl, pH 7.5, 150 mM NaCl, 1% sodium deoxycholate, 1% Triton-X-100, 0.1% SDS, 1 mM DTT, 1 mM EDTA, 1 mM PMSF) containing 1:200 protease

inhibitor cocktail (Sigma-Aldrich Canada Ltd.), by repeatedly passing through a 26G needle. Homogenates were then centrifuged (20 min at 20,000 x g, 4°C). Following centrifugation, the supernatants were collected and protein concentration was determined using the Bradford assay (Sigma-Aldrich Canada Ltd.). Western blot analysis of occludin and β -actin was conducted according to procedures outlined in Chapter 2, using 10 μ g of protein from each insert sampled, a 1:1,000 dilution of a rabbit polyclonal anti-occludin antibody (Zymed Laboratories, Inc.) and a 1:20,000 dilution of mouse monoclonal anti- β -actin antibody (Sigma-Aldrich Canada Ltd.). Occludin and β -actin abundance was quantified using a Molecular Imager Gel Doc XR+ System and Quantity One 1D analysis software (Bio-Rad Laboratories Canada Ltd.). Occludin protein abundance is expressed as a normalized value relative to β -actin abundance. Occludin protein abundance in epithelia exposed to FW/L15 conditions are expressed relative to occludin protein abundance in epithelia held under symmetrical control conditions which was assigned a value of 100.

5.3.8 Statistical analysis: All data are expressed as mean values \pm s.e.m. (n), where n represents the number of inserts, except in Fig. 5-4, where n represents the number of fish sampled. A one-way or two-way analysis of variance (ANOVA) followed by a Student-Newman-Keuls test was used to determine significant differences ($P < 0.05$) between groups. When appropriate, a Student's t -test was also used. All statistical analyses were conducted using Sigmastat Software (Systat Software Inc., San Jose, CA, USA).

5.4 Results

5.4.1 Characterization of primary cultured goldfish gill epithelia

5.4.1.1 *General epithelial morphology:* When enzymatically isolated gill cells were seeded into uncoated cell culture flasks, cell attachment was rare and those cells that did attach did not proliferate (i.e. detached within 2 – 3 days in culture). Pre-coating flasks with collagen enhanced cell attachment and survival (see Fig. 5-1A,B). Cell seeding densities of $0.24 - 0.28 \times 10^6$ cells/cm² yielded flasks that were ~ 50 – 70% confluent after 24 h (Fig. 5-1A). A further 24 h in culture resulted in flasks that were ~ 85 – 100% confluent (Fig. 5-1B). During culture in flasks, most cells exhibit an irregular and elongated morphology, however colonies of cells with a more rounded appearance were also observed. When harvested from collagen-coated flasks, gill cells readily attach to the surface of PET filters in culture inserts and achieve 100% confluence within 6 – 8 h. Approximately 36 - 42 h after seeding gill cells in inserts, preparations exhibit a typical epithelial morphology. More specifically, cultured cells take on a flattened polygonal morphology with well-defined intercellular junctions (see Fig. 5-1C,D). When viewed at higher magnification, the apical surfaces of cultured gill cells exhibit occasional microvilli and prominent microridges (Fig. 5-1E,F,H). These structures are characteristic of goldfish gill PVCs as seen *in vivo* (Fig. 5-1G). MRC apical openings observed *in vivo* by SEM were not observed in cultured gill epithelia *in vitro* (Fig. 5-1E,G).

TEM sections demonstrated that cultured goldfish epithelia were typically composed of 1 – 2 (occasionally 3) overlapping cell layers (e.g. Fig. 5-1H). Furthermore, epithelia exhibited TJs between cells on the apical surface cell layer, desmosomes near

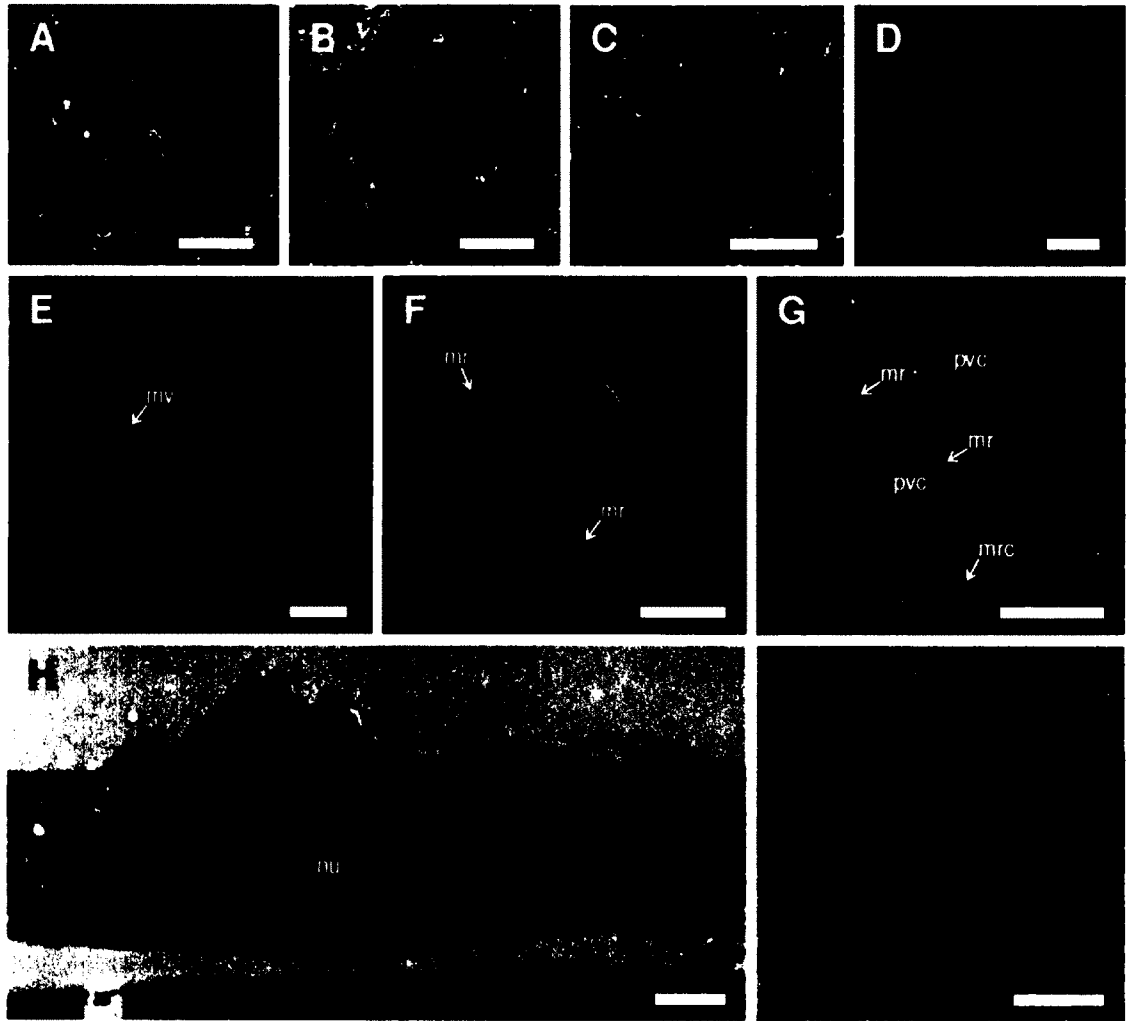


Figure 5-1: Phase contrast micrographs of cultured goldfish gill cells at (A) 24 h post-seeding in flasks, (B) 48 h post-seeding in flasks, and (C,D) 48 h post-seeding in culture inserts under symmetrical (L15/L15) conditions. Scanning electron microscope (SEM) images of the apical surfaces of (E,F) a cultured goldfish gill epithelium at 48 h post-seeding in inserts under L15/L15 conditions, and (G) a goldfish gill filament. (H, I) Transmission electron microscope (TEM) images of a cultured goldfish gill epithelium at 48 h post-seeding in culture inserts under L15/L15 conditions. mv, microvilli; mr, microridge; pvc, pavement cell; mrc, mitochondria-rich cell; ap, apical surface; tj, tight junction; nu, nucleus; pet, polyethylene terephthalate filter; ds, desmosome; rer, rough endoplasmic reticulum. Scale bars: (A,B,C) 100 μ m; (D) 20 μ m; (E,F,G) 10 μ m; (H) 1 μ m; (I) 500 nm.

the apical surface as well as between cell layers, few mitochondria and abundant rough endoplasmic reticulum (Fig. 5-1H,I).

5.4.1.2 Immunocytological analysis: Occludin immunostaining was observed at intercellular junctions along the borders of adjacent cultured gill cells (Fig. 5-2A). NKA immunostaining was absent in cultured gill preparations (Fig. 5-2B). Occludin immunostaining was absent in negative control preparations (i.e. primary antibody omitted) (Fig. 5-2C). As a positive control, robust NKA immunoreactivity could be observed in putative MRCs *in vivo* (Fig. 5-2D). Consistent with TEM images, live and fixed cultured goldfish gill epithelia pre-treated with Mitotracker[®] showed no appreciable mitochondrial staining (data not shown).

5.4.1.3 Transepithelial resistance (TER): Goldfish gill epithelia cultured under symmetrical (L15/L15) conditions exhibit a sigmoidal increase in TER over time (Fig. 5-3A). TER typically plateaus 36 - 42 h after seeding cells in inserts and this corresponds with the appearance of a more distinct epithelial-like morphology with well-defined intercellular junctions (see Section 5.4.1.1 above; Fig. 5-1C,D). The plateau in TER that cultured goldfish gill epithelia exhibit has proven to be quite consistent between fish. Based on 331 inserts generated from 41 goldfish, TER stabilizes at $1150 \pm 46 \Omega\text{cm}^2$ ($n = 41$) and these levels are maintained for at least 30 h (data not shown). Goldfish gill epithelia were also tolerant of asymmetrical (FW/L15) conditions. Abrupt apical FW exposure resulted in a significant increase in TER (to more than sevenfold pre-exposure values) within 0.5 h. TER then decreased sharply after 1 h (to ~ fourfold initial values) and remained stable for at least another 2 h (Fig. 5-3B). Upon restoration of symmetrical

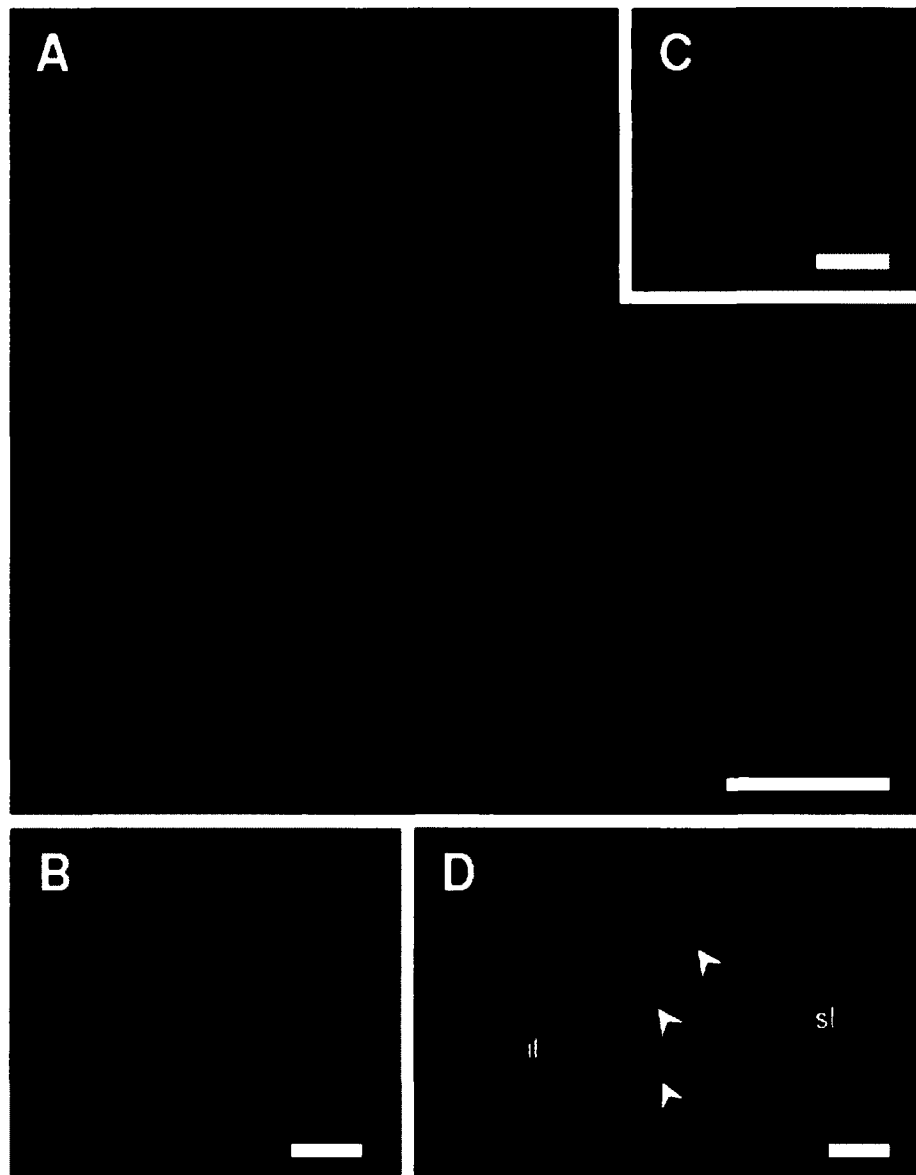


Figure 5-2: Immunolocalization of (A) occludin (red) and (B) $\text{Na}^+\text{-K}^+\text{-ATPase}$ (NKA, green) in a cultured goldfish gill epithelium at 48 h post-seeding in a culture insert under symmetrical (L15/L15) conditions. Note that no NKA immunostaining is observed in cultured goldfish gill epithelia. A negative control for occludin immunoreactivity (primary antibody omitted) is shown in (C). Putative mitochondria-rich cell localization (arrowhead) via NKA immunostaining in goldfish gill tissue is also shown in (D). il, interlamellar region of a primary gill filament; sl, secondary lamellae. Scale bars: 20 μm .

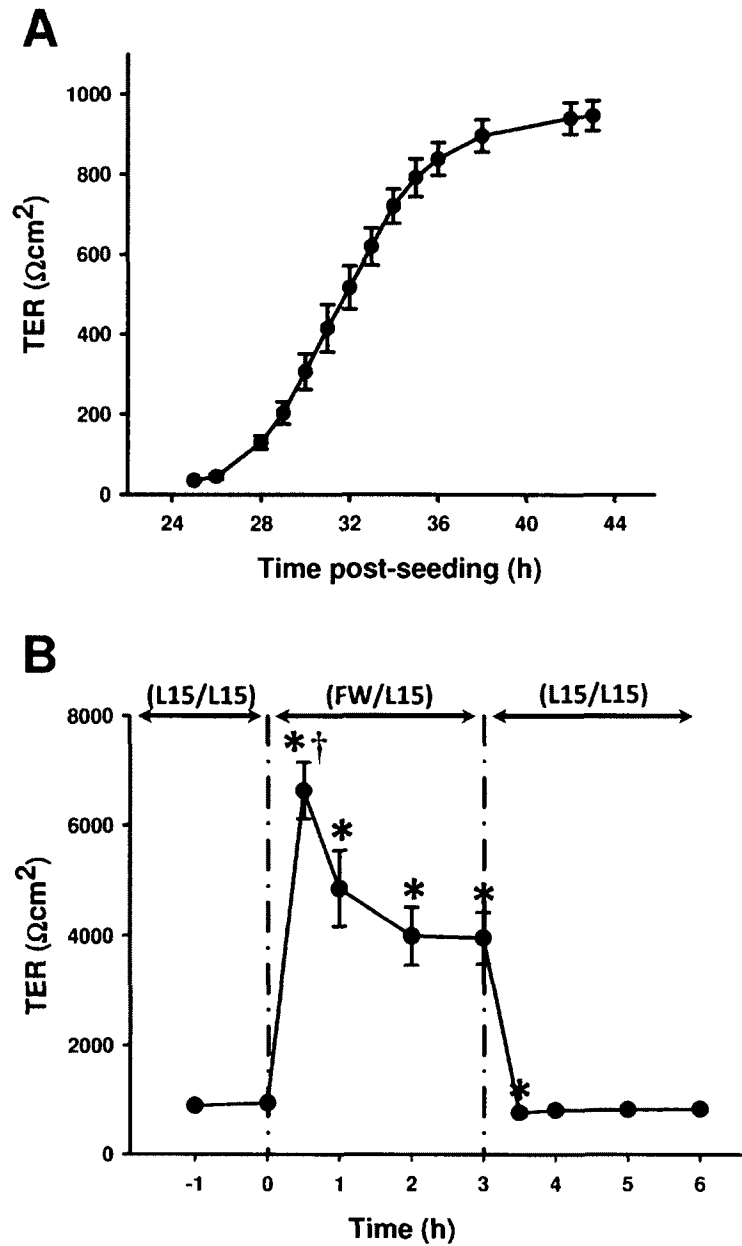


Figure 5-3: (A) Changes in transepithelial resistance (TER) of cultured goldfish gill epithelia post-seeding in culture inserts. Epithelia were cultured under symmetrical (L15/L15) conditions. (B) The effect of short-term (3-h) asymmetrical (FW/L15) conditions and subsequent recovery under L15/L15 on the TER of goldfish gill epithelia cultured in inserts. Data are expressed as mean values \pm s.e.m. ($n = 6$). * Significant difference ($P < 0.05$) from pre-FW exposure values. † Significant difference ($P < 0.05$) from all other FW exposure values.

conditions, TER significantly dropped below pre-exposure values, but then steadily (after 1 h) recovered to pre-exposure values where it remained stable for at least a further 2 h (Fig. 5-3B).

5.4.2 Cloning of goldfish occludin cDNA and occludin mRNA tissue expression profile:

Cloning and sequence analysis of the 1503-bp protein coding region for goldfish occludin revealed an open reading frame for a 500-amino acid protein with a molecular weight of ~ 56 kDa. Goldfish occludin exhibited ~ 89% amino acid sequence similarity (identical matches plus mismatches with similar amino acids) with zebrafish occludin (GenBank accession number NP_997997), ~ 75% similarity with rainbow trout occludin (NP_001177375) and 58 – 61% similarity with mammalian occludin (i.e. human [NP_002529], mouse [NP_032782], rat [NP_112619], dog [NP_001003195], pig [NP_001157119] and cow [NP_001075902]). Using qRT-PCR to measure transcript abundance, occludin mRNA was found to be widely expressed in goldfish tissues (Fig. 5-4). Transcript abundance was highest in the gill, followed by the gallbladder, kidney and skin. Transcript was absent from the heart, spleen, muscle and blood (Fig. 5-4).

5.4.3 Effects of 24 h exposure to asymmetrical culture conditions on cultured gill epithelia

5.4.3.1 TER and [³H]PEG-4000 flux: When exposed to asymmetrical culture conditions (i.e. FW apical/L15 basolateral) for a period of 24 h, TER initially exhibited a rapid and significant increase that was relatively stable for the first few hours of the exposure period (Fig. 5-5A). These were consistent with changes in TER previously observed

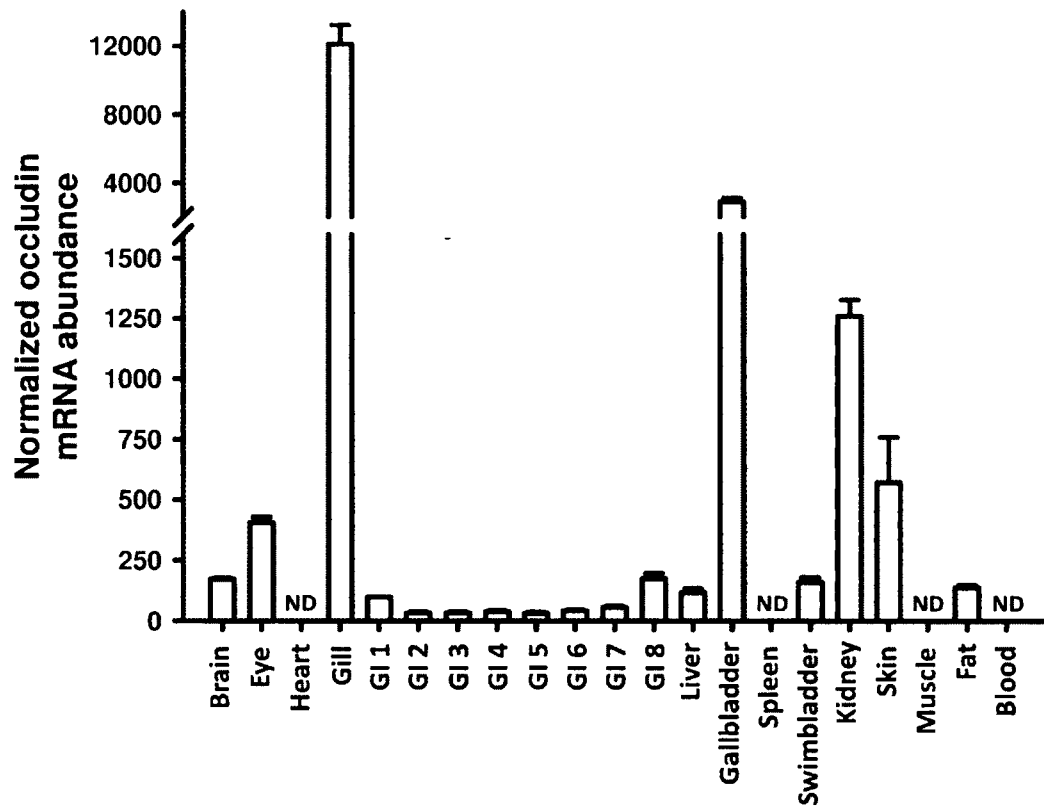


Figure 5-4: Occludin mRNA expression profile for discrete goldfish tissues as generated by qRT-PCR. Occludin mRNA abundance was normalized to β -actin abundance. Occludin mRNA abundance in each goldfish tissue was expressed relative to GI 1 which was assigned a value of 100. Data are expressed as mean values \pm s.e.m. ($n = 3-4$). ND = not detected.

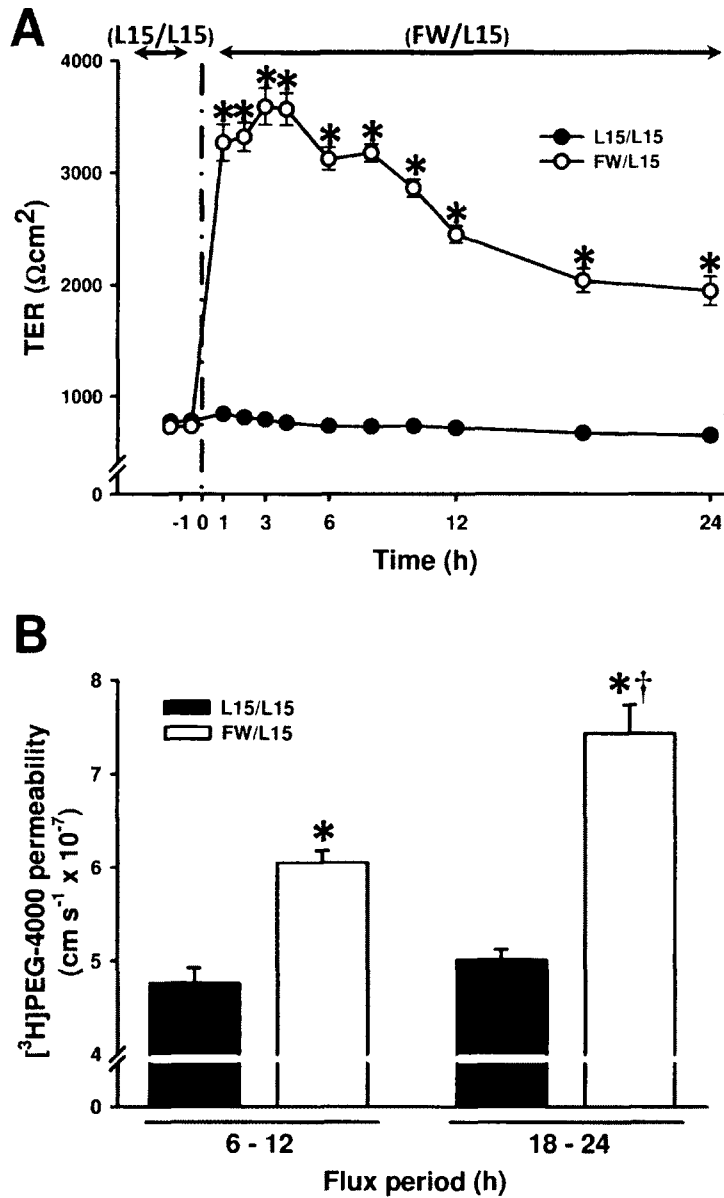


Figure 5-5: Effect of long-term (24-h) asymmetrical (FW/L15) conditions on (A) transepithelial resistance (TER) and (B) $[^3\text{H}]\text{PEG-4000}$ permeability across goldfish gill epithelia cultured in inserts. $[^3\text{H}]\text{PEG-4000}$ fluxes were conducted over 6 h periods between 6–12 h and 18–24 h post-FW exposure. Data are expressed as mean values \pm SEM ($n = 6-12$). * Significant difference ($P < 0.05$) between L15/L15 and FW/L15 groups at the same time point or within the same flux period. † Significant difference ($P < 0.05$) from the FW/L15 group within the 6 - 12 h flux period.

during short-term exposure to asymmetrical culture conditions (see Section 5.4.1.3 above). Following this early response, TER remained significantly elevated throughout the entire course of the 24-h asymmetrical experiment (Fig. 5-5A). However, although TER remained significantly elevated relative to L15/L15 preparations throughout the duration of the experiment, TER exhibited a gradual decline that was greater during the 3 – 12 h post-FW exposure period (~ 32% reduction) than during the 12 – 24 h post-FW exposure period (~ 14% decline) (Fig. 5-5A).

[³H]PEG-4000 permeability significantly elevated in response to asymmetrical culture conditions. [³H]PEG-4000 flux exhibited an ~ 27% and ~ 48% increase relative to control epithelia during the 6 – 12 h and 18 – 24 h flux periods respectively (Fig. 5-5B). Cultured epithelia were routinely examined by phase-contrast microscopy throughout the 24-h asymmetrical experiment and no signs of significant morphological change or epithelial deterioration were observed. Within a treatment group (i.e. L15/L15 or FW/L15), TER across epithelia 24 h following the start of the experiment was moderately but significantly lower than TER measurements recorded at 12 h (Fig. 5-6A).

5.4.3.2 Occludin mRNA and protein abundance: The introduction of asymmetrical (FW/L15) conditions had no significant effect on occludin mRNA abundance in cultured goldfish gill epithelia relative to control L15/L15 preparations (Fig. 5-6B). Transcript abundance, however, was significantly altered over time regardless of culture conditions. Samples (both symmetrical and asymmetrical) collected at the 24 h time point exhibited significantly lower levels of occludin mRNA when compared to samples collected at 12 h (Fig. 5-6B).

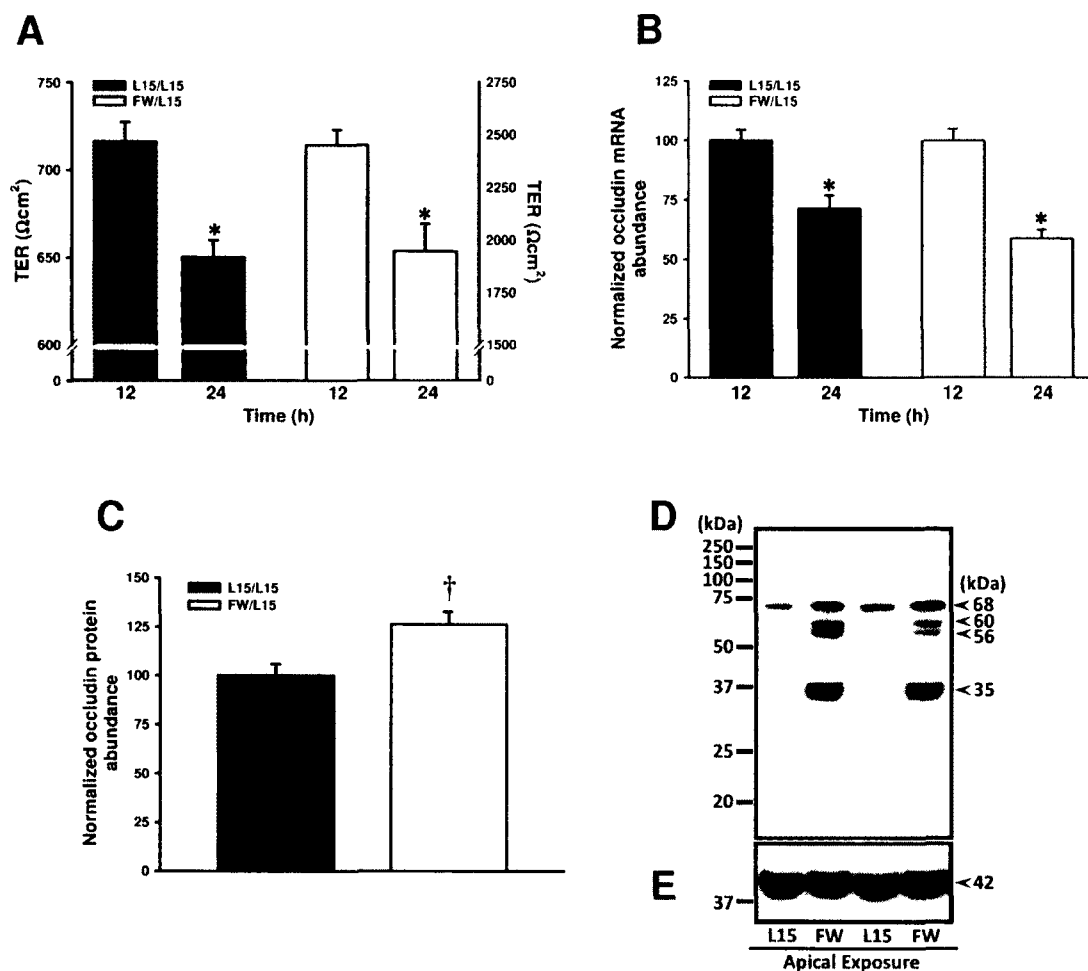


Figure 5-6: Effect of long-term asymmetrical (FW/L15) culture conditions on (A) TER, (B) occludin mRNA abundance and (C) occludin protein abundance in primary cultured goldfish gill epithelia. Representative western blots of (D) occludin and (E) β -actin from cultured goldfish gill epithelia exposed to L15/L15 or FW/L15 conditions are shown. Note that occludin-immunoreactive bands resolve at ~ 60, 56 and 35 kDa in the FW/L15 cultured epithelia in addition to the dominant ~ 68 kDa form expressed by L15/L15 cultured epithelia. Plate (C) illustrates the quantification of the 68 kDa form of occludin shown in (D). mRNA samples were collected at 12 h and 24 h, and protein samples were collected 24 h post-FW exposure. Occludin mRNA or protein abundance was normalized to β -actin mRNA or protein abundance respectively. All occludin mRNA data are expressed relative to occludin mRNA abundance in epithelia held under L15/L15 conditions at 12 h which was assigned a value of 100. Data are expressed as mean values \pm s.e.m. ($n = 6-8$). * Significant difference ($P < 0.05$) from the 12 h sampling point within the same treatment group (L15/L15 or FW/L15). † Significant difference ($P < 0.05$) from the L15/L15 group.

Neither asymmetrical conditions nor time significantly altered ($P > 0.05$) β -actin mRNA abundance. Conversely, protein abundance of the 68 kDa occludin form was marginally but significantly elevated by 24-h apical FW exposure relative to control L15/L15 preparations (Fig. 5-6C). By western blot analysis, both L15/L15 and FW/L15 cultured gill epithelia expressed the dominant 68 kDa form of occludin, however FW/L15 cultured epithelia also exhibited three additional occludin-immunoreactive bands which resolved at ~ 60, 56 and 35 kDa respectively (Fig. 5-6D). β -Actin protein resolved at ~ 42 kDa and its abundance was not significantly altered ($P > 0.05$) by apical FW exposure (Fig. 5-6E).

5.5 Discussion

5.5.1 General characterization of primary cultured goldfish gill epithelia: Cultured goldfish gill epithelia appear to be composed exclusively of PVCs. More specifically, electron microscopy demonstrated that cultured goldfish gill preparations comprise cells which exhibit morphological characteristics typical of PVCs. These cells are polygonal, squamous, and possess apical surface microridges identical to those observed in goldfish gill PVCs *in vivo* (Fig. 5-1E-H). The cells also possess few mitochondria and abundant rough endoplasmic reticulum. In addition to these morphological observations, immunocytochemistry results indicated that cultured goldfish gill epithelia did not possess any cells exhibiting robust NKA-immunoreactivity or Mitotracker[®] staining. Both NKA-immunoreactivity and staining with a mitochondrial dye such as Mitotracker[®] are reliable markers of MRC presence in fish gill epithelia (see Fig. 5-2D; Chapter 2; Mitrovic and Perry 2009). The observations made of goldfish epithelia in this study are consistent with the morphological characteristics of other cultured PVC epithelia generated from species such as the sea bass (Avella and Ehrenfeld, 1997), rainbow trout (Wood and Pärt, 1997) and tilapia (Kelly and Wood, 2002). It remains to be determined whether isolated goldfish gill cells can be used to generate double seeded insert (DSI) epithelia containing MRCs (see Fletcher et al., 2000). In this regard, preliminary attempts to generate single direct seeded inserts (SDSI; see Wood et al., 2003) using freshly isolated goldfish gills cells were not successful.

Approximately 24 h after seeding cells in inserts, and over a period of ~ 14 h (i.e. ~ 24 – 38 h post-seeding; see Fig. 5-3A), goldfish gill epithelia exhibit a sigmoidal

increase in TER. The development of a sigmoidal TER curve is characteristic of many epithelia in culture including PVC epithelial preparations from rainbow trout (Wood and Part, 1997; Kelly et al., 2000) and tilapia (Kelly and Wood, 2002). However, in trout and tilapia preparations, the development of a stable plateau in TER usually takes days rather than hours (see Wood and Part, 1997; Kelly et al., 2000; Kelly and Wood, 2002). This observed difference in time taken to develop a stable plateau in TER (i.e. ~ 36 - 42 h for goldfish versus 5 -7 days for rainbow trout and tilapia preparations) is consistent with the general observation that development rates exhibited by cultured goldfish gill preparations were much faster than those demonstrated by cultured rainbow trout and tilapia gill models. For example, cultured goldfish gill cells were ready to be harvested and seeded into inserts following 2 days of culture in flasks (Fig. 5-1A,B) versus 4 – 5 days flask culture for cultured rainbow trout and tilapia gill cells (Kelly et al., 2000; Kelly and Wood, 2002). However, goldfish preparations maintain a stable TER for less time after plateau (usually ~ 30 h; data not shown) than rainbow trout preparations (several days; Wood and Part, 1997; Kelly and Wood, 2001). Therefore, although the accelerated development of cultured goldfish gill epithelia can save a considerable amount of time when compared to other *in vitro* FW fish gill models, the optimal experimental time window for conducting analyses may be shortened. The differences observed in development of epithelia and duration of culture could be species-specific but may also be influenced by factors such as difference in culture incubation temperature (e.g. 18 – 20°C for trout and tilapia versus 27°C for goldfish). However, primary cultured gill epithelia generated from euryhaline puffer fish (*Tetraodon nigroviridis*) are also

incubated at 27°C and develop a stable TER following 5 - 7 days in culture (Bui and Kelly, unpublished observations). Therefore, despite temperature differences, cultured puffer fish gill epithelia develop in a manner similar to cultured rainbow trout and tilapia preparations. This strongly supports the idea that species-specific differences could play an important role in the physiological diversity of cultured gill epithelia.

Irrespective of time taken to develop, the sigmoidal TER curve can be attributed to the gradual formation of TJs between cells which limit the paracellular electrical conductance across an epithelium (Cerejido et al., 1981). In this regard, a positive linear relationship between [³H]PEG-4000 flux (a measurement of paracellular permeability and thus TJ 'tightness') and epithelial conductance (inverse of TER) across cultured rainbow trout preparations has previously been demonstrated by Wood et al. (1998). TER across cultured goldfish gill epithelia stabilizes at ~ 1150 Ωcm² and this value falls within the range of stable resistance measurements reported for other gill PVC epithelial preparations derived from fish held in FW such as rainbow trout (1000 - 5000 Ωcm², Kelly et al., 2000) and tilapia (1000 – 3000 Ωcm², Kelly and Wood, 2002). In addition, a value of ~ 1150 Ωcm² in the current study is also very similar to the TER across a PVC-rich opercular epithelium isolated from FW brook trout (i.e. ~ 1170 Ωcm²) as reported by Marshall (1985). It is also of interest to note that in cultured goldfish epithelia, an increase and plateau in TER occurs in conjunction with the appearance of well-defined intercellular junctions between cultured cells (Fig. 5-1C,D,H,I). This provides a convenient tool for visually monitoring the development of cultured goldfish gill epithelia (i.e. a morphological indicator of TER development and electrophysiological

integrity) and also provides further support for a correlation between TJ assembly and TER development as discussed previously.

5.5.2 Goldfish occludin mRNA distribution and protein immunolocalization: Occludin is a transmembrane TJ protein that contributes significantly to TJ barrier function and thus the permeability of the paracellular pathway across an epithelium (for review, see Feldman et al., 2005). Occludin mRNA is widely expressed in goldfish tissues and is particularly abundant in the gill as well as other tissues involved in the maintenance of hydromineral balance (i.e. kidney and skin; see Fig. 5-4). Broad occludin distribution and high levels of mRNA in gill tissue have also recently been described in rainbow trout (see Chapter 4), and the widespread presence of occludin has additionally been demonstrated in other non-aquatic vertebrate species (Saitou et al., 1997; Feldman et al., 2005). With regard to gill tissue, a recent study has reported that occludin immunolocalizes to areas of cell-to-cell contact (presumably PVCs-PVCs and PVCs-MRCs) in the gill epithelium of the goldfish (see Chapter 2). Therefore, observations in the current study that reveal occludin immunostaining restricted quite distinctly to intercellular junctions along the borders of adjacent polygonal PVCs in a cultured goldfish gill model confirm that occludin does indeed localize between goldfish gill PVCs at least. This pattern of localization *in vitro* is consistent with observations of occludin immunostaining in various vertebrate epithelial cell lines (e.g. McCarthy et al., 1996; Wong and Gumbiner, 1997; Finamore et al., 2008; Benedicto et al., 2009; Vermeer et al., 2009). Furthermore, these observations are also consistent with a recent report on occludin immunolocalization between PVCs in a cultured trout gill epithelium (see Chapter 4).

However, a particular advantage of the cultured goldfish gill model pertains to our observations in Chapter 2, that in addition to localizing to the gill epithelium, occludin also localizes to the goldfish gill capillary endothelium. In the currently described culture preparation, there is no capillary endothelium. Therefore, alterations in molecular factors that may play a role in the regulation of gill permeability, such as occludin, can be examined in the absence of any contribution from the vasculature.

In contrast to the abundance of occludin mRNA in osmoregulatory tissues such as the gill and kidney, occludin mRNA abundance was relatively low along the GI tract of goldfish (see Fig. 5-4). However, TER measurements across the goldfish intestine suggest that this is not a tight epithelium (i.e. $\sim 24 \Omega\text{cm}^2$; Siegenbeek van Heukelom et al., 1982). Therefore, low levels of occludin transcript may be expected.

5.5.3 Effects of asymmetrical conditions

5.5.3.1 Measurements of epithelial permeability: Conditions that occur *in vivo* were mimicked *in vitro* by introducing FW to the apical side of the cultured goldfish gill epithelium. Exposure to apical FW resulted in a sharp increase in TER (Figs. 5-3B, 5-5A). This type of response to apical FW exposure has previously been noted in other cultured gill epithelia (Wood and Pärt, 1997; Kelly and Wood, 2002), as well as opercular epithelia isolated from a FW fish (Marshall, 1985). In cultured trout gill epithelia, elevated TER in response to apical FW exposure appears to predominantly reflect decreased transcellular permeability since it occurs in conjunction with a paradoxical increase in paracellular permeability (i.e. increased [^3H]PEG-4000 flux; see Wood et al., 1998). This is not the case in cultured tilapia gill epithelia which exhibit both

an increase in TER and decrease in [³H]PEG-4000 upon apical FW exposure (Kelly and Wood, 2002). Consistent with the response of cultured trout gill epithelia, cultured goldfish gill preparations exhibit an increase in [³H]PEG-4000 flux when FW is present on the apical side of the epithelium (Fig. 5-5B). Therefore it seems likely that elevated TER in goldfish gill epithelia also primarily reflects changes in transcellular permeability since the paracellular pathway becomes “leakier” to [³H]PEG-4000 movement.

TER across goldfish gill preparations exhibited a gradual decline during prolonged apical FW exposure and this has also been observed in cultured rainbow trout and tilapia gill epithelia (Fig. 5-5A; Kelly and Wood, 2001, 2002). Taking into account that [³H]PEG-4000 flux elevates even further during long-term (24-h) asymmetrical culture (Fig. 5-5B), it is possible that the increasingly “leaky” paracellular barrier properties of the preparation may contribute to the gradual decline in TER, although to what extent remains unclear.

5.5.3.2 Occludin mRNA and protein abundance: Recent studies have reported that occludin abundance alters in the gill tissue of goldfish under conditions where hydromineral status is challenged (see Chapters 2 and 3). However, alterations in occludin abundance have yet to be reported in conjunction with measured changes in epithelial permeability in goldfish. Therefore to gain insight into the potential contribution of occludin to alterations in cultured goldfish gill permeability characteristics, occludin abundance was examined following the introduction of asymmetrical culture conditions (see Fig. 5-6). Exposure to asymmetrical culture conditions for 12 or 24 h had no significant effect on occludin mRNA abundance relative

to control preparations held under symmetrical conditions (Fig. 5-6B). This occurred despite a significant increase in paracellular permeability (Fig. 5-5B). These observations are consistent with unaltered occludin mRNA levels in cultured rainbow trout gill epithelia exposed to asymmetrical culture conditions which also exhibited an increase in paracellular permeability (see Chapter 4). Of interest, however, was a significant decline in occludin mRNA abundance in both symmetrical and asymmetrical epithelia 24 h following the start of the experiment (see Fig. 5-6B). This data corresponds with reductions in TER between the 12 and 24 h time-points (Fig. 5-6A), and in the case of epithelia held under asymmetrical conditions, a reduction in occludin mRNA abundance also corresponds with an increase in paracellular permeability (see Figs. 5-5B, 5-6B). Although there is no significant difference in [³H]PEG-4000 flux between symmetrical epithelia at the 6 – 12 h versus 18 – 24 h time points, it should be remembered that mRNA data is generated from tissue collected at the end of the flux period (i.e. at 12 h or 24 h) and in this particular case, transcript abundance may not represent the entire 6 h flux period. Therefore in cultured goldfish epithelia, occludin mRNA does not decline in association with an apical FW exposure-mediated increase in paracellular permeability, however over time in culture, occludin mRNA does change in a manner that reflects changes in permeability. This temporal change most likely reflects the general decline in TER that can be observed in cultured epithelial preparations as the culture time progresses after TER plateau.

Despite no observable difference in transcript abundance upon exposure to asymmetrical culture conditions, western blot analysis was used to examine if any

alterations in protein abundance could be detected at 24 h. A slight but significant increase in occludin protein abundance was observed (i.e. 100 versus 120; Fig. 5-6C) despite an absence of change at the transcript level. The physiological significance of this modest change is not clear and since it is not coupled with changes in mRNA, it could reflect differences in protein degradation rates. However, of far more interest were the changes observed in occludin-immunoreactive band position following electrophoresis that was evident under asymmetrical conditions. More specifically, under symmetrical culture conditions, occludin resolved as a 68 kDa band that was identical to the occludin-immunoreactive band found in the goldfish gill *in vivo* (see Chapter 2). However under asymmetrical culture conditions, goldfish gill preparations were found to possess both the dominant 68 kDa (high molecular weight; HMW) form of occludin as well as three additional low molecular weight (LMW) occludin-immunoreactive bands at ~ 60, 56 and 35 kDa respectively (Fig. 5-6D). Since apical FW exposure did not significantly alter occludin mRNA abundance in cultured goldfish gill epithelia (Fig. 5-6B), it is likely that the observed 60 and 56 kDa LMW immunoreactive bands reflect post-translational modifications of existing occludin protein. In this regard, multiple differentially phosphorylated forms of occludin, ranging from ~ 50 – 82 kDa have previously been detected by western blot in a variety of vertebrate epithelia, which upon treatment with phosphatases converge to LMW forms, thereby demonstrating that HMW forms of occludin are in fact hyperphosphorylated LMW forms (Sakakibara et al., 1997; Wong, 1997; Feldman et al., 2005; Zeng et al., 2004). Furthermore, a growing body of research seems to indicate that occludin phosphorylation status may regulate TJ complex assembly

and disassembly (reviewed by Rao, 2009), whereby hyperphosphorylated HMW forms of occludin are recruited into TJ complexes to “tighten” TJs, while dephosphorylation of occludin disrupts TJs by relocalizing resultant LMW forms out of the complex (Wong, 1997). This general trend was clearly demonstrated in a human cervical epithelial cell line where estrogen-mediated reductions in TER closely correlated with a decrease in HMW occludin and simultaneous increase in LMW occludin in a time- and dose-dependent manner, and in the absence of a change in occludin mRNA abundance (Zeng et al., 2004). Therefore the additional 60 and 56 kDa LMW forms of occludin and observed increase in [³H]PEG-4000 flux during the asymmetrical culture of goldfish gill epithelia (Figs. 5-5B, 5-6D) may involve a disruption in TJ integrity by occludin dephosphorylation. The significance of the 35 kDa LMW form of occludin (Fig. 5-6D) with respect to TJ barrier function is currently unclear, as its appearance cannot be attributed to dephosphorylation. But it should be noted that similar occludin-immunoreactive bands (i.e. 30 - 35 kDa) have previously been reported in other epithelia (e.g. Wu et al., 2000; Minagar et al., 2003) and likely reflect protein degradation or some other uncharacterized post-translational modification.

5.5.4 Conclusion: To conclude, methodology for the primary culture of a goldfish gill epithelium composed exclusively of PVCs is described. Epithelia generate an appreciable TER under symmetrical culture conditions and tolerate exposure to FW. The physiological response of the cultured goldfish gill epithelium to asymmetrical culture conditions was qualitatively similar to responses previously reported for rainbow trout PVC cultures (Wood and Pärt, 1997), and in this regard, no differences based on

stenohalinity versus euryhalinity were obvious. In future studies, it will be interesting to examine if stenohaline versus euryhaline distinctions will become apparent when osmoregulatory hormones are introduced to cultured goldfish gill epithelial preparations. For example, it has recently been reported that occludin mRNA and protein abundance increase in response to cortisol treatment in cultured gill epithelia from a euryhaline fish (i.e. rainbow trout, see Chapter 4). Whether epithelia derived from a stenohaline fish, such as the goldfish, respond in a similar manner has yet to be determined. In addition, it will also be of interest to examine other proteins involved in the regulation of permeability in vertebrate epithelia such as the claudin family or cortical proteins such as ZO-1. This provides momentum for further study.

5.6 References

Avella M, Ehrenfeld, J. 1997. Fish gill respiratory cells in culture: a new model for Cl⁻ secreting epithelia. *J Membr Biol* 156:87-97.

Benedicto I, Molina-Jiménez F, Bartosch B, Cosset FL, Lavillette D, Prieto J, Moreno-Otero R, Valenzuela-Fernández A, Aldabe R, López-Cabrera M, Majano PL. 2009. The tight junction-associated protein occludin is required for a postbinding step in hepatitis C virus entry and infection. *J Virol* 83:8012-8020.

Bui P, Bagherie-Lachidan M, Kelly SP. 2010. Cortisol differentially alters claudin isoforms in cultured puffer fish gill epithelia. *Mol Cell Endocrinol* 317:120-126.

Cerejido M, Meza I, Martínez-Palomo A. 1981. Occluding junctions in cultured epithelial monolayers. *Am J Physiol* 240:C96-C102.

Evans DH, Piermarini PM, Choe KP. 2005. The multifunctional fish gill: dominant site of gas exchange, osmoregulation, acid-base regulation, and excretion of nitrogenous waste. *Physiol Rev* 85:97-177.

Feldman GJ, Mullin JM, Ryan MP. 2005. Occludin: structure, function and regulation. *Adv Drug Deliv Rev* 57:883-917.

Finamore A, Massimi M, Conti Devirgiliis L, Mengheri E. 2008. Zinc deficiency induces membrane barrier damage and increases neutrophil transmigration in Caco-2 cells. *J Nutr* 138:1664-1670.

Fletcher M, Kelly SP, Pärt P, O'Donnell MJ, Wood CM. 2000. Transport properties of cultured branchial epithelia from freshwater rainbow trout: a novel preparation with mitochondria-rich cells. *J Exp Biol* 203:1523-1537.

Kelly SP, Fletcher M, Pärt P, Wood CM. 2000. Procedures for the preparation and culture of 'reconstructed' rainbow trout branchial epithelia. *Methods Cell Sci* 22:153-163.

Kelly SP, Wood CM. 2001. Effect of cortisol on the physiology of cultured pavement cell epithelia from freshwater trout gills. *Am J Physiol Integrative Comp Physiol* 281:R811-R820.

Kelly SP, Wood CM. 2002. Cultured gill epithelia from freshwater tilapia (*Oreochromis niloticus*): effect of cortisol and homologous serum supplements from stressed and unstressed fish. *J Membr Biol* 190:29-42.

Marshall WS. 1985. Paracellular ion transport in trout opercular epithelium models osmoregulatory effects of acid precipitation. *Can J Zool* 63:1816-1822.

McCarthy KM, Skare IB, Stankewich MC, Furuse M, Tsukita S, Rogers RA, Lynch RD, Schneeberger EE. 1996. Occludin is a functional component of the tight junction. *J Cell Sci* 109:2287-2298.

Minagar A, Ostanin D, Long AC, Jennings M, Kelley RE, Sasaki M, Alexander JS. 2003. Serum from patients with multiple sclerosis downregulates occludin and VE-cadherin expression in cultured endothelial cells. *Mult Scler* 9:235-238.

Mitrovic D, Perry SF. 2009. The effects of thermally induced gill remodeling on ionocyte distribution and branchial chloride fluxes in goldfish (*Carassius auratus*). *J Exp Biol* 212:843-852.

Rao R. 2009. Occludin phosphorylation in regulation of epithelial tight junctions. *Ann N Y Acad Sci* 1165:62-68.

Saitou M, Ando-Akatsuka Y, Itoh M, Furuse M, Inazawa J, Fujimoto K, Tsukita S. 1997. Mammalian occludin in epithelial cells: its expression and subcellular distribution. *Eur J Cell Biol* 73:222-231.

Sakakibara A, Furuse M, Saitou M, Ando-Akatsuka Y, Tsukita S. 1997. Possible involvement of phosphorylation of occludin in tight junction formation. *J Cell Biol* 137:1393-1401.

Siegenbeek van Heukelom J, van den Ham MD, Dekker K. 1982. The modulation by glucose transport of the electrical responses to hypertonic solutions of the goldfish intestinal epithelium. *Pflügers Arch* 395:65-70.

Vermeer PD, Denker J, Estin M, Moninger TO, Keshavjee S, Karp P, Kline JN, Zabner J. 2009. MMP6 modulates tight junction integrity and cell viability in human airway epithelia. *Am J Physiol Lung Cell Mol Physiol* 296:L751-L762.

Wong V. 1997. Phosphorylation of occludin correlates with occludin localization and function at the tight junction. *Am J Physiol Cell Physiol* 273:C1859-1867.

Wong V, Gumbiner BM. 1997. A synthetic peptide corresponding to the extracellular domain of occludin perturbs the tight junction permeability barrier. *J Cell Biol* 136:399-409.

Wood CM, Pärt P. 1997. Cultured branchial epithelia from freshwater fish gills. *J Exp Biol* 200:1047-1059.

Wood CM, Gilmour KM, Pärt P. 1998. Passive and active transport properties of a gill model, the cultured branchial epithelium of the freshwater rainbow trout (*Oncorhynchus mykiss*). *Comp Biochem Physiol A Mol Integr Physiol* 119:87-96.

Wood CM, Kelly SP, Zhou B, Fletcher M, O'Donnell M, Eletti B, Pärt P. 2002. Cultured gill epithelia as models for the freshwater fish gill. *Biochim Biophys Acta* 1566:72-83.

Wood CM, Eletti B, Pärt P. 2003. New methods for the primary culture of gill epithelia from freshwater rainbow trout. *Fish Physiol Biochem* 26: 329-344.

Wu Z, Nybom P, Magnusson KE. 2000. Distinct effects of *Vibrio cholera* haemagglutinin/protease on the structure and localization of the tight junction-associated proteins occludin and ZO-1. *Cell Microbiol* 2:11-17.

Zeng R, Li X, Gorodeski GI. 2004. Estrogen abrogates transcervical tight junctional resistance by acceleration of occludin modulation. *J Clin Endocrinol Metab* 89:5145-5155.

CHAPTER 6:

EFFECT OF CORTISOL ON PERMEABILITY AND TIGHT JUNCTION PROTEIN TRANSCRIPT ABUNDANCE IN PRIMARY CULTURED GILL EPITHELIA FROM STENOHALINE GOLDFISH AND EURYHALINE TROUT

Helen Chasiotis and Scott P. Kelly

Department of Biology, York University, Toronto, Ontario, Canada M3J 1P3

This chapter has been published and reproduced with permission:

Chasiotis H, Kelly SP. 2011. Effect of cortisol on permeability and tight junction protein transcript abundance in primary cultured gill epithelia from stenohaline goldfish and euryhaline trout. *Gen Comp Endocrinol* 172:494-504.

6.1 Abstract

Primary cultured gill epithelia from goldfish and rainbow trout were used to investigate a role for cortisol in the regulation of paracellular permeability and tight junction (TJ) protein transcript abundance in representative stenohaline versus euryhaline freshwater (FW) fish gills. Glucocorticoid and mineralocorticoid receptors are expressed in cultured goldfish gill preparations and cortisol treatment (100, 500 and 1000 ng/mL) dose-dependently elevated transepithelial resistance (TER) and reduced paracellular [³H]PEG-4000 flux across cultured goldfish gill epithelia. Despite these dose-dependent “tightening” effects of cortisol, the response of goldfish TJ protein transcripts (i.e. occludin, claudin b, c, d, e, h, 7, 8d and 12, and ZO-1) were surprisingly small, with only claudin c and h, and ZO-1 transcript levels significantly decreasing at a dose of 1000 ng/mL. Extending the duration of cortisol exposure from 24 h to 48 or 96 h (at 500 ng/mL) did little to alter this phenomenon. By comparison, exposing primary cultured trout gill epithelia (i.e. a euryhaline fish gill model) to 500 ng/mL cortisol resulted in a qualitatively similar, but quantitatively stronger epithelial “tightening” response. Furthermore, transcript abundance of orthologous trout TJ proteins (i.e. occludin, and claudin 30, 28b, 3a, 7, 8d and 12) significantly elevated as would be expected in a “tighter” epithelium. Taken together, data suggest a conservative role for cortisol in the endocrine regulation of paracellular permeability across the goldfish gill that may relate to stenohalinity.

6.2. Introduction

Cortisol is the main corticosteroid in fishes, functioning as both a glucocorticoid and mineralocorticoid hormone (reviewed by Mommsen et al., 1999). Although cortisol is involved in the stress response, growth and reproduction, this remarkably versatile hormone also has a well-established role in the endocrine control of osmoregulation (Mommsen et al., 1999; McCormick, 2001). In this regard, cortisol appears to possess a dual function, as it has long been associated with salt secretion across the gills of fishes under hyper-osmotic conditions (i.e. seawater, SW) and has more recently been linked to ion uptake across the gill epithelium in a hypo-osmotic setting (i.e. freshwater, FW) (McCormick, 2001; Evans et al., 2005). These observations have been generated largely by studies that have focused on the role of cortisol in altering elements of the transcellular transport pathway in gill tissue (Evans et al., 2005). However, there is also evidence to suggest that cortisol may play an important role in regulating the physiological properties of the paracellular pathway in gill epithelia (see Chapter 4; Kelly and Wood, 2001, 2002) and that tight junction (TJ) proteins may be integrally involved in this endocrine mediated event (see Chapter 4; Tipsmark et al., 2009; Bui et al., 2010).

TJs comprise transmembrane and cytoplasmic protein networks encircling the apical-most domain of vertebrate epithelial cells and form a semi-permeable seal that limits the movement of water and solutes along the paracellular pathway. While transmembrane TJ proteins, such as occludin and claudins, form the physical paracellular barrier that selectively restricts the passage of ions and solutes between epithelial cells, the cytoplasmic adaptor or “scaffolding” TJ proteins, such as ZO-1, tether occludin and

claudins to actin filaments within the cytoskeleton. This link between the “sealing” transmembrane TJ proteins and the actin cytoskeleton allows signals from the external environment to be transmitted to the inside of the cell in order to influence transcriptional pathways that regulate TJ permeability and thus the “tightness” or “leakiness” of the epithelium (reviewed by González-Mariscal et al., 2003).

Corticosteroids have a well documented ability to alter the permeability characteristics of cultured vertebrate epithelia and endothelia (e.g. Zettl et al., 1992; Stelwagen et al., 1999; Förster et al., 2008), including the gill epithelia of euryhaline fishes such as the rainbow trout (Kelly and Wood, 2001) and tilapia (Kelly and Wood, 2002). These latter observations are in line with a growing body of evidence that suggests an important role for TJ proteins in the regulation and maintenance of hydromineral balance in fishes, particularly during conditions of altered environmental salinity. In this regard, significant changes in occludin and claudin transcript and/or protein abundance in the teleost gill have been demonstrated following acclimation to ion-poor water (see Chapter 3; Duffy et al., 2011), SW (Tipsmark et al., 2008; Bagherie-Lachidan et al., 2008, 2009; Duffy et al., 2011) as well as hypersaline SW (Bagherie-Lachidan et al., 2008). However, the majority of the aforementioned studies and all *in vitro* studies that have examined the effects of cortisol on gill permeability have been conducted using either euryhaline fishes or gill epithelial models derived from euryhaline fishes. To the best of our knowledge, no studies have examined the effects of cortisol on the permeability characteristics and TJ components of a stenohaline FW fish gill, or compared these with a euryhaline fish gill.

Therefore, the first objective of the present study was to utilize a recently developed cultured gill epithelium derived from the goldfish (see Chapter 5) to investigate a role for cortisol in the endocrine regulation of gill permeability in a representative stenohaline FW fish. A second objective was to compare results obtained in the goldfish gill model to those observed in a cultured euryhaline fish gill epithelium derived from rainbow trout (Kelly and Wood, 2001). Since corticosteroid-induced alterations in the permeability characteristics of vertebrate epithelia have been linked to alterations in the transcriptional and post-translational abundance of TJ proteins (e.g. see Chapter 4; Stelwagen et al., 1999; Felinski et al., 2008; Förster et al., 2008), a third objective was to identify and examine the transcript abundance of select TJ proteins in goldfish and rainbow trout gill preparations that are associated with changes in epithelial permeability in other vertebrates. Where possible, these TJ components were selected on the basis that they have already been associated with changes in the hydromineral status of fishes, such as occludin (see Chapters 2, 3 and 4), claudin h (which is a claudin 3a ortholog; see (Bagherie-Lachidan et al., 2008; Bui et al., 2010; Duffy et al., 2011), claudin 8d (see Bagherie-Lachidan et al., 2009; Bui et al., 2010; Duffy et al., 2011), and claudin b and e (orthologs of claudin 30 and 28b respectively; see Tipsmark et al., 2008, 2009). It is our view that in order to gain broader insight into the various mechanisms that regulate gill permeability in fishes, it is important to consider the physiology and molecular components of a stenohaline model in addition to the traditional euryhaline archetype.

6.3. Materials and Methods

6.3.1 *Animals*: Goldfish (*Carassius auratus*, 18 - 30 g) and rainbow trout (*Oncorhynchus mykiss*, ~ 125 g) were obtained from local suppliers (Aleongs International, Mississauga, ON, Canada; Humber Springs Trout Club and Hatchery, Orangeville, ON, Canada) and held in either 200-L (goldfish) or 600-L (trout) opaque polyethylene tanks. Tanks were supplied with flow-through dechlorinated FW (approximate composition in mM: [Na⁺] 0.59, [Cl⁻] 0.92, [Ca²⁺] 0.76, [K⁺] 0.43, pH 7.35) at 25 ± 1°C for goldfish and 10 ± 2°C for rainbow trout. All fish were held under the above described conditions for at least 3 weeks prior to use and fed *ad libitum* once daily with commercial pellets (Martin Profishent, Elmira, ON, Canada).

6.3.2 *Preparation of cultured gill epithelia*: Procedures for goldfish gill cell isolation and the culture of goldfish gill epithelia (composed of pavement cells only) were conducted according to previously described methods (see Chapter 5). Methods for rainbow trout gill cell isolation and the preparation of rainbow trout gill epithelia (composed of pavement cells only) were conducted according to procedures originally developed by Wood and Pärt (1997) and described in detail by Kelly et al. (2000). In brief, isolated goldfish or rainbow trout gill cells were initially cultured in flasks with Leibovitz's L-15 culture medium supplemented with 2 mM L-glutamine (L15) and 6% fetal bovine serum (FBS). At confluence (~ 2 days for goldfish; ~ 4 - 5 days for rainbow trout), cells were harvested from flasks by trypsination and seeded into cell culture inserts (polyethylene terephthalate filters, 0.9 cm² growth area, 0.4 µm pore size, 1.6 x 10⁶ pore/cm² pore density; BD Falcon™, BD Biosciences, Mississauga, ON, Canada). Epithelia were

allowed to develop under symmetrical culture conditions (i.e. with FBS-supplemented L15 culture medium bathing both apical and basolateral surfaces of the epithelial preparations) and were maintained in an air atmosphere at either 27°C or 18°C for cultured goldfish and rainbow trout gill epithelia respectively. All experimental procedures conformed to the guidelines of the Canadian Council on Animal Care and were approved by the York University Animal Care Committee.

6.3.3 Transepithelial resistance (TER) and [³H]PEG-4000 flux measurements:

Measurements of TER were conducted using chopstick electrodes (STX-2) connected to a custom-modified EVOM epithelial voltohmmeter (World Precision Instruments, Sarasota, FL, USA). All TER measurements are expressed as $k\Omega\text{cm}^2$ and background-corrected for TER measured across “vacant” culture inserts containing appropriate media. Paracellular permeability across cultured epithelia was determined using the paracellular marker, [³H] polyethylene glycol (molecular mass 4000 Da; PEG-4000; PerkinElmer, Woodbridge, ON, Canada) according to previously described methods and calculations (Wood et al., 1998). Briefly, the appearance of [³H]PEG-4000 in the apical compartment was monitored as a function of time and epithelial surface area after the addition of 1 μCi of [³H]PEG-4000 to basolateral culture media.

6.3.4 Cortisol treatment:

Single-use aliquots of a stock cortisol solution were prepared by dissolving cortisol (hydrocortisone 21-hemisuccinate sodium salt; Sigma-Aldrich Canada Ltd., Oakville, ON, Canada) in sterile phosphate-buffered saline (PBS; pH 7.7). Aliquots were stored at -30°C until use. Cortisol treatment of cultured goldfish and rainbow trout gill epithelia commenced at ~ 24 h after seeding cells in culture inserts when TER

measurements were $\sim 100 - 200 \Omega\text{cm}^2$ above background levels (see Section 6.3.3). Inserts were randomly assigned to either a control group or a cortisol-treated group. In the cortisol-treated group, basolateral culture media were supplemented with an appropriate amount of thawed stock cortisol in order to achieve the desired concentration of hormone. Control media contained no cortisol supplement.

Series 1. To investigate the dose-dependent effects of cortisol on cultured goldfish gill epithelia, basolateral media were supplemented with three concentrations of cortisol (100, 500 and 1000 ng/mL), the lower two of which are within the physiological range for goldfish (see Pottinger, 2010). Once control and hormone-treated preparations developed a stable plateau in TER (~ 21 h after the addition of cortisol), [^3H]PEG-4000 permeability was measured over a 3 h flux period and then epithelia were collected for RNA extraction (see Section 6.3.5). Therefore, in these experiments, epithelia were treated with cortisol for a total of 24 h.

Series 2. To examine the time-course effects of cortisol on cultured goldfish gill epithelia, basolateral media were supplemented with 500 ng/mL cortisol, and control and cortisol-treated preparations were collected for RNA extraction at 48 h and 96 h after the addition of cortisol. To confirm that cortisol was having the desired effect, the TER across epithelia was monitored periodically throughout the incubation period. A single dose of 500 ng/ml cortisol was used in this series based on physiological relevance and observations made in *series 1*. Control and cortisol-supplemented media were renewed once at 48 h for epithelia collected at 96 h.

Series 3. In a side-by-side comparison of the effects of cortisol on cultured goldfish and rainbow trout gill epithelia respectively, basolateral media of goldfish and rainbow trout preparations were supplemented with 500 ng/mL cortisol. This cortisol concentration was selected based on observations made in *series 1* and *series 2*, the results of previous *in vitro* studies conducted in cultured rainbow trout gill epithelia (see Chapter 4; Kelly and Wood, 2001), and the physiological relevance of this cortisol dose as it pertains to both goldfish and rainbow trout (Pottinger, 2010). When control and cortisol-treated preparations exhibited a plateau in TER, [³H]PEG-4000 permeability was determined, following which epithelia were collected for RNA extraction. The period of cortisol exposure was 24 h for goldfish gill epithelia and ~ 96 h for rainbow trout gill epithelia.

6.3.5 RNA extraction and cDNA synthesis: Total RNA was isolated from goldfish gill tissue and cultured goldfish and rainbow trout gill epithelia using TRIzol[®] Reagent (Invitrogen Canada Inc., Burlington, ON, Canada) according to manufacturer's instructions. Extracted RNA was treated with DNase I (Amplification Grade; Invitrogen Canada Inc.) and then first-strand cDNA was synthesized using SuperScript[™] III Reverse Transcriptase and Oligo(dT)₁₂₋₁₈ primers (Invitrogen Canada Inc.).

6.3.6 Cloning of goldfish corticosteroid receptor, claudin and ZO-1 cDNA: Using ClustalX multiple sequence alignments (Larkin et al., 2007) of known coding sequences for corticosteroid receptors, claudins and ZO-1 from various species, degenerate primers were designed based on highly conserved regions. For example, degenerate primers for corticosteroid receptors were designed based on highly conserved regions identified

within the aligned coding sequences for zebrafish, common carp and rainbow trout glucocorticoid receptor 1 (GR1), glucocorticoid receptor 2 (GR2) and mineralocorticoid receptor (MR) orthologs (see Table 6-1 for ortholog accession nos.). For claudin b, c, d, e, h, 7 and 12 degenerate primer design, coding sequences for appropriate *Takifugu* (= *Fugu*) *rubripes* and zebrafish claudin orthologs, as defined by Loh (2004) and Clelland and Kelly (2010), were aligned (see Table 6-2 for ortholog accession nos.). For claudin 8d degenerate primer design, coding sequences for *Fugu* and rainbow trout claudin 8d orthologs were aligned (see Table 6-2 for ortholog accession nos.). Finally, for ZO-1 (= tight junction protein-1; TJPI) degenerate primer design, coding sequences for mouse (NM_009386), rat (NM_001106266), human (NM_003257), dog (NM_001003140), chicken (XM_413773) and zebrafish (XM_001922655) ZO-1 orthologs were aligned. Degenerate primers were used in reverse transcriptase PCR (RT-PCR) to amplify partial goldfish corticosteroid receptor, claudin or ZO-1 cDNA fragments from a goldfish gill cDNA template. The following RT-PCR reaction conditions were utilized: 1 cycle of denaturation (95°C, 4 min), 40 cycles of denaturation (95°C, 30 sec), annealing (53 - 62°C, 30 sec) and extension (72°C, 30 sec) respectively, final single extension cycle (72°C, 5 min). Gel electrophoresis (1% agarose stained with ethidium bromide) verified PCR products at predicted amplicon sizes. Putative cDNA fragments were then excised, purified using a QIAquick Gel Extraction Kit (QIAGEN Inc., Mississauga, ON, Canada) and sequenced in the York University Core Molecular Biology and DNA Sequencing Facility (Department of Biology, York University, ON, Canada). Partial goldfish GR1, GR2, MR, claudin b, c, d, e, h, 7, 8d and 12, and ZO-1 sequences were confirmed using a

Table 6-1: Primer sequences and corresponding fish orthologs for goldfish corticosteroid receptors.

Goldfish Gene (accession no.)	Primer Sequence (5' → 3')	Amplicon Size (bp)	Fish Ortholog (accession no.)
GR1 (HQ656017)	FOR: GATGCGATTACAGGGTCATTC REV: CTCCGTTACACTGCTGGTAGG	368	zf nr3c1 (NM_001020711) crp GR1a (AJ879149) rt GR (NM_001124730)
GR2 (HQ656018)	FOR: TTACAGCAACAGCCCAGTC REV: CCACCAATCAAGGAGTCTG	351	zf GR β (EF436285) crp GR2 (AM183668) rt GR2 (NM_001124482)
MR (HQ656019)	FOR: AGGTGAGCCAGGAGTTTGTC REV: TGGTCGCTGATTATTTCCAC	340	zf nr3c2 (NM_001100403) crp MR (AJ783704) rt MRa (AY495584)

GR1, glucocorticoid receptor 1; GR2, glucocorticoid receptor 2; MR, mineralocorticoid receptor; zf, zebrafish; crp, carp; rt, rainbow trout.

Table 6-2: Primer sequences and corresponding fish orthologs for goldfish claudins and ZO-1.

Goldfish Gene (accession no.)	Primer Sequence (5' → 3')	Amplicon Size (bp)	Fish Ortholog (accession no.)
claudin b (HQ656008)	FOR: GTGCCCTCACCATCATTTC REV: GCTCTCTCTTCTGTGCTTGGTTC	237	zf claudin b (AF359426) fu claudin 30d (AY554376)
claudin c (HQ656009)	FOR: CATTGTGGGTGTCCTAGCG REV: CAATACGACTTTGCGGTGG	335	zf claudin c (AF359432) fu claudin 3d (AY554368)
claudin d (HQ656010)	FOR: AATCCTCGTGACCTTCTTGG REV: CCAGCCGATGAACAGAGAC	244	zf claudin d (BC078260) fu claudin 29a (AY554372)
claudin e (HQ656011)	FOR: TCTGTGGATGACCTGTGTGG REV: CCCTGACGATGGTGTTAGTTG	289	zf claudin e (AF359425) fu claudin 28b (AY554375)
claudin h (HQ656012)	FOR: ACCTTCAGGCTTCCAGAGC REV: CAGCGCAAACCTATGTAG	285	zf claudin h (BC053223) fu claudin 3a (AY554377)
claudin 7 (HQ656013)	FOR: GCAAGGTGTACGACTCCATC REV: TGTGTTGACTGGTGTGAAGG	281	zf claudin 7 (BC066408) fu claudin 7b (AY554347)
claudin 8d (HQ656014)	FOR: GAGGGACTGTGGATGAACTGC REV: GACACGGGAATAATGGTGGTC	272	fu claudin 8d (AY554390) rt claudin 8d (BK007966)
claudin 12 (HQ656015)	FOR: TTTCCAGCTTGGCTCTTCTG REV: GCTAAGATCAGACCACCAGCAC	280	zf claudin 12 (BC075744) fu claudin 12 (AY554346)
ZO-1 (HQ656016)	FOR: CTGGCTGGAGGAAATGATGTG REV: CCACCACTCTGAACACCTCTCC	330	zf TJPI (XM_001922655)

zf, zebrafish; fu, *Fugu*; rt, rainbow trout.

BLAST search (Altschul et al., 1997) and submitted to GenBank (accession nos. are shown in Tables 6-1 and 6-2).

6.3.7 Identification of rainbow trout claudins: Full-length and partial coding sequences for rainbow trout claudin 3a, 7, 8d, 12 and 30 were assembled from overlapping rainbow trout EST sequences using ClustalX multiple sequence alignments. Rainbow trout EST sequences were identified by submitting known *Fugu* and/or Atlantic salmon claudin coding sequences (see Table 6-3 for ortholog accession nos.) to a BLAST search against a rainbow trout EST database available at the NCBI (www.ncbi.nlm.nih.gov). Assembled sequences for rainbow trout claudins were submitted to the Third Party Annotation (TPA) database (accession nos. are shown in Table 6-3).

6.3.8 RT-PCR of goldfish corticosteroid receptors: Expression of goldfish corticosteroid receptor mRNA in goldfish gill tissue and cultured goldfish gill epithelia was examined by routine RT-PCR under reaction conditions described above (see Section 6.3.6) using gene-specific primer sets for goldfish corticosteroid receptors (see Table 6-1). Primers were designed based on the partial coding sequences determined above (see Section 6.3.6). The sequence identities of RT-PCR products were confirmed by sequence analysis (Department of Biology, York University) to verify that the gene-specific primer sets were targeting the correct genes. β -actin mRNA abundance was used as a loading control and was amplified using primers previously reported in Chapter 5. Resulting RT-PCR amplicons were resolved by gel electrophoresis (1% agarose stained with ethidium bromide), and images were captured using a Molecular Imager Gel Doc XR+ System and

Table 6-3: Primer sequences and corresponding fish orthologs for trout claudins.

Trout Gene (accession no.)	Primer Sequence (5' → 3')	Amplicon Size (bp)	Fish Ortholog (accession no.)
claudin 3a (BK007964)	FOR: TGGATCATTGCCATCGTGTC REV: GCCTCGTCCTCAATACAGTTGG	285	fu claudin 3a (AY554377) sl claudin 3a (BK006381)
claudin 7 (BK007965)	FOR: CGTCCTGCTGATTGGATCTC REV: CAAACGTA CTCTTGCTGCTG	261	fu claudin 7b (AY554347) sl claudin 7 (BK006387)
claudin 8d (BK007966)	FOR: GCAGTGTAAGTGTACGACTCTCTG REV: CACGAGGAACAGGCATCC	200	fu claudin 8d (AY554390)
claudin 12 (BK007967)	FOR: CTTCATCATCGCCTTCATCTC REV: GAGCCAAACAGTAGCCAGTAG	255	fu claudin 12 (AY554346) sl claudin 12 (NM_001140081)
claudin 30 (BK007968)	FOR: CGGCGAGAACATAATCACAG REV: GGGATGAGACACAGGATGC	297	sl claudin 30 (BK006405)

fu, *Fugu*; sl, Atlantic salmon.

Quantity One 1D analysis software (Bio-Rad Laboratories Canada Ltd., Mississauga, ON, Canada).

6.3.9 Quantitative real-time PCR analysis: TJ protein mRNA abundance in goldfish gill tissue and cultured goldfish and rainbow trout gill epithelia was examined by quantitative real-time PCR analysis (qRT-PCR). Based on the coding sequences determined above (see Sections 6.3.6 and 6.3.7), gene-specific primer sets for goldfish claudins and ZO-1 (see Table 6-2) and rainbow trout claudins (see Table 6-3) were designed for use in qRT-PCR. The sequence identities of amplicons generated using gene-specific primer sets were confirmed by sequence analysis (Department of Biology, York University). Goldfish and rainbow trout occludin mRNA were also amplified using primers previously reported in Chapters 4 and 5. Primers for rainbow trout claudin 28b (forward: 5' CTTTCATCGGAGCCAACATC 3' and reverse: 5' CAGACAGGGACCAGAACCAG 3', amplicon size ~ 310 bp) were designed based on GenBank accession number EU921670. qRT-PCR analysis of TJ protein mRNA was conducted using SYBR Green I Supermix (Bio-Rad Laboratories Canada Ltd.) and a Chromo4™ Detection System (CFB-3240; Bio-Rad Laboratories Canada Ltd.) under the following reaction conditions: 1 cycle denaturation (95°C, 4 min) followed by 40 cycles of denaturation (95°C, 30 sec), annealing (51 - 61°C, 30 sec) and extension (72°C, 30 sec) respectively. A standard curve was constructed for each TJ gene examined in order to optimize the template cDNA concentration used and to ensure that the threshold cycle for each gene occurred within an acceptable range. A melting curve was also carried out after each qRT-PCR run to ensure that a single product was synthesized during reactions.

For all qRT-PCR analyses, TJ protein mRNA abundance was normalized to β -actin transcript abundance after verifying that β -actin did not alter in response to experimental conditions. Goldfish and rainbow trout β -actin mRNA was amplified using primers previously described in Chapters 4 and 5.

6.3.10 Statistical analysis: All data are expressed as mean values \pm s.e.m. (n), where n represents the number of inserts, except in Fig. 6-2B, where n represents the number of fish sampled. A one-way or two-way analysis of variance (ANOVA) followed by a Student-Newman-Keuls test was used to determine significant differences ($P < 0.05$) between groups. When appropriate, a Student's t -test was also used. All statistical analyses were conducted using SigmaStat 3.5 software (Systat Software Inc., San Jose, CA, USA).

6.4 Results

6.4.1 Corticosteroid receptor mRNA expression and dose-dependent effects of cortisol on permeability in cultured goldfish gill epithelia: Using degenerate primers, partial coding sequences for goldfish corticosteroid receptors (GR1, GR2 and MR) were cloned. Translated goldfish GR1, GR2 and MR fragments shared ~ 99% amino acid sequence similarity (identical matches plus mismatches with similar amino acids) with aligned regions of corresponding carp, zebrafish and trout corticosteroid receptor orthologs (see Table 6-1 for ortholog accession nos.). Using RT-PCR and gel electrophoresis, cultured gill cells were examined for the presence of goldfish GR1, GR2 and MR expression. As a positive control, corticosteroid receptor mRNA in goldfish gill tissue was also evaluated. Transcripts for all three goldfish corticosteroid receptors were found to be present in both goldfish gill tissue and cultured gill cells (Fig. 6-1A).

To examine the dose-dependent effects of cortisol on the permeability characteristics of cultured goldfish gill epithelia, basolateral media were supplemented with 100, 500 and 1000 ng/mL of cortisol. Following 24 h of cortisol treatment, all three tested doses significantly elevated TER when compared to untreated control preparations (Fig. 6-1B). All tested cortisol doses also significantly reduced [³H]PEG-4000 flux across cultured goldfish gill preparations (Fig. 6-1C). [³H]PEG-4000 permeability appeared to decrease in a stepwise manner with increasing cortisol concentration, however flux across 500 ng/mL cortisol-treated preparations was not significantly different ($P > 0.05$) from 100 ng/mL cortisol-treated epithelia (Fig. 6-1C).

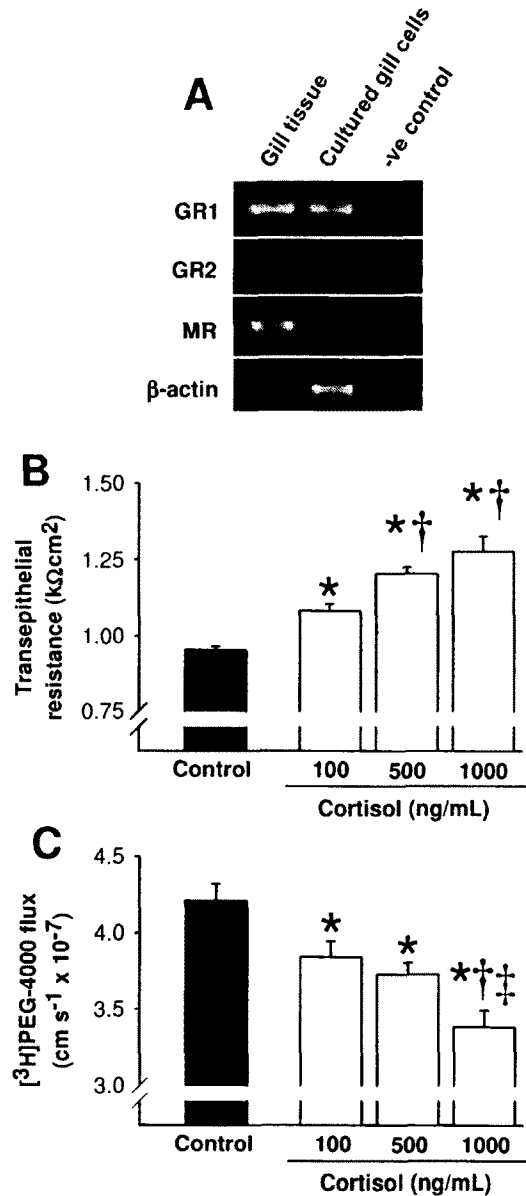


Figure 6-1: (A) Corticosteroid receptor mRNA expression in goldfish gill tissue and cultured goldfish gill cells by routine RT-PCR and gel electrophoresis. β -actin mRNA was used as a loading control. Dose-dependent effects of 24 h cortisol treatment on (B) transepithelial resistance and (C) [³H]PEG-4000 flux across cultured goldfish gill epithelia. Data are expressed as mean values \pm s.e.m. ($n = 8-11$). * Significant difference ($P < 0.05$) from the untreated control (0 ng/mL) group. † Significant difference ($P < 0.05$) from the 100 ng/mL cortisol group. ‡ Significant difference ($P < 0.05$) from the 500 ng/mL cortisol group. GR1, glucocorticoid receptor 1; GR2, glucocorticoid receptor 2; MR, mineralocorticoid receptor.

6.4.2 TJ protein mRNA expression in cultured goldfish gill epithelia and goldfish gill tissue: Using degenerate primers, partial coding sequences for goldfish claudins and ZO-1 were cloned. Translated goldfish claudin fragments exhibited ~ 94 - 99% and ~ 84 - 92% amino acid sequence similarity with aligned regions of corresponding zebrafish and *Fugu* claudin orthologs respectively (see Table 6-2 for ortholog accession nos.). Goldfish claudins were therefore designated a single letter or number based on the nomenclature of the zebrafish claudin family originally described by Kollmar (2001), except for goldfish claudin 8d which was named according to *Fugu* terminology (outlined by Loh et al., 2004) since a zebrafish ortholog for claudin 8d has yet to be identified. The translated goldfish ZO-1 fragment exhibited 100% and 97 - 98% amino acid sequence similarity with aligned regions of zebrafish and mammalian (e.g. mouse, rat, human, dog) ZO-1 orthologs respectively.

Because all TJ protein genes were expressed in gill tissue and the cultured gill epithelium, the relative abundance of TJ protein mRNA was compared within each tissue to examine whether tissue-specific levels of TJ protein mRNA in the *in vitro* preparation matched native gill tissue (see Fig. 6-2). In broad terms, the relative abundance of TJ protein mRNA in each tissue matched well. For example, claudin 7, b, e and 8d mRNA were the most abundant in both tissues and claudin d and c were the least abundant. However, subtle differences were also noted. Claudin b, for example, was the most abundant transcript in gill tissue, but in cultured gill epithelia, both claudin b and claudin 7 were the most abundant (Fig. 6-2).

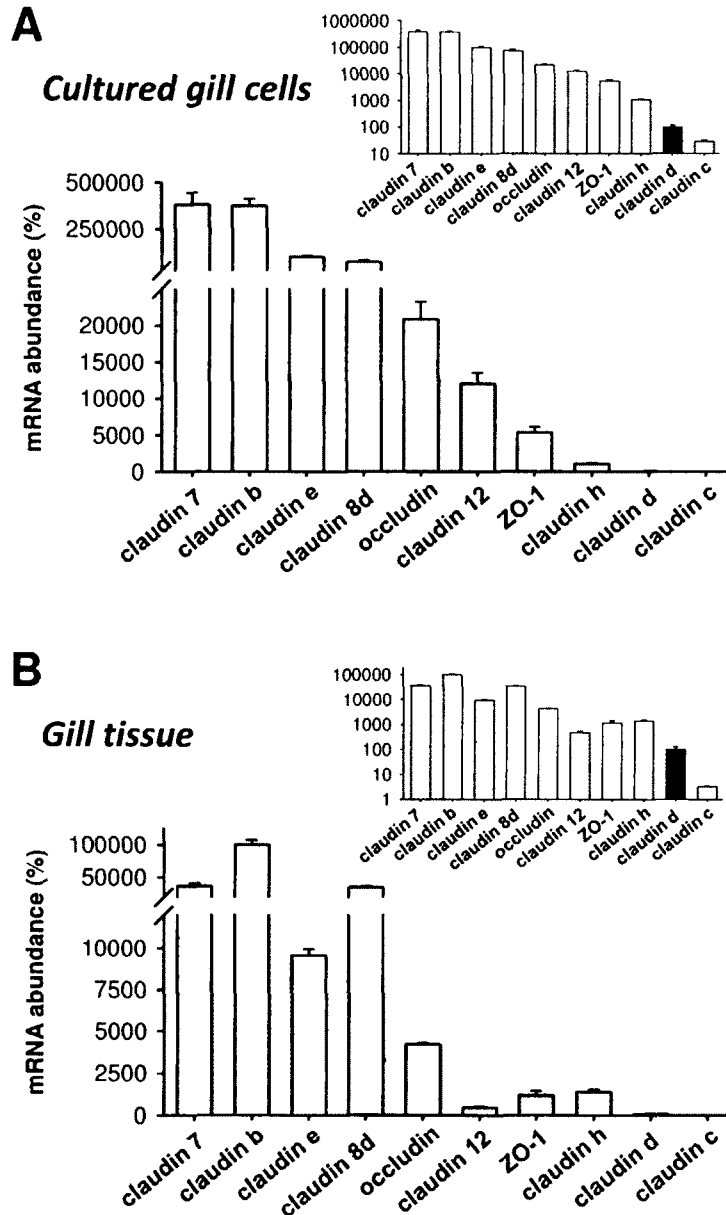


Figure 6-2: Goldfish occludin, claudin and ZO-1 mRNA abundance in (A) cultured gill cells and (B) gill tissue by qRT-PCR analysis. Inset graphs show data re-expressed on a semi-logarithmic scale. Transcript abundance was normalized to β -actin mRNA abundance, and mRNA abundance for each gene examined was expressed relative to claudin d transcript abundance (indicated by the solid bar) which was assigned a value of 100%. In (A) and (B), transcripts for TJ proteins are shown in descending order of abundance (left to right) as found in the primary cultured goldfish gill epithelium. Data are expressed as mean values \pm s.e.m. (A, $n = 6$; B, $n = 3-4$).

6.4.3 Dose-dependent effects of cortisol on TJ protein mRNA abundance in cultured goldfish gill epithelia: In *series 1* experiments, cultured goldfish gill epithelia were treated with 100, 500 and 1000 ng/mL of cortisol for 24 h to examine the dose-dependent effects of the hormone on TJ protein mRNA abundance. Occludin and claudin b, d, e, 7, 8d and 12 levels did not significantly alter in response to cortisol treatment ($P > 0.05$) (Fig. 6-3A,B,D,E,G,H,I). Cortisol doses of 500 and 1000 ng/mL however significantly reduced claudin c mRNA abundance by ~ 28 and 44% respectively when compared to untreated control epithelia (Fig. 6-3C). Similarly, treatment with 1000 ng/mL cortisol significantly reduced claudin h and ZO-1 transcript abundance by ~ 42 and 39% respectively (Fig. 6-3F, J). β -actin mRNA abundance was not significantly altered by cortisol treatment ($P = 0.994$).

6.4.4 Time-course effects of cortisol on permeability and TJ protein mRNA abundance in cultured goldfish gill epithelia: In *series 2* experiments, cultured goldfish gill epithelia were treated with 500 ng/mL of cortisol for 48 and 96 h to examine the response of epithelia to prolonged cortisol exposure. TER was significantly elevated after 48 and 96 h of cortisol treatment when compared to untreated control preparations within the same time group (Fig. 6-4A). Over time, TER within the control group significantly decreased, however TER within the cortisol-treated group remained unchanged ($P > 0.05$; Fig. 6-4A). Neither cortisol treatment nor time significantly altered claudin b, d, e and 8d transcript abundance ($P > 0.05$; data not shown). Claudin 7 mRNA abundance however, was significantly decreased over time but was not dependent on cortisol treatment as

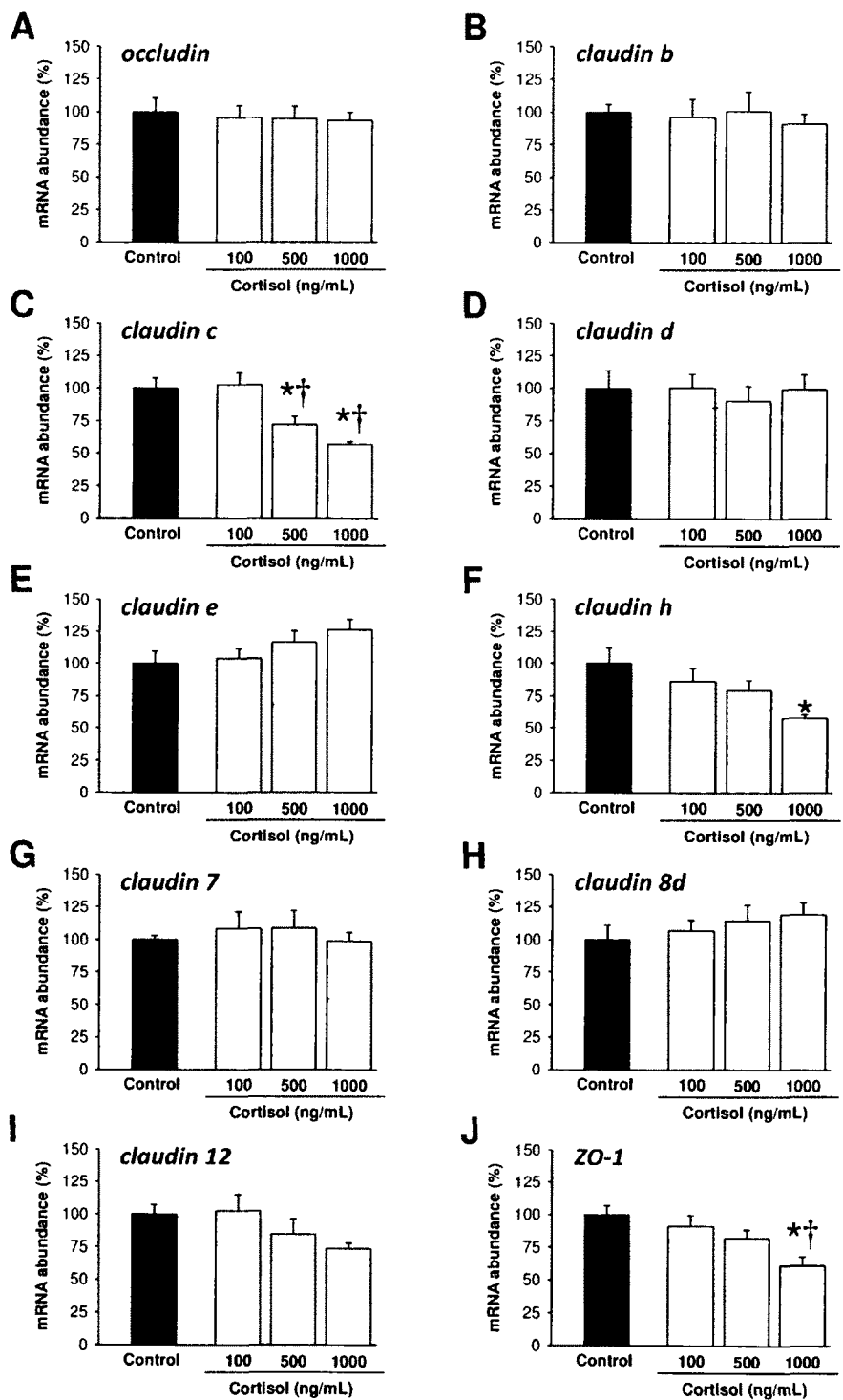


Figure 6-3: (see legend on next page)

Figure 6-3: Dose-dependent effects of 24 h cortisol treatment on (A) occludin, (B) claudin b, (C) claudin c, (D) claudin d, (E) claudin e, (F) claudin h, (G) claudin 7, (H) claudin 8d, (I) claudin 12 and (J) ZO-1 mRNA abundance in cultured goldfish gill epithelia. Occludin, claudin and ZO-1 transcript abundance were normalized to β -actin mRNA abundance. Data are expressed as mean values \pm s.e.m. ($n = 5-6$). * Significant difference ($P < 0.05$) from the untreated control (0 ng/mL) group. † Significant difference ($P < 0.05$) from the 100 ng/mL cortisol group.

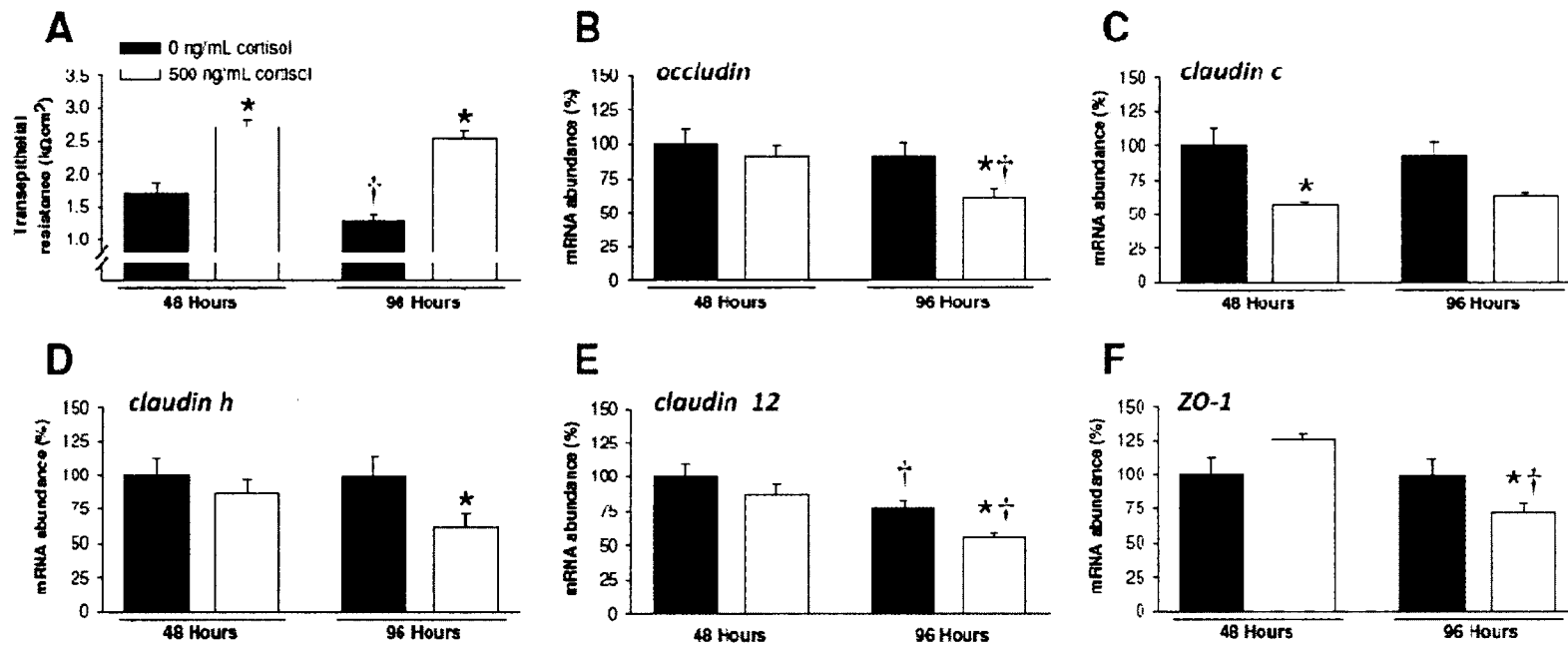


Figure 6-4: (see legend on next page)

Figure 6-4: Time-course effects of 48 and 96 h cortisol treatment on (A) transepithelial resistance and (B) occludin, (C) claudin c, (D) claudin h, (E) claudin 12 and (F) ZO-1 mRNA abundance in cultured goldfish gill epithelia. Occludin, claudin and ZO-1 transcript abundance were normalized to β -actin mRNA abundance, and mRNA data were expressed relative to transcript abundance for control (0 ng/mL cortisol) epithelia collected at 48 h which were assigned a value of 100%. Data are expressed as mean values \pm s.e.m. ($n = 5-6$). * Significant difference ($P < 0.05$) between control and cortisol groups within the same time period (e.g. control versus cortisol at 48 h). † Significant difference ($P < 0.05$) between time periods within a treatment group (e.g. control at 48 h versus control at 96 h).

there was no statistically significant interaction between hormone treatment and time ($P > 0.05$; data not shown). Although occludin, claudin h and 12, and ZO-1 transcript abundance remained unchanged ($P > 0.05$) relative to control preparations after 48 h cortisol treatment, mRNA expression levels were significantly reduced by cortisol following 96 h (Fig. 6-4B,D,E,F). Occludin, claudin 12 and ZO-1 mRNA expression were also significantly reduced after 96 h cortisol treatment relative to cortisol-treated epithelia at 48 h (Fig. 6-4B,E,F). Furthermore, control epithelia collected at 96 h exhibited significantly lower levels of claudin 12 mRNA when compared to control preparations collected at 48 h (Fig. 6-4E). Finally, cortisol supplementation reduced claudin c mRNA abundance following both 48 h ($P < 0.05$) and 96 h ($P = 0.139$), however this was only significant following 48 h (Fig. 6-4C). Neither cortisol treatment nor time significantly altered ($P > 0.05$) β -actin mRNA abundance.

6.4.5 Comparative effects of cortisol on permeability and TJ protein mRNA abundance in cultured goldfish and rainbow trout gill epithelia: To compare changes in TJ protein mRNA abundance in cultured goldfish and rainbow trout gill epithelia, several trout claudin orthologs were identified using a BLAST search to compare known *Fugu* and/or Atlantic salmon sequences to a rainbow trout EST database. Translated rainbow trout claudin 3a, 7, 12 and 30 fragments exhibited ~ 85 – 99% and 99 – 100% amino acid sequence similarity with aligned regions of corresponding *Fugu* and Atlantic salmon orthologs respectively (see Table 6-3 for ortholog accession nos.), and were therefore named according to previously reported Atlantic salmon claudin nomenclature (see Tipsmark et al., 2008). Since an Atlantic salmon claudin 8d ortholog has yet to be

identified, rainbow trout claudin 8d was named after *Fugu* claudin 8d (see Loh et al., 2004) which shares ~ 89% amino acid sequence similarity with aligned regions of the trout ortholog. Taken together, this allowed a comparison of seven TJ orthologs. Specifically, rainbow trout occludin, claudin 30, 28b, 3a, 7, 8d and 12 genes are orthologs of goldfish occludin, claudin b, e, h, 7, 8d and 12 genes respectively.

In *series 3* experiments, cultured goldfish and rainbow trout gill epithelia were supplemented with a single dose of 500 ng/mL cortisol. When compared to control preparations, cortisol treatment significantly elevated TER by ~ 35% and 530% in cultured goldfish and rainbow trout gill epithelia respectively (Fig. 6-5A,C). Cortisol also significantly reduced [³H]PEG-4000 flux by ~ 22% and 42% in cultured goldfish and rainbow trout gill epithelia respectively (Fig. 6-5B,D). Transcripts encoding for goldfish TJ proteins were unaltered ($P > 0.05$) by cortisol treatment, except for claudin e mRNA abundance, which exhibited a marginal but significant increase in response to cortisol (Fig. 6-5E). In contrast, cortisol treatment significantly elevated the transcript abundance of all rainbow trout TJ orthologs examined. In both cultured goldfish and rainbow trout gill epithelia, β -actin mRNA abundance was not significantly altered ($P = 0.478$ and 0.6806 respectively) by cortisol treatment.

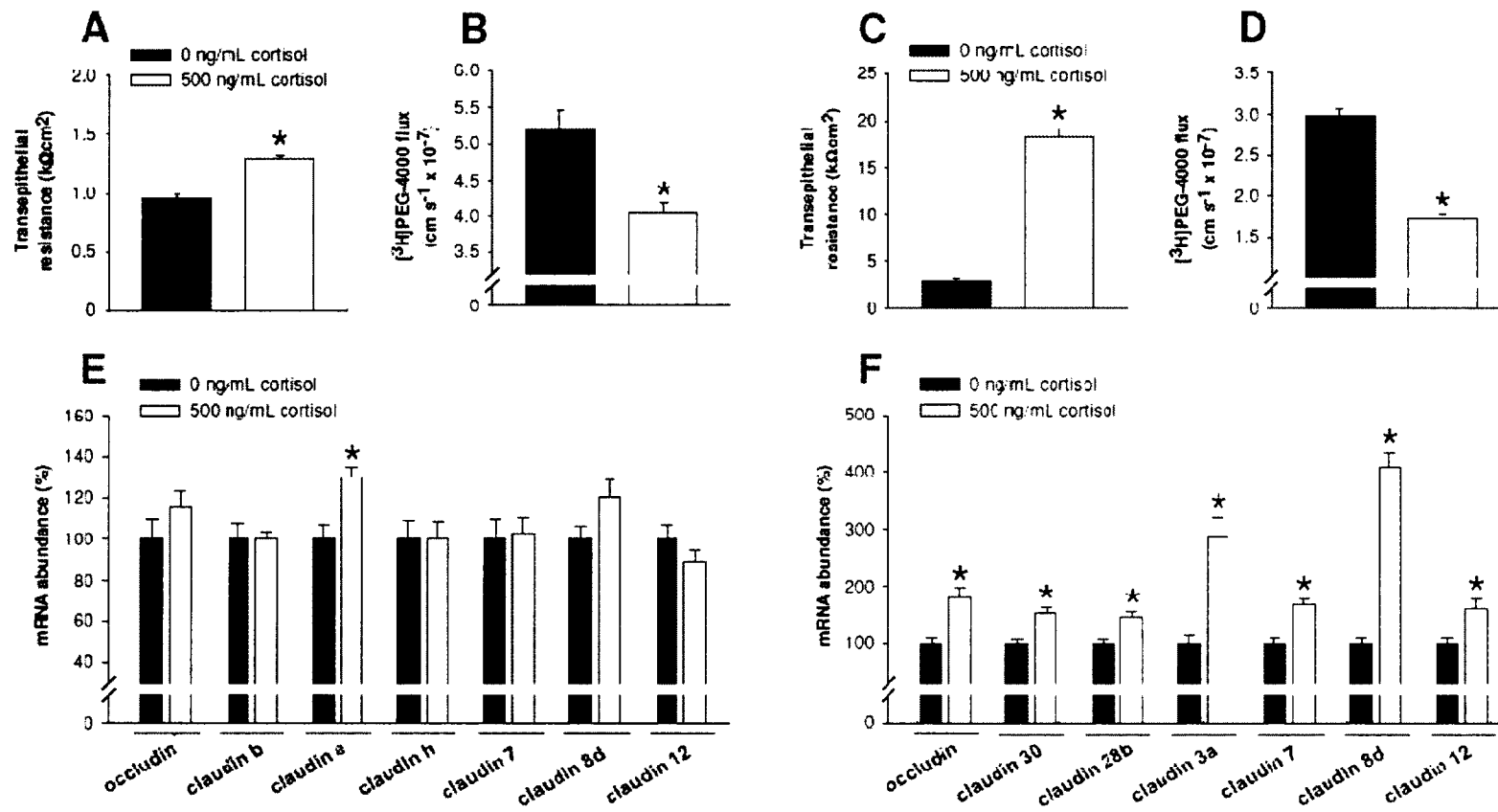


Figure 6-5: (see legend on next page)

Figure 6-5: Comparative effects of cortisol on (A,C) transepithelial resistance, (B,D) [³H]PEG-4000 flux and (E,F) TJ protein mRNA abundance in cultured (A,B,E) goldfish and (C,D,F) rainbow trout gill epithelia. Note: goldfish occludin, claudin b, e, h, 7, 8d and 12 genes are orthologs of rainbow trout occludin, claudin 30, 28b, 3a, 7, 8d and 12 genes respectively. Goldfish and rainbow trout occludin and claudin transcript abundance were normalized to β -actin mRNA abundance. Data are expressed as mean values \pm s.e.m. ($n = 5-8$). * Significant difference ($P < 0.05$) from the untreated control (0 ng/mL) group.

6.5 Discussion

6.5.1 Overview: During SW acclimation of euryhaline fishes, circulating cortisol levels have been shown to rapidly elevate (e.g. Marshall et al., 1999; Craig et al., 2005). Under these circumstances, elevated cortisol levels help to increase salinity tolerance by stimulating active ion extrusion mechanisms in the gill (e.g. Jacob and Taylor, 1983; Evans et al., 2005). The ability of fishes to acclimate to ion-poor surroundings has also been linked to elevated cortisol levels (Perry and Laurent, 1989). In studies conducted on euryhaline rainbow trout, hypercortisolaemia was proposed to enhance acclimation to ion-poor surroundings by enlarging gill mitochondria-rich cells and enhancing ion uptake (Perry and Laurent, 1989). However a decrease in ion efflux rate was also reported to occur (Perry and Laurent, 1989), an observation that is consistent with the ability of cortisol to reduce ion efflux rates and increase the abundance of the TJ protein occludin in cultured gill epithelia derived from FW rainbow trout (see Chapter 4; Kelly and Wood, 2001). In contrast, the goldfish is a stenohaline FW fish that cannot survive in SW (Lahlou et al., 1969). However, when gradually acclimated to elevated salinity, it has been reported that goldfish can survive indefinitely in half-strength SW (Lahlou et al., 1969). Interestingly, goldfish serum cortisol levels have also been shown to significantly elevate when acclimated to a tolerable saline environment (Singley and Chavin, 1975). Furthermore, goldfish are able to acclimate to ion-poor surroundings (see Chapter 3). Serum cortisol levels have not been described in goldfish during ion-poor water exposure however increased ion influx and reductions in ion efflux across the gills have been observed (Cuthbert and Maetz, 1972). Correspondingly, occludin TJ protein abundance is

markedly elevated in the gills of goldfish when acclimated to ion-poor water (see Chapter 3). Therefore, the literature appears to indicate that cortisol may be a common link between the ionoregulatory response of euryhaline and stenohaline species to altered environmental salinity. However, the current set of studies does not entirely support this view. In contrast, the modest (or absent) response of cultured goldfish gill epithelia to cortisol treatment seems to suggest that cortisol may play a less important role in controlling salt and water balance in goldfish and introduces the idea that the stenohaline nature of goldfish may be related to this phenomenon.

6.5.2 Dose-dependent effects of cortisol on permeability: Cultured goldfish gill epithelia are composed exclusively of pavement cells, therefore goldfish corticosteroid receptors were cloned to establish their presence in cultured preparations. Transcripts for all three goldfish corticosteroid receptors (GR1, GR2 and MR) examined were found in goldfish gill tissue and cultured gill epithelia (Fig. 6-1A). In view of this, it seemed reasonable to conclude that cultured goldfish gill epithelia would be capable of mounting a response to cortisol treatment. Therefore three cortisol concentrations were tested, using doses (100, 500 and 1000 ng/mL) that were selected based on the reported physiological range for plasma cortisol in goldfish and other cyprinids subjected to various stressors (e.g. noise stress, air exposure) (Smith et al., 2004; Dror et al., 2006; Pottinger et al., 2010).

Cortisol treatment elicited a distinct epithelial “tightening” effect by significantly elevating TER and reducing [³H]PEG-4000 flux across cultured goldfish gill epithelia in a dose-dependent manner (Figs. 6-1B,C). This “tightening” of cultured goldfish gill preparations is in accordance with observed glucocorticoid-mediated reductions in

permeability across other cultured vertebrate epithelia and endothelia (e.g. Zettl et al., 1992; Stelwagen et al., 1999; Förster et al., 2008), including primary cultured fish gill models derived from rainbow trout and tilapia (Kelly and Wood, 2001, 2002). However, although the effect of cortisol on cultured goldfish gill preparations was qualitatively similar to those observed in cultured trout gill epithelia (see Kelly and Wood, 2001), the response of trout preparations to cortisol treatment was quantitatively different. For example, when compared to untreated controls, cortisol concentrations of 100 and 1000 ng/mL elevated TER measurements by ~ 13% and 34% respectively in cultured goldfish gill epithelia (Fig. 6-1B) versus ~ 475% and 1900% respectively in cultured trout preparations (Kelly and Wood, 2001). Similarly, cortisol doses of 100 and 1000 ng/mL reduced paracellular [³H]PEG-4000 flux by ~ 10% and 20% respectively in cultured goldfish gill epithelia (Fig. 6-1C) versus ~ 40% and 68% respectively in cultured trout preparations (Kelly and Wood, 2001). In terms of the corticosteroid regulation of epithelial permeability, this provides unique insight into species-specific differences that could relate to the environmental physiology of these organisms (i.e. euryhaline versus stenohaline).

6.5.3 Expression patterns of TJ protein transcripts in a cultured goldfish gill epithelium and goldfish gill tissue: A comparison of occludin, claudins and ZO-1 within gill tissue indicated that transcript abundance of the TJ proteins claudin b, e, 7, 8d and occludin were considerably greater than claudin c, d, 3a and 12, and ZO-1 (Fig. 6-2B). With the exception of a few subtle differences, the same pattern of abundance was present in the primary cultured goldfish gill model (see Fig. 6-2A). Therefore, although the TJ mRNA

abundance profile in the *in vitro* model was largely the same as native gill tissue, it is likely that the few observed differences relate to the cultured gill epithelium being composed of pavement cells only whereas in gill tissue there would be TJs between other cell types (e.g. pavement cells with mitochondria-rich cells and/or junctions between cells of the capillary endothelium).

6.5.4 Dose-dependent and time-course effects of cortisol on TJ protein mRNA abundance: Of the ten goldfish TJ genes evaluated in *series 1* experiments, only three TJ protein transcripts, claudin c and h, and ZO-1, were significantly altered by 24 h cortisol exposure (Fig. 6-3C,F,J). Furthermore, only claudin c mRNA abundance was significantly altered by a physiologically relevant dose of cortisol (i.e. 500 ng/mL) (Fig. 6-3C). It is interesting that transcript abundance of goldfish claudin c and h genes decreased as they are both orthologs of claudin 3d and 3a genes respectively within the claudin 3 family of TJ protein genes in puffer fish, as well as orthologs of the single claudin 3 gene in mammals. Several lines of evidence in both fish (Bagherie-Lachidan et al., 2008; Duffy et al., 2011) and mammals (Kiuchi-Saishin et al., 2002; Markov et al., 2010; Milatz et al., 2010) strongly support a role for claudin 3 orthologs as barrier-forming or “tightening” TJ proteins. However, contrary to this strongly supported function, cultured puffer fish gill epithelia have also been reported to exhibit a significant reduction in claudin 3a (and no change in claudin 3d) transcript abundance in response to cortisol treatment (Bui et al., 2010). In addition to the aforementioned claudins, the observed reduction in ZO-1 mRNA abundance also conflicts with a previous study that

reported glucocorticoid treatment of mouse mammary epithelia to significantly augment ZO-1 protein levels in association with elevated TER (Singer et al., 1994).

Despite unchanged expression or the paradoxically observed decrease in transcript abundance of barrier-forming TJ genes, the paracellular barrier across cultured goldfish gill epithelia was significantly enhanced by cortisol treatment (Fig. 6-1C). It is possible that the observed reductions in paracellular [³H]PEG-4000 flux were due to non-genomic actions, such as alterations in TJ protein turnover rates, recruitment of existing TJ proteins from the cytosolic pool to the TJ complex, or TJ assembly and disassembly by rapid phosphorylation or dephosphorylation of TJ proteins. To address the possibility that the duration of cortisol treatment was not long enough to elicit a genomic response, in *series 2* experiments the cortisol treatment period was extended to 48 and 96 h. In this experimental set, a single dose of 500 ng/mL cortisol was used as this was the only physiologically relevant dose that significantly altered TJ protein mRNA abundance in *series 1* experiments (Fig. 6-3). In addition, this dose and these exposure times are similar to those reported to elicit alterations in the transcript abundance of TJ proteins in cultured gill epithelia derived from euryhaline fishes (i.e. 44 h at 500 ng/mL, *Tetraodon nigroviridis*, see Bui et al., 2010; ~ 96 h at 500 ng/mL, *Oncorhynchus mykiss*, this study, see Section 6.5.5 below). Within the same time group (i.e. 48 h or 96 h), TER was significantly elevated by cortisol treatment relative to untreated controls (Fig. 6-4A). Therefore prolonged cortisol treatment significantly “tightened” goldfish gill preparations as was seen following 24 h exposure. However, and also consistent with *series 1* experiments, minimal alterations in TJ protein mRNA abundance were elicited. At 48 h,

only claudin c mRNA was significantly altered in response to cortisol while the abundance of transcripts encoding for occludin, claudin b, d, e, h, 7, 8d and 12, and ZO-1 did not change (Fig. 6-4). Following 96 h exposure to cortisol, claudin b, d, e, 7 and 8d transcript abundance continued to be unaffected by cortisol, but significant reductions in occludin, claudin h and 12, and ZO-1 mRNA were observed. Therefore, although some additional changes in TJ protein mRNA abundance were observed after a longer duration of cortisol exposure, these alterations were contrary to what may have been expected (i.e. decreased mRNA rather than increased) based on the physiological characteristics of the cortisol-treated preparations at 96 h (i.e. elevated TER) and our understanding of the barrier-enhancing roles these TJ proteins play in other epithelia (e.g. Bagherie-Lachidan et al., 2008; Van Itallie et al., 2009; Milatz et al., 2010; Duffy et al., 2011; see discussion above).

6.5.5 Comparative effects of cortisol on permeability and TJ protein mRNA abundance in cultured goldfish and rainbow trout gill epithelia: Despite its epithelial “tightening” effect, cortisol treatment elicited limited alterations in TJ protein mRNA abundance in goldfish gill preparations in *series 1* and *series 2* experiments. Furthermore, in instances when TJ protein transcript levels were altered (either by high concentrations of cortisol or prolonged cortisol treatment), these were decreased rather than increased as would be anticipated to match the observed reductions in epithelial permeability and the understood functions of orthologous mammalian and fish TJ proteins (see discussion in Section 6.5.4 above). It seems reasonable to assume that the molecular TJ components that contribute to alterations in the paracellular permeability properties of the cultured

goldfish epithelium still require identification. However, it is also of interest to consider the possibility that species-specific differences could be a factor in the somewhat unusual observations from *series 1* and *2* experiments, and that these could relate to the stenohaline nature of goldfish. Indeed, the literature already supports this idea to some extent as occludin transcript and protein abundance have been reported to increase in cultured trout gill epithelia treated with cortisol (see Chapter 4) and mRNA encoding for a number of claudin isoforms have been reported to alter in response to cortisol treatment in a cultured puffer fish gill epithelium (see Bui et al., 2010). Therefore, to explore this idea further, *series 3* experiments sought to use a comparable system derived from a euryhaline fish (the rainbow trout) to conduct a side-by-side comparison of cortisol-mediated alterations in orthologous TJ protein transcripts. These studies were conducted using comparable doses of cortisol (i.e. 500 ng/mL), and although the time-frame for cortisol exposure was different (i.e. 24 h for goldfish versus ~ 96 h for trout, as is necessitated by the differences in epithelium development between the two preparations, see Chapter 5), *series 2* experiments indicated that time did little to further alter the effects of cortisol on goldfish gill preparations.

As previously noted, a single physiologically relevant dose of cortisol significantly elevated TER measurements and reduced [³H]PEG-4000 flux across cultured gill epithelia derived from both goldfish and rainbow trout (Fig. 6-5 A-D; see Chapter 4; Kelly and Wood, 2001). This “tightening” effect, however, was much more pronounced in trout gill preparations, where elevations in TER were almost 15-fold

higher and reductions in [³H]PEG-4000 flux were 2-fold lower than those observed across goldfish gill preparations (Fig. 6-5 A-D).

In accordance with the results of *series 1*, cortisol treatment did not significantly alter TJ protein transcript abundance in goldfish gill preparations, except for claudin e mRNA, which was marginally elevated (Fig. 6-5E). An equivalent dose of cortisol, however significantly elevated all orthologous trout TJ protein transcripts examined (Fig. 6-5F). Up-regulated occludin mRNA expression in the rainbow trout gill model in response to cortisol treatment confirms earlier results reported in Chapter 4 and is in agreement with a barrier-forming role for occludin (see Chapter 3; Feldman et al., 2005). Furthermore, the cortisol-mediated elevation in claudin 30 mRNA abundance is consistent with the observations of Tipsmark et al. (2009) where claudin 30 transcript abundance was significantly increased in whole gill tissue from Atlantic salmon following *in vitro* incubation with cortisol. These observations are also in line with a role for claudin 30 as a “tightening” TJ protein, as claudin 30 mRNA abundance was significantly reduced in the Atlantic salmon gill following SW acclimation (Tipsmark et al., 2008). Rainbow trout claudin 28b mRNA abundance significantly increased in the present study and interestingly, orthologous goldfish claudin e mRNA was also increased in response to cortisol treatment (Fig. 6-5E,F). Goldfish claudin e was the only goldfish TJ gene examined in the present study that exhibited a significant elevation following cortisol treatment (Fig. 6-5E) and (although not significant) also appeared to be elevated in response to cortisol in a dose-dependent manner in *series 1* experiments (Fig. 6-3E). Claudin 28b mRNA abundance in the Atlantic salmon gill has been reported to

transiently decrease during the early stages of SW acclimation (Tipsmark et al., 2008), therefore it is possible that rainbow trout claudin 28b and orthologous goldfish claudin e proteins may contribute to the TJ barrier. Cortisol treatment significantly elevated rainbow trout claudin 3a mRNA abundance in accordance with a well-supported barrier role for orthologous mammalian and fish claudin 3 (Bagherie-Lachidan et al., 2008; Milatz et al., 2010; Duffy et al., 2011; see discussion in Section 6.5.4 above), and out of the seven rainbow trout TJ genes examined in this study, claudin 8d exhibited the greatest increase in mRNA abundance in response to cortisol treatment (i.e. an ~ 310% elevation relative to untreated controls; Fig. 6-5F). A large body of research suggests a barrier-forming role for mammalian claudin 8 (Kiuchi-Saishin et al., 2002; Yu et al., 2003; Li et al., 2004; Fujita et al., 2006; Markov et al., 2010) and in fishes a similar barrier role for claudin 8 isoforms has also been proposed to exist (Bagherie-Lachidan et al., 2009; Duffy et al., 2011). Claudin 7 is a peculiar TJ protein as siRNA knockdown studies have demonstrated that it can form a barrier to the paracellular movement of Na⁺ ions or facilitate the permeability of Cl⁻ ions by formation of Cl⁻-selective paracellular pores (Hou et al., 2006). In the present study, rainbow trout claudin 7 transcript abundance was significantly elevated in response to cortisol (Fig. 6-5F), and correspondingly it has previously been demonstrated that cortisol treatment significantly reduces both net Na⁺ and Cl⁻ flux across cultured rainbow trout gill preparations in a dose-dependent manner (see Chapter 4; Kelly and Wood, 2001). Therefore, it seems likely that rainbow trout claudin 7 may function as a barrier to Na⁺ permeability. Taken together, the response of rainbow trout TJ protein orthologs appears to be very much in line with the physiological

changes that occur in response to cortisol (i.e. epithelial “tightening”). In addition, the changes in trout transcript abundance that take place fit well with what we currently know about the physiological role of these TJ components in fishes and other vertebrates. Therefore, it would seem that the conservative response in goldfish preparations at the physiological and molecular level represents a species-specific phenomenon that could be linked to differences between how a stenohaline and euryhaline fish may respond to the osmoregulatory actions of cortisol.

6.5.6 Conclusions: In the present study, data clearly support a role for cortisol in the endocrine regulation of paracellular permeability across the euryhaline rainbow trout gill, as cortisol treatment elicited significant alterations in several genes encoding for TJ proteins. Whether a similar role for cortisol in the stenohaline goldfish gill exists however is far less evident. Although cortisol treatment significantly reduced the epithelial permeability of cultured goldfish gill epithelia in a manner that was qualitatively similar to trout preparations, quantitatively these modifications in permeability were very different from those exhibited by the trout model. Furthermore, alterations in goldfish TJ components in response to cortisol were either entirely absent or did not correlate with the observed changes in epithelial permeability and our current understanding of the specific functions of the TJ proteins examined. In this regard, we introduce the notion that perhaps, at least in goldfish, stenohalinity is in part a consequence of a reduced capacity to limit diffusional salt influx by altering requisite TJ components as a result of an inability to adequately respond to cortisol during SW acclimation. Clearly more work is required, including the complete enumeration and analysis of goldfish TJ proteins

(particularly members of the claudin family), an examination of the effects of other osmoregulatory hormones (e.g. prolactin, growth hormone) on epithelial permeability, as well as similar comparison studies in other stenohaline and euryhaline species. Furthermore, future studies examining the effects of cortisol on a cultured stenohaline gill epithelium composed of both pavement and mitochondria-rich cells may also be revealing.

6.6 References

Altschul SF, Madden TL, Schäffer AA, Zhang J, Zhang Z, Miller W, Lipman DJ. 1997. Gapped BLAST and PSI-BLAST: a new generation of protein database search programs. *Nucleic Acids Res* 25:3389-3402.

Bagherie-Lachidan M, Wright SI, Kelly SP. 2008. Claudin-3 tight junction proteins in *Tetraodon nigroviridis*: cloning, tissue specific expression and a role in hydromineral balance. *Am J Physiol Integr Comp Physiol* 294:R1638-R1647.

Bagherie-Lachidan M, Wright SI, Kelly SP. 2009. Claudin-8 and -27 tight junction proteins in puffer fish *Tetraodon nigroviridis* acclimated to freshwater and seawater. *J Comp Physiol B* 179:419-431.

Bui P, Bagherie-Lachidan M, Kelly SP. 2010. Cortisol differentially alters claudin isoforms in cultured puffer fish gill epithelia. *Mol Cell Endocrinol* 317:120-126.

Clelland E, Kelly SP. 2010. Tight junction proteins in zebrafish ovarian follicles: stage specific mRNA abundance and response to 17β -estradiol, human chorionic gonadotropin, and maturation inducing hormone. *Gen Comp Endocrinol* 168:388-400.

Craig PM, Al-Timimi H, Bernier NJ. 2005 Differential increase in forebrain and caudal neurosecretory system corticotrophin-releasing factor and urotensin I gene expression associated with seawater transfer in rainbow trout. *Endocrinology* 146:3851-3860.

Cuthbert AW, Maetz J. 1972. The effects of calcium and magnesium on sodium fluxes through gills of *Carassius auratus*, L. *J Physiol* 221:633-643.

Dror M, Sinyakov MS, Okun E, Dym M, Sredni B, Avtalion RR. 2006. Experimental handling stress as infection-facilitating factor for the goldfish ulcerative disease. *Vet Immunol Immunopathol* 109:279-287.

Duffy NM, Bui P, Bagherie-Lachidan M, Kelly SP. 2011. Epithelial remodeling and claudin mRNA abundance in the gill and kidney of puffer fish (*Tetraodon biocellatus*) acclimated to altered environmental ion levels. *J Comp Physiol B* 181:219-238.

Evans DH, Piermarini PM, Choe KP. 2005. The multifunctional fish gill: dominant site of gas exchange, osmoregulation, acid-base regulation, and excretion of nitrogenous waste. *Physiol Rev* 85:97-177.

Feldman GJ, Mullin JM, Ryan MP. 2005. Occludin: structure, function and regulation. *Adv Drug Deliv Rev* 57:883-917.

Felinski EA, Cox AE, Phillips BE, Antonetti DA. 2008. Glucocorticoids induce transactivation of tight junction genes occludin and claudin-5 in retinal endothelial cells via a novel cis-element. *Exp Eye Res* 86:867-878.

Förster C, Burek M, Romero IA, Weksler B, Couraud PO, Drenckhahn D. 2008. Differential effects of hydrocortisone and TNF α on tight junction proteins in an *in vitro* model of the human blood-brain barrier. *J Physiol* 586:1937-1949.

Fujita H, Chiba H, Yokozaki H, Sakai N, Sugimoto K, Wada T, Kojima T, Yamashita T, Sawada N. 2006. Differential expression and subcellular localization of claudin-7, -8, -12, -13, and -15 along the mouse intestine. *J Histochem Cytochem* 54:933-944.

González-Mariscal L, Betanzos A, Nava P, Jaramillo BE. 2003. Tight junction proteins. *Prog Biophys Mol Biol* 81:1-44.

Hou J, Gomes AS, Paul DL, Goodenough DA. 2006. Study of claudin function by RNA interference. *J Biol Chem* 281:36117-36123.

Jacob WF, Taylor MH. 1983. The time course of seawater acclimation in *Fundulus heteroclitus* L. *J Exp Zool* 228:33-39.

Kelly SP, Fletcher M, Pärt P, Wood CM. 2000. Procedures for the preparation and culture of 'reconstructed' rainbow trout branchial epithelia. *Methods Cell Sci* 22:153-163.

Kelly SP, Wood CM. 2001. Effect of cortisol on the physiology of cultured pavement cell epithelia from freshwater trout gills. *Am J Physiol Regul Integr Comp Physiol* 281:R811-R820.

Kelly SP, Wood CM. 2002. Cultured gill epithelia from freshwater tilapia (*Oreochromis niloticus*): effect of cortisol and homologous serum supplements from stressed and unstressed fish. *J Membr Biol* 190:29-42.

Kiuchi-Saishin Y, Gotoh S, Furuse M, Takasuga A, Tano Y, Tsukita S. 2002. Differential expression patterns of claudins, tight junction membrane proteins, in mouse nephron segments. *J Am Soc Nephrol* 13:875-886.

Kollmar R, Nakamura SK, Kappler JA, Hudspeth AJ. 2001. Expression and phylogeny of claudins in vertebrate primordia. *Proc Natl Acad Sci USA* 98:10196-10201.

Lahlou B, Henderson IW, Sawyer WH. 1969. Sodium exchanges in goldfish (*Carassius auratus L.*) adapted to a hypertonic saline solution. *Comp Biochem Physiol* 28:1427-1433.

Larkin MA, Blackshields G, Brown NP, Chenna R, McGettigan PA, McWilliam H, Valentin F, Wallace IM, Wilm A, Lopez R, Thompson JD, Gibson TJ, Higgins DG. 2007. Clustal W and Clustal X version 2.0. *Bioinformatics* 23:2947-2948.

Li WY, Huey CL, Yu AS. 2004. Expression of claudin-7 and -8 along the mouse nephron. *Am J Physiol Renal Physiol* 286:F1063-1071.

Loh YH, Christoffels A, Brenner S, Hunziker W, Venkatesh B. 2004. Extensive expansion of the claudin gene family in the teleost fish, *Fugu rubripes*. *Genome Res* 14:1248-1257.

Markov AG, Veshnyakova A, Fromm M, Amasheh M, Amasheh S. 2010. Segmental expression of claudin proteins correlates with tight junction barrier properties in rat intestine. *J Comp Physiol B* 180:591-598.

Marshall WS, Emberley TR, Singer TD, Bryson SE, McCormick SD. 1999. Time course of salinity adaptation in a strongly euryhaline estuarine teleost, *Fundulus heteroclitus*: a multivariable approach. *J Exp Biol* 202:1535-1544.

McCormick SD. 2001. Endocrine control of osmoregulation in teleost fish. *Amer Zool* 41:781-794.

Milatz S, Krug SM, Rosenthal R, Günzel D, Müller D, Schulzke JD, Amasheh S, Fromm M. 2010. Claudin-3 acts as a sealing component of the tight junction for ions of either charge and uncharged solutes. *Biochim Biophys Acta* 1798:2048-2057.

Mommsen TP, Vijayan MM, Moon TW. 1999. Cortisol in teleosts: dynamics, mechanisms of action, and metabolic regulation. *Rev Fish Biol Fisher* 9:211-268.

Perry SF, Laurent P. 1989. Adaptational responses of rainbow trout to lowered external NaCl concentration: contribution of the branchial chloride cell. *J Exp Biol* 147:147-168.

Pottinger TG. 2010. A multivariate comparison of the stress response in three salmonid and three cyprinid species: evidence for inter-family differences. *J Fish Biol* 76:601-621.

Singer KL, Stevenson BR, Woo PL, Firestone GL. 1994. Relationship of serine/threonine phosphorylation/dephosphorylation signaling to glucocorticoid regulation of tight junction permeability and ZO-1 distribution in nontransformed mammary epithelial cells. *J Biol Chem* 269:16108-16115.

Singley JA, Chavin W. 1975. The adrenocortical-hypophyseal response to saline stress in the goldfish, *Carassius auratus L.* *Comp Biochem Physiol A Comp Physiol* 51:749-756.

Smith ME, Kane AS, Popper AN. 2004. Noise-induced stress response and hearing loss in goldfish (*Carassius auratus*). *J Exp Biol* 207:427-435.

Stelwagen K, McFadden HA, Demmer J. 1999. Prolactin, alone or in combination with glucocorticoids, enhances tight junction formation and expression of the tight junction protein occludin in mammary cells. *Mol Cell Endocrinol* 156:55-61.

Tipsmark CK, Kiilerich P, Nilsen TO, Ebbesson LOE, Stefansson SO, Madsen SS. 2008. Branchial expression patterns of claudin isoforms in Atlantic salmon during seawater acclimation and smoltification. *Am J Physiol Regul Integr Comp Physiol* 294:R1563-R1574.

Tipsmark CK, Jorgensen C, Brande-Lavridsen N, Engelund M, Olesen JH, Madsen SS. 2009. Effects of cortisol, growth hormone and prolactin on gill claudin expression in Atlantic salmon. *Gen Comp Endocrinol* 163:270-277.

Van Itallie CM, Fanning AS, Bridges A, Anderson JM. 2009. ZO-1 stabilizes the tight junction solute barrier through coupling to the perijunctional cytoskeleton. *Mol Biol Cell* 20:3930-3940.

Wood CM, Pärt P. 1997. Cultured branchial epithelia from freshwater fish gills. *J Exp Biol* 200:1047-1059.

Wood CM, Gilmour KM, Pärt P. 1998. Passive and active transport properties of a gill model, the cultured branchial epithelium of the freshwater rainbow trout (*Oncorhynchus mykiss*). *Comp Biochem Physiol A Mol Integr Physiol* 119:87-96.

Yu AS, Enck AH, Lencer WI, Schneeberger EE. 2003. Claudin-8 expression in Madin-Darby canine kidney cells augments the paracellular barrier to cation permeation. *J Biol Chem* 278:17350-17359.

Zettl KS, Sjaastad MD, Riskin PM, Parry G, Machen TE, Firestone GL. 1992. Glucocorticoid-induced formation of tight junctions in mouse mammary epithelial cells *in vitro*. *Proc Natl Acad Sci USA* 89:9069-9073.

CHAPTER 7:

EFFECTS OF ELEVATED CIRCULATING CORTISOL LEVELS ON HYDROMINERAL STATUS AND GILL TIGHT JUNCTION PROTEIN ABUNDANCE IN STENOHALINE GOLDFISH

Helen Chasiotis and Scott P. Kelly

Department of Biology, York University, Toronto, Ontario, Canada M3J 1P3

7.1 Abstract

A role for cortisol in the regulation of hydromineral balance and gill tight junction (TJ) protein transcript abundance in the stenohaline freshwater goldfish was investigated using intraperitoneal cortisol implants (50, 100, 200, 400 μg cortisol/g body weight) to dose-dependently elevate circulating cortisol levels over a four day period. Elevated cortisol did not significantly alter serum osmolality, serum Na^+ or muscle water content, however serum glucose and gill $\text{Na}^+\text{-K}^+\text{-ATPase}$ activity significantly increased and serum Cl^- levels significantly decreased when compared to control groups. Transcripts for glucocorticoid receptor 1 (GR1) and mineralocorticoid receptor (MR) in the gill remained unchanged by cortisol treatment, however glucocorticoid receptor 2 (GR2) mRNA was significantly down-regulated. Conversely, cortisol treatment significantly increased transcript and protein abundance of the TJ protein occludin in goldfish gill tissue, as well as mRNA encoding for claudin e, 7 and 8d. These claudins have previously been characterized as barrier-forming TJ proteins and goldfish tissue expression profiles demonstrated that all exhibit foremost abundance in the gill. Overall results suggest enhanced salt uptake by the gill as well as a “tightened” gill epithelium in response to elevated cortisol levels in the goldfish. These data support a role for cortisol in the endocrine regulation of hydromineral status and gill permeability of a stenohaline freshwater fish. However, reduced systemic Cl^- levels also suggest that sustained cortisol elevation in goldfish may have a detrimental effect on other ionoregulatory tissues.

7.2 Introduction

In vertebrate organisms, the tight junction (TJ) complex plays a fundamental role in the formation of epithelial and endothelial barriers (reviewed by González-Mariscal et al., 2003). Comprising networks of transmembrane and cytoplasmic proteins encircling the apical-most domain of cells, TJs assist in the maintenance of tissue homeostasis and function by regulating the paracellular movement of solutes across epithelia and endothelia. Transmembrane TJ proteins, such as occludin and members of the claudin superfamily, limit paracellular solute movement via homotypic and heterotypic associations with other transmembrane TJ proteins of adjacent cells (Nusrat et al., 2005; Krause et al., 2008). The diversity of claudins imparts selectivity to the paracellular barrier by allowing the formation of charge and/or size-selective paracellular pores within the TJ complex, and based on their distinct tissue-specific expression patterns, claudins are also believed to bestow the wide-ranging barrier properties exhibited by different types of epithelia and endothelia (reviewed by Krause et al., 2008). The cytoplasmic (or “scaffolding”) TJ proteins, such as ZO-1, anchor the transmembrane TJ proteins to the actin cytoskeleton to provide a basis for TJ assembly and structural stability, but also participate in signal transduction pathways involved in epithelial and endothelial cell proliferation, differentiation and gene expression (González-Mariscal et al., 2003).

The underlying endocrine pathways modulating TJ permeability and expression of components associated with the TJ complex are far from being fully understood, however corticosteroid-mediated alterations in the permeability of various mammalian epithelial and endothelial models are well documented. For example, corticosteroids have

been shown to elicit a clear “tightening” effect in association with alterations in TJ protein localization or TJ transcript and/or protein expression in cultured corneal epithelial cells (Kimura et al., 2011), mammary epithelial cell lines (Stelwagen et al., 1999; Singer et al., 1994; reviewed by Casey and Plaut, 2007), retinal endothelia (Antonetti et al., 2002; Felinski et al., 2008), endothelial cells of the blood-nerve-barrier (Kashiwamura et al., 2011) and brain endothelial cells (Romero et al., 2003; Förster et al., 2005; Förster et al., 2008). Furthermore, putative glucocorticoid-response elements within the promoter sequences of human occludin and murine claudin 5 genes have been identified and can induce the expression of occludin and claudin 5 transcripts respectively when activated by glucocorticoid treatment (Harke et al., 2008; Burek and Förster, 2009).

Cortisol, the principal corticosteroid and stress hormone in teleost fishes, has a well documented role in the regulation of salt and water balance in euryhaline fishes, and this is mediated in part by significant alterations in the structure and function of the gill epithelium (reviewed by Evans et al., 2005). During seawater (SW) or freshwater (FW) acclimation of euryhaline fishes, circulating cortisol levels have been shown to rapidly elevate and contribute to alterations in the growth and differentiation of gill ionocytes for salt secretion in a hyper-osmotic setting or ion uptake in a hypo-osmotic environment (Evans et al., 2005). Cortisol however has also been shown to alter the paracellular permeability characteristics of primary cultured gill epithelia (e.g. see Chapters 4 and 6; Kelly and Wood, 2001a, 2002; Bui et al., 2010; Kelly and Chasiotis, 2011). When treated with physiologically relevant doses of cortisol, cultured gill epithelia composed exclusively of gill pavement cells (PVCs) or both gill PVCs and mitochondria-rich cells

(MRCs) exhibit elevated transepithelial resistance (TER) and reduced flux to a radiolabeled paracellular marker in a dose-dependent manner, along with decreased unidirectional flux to Na⁺ and Cl⁻ (Kelly and Wood, 2001a, 2002; Wood et al., 2002). Correspondingly, in a cultured rainbow trout gill model, transcripts encoding for occludin and several claudins that have been characterized as “tightening” TJ proteins are up-regulated (see Chapters 4 and 6; Kelly and Chasiotis, 2011) and TJ depth, as revealed by transmission electron microscopy, is significantly increased (Sandbichler et al., 2011) in association with the cortisol-mediated reductions in permeability. In addition, alterations in TJ protein transcript abundance following cortisol treatment of primary cultured PVC epithelia derived from puffer fish (*Tetraodon nigroviridis*) and gill explants taken from Atlantic salmon have been reported (Tipsmark et al., 2009; Bui et al., 2010), as well as in gill tissue of cortisol-injected Atlantic salmon (Tipsmark et al., 2009). Taken together, these studies strongly suggest that cortisol may additionally enhance the function of the euryhaline gill during osmotic stress by “tightening” TJs between PVCs (cells which comprise over 90% of the gill epithelium) in order to limit passive salt gain or loss during SW or FW acclimation respectively.

In a recent study (see Chapter 6), a cultured PVC epithelium derived from stenohaline FW goldfish gills was demonstrated to exhibit significant but marginal changes in permeability in response to cortisol treatment. Furthermore, no alterations were observed in orthologous TJ protein transcripts that were previously shown to change in gill preparations from FW euryhaline species (e.g. rainbow trout, pufferfish, Atlantic salmon) (see Chapter 4 and 6; Tipsmark et al., 2009; Bui et al., 2010). It was therefore

postulated that the modest (or absent) response to cortisol in a cultured goldfish gill epithelium, as compared to other salt tolerant species, may relate to stenohalinity, such that goldfish are unable to effectively osmoregulate during hyper-osmotic stress in part because they cannot adequately respond to cortisol in order to adjust branchial permeability (see Chapter 6). In this regard, early studies examining goldfish acclimation to saline environments allude to a possible inability to limit diffusional salt influx despite elevated serum cortisol levels (Lahlou et al., 1969; Singley and Chavin, 1975). Therefore, in light of these observations, the objective of the current study was to investigate the effects of cortisol in FW stenohaline goldfish as it pertains to hydromineral status and gill permeability *in vivo*. Intraperitoneal cortisol implants were used to elicit a dose-dependent increase in circulating cortisol, following which endpoints of hydromineral status as well as alterations in gill TJ protein and TJ protein transcript abundance could be examined. The current *in vivo* study will enable a potential role (or lack thereof) for cortisol in regulating the permeability properties of the stenohaline goldfish gill to be further examined.

7.3 Materials and Methods

7.3.1 Experimental animals: Goldfish (*Carassius auratus*, 18 - 30 g) were obtained from a local supplier (Aleongs International, Mississauga, ON, Canada) and held in 200-L opaque polyethylene tanks supplied with flow-through dechlorinated FW (approximate composition in mM: [Na⁺] 0.59, [Cl⁻] 0.92, [Ca²⁺] 0.76, [K⁺] 0.043, pH 7.35) at 18 ± 1°C. Fish were fed *ad libitum* once daily with commercial koi and goldfish pellets (Martin Profishent, Elmira, ON, Canada).

7.3.2 Cortisol implantation and tissue collection: Goldfish were randomly separated into six groups and acclimated to conditions outlined above (see Section 7.3.1). Following a one week settling period, four groups of goldfish were administered intraperitoneal cortisol (hydrocortisone 21-hemisuccinate sodium salt; Sigma-Aldrich Canada Ltd., Oakville, ON, Canada) implants using coconut oil as a vehicle. Implants were administered in a manner similar to that described by Gregory and Wood (1999) and doses were selected based on circulating cortisol levels achieved in previous goldfish implantation studies (i.e. Bernier et al., 1999; Bernier et al., 2004). Briefly, individual goldfish were anaesthetized in 0.25 g/L tricaine methanesulfonate (MS-222; Syndel Laboratories Ltd., Qualicum Beach, BC, Canada), weighed and then placed on ice for ~ 30 sec prior to being given a single intraperitoneal injection (5 µL/g body weight) of 50, 100, 200 or 400 µg/g body weight of cortisol dissolved in warm (~ 28°C) coconut oil. Injections were administered at a site anterior and dorsal to the pelvic fin. Following injection, goldfish were left on ice for ~ 1 min to allow the coconut oil to solidify and were then returned to their original tanks. A fifth group of goldfish was sham implanted

with intraperitoneal injections (5 μ L/g body weight) of warm coconut oil only. A sixth group of goldfish remained untreated and received no injections. During the experimental period, goldfish were provided with pellets at a ration of 1.5% their body mass once daily. Four days following implantation, blood and tissue samples from goldfish were collected following rapid net capture and immersion in 1 g/L MS-222. Blood was promptly sampled (within ~ 2 min) from caudal vessels, allowed to clot (4°C for 1 h) and then centrifuged (10,600 g for 10 min at 4°C). The resulting serum was collected, frozen with liquid nitrogen and stored at – 80°C until further analysis. Following blood collection, fish were killed by spinal transection and gills were removed, frozen with liquid nitrogen and stored at – 80°C until further analysis for Na⁺-K⁺-ATPase activity. A standardized region of epaxial white muscle was also collected for analysis of muscle water content.

In a second experiment, using the same conditions and procedures described above, goldfish were randomly separated into three groups that received either sham or high cortisol dose (i.e. 400 μ g cortisol/g body weight) implants or remained untreated (no implants). Four days following implantation, untreated, sham and high cortisol dose implanted goldfish were sampled as previously described. Gills were removed, frozen with liquid nitrogen and stored at – 80°C until further processing for RNA extraction or western blotting.

7.3.3 Serum analysis, muscle water content and gill Na⁺-K⁺-ATPase enzyme activity: Goldfish serum cortisol levels were measured using a commercial cortisol enzyme immunoassay (EIA) kit (Cayman Chemical Company, Ann Arbor, Michigan, USA)

according to manufacturer's instructions. The EIA kit was validated for use with goldfish serum by generating parallelism curves using serial dilutions of serum collected from untreated and 400 µg cortisol/g body weight implanted goldfish (see Appendix A.2). Serum osmolality was determined using a Model 5500 vapor pressure osmometer (Wescor, Inc., Logan, UT, USA) and serum Na⁺ was measured by atomic absorption spectroscopy using an AAnalyst 200 spectrometer (PerkinElmer Life and Analytical Sciences, Woodbridge, ON, Canada). Serum Cl⁻ was determined using a colorimetric assay previously described by Zall et al. (1956) and serum glucose was measured using PGO Enzymes according to manufacturer's instructions (Sigma-Aldrich Canada Ltd.). To determine muscle water content, muscle tissue was weighed and then dried to a constant mass in an oven at 60°C. Gill Na⁺-K⁺-ATPase activity was determined using the methodology of McCormick (1993) with modifications as described in Chapter 2.

7.3.4 Sample collection for goldfish tissue expression profiles: Goldfish were randomly selected, anaesthetized using 1 g/L MS-222 and then killed by spinal transection. The following discrete goldfish tissues were removed, frozen in liquid nitrogen and stored at -80°C until further processing: brain, eye, gill, anterior gastrointestinal (aGI) tract, middle GI tract (mGI), posterior GI tract (pGI), liver, gallbladder, swimbladder, kidney and skin. Because the goldfish GI tract is not separated into morphologically distinct regions, the total length of the GI tract was measured and then cut into eight equal segments which were numbered as segments 1 – 8 (1 = anterior-most GI tract segment and 8 = posterior-most GI tract segment). Segments 1, 5 and 8 of the GI tract were designated as the aGI, mGI and pGI respectively.

7.3.5 RNA extraction and cDNA synthesis: Total RNA was isolated from goldfish tissues for expression profile studies, and gills from untreated, sham and high cortisol dose implanted goldfish using TRIzol[®] Reagent (Invitrogen Canada Inc., Burlington, ON, Canada) according to manufacturer's instructions. Extracted RNA was then treated with DNase I (Amplification Grade; Invitrogen Canada Inc.) and first-strand cDNA was synthesized using SuperScript[™] III Reverse Transcriptase and Oligo(dT)₁₂₋₁₈ primers (Invitrogen Canada Inc.).

7.3.6 Quantitative real-time PCR analysis: For expression profile studies, the mRNA abundance of the following TJ protein genes was analyzed in discrete goldfish tissues by quantitative real-time PCR analysis (qRT-PCR): claudin b, c, d, e, h, 7, 8d and 12, and ZO-1. For cortisol implantation studies, the mRNA abundance of the following TJ protein and corticosteroid receptor genes was examined in the gills of untreated, sham and high cortisol dose implanted goldfish by qRT-PCR: occludin, claudin b, c, d, e, h, 7, 8d and 12, ZO-1, glucocorticoid receptor 1 (GR1), glucocorticoid receptor 2 (GR2) and mineralocorticoid receptor (MR). qRT-PCR was performed using SYBR Green I Supermix (Bio-Rad Laboratories Canada Ltd.), a Chromo4[™] Detection System (CFB-3240; Bio-Rad Laboratories Canada Ltd.) and primer sets described in Chapters 5 and 6. The following qRT-PCR reaction conditions were used: 1 cycle denaturation (95°C, 4 min), followed by 40 cycles of denaturation (95°C, 30 sec), annealing (51 - 61°C, 30 sec) and extension (72°C, 30 sec) respectively. A melting curve was carried out after each qRT-PCR run to ensure that a single product was synthesized during reactions. For all qRT-PCR analyses, mRNA abundance was normalized to either β -actin transcript

abundance (for tissue expression profiles) or elongation factor 1-alpha (EF1 α) transcript abundance (for cortisol implantation studies). Goldfish β -actin mRNA was amplified using primers previously described in Chapter 5. Primers for goldfish EF1 α (forward: 5' CAAGAAAATCGGCTACAACC 3' and reverse: 5' CAAAGGTCACAACCATACCAG 3', amplicon size: 308 bp) were designed based on GenBank accession number AB056104.

7.3.7 Western blotting: Occludin and β -actin protein abundance was examined in the gills of untreated, sham and high cortisol dose implanted goldfish by western blot analysis according to procedures outlined in Chapter 2, and using 75 μ g of gill protein from each fish sampled, a 1:1,000 dilution of a rabbit polyclonal anti-occludin antibody (Zymed laboratories, Inc.) and a 1: 50,000 dilution of mouse monoclonal anti- β -actin antibody (Sigma-Aldrich Canada Ltd.). Occludin and β -actin protein abundance were quantified using a Molecular Imager Gel Doc XR+ System and Quantity One 1D analysis software (Bio-Rad Laboratories Canada Ltd.). Occludin protein abundance was expressed as a normalized value relative to β -actin protein abundance.

7.3.8 Statistical analysis: All data are expressed as mean values \pm s.e.m. (n), where n represents the number of fish sampled. A one-way analysis of variance (ANOVA) followed by a Student-Newman-Keuls test was used to determine significant differences ($P < 0.05$) between groups. Statistical analyses were conducted using SigmaStat 3.5 software (Systat Software Inc., San Jose, CA, USA).

7.4 Results

7.4.1 Effects of cortisol implants on goldfish serum cortisol, glucose and ion levels, muscle water content and gill Na⁺-K⁺-ATPase activity: Goldfish that received sham implants (coconut oil only) had serum cortisol levels that were not significantly different from untreated (no implant) fish (i.e. 32±15 versus 24±10 ng/mL). Cortisol implantation (for four days) elevated goldfish serum cortisol levels in a dose dependent manner, however only the 200 and 400 µg cortisol/g body weight implanted fish showed serum cortisol levels that were significantly elevated relative to controls (i.e. untreated and sham groups) (Fig. 7-1). For serum ion and glucose levels, muscle water content and gill Na⁺-K⁺-ATPase enzyme activity analyses, the untreated group did not significantly differ from the sham implant group (Fig. 7-2). Additionally, serum osmolality and muscle water content were not significantly affected by any of the cortisol implant doses tested (Fig. 7-2A, E). Although not quite statistically significant (P = 0.0596), serum Na⁺ levels appeared to slightly decline with increasing cortisol implant dose (Fig. 7-2B). The two highest cortisol implant doses however significantly decreased serum Cl⁻ levels relative to untreated and sham implant groups (Fig. 7-2C). Furthermore, serum glucose levels were significantly elevated by all cortisol implant doses tested when compared to control levels (Fig. 7-2D). Only the highest cortisol implant dose (i.e. 400 µg cortisol/g body weight) significantly elevated gill Na⁺-K⁺-ATPase activity relative to control groups (Fig. 7-2F).

7.4.2 Goldfish tissue expression profiles for TJ protein transcripts: Using qRT-PCR analysis, claudin and ZO-1 mRNA expression patterns in various goldfish tissues were

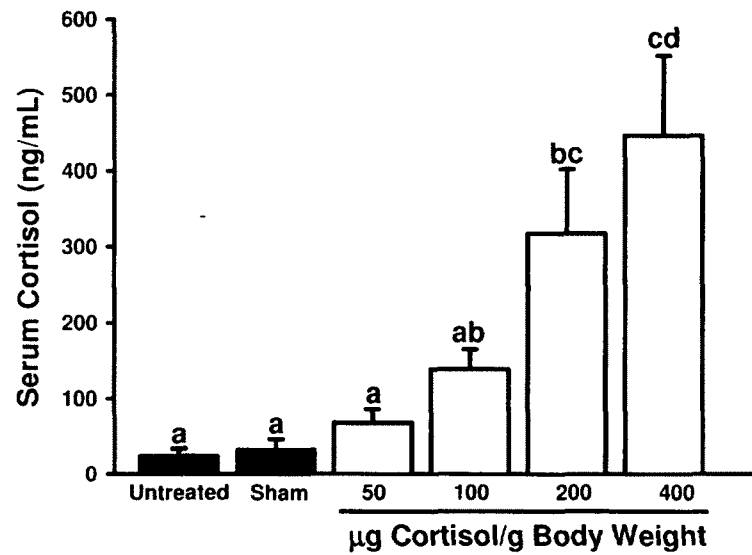


Figure 7-1: Dose-dependent effects of cortisol implants on goldfish serum cortisol levels. Goldfish were implanted intraperitoneally with four doses of cortisol (i.e. 50, 100, 200, 400 µg cortisol/g body weight) using coconut oil as the implant vehicle. Sham implanted goldfish received implants containing coconut oil only, while untreated goldfish received no implants. Serum was collected four days post-implantation. Data are expressed as mean values \pm s.e.m. ($n = 6-7$). Different lowercase letters denote significant differences ($P < 0.05$) between groups.

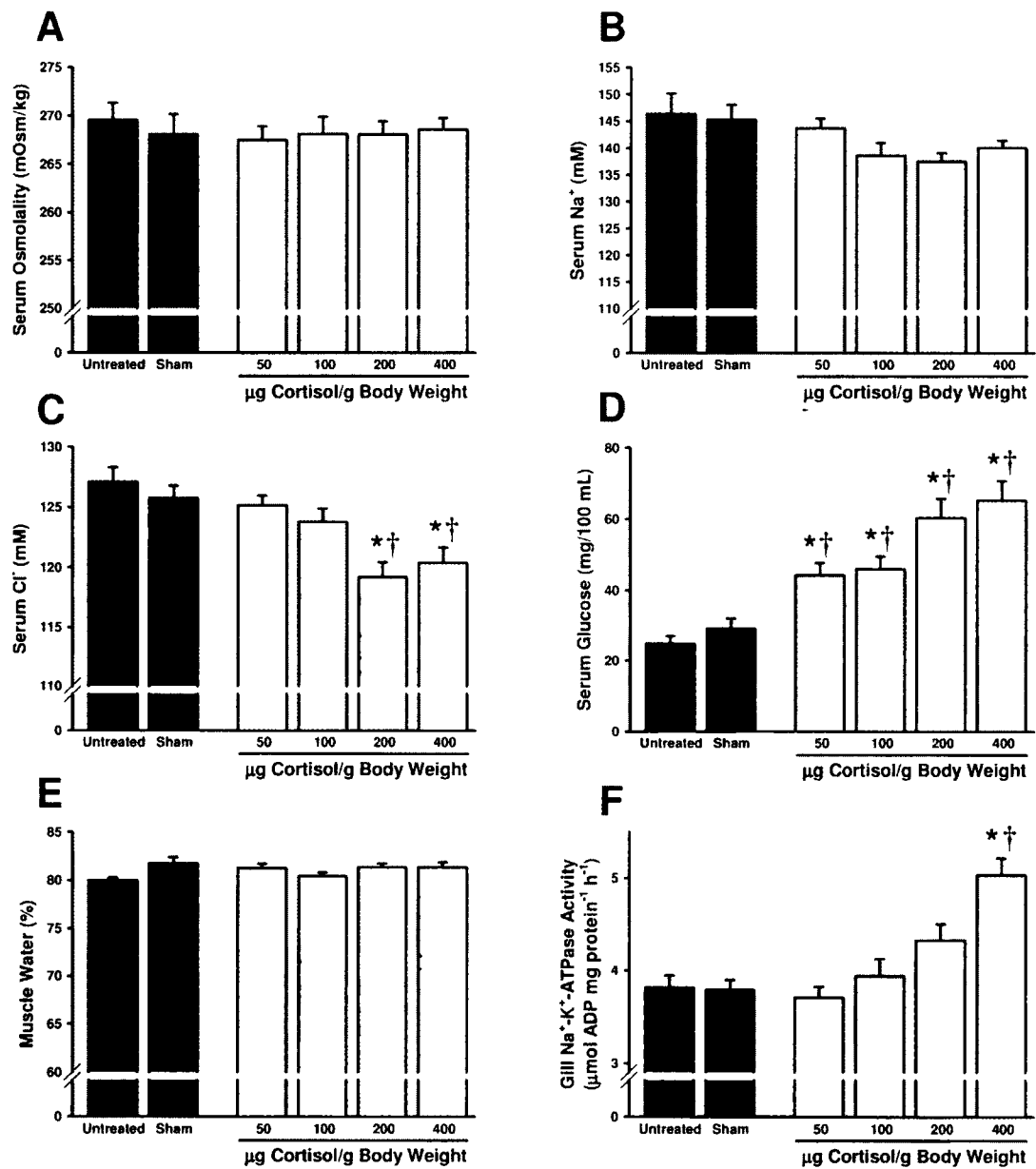


Figure 7-2: Effect of elevated circulating cortisol levels on goldfish (A) serum osmolality, (B) serum Na⁺, (C) serum Cl⁻, (D) serum glucose, (E) muscle water content and (F) gill Na⁺-K⁺-ATPase activity. Data are expressed as mean values ± s.e.m. (*n* = 28-32). * Significant difference (*P* < 0.05) from untreated group. † Significant difference (*P* < 0.05) from sham group.

examined. Goldfish claudin transcripts were widely but differentially expressed in discrete goldfish tissues (Fig. 7-3). Claudin b, e, h, 7 and 8d transcript abundance was highest in the goldfish gill (Fig. 7-3A, D, E, F, G). Conversely, claudin c and d were least abundant in the gill (Fig. 7-3B, C). Claudin c however was notably most abundant within tissues of the goldfish GI tract and kidney (Fig. 7-3B). Claudin 12 transcript was ubiquitously expressed at more or less similar levels amongst all goldfish tissues examined except for the brain and liver (Fig. 7-3H). Similarly, ZO-1 mRNA was also ubiquitously expressed in goldfish tissues, however slightly greater transcript abundance was detected in the brain, gallbladder and swimbladder (Fig. 7-3I). β -actin mRNA abundance, which was used to normalize claudin and ZO-1 mRNA abundance in goldfish tissue expression profiles, was not significantly different between the tissues examined ($P = 0.6299$)

7.4.3 Effects of a high cortisol implant dose on corticosteroid receptor and TJ protein mRNA abundance and occludin protein abundance in goldfish gills: Since alterations in hydromineral endpoints and enzyme activity occurred only in goldfish implanted with a high cortisol dose, receptor and TJ protein transcript abundance were analyzed in gills collected from untreated, sham and 400 μ g cortisol/g body weight implanted goldfish only. Corticosteroid receptor (i.e. GR1, GR2, MR) mRNA abundance in the gills of goldfish that received sham implants was not significantly different from the untreated group (Table 7-1). Although gill GR1, GR2 and MR mRNA abundance appeared to decrease in the high cortisol dose implant (i.e. 400 μ g cortisol/g body weight) group when compared to controls (i.e. untreated and sham groups), only the reduction in GR2

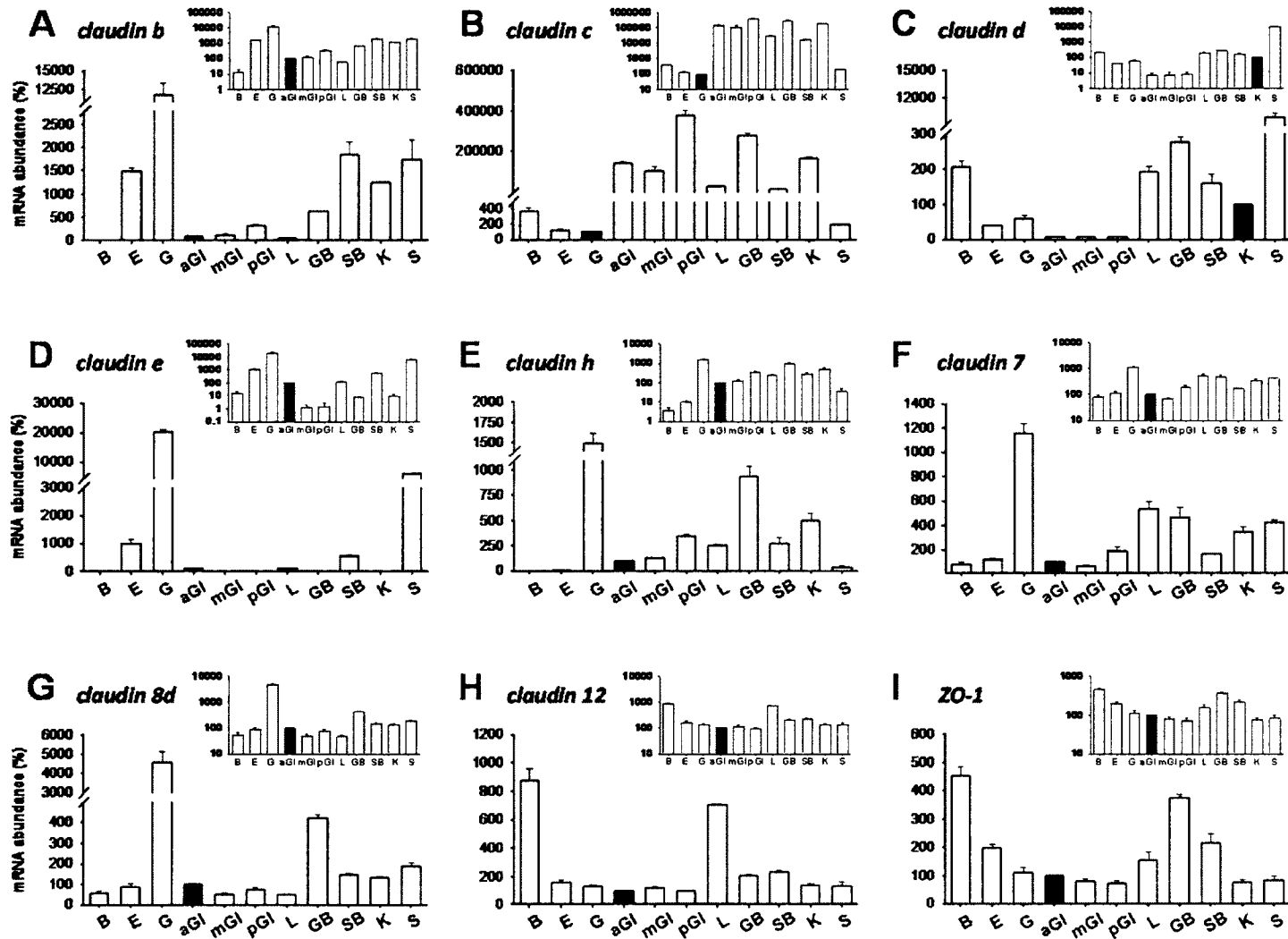


Figure 7-3: (see legend on next page)

Figure 7-3: qRT-PCR generated mRNA expression profiles for (A) claudin b, (B) claudin c, (C) claudin d, (D) claudin e, (E) claudin h, (F) claudin 7, (G) claudin 8d, (H) claudin 12 and (I) ZO-1 in discrete goldfish tissues. Inset graphs show data re-expressed on a semi-logarithmic scale. Claudin and ZO-1 transcript abundance were normalized to β -actin mRNA abundance, and mRNA abundance in each tissue was expressed relative to the tissue indicated by the solid bar which was assigned a value of 100%. Data are expressed as mean values \pm s.e.m. ($n = 3-4$). B, brain; E, eye; G, gill; aGI, anterior GI tract; mGI, middle GI tract; pGI, posterior GI tract; L, liver; GB, gallbladder; SB, swimbladder; K, kidney; S, skin.

Table 7-1: Effects of elevated circulating cortisol levels on corticosteroid receptor mRNA abundance in goldfish gills

Receptor	Untreated	Sham	Cortisol
GR1	100 ± 11.6	96.4 ± 11.2	71.7 ± 8.5
GR2	100 ± 14.0	93.9 ± 11.0	60.0 ± 7.0*
MR	100 ± 10.9	108.7 ± 10.6	74.4 ± 7.2

Data are expressed as mean values ± s.e.m. (*n* = 6-8). Corticosteroid receptor mRNA abundance was normalized to EF1 α transcript abundance, and mRNA data were expressed relative to transcript abundance for the untreated group which was assigned a value of 100. Note: cortisol group = 400 μ g cortisol/g body weight implant group. * Significant difference (*P* < 0.05) from untreated and sham groups.

mRNA abundance was statistically significant ($P = 0.038$) (Table 7-1).

For all gill TJ protein transcripts examined, mRNA abundance did not differ between control groups (Fig. 7-4). Furthermore, high cortisol dose implants had no effect on the mRNA abundance of claudin b, c, d, h and 12, and ZO-1 in the gill when compared to controls (Fig. 7-4). Occludin, claudin e, 7 and 8d mRNA abundance however was significantly elevated in the gills of the high cortisol dose implant group when compared to untreated and sham fish (Fig. 7-4). Correspondingly, occludin protein abundance in untreated and sham implanted goldfish gills did not differ, however gills from the high cortisol dose implanted group exhibited significantly elevated occludin protein abundance relative to the gills of controls (Fig. 7-5). EF1 α mRNA abundance was used to normalize corticosteroid receptor and TJ protein transcript data and did not significantly alter ($P = 0.2845$) in response to sham and cortisol implantation. Similarly, β -actin protein was used to normalize occludin protein abundance and was not significantly altered ($P = 0.7242$) by implantation procedures or cortisol treatment.

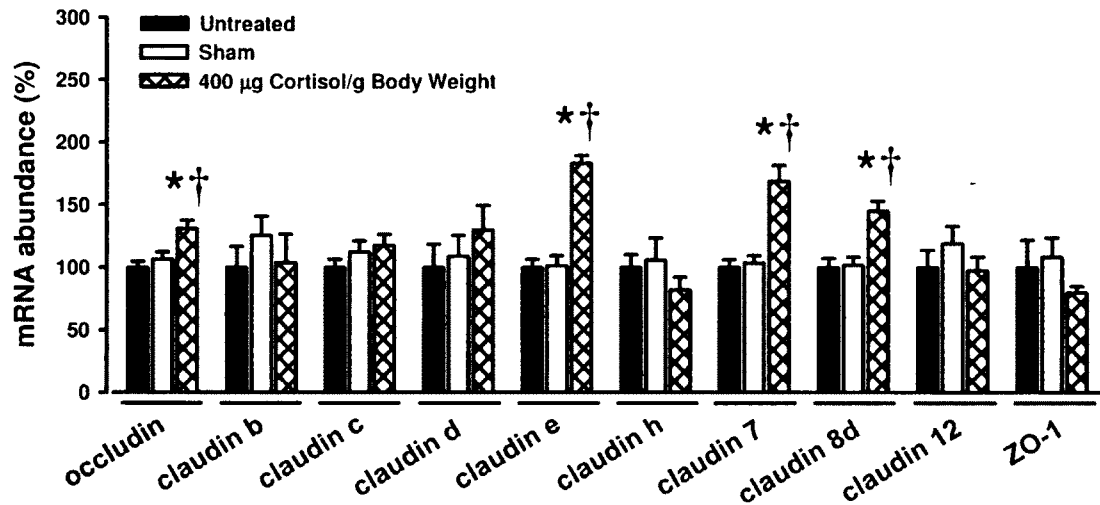


Figure 7-4: Effect of elevated circulating cortisol levels on TJ protein mRNA abundance in goldfish gills. TJ protein transcript abundance was normalized to EF1 α mRNA abundance, and mRNA data were expressed relative to transcript abundance for the untreated group which was assigned a value of 100%. Data are expressed as mean values \pm s.e.m. ($n = 8$). * Significant difference ($P < 0.05$) from untreated group. † Significant difference ($P < 0.05$) from sham group.

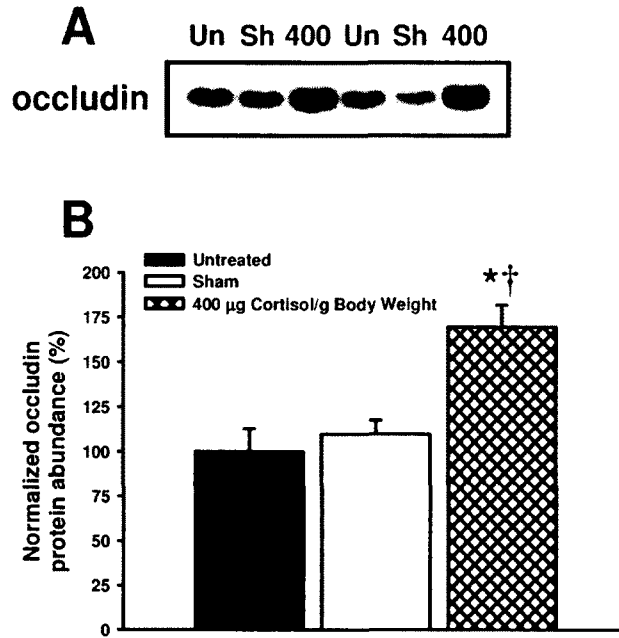


Figure 7-5: Effect of elevated circulating cortisol levels on occludin protein abundance in goldfish gills. (A) shows a representative western blot where occludin immunoreactivity can be observed at ~ 68 kDa. Note: Un = untreated group, Sh = sham implant group, 400 = 400 µg cortisol/g body weight implant group. (B) presents occludin protein abundance normalized to β -actin protein abundance, and expressed relative to the untreated group which was assigned a value of 100%. Data are expressed as mean values \pm s.e.m. ($n = 17$). * Significant difference ($P < 0.05$) from untreated group. † Significant difference ($P < 0.05$) from sham group.

7.5 Discussion

The present study examined the effects of elevated circulating cortisol levels on the hydromineral status of stenohaline FW goldfish, as well as endpoints of branchial permeability (i.e. alterations in TJ transcript and protein abundance). Results demonstrate that the cortisol implantation methods utilized in this study can effectively elevate goldfish serum cortisol levels to within the physiological range of stressed cyprinids (i.e. ~ 70 - 450 ng/ml; see Pottinger, 2010) with no apparent effect of the implantation procedure itself on circulating cortisol (see Fig. 7-1) or other parameters examined (Fig. 7-2, 7-4, 7-5). Correspondingly, all cortisol implant doses tested resulted in hyperglycemia (Fig. 7-2D), a response often elicited by elevated cortisol levels in teleost fishes, including goldfish (Umminger and Gist, 1973; reviewed by Mommsen et al., 1999).

Of the ten TJ protein genes examined in goldfish gills, only four showed altered transcript levels in response to cortisol implantation. Occludin mRNA and protein, and claudin e, 7 and 8d transcripts were all significantly elevated in the gills of cortisol-treated goldfish (Fig. 7-4, 7-5). Tissue expression profiles in this study (Fig. 7-3D, F, G) as well as in a previous report (see Chapter 5) show that transcripts encoding for all four of these TJ proteins are predominantly found in the gills of goldfish. This is consistent with the dominant abundance of these TJ constituents in the gills of other fish species (see Chapter 4; Loh et al., 2004; Bagherie-Lachidan et al., 2009; Tipsmark et al., 2008; Clelland and Kelly, 2010; Kumai et al., 2011) and suggests that these TJ proteins play an important role in the regulation of gill permeability. In addition, numerous studies have

characterized occludin and claudin e, 7 and 8d orthologs as barrier-forming TJ proteins in vertebrates (e.g. see Chapters 2, 3 4 and 6; Yu et al., 2003; Feldman et al., 2005; Hou et al., 2006; Bagherie-Lachidan et al., 2009; Chasiotis and Kelly, 2009). Up-regulation of these TJ transcripts, as observed in this study, therefore suggests a “tightened” gill epithelium. In support of this idea, cortisol has previously been reported to significantly increase claudin e mRNA abundance in association with a significant reduction in paracellular permeability in a primary cultured goldfish gill epithelium (see Chapter 6), and this is consistent with a cortisol-induced elevation in the mRNA abundance of claudin 28b (a claudin e ortholog) and reduction in paracellular permeability across a cultured gill epithelial model from trout (see Chapter 6; Kelly and Chasiotis, 2011). In addition, cortisol-mediated elevations in gill occludin mRNA and protein abundance (see Chapters 4 and 6), as well as claudin 7 and 8d transcripts in association with reductions in epithelial permeability have previously been reported in cultured PVCs from FW rainbow trout (see Chapters 4 and 6; Kelly and Chasiotis, 2011). However, occludin, claudin 7 and 8d were not significantly elevated following *in vitro* cortisol treatment of cultured goldfish gill epithelia (see Chapter 6). A possible explanation for this latter discrepancy is that the molecular components of the goldfish gill TJ complex may be more responsive to elevated cortisol *in vivo* due to the presence of endogenous endocrine factors that enhance the actions of this corticosteroid. In this regard, corticosteroid-induced alterations in the form and function of fish gills have previously been documented to be altered when other endocrine factors are simultaneously present and/or elevated (e.g. Bindon et al., 1994; McCormick, 1996). Furthermore, in cultured gill epithelia,

corticosteroid-induced alterations in the permeability properties of preparations have been reported to be altered in the presence of hormones such as 3,5',3'-triiodo-L-thyronine (Kelly and Wood, 2001b) and prolactin (Zhou et al., 2004).

Despite previous observations of cortisol-induced reductions in the paracellular permeability of goldfish gill epithelia (see Chapter 6), and strong evidence in the current study suggesting that elevated cortisol levels reduce the paracellular permeability of goldfish gills *in vivo*, the overall balance of hydromineral endpoints (i.e. circulating electrolytes such as Na^+ and Cl^- , serum osmolality, muscle water content and gill Na^+ - K^+ -ATPase) does not provide an unequivocal picture of how reduced gill permeability aids salt and water balance in the stenohaline goldfish. More specifically, serum osmolality and Na^+ levels as well as muscle water content do not significantly alter in response to cortisol treatment. However, goldfish implanted with the two highest cortisol doses exhibited significantly declined serum Cl^- levels (Fig. 7-2C). In addition, gill Na^+ - K^+ -ATPase, which is presumed to be a major driving force behind salt uptake by FW gill MRCs, exhibited significantly elevated activity in high cortisol dose implanted goldfish (Fig. 7-2F). Based on available literature, the effect of cortisol on the salt and water status of stenohaline FW teleosts appears to vary. For example, serum osmolality and ion levels have been shown to either increase, decrease or remain unaltered following exogenous cortisol treatment in species of catfish, common carp and goldfish (Umminger and Gist, 1973; De Boeck et al., 2001; Eckert et al., 2001; Sherwani and Parwez, 2008; Babitha and Peter, 2010). The reasons for these inconsistencies are unclear, but likely relate to differences among species or reflect different treatment periods, sampling regimes,

methods used for cortisol administration (i.e. injections vs. diet), or the composition of the FW used for holding fishes. Nevertheless, in the current study, hypochloremia in cortisol-injected goldfish is consistent with the observations of Umminger and Gist (1973), and elevated gill $\text{Na}^+\text{-K}^+\text{-ATPase}$ in high cortisol dose implanted goldfish is in line with previous reports of elevated gill $\text{Na}^+\text{-K}^+\text{-ATPase}$ activity in other species of stenohaline and euryhaline FW fishes treated with cortisol (e.g. De Boeck et al., 2001; Eckert et al., 2001; Metz et al., 2003; Sherwani and Parwez, 2008; Babitha and Peter, 2010; see Evans et al., 2005 for review). Therefore, taken together with the alterations observed in TJ protein and TJ protein mRNA abundance, elevated gill $\text{Na}^+\text{-K}^+\text{-ATPase}$ activity suggests that in the gills of goldfish, cortisol not only stimulates a restructured epithelium with respect to reduced paracellular ion loss (see discussion above), but also alters transcellular transport processes in order to enhance active ion acquisition. In this regard, cortisol administration has been reported to elevate whole body Na^+ and Cl^- uptake in correlation with increased gill MRC fractional area in several species of FW fish, including FW stenohaline catfish (Perry et al., 1992). Furthermore, enhanced gill MRC fractional area has been shown to result in an increase in ion uptake across the gills of goldfish acclimated to an artificial ion-poor environment (Chang et al., 2002). However, if these observations are juxtaposed with reduced serum Cl^- levels in this study, it would appear that despite enhanced hyper-osmoregulatory function in gill tissue, four days of high circulating levels of cortisol may be having a deleterious effect on other epithelia where ion loss or reduced ion uptake/re-absorption could potentially occur (e.g. across the kidney, gut or skin). This contention is supported by the recent observations of

Babitha and Peter (2010), who reported that cortisol-injected catfish exhibited significantly decreased renal Na⁺-K⁺-ATPase activity in conjunction with decreased Na⁺ levels and elevated gill Na⁺-K⁺-ATPase activity, thus offering the possibility of salt loss due to cortisol-mediated reductions in salt re-absorption by the kidney followed by compensatory uptake of salt by the gill. Therefore, further studies that examine the effects of cortisol on other osmoregulatory organs that contribute to Na⁺ and Cl⁻ homeostasis in goldfish would be revealing.

To investigate the effect of elevated circulating cortisol levels on corticosteroid receptors of the gill, GR1, GR2 and MR transcript abundance was examined in cortisol-implanted goldfish. All corticosteroid receptor transcripts examined in the goldfish gill showed a slight decline in abundance (Table 7-1), suggesting a negative autoregulatory response to cortisol. These observations are in line with previous studies in the gills of cortisol-treated coho salmon (Maule and Schreck, 1991; Shrimpton and Randall, 1994). Negative autoregulation of corticosteroid receptors is believed to dampen the potentially maladaptive effects of chronic stress on physiological processes such growth, immune function and hydromineral status (Barton, 2002). Interestingly, transactivation analyses of rainbow trout GRs have characterized GR2 as having greater sensitivity to cortisol when compared to GR1 (Bury et al., 2003). In the present study, only transcript encoding for goldfish GR2 was significantly down-regulated in response to cortisol (Table 7-1), suggesting that goldfish GR2 may also be more sensitive to cortisol than goldfish GR1.

To summarize, cortisol implants were used to investigate the effects of elevated circulating cortisol on hydromineral status and TJ transcript and protein abundance in the

gills of goldfish, a stenohaline FW fish model. Elevated cortisol levels appeared to have no significant effect on overall hydromineral status as determined by measurements of serum osmolality, Na^+ and muscle water content. However, serum Cl^- levels were significantly reduced despite increased gill Na^+ - K^+ -ATPase activity and elevations in occludin and claudin transcripts that have been characterized as “tightening” TJ proteins. Clearly, cortisol plays a complex role in the endocrine regulation of paracellular permeability across the teleost gill. Although studies conducted to date allude to species-specific differences in cortisol-mediated alterations of gill permeability and TJ proteins, there is still a significant paucity of information in this area. Future studies in a wider scope of teleosts would certainly provide greater insight into the species-specific differences in the endocrine regulation of gill permeability that could relate to the environmental physiology of euryhaline versus stenohaline fishes.

7.6 References

Antonetti DA, Wolpert EB, DeMaio L, Harhaj NS, Scaduto Jr RC. 2002. Hydrocortisone decreases retinal endothelial cell water and solute flux coincident with increased content and decreased phosphorylation of occludin. *J Neurochem* 80:667-677.

Babitha GS, Peter MCS. 2010. Cortisol promotes and integrates the osmotic competence of the organs in North African catfish (*Clarias gariepinus* Burchell): Evidence from *in vivo* and *in situ* approaches. *Gen Comp Endocrinol* 168:14-21.

Bagherie-Lachidan M, Wright SI, Kelly SP. 2009. Claudin-8 and -27 tight junction proteins in puffer fish *Tetraodon nigroviridis* acclimated to freshwater and seawater. *J Comp Physiol B* 179:419-431.

Barton BA. 2002. Stress in fishes: A diversity of responses with particular reference to changes in circulating corticosteroids. *Integr Comp Biol* 42:517-525.

Bernier NJ, Lin X, Peter RE. 1999. Differential expression of corticotropin-releasing factor (CRF) and urotensin I precursor genes, and evidence of CRF gene expression regulated by cortisol in goldfish brain. *Gen Comp Endocrinol* 116:461-477.

Bernier NJ, Bedard N, Peter RE. 2004. Effects of cortisol on food intake, growth, and forebrain neuropeptide Y and corticotropin-releasing factor gene expression in goldfish. *Gen Comp Endocrinol* 135:230-240.

Bindon SD, Fenwick JC, Perry SF. 1994. Branchial chloride cell proliferation in the rainbow trout, *Oncorhynchus mykiss*: implications for gas transfer. *Can J Zool* 72:1395-1402.

Bui P, Bagherie-Lachidan M, Kelly SP. 2010. Cortisol differentially alters claudin isoforms in cultured puffer fish gill epithelia. *Mol Cell Endocrinol* 317:120-126.

Burek M, Förster C. 2009. Cloning and characterization of the murine claudin-5 promoter. *Mol Cell Endocrinol* 298:19-24.

Bury NR, Sturm A, Le Rouzic P, Lethimonier C, Ducouret B, Guiguen Y, Robinson-Rechavi M, Laudet V, Rafestin-Oblin ME, Prunet P. 2003. Evidence for two distinct functional glucocorticoid receptors in teleost fish. *J Mol Endocrinol* 31:141-156.

Casey TM, Plaut K. 2007. The role of glucocorticoids in secretory activation and milk secretion, a historical perspective. *J Mammary Gland Biol Neoplasia* 12:293-304.

Chang IC, Lee TH, Wu HC, Hwang PP. 2002. Effects of environmental Cl⁻ levels on Cl⁻ uptake and mitochondria-rich cell morphology in gills of the stenohaline goldfish, *Carassius auratus*. *Zool Stud* 41:236-243.

Chasiotis H, Kelly SP. 2009. Occludin and hydromineral balance in *Xenopus laevis*. *J Exp Biol* 212:287-296.

Clelland ES, Kelly SP. 2010. Tight junction proteins in zebrafish ovarian follicles: stage specific mRNA abundance and response to 17 β -estradiol, human chorionic gonadotropin, and maturation inducing hormone. *Gen Comp Endocrinol* 168:388-400.

De Boeck G, Vlaeminck A, Balm PH, Lock RA, De Wachter B, Blust R. 2001. Morphological and metabolic changes in common carp, *Cyprinus carpio*, during short-term copper exposure: interactions between Cu²⁺ and plasma cortisol elevation. *Environ Toxicol Chem* 20:374-81.

Eckert SM, Yada T, Shepherd BS, Stetson MH, Hirano T, Grau EG. 2001. Hormonal control of osmoregulation in the channel catfish *Ictalurus punctatus*. *Gen Comp Endocrinol* 122:270-286.

Evans DH, Piermarini PM, Choe KP. 2005. The multifunctional fish gill: dominant site of gas exchange, osmoregulation, acid-base regulation, and excretion of nitrogenous waste. *Physiol Rev* 85:97-177.

Feldman GJ, Mullin JM, Ryan MP. 2005. Occludin: structure, function and regulation. *Adv Drug Deliv Rev* 57:883-917.

Felinski EA, Cox AE, Phillips BE, Antonetti DA. 2008. Glucocorticoids induce transactivation of tight junction genes occludin and claudin-5 in retinal endothelial cells via a novel cis-element. *Exp Eye Res* 86:867-878.

Förster C, Silwedel C, Golenhofen N, Burek M, Kietz S, Mankertz J, Drenckhahn D. 2005. Occludin as direct target for glucocorticoid-induced improvement of blood-brain barrier properties in a murine *in vitro* system. *J Physiol* 565:475-486.

Förster C, Burek M, Romero IA, Weksler B, Couraud PO, Drenckhahn D. 2008. Differential effects of hydrocortisone and TNF α on tight junction proteins in an *in vitro* model of the human blood-brain barrier. *J Physiol* 586:1937-1949.

González-Mariscal L, Betanzos A, Nava P, Jaramillo BE. 2006. Tight junction proteins. *Prog Biophys Mol Biol* 81:1-44.

Gregory TR, Wood CM. 1999. The effects of chronic plasma cortisol elevation on the feeding behaviour, growth, competitive ability, and swimming performance of juvenile rainbow trout. *Physiol Biochem Zool* 72:286-295.

Harke N, Leers J, Kietz S, Drenckhahn D, Förster C. 2008. Glucocorticoids regulate the human occludin gene through a single imperfect palindromic glucocorticoid response element. *Mol Cell Endocrinol* 295:39-47.

Hou J, Gomes AS, Paul DL, Goodenough DA. 2006. Study of claudin function by RNA interference. *J Biol Chem* 281:36117-36123.

Kashiwamura Y, Sano Y, Abe M, Shimizu F, Haruki H, Maeda T, Kawai M, Kanda T. 2011. Hydrocortisone enhances the function of the blood-nerve barrier through the up-regulation of claudin-5. *Neurochem Res* 36:849-855.

Kelly SP, Chasiotis H. 2011. Glucocorticoid and mineralocorticoid receptors regulate paracellular permeability in a primary cultured gill epithelium. *J Exp Biol* 214:2308-2318.

Kelly SP, Wood CM. 2001a. Effect of cortisol on the physiology of cultured pavement cell epithelia from freshwater trout gills. *Am J Physiol Regul Integr Comp Physiol* 281:R811-R820.

Kelly SP, Wood CM. 2001b. The physiological effects of 3,5',3'-triiodo-L-thyronine alone or combined with cortisol on cultured pavement cell epithelia from freshwater rainbow trout gills. *Gen Comp Endocrinol* 123:280-294.

Kelly SP, Wood CM. 2002. Cultured gill epithelia from freshwater tilapia (*Oreochromis niloticus*): effect of cortisol and homologous serum supplements from stressed and unstressed fish. *J Membr Biol* 190:29-42.

Kimura K, Teranishi S, Kawamoto K, Nishida T. 2011. Protective effect of dexamethasone against hypoxia-induced disruption of barrier function in human corneal epithelial cells. *Exp Eye Res* 92:388-393.

Krause K, Winkler L, Mueller SL, Haseloff RF, Piontek J, Blasig IE. 2008. Structure and function of claudins. *Biochim Biophys Acta* 1778:631-645.

Kumai Y, Bahubeshi A, Steele S, Perry SF. 2011. Strategies for maintaining Na⁺ balance in zebrafish (*Danio rerio*) during prolonged exposure to acidic water. *Comp Biochem Physiol A Mol Integr Physiol* 160:52-62.

Lahlou B, Henderson IW, Sawyer WH. 1969. Sodium exchanges in goldfish (*Carassius auratus L.*) adapted to a hypertonic saline solution. *Comp Biochem Physiol* 28:1427-1433.

Loh YH, Christoffels A, Brenner S, Hunziker W, Venkatesh B. 2004. Extensive expansion of the claudin gene family in the teleost fish *Fugu rubripes*. *Genome Res* 14:1248-1257.

Maule AG, Schreck CB. 1991. Stress and cortisol treatment changed affinity and number of glucocorticoid receptors in leukocytes and gill of coho salmon. *Gen Comp Endocrinol* 84:83-93.

McCormick SD. 1993. Methods for nonlethal gill biopsy and measurement of Na⁺, K⁺-ATPase activity. *Can J Fish Aquat Sci* 50:656-658.

McCormick SD. 1996. Effects of growth hormone and insulin-like growth factor I on salinity tolerance and gill Na⁺,K⁺-ATPase in Atlantic salmon (*Salmo salar*): interaction with cortisol. *Gen Comp Endocrinol* 101:3-11.

Metz JR, van den Burg EH, Wendelaar Bonga SE, Flik G. 2003. Regulation of branchial Na⁺/K⁺-ATPase in common carp *Cyprinus carpio L.* acclimated to different temperatures. *J Exp Biol* 206:2273-2280.

Mommsen TP, Vijayan MM, Moon TW. 1999. Cortisol in teleosts: dynamics, mechanisms of action, and metabolic regulation. *Rev Fish Biol Fisher* 9:211-268.

Nusrat A, Brown GT, Tom J, Drake A, Bui TT, Quan C, Mrsnys RJ. 2005. Multiple protein interactions involving proposed extracellular loop domains of the tight junction protein occludin. *Mol Biol Cell* 16:1725-1734.

Perry SF, Goss GG, Laurent P. 1992. The interrelationships between gill chloride cell morphology and ionic uptake in four freshwater teleosts. *Can J Zool* 70:1775-1786.

Pottinger TG. 2010. A multivariate comparison of the stress response in three salmonid and three cyprinid species: evidence for inter-family differences. *J Fish Biol* 76:601-621.

Romero IA, Radewicz K, Jubin E, Michel CC, Greenwood J, Couraud PO, Adamson P. 2003. Changes in cytoskeletal and tight junctional proteins correlate with decreased permeability induced by dexamethasone in cultured rat brain endothelial cells. *Neurosci Lett* 344:112-116.

Sandbichler AM, Farkas J, Salvenmoser W, Pelster B. 2011. Cortisol affects tight junction morphology between pavement cells of rainbow trout gills in single-seeded insert culture. *J Comp Physiol B* (In Press).

Sherwani FA, Parwez I. 2008. Plasma thyroxine and cortisol profiles and gill and kidney Na^+/K^+ -ATPase and SDH activities during acclimation of the catfish *Heteropneustes fossilis* (bloch) to higher salinity, with special reference to the effects of exogenous cortisol on hypo-osmoregulatory ability of the catfish. *Zoolog Sci* 25:164-71.

Shrimpton JM, Randall DJ. 1994. Downregulation of corticosteroid receptors in gills of coho salmon due to stress and cortisol treatment. *Am J Physiol Regul Integr Comp Physiol* 267:R432-R438.

Singer KL, Stevenson BR, Woo PL, Firestone GL. 1994. Relationship of serine/threonine phosphorylation/dephosphorylation signaling to glucocorticoid regulation of tight junction permeability and ZO-1 distribution in non-transformed mammary epithelial cells. *J Biol Chem* 269:16108-16115.

Singley JA, Chavin W. 1975. The adrenocortical–hypophyseal response to saline stress in the goldfish *Carassius auratus L.* *Comp Biochem Physiol A Comp Physiol* 51:749–756.

Stelwagen K, McFadden HA, Demmer J. 1999. Prolactin alone or in combination with glucocorticoids enhances tight junction formation and expression of the tight junction protein occludin in mammary cells. *Mol Cell Endocrinol* 156:55-61.

Tipsmark CK, Kiilerich P, Nilsen TO, Ebbesson LOE, Stefansson SO, Madsen SS. 2008. Branchial expression patterns of claudin isoforms in Atlantic salmon during seawater acclimation and smoltification. *Am J Physiol Regul Integr Comp Physiol* 294:R1563-R1574.

Tipsmark CK, Jorgensen C, Brande-Lavridsen N, Engelund M, Olesen JH, Madsen SS. 2009. Effects of cortisol, growth hormone and prolactin on gill claudin expression in Atlantic salmon. *Gen Comp Endocrinol* 163:270-277.

Umminger BL, Gist DH. 1973. Effects of thermal acclimation on physiological responses to handling stress, cortisol and aldosterone injections in the goldfish, *Carassius auratus*. *Comp Biochem Physiol A Comp Physiol* 44:967-977.

Wood CM, Kelly SP, Zhou B, Fletcher M, O'Donnell M, Eletti B, Pärt P. 2002. Cultured gill epithelia as models for the freshwater fish gill. *Biochim Biophys Acta* 1566:72-83.

Yu AS, Enck AH, Lencer WI, Schneeberger EE. 2003. Claudin-8 expression in Madin-Darby canine kidney cells augments the paracellular barrier to cation permeation. *J Biol Chem* 278:17350-17359.

Zall DM, Fisher D, Garner MD. 1956. Photometric determination of chlorides in water. *Anal Chem* 28:1665-1678.

Zhou B, Kelly SP, Ianowski JP, Wood CM. 2003. Effects of cortisol and prolactin on Na⁺ and Cl⁻ transport in cultured branchial epithelia from FW rainbow trout. *Am J Physiol Regul Integr Comp Physiol* 285:R1305-R1316.

CHAPTER 8:

**PERMEABILITY PROPERTIES OF THE GOLDFISH GILL
EPITHELIUM UNDER ION-POOR CONDITIONS**

Helen Chasiotis, Dennis Kolosov and Scott P. Kelly

Department of Biology, York University, Toronto, Ontario, Canada M3J 1P3

8.1 Abstract

Permeability properties of the goldfish gill epithelium were examined *in vivo* and *in vitro* following exposure to ion-poor water (IPW) conditions. In gill tissue of IPW-acclimated goldfish, transcript abundance of tight junction (TJ) proteins occludin, claudin b, d, e, h, 7 and 8d increased, while claudin 12 and ZO-1 decreased, and claudin c was unaltered. This occurred in association with an increase in TJ depth between pavement cells (PVCs). To examine the PVC specific response of TJ transcripts, the PVC fraction of the goldfish gill epithelium was isolated using Percoll™. Transcripts encoding for occludin, claudin b, c, d, e, h, 7, 8d and 12, and ZO-1 were all present in the PVC fraction, and mRNA encoding for occludin, claudin b, e and 8d, and ZO-1 significantly increased in PVCs isolated from IPW-acclimated goldfish. To examine a functional relationship between PVC TJ molecular physiology and measurements of epithelial permeability, primary cultured goldfish PVC epithelia were exposed to homologous IPW-acclimated goldfish serum. Supplementation of cultured gill epithelia with IPW goldfish serum elevated transepithelial resistance, reduced paracellular [³H]PEG-4000 permeability and enhanced epithelial integrity following *in vitro* exposure to apical IPW. In addition, increased mRNA abundance of occludin, claudin e and h were observed *in vitro*. These studies demonstrate the PVC-specific response of TJ proteins to IPW in goldfish gill epithelia and support the idea that TJ proteins play an important role in regulating gill permeability in IPW.

8.2 Introduction

The teleost fish gill is an architecturally complex multifunctional organ composed of a heterogeneous epithelium overlying a rich vasculature (Wilson and Laurent, 2002). It is directly exposed to the surrounding medium of water and presents a large surface area across which gas exchange, ion and acid/base balance as well as nitrogenous waste elimination takes place. In this regard, the fish gill epithelium functions as a complex and pivotal transport site, and has evolved a broad-spectrum of transport mechanisms for the balance and maintenance of gradients (concentration/electrochemical) between fluid compartments of enormously different composition (i.e. blood versus a fluctuating aquatic environment). In fishes that reside in freshwater (FW), the gill epithelium contributes to the maintenance of hydromineral balance by actively acquiring ions from the surrounding water and restricting passive (obligatory) ion loss. Mechanisms of ion acquisition are complex and occur through the transcellular pathway which has been the focal point of numerous studies (for review see Evans et al., 2005; Hwang et al., 2011). In contrast, considerably less is known about the regulation of passive ion loss across the gill epithelium of FW fishes. However, it is broadly acknowledged that passive ion efflux occurs primarily through the paracellular pathway of FW fish gills, and that ion loss is held in check by the properties and components of the epithelial tight junction (TJ) complex (Marshall and Grosell, 2005).

The TJ complex forms the principal barrier to the passive paracellular movement of solutes across vertebrate epithelia (González-Mariscal et al., 2003). It is composed of transmembrane and cytoplasmic TJ proteins, however the overall composition of the

transmembrane component appears to play a crucial role in determining the permeability properties of the paracellular pathway. Variations in the composition of TJ complexes occur primarily due to heterogeneity in the distribution and abundance of claudin transmembrane TJ proteins. In mammals there are ~ 24 claudin proteins (Krause et al., 2008) and in fishes, as many as 56 genes encoding for claudin proteins have been described (Loh et al., 2004). Furthermore, select claudins are reported to be barrier-forming while others seem to possess pore-forming characteristics (Krause et al., 2008). In contrast to most claudins, the transmembrane TJ protein occludin is ubiquitously expressed in vertebrate epithelia and its abundance can vary considerably between tissues (Chapters 4 and 5; Saitou et al., 1997; Feldman et al., 2005). Given that increased occludin abundance is strongly associated with decreased epithelial permeability (Feldman et al., 2005), this protein also appears to play an important role in regulating the barrier properties of the vertebrate epithelium.

A role for TJ proteins in regulating the permeability properties of the fish gill epithelium has recently been proposed. For example, alterations in the mRNA abundance of select claudin isoforms have been reported in whole gill tissue taken from euryhaline fishes acclimated to FW or seawater (SW) (Bagherie-Lachidan et al., 2008, 2009; Duffy et al., 2011; Tipsmark et al., 2008; Whitehead et al., 2011). Furthermore, hormone-induced alterations in occludin and claudin transcript/protein abundance have been described in association with alterations in the paracellular permeability of primary cultured gill epithelia (Chapters 4 and 6; Kelly and Chasiotis, 2011). However to date, no study has attempted to directly relate measured changes in permeability and TJ molecular

physiology of gill epithelia *in vitro* with the molecular physiology of TJs within the gill epithelium *in vivo*. To address this, a series of experiments was conducted to examine the properties and TJ molecular physiology of the goldfish gill epithelium exposed to ion-poor water (IPW) conditions *in vivo* and *in vitro*. Acclimation of fishes (including goldfish) to IPW has been reported to result in a very significant reduction in ion efflux rates across the gills (Cuthbert and Maetz, 1972; Perry and Laurent, 1989). This presumably occurs, at least in part, by means of a TJ-mediated reduction in paracellular permeability. Reduced gill permeability in IPW would curb ion loss in surroundings that not only limit ion acquisition but also significantly increase ion concentration gradients between the internal and external environment. In this regard, recent studies provide evidence to support the idea that gill TJ proteins perform an important physiological role in the regulation of ionoregulatory homeostasis in IPW. More specifically, occludin abundance is significantly increased in goldfish gill tissue (Chapter 3), and transcripts encoding for claudin 3a, 3c and 27a are elevated in the gills of a FW puffer fish (*Tetraodon biocellatus*; Duffy et al., 2011) following acclimation to IPW. In this latter study, changes in the molecular components of the TJ complex occurred in association with increased TJ depth between gill epithelial cells (Duffy et al., 2011). Therefore, by directly comparing the effects of IPW conditions on the molecular physiology of gill TJs *in vivo* and *in vitro*, significant insight into the importance of TJ proteins in gill tissue and ionoregulatory homeostasis in FW teleost fishes can be attained.

8.3 Materials and Methods

8.3.1 Experimental animals: Stock goldfish (*Carassius auratus*, 25-30 g) were obtained from a local supplier (Aleongs International, Mississauga, ON, Canada) and held in 60-L glass tanks supplied with flow-through dechlorinated FW (approximate composition in μM : $[\text{Na}^+]$ 590, $[\text{Cl}^-]$ 920, $[\text{Ca}^{2+}]$ 760, $[\text{K}^+]$ 43, pH 7.35). Water temperature was maintained at $20\pm 1^\circ\text{C}$ for goldfish utilized in IPW acclimation experiments (see Sections 8.3.2.1 and 8.3.4.1) or $25\pm 1^\circ\text{C}$ for goldfish used in the preparation of primary cultured gill epithelia (see Section 8.3.4.2). Fish were held under a simulated natural photoperiod of 12h light:12h dark and fed *ad libitum* once daily with commercial koi and goldfish pellets (Martin Profishent, Elmira, ON, Canada).

8.3.2 Isolation and separation of gill cells from FW and IPW-acclimated goldfish

8.3.2.1 Acclimation of goldfish to IPW: Stock goldfish were randomly transferred into 240-L opaque polyethylene tanks and maintained under FW conditions identical to those outlined above (see Section 8.3.1). After a 1 week settling period, goldfish were introduced to ion-poor conditions by gradually replacing FW with IPW over a 24 h period. The approximate composition of IPW (in μM) was as follows: $[\text{Na}^+]$ 20, $[\text{Cl}^-]$ 40, $[\text{Ca}^{2+}]$ 2, $[\text{K}^+]$ 0.4, pH 6.5. To confirm that ion-poor conditions were in fact achieved and maintained throughout the acclimation period, Cl^- concentrations in the IPW tank were periodically monitored using the colorimetric assay described by Zall et al. (1956). As a control, a second group of goldfish were held under the initial FW holding conditions described above (see Section 8.3.1). All goldfish were provided with pellets at a ration of

2% their body mass once daily and sacrificed for gill cell isolation and separation (see Section 8.3.2.2) following at least two weeks of acclimation to FW or IPW conditions.

8.3.2.2 Goldfish gill cell isolation and separation: Methods for goldfish gill cell isolation and separation were based on procedures for rainbow trout gills, detailed by Goss et al. (2001) and Galvez et al. (2002), with modifications described below. Briefly, goldfish gills were perfused through the bulbus arteriosus with a 0.8% saline solution to remove blood cells, following which all eight gill arches were excised from the fish. One arch was immediately frozen with liquid nitrogen and stored at -80°C until further processing for RNA extraction (see Section 8.3.5), while a second arch was fixed in 2.5% glutaraldehyde for transmission electron microscopy (TEM) (see Section 8.3.3). The remaining six arches were washed (3 x 10 min at 4°C) in phosphate-buffered saline (PBS; 137 mM NaCl, 8.1 mM Na₂HPO₄, 2.68 mM KCl, 1.47 mM KH₂PO₄, pH 7.7), and then gill cells were isolated from gill filaments using four consecutive cycles of digestion (8 min each) at room temperature (RT) with 0.1 mg/ml collagenase (Sigma-Aldrich Canada Ltd., Oakville, ON, Canada) and continuous circular agitation. At the end of each 8 min collagenase cycle, cells were filtered through a 100 µm cell strainer to yield a mixed population of isolated gill cells. This total cell isolate was then centrifuged (500 g for 10 min at 4°C), re-suspended in PBS and placed over a stacked three-stage discontinuous Percoll® (Sigma-Aldrich Canada Ltd.) gradient consisting of a 1.03 g/ml top layer, a 1.06 g/ml middle layer and a 1.13 g/ml the bottom layer. The stacked cell suspension was then centrifuged (2000 g for 45 min at 4°C) and an inter-phase fraction of

putative gill pavement cells (PVCs) was collected in TRIzol Reagent® (Invitrogen Canada Inc.) and stored at -80°C for RNA extraction (see Section 8.3.5).

The purity of the inter-phase PVC fraction was confirmed by mitochondrial staining. Briefly, a small sample of the inter-phase cell fraction was taken just prior to collection for RNA extraction and stained with the mitochondria specific dye Mitotracker® Deep Red FM (100 nM for 20 min at RT; Invitrogen Canada Inc., Burlington, ON, Canada). The stained cells then were centrifuged (500 g, 10 min at RT), re-suspended and fixed with 3% paraformaldehyde (20 min at RT), centrifuged once more, resuspended in PBS, mounted on glass slides and then examined using a Reichert Polyvar microscope (Reichert Microscope services, Depew, NY, USA).

8.3.3 Electron microscopy and gill cell morphometrics

8.3.3.1 TEM: Goldfish gill tissues collected from FW and IPW-acclimated goldfish (see Section 8.3.2.2) were fixed in 2.5% glutaraldehyde (4 hours at RT) for TEM. Subsequent tissue preparation and procedures for TEM followed those described in Chapter 5. TEM samples were examined using a Philips EM 201 transmission electron microscope (Philips, Eindhoven, NB, Netherlands), and images were captured on film and scanned using Adobe Photoshop CS2 software (Adobe Systems Canada, Toronto, ON, Canada).

8.3.3.2 PVC morphometrics: The depth of TJ complexes formed by adjacent PVCs (PVC-PVC) was measured using ten TEM images of different gill filaments from each FW and IPW-acclimated fish sampled. TJ depth was defined as the distance between the apical-most point of the cell-to-cell junction and the beginning of the adherens junction. Morphometric measurements were performed using ImageJ software.

8.3.4 Supplementation of cultured goldfish gill epithelia with homologous serum

8.3.4.1 Preparation of homologous serum: Goldfish serum (GFS) was obtained from a separate stock of fish (80-200 g) that were acclimated to FW or IPW conditions as detailed in Sections 8.3.1 and 8.3.2.1. Following at least two weeks of FW or IPW acclimation, goldfish were quickly net captured and blood was rapidly sampled (within ~ 2 min) by caudal puncture. Blood samples that were collected from several fish within an acclimation group (i.e. FW or IPW) were pooled and then allowed to clot for 30 min at RT prior to centrifugation (3220 g for 10 min at 4°C). Resulting serum from FW or IPW-acclimated goldfish was collected and sterilized by passing once through a 0.2 µm filter and then stored at -30°C as single-use aliquots.

8.3.4.2 Preparation of primary cultured goldfish gill epithelia: Procedures for goldfish gill cell isolation and the primary culture of goldfish gill epithelia, composed of PVCs only, were conducted according to the methods described in Chapter 5. Briefly, isolated goldfish gill cells were initially cultured in flasks with Leibovitz's L-15 culture medium supplemented with 2 mM L-glutamine (L15) and 6% fetal bovine serum (FBS) in an air atmosphere at 27°C. At confluence (~ 2 days in culture), cells were harvested from flasks by trypsination and seeded into cell culture inserts (polyethylene terephthalate filters, 0.9 cm² growth area, 0.4 µm pore size, 1.6 x 10⁶ pore/cm² pore density; BD Falcon TM, BD Biosciences, Mississauga, ON, Canada).

8.3.4.3 Transepithelial resistance (TER) and [³H]PEG-4000 permeability: Measurements of TER were conducted using chopstick electrodes (STX-2) connected to a custom-modified EVOM epithelial voltohmmeter (World Precision Instruments, Sarasota, FL,

USA). All TER measurements are expressed as $k\Omega\text{cm}^2$ after correcting for TER measured across “blank” culture inserts bathed with appropriate media. Paracellular permeability across cultured epithelia was determined using the paracellular marker [^3H]polyethylene glycol (molecular mass 4000 Da; PEG-4000; PerkinElmer, Woodbridge, ON, Canada) according to methods and calculations previously described by Wood et al. (1998).

8.3.4.4 Supplementation with homologous goldfish serum: Cultured goldfish gill epithelia (prepared in Section 8.3.4.2) were allowed to develop in inserts under symmetrical culture conditions (i.e. with FBS-supplemented L15 bathing both apical and basolateral surfaces of epithelial preparations). When TER measurements were $\sim 50\text{-}100 \Omega\text{cm}^2$ above background levels, inserts were randomly separated into three groups. Using thawed GFS aliquots (prepared in Section 8.3.4.1), two groups of inserts were cultured under symmetrical conditions in L15 media supplemented with either 10% FW-acclimated GFS (FW serum group) or 10% IPW-acclimated GFS (IPW serum group) in place of FBS. A third control group was cultured under symmetrical conditions with 10% FBS-supplemented L15 media (FBS group). Once control and GFS supplemented preparations had developed a stable plateau in TER (at ~ 20 h post-serum change), [^3H]PEG-4000 permeability was measured over a 4 h flux period. Epithelia were then collected (at ~ 24 h) and stored at -80°C for RNA extraction (see Section 8.3.5). When the effects of asymmetrical culture conditions were tested in combination with homologous serum supplementation, FW and IPW GFS and FBS-treated gill preparations were first allowed to develop stable TER under symmetrical conditions (as described

above). Apical media were then replaced with temperature-equilibrated sterile FW or IPW after several careful rinses to ensure the complete removal of residual medium. FW and IPW were sterilized by passing through a 0.2 µm filter and were the same composition as the holding water detailed in Sections 8.3.1 and 8.3.2.1. Control and GFS supplemented preparations were held under asymmetrical culture conditions for 3 h, during which TER and [³H]PEG-4000 flux across epithelia were measured.

8.3.5 RNA extraction and cDNA synthesis: Total RNA was isolated from whole goldfish gill tissue, PVC fractions, and cultured goldfish gill epithelia using TRIzol Reagent® (Invitrogen Canada Inc.) according to manufacturer's instructions. Extracted RNA was treated with DNase I (Amplifications Grade, Invitrogen Canada, Inc.) and then first-strand cDNA was synthesized using SuperScript™ III Reverse Transcriptase and Oligo(dT)₁₂₋₁₈ primers (Invitrogen Canada, Inc.).

8.3.6 Quantitative real-time PCR analysis: Transcript abundance of the following TJ genes were analyzed in whole goldfish gill tissue, PVC fractions and cultured goldfish gill epithelia using quantitative real-time PCR (qRT-PCR): occludin, claudin b, c, d, e, h, 7, 8d and 12, and ZO-1. qRT-PCR was performed using SYBR Green I Supermix (Bio-Rad Laboratories Canada Ltd., Mississauga, ON, Canada), primer sets described in Chapters 5 and 6, and a Chromo4™ Detection System (CFB-3240; Bio-Rad Laboratories Canada Ltd.). The following reaction conditions were used: 1 cycle denaturation (95°C, 4 min), followed by 40 cycles of denaturation (95°C, 30 sec), annealing (51-61°C, 30 sec) and extension (72°C, 30 sec) respectively. To ensure that a single PCR product was synthesized during reactions, a melting curve was carried out after each qRT-PCR run.

For all qRT-PCR analyses, TJ protein mRNA abundance was normalized to either β -actin or elongation factor 1-alpha (EF1 α) transcript abundance. Goldfish β -actin and EF1 α mRNA were amplified using primers previously described in Chapters 5 and 7 respectively.

8.3.7 Statistical analysis: All data are expressed as mean values \pm s.e.m. (n), where n represents the number of fish sampled (Figs. 8-1, 8-2 and 8-3) or the number of inserts sampled (Figs. 8-4, 8-5 and 8-6). A Student's t -test was used to determine significant differences ($P < 0.05$) between groups (Figs. 8-1, 8-2 and 8-3). Where appropriate (Figs. 8-4, 8-5 and 8-6), significant differences ($P < 0.05$) were also determined using an analysis of variance (ANOVA) followed by a Student-Newman-Keuls test. All statistical analyses were conducted using SigmaStat 3.5 software (Systat Software Inc., San Jose, CA, USA).

8.4 Results

8.4.1 Effects of IPW acclimation on TJ mRNA abundance and PVC-PVC TJ depth in whole goldfish gill tissue: Of the ten TJ protein genes examined in whole goldfish gill tissue, nine genes showed altered transcript abundance in response to IPW acclimation when compared to levels in the gills of FW-acclimated fish. Occludin, claudin b, d, e, h, 7 and 8d mRNA abundance was significantly elevated, and claudin 12 and ZO-1 were significantly reduced in the gills of IPW-acclimated goldfish (Fig. 8-1). Claudin c transcript abundance was unchanged by IPW acclimation (Fig. 8-1). β -actin mRNA abundance was used to normalize TJ protein transcript data and was not significantly altered ($P = 0.127$) by IPW acclimation.

TEM images were used to measure PVC-PVC TJ depth in response to IPW acclimation. PVC-PVC TJ depth was significantly elevated (~ 2-fold) in IPW-acclimated goldfish gills relative to gills from FW-acclimated fish (Fig. 8-2).

8.4.2 Isolation and separation of goldfish gill PVCs: Goldfish gills were perfused with saline to prevent contamination of cell fractions with blood cells. Examination of total cell isolates confirmed the absence of blood cells (not shown). Procedures were found to yield a pure inter-phase fraction that contains 99.4% PVCs as determined by Mitotracker® staining (not shown).

8.4.3 Effects of IPW acclimation on TJ protein mRNA abundance in isolated goldfish gill PVCs: TJ protein transcript abundance was analyzed by qRT-PCR in PVC fractions isolated from FW and IPW-acclimated goldfish gills. Occludin, claudin b, e and 8d, and ZO-1 mRNA abundance was significantly elevated in PVC fractions in response to IPW

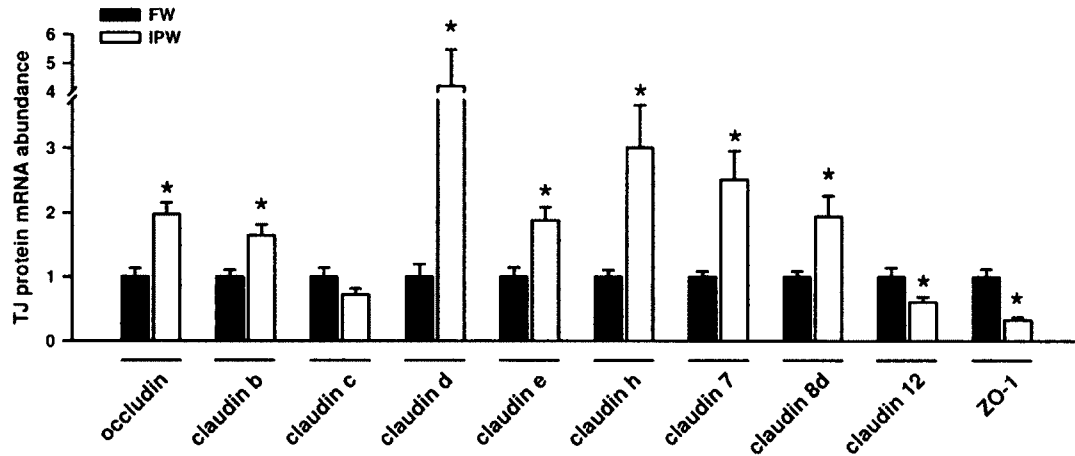


Figure 8-1: Effect of ion-poor water (IPW) acclimation on tight junction (TJ) protein mRNA abundance in goldfish gills. TJ protein transcript abundance was normalized to β -actin mRNA abundance, and mRNA data were expressed relative to transcript abundance for the freshwater (FW) group which was assigned a value of 1.0. Data are expressed as mean values \pm s.e.m. ($n = 9-13$). * Significant difference ($P < 0.05$) from the FW group.

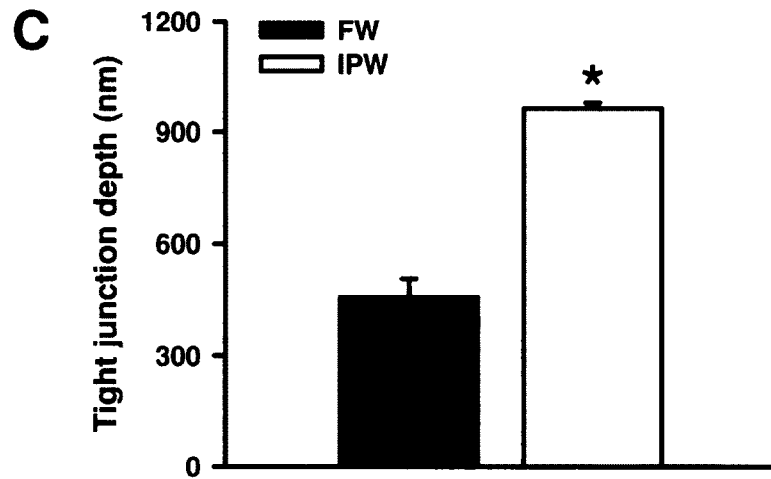
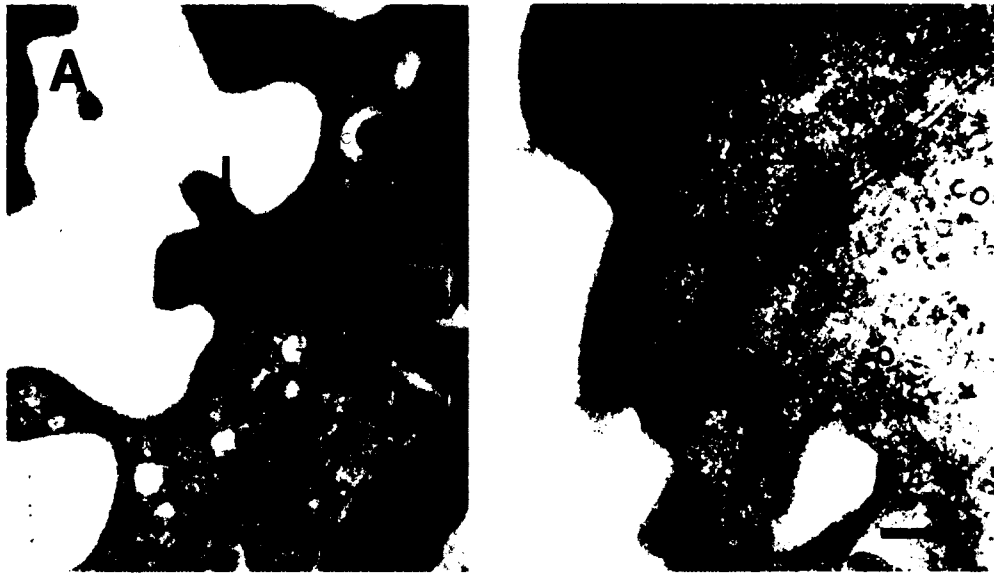


Figure 8-2: Transmission electron microscope (TEM) images of tight junctions (TJs) between pavement cells (PVCs) in the gills of goldfish acclimated to (A) freshwater (FW) and (B) ion-poor water (IPW). (C) Measurements of TJ depth between adjacent PVCs in the gills of goldfish acclimated to FW and IPW. Data are expressed as mean values \pm s.e.m. ($n = 4$). * Significant difference ($P < 0.05$) from the FW group. Black arrows denote the deepest point of the TJ complex. Scale bars = 500 nm.

acclimation (Fig. 8-3). Claudin c, d, h, 7 and 12 transcript abundance was unchanged in the PVC fraction of IPW-acclimated goldfish gills (Fig. 8-3). IPW acclimation did not significantly alter ($P = 0.202$) EF1 α transcript abundance in PVC fractions.

8.4.4 Effects of GFS from FW and IPW-acclimated goldfish on the permeability properties and TJ protein mRNA abundance of cultured goldfish gill epithelia:

Supplementation of cultured goldfish gill epithelia, comprising PVCs only, with homologous serum (harvested from either FW or IPW-acclimated goldfish) significantly elevated TER and reduced [^3H]PEG-4000 flux when compared to gill preparations supplemented with FBS (Fig. 8-4). Furthermore, TER was significantly increased and [^3H]PEG-4000 permeability was significantly decreased in the IPW serum group relative to the FW serum group (Fig. 8-4).

Occludin, claudin e, h and 8d mRNA abundance was significantly elevated in GFS supplemented cultured gill epithelia when compared to those supplemented with FBS (Fig. 8-5). Furthermore, occludin and claudin e and h transcript abundance was significantly increased in the IPW serum group relative to the FW serum group (Fig. 8-5). Conversely, claudin d and ZO-1 mRNA abundance was significantly decreased in both FW and IPW serum groups when compared to the FBS group (Fig. 8-5). Claudin b, c, 7 and 12 transcript abundance was unaffected by homologous serum supplementation (Fig. 8-5). EF1 α mRNA abundance was used to normalize TJ protein transcript data and was not significantly altered ($P = 0.262$) by GFS supplementation.

8.4.5 Effects of apical FW and IPW exposure on the permeability properties of cultured goldfish gill epithelia supplemented with serum from FW and IPW-acclimated goldfish:

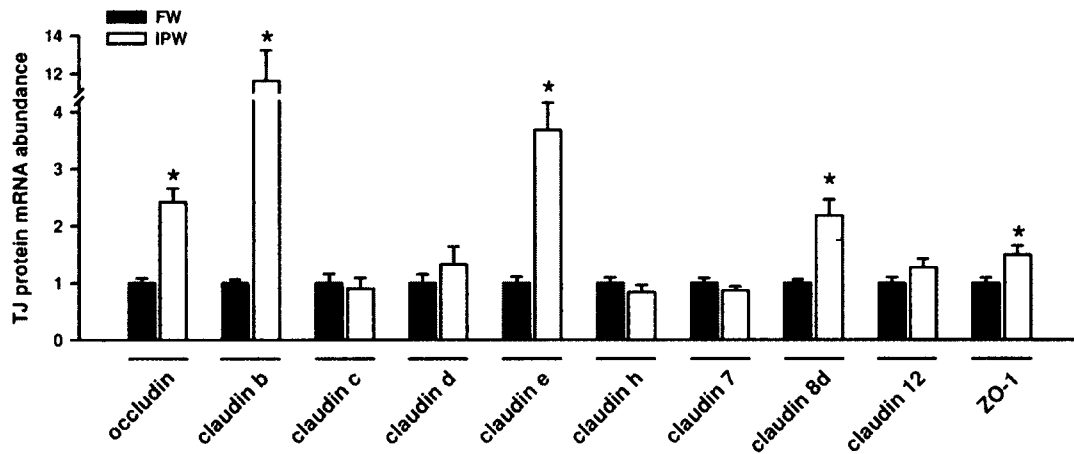


Figure 8-3: Effect of ion-poor water (IPW) acclimation on tight junction (TJ) protein mRNA abundance in pavement cells (PVCs) isolated from goldfish gills. TJ protein transcript abundance was normalized to EF1 α mRNA abundance, and mRNA data were expressed relative to transcript abundance for the freshwater (FW) group which was assigned a value of 1.0. Data are expressed as mean values \pm s.e.m. ($n = 13-15$). * Significant difference ($P < 0.05$) from the FW group.

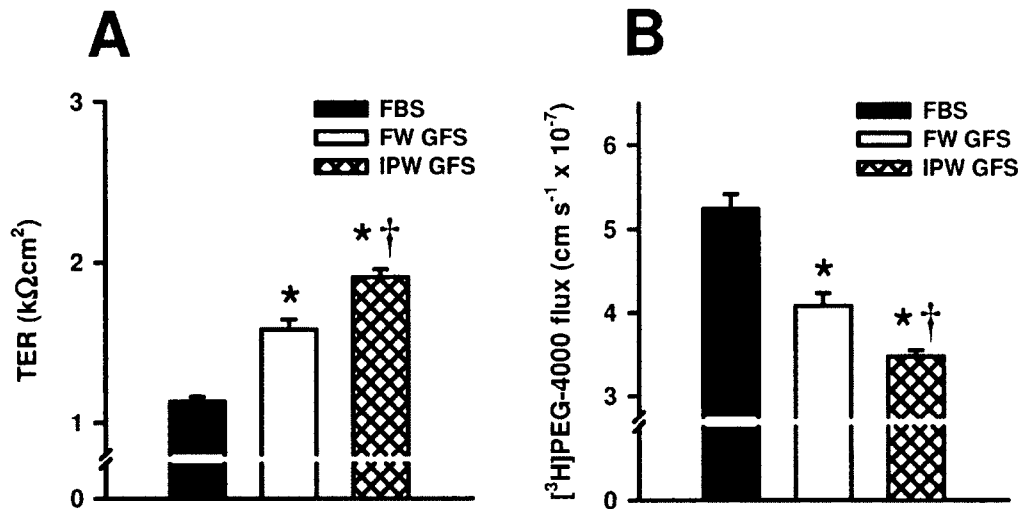


Figure 8-4: Effect of fetal bovine serum (FBS) or goldfish serum (GFS) derived from fish acclimated to freshwater (FW) or ion-poor water (IPW) on (A) transepithelial resistance (TER) and (B) [³H]PEG-4000 flux across primary cultured goldfish gill epithelia composed of pavement cells. Gill epithelia were maintained under symmetrical culture conditions (L15 apical/L15 basolateral) and exposed to homologous serum supplements for ~ 24 h. Data are expressed as mean values ± s.e.m. (*n* = 9-12). * Significant difference (*P* < 0.05) from the FBS group. † Significant difference (*P* < 0.05) from the FW GFS group.

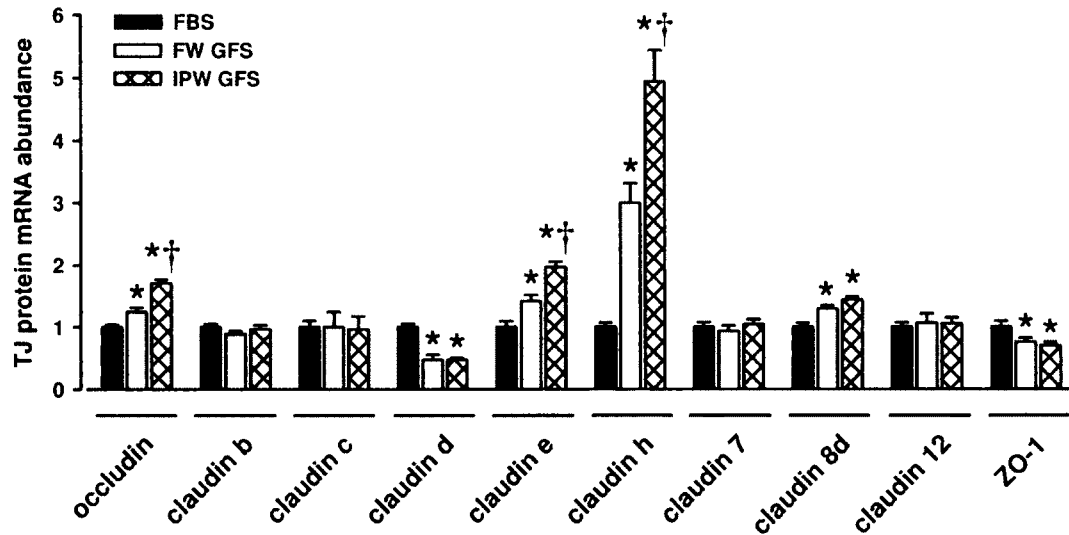


Figure 8-5: Effect of fetal bovine serum (FBS) or goldfish serum (GFS) derived from fish acclimated to freshwater (FW) or ion-poor water (IPW) on tight junction (TJ) protein mRNA abundance in primary cultured goldfish gill epithelia composed of pavement cells. Gill epithelia were maintained under symmetrical culture conditions (L15 apical/L15 basolateral) and exposed to homologous serum supplements for ~ 24 h. TJ protein transcript abundance was normalized to EF1 α mRNA abundance, and mRNA data were expressed relative to transcript abundance for the FBS group which was assigned a value of 1.0. Data are expressed as mean values \pm s.e.m. ($n = 6$). * Significant difference ($P < 0.05$) from the FBS group. † Significant difference ($P < 0.05$) from the FW GFS group.

Within the FBS group, TER was significantly elevated by apical IPW exposure when compared to apical FW exposure, however [³H]PEG-4000 permeability was unchanged (Fig. 8-6). Within the FW serum group, apical IPW exposure significantly increased TER and decreased [³H]PEG-4000 flux relative to apical FW exposure (Fig. 8-6). With respect to apical FW exposure, the FW serum group exhibited significantly elevated TER, but no change in [³H]PEG-4000 permeability when compared to the FBS group (Fig. 8-6). On the other hand, the FW serum group showed significantly increased TER and reduced [³H]PEG-4000 flux relative to the FBS group during apical IPW exposure (Fig. 8-6). When exposed to apical IPW, the IPW serum group exhibited significantly elevated TER and reduced [³H]PEG-4000 permeability when compared to all other treatment groups (i.e. FW serum and FBS groups during apical FW or IPW exposure) (Fig. 8-6).

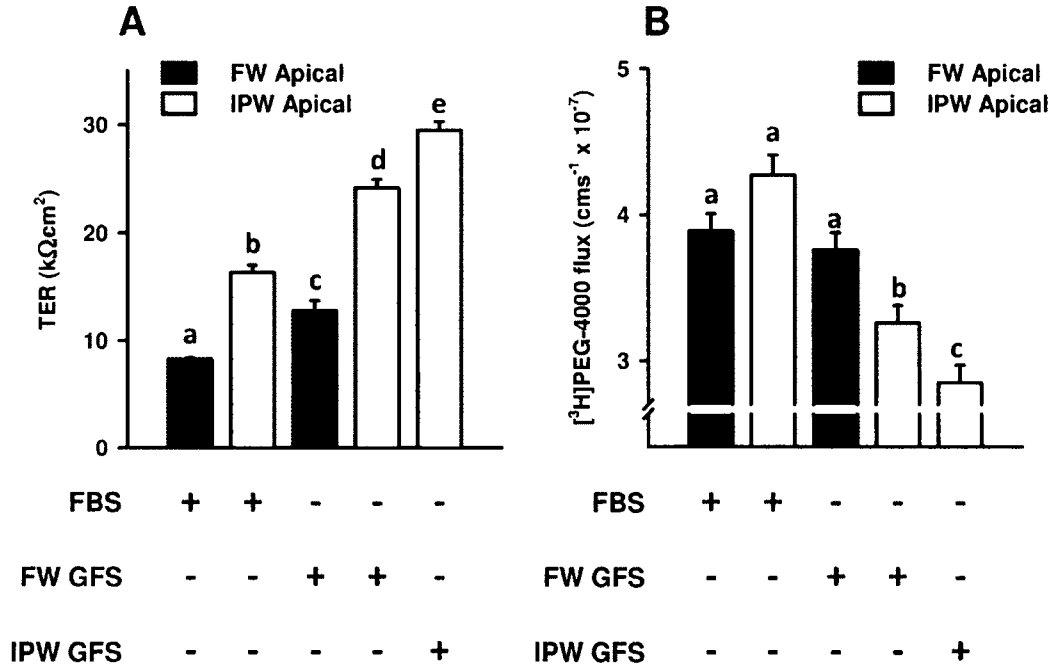


Figure 8-6: Effect of fetal bovine serum (FBS) or goldfish serum (GFS) derived from fish acclimated to freshwater (FW) or ion-poor water (IPW) on (A) transepithelial resistance (TER) and (B) [³H]PEG-4000 flux across primary cultured goldfish gill epithelia, composed of pavement cells, following exposure to asymmetrical culture conditions (FW apical/L15 basolateral or IPW apical/L15 basolateral). Data are expressed as mean values ± s.e.m (*n* = 6-9). Different letters denote significant differences (*P* < 0.05) between treatment groups.

8.5 Discussion

8.5.1 Overview: The current work strongly supports the view that altered paracellular permeability across the gill plays a crucial role in the maintenance of salt and water balance under conditions where (1) the acquisition of ions is severely limited and (2) the internal hyper-osmotic/external hypo-osmotic gradient is greater than in regular FW. In this particular suite of studies, goldfish were acclimated to ion-poor surroundings to introduce the aforementioned conditions. Based on the observed results, it seems that the response of the paracellular pathway to these environmental circumstances can also be mimicked *in vitro* by supplementing a primary cultured “reconstructed” gill epithelium with homologous serum. Although the primary cultured gill preparation is composed of PVCs only, separation of whole gill cells into a PVC population revealed that PVCs, both *in vivo* and *in vitro*, respond to ion-poor conditions in a similar manner – i.e. with generally similar alterations in molecular TJ components. Taken together with the observed morphological and physiological changes in PVCs from both *in vivo* and *in vitro* studies, alterations in response to ion-poor conditions appear to indicate reduced gill epithelial permeability. This may not be unexpected and would in fact be advantageous for the animal, as the gill represents a very large surface area of direct exposure to the external environment, and gill PVCs are estimated to comprise over 90% of this epithelial interface (Evans et al., 2005). Therefore a reduction in PVC-PVC paracellular permeability would contribute greatly to a decline in passive ion loss. This provides valuable insight into strategies for maintaining salt and water balance in fishes under conditions where the capacity for ion uptake is severely limited due to extrinsic factors.

8.5.2 TJ protein mRNA abundance in whole gill tissue and isolated PVCs following acclimation to IPW: A significant increase in the transcript abundance of gill TJ proteins occludin, claudin b, d, e, h, 7 and 8d was found following acclimation of goldfish to IPW (Fig. 8-1). Similarly, occludin, claudin b, e and 8d mRNA abundance was increased in PVCs isolated from the gills of IPW-acclimated goldfish (Fig. 8-3). These observations are consistent with previous studies that reported an increase in the protein abundance of gill occludin in goldfish (Chapter 3) and mRNA abundance of several claudin isoforms in gill tissue of puffer fish (Duffy et al., 2011) following acclimation to IPW. Furthermore, occludin, claudin b, e, h, 7 and 8d have all previously been characterized as barrier-forming TJ elements in vertebrate epithelia or have been associated with reduced paracellular permeability across the gill epithelia of fishes (Chapters 4 and 6; Yu et al., 2003; Bagherie-Lachidan et al., 2008, 2009; Milatz et al., 2010; Kelly and Chasiotis, 2011). Therefore, an increase in the abundance of these proteins in goldfish gills following acclimation to IPW seems very likely to be involved in reducing paracellular permeability across gill tissue. Accordingly, TJ depth between adjacent PVCs in goldfish gill tissue was also significantly increased following IPW acclimation (Fig. 8-2). Together, these changes would result in a beneficial reduction in passive ion loss in an ion-poor environment. Indeed, reduced ion efflux has previously been reported to occur across the gills of goldfish under ion-poor conditions (Cuthbert and Maetz, 1972).

In contrast to the above, claudin 12 and ZO-1 mRNA abundance was significantly decreased in whole gill tissue of goldfish following acclimation to IPW (Fig. 8-1). Since claudin 12 and ZO-1 mRNA abundance were unaltered and significantly elevated

respectively in isolated PVCs (see Fig. 8-3), it seems likely that these variations in whole gill tissue may have been driven by alterations in TJ components between other gill epithelial cell types (i.e. mitochondria-rich cells, MRCs) and/or endothelial cells of the goldfish gill. A similar line of reasoning can be made for the observed elevations in transcript abundance for claudin d, h, and 7 in whole gill tissue in response to IPW acclimation (Fig. 8-1), but no observed changes in mRNA for these same genes within isolated gill PVCs (Fig. 8-3). These observations highlight the importance of considering and not overlooking the heterogeneous nature of the gill epithelium as well as the potential contribution of the capillary endothelium when studying alterations in TJ protein or transcript abundance in whole gill tissue.

8.5.3 Cultured gill epithelia and homologous serum supplementation

8.5.3.1 Permeability properties under symmetrical culture conditions: Under symmetrical culture conditions (i.e. L15 apical/L15 basolateral), an increase in TER and reduction in [³H]PEG-4000 permeability was observed in cultured gill epithelia supplemented with GFS instead of FBS (Fig. 8-4). These changes suggest that homologous serum supplements derived from a FW fish may contain inherent factors that promote a reduction in cultured gill epithelial permeability. This may not be unexpected since FW fishes would need to maintain adequate levels of circulating signaling molecules in order to mediate reductions in paracellular permeability across tissues that interface with the surrounding environment (e.g. the gill). Under natural *in vivo* conditions, this would help to minimize passive ion loss to the hypo-osmotic environment. This idea is further strengthened by the observation that IPW-acclimated GFS reduced epithelial

permeability to a greater extent than serum from fish held in regular FW (Fig. 8-4), and is consistent with previous studies that have reported reduced ion loss (efflux) across the gill epithelium of goldfish (Cuthbert and Maetz, 1972) and other FW fish species (Perry and Laurent, 1989) acclimated to ion-poor conditions. In contrast, the current results differ from a previous study that reported a reduction in TER across primary cultured sea bass gill epithelia when homologous serum was used instead of FBS (Avella and Ehrenfeld, 1997). However, key differences are noted; the cultured sea bass gill preparation was generated from a marine fish, and the serum used for supplementation was derived from sea bass residing in SW (Avella and Ehrenfeld, 1997). It is broadly accepted that the gill epithelium of marine fishes is considerably “leakier” than the gill epithelium of FW fishes (see Marshall and Grosell, 2005). Furthermore, in surrogate models of the SW fish gill epithelium, TER is substantially lower than TER across equivalent preparations isolated from FW fish (e.g. Foskett et al., 1981). Therefore, it seems plausible that, in contrast to the “tightening” influence of FW fish serum, SW fish serum may contain factors that promote an increase in permeability. It would be interesting to develop this idea further given that the cultured sea bass gill preparation was composed exclusively of PVCs, whereas SW fish gill “leakiness” is largely attributed to the presence of shallow “leaky” TJs between gill MRCs and accessory cells (Marshall and Grosell, 2005). However, paracellular permeability between PVCs of a euryhaline species of fish acclimated to FW or SW has never been directly compared.

8.5.3.2 TJ protein mRNA abundance in cultured gill epithelia: For the most part, alterations in TJ components match up well when comparing the *in vivo* and *in vitro*

response of PVCs to “ion-poor conditions”. For example, occludin, claudin e and 8d mRNA abundance increased in isolated PVCs from IPW-acclimated goldfish gills (Fig. 8-3) and in cultured PVC epithelia after treatment with IPW GFS *in vitro* (Fig. 8-5). Furthermore in isolated gill PVCs, transcripts encoding for claudin c, 7 and 12 were unaltered by IPW acclimation (Fig. 8-3), and mRNA encoding for these same TJ components did not change in cultured PVC epithelia following treatment with either FW or IPW GFS (Fig. 8-5). The alterations observed in occludin, claudin e and 8d, in association with increased TER and decreased [³H]PEG-4000 flux, further strengthen the suggestion these TJ elements are involved in reducing paracellular permeability in gill tissue. These results are also consistent with previous reports of increased occludin, claudin e (= claudin 28b) and claudin 8d protein and/or mRNA abundance in association with corticosteroid-induced reductions in the paracellular permeability of primary cultured gill epithelia (Chapters 4 and 6; Kelly and Chasiotis, 2011).

Not all alterations in PVC TJ components however corresponded when *in vivo* and *in vitro* results were compared. Notably, claudin d and ZO-1 mRNA abundance decreased in cultured PVC epithelia following GFS treatment (Fig. 8-5), whereas PVCs isolated from fish acclimated to IPW showed unaltered and increased claudin d and ZO-1 mRNA abundance respectively (Fig. 8-3). At this stage, the specific reasons for this discrepancy are unclear. However, it is noteworthy that the decline in claudin d and ZO-1 mRNA abundance *in vitro* following exposure to GFS did not vary between FW GFS and IPW GFS treatments (Fig. 8-5). Therefore, the effect appears to occur irrespective of the physiological state of the fish from which the serum was derived. This response to GFS

differs from TJ protein mRNA changes that match between *in vivo* and *in vitro* studies (e.g. occludin and claudin e), where mRNA abundance alters in response to IPW GFS to a greater extent than FW GFS treatment (Fig. 8-5). Previous studies using mammalian cell lines have reported that serum-derived factors can weaken the TJ complex and this has been associated with an increase in permeability, reduction in ZO-1 abundance, and delocalization of ZO-1 (Chang et al., 1997; Nitz et al., 2003). Under certain circumstances, this appears to occur when cultured epithelia or endothelia express a pathophysiological response to the presence of serum where it is normally absent (e.g. basolateral side of brain capillary endothelial cells; Nitz et al., 2003). In these cases, the deleterious effects of serum match the *in vivo* pathological response of tissue when disease or injury results in serum leakage and contamination of the normally serum-free compartment (Chang et al., 1997; Nitz et al., 2008). Although the presence of GFS reduces ZO-1 (and claudin d) mRNA abundance in the current study, GFS does not have a deleterious effect on the physiological properties of the epithelium (see Fig. 8-4). Nevertheless, the fact that the apical surface of the gill epithelium *in vivo* is serum-free (i.e. exposed directly to water) under natural conditions suggests that in future studies it may be interesting to reduce the presence of GFS on the apical side of cultured gill epithelia to see if this curtails the observed reduction in ZO-1 or claudin d transcript abundance.

A final curious discrepancy between PVC TJ protein mRNA alterations following GFS treatment *in vitro* versus ion-poor conditions *in vivo*, is the response of claudin b and h. More specifically, transcript encoding for claudin b is greatly elevated in PVCs

isolated from the gills of fish acclimated to IPW (Fig. 8-3), but does not alter *in vitro* following GFS treatment (Fig. 8-5). In a reverse situation, claudin h does not exhibit any change in mRNA abundance in PVCs isolated from the gills of IPW-acclimated fish (Fig. 8-3), but is significantly increased *in vitro* in response to FW GFS and, in a more pronounced manner, IPW GFS treatment (Fig. 8-5). Once again, the specific reasons for this discrepancy are currently unknown and will require further study, however, a number of factors could contribute. For example, cultured PVC epithelia were exposed to 10% GFS, which represents a 90% reduction in any element that, *in vivo*, may be stimulating (or suppressing) claudin TJ protein abundance. Also, temporal factors could play a role since cultured PVC epithelia were exposed to GFS for 24 hours, whereas PVCs were isolated from the gills of goldfish that had been acclimated to IPW for at least 14 days. Nevertheless, an increase in claudin h (= claudin 3a) abundance could also contribute to the observed reductions in the permeability of GFS-treated epithelia, since claudin 3 is generally considered to be a barrier-promoting TJ protein (Milatz et al., 2010).

8.5.3.3 Permeability properties under asymmetrical culture conditions: When exposed to apical IPW, a significant difference between epithelia supplemented with GFS derived from FW- and IPW-acclimated fish was, once again, apparent. The highest TER and lowest [³H]PEG-4000 flux measurements were observed to occur across epithelia treated with IPW GFS (Fig. 8-6). This distinction clearly suggests that the presence of IPW GFS allows epithelia to tolerate and better respond to *in vitro* IPW exposure. This, as well as the response of epithelia to IPW GFS supplementation under symmetrical culture conditions (see above), strongly supports the idea that IPW GFS contains factors that lead

to the differentiation of an IPW-like epithelial phenotype *in vitro*. As previously discussed, the serum components responsible for this effect are currently unknown, however it seems reasonable to anticipate that osmoregulatory endocrine factors most likely play a pivotal role. In this regard, hormones that are linked to vertebrate salt and water balance have previously been demonstrated to significantly impact the permeability of cultured gill epithelia (Chapter 6; Kelly and Wood, 2001a, 2001b, 2002a, 2002b; Kelly and Chasiotis, 2011) as well as molecular components of the TJ complex in the gill (Chapters 4, 6 and 7; Tipsmark et al., 2009; Bui et al., 2010; Kelly and Chasiotis, 2011). For example, elevated circulating levels of the osmoregulatory hormone cortisol in goldfish were reported to significantly increase gill protein and/or mRNA abundance of the same TJ components that have been shown to respond to ion-poor conditions in the current *in vivo* and *in vitro* studies (i.e. occludin and claudin e; Chapter 7). The observation that cultured goldfish gill epithelia exhibit a differential response to homologous serum derived from fish in different physiological states is also consistent with a previous report where cultured tilapia gill epithelia were shown to respond very differently to homologous serum derived from fish that were unstressed versus serum from fish that had been stressed (i.e. intermittently net chased over a 20 min period; see Kelly and Wood, 2002a). In the tilapia study, the stress (and osmoregulatory) hormone cortisol was also found to be largely responsible for the differential response of the cultured gill preparations (Kelly and Wood, 2002a).

8.5.4 Perspectives: The current studies reinforce the notion that TJs play a central role in maintaining salt and water balance in fishes, specifically in an ion-poor environment

where salt acquisition from the external milieu is limited. These studies also demonstrate that supplementation of primary cultured “reconstructed” gill epithelia with homologous serum provides an appropriate means by which alterations in epithelial permeability and molecular TJ components can be correlated with changes in the physiological state of the fish. In this regard, the observed morphological and biochemical reorganization of TJs between PVCs in the gill epithelium, in response to *in vivo* and *in vitro* “ion-poor conditions”, strongly supports a significant contribution for TJs in the management of passive ion movement across the gill epithelium, whereby obligatory salt loss to the hypo-osmotic environment is reduced. A more complete understanding of this contribution however can be obtained in future studies by isolating and examining alterations in the molecular TJ components of the MRC fraction of the gill epithelium in addition to the PVCs. Although MRCs represent a much smaller percentage of the gill epithelial surface area (less than ~ 10%), these ionocytes are the primary site for active ion uptake (Evans et al., 2005). Therefore, further studies in MRCs may provide additional insight into interactions between transcellular and paracellular ionoregulatory strategies within the gill epithelium. A recent study has furthermore demonstrated the expression of MRC-specific claudins in gills of the euryhaline FW puffer fish (*Tetraodon nigroviridis*; see Bui et al., 2010). It would be of interest to see if similar TJ heterogeneity exists within the PVCs and MRCs of the stenohaline FW fish gill epithelium and if TJ components will show differential response between PVCs and MRCs following acclimation to ion-poor conditions.

8.6 References

Avella M, Ehrenfeld J. 1997. Fish gill respiratory cells in culture: a new model for Cl⁻ secreting epithelia. *J Membr Biol* 156:87-97.

Bagherie-Lachidan M, Wright SI, Kelly SP. 2008. Claudin-3 tight junction proteins in *Tetraodon nigroviridis*: cloning, tissue specific expression and a role in hydromineral balance. *Am J Physiol Integr Comp Physiol* 294:R1638-R1647.

Bagherie-Lachidan M, Wright SI, Kelly SP. 2009. Claudin-8 and -27 tight junction proteins in puffer fish *Tetraodon nigroviridis* acclimated to freshwater and seawater. *J Comp Physiol B* 179:419-431.

Bui P, Bagherie-Lachidan M, Kelly SP. 2010. Cortisol differentially alters claudin isoform mRNA abundance in a cultured gill epithelium from puffer fish (*Tetraodon nigroviridis*). *Mol Cell Endocrinol* 317:120-126.

Chang CW, Wang X, Caldwell RB. 1997. Serum opens tight junctions and reduces ZO-1 protein in retinal epithelial cells. *J Neurochem* 69:859-867.

Cuthbert AW, Maetz J. 1972. The effects of calcium and magnesium on sodium fluxes through gills of *Carassius auratus*, L. *J Physiol* 221:633-643.

Duffy NM, Bui P, Bagherie-Lachidan M, Kelly SP. 2011. Epithelial remodeling and claudin mRNA abundance in the gill and kidney of puffer fish (*Tetraodon biocellatus*) acclimated to altered environmental ion levels. *J Comp Physiol B* 181:219-238.

Evans DH, Piermarini PM, Choe KP. 2005. The multifunctional fish gill: dominant site of gas exchange, osmoregulation, acid-base regulation, and excretion of nitrogenous waste. *Physiol Rev* 85: 97-177.

Feldman GJ, Mullin JM, Ryan MP. 2005. Occludin: structure, function and regulation. *Adv Drug Deliv Rev* 57:883-917.

Foskett KJ, Logsdon CD, Turner T, Machen TE, Bern HA. 1981. Differentiation of the chloride extrusion mechanism during seawater adaptation of a teleost fish, the cichlid *Sarotherodon mossambicus*. *J Exp Biol* 93:209-224.

Galvez F, Reid SD, Hawkings G, Goss GG. 2002. Isolation and characterization of mitochondria-rich cell types from the gill of freshwater rainbow trout. *Am J Physiol Regul Integr Comp Physiol* 282:R658-R668.

González-Mariscal L, Betanzos A, Nava P, Jaramillo BE. 2003. Tight junction proteins. *Prog Biophys Mol Biol* 81:1-44.

Goss GG, Adamia S, Galvez F. 2001. Peanut lectin binds to a subpopulation of mitochondria-rich cells in the rainbow trout gill epithelium. *Am J Physiol Regul Integr Comp Physiol* 281:R1718-R1725.

Hwang PP, Lee TH, Lin LY. 2011. Ion regulation in fish gills: recent progress in the cellular and molecular mechanisms. *Am J Physiol Regul Integr Comp Physiol* 301:R28-R47.

Kelly SP, Chasiotis H. 2011. Glucocorticoid and mineralocorticoid receptors regulate paracellular permeability in a primary cultured gill epithelium. *J Exp Biol* 214:2308-2318.

Kelly SP, Wood CM. 2001a. The physiological effects of 3,5',3'-triiodo-L-thyronine alone or combined with cortisol on cultured pavement cell epithelia from freshwater rainbow trout gills. *Gen Comp Endocrinol* 123:280-294.

Kelly SP, Wood CM. 2001b. Effect of cortisol on the physiology of cultured pavement cell epithelia from freshwater trout gills. *Am J Physiol Regul Integr Comp Physiol* 281:R811-R820.

Kelly SP, Wood CM. 2002a. Cultured gill epithelia from freshwater tilapia (*Oreochromis niloticus*): effect of cortisol and homologous serum supplements from stressed and unstressed fish. *J Membr Biol* 190:29-42.

Kelly SP, Wood CM. 2002b. Prolactin effects on cultured pavement cell epithelia and pavement cell plus mitochondria-rich cell epithelia from freshwater rainbow trout gills. *Gen Comp Endocrinol* 128:44-56.

Krause G, Winkler L, Mueller SL, Haseloff RF, Piontek J, Blasig IE. 2008. Structure and function of claudins. *Biochim Biophys Acta* 1778:631-645.

Loh YH, Christoffels A, Brenner S, Hunziker W, Venkatesh B. 2004. Extensive expansion of the claudin gene family in the teleost fish, *Fugu rubripes*. *Genome Res* 14:1248-1257.

Marshall WS, Grosell M. 2005. Ion transport, osmoregulation and acid-base balance. In: *The Physiology of Fishes*, 3rd edition (ed. DH Evans, JB Claiborne), pp 177-230. New York: CRC Press.

Milatz S, Krug SM, Rosenthal R, Günzel D, Müller D, Schulzke JD, Amasheh S, Fromm M. 2010. Claudin-3 acts as a sealing component of the tight junction for ions of either charge and uncharged solutes. *Biochim Biophys Acta* 1798:2048-2057.

Nitz T, Eisenblätter T, Psathaki K, Galla HJ. 2003. Serum-derived factors weaken the barrier properties of cultured porcine brain capillary endothelial cells *in vitro*. *Brain Res* 981:30-40.

Perry SF, Laurent P. 1989. Adaptational responses of rainbow trout to lowered external NaCl concentration: contribution of the branchial chloride cell. *J Exp Biol* 147:147-168.

Saitou M, Ando-Akatsuka Y, Itoh M, Furuse M, Inazawa J, Fujimoto K, Tsukita S. 1997. Mammalian occludin in epithelial cells: its expression and subcellular distribution. *Eur J Cell Biol* 73:222-231.

Tipsmark CK, Kiilerich P, Nilsen TO, Ebbesson LOE, Stefansson SO, Madsen SS. 2008. Branchial expression patterns of claudin isoforms in Atlantic salmon during seawater acclimation and smoltification. *Am J Physiol Regul Integr Comp Physiol* 294:R1563-R1574.

Tipsmark CK, Jorgensen C, Brande-Lavridsen N, Engelund M, Olesen JH, Madsen SS. 2009. Effects of cortisol, growth hormone and prolactin on gill claudin expression in Atlantic salmon. *Gen Comp Endocrinol* 163:270-277.

Whitehead A, Roach JL, Zhang S, Galvez F. 2011. Genomic mechanisms of evolved physiological plasticity in killifish distributed along an environmental salinity gradient. *Proc Natl Acad Sci USA* 108:6193-6198.

Wilson JM, Laurent P. 2002. Fish gill morphology: inside out. *J Exp Zool* 293:192-213.

Wood CM, Gilmour KM, Pärt P. 1998. Passive and active transport properties of a gill model, the cultured branchial epithelium of the freshwater rainbow trout (*Oncorhynchus mykiss*). *Comp Biochem Physiol A Mol Integr Physiol* 119A:87-96.

Yu ASL, Enck AH, Lencer WI, Schneeberger EE. 2003. Claudin-8 expression in Madin-Darby canine kidney cells augments the paracellular barrier to cation permeation. *J Biol Chem* 278:17350-17359.

Zall DM, Fisher D, Garner MD. 1956. Photometric determination of chlorides in water. *Anal Chem* 28:1665-1678.

CHAPTER 9:

**siRNA-MEDIATED REDUCTIONS IN OCCLUDIN EXPRESSION
INCREASES PERMEABILITY ACROSS GOLDFISH GILL EPITHELIA**

Helen Chasiotis and Scott P. Kelly

Department of Biology, York University, Toronto, Ontario, Canada M3J 1P3

9.1 Rationale and methodology

In Chapters 4, 6 and 8, a mechanistic role for occludin in the regulation of gill permeability was investigated. In these studies, hormone or homologous fish serum treatment were used as tools to firstly manipulate cultured gill epithelial permeability, following which subsequent changes in occludin transcript and/or protein abundance were examined. In the mini-study presented in this section, the opposite approach was used, that is, short interfering RNAs (siRNAs) were utilized as tools to firstly manipulate occludin transcript and protein abundance in cultured goldfish gill epithelia, following which subsequent alterations in epithelial permeability were examined. siRNAs are double-stranded RNA molecules that bind to and direct the degradation of target mRNA to effectively reduce or “knockdown” expression of a gene of interest. siRNA-mediated gene “knockdown” therefore can provide valuable insight into the function of a gene.

As described in the Materials and Methods of Chapter 5, goldfish gill cells were isolated and cultured on cell culture inserts under symmetrical conditions (i.e. with FBS-supplemented L15 culture medium bathing both apical and basolateral surfaces of preparations). Once cells had formed confluent epithelia (~ 8 h post-seeding cells in inserts), they were transfected on apical surfaces with Endo-Porter Delivery Reagent (6 μ M; Gene Tools, LLC, Philomath, OR, USA) and either custom goldfish occludin siRNA or custom scrambled control siRNA (1000 nM; Shanghai GenePharma Co., Ltd., Shanghai, China). The custom goldfish occludin siRNA (5' CCAGUGAAUUCCCUCCCAUTT 3'; 5' AUGGGAGGGAAUUCACUGGTT 3') were designed to target a specific sequence starting at nucleotide 1,187 within the 1,500-

nucleotide goldfish occludin gene. The scrambled siRNA (5' GCACACCCCUUCGUUACAUTT 3'; AUGUAACGAAGGGGUGUGCTT 3') were used as a negative control to account for any changes in gene expression caused by the siRNA delivery method. Epithelia were collected for RNA and protein extraction according to methods described in Chapter 5 at ~ 86 h post-transfection. TER measurements were conducted periodically throughout the course of the experiment and paracellular permeability across cultured epithelia was also determined prior to sample collection using the paracellular marker, [³H] polyethylene glycol (molecular mass 4000 Da; PEG-4000). Alterations in occludin transcript and protein abundance were determined by quantitative real-time PCR (qRT-PCR) and western blotting respectively. Procedures and/or calculations for TER and [³H]PEG-4000 flux measurements, qRT-PCR and western blotting are described in the Material and Methods of Chapter 5.

9.2 Results and discussion

Transfection of cultured goldfish gill epithelia with occludin siRNA resulted in an ~ 60% reduction in goldfish occludin transcript abundance and an ~ 50% decrease in occludin protein levels (Fig. 9-1). Despite these significant reductions in occludin expression, TER across goldfish gill epithelia was unaltered (Fig. 9.2A). A significant increase in flux to the paracellular marker [³H]PEG-4000 however was observed (Fig. 9.2B), indicating that the paracellular pathway did indeed become “leakier” as a result of occludin loss. Since TER represents measurements of resistance to the flow of charged solutes (e.g. ions), the results suggest that occludin may only regulate the paracellular movement of uncharged or large molecules rather than ions. However, it is also possible that changes in TER were not observed because other TJ proteins (e.g. claudins) were up-regulated in order to compensate for the occludin loss. In a recent study in an intestinal epithelial cell line (i.e. Caco-2), siRNA-mediated occludin “knockdown” was shown to significantly increase paracellular flux to various sized macromolecules without altering TER (Al-Sadi et al., 2011). Claudin-2 transcript and protein abundance were furthermore shown to be elevated in response to occludin loss (Al-Sadi et al., 2011). Based on the results of this mini-report, occludin clearly plays a barrier-forming or “tightening” role in the regulation of gill permeability, however further studies are required to delineate the selectivity of occludin and the degree of its contribution to the paracellular barrier.

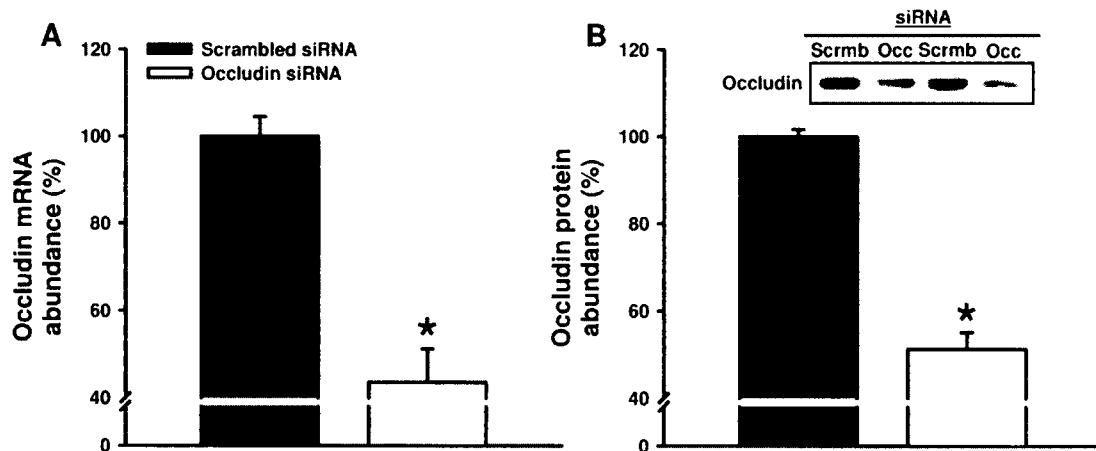


Figure 9-1: Effect of goldfish occludin siRNA transfection on occludin (A) mRNA and (B) protein abundance in cultured goldfish gill epithelia. A representative western blot, where occludin immunoreactivity can be observed at ~ 68 kDa, is also shown in (B). Note: Scrb = scrambled siRNA group, Occ = occludin siRNA group. Occludin transcript abundance was normalized to elongation factor 1-alpha (EF1 α) mRNA abundance, and occludin protein abundance was normalized to β -actin protein abundance. Occludin mRNA and protein data were also expressed relative to transcript and protein abundance respectively for the scrambled siRNA group which was assigned a value of 100%. Data are expressed as means \pm s.e.m. ($n = 3-4$). * Significant difference ($P < 0.05$) from the scrambled siRNA group. EF1 α transcript and β -actin protein abundance were not significantly altered ($P > 0.05$) by transfection procedures when compared to the scrambled siRNA group (data not shown).

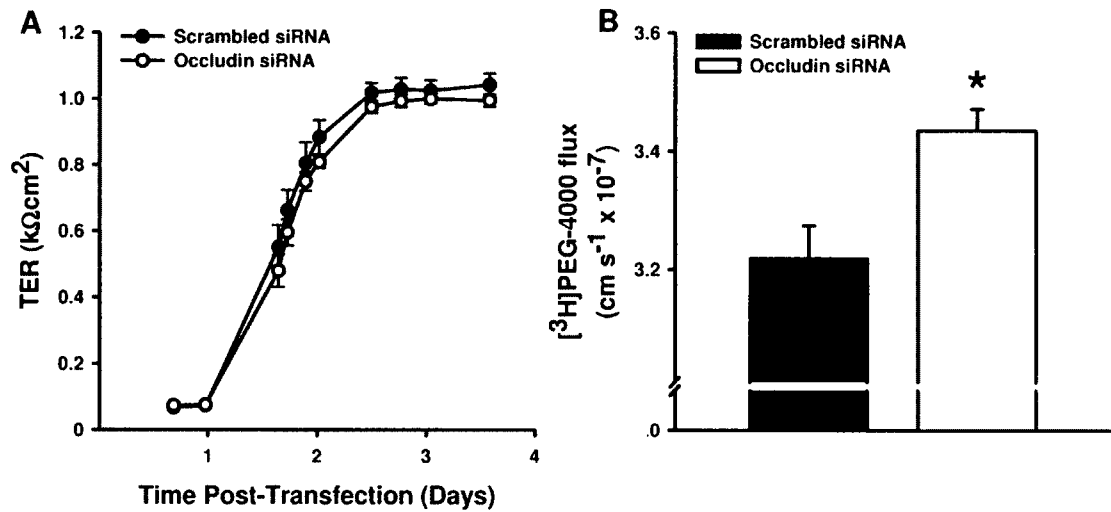


Figure 9-2: Effect of goldfish occludin siRNA transfection on (A) transepithelial resistance (TER) and (B) [³H]PEG-4000 flux across cultured goldfish gill epithelia. [³H]PEG-4000 flux was measured over a 12 h period (between 74 and 86 h post-transfection). Data are expressed as mean values ± s.e.m. (*n* = 6). * Significant difference (*P* < 0.05) from the scrambled siRNA group.

9.3 References

Al-Sadi R, Khatib K, Guo S, Ye D, Youssef M, Ma T. 2011. Occludin regulates macromolecule flux across the intestinal epithelial tight junction barrier. *Am J Physiol Gastrointest Liver Physiol* 300:G1054-1064.

CHAPTER 10:
SUMMARY AND FUTURE DIRECTIONS

10.1 Summary

At the onset of these studies, the contribution of tight junction (TJ) proteins to the barrier properties of fish tissues was not known. Since then, a considerable amount of new and exciting research in this area has emerged. Several TJ proteins, particularly claudins, have been identified in fish osmoregulatory tissues, and roles have been proposed, with respect to their homeostatic control of salt and water movement across epithelia, in a wide variety of teleost fishes, such as the rainbow trout (Kelly and Chasiotis, 2011), Atlantic salmon (Tipsmark et al., 2008c, 2009, 2010), tilapia (Tipsmark et al., 2008a), Southern flounder (Tipsmark et al., 2008b), puffer fish (Bagherie-Lachidan et al., 2008, 2009; Clelland et al., 2010; Bui et al., 2010; Duffy et al., 2011) and zebrafish (Kumai et al., 2011). The collection of studies examining occludin in the current dissertation however presents the most comprehensive characterization and in depth mechanistic understanding of a single TJ protein in fishes to date. With regard to the specific aims of these studies (outlined in Chapter 1), key findings are summarized below.

10.1.1 Occludin is a component of the TJ complex in fish tissues

Using molecular techniques, full-length coding sequences for occludin genes from both stenohaline goldfish and euryhaline rainbow trout were cloned (Chapters 4 and 5). Occludin transcript was found to be widely expressed in fish tissues, but was predominantly abundant in the gills of both rainbow trout and goldfish, thus suggesting an important role for occludin in the regulation of gill permeability (Chapters 4 and 5). Sequences for several claudin genes in both goldfish and rainbow trout were additionally cloned and identified (Chapter 6). Claudin orthologs, which had previously been

characterized by mammalian studies as barrier-forming TJ proteins, were also found to be principally expressed in the goldfish gill (Chapter 7). Using immunohistochemical methods, occludin immunolocalization patterns within the gills, intestine and kidney of the goldfish were also characterized (Chapter 2). For example, occludin immunostaining was shown to be associated with both pavement cells (PVCs) and mitochondria-rich cells (MRCs) of the gill epithelium (Chapter 2). It is noteworthy that occludin was differentially expressed in discrete regions of the goldfish nephron, and that the observed expression patterns correlated with segment-specific permeability, whereby only the “tight” distal tubules and collecting ducts expressed occludin (Chapter 2).

When taken together, these data present novel information on the sequence orthology of occludin and claudin genes in vertebrates, and provide the first notion of functional conservation for occludin as a barrier-forming or “tightening” TJ protein in vertebrate epithelia. The prevailing expression of occludin and certain claudins in the goldfish gill also supports the widely-accepted concept of a “tight” gill epithelium in FW teleost fishes that reduces passive ion loss to the dilute environment (reviewed by Evans et al., 2005). This generally-accepted concept had been proposed based on the multi-stranded and “deep” TJ networks observed between PVC-PVC and PVC-MRC contacts within the FW gill (Sardet et al., 1979; Evans et al., 2005).

10.1.2 A role for occludin in FW teleost osmoregulation

To establish a potential role for occludin in the regulation of salt and water balance in FW fishes, alterations in systemic hydromineral endpoints were related to *in vivo* changes in occludin abundance. To this end, goldfish were subjected to varying periods of food

deprivation in order to disturb the active and passive transport properties of their osmoregulatory epithelia (Chapter 2). In response to food deprivation, occludin expression was shown to alter in a tissue-specific manner and in association with time-dependent variations in hydromineral endpoints (Chapter 2). These published observations were amongst the first to suggest a potential role for a TJ protein in the regulation of salt and water balance in teleosts. The biphasic but inverse alterations exhibited by goldfish gill $\text{Na}^+\text{-K}^+\text{-ATPase}$ activity and kidney occludin expression in response to varying periods of food deprivation also provide interesting evidence for an interplay of transcellular and paracellular ionoregulatory strategies between different epithelia (Chapter 2).

A role for occludin in FW fish osmoregulation was particularly highlighted in Chapter 3, when goldfish were acclimated to ion-poor water (IPW). Occludin abundance in the goldfish gill was shown to significantly elevate in response to long-term IPW acclimation (Chapter 3). This occurred in accordance with increased TJ depth between gill PVCs of IPW-acclimated goldfish (Chapter 8) and is in agreement with a previous study that reported significant reductions in Na^+ efflux across the gills of goldfish acclimated to similar conditions (Cuthbert and Maetz, 1972). Given that gill $\text{Na}^+\text{-K}^+\text{-ATPase}$ activity remained unaltered in response to long-term IPW exposure (Chapter 3), these observations appear to indicate that reductions in passive ion loss via changes in TJ physiology may be especially important in a dilute environment where active ion acquisition by the gill is limited.

Since the endocrine system is believed to mediate physiological adjustments in osmoregulatory processes in response to environmental change (reviewed by McCormick, 2001), it was postulated that the observed alterations in occludin during IPW acclimation were perhaps under hormonal control (Chapter 3). The osmoregulatory hormone cortisol appeared to be a good candidate as it had previously been shown to become elevated in fish blood during acclimation to IPW (Perry and Laurent, 1989). Indeed, when intraperitoneal cortisol implants were used to chronically elevate circulating cortisol levels in goldfish, occludin mRNA and protein abundance were significantly increased in the gills (Chapter 7). Transcripts for putative barrier-forming claudins were additionally up-regulated in gill tissue (Chapter 7). Since corticosteroid-mediated alterations in TJ protein expression are well-documented in various mammalian epithelial and endothelial models (e.g. Stelwagen et al., 1999; Felinski et al., 2008; Förster et al., 2008), the results of this study suggest that the endocrine regulation of TJ proteins in vertebrates may also be evolutionarily conserved.

10.1.3 Primary cultured gill model from the stenohaline FW goldfish

The evaluation of gill permeability *in vivo* is particularly challenging due to the complex three-dimensional architecture of the gill, as well as the multicellular nature of the gill epithelium. Furthermore, immunolocalization studies in goldfish gills demonstrated occludin immunostaining within gill endothelia (Chapter 2), thus making it difficult to interpret *in vivo* alterations in gill occludin abundance as changes between cells of the gill epithelium (i.e. PVCs and/or MRCs) or endothelial cells of the gill vasculature. To circumvent these *in vivo* limitations, reliable and reproducible methodology for the

primary culture of a model gill epithelium from the FW goldfish was developed, the first such model derived from a stenohaline fish species (Chapter 5). Isolated goldfish gill cells were shown to form a flat and polarized epithelium, composed exclusively of PVCs, that can withstand prolonged apical FW exposure as experienced *in vivo* (Chapter 5; Appendix A.1). By furthermore demonstrating that the cultured gill preparations allow changes in occludin to be simultaneously examined with alterations in epithelial permeability [e.g. transepithelial resistance (TER) and flux to a paracellular permeability marker], it was shown that these cultured epithelia would provide appropriate *in vitro* models for studying TJ protein physiology and function in the gill (Chapter 5).

10.1.4 Occludin is a barrier-forming TJ protein in the teleost gill

To determine a functional role for occludin in the regulation of the paracellular barrier across the gill epithelium, primary cultured gill models composed exclusively of PVCs were utilized to correlate changes in permeability with alterations in occludin abundance. Cortisol has a well documented role in the regulation of salt and water balance in euryhaline fishes, and this is mediated in part by significant alterations in the growth and differentiation of gill MRCs for salt secretion in a hyper-osmotic setting or ion-uptake in a hypo-osmotic environment (Evans et al., 2005). Cortisol however has also been shown to modulate the paracellular permeability characteristics of primary cultured gill epithelia comprising PVCs (e.g. Kelly and Wood, 2001, 2002). Accordingly, when cortisol treatment was used as a tool to manipulate the paracellular barrier properties of cultured gill epithelia from euryhaline rainbow trout, significant alterations in occludin abundance were observed. More specifically, cortisol-mediated reductions in epithelial permeability

occurred in association with significantly elevated occludin mRNA and protein abundance, thus strongly supporting a barrier-forming role for occludin (Chapter 4). Transcripts for putative barrier-forming claudins however were also up-regulated in response to cortisol treatment (Chapter 6). Taken together, the results of these studies suggest that cortisol may additionally enhance the function of the euryhaline gill during osmotic stress by “tightening” TJs between PVCs in order to limit passive salt gain or loss during seawater (SW) or FW acclimation respectively. On the other hand, cortisol treatment of cultured gill epithelia derived from the stenohaline FW goldfish elicited only a small “tightening” effect and little alterations in occludin or claudin abundance (Chapter 6), suggesting that in stenohaline fishes, cortisol may play a limited role in the endocrine regulation of paracellular permeability. These results provide unique insight into species-specific differences in the endocrine control of TJs that may relate to the environmental physiology of euryhaline versus stenohaline fishes. Nevertheless, exogenously elevated cortisol levels in goldfish serum (as discussed above; Chapter 7), significantly altered both occludin and claudin expression in intact gills. This discrepancy suggests that *in vivo*, several endocrine factors may function together to synergistically mediate the physiological adjustments necessary for acclimation.

In this regard, a follow-up study was conducted using cultured goldfish gill epithelia supplemented with either FW or IPW-acclimated goldfish serum (Chapter 8). It was reasoned that the homologous fish serum would provide a more complete and realistic complement of endocrine factors involved in IPW acclimation, and would thus give greater mechanistic insight into the role of TJ proteins in gill permeability during

this event. Indeed, cultured gill preparations supplemented with IPW-acclimated goldfish serum were significantly “tighter” and exhibited a greater paracellular barrier to passive diffusion than those treated with FW-acclimated goldfish serum (Chapter 8). Correspondingly, occludin abundance was up-regulated in the IPW-serum supplemented gill preparations, but also in whole gill tissue and PVCs separated from IPW-acclimated goldfish (Chapter 8). These observations provide solid mechanistic support of a “tightened” gill epithelium upon acclimation to a hypo-osmotic environment.

The studies described above demonstrate a well-defined correlation between elevated occludin expression and reductions in epithelial permeability. Several claudins however were also shown to simultaneously alter in response to treatments. It is possible therefore that the alterations in claudin expression may have masked the actual contribution of occludin to the paracellular barrier. To substantiate a function for occludin, a mini-study was conducted using small interfering RNAs (siRNAs) to disrupt or “knockdown” occludin expression in cultured goldfish gill epithelia (Chapter 9). siRNA-mediated reductions in occludin abundance resulted in significantly increased permeability to a paracellular tracer molecule (Chapter 9), thus confirming a barrier-forming role for occludin in the TJs of gill epithelia.

Collectively, the current studies suggest that occludin may provide a simple and reliable marker for assessing overall gill integrity or “tightness”. While this type of marker would certainly be useful for future studies examining the osmoregulatory status of fishes, it may also have practical applications in other disciplines. In aquatic

toxicology and disease transmission studies for example, occludin expression may prove to be a useful marker for tracking gill vulnerability to pollutants and pathogens.

10.2 Future directions

The present studies have significantly improved our fundamental understanding of the role that occludin, and TJ proteins in general, play in the regulation of salt and water balance in FW fishes. Significant insight into the physiology and function of occludin in teleost fish tissues has also been gained. Nevertheless, the permselectivity of occludin in fish epithelia is still unclear. siRNA-mediated reductions in occludin abundance did not affect TER, suggesting that occludin may only regulate the paracellular movement of uncharged molecules and/or that other TJ components (e.g. claudins) may be up- or down-regulated in order to compensate for the occludin loss (Chapter 9). Future studies that profile claudin expression in response to occludin “knockdown” and that utilize paracellular markers that vary in size and charge would be helpful.

Studies examining a role for occludin during hypo-osmoregulation in SW are also currently lacking. As a barrier-forming TJ protein, it would be interesting to see if occludin abundance will be down-regulated in the euryhaline gill upon SW acclimation in order to confer the proposed “leaky” phenotype required for salt extrusion. In this respect, supplementation of the cultured euryhaline rainbow trout gill model with homologous serum from SW-acclimated fish may be revealing.

Although the primary focus of the current research was clearly occludin, several orthologous claudins were also identified in goldfish and rainbow trout tissues, and alterations in their expression were additionally observed (Chapters 6, 7 and 8). Based on

the current studies and available literature (e.g. Bagherie-Lachidan et al., 2008, 2009; Duffy et al., 2011), claudins also appear to contribute to FW as well as SW fish osmoregulation. Mechanistic understanding of the barrier- or pore-forming roles of these claudins in fish tissues however is lacking. Complete enumeration, immunolocalization and distribution of claudins in fish tissues, as well as loss-of-function studies (e.g. utilizing siRNAs or morpholinos to disrupt claudin expression) are required in order to ascertain specific claudin contributions to the paracellular barrier of fish epithelia. In a recent study in the FW puffer fish, MRC-specific claudins in the gill were identified by comparing claudin expression patterns in cultured PVCs with whole gill tissue (Bui et al., 2010). Future studies using cultured gill epithelia comprising both PVCs and MRCs would therefore be helpful for delineating differences in the molecular composition and permeability of PVC-PVC and PVC-MRC TJs within the gill epithelium.

Future studies utilizing a broader scope of osmoregulatory hormones (e.g. prolactin, growth hormone) would certainly help to elucidate the complex endocrine regulation of TJ proteins and gill permeability in teleosts. Along the same lines, studies in a wider variety of fishes would provide greater insight into variations in molecular TJ components that may allow teleosts to reside in such diverse environments.

10.3 References

Bagherie-Lachidan M, Wright SI, Kelly SP. 2008. Claudin-3 tight junction proteins in *Tetraodon nigroviridis*: cloning, tissue-specific expression and a role in hydromineral balance. *Am J Physiol Regul Integr Comp Physiol* 294:R1638-R1647.

Bagherie-Lachidan M, Wright SI, Kelly SP. 2009. Claudin-8 and -27 tight junction proteins in puffer fish *Tetraodon nigroviridis* acclimated to freshwater and seawater. *J Comp Physiol B* 179:419-431.

Bui P, Bagherie-Lachidan M, Kelly SP. 2010. Cortisol differentially alters claudin isoforms in cultured puffer fish gill epithelia. *Mol Cell Endocrinol* 317:120-126.

Clelland ES, Bui P, Bagherie-Lachidan M, Kelly SP. 2010. Spatial and salinity-induced alterations in claudin-3 isoform mRNA along the gastrointestinal tract of the pufferfish, *Tetraodon nigroviridis*. *Comp Biochem Physiol A Mol Integr Physiol* 155:154-163.

Cuthbert AW, Maetz J. 1972. The effects of calcium and magnesium on sodium fluxes through gills of *Carassius auratus*, L. *J Physiol* 221:633-643.

Duffy NM, Bui P, Bagherie-Lachidan M, Kelly SP. 2011. Epithelial remodeling and claudin mRNA abundance in the gill and kidney of puffer fish (*Tetraodon biocellatus*) acclimated to altered environmental ion levels. *J Comp Physiol B* 181:219-238.

Evans DH, Piermarini PM, Choe KP. 2005. The multifunctional fish gill: dominant site of gas exchange, osmoregulation, acid-base regulation, and excretion of nitrogenous waste. *Physiol Rev* 85: 97-177.

Felinski EA, Cox AE, Phillips BE, Antonetti DA. 2008. Glucocorticoids induce transactivation of tight junction genes occludin and claudin-5 in retinal endothelial cells via a novel cis-element. *Exp Eye Res* 86:867-878.

Förster C, Burek M, Romero IA, Weksler B, Couraud PO, Drenckhahn D. 2008. Differential effects of hydrocortisone and TNF α on tight junction proteins in an *in vitro* model of the human blood–brain barrier. *J Physiol* 586:1937-1949.

Kelly SP, Chasiotis H. 2011. Glucocorticoid and mineralocorticoid receptors regulate paracellular permeability in a primary cultured gill epithelium. *J Exp Biol* 214:2308-2318.

Kelly SP, Wood CM. 2001. Effect of cortisol on the physiology of cultured pavement cell epithelia from freshwater trout gills. *Am J Physiol Regul Integr Comp Physiol* 281:R811-R820.

Kelly SP, Wood CM. 2002. Cultured gill epithelia from freshwater tilapia (*Oreochromis niloticus*): effect of cortisol and homologous serum supplements from stressed and unstressed fish. *J Membr Biol* 190:29-42.

Kumai Y, Bahubeshi A, Steele S, Perry SF. 2011. Strategies for maintaining Na⁺ balance in zebrafish (*Danio rerio*) during prolonged exposure to acidic water. *Comp Biochem Physiol A Mol Integr Physiol* 160:52-62.

McCormick SD. 2001. Endocrine control of osmoregulation in teleost fish. *Amer Zool* 41:781-794.

Perry SF, Laurent P. 1989. Adaptational responses of rainbow trout to lowered external NaCl concentration: contribution of the branchial chloride cell. *J Exp Biol* 147:147-168.

Stelwagen K, McFadden HA, Demmer J. 1999. Prolactin alone or in combination with glucocorticoids enhances tight junction formation and expression of the tight junction protein occludin in mammary cells. *Mol Cell Endocrinol* 156:55-61.

Tipsmark CK, Baltzegar DA, Ozden O, Grubb BJ, Borski RJ. 2008a. Salinity regulates claudin mRNA and protein expression in the teleost gill. *Am J Physiol Regul Integr Comp Physiol* 294:R1004-R1014.

Tipsmark CK, Luckenbach JA, Madsen SS, Kiilerich P, Borski RJ. 2008b. Osmoregulation and expression of ion transport proteins and putative claudins in the gill of Southern flounder (*Paralichthys lethostigma*). *Comp Biochem Physiol A Mol Integr Physiol* 150:265-273.

Tipsmark CK, Kiilerich P, Nilsen TO, Ebbesson LOE, Stefansson SO, Madsen SS. 2008c. Branchial expression patterns of claudin isoforms in Atlantic salmon during seawater acclimation and smoltification. *Am J Physiol Regul Integr Comp Physiol* 294:R1563-R1574.

Tipsmark CK, Jørgensen C, Brande-Lavridsen N, Engelund M, Olesen JH, Madsen SS. 2009. Effects of cortisol, growth hormone and prolactin on gill claudin expression in Atlantic salmon. *Gen Comp Endocrinol* 163:270-277.

Tipsmark CK, Sørensen KJ, Hulgard K, Madsen SS. 2010. Claudin-15 and -25b expression in the intestinal tract of Atlantic salmon in response to seawater acclimation, smoltification and hormone treatment. *Comp Biochem Physiol A Mol Integr Physiol* 155:361-370.

APPENDIX A:
SUPPLEMENTARY DATA

A.1 Primary cultured goldfish gill cells form polarized epithelia

A.1.1 Rationale and methodology: In this section, the *in vitro* goldfish gill model was further characterized by demonstrating that cultured goldfish gill cells form functionally polarized epithelia.

As outlined in the Materials and Methods of Chapter 5, goldfish gill cells were isolated and cultured on cell culture inserts under symmetrical conditions (i.e. with FBS-supplemented L15 culture medium bathing both apical and basolateral surfaces of preparations; L15/L15). Once a stable plateau in transepithelial resistance (TER) had developed, inserts were randomly separated into three groups. Two of these groups were switched to asymmetrical culture conditions by adding temperature-equilibrated sterile dechlorinated freshwater (FW) to either the apical side of inserts (i.e. FW/L15 group) or the basolateral side of inserts (L15/FW group) after several careful rinses to ensure the removal of residual medium. The third group of inserts was maintained under symmetrical conditions (L15/L15 group) and served as a control. After 3.5 h of FW exposure, all groups were switched back to symmetrical (L15/L15) culture conditions and epithelia were allowed to recover for 5 h. Measurements of TER were conducted at 0.5 h intervals throughout the pre-exposure, FW exposure and recovery periods according to methods described in Chapter 5. Inserts were also routinely examined by phase contrast microscopy (see Chapter 5 for details) and phase contrast images of epithelia were captured to document any changes in epithelial morphology.

A.1.2 Results and discussion: In the pre-exposure period, all cultured goldfish gill cells exhibited a flattened polygonal morphology with well-defined intercellular junctions that

are characteristic of these epithelia (Fig. A-1A, see Chapter 5). Control L15/L15 inserts maintained this typical morphology as well as stable TER levels throughout the course of the experiment (Fig. A-2). As previously shown in Chapter 5, goldfish gill epithelia are tolerant of asymmetrical FW/L15 conditions. Abrupt apical FW exposure resulted in a rapid increase and stabilization of TER followed by an immediate recovery to control TER levels upon restoration of L15/L15 culture conditions (Fig. A-2). Furthermore, the characteristic epithelial morphology of cultured goldfish gill cells was unchanged by FW/L15 culture conditions and maintained during the L15/L15 recovery period (Fig. A-1B,C). On the other hand, abrupt basolateral FW exposure resulted in a rapid collapse in TER to almost zero levels (Fig. A-2). Within 15 min of switching to L15/FW culture conditions, the characteristic intercellular junctions between cells were no longer visible and the cultured epithelia began to tear and form large clumps (Fig. A-1D). After 3 h, the underlying polyethylene terephthalate (PET) filters became visible through gaping holes in the epithelia and detached cells were floating in the culture medium (Fig. A-1E). Surprisingly, upon restoration of L15/FW inserts to L15/L15 culture conditions, TER steadily recovered to control levels within 5 h (Fig. A-2). Furthermore, holes and tears in the epithelia were repaired within 1.5 h of the recovery period, and the characteristic epithelial morphology with defined intercellular junctions began to return ~ 5 h into the recovery period (Fig. A-1F). The TER observations in the present study are in accordance with those reported for cultured rainbow trout gill epithelia exposed to basolateral FW, however TER in the rainbow trout gill preparations did not recover upon restoration of

basolateral L15 media (Wood et al., 2000). Clearly, the cultured goldfish gill epithelia are polarized such that FW exposure is only tolerated on apical surfaces.

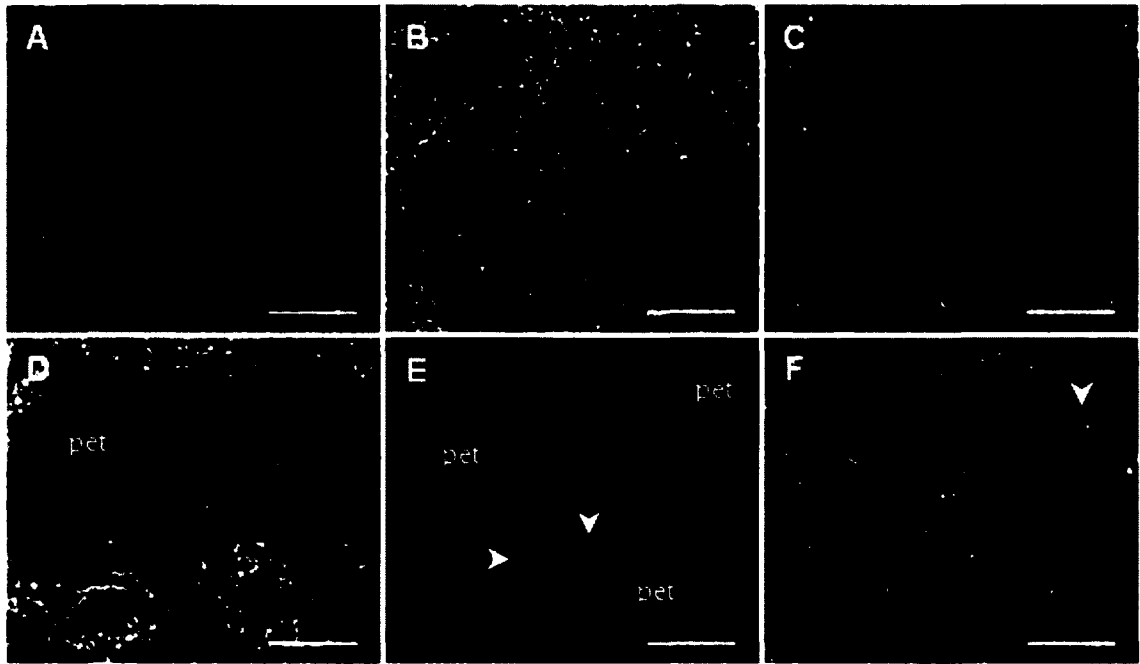


Figure A-1: Effect of abrupt apical FW exposure (FW/L15) or basolateral FW exposure (L15/FW) and subsequent recovery under symmetrical (L15/L15) culture conditions on cultured goldfish gill epithelial cell morphology. (A) Cultured gill epithelia in the pre-exposure period under L15/L15 exhibit characteristic polygonal morphology with well-defined intercellular junctions. (B) Cultured gill epithelia after 3 h of FW/L15. (C) Cultured gill epithelia recovering under L15/L15 after 3.5 h of FW/L15. Cultured gill epithelia following (D) 1.5 h and (E) 3 h of L15/FW. (F) Cultured gill epithelia recovering under L15/L15 after 3.5 h of L15/FW. Note: pet = polyethylene terephthalate filter underlying the epithelia; * = clumping epithelial cells; white arrowhead = detached and floating cells. Scale bar = 10 μ m.

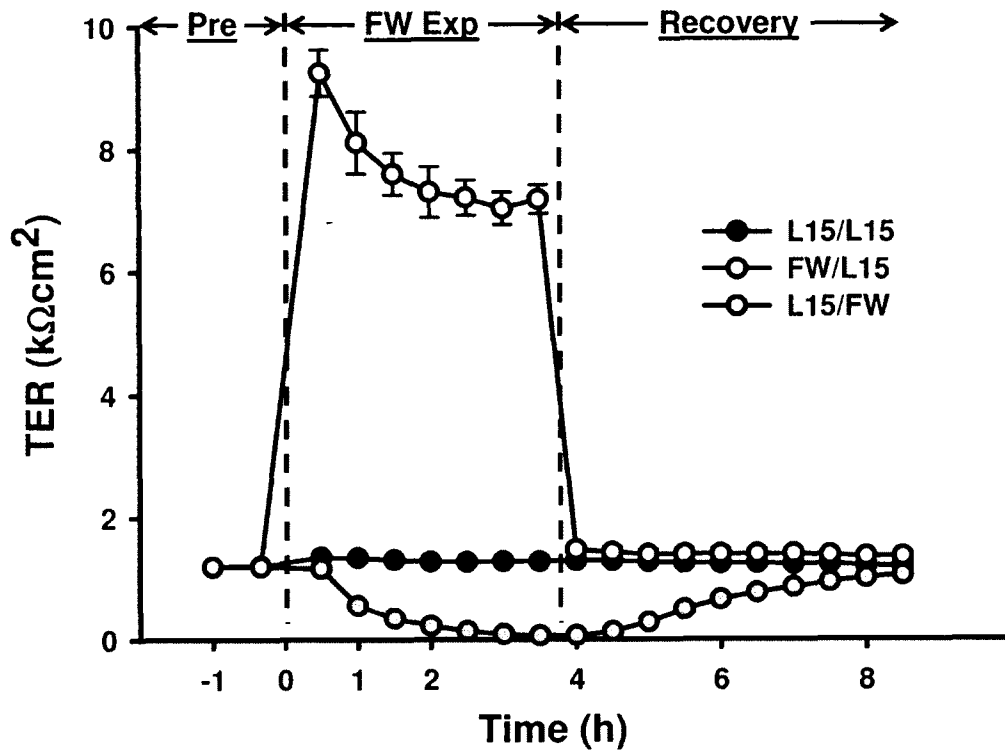


Figure A-2: Effect of abrupt apical FW exposure (FW/L15) or basolateral FW exposure (L15/FW) and subsequent recovery under symmetrical (L15/L15) culture conditions on the transepithelial resistance (TER) of cultured goldfish gill epithelia. Note: Pre = pre-exposure period under L15/L15; FW Exp = abrupt FW exposure period under FW/L15 or L15/FW; Recovery = recovery period under L15/L15. The control L15/L15 group was maintained under symmetrical conditions throughout the course of the experiment. Data are expressed as mean values \pm s.e.m. ($n = 6$).

A.2 Validation of a commercial cortisol EIA kit for measuring cortisol titres in goldfish serum

A.2.1 Rationale, methodology and results: In Chapter 7, goldfish serum cortisol levels were measured using a commercial cortisol enzyme immunoassay (EIA) kit intended for use with mammalian serum. To ensure that changes in goldfish serum cortisol could be measured accurately using this kit, curves generated by serial dilution of serum from untreated and 400 µg cortisol/g body weight implanted goldfish (from experiments in Chapter 7) were compared against a standard curve generated with cortisol standards provided in the kit. The EIA kit was validated for measuring cortisol levels in goldfish serum by demonstrating that the dilution curves of cortisol in goldfish serum were parallel to the cortisol standard curve (Fig. A-3).

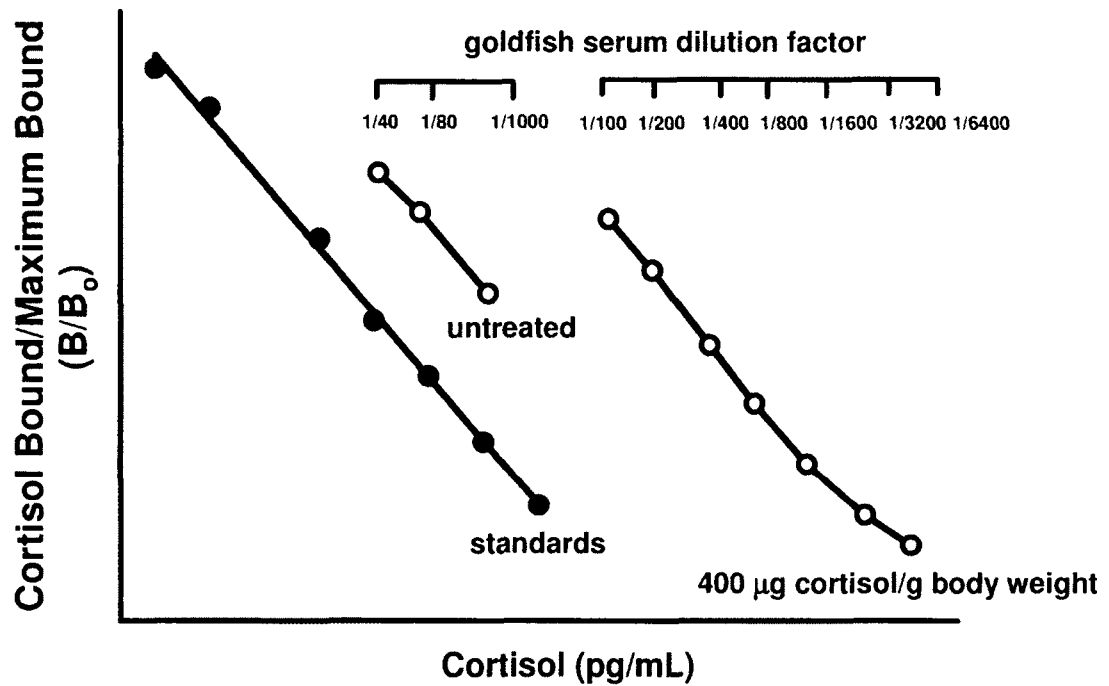


Figure A-3: In Chapter 7, goldfish serum cortisol was measured using a commercial cortisol enzyme immunoassay (EIA) kit intended for use with mammalian serum. To ensure that changes in goldfish serum cortisol levels could be measured accurately using this kit, parallelism was demonstrated by comparison of a cortisol standard curve with curves generated by serial dilution of serum from untreated and 400 µg cortisol/g body weight implanted goldfish from experiments in Chapter 7.

A.3 References

Wood CM, Kelly SP, Zhou B, Fletcher M, O'Donnell M, Eletti B, Pärt P. 2002. Cultured gill epithelia as models for the freshwater fish gill. *Biochim Biophys Acta* 1566:72-83.



APPENDIX B:
PUBLICATIONS

Date: Tue, 02 Aug 2011 10:25:03 +0100

From: Sue Chamberlain <sue@biologists.com>

To: helench@yorku.ca

Subject: Re: Would like written permission to use my article in my PhD dissertation

 2 unnamed text/html 3.90 KB 

Helen Chasiotis and Scott P. Kelly
Occludin immunolocalization and protein expression in goldfish
J Exp Biol 2008 211:1524-1534. doi:10.1242/jeb.014894

Dear Helen,

Permission is granted with no charge.

The acknowledgement should state "reproduced / adapted with permission" and give the source journal name - the acknowledgement should either provide full citation details or refer to the relevant citation in the article reference list - the full citation details should include authors, journal, year, volume, issue and page citation.

Where appearing online or in other electronic media, a link should be provided to the original article (e.g. via DOI):-

The Journal of Experimental Biology: jeb.biologists.org

Best wishes,
Sue Chamberlain

On 2/8/11 04:40, "helench@yorku.ca" helench@yorku.ca wrote:

> Hello,
>
> I would like to obtain written permission to include the following publication
> in my PhD dissertation:
>
> Chasiotis H, Kelly SP (2008) Occludin immunolocalization and protein
> expression
> in goldfish. Journal of Experimental Biology: 211, 1524 - 1594.
>
> Thank you in advance for your time.
>
> Best,
> Helen Chasiotis

This email was sent by Sue Chamberlain on behalf of the Company of Biologists.

permissions@biologists.com

Sue Chamberlain
For and on behalf of The Company of Biologists
Bidder Building
140 Cowley Road
Cambridge
CB4 0DL
UK

Tel: +44 (0)1223 425 525

Occludin immunolocalization and protein expression in goldfish

Helen Chasiotis* and Scott P. Kelly

Department of Biology, York University, Toronto, ON, Canada, M3J 1P3

*Author for correspondence (e-mail: helench@yorku.ca)

Accepted 25 March 2008

SUMMARY

Tight junctions (TJs) are an integral component of models illustrating ion transport mechanisms across fish epithelia; however, little is known about TJ proteins in fishes. Using immunohistochemical methods and Western blot analysis, we examined the localization and expression of occludin, a transmembrane TJ protein, in goldfish tissues. In goldfish gills, discontinuous occludin immunostaining was detected along the edges of secondary gill lamellae and within parts of the interlamellar region that line the lateral walls of the central venous sinus. In the goldfish intestine, occludin immunolocalized in a TJ-specific distribution pattern to apical regions of columnar epithelial cells lining the intestinal lumen. In the goldfish kidney, occludin was differentially expressed in discrete regions of the nephron. Occludin immunostaining was strongest in the distal segment of the nephron, moderate in the collecting duct and absent in the proximal segment. To investigate a potential role for occludin in the maintenance of the hydromineral balance of fishes, we subjected goldfish to 1, 2 and 4 weeks of food deprivation, and then examined the endpoints of hydromineral status, Na⁺,K⁺-ATPase activity and occludin protein expression in the gills, intestine and kidney. Occludin expression altered in response to hydromineral imbalance in a tissue-specific manner suggesting a dynamic role for this TJ protein in the regulation of epithelial permeability in fishes.

Key words: occludin, tight junction, osmoregulation, permeability, epithelium, Na⁺,K⁺-ATPase, gills, kidney, intestine, food deprivation.

INTRODUCTION

Hydromineral balance in freshwater (FW) fishes is regulated by strategies of ion retention and ion acquisition across ionoregulatory epithelia. While ion retention mechanisms limit outwardly directed solute movement across epithelia, ion acquisition compensates for obligatory losses to the environment (e.g. ion loss to FW due to epithelial permeability). Studies examining the role of ionoregulatory epithelia in the maintenance of hydromineral status in fishes have generally focused on transcellular mechanisms/routes of ion movement, through which actively driven ion transport takes place. In contrast, far less emphasis has been placed on mechanisms that enhance ion retention, i.e. those that limit paracellular ion loss. As a result, while transcellular pathways are well characterized and are known to incorporate a multifaceted suite of pumps, exchangers and channels that associate with either apical or basolateral cell membranes (Loretz, 1995; Marshall, 2002; Evans et al., 2005), the paracellular pathway, which is controlled by the tight junction (TJ) complex, remains poorly understood in aquatic vertebrates.

TJs are composed of transmembrane and cytosolic protein complexes that form strands around the apical domain of an epithelial cell. TJ proteins of adjacent epithelial cells associate with one another to form a semi-permeable paracellular seal that restricts solute movement between cells (Cerejido and Anderson, 2001). In addition to regulating paracellular permeability and limiting solute movement, TJs also demarcate apicobasal polarity and establish cell–cell contacts, which aid in the regulation of cellular processes such as transcription and proliferation (reviewed by Schneeberger and Lynch, 2004). To date, over 40 TJ and TJ-associated proteins have been identified at the epithelial TJ complex (González-Mariscal et al., 2003). Isolated from chick liver, occludin was the first transmembrane TJ protein identified (Furuse et al., 1993). The presence of this tetraspan protein within TJ fibrils (Fujimoto, 1995)

and its capacity to form TJ-like strands when transfected into cells lacking TJs (Furuse et al., 1998) quickly underscored a structural role for occludin within TJ complexes. Several other lines of evidence, however, also suggested a vital functional role for occludin in TJ sealing and the regulation of solute movement through the paracellular pathway. For example, the over-expression of chick occludin in Madin–Darby canine kidney (MDCK) epithelial cells led to an increase in transepithelial resistance (TER) (Balda et al., 1996; McCarthy et al., 1996). In contrast, treatment of *Xenopus* A6 epithelial cells with a synthetic peptide designed to disrupt occludin associations between adjacent cells led to a significant decrease in TER and an increase in permeability to paracellular markers (e.g. [³H]mannitol, [¹⁴C]inulin and dextrans) (Wong and Gumbiner, 1997). Moreover, microinjection of mRNA encoding C-terminally truncated occludin into *Xenopus* embryos resulted in TJs exhibiting a ‘leaky’ phenotype (Chen et al., 1997). This ‘leaky’ phenotype could be rescued by co-injection with full-length occludin mRNA (Chen et al., 1997).

While various TJ forms (e.g. ‘leaky’ versus ‘tight’) are widely accepted to play critical roles in the way fish epithelia function (for reviews, see Loretz, 1995; Marshall, 2002; Evans et al., 2005), little is known about TJ proteins in fishes. Given its role in regulating TJ barrier function and its use as an indicator of changes in paracellular permeability, we conducted studies on the integral TJ protein occludin in goldfish to investigate a potential role for occludin in the maintenance of the hydromineral balance of fishes. Using Western blot analysis and immunohistochemistry, we first examined occludin protein expression and localization in select goldfish epithelial tissues (i.e. gill, intestine and kidney). We then hypothesized that occludin protein expression would alter in response to hydromineral imbalance. To test this hypothesis we subjected goldfish to varying periods of food deprivation, working

on the assumption that the restricted nutritional state would disrupt normal, energy-dependent mechanisms of ion acquisition in a time-dependent manner. Using endpoint measurements of hydromineral status and Na^+, K^+ -ATPase activity, we characterized the response of goldfish to negative energy status in conjunction with measurements of occludin protein expression.

MATERIALS AND METHODS

Experimental animals

Goldfish *Carassius auratus* L. were obtained from a local supplier and held at 18–19°C under a simulated natural photoperiod (12h light:12h dark) in aerated 200l opaque polyethylene tanks at a density of 10–12 fish per tank. Each tank was supplied with flow through dechlorinated FW (approximate composition in mmol l^{-1} : $[\text{Na}^+] 0.59$, $[\text{Cl}^-] 0.92$, $[\text{Ca}^{2+}] 0.76$ and $[\text{K}^+] 0.43$) at a rate of ~250–300 ml min^{-1} . Fish were held for at least 4 weeks prior to experimentation and during this period were fed *ad libitum* once daily with commercial koi and goldfish pellets (Martin Profishent, Elmira, ON, Canada).

Immunohistochemistry and Western blot analysis

Tissue collection

Fish were randomly selected and anaesthetized using 1 g l^{-1} MS-222 (Syndel Laboratories Ltd, Qualicum Beach, BC, Canada). For immunohistochemistry, gill and kidney tissues were carefully isolated and fixed in Bouin's solution for 3–4 h. A standardized region of the intestine (i.e. a section approximately one-third from the anterior-most region, relative to full gastrointestinal tract length), was also isolated and gently flushed of any gut contents with Bouin's solution. The tissue was then immersed in Bouin's solution and fixed for 3–4 h. Following fixation, all tissues were rinsed twice with 70% ethanol and stored in 70% ethanol at 4°C until further processing. For Western blot analysis, samples of goldfish blood cells, gill, kidney and intestine were collected. Blood was sampled from anesthetized fish *via* caudal puncture using a 25 gauge needle, following which fish were killed by spinal transection. Blood was allowed to clot at 4°C for 1 h and was then centrifuged at 10 600 g for 5 min at 4°C. The resulting serum was discarded and the pellet of packed blood cells was quick-frozen in liquid nitrogen and stored at –85°C until further processing. The intestinal segment collected for Western blot analysis was the same as that described above; however, any residual gut contents were gently flushed out with 0.7% NaCl (i.e. not flushed with Bouin's solution). Rat kidney tissue was donated by G. Sweeney (York University, Toronto, ON, Canada). After collection, all tissues were quick-frozen in liquid nitrogen and stored at –85°C until further analysis.

Immunohistochemistry

Fixed tissues were dehydrated through an ascending series of ethanol rinses (70–100%), cleared with xylene and infiltrated and embedded in Paraplast Plus Tissue Embedding Medium (Oxford Worldwide, LLC, Memphis, TN, USA). Sections (3 μm thick) were cut using a Leica RM 2125RT manual rotary microtome (Leica Microsystems Inc., Richmond Hill, ON, Canada), collected on 2% bovine serum albumin (BSA; BioShop Canada Inc., Burlington, ON, Canada)-coated glass slides and incubated overnight at 45°C. Sections were deparaffinized with xylene, rehydrated to water *via* a descending series of ethanol rinses (100–50%), and subjected to heat-induced epitope retrieval (HIER). HIER was accomplished by immersing slides in a sodium citrate buffer (10 mmol l^{-1} , pH 6.0) and heating both solution and slides in a microwave oven for 4 min. The solution was allowed to cool for 20 min, reheated for 2 min and cooled for

a further 15 min. Slides were then washed three times with phosphate-buffered saline (PBS, pH 7.4) and quenched for 30 min in 3% H_2O_2 in PBS. Following quenching, slides were then successively washed with 0.4% Kodak Photo-Flo 200 in PBS (PF/PBS, 10 min), 0.05% Triton X-100 in PBS (TX/PBS, 10 min), and 10% antibody dilution buffer (ADB; 10% goat serum, 3% BSA and 0.05% Triton X-100 in PBS) in PBS (ADB/PBS, 10 min). Slides were incubated overnight at room temperature with rabbit polyclonal anti-occludin antibody (1:100 dilution in ADB; Zymed Laboratories, Inc., South San Francisco, CA, USA) and mouse monoclonal anti- Na^+, K^+ -ATPase α -subunit antibody ($\alpha 5$, 1:10 in ADB; Developmental Studies Hybridoma Bank, Iowa City, IA, USA). The anti-occludin antibody is epitope-affinity purified and directed against the C-terminal region of the human occludin protein. As negative controls, two sets of slides were also incubated overnight with ADB alone or with normal rabbit serum. Normal rabbit serum was donated by P. Moens (York University, Toronto, ON, Canada). Following overnight incubation, sections were successively washed with PF/PBS, TX/PBS and ADB/PBS (10 min each) as described above, and incubated with tetramethyl rhodamine isothiocyanate (TRITC)-labelled goat anti-rabbit antibody (1:500 in ADB; Jackson ImmunoResearch Laboratories, Inc., West Grove, PA, USA) and fluorescein-isothiocyanate (FITC)-labelled goat anti-mouse antibody (1:500 in ADB; Jackson ImmunoResearch Laboratories, Inc.) for 1 h at 37°C. Slides were then successively washed with PF/PBS, TX/PBS and ADB/PBS (10 min each) and rinsed 3 times with 0.4% PF in distilled water (PF/dH₂O, 1 min each). Slides were air dried for 1 h and mounted with Molecular Probes ProLong Antifade (Invitrogen Canada Inc., Burlington, ON, Canada) containing $5 \mu\text{g ml}^{-1}$ 4',6-diamidino-2-phenylindole (DAPI; Sigma-Aldrich Canada Ltd, Oakville, ON, Canada). Fluorescence images were captured using a Reichert Polyvar microscope (Reichert Microscope Services, Depew, NY, USA) and Olympus DP70 camera (Olympus Canada Inc., Markham, ON, Canada), and merged using Adobe Photoshop CS2 software (Adobe Systems Canada, Toronto, ON, Canada).

Western blotting

Goldfish tissues (blood pellet, gills, intestine, kidney) and rat kidney were thawed and homogenized on ice in chilled homogenization buffer (200 mmol l^{-1} sucrose, 1 mmol l^{-1} EDTA, 1 mmol l^{-1} PMSF, 1 mmol l^{-1} DTT in 0.7% NaCl) containing 1:200 protease inhibitor cocktail (Sigma-Aldrich Canada Ltd). Tissues were homogenized at a 1:3 w:v tissue to homogenization buffer ratio using a PRO250 homogenizer (PRO Scientific Inc., Oxford, CT, USA). Homogenates were centrifuged at 3200 g for 20 min at 4°C and supernatants were collected after centrifugation. Protein content was quantified using the Bradford assay (Sigma-Aldrich Canada Ltd) according to the manufacturer's guidelines with BSA as a standard. Samples were prepared for SDS-PAGE by boiling at 100°C with 6 \times sample buffer (360 mmol l^{-1} Tris-HCl, 30% glycerol, 12% SDS, 600 mmol l^{-1} DTT, 0.03% Bromophenol Blue); 20 μg of rat kidney and 75 μg of goldfish blood pellet, gill, intestine and kidney were electrophoretically separated by SDS-PAGE in 12% acrylamide gels at 150 V. After electrophoresis, protein was transferred to a Hybond-P polyvinylidene difluoride (PVDF) membrane (GE Healthcare Bio-Sciences Inc., Baie d'Urfé, QC, Canada) over a 2 h period using a TE70 Semi-Dry Transfer unit (GE Healthcare Bio-Sciences Inc.). Following transfer, the membrane was washed in Tris-buffered saline with Tween-20 [TBS-T; TBS (10 mmol l^{-1} Tris, 150 mmol l^{-1} NaCl, pH 7.4) with 0.05% Tween-20], and blocked for 1 h in 5% non-fat dried skimmed milk powder in TBS-T (5% skimmed milk

TBS-T). The membrane was then incubated for ~16 h at 4°C with rabbit polyclonal anti-occludin antibody (1:1000 dilution in 5% skimmed milk TBS-T; Zymed Laboratories, Inc.). Following incubation with primary antibody, the membrane was washed with TBS-T and incubated at room temperature with horseradish peroxidase (HRP)-conjugated goat anti-rabbit antibody (1:5000 in 5% skimmed milk TBS-T; Bio-Rad Laboratories, Inc., Mississauga, ON, Canada) for 1 h, and then washed with TBS-T and TBS, respectively. Protein bands were visualized using Enhanced Chemiluminescence Plus Western blotting detection system (GE Healthcare Bio-Sciences Inc.).

Food deprivation experiments

Experimental animals and tissue sampling

Goldfish (mean mass 19.2±0.7 g, *N*=60), were acclimated to conditions as outlined above and randomly assigned to one of six experimental groups. Fish were food deprived for 1, 2 or 4 weeks, and for each unfed group a corresponding fed control group was run. Fed control fish were provided with pellets at a ration of 1.5% their body mass once daily. Control fish were not fed 24 h prior to sampling. Goldfish were weighed immediately prior to commencing experiments and at the end of each experimental period (i.e. at the time of tissue sampling), enabling calculation of body mass change. Individual fish were identified by unique markings. At 1, 2 and 4 weeks, fed and unfed fish were anaesthetized using 1 g l⁻¹ MS-222 and blood was rapidly sampled (within ~2 min) *via* caudal puncture using a 25 gauge needle. Blood was processed as described above and serum was collected, quick-frozen in liquid nitrogen and stored at -85°C until further analysis. For analysis of muscle moisture content, a standardized region of epaxial white muscle was removed. Gill, kidney and intestinal tissues for enzyme and Western blot analyses were removed, frozen in liquid nitrogen and stored at -85°C until further processing.

Muscle moisture content and serum analysis

Pre-weighed muscle tissue was placed in an oven and dried to a constant mass at 60°C. Muscle moisture content was subsequently determined gravimetrically. Serum osmolality was measured using a Model 5500 vapor pressure osmometer (Wescor, Inc., Logan, UT, USA). Serum Na⁺ concentration was determined by atomic absorption spectroscopy using an AAnalyst 200 spectrometer (PerkinElmer Life and Analytical Sciences, Woodbridge, ON, Canada). Serum Cl⁻ concentration was determined using a colorimetric assay as previously described (Zall et al., 1956) and measured using a Multiskan Spectrum microplate reader (Thermo Fisher Scientific, Nepean, ON, Canada).

Na⁺,K⁺-ATPase enzyme activity

Na⁺,K⁺-ATPase activity was examined using methods previously outlined (McCormick, 1993), with some minor modifications. Briefly, gill, kidney or intestinal tissues were homogenized at 4°C in a 1:10 w:v pre-chilled SEI (150 mmol l⁻¹ sucrose, 10 mmol l⁻¹ EDTA, 50 mmol l⁻¹ imidazole, pH 7.3):SEID (0.5 g sodium deoxycholate/100 ml SEI) buffer mixture (4:1 mixture of SEI:SEID) using a PRO250 homogenizer. Homogenates were centrifuged at 3200 g for 10 min at 4°C and supernatants were collected, quick-frozen in liquid nitrogen and stored at -85°C until enzyme analysis. For analysis, supernatants were thawed on ice and assayed for Na⁺,K⁺-ATPase activity using solutions that couple ATP hydrolysis to ADP with the oxidation of NADH. The sensitivity of goldfish Na⁺,K⁺-ATPase activity to ouabain inhibition varies from tissue to tissue (see Busacker and Chavin, 1981). Therefore, to distinguish

Na⁺,K⁺-ATPase activity from total ATPase activity, samples were run in assay solutions either with or without K⁺ present, under the assumption that K⁺-dependent ATPase activity is almost exclusively Na⁺,K⁺-ATPase activity. The use of K⁺-free assay solutions yielded equivalent results to using 0.5 mmol l⁻¹ and 10 mmol l⁻¹ ouabain for kidney and gill/intestine tissues, respectively. This corresponds with the observations in a previous report (Busacker and Chavin, 1981) that maximal inhibition of gill and kidney Na⁺,K⁺-ATPase activity occurred at an ouabain concentration of 10 mmol l⁻¹, but that gill activity was less sensitive to higher ouabain concentrations than kidney tissue. Na⁺,K⁺-ATPase activity was standardized to ADP release and was expressed as μmol ADP mg protein⁻¹ h⁻¹. The protein content of supernatants used for analysis was measured using a Bradford assay with BSA as a standard, as described above.

Western blot analysis

Western blots for occludin were carried out as outlined above using equal amounts of protein from each tissue sampled. As a loading control, membranes were subsequently stripped with stripping buffer (100 mmol l⁻¹ glycine, 30 mmol l⁻¹ KCl, 20 mmol l⁻¹ sodium acetate, pH 2.2), washed with TBS-T, blocked with 5% skimmed milk TBS-T and incubated for ~16 h at 4°C with mouse monoclonal anti-α-tubulin antibody (12G10; 1:10000 in 5% skimmed milk TBS-T; Developmental Studies Hybridoma Bank). Membranes were then washed with TBS-T and incubated at room temperature with HRP-conjugated goat anti-mouse antibody (1:5000 in 5% skimmed milk TBS-T; Bio-Rad Laboratories, Inc.) for 1 h, washed with TBS-T then TBS, and visualized as described above. Occludin and α-tubulin protein expression were quantified using Labworks image acquisition and analysis software (UVP Bioluminescence Systems and Analysis Systems, Upland, CA, USA), and α-tubulin was used for normalization of occludin expression.

Statistical analyses

All data are presented as mean values ± s.e.m. A one-way ANOVA was used to examine for significant differences between control groups at 1, 2 or 4 weeks. In all cases no significant differences were found. Therefore, data were subsequently analysed using Student's *t*-test to examine for significant differences (*P*<0.05) between control (fed) and experimental (unfed) groups within a time point. A one-way ANOVA was also used to examine for significant differences between experimental (unfed) groups at 1, 2 or 4 weeks. All statistical analyses were run using Graphpad Instat software version 3.00 (GraphPad Software, Inc., San Diego, CA, USA).

RESULTS

Immunohistochemistry

Occludin and Na⁺,K⁺-ATPase immunolocalization in the gill Na⁺,K⁺-ATPase immunolocalized to select cells within the interlamellar (IL) region of primary filaments and at the base of the secondary gill lamellae of goldfish gills (Fig. 1A). Immunofluorescence microscopy revealed pronounced and discontinuous occludin immunostaining along the edges of secondary lamellae and medial parts of lamellae that are embedded within the body of the primary filament (Fig. 1B,C,E). In addition, occludin immunostaining appeared to be associated with cells of the secondary lamellae that also express Na⁺,K⁺-ATPase (Fig. 1C,D). Furthermore, occludin immunofluorescence was also prominent in parts of the IL region that line the lateral walls of the central venous sinus (CVS; Fig. 1B). While there appeared to be no difference in staining for occludin between the afferent and efferent edges of gill filaments, Na⁺,K⁺-ATPase immunostaining was generally prominent

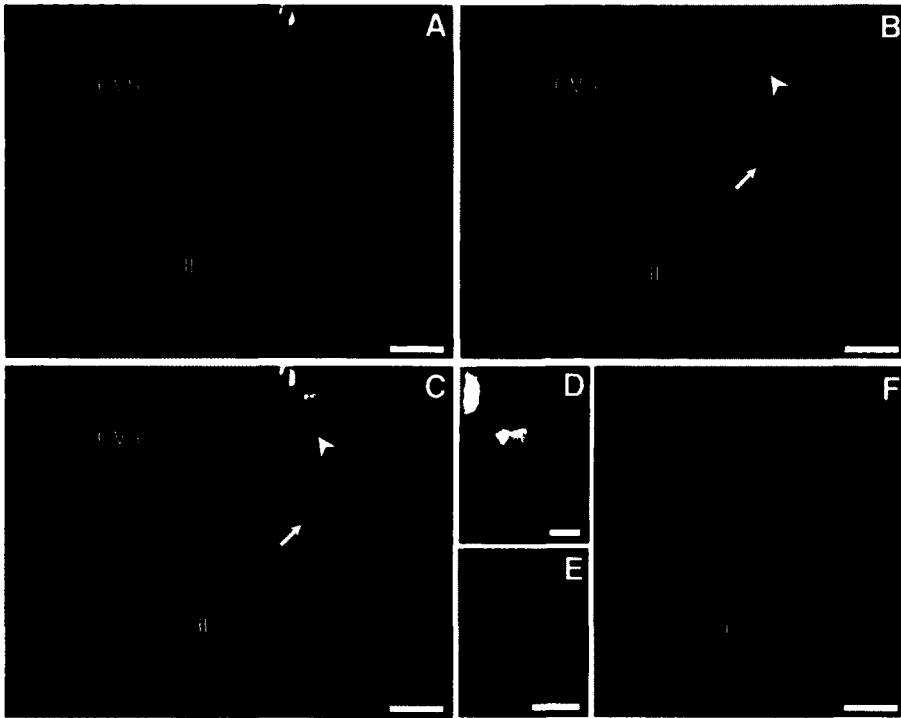


Fig. 1. Immunofluorescence staining of (A) Na^+, K^+ -ATPase (green) and (B) occludin (red) in longitudinal sections of a goldfish gill filament. Nuclei are stained with DAPI (blue) in A and F. C is a merged image of A and B. In A, Na^+, K^+ -ATPase immunolocalizes to select cells within the interlamellar (IL) region of the primary filament and at the base of secondary gill lamellae. In B, discontinuous occludin immunostaining is concentrated along the edges of secondary gill lamellae (white arrow), including medial parts of lamellae that are embedded within the body of the primary filament, and is associated with cells that also stain for Na^+, K^+ -ATPase (white arrowhead). Occludin immunostaining is also prominent in parts of the IL region that line the lateral walls of the central venous sinus (CVS). D and E show, at higher magnification, areas from C that are indicated by the white arrowhead and white arrow, respectively. Control sections probed with secondary antibody only show DAPI fluorescence (F). Scale bars in A, B, C and F are $20 \mu\text{m}$. Scale bars in D and E are $5 \mu\text{m}$.

along the trailing edge of primary gill filaments (cross-sections not shown). No co-localization of occludin and Na^+, K^+ -ATPase was found, and no TRITC or FITC fluorescence was observed in control sections that had been probed with secondary antibody only (Fig. 1F) or with normal rabbit serum (not shown).

Occludin and Na^+, K^+ -ATPase immunolocalization in the intestine
 Immunohistochemical analysis of goldfish intestine revealed prominent basolateral Na^+, K^+ -ATPase immunostaining and distinct apical occludin immunostaining in columnar epithelial cells lining the intestinal lumen (Fig. 2A,B,C). While basolateral Na^+, K^+ -ATPase immunostaining also extended to epithelial cells lining the base of intestinal villi, apical occludin immunostaining appeared less prominent in this region (Fig. 2A). Observation of intestinal

villi and occludin immunostaining at higher magnification revealed a honeycomb-like TJ protein apical distribution pattern facing the intestinal lumen (Fig. 2C). No TRITC or FITC fluorescence was observed in control sections probed with secondary antibody only (Fig. 2E) or with normal rabbit serum (not shown).

Occludin and Na^+, K^+ -ATPase immunolocalization in the kidney
 Immunofluorescence microscopy of the goldfish kidney revealed differential immunostaining patterns in discrete regions of the nephron for both occludin and Na^+, K^+ -ATPase (Fig. 3B). No TRITC or FITC fluorescence was observed in control sections probed with secondary antibody only (Fig. 3C) or with normal rabbit serum (not shown). Within the proximal region of the nephron, immunostaining for Na^+, K^+ -ATPase appeared to be restricted primarily to basal

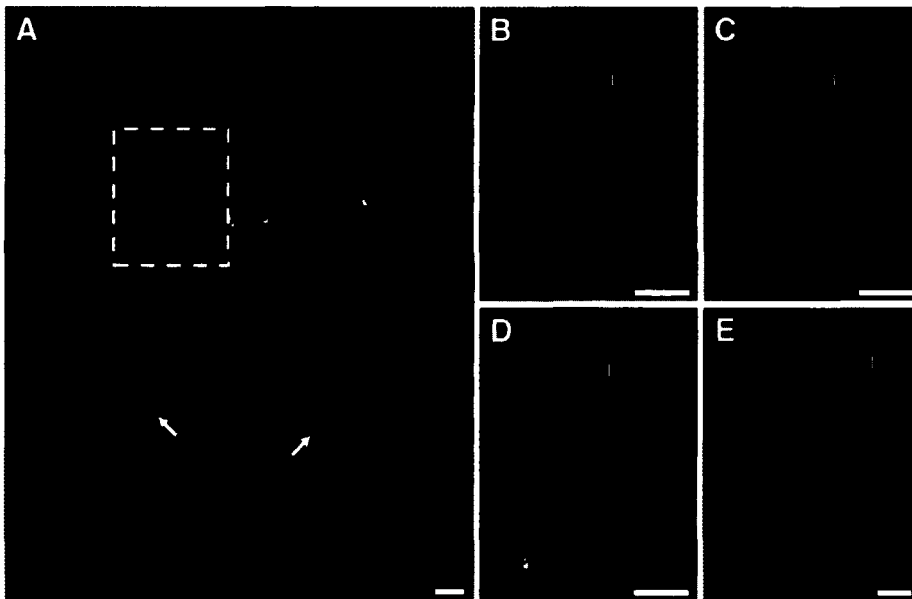


Fig. 2. Immunofluorescence staining of (A,B) Na^+, K^+ -ATPase (green) and (A,C) occludin (red) in cross-sections of goldfish intestine. D is a merged image of B and C. In A, immunostaining for Na^+, K^+ -ATPase is concentrated to basolateral regions and occludin immunostaining is apparent in apical regions of epithelia lining the intestinal lumen (L). Occludin immunostaining appears less prominent in epithelial cells at the base of the intestinal villi (see white arrows in A). At higher magnification (see dashed box in A, which outlines area magnified in C,D), occludin immunostaining appears as a typical honeycomb-like tight junction (TJ) pattern. Nuclei are stained with DAPI (blue), and only DAPI staining is observed in sections probed with secondary antibody alone (E). All scale bars are $20 \mu\text{m}$.

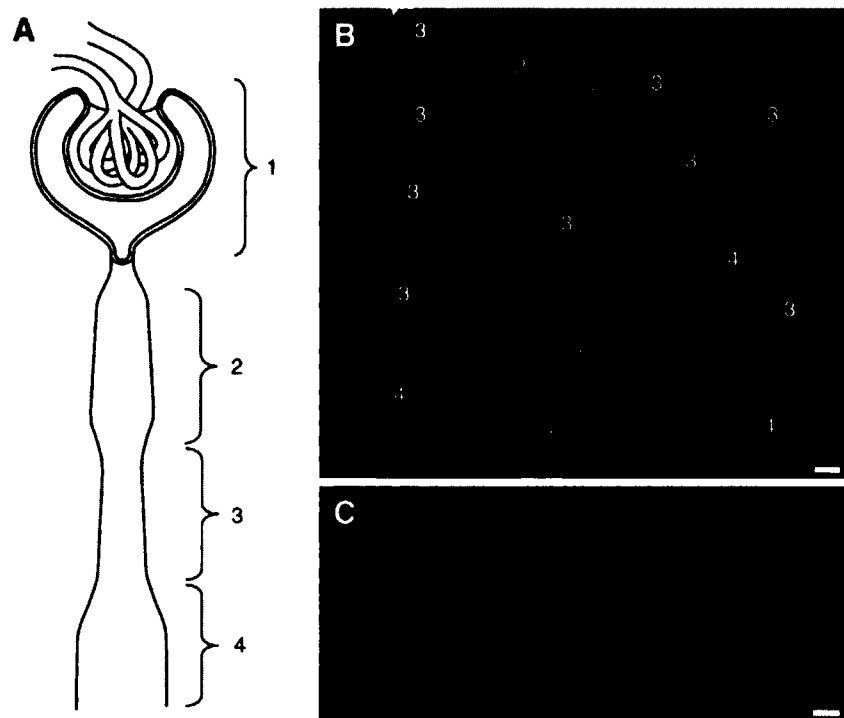


Fig. 3. (A) Schematic illustration of a goldfish nephron based on morphological criteria previously outlined (Sakai, 1985). The goldfish nephron can be divided into the following regions: 1, renal corpuscle (Bowman's capsule and glomerulus); 2, proximal tubule; 3, distal tubule; and 4, collecting duct. (B) Cross-section of goldfish kidney immunostained for occludin (red) and Na^+, K^+ -ATPase (green). Occludin and Na^+, K^+ -ATPase show region-specific immunostaining along the nephron. Numbered labels indicate regions of the nephron as defined in A. No occludin or Na^+, K^+ -ATPase immunostaining was found in the renal corpuscle. A control section can be seen in C (i.e. DAPI fluorescence only). All scale bars are $20 \mu\text{m}$.

regions of the plasma membrane of renal epithelial cells (Fig. 3B, Fig. 4A). In contrast, Na^+, K^+ -ATPase immunostaining in renal epithelial cells of the distal tubule and collecting duct exhibited patterns consistent with localization in basolateral regions of the plasma membrane (Fig. 3B, Fig. 4B,C). An observable difference

in Na^+, K^+ -ATPase immunostaining between the distal tubule and collecting duct was the intensity of immunoreactivity; basolateral Na^+, K^+ -ATPase immunostaining was consistently weaker in the collecting duct (Fig. 3B, Fig. 4C) than in the distal tubule (Fig. 3B, Fig. 4B). While no occludin immunostaining could be observed in

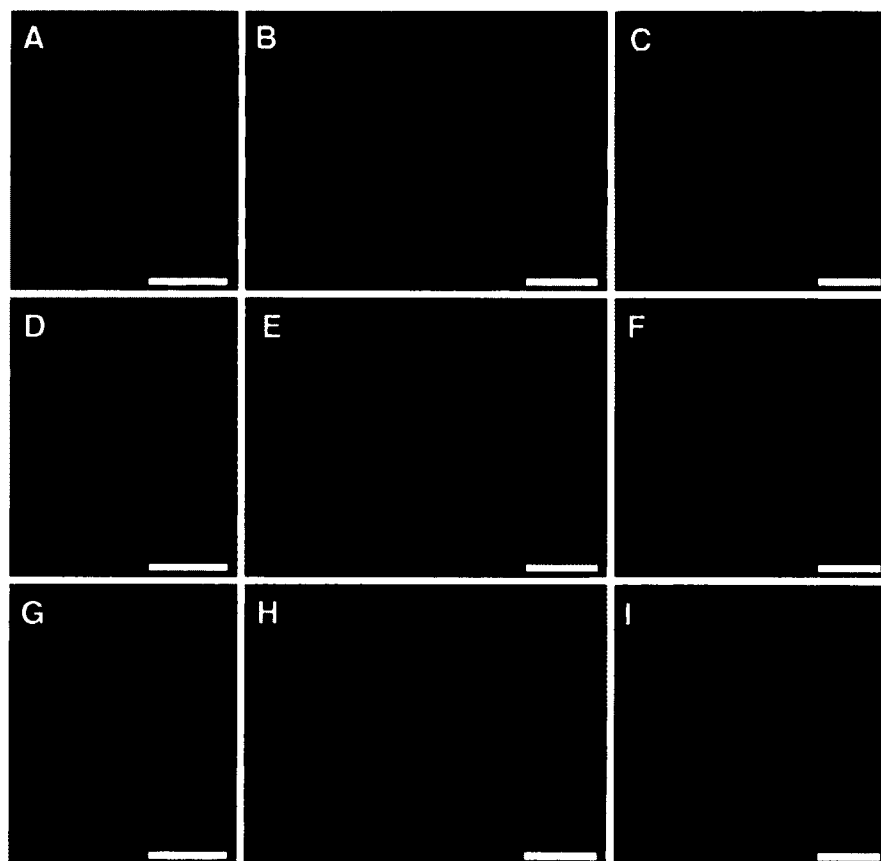


Fig. 4. Immunofluorescence staining of (A–C) Na^+, K^+ -ATPase (green) and (D–F) occludin (red) in cross-sections of goldfish proximal tubule (A, D, G), distal tubule (B, E, H) and collecting duct (C, F, I). Nuclei are stained with DAPI (blue) in A–C. G, H and I are merged images of A and D, B and E, and C and F, respectively. Immunostaining for Na^+, K^+ -ATPase is restricted primarily to the basal membrane of renal epithelial cells in the proximal region of the nephron (A) and to the basolateral membrane of renal epithelial cells in distal and collecting segments (B, C). No occludin immunostaining is observed in proximal segments of the nephron (D). Strong and moderate occludin immunostaining is concentrated at the apical membrane of renal epithelial cells lining the lumen of the distal tubule and collecting duct, respectively (E, F). All scale bars are $20 \mu\text{m}$.

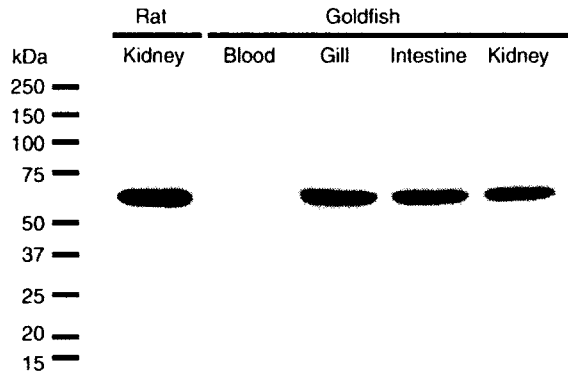


Fig. 5. Western blot analysis of occludin expression in goldfish gill, intestine and kidney. Single occludin immunoreactive bands (at ~68 kDa) always appeared for goldfish epithelial tissue. A non-epithelial negative control tissue (goldfish blood cells) was not immunoreactive. A positive tissue control (rat kidney) was found to resolve at ~65 kDa.

proximal segments of the goldfish nephron (Fig. 3B, Fig. 4D), strong and moderate occludin immunostaining occurred at the apical membrane of renal epithelial cells lining the lumen of the distal tubule and collecting duct, respectively (Fig. 3B, Fig. 4E,F). There appeared to be no occludin or Na⁺,K⁺-ATPase immunostaining at the goldfish renal corpuscle.

Western blot analysis

Western blot analysis of protein isolated from goldfish gill, intestine and kidney revealed single occludin immunoreactive bands at ~68 kDa; however, no immunoreactive bands were detected for protein isolated from goldfish blood cells (Fig. 5). A single occludin immunoreactive band for protein isolated from rat kidney resolved at ~65 kDa (Fig. 5).

Food deprivation experiments

Body mass changes

The effects of 1, 2 and 4 weeks of food deprivation on goldfish body mass are shown in Fig. 6. Control fish, fed 1.5% their initial body mass, gained an average (\pm s.e.m.) of 4.5 \pm 0.6%, 13.5 \pm 1.7% and

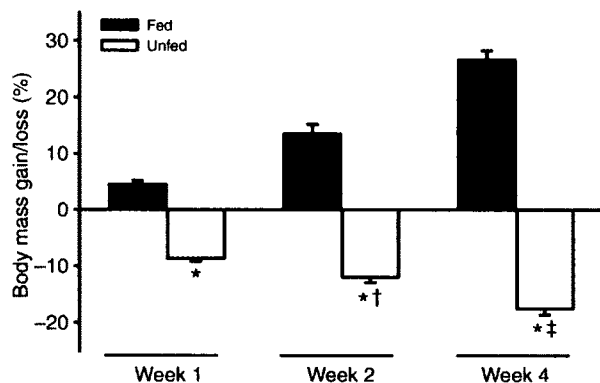


Fig. 6. Effects of 1, 2 and 4 weeks feeding and food deprivation on relative mass gain/loss in goldfish. Data are expressed as mean values \pm s.e.m. ($N=10$ per group). *Significant difference ($P<0.05$) between fed and unfed groups at the same time point. †Significant difference ($P<0.05$) from 1 week unfed group. ‡Significant difference ($P<0.05$) from 2 weeks unfed group.

26.6 \pm 1.6% of their initial body mass during the 1, 2 and 4 week experimental periods, respectively. In contrast, food-deprived fish lost an average of 8.6 \pm 0.6% (1 week), 12 \pm 1% (2 weeks) and 17.5 \pm 1.1% (4 weeks) their initial body mass.

Serum osmolality, electrolytes and muscle moisture content

After 1 week of food deprivation, no significant ($P>0.05$) alterations in serum osmolality and Na⁺ or Cl⁻ levels were observed (Fig. 7A,B,C). Similarly, 1 week of food deprivation had no significant ($P>0.05$) effect on muscle moisture content (Fig. 7D). In contrast, following 2 and 4 weeks of food deprivation, serum osmolality, and Na⁺ and Cl⁻ levels significantly ($P<0.05$) decreased, while muscle water content significantly ($P<0.05$) increased (Fig. 7).

Na⁺,K⁺-ATPase enzyme activity and occludin protein expression

When compared with fed fish groups, goldfish gill Na⁺,K⁺-ATPase activity significantly ($P<0.05$) decreased (~16%) following 1 week of food deprivation, increased (~11%, $P>0.05$) following 2 weeks of food deprivation and significantly ($P<0.05$) increased (~13%) following 4 weeks of food deprivation (Fig. 8A). Gill occludin protein expression in food-deprived goldfish was significantly ($P<0.05$) lower than in control groups by ~41%, ~58% and ~31% following 1, 2 and 4 weeks of food deprivation, respectively (Fig. 8B). Intestinal Na⁺,K⁺-ATPase activity in goldfish following 1, 2 and 4 weeks of food deprivation significantly ($P<0.05$) decreased by ~46%, ~66% and ~44%, respectively, when compared with fed fish (Fig. 9A). Intestinal occludin protein expression did not significantly ($P>0.05$) alter in goldfish following 1 and 2 weeks of food deprivation when compared with control groups; however, intestinal occludin protein expression significantly ($P<0.05$) decreased by ~34% following 4 weeks of food deprivation when compared with fed fish (Fig. 9B). Food deprivation did not significantly ($P>0.05$) alter goldfish kidney Na⁺,K⁺-ATPase activity at any point during the experiment (Fig. 10A); however, goldfish kidney occludin protein expression significantly ($P<0.05$) increased by ~640% and ~160% following 1 and 2 weeks of food deprivation, respectively, and significantly ($P<0.05$) decreased by ~60% following 4 weeks of food deprivation when compared with fed groups (Fig. 10B). The loading control, α -tubulin, was detected at ~52 kDa and its expression did not change following 1, 2 and 4 weeks of food deprivation (not shown).

DISCUSSION

Overview

Despite the universal inclusion of TJs in illustrative models of ion transport across fish epithelia, studies specifically investigating TJs in fishes have largely been limited to morphological analyses by electron microscopy (Sardet et al., 1979; Bartels and Potter, 1991; Freda et al., 1991; McDonald et al., 1991). To the best of our knowledge, no studies have examined the immunohistochemical localization and protein expression of any integral TJ protein in fish gill, intestine or renal epithelial tissue, although the localization of zonula occludens-1 (ZO-1, a cytosolic TJ-related protein) was recently described in puffer fish gills (Kato et al., 2007). Furthermore, no studies have examined whether or how TJ protein expression may adjust in response to altered hydromineral status in aquatic vertebrates. We have examined the localization and expression of the integral transmembrane TJ protein occludin in fish tissues for the first time. Our observations suggest a role for occludin in the maintenance of hydromineral balance and that its regulation of epithelial 'tightness' may be tissue specific. Furthermore, within tissue composed of heterogeneous regions of

physiological function, such as the nephron, the role of occludin is likely to vary between discrete zones. Overall, alterations in occludin

protein expression in response to hydromineral imbalance suggest that occludin may play a dynamic role in the regulation of epithelial permeability in fish.

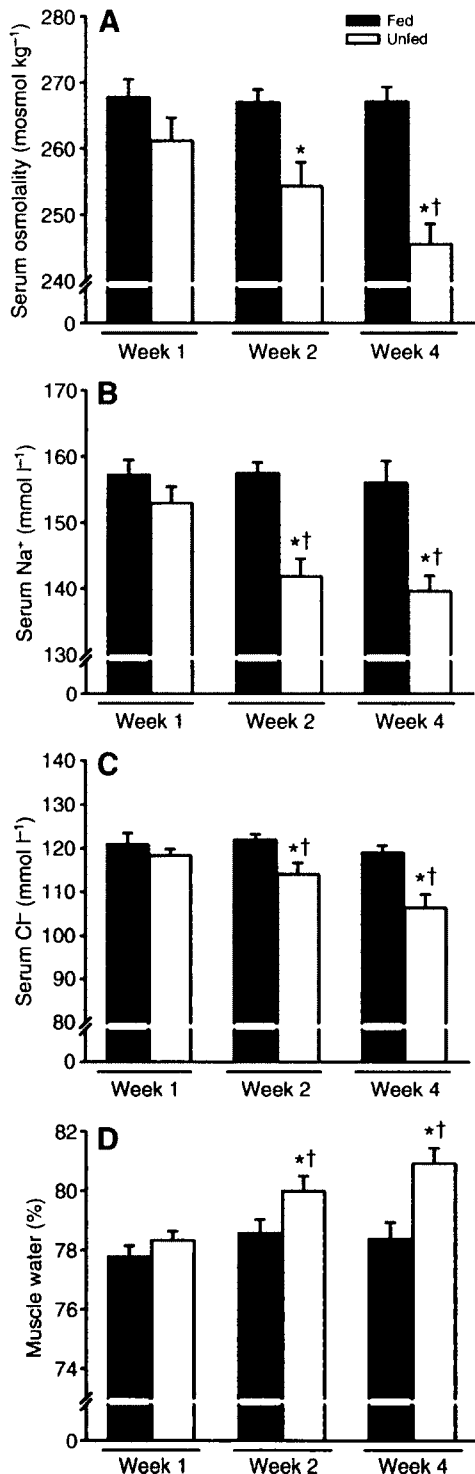


Fig. 7. Effects of 1, 2 and 4 weeks feeding and food deprivation on (A) serum osmolality, (B) serum Na⁺, (C) serum Cl⁻ and (D) muscle water content in goldfish. Data are expressed as mean values \pm s.e.m. ($N=10$ per group). *Significant difference ($P < 0.05$) between fed and unfed groups at the same time point. †Significant difference ($P < 0.05$) from 1 week unfed group.

Immunolocalization and Western blot analysis of occludin

Na⁺,K⁺-ATPase immunolocalization to cells within the IL region of goldfish primary filaments and at the base of the secondary gill filaments (particularly along the trailing edge of primary gill filaments; Fig. 1A) corresponds with the location of mitochondria-rich cells (MRCs) in goldfish gills (Kikuchi, 1977) and FW fish gills in general (Perry, 1997; Wilson et al., 2000). Pronounced and discontinuous occludin immunostaining along the edges of goldfish gill secondary lamellae (Fig. 1B,E), and along the edges of gill epithelial cells that immunostain for Na⁺,K⁺-ATPase (and are thus presumed to be MRCs; Fig. 1D), suggests that occludin may be associated with TJs between cells of the lamellar epithelium (e.g. pavement cells or MRCs) and/or with TJs between pillar cells that surround and form the lamellar blood spaces. This generally agrees with previous reports in which freeze fracture and electron microscopy observations of fish gill epithelia have shown that

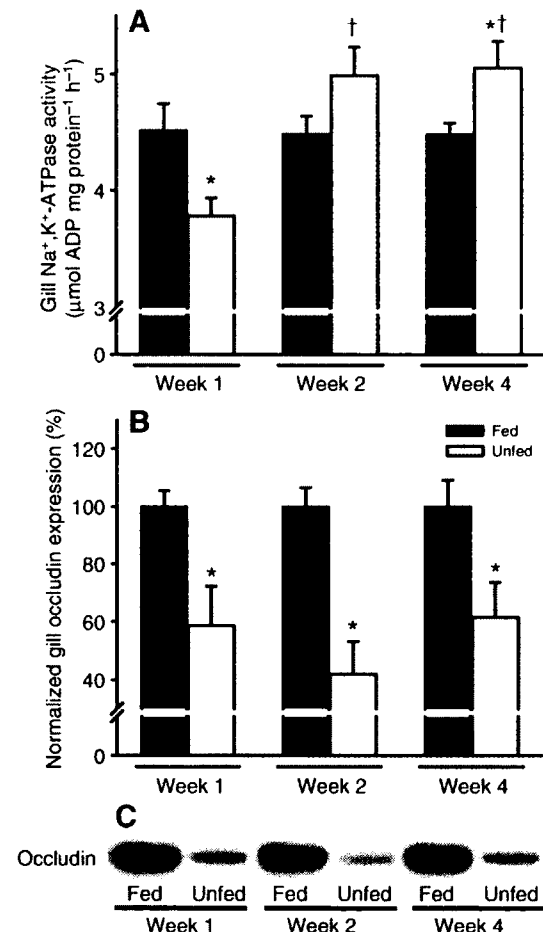


Fig. 8. Effects of 1, 2 and 4 weeks feeding and food deprivation on (A) gill Na⁺,K⁺-ATPase activity and (B) normalized gill occludin expression in goldfish determined by Western blot analyses. (C) Representative Western blot of gill occludin protein expression in fed and unfed goldfish. Data are expressed as mean values \pm s.e.m. ($N=8-10$ per group). *Significant difference ($P < 0.05$) between fed and unfed groups at the same time point. †Significant difference ($P < 0.05$) from 1 week unfed group.

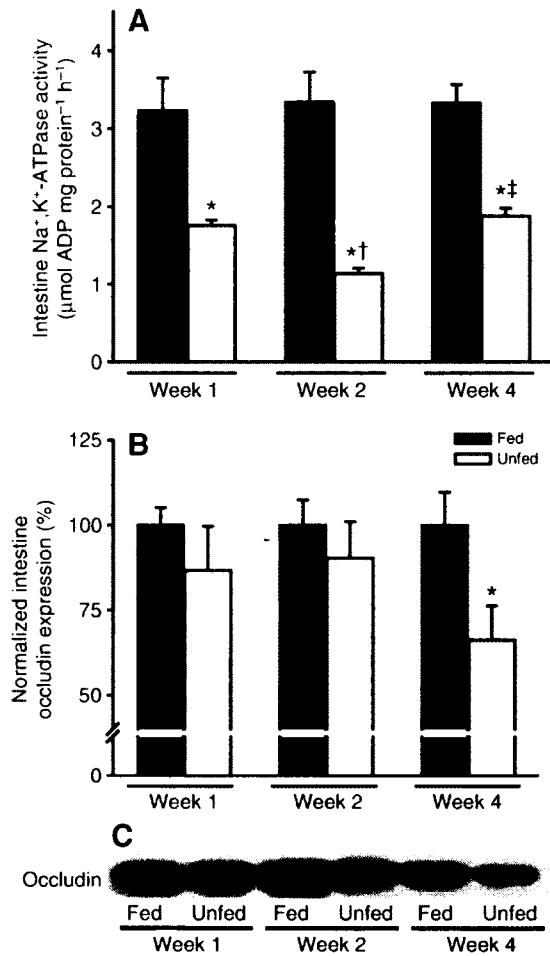


Fig. 9. Effects of 1, 2 and 4 weeks feeding and food deprivation on (A) intestine Na⁺,K⁺-ATPase activity and (B) normalized intestine occludin expression in goldfish determined by Western blot analyses. (C) Representative Western blot of intestine occludin protein expression in fed and unfed goldfish. Data are expressed as mean values ± s.e.m. (*N*=8–10 per group). *Significant difference (*P*<0.05) between fed and unfed groups at the same time point. †Significant difference (*P*<0.05) from 1 week unfed group. ‡Significant difference (*P*<0.05) from 2 weeks unfed group.

pavement cells (PVCs), MRCs and pillar cells all form TJ complexes with adjacent cells – i.e. PVCs with adjacent PVCs, PVCs with MRCs, or pillar cells with adjacent pillar cells (Hughes and Grimstone, 1965; Sardet et al., 1979; Bartels and Potter, 1991; Kudo et al., 2007). Furthermore, a recent study has immunolocalized ZO-1, which is believed to associate with the C-terminal region of occludin (Furuse et al., 1994), to pillar cells within the gills of marine puffer fish (Kato et al., 2007). When taken together, the results of our study combined with the immunolocalization of ZO-1 in puffer fish gills (Kato et al., 2007) indicate that the close association between ZO-1 and occludin that has been observed in mammals is likely to exist in fishes as well. While our data suggest a potential role for occludin in gill permeability, future studies using higher resolution microscopy techniques will be beneficial to ascertain the exact nature of occludin expression and interaction between gill cells (e.g. PVCs, MRCs and/or pillar cells) within branchial lamellae.

Similar to immunohistochemical studies in other fish species (Giffard-Mena et al., 2006), Na⁺,K⁺-ATPase immunostaining in the

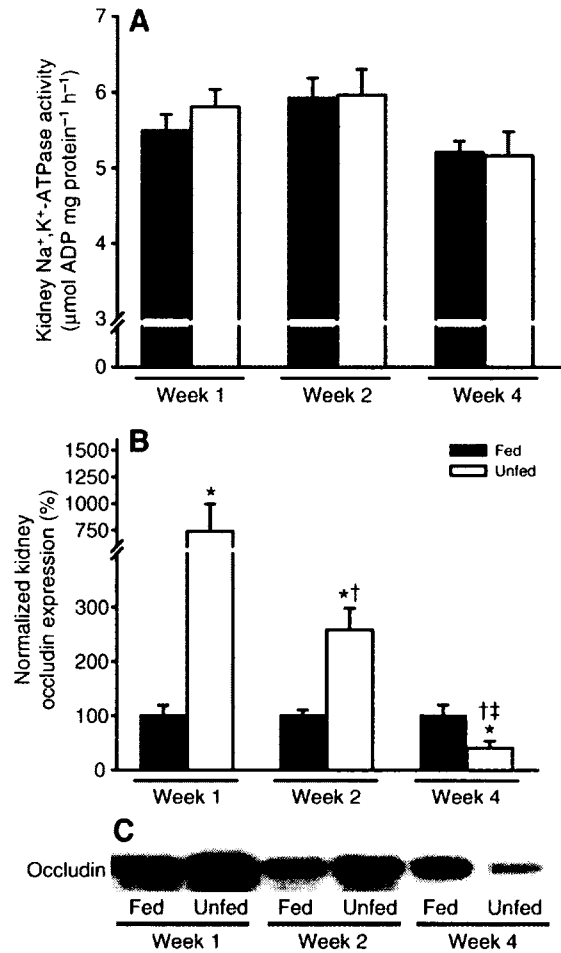


Fig. 10. Effects of 1, 2 and 4 weeks feeding and food deprivation on (A) kidney Na⁺,K⁺-ATPase activity and (B) normalized kidney occludin expression in goldfish determined by Western blot analyses. (C) Representative Western blot of kidney occludin protein expression in fed and unfed goldfish. Data are expressed as mean values ± s.e.m. (*N*=8–10 per group). *Significant difference (*P*<0.05) between fed and unfed groups at the same time point. †Significant difference (*P*<0.05) from 1 week unfed group. ‡Significant difference (*P*<0.05) from 2 weeks unfed group.

goldfish intestine was concentrated along the basolateral membrane of columnar epithelial cells lining the intestinal lumen (Fig. 2A,B). In contrast, occludin immunostaining was most prominent in apical regions of intestinal epithelial cells (Fig. 2A,C). When observed more closely, occludin immunostaining along the apical membrane of intestinal epithelial cells appeared to be distributed in a honeycomb-like arrangement (Fig. 2C), a typical TJ protein distribution pattern that has been observed along the gastrointestinal tract of other vertebrates (Inoue et al., 2006; Ridyard et al., 2007).

The goldfish kidney revealed differential immunostaining patterns in discrete regions of the nephron for both Na⁺,K⁺-ATPase and occludin (Fig. 3B). Similar differential Na⁺,K⁺-ATPase staining patterns have been observed in other fish species and basolateral localization of Na⁺,K⁺-ATPase concurs with models illustrating region-specific ion transport mechanisms in fish renal epithelia (Nebel et al., 2005; Beyenbach, 2004). Furthermore, specific patterns of Na⁺,K⁺-ATPase distribution along the nephron have also been reported for several other vertebrate groups (Piepenhagen et

al., 1995; Kwon et al., 1998; Sabolić et al., 1999; Sturla et al., 2003). The differential occludin expression patterns observed in the goldfish nephron were similar to those observed in the mammalian kidney (Kwon et al., 1998; González-Mariscal et al., 2000). In mammals, differential occludin immunostaining patterns correlate with renal epithelial 'tightness', such that 'tighter' nephron segments (as determined by TER measurements) express higher levels of occludin protein than 'leakier' nephron regions. In human and rabbit renal tubules, occludin immunostaining was weakest in 'leaky' proximal tubules and strongest in 'tight' distal tubules (Kwon et al., 1998; González-Mariscal et al., 2000). Furthermore, Western blot analysis of microdissected rabbit renal tubules revealed low occludin protein expression in 'leaky' proximal tubules and significantly higher occludin protein expression in 'tight' distal and collecting segments (González-Mariscal et al., 2000). The proximal tubule of the FW fish nephron is characterized as a relatively water-permeable and 'leaky' epithelium that reabsorbs a small percentage of Na^+ and Cl^- ions, as well as glucose and other organic solutes, from glomerular filtrate (Logan et al., 1980; Dantzer, 2003). The distal tubule and collecting duct of the FW teleost nephron, on the other hand, reabsorb the majority of salts from glomerular filtrate and are characterized as 'tight' epithelia (Nishimura et al., 1983; Dantzer, 2003). In the goldfish nephron, no occludin immunostaining was observed in 'leaky' proximal regions (Fig. 4D); however, strong apical occludin immunoreactivity was detected in the 'tighter' distal regions and moderate expression was observed in the collecting segments (Fig. 4E,F). These observations suggest that occludin may regulate goldfish renal epithelial 'tightness' in a manner similar to mammals, and may thus influence the re-absorptive capacity of the different segments of the nephron.

Western blot analysis of occludin protein expression in homogenized rat kidney revealed a single immunoreactive band at ~65 kDa, while single immunoreactive bands at ~68 kDa were detected for homogenized goldfish gills, intestine and kidney (Fig. 5). No occludin immunoreactivity was detected for goldfish blood cells, a non-epithelial tissue (Fig. 5). Although predominantly detected as a 65 kDa protein in mammals, many reports have identified several occludin immunoreactive bands between ~62 and 82 kDa (Sakakibara et al., 1997; Wong, 1997), therefore the occludin immunoreactive band found for goldfish epithelial tissue is consistent with the molecular mass range found in other vertebrates.

Hydromineral balance and occludin expression in food-deprived goldfish

Food deprivation in goldfish resulted in a negative energy balance (negative changes in fish mass) at all time periods examined in the current study (Fig. 6). However, only fish that were food deprived for 2 weeks or longer exhibited alterations in the endpoints associated with salt and water balance. The observed reductions in serum osmolality, and Na^+ and Cl^- levels and a concomitant increase in muscle hydration (Fig. 7) indicate that food deprivation can elicit changes in the hydromineral status of goldfish. These observations are in line with other studies that have described the reorganization of ionoregulatory machinery in response to restricted dietary regimes or food deprivation (Kültz and Jürss, 1991; Vijayan et al., 1996; Kelly et al., 1999).

Short-term food deprivation (1 week) in goldfish resulted in a significant reduction in gill Na^+, K^+ -ATPase activity while a longer period without feeding (e.g. 4 weeks) resulted in a significant increase in gill Na^+, K^+ -ATPase activity (Fig. 8A), suggesting an initial (temporary) down-regulation of active ion transport across the gills followed by a significant up-regulation. An up-regulation

of gill Na^+, K^+ -ATPase activity after 4 weeks of food deprivation was unexpected. A previous study (Kültz and Jürss, 1991) reported that food deprivation (albeit 6 weeks) in FW tilapia caused a reduction in gill Na^+, K^+ -ATPase activity. However, results may be time or species specific as another study (Vijayan et al., 1996) reported no change in gill Na^+, K^+ -ATPase activity after 2 weeks of food deprivation in the same species. In contrast to Na^+, K^+ -ATPase activity, occludin protein expression decreased in response to food deprivation after 1 week and remained consistently low after 2 and 4 weeks (Fig. 8B). Although these results allow us to accept our original hypothesis, that occludin protein expression would alter in response to hydromineral imbalance, it is difficult to rationalize a reduction in occludin protein expression, as opposed to an increase that might be expected to occur in association with gill epithelial tightening and reduced passive ion loss. There are several possible explanations: (1) gill epithelia may become 'leakier' in food-deprived goldfish; however, this would seem maladaptive [furthermore, a previous study (Nance et al., 1987) reported reductions in gill epithelial permeability in response to food deprivation in a FW fish]; (2) the role of occludin in regulating gill epithelial permeability during periods of food deprivation may be overshadowed by other TJ proteins such as claudins, a family of transmembrane TJ proteins that also significantly contribute to the TJ barrier function (for a review, see Koval, 2006); or (3) the use of whole-gill homogenates and the heterogeneous nature of the gill epithelium may mask specific changes in occludin expression between specific gill cell types. For example, an earlier study reported (Kültz and Jürss, 1991) a significant reduction in MRC number in response to food deprivation in a FW fish. A reduction in MRC number, and thus a reduction in MRC-PVC TJ interactions, could potentially result in an overall reduction in gill occludin expression with little to no change in gill permeability, since PVC-PVC TJs would presumably remain intact. Regardless, the exact reason(s) for a reduction in gill occludin expression in food-deprived goldfish requires further study.

Dietary Na^+ and Cl^- as well as nutrient absorption by intestinal epithelial cells of FW fishes is dependent upon an electrochemical gradient generated by Na^+, K^+ -ATPase (Loretz, 1995). Food deprivation at all time points resulted in a significant reduction in goldfish intestinal Na^+, K^+ -ATPase activity (Fig. 9A), suggesting a diminished capacity for active dietary salt and nutrient absorption by starved fish. Reduced intestinal Na^+, K^+ -ATPase activity as a result of food deprivation has also been reported in FW tilapia (Kültz and Jürss, 1991) and may be indicative of a depletion of the intestinal absorptive mucosa, a starvation-associated condition observed in other fish species (Bogé et al., 1981; Avella et al., 1992). Intestinal occludin expression significantly decreased following 4 weeks of food deprivation only (Fig. 9B), suggesting that over longer periods of dietary restriction, occludin may become involved in modifications of the barrier function of the goldfish intestine. Significant reductions in intestine epithelial TER and increased Na^+ -independent intestinal influx of proline in FW-adapted coho salmon following 2 weeks of food deprivation have previously been reported (Collie, 1985), indicating impairment of barrier function in response to starvation in a FW fish. In other vertebrates, occludin down-regulation occurs in association with decreased intestine epithelial resistance, TJ protein re-distribution and intestinal barrier dysfunction (Zeissig et al., 2007; Musch et al., 2006). These areas require further attention.

The FW fish kidney actively reabsorbs salts from glomerular filtrate producing dilute urine. Solute reabsorption across proximal and distal tubules of the nephron is driven by an electrochemical

gradient of Na^+ generated by Na^+, K^+ -ATPase (Dantzler, 2003). Although, in the current study, negative energy balance appeared to have no overall effect on kidney Na^+, K^+ -ATPase activity (Fig. 10A), it is possible that food deprivation may have resulted in nephron-specific alterations in Na^+, K^+ -ATPase activity such that there was no observable alteration in 'total' activity. For example, in humans, dietary restriction and food deprivation are associated with reduced Na^+ reabsorption across the proximal tubule of the nephron and a concomitant increase in Na^+ reabsorption by distal segments to counterbalance natriuresis, presumably both of which are associated with opposing alterations in ionomotive enzyme activity (Satta et al., 1984). Occludin protein expression in the goldfish kidney, however, exhibited an apparent biphasic pattern in food-deprived fish, markedly increasing after 1 week and significantly decreasing after 4 weeks (Fig. 10B), suggesting that food deprivation provokes a biphasic effect on renal function in the goldfish. A starvation-induced biphasic response in renal function has previously been documented in both humans and rats (Boulter et al., 1973; Boim et al., 1992; Wilke et al., 2005), where short-term starvation can result in natriuresis and polyuria that are eventually corrected and compensated for over longer experimental periods (Boulter et al., 1973; Wilke et al., 2005). Assuming the observed biphasic alterations in kidney occludin expression in food-deprived goldfish lead to adaptive function, one can rationalize that resulting regional changes in nephron permeability would enhance ion reabsorption and augment water elimination. In this regard, it is noteworthy that the highest and lowest renal expression of occludin in food-deprived goldfish occur in association with reduced and elevated gill Na^+, K^+ -ATPase activity, respectively, indicating an interplay of strategies worthy of further investigation.

Conclusion

To summarize, we have immunolocalized occludin in goldfish ionoregulatory epithelia and demonstrated that occludin protein expression levels alter in response to hydromineral imbalance. The changes that occur in occludin protein abundance in response to starvation-induced hydromineral imbalance are tissue specific and, based on morphological evidence, are likely to be regionally different within specific tissues. The current study suggests that occludin should be expected to play an important role in the regulation of paracellular solute movement in aquatic vertebrates. While the response of occludin to hydromineral imbalance in goldfish often fits with its currently accepted role as an integral transmembrane TJ protein involved in regulating epithelial permeability, alterations in gill tissue are less easily explained. This underscores the paucity of information in the area of TJ physiology and the role these proteins play in the homeostatic control of hydromineral balance in aquatic vertebrates. This alone is an impetus for further study.

This work was supported by an NSERC Discovery Grant and a CFI New Opportunities Fund to S.P.K. H.C. was supported by an Ontario Graduate Scholarship from the Government of Ontario. All procedures conformed to the guidelines of the Canadian Council of Animal Care. The monoclonal antibodies developed by D. M. Fambrough ($\alpha 5$) and J. Frankel and E. M. Nelsen (12G10) were obtained from the Developmental Studies Hybridoma Bank developed under the auspices of the NICHD and maintained by The University of Iowa, Department of Biological Sciences, Iowa City, IA, 52242, USA.

REFERENCES

- Avella, M., Blaise, O. and Berhaut, J. (1992). Effects of starvation on valine and alanine transport across the intestinal mucosal border in sea bass, *Dicentrarchus labrax*. *J. Comp. Physiol. B* 162, 430-435.
- Balda, M. S., Whitney, J. A., Flores, C., González, S., Cerejildo, M. and Matter, K. (1996). Functional dissociation of paracellular permeability and transepithelial electrical resistance and disruption of the apical-basolateral intramembrane diffusion barrier by expression of a mutant tight junction membrane protein. *J. Cell Biol.* 134, 1031-1049.
- Bartels, H. and Potter, I. C. (1991). Structural changes in the zonulae occludentes of the chloride cells of young adult lampreys following acclimation to seawater. *Cell Tissue Res.* 265, 447-457.
- Beyenbach, K. W. (2004). Kidney sans glomeruli. *Am. J. Physiol.* 286, F811-F827.
- Bogé, G., Rigal, A. and Pérès, G. (1981). A study of *in vivo* glycine absorption by fed and fasted rainbow trout (*Salmo gairdneri*). *J. Exp. Biol.* 91, 285-292.
- Boim, M. A., Ajzen, H., Ramos, O. L. and Schor, N. (1992). Glomerular hemodynamics and hormonal evaluation during starvation in rats. *Kidney Int.* 42, 567-572.
- Boulter, P. R., Hoffman, R. S. and Arky, R. A. (1973). Pattern of sodium excretion accompanying starvation. *Metabolism* 22, 675-683.
- Busacker, G. P. and Chavin, W. (1981). Characterization of $\text{Na}^+ + \text{K}^+$ -ATPases and Mg^{2+} -ATPases from the gill and the kidney of the goldfish (*Carassius auratus* L.). *Comp. Biochem. Physiol.* 69B, 249-256.
- Cerejildo, M. and Anderson, J. M. (2001). Introduction: evolution of ideas on the tight junction. In *Tight Junctions* (ed. M. Cerejildo and J. M. Anderson), pp. 1-18. Boca Raton: CRC Press.
- Chen, Y., Merzdorf, C., Paul, D. L. and Goodenough, D. A. (1997). COOH terminus of occludin is required for tight junction barrier function in early *Xenopus* embryos. *J. Cell Biol.* 138, 891-899.
- Collie, N. L. (1985). Intestinal nutrient transport in coho salmon (*Oncorhynchus kisutch*) and the effects of development, starvation, and seawater adaptation. *J. Comp. Physiol. B* 156, 163-174.
- Dantzler, W. H. (2003). Regulation of renal proximal and distal tubule transport: sodium, chloride and organic anions. *Comp. Biochem. Physiol.* 136A, 453-478.
- Evans, D. H., Piermarini, P. M. and Choe, K. P. (2005). The multifunctional fish gill: dominate site of gas exchange, osmoregulation, acid-base regulation, and excretion of nitrogenous waste. *Physiol. Rev.* 85, 97-177.
- Freda, J., Sanchez, D. A. and Bergman, H. L. (1991). Shortening of branchial tight junctions in acid-exposed rainbow trout (*Oncorhynchus mykiss*). *Can. J. Fish. Aquat. Sci.* 48, 2028-2033.
- Fujimoto, K. (1995). Freeze-fracture replica electron microscopy combined with SDS digestion for cytochemical labeling of integral membrane proteins. Application to the immunogold labeling of intercellular junctional complexes. *J. Cell Sci.* 108, 3443-3449.
- Furuse, M., Hirase, T., Itoh, M., Nagafuchi, A., Yonemura, S., Tsukita, S. and Tsukita, S. (1993). Occludin: a novel integral membrane protein localizing at tight junctions. *J. Cell Biol.* 123, 1777-1788.
- Furuse, M., Itoh, M., Hirase, T., Nagafuchi, A., Yonemura, S., Tsukita, S. and Tsukita, S. (1994). Direct association of occludin with ZO-1 and its possible involvement in the localization of occludin at tight junctions. *J. Cell Biol.* 127, 1617-1626.
- Furuse, M., Sasaki, H., Fujimoto, K. and Tsukita, S. (1998). A single gene product, claudin-1 or -2, reconstitutes tight junction strands and recruits occludin in fibroblasts. *J. Cell Biol.* 143, 391-401.
- Giffard-Mena, I., Charmantier, G., Grousset, E., Aujoulat, F. and Castille, R. (2006). Digestive tract ontogeny of *Dicentrarchus labrax*: implication in osmoregulation. *Dev. Growth Differ.* 48, 139-151.
- González-Mariscal, L., Namorado, M. C., Martín, D., Luna, J., Alarcon, L., Islas, S., Valencia, L., Muriel, P., Ponce, L. and Reyes, J. L. (2000). Tight junction proteins ZO-1, ZO-2, and occludin along isolated renal tubules. *Kidney Int.* 57, 2386-2402.
- González-Mariscal, L., Betanzos, A., Nava, P. and Jaramillo, B. E. (2003). Tight junction proteins. *Prog. Biophys. Mol. Biol.* 81, 1-44.
- Hughes, G. M. and Grimstone, A. V. (1965). The fine structure of the secondary lamellae of the gills of *Gadus pollachius*. *Q. J. Microsc. Sci.* 106, 343-353.
- Inoue, K., Oyama, M., Mitsufuji, S., Okanoue, T. and Takamatsu, T. (2006). Different changes in the expression of multiple kinds of tight-junction proteins during ischemia-reperfusion injury of the rat ileum. *Acta Histochem. Cytochem.* 39, 35-45.
- Kato, A., Nakamura, K., Kudo, H., Tran, Y. H., Yamamoto, Y., Doi, H. and Hirose, S. (2007). Characterization of the column and autocolar junctions that define the vasculature of gill lamellae. *J. Histochem. Cytochem.* 55, 941-953.
- Kelly, S. P., Chow, I. N. K. and Woo, N. Y. S. (1999). Alterations in Na^+/K^+ -ATPase activity and gill chloride cell morphometrics of juvenile black sea bream (*Mylio macrocephalus*) in response to salinity and ration size. *Aquaculture* 172, 351-367.
- Kikuchi, S. (1977). Mitochondria-rich (chloride) cells in the gill epithelia from four species of stenohaline fresh water teleosts. *Cell Tissue Res.* 180, 87-98.
- Koval, M. (2006). Claudins – key pieces in the tight junction puzzle. *Cell Commun. Adhes.* 13, 127-138.
- Kudo, H., Kato, A. and Hirose, S. (2007). Fluorescence visualization of branchial collagen columns embraced by pillar cells. *J. Histochem. Cytochem.* 55, 57-62.
- Kültz, D. and Jürss, K. (1991). Acclimation of chloride cells and Na^+/K^+ -ATPase to energy deficiency in tilapia (*Oreochromis mossambicus*). *Zool. Jb. Physiol.* 95, 39-50.
- Kwon, O., Myers, B. D., Sibley, R., Dafoe, D., Altrey, E. and Nelson, W. J. (1998). Distribution of cell membrane-associated proteins along the human nephron. *J. Histochem. Cytochem.* 46, 1423-1434.
- Logan, A. G., Moriarty, R. J. and Rankin, J. C. (1980). A micropuncture study of kidney function in the river lamprey, *Lampetra fluviatilis*, adapted to fresh water. *J. Exp. Biol.* 85, 137-147.
- Loretz, C. A. (1995). Electrophysiology of ion transport in teleost intestinal cells. In *Fish Physiology, Volume 14, Cellular and Molecular Approaches to Fish Ionic Regulation* (ed. C. M. Wood and T. J. Shuttleworth), pp. 25-56. San Diego: Academic Press.
- Marshall, W. S. (2002). Na^+ , Cl^- , Ca^{2+} and Zn^{2+} transport by fish gills: retrospective review and prospective synthesis. *J. Exp. Zool.* 293, 264-283.
- McCarthy, K. M., Skare, I. B., Stankewich, M. C., Furuse, M., Tsukita, S., Rogers, R. A., Lynch, R. D. and Schneeberger, E. E. (1996). Occludin is a functional component of the tight junction. *J. Cell Sci.* 109, 2287-2298.
- McCormick, S. D. (1993). Methods for nonlethal gill biopsy and measurement of Na^+ , K^+ -ATPase activity. *Can. J. Fish. Aquat. Sci.* 50, 656-658.

- McDonald, D. G., Freda, J., Cavdek, V., Gonzalez, R. and Zia, S. (1991). Interspecific differences in gill morphology of freshwater fish in relation to tolerance of low-pH environments. *Physiol. Zool.* **64**, 124-144.
- Musch, M. W., Walsh-Reitz, M. M. and Chang, E. B. (2006). Roles of ZO-1, occludin, and actin in oxidant-induced barrier disruption. *Am. J. Physiol.* **290**, G222-G231.
- Nance, J. M., Masoni, A., Sola, F. and Bornancin, M. (1987). The effects of starvation and sexual maturation on Na⁺ transbranchial fluxes following direct transfer from fresh water to sea-water in rainbow trout (*Salmo gairdneri*). *Comp. Biochem. Physiol.* **87A**, 613-622.
- Nebel, C., Romestand, B., Nègre-Sadargues, G., Grousset, E., Aujoulat, F., Bacal, J., Bonhomme, F. and Charmantier, G. (2005). Differential freshwater adaptation in juvenile sea-bass *Dicentrarchus labrax*: involvement of gills and urinary system. *J. Exp. Biol.* **208**, 3859-3871.
- Nishimura, H., Imai, M. and Ogawa, M. (1983). Sodium chloride and water transport in the renal distal tubule of the rainbow trout. *Am. J. Physiol.* **244**, F247-F254.
- Perry, S. F. (1997). The chloride cell: structure and function in the gills of freshwater fishes. *Annu. Rev. Physiol.* **59**, 325-347.
- Piepenhagen, P. A., Peters, L. L., Lux, S. E. and Nelson, W. J. (1995). Differential expression of Na⁺-K⁺-ATPase, ankyrin, fodrin, and E-cadherin along the kidney nephron. *Am. J. Physiol.* **269**, C1417-C1432.
- Ridyard, A. E., Brown, J. K., Rhind, S. M., Else, R. W., Simpson, J. W. and Miller, H. R. P. (2007). Apical junction complex protein expression in the canine colon: differential expression of claudin-2 in the colonic mucosa in dogs with idiopathic colitis. *J. Histochem. Cytochem.* **55**, 1049-1058.
- Sabolík, I., Herak-Kramberger, C. M., Breton, S. and Brown, D. (1999). Na⁺/K⁺-ATPase in intercalated cells along the rat nephron revealed by antigen retrieval. *J. Am. Soc. Nephrol.* **10**, 913-922.
- Sakai, T. (1985). The structure of the kidney from the freshwater teleost *Carassius auratus*. *Anat. Embryol.* **171**, 31-39.
- Sakakibara, A., Furuse, M., Saitou, M., Ando-Akatsuka, Y. and Tsukita, S. (1997). Possible involvement of phosphorylation of occludin in tight junction formation. *J. Cell Biol.* **137**, 1393-1401.
- Sardet, C., Pisam, M. and Maetz, J. (1979). The surface epithelium of teleostean fish gills. Cellular and junctional adaptations of the chloride cell in relation to salt adaptation. *J. Cell Biol.* **80**, 96-117.
- Satta, A., Faedda, R., Olmeo, N. A., Soggia, G., Branca, G. F. and Bartoli, E. (1984). Studies on the nephron segment with reduced sodium reabsorption during starvation natriuresis. *Ren. Physiol.* **7**, 283-292.
- Schneeberger, E. E. and Lynch, R. D. (2004). The tight junction: a multifunctional complex. *Am. J. Physiol. Cell Physiol.* **286**, C1213-C1228.
- Sturla, M., Prato, P., Masini, M. A. and Uva, B. M. (2003). Ion transport proteins and aquaporin water channels in the kidney of amphibians from different habitats. *Comp. Biochem. Physiol.* **136C**, 1-7.
- Vijayan, M. M., Morgan, J. D., Sakamoto, T., Grau, E. G. and Iwama, G. K. (1996). Food-deprivation affects seawater acclimation in tilapia: hormonal and metabolic changes. *J. Exp. Biol.* **199**, 2467-2475.
- Wilke, C., Sheriff, S., Soleimani, M. and Amial, H. (2005). Vasopressin-independent regulation of collecting duct aquaporin-2 in food deprivation. *Kidney Int.* **67**, 201-216.
- Wilson, J. M., Laurent, P., Tufts, B. L., Benos, D. J., Donowitz, M., Vogl, A. W. and Randall, D. J. (2000). NaCl uptake by the branchial epithelium in freshwater teleost fish: an immunological approach to ion-transport protein localization. *J. Exp. Biol.* **203**, 2279-2296.
- Wong, V. (1997). Phosphorylation of occludin correlates with occludin localization and function at the tight junction. *Am. J. Physiol.* **273**, C1859-C1867.
- Wong, V. and Gumbiner, B. M. (1997). A synthetic peptide corresponding to the extracellular domain of occludin perturbs the tight junction permeability barrier. *J. Cell Biol.* **136**, 399-409.
- Zall, D. M., Fisher, D. and Garner, M. D. (1956). Photometric determination of chlorides in water. *Anal. Chem.* **28**, 1665-1678.
- Zeissig, S., Bürgel, N., Günzel, D., Richter, J., Mankertz, J., Wahnschaffe, U., Kroesen, A. J., Zeltz, M., Fromm, M. and Schulzke, J. D. (2007). Changes in expression and distribution of claudin-2, -5 and -8 lead to discontinuous tight junctions and barrier dysfunction in active Crohn's disease. *Gut* **56**, 61-72.

**SPRINGER LICENSE
TERMS AND CONDITIONS**

Sep 20, 2011

This is a License Agreement between Helen Chasiotis ("You") and Springer ("Springer") provided by Copyright Clearance Center ("CCC"). The license consists of your order details, the terms and conditions provided by Springer, and the payment terms and conditions.

All payments must be made in full to CCC. For payment instructions, please see information listed at the bottom of this form.

License Number	2753371204016
License date	Sep 20, 2011
Licensed content publisher	Springer
Licensed content publication	Journal of Comparative Physiology B
Licensed content title	Occludin expression in goldfish held in ion-poor water
Licensed content author	Helen Chasiotis
Licensed content date	Feb 1, 2009
Volume number	179
Issue number	2
Type of Use	Thesis/Dissertation
Portion	Full text
Number of copies	1
Author of this Springer article	Yes and you are the sole author of the new work
Order reference number	
Title of your thesis / dissertation	The role of occludin tight junction protein in freshwater teleost fish osmoregulation
Expected completion date	Oct 2011
Estimated size(pages)	350
Total	0.00 USD

Terms and Conditions

Introduction

The publisher for this copyrighted material is Springer Science + Business Media. By clicking "accept" in connection with completing this licensing transaction, you agree that the following terms and conditions apply to this transaction (along with the Billing and Payment terms and conditions established by Copyright Clearance Center, Inc. ("CCC"), at the time that you opened your Rightslink account and that are available at any time at <http://myaccount.copyright.com>).

Limited License

With reference to your request to reprint in your thesis material on which Springer Science

Occludin expression in goldfish held in ion-poor water

Helen Chasiotis · Jennifer C. Effendi · Scott P. Kelly

Received: 30 June 2008 / Revised: 3 August 2008 / Accepted: 1 September 2008 / Published online: 18 September 2008
© Springer-Verlag 2008

Abstract With an emphasis on the tight junction protein occludin, the response of goldfish following abrupt exposure (0–120 h) as well as long-term acclimation (14 and 28 days) to ion-poor water (IPW) was examined. Both abrupt and long-term exposure to IPW lowered serum osmolality, $[Na^+]$ and $[Cl^-]$, and elevated serum glucose. After abrupt exposure to IPW, gill tissue exhibited a prompt and sustained decrease in Na^+K^+ -ATPase activity, and a transient increase in occludin expression that returned to control levels by 6 h. Following 14 and 28 days in IPW, gill occludin expression was markedly elevated, while Na^+K^+ -ATPase activity was only significantly different (elevated) at day 14. Kidney tissue exhibited an elevation in both Na^+K^+ -ATPase activity and occludin expression after 28 days; however, in the intestine, occludin expression declined at day 14 but did not differ from FW fish at day 28. These studies demonstrate that goldfish can tolerate abrupt as well as sustained exposure to ion-poor surroundings. Data also suggests that occludin may play an adaptive role in fishes acclimated to ion-poor conditions by contributing to the modulation of epithelial barrier properties in ionoregulatory tissues.

Keywords Tight junction · Gill · Kidney · Paracellular permeability · Osmoregulation

Introduction

Fishes are often found in environments that vary greatly in ionic composition. To maintain internal homeostasis, these organisms have evolved a complex suite of ionoregulatory mechanisms that control water and solute movement across epithelial surfaces. The passage of water and dissolved solutes across epithelia can occur through the transcellular and/or paracellular pathway. The permeability of the paracellular route is regulated by the tight junction (TJ) complex. Composed of integral transmembrane as well as cytoplasmic scaffolding TJ proteins, the TJ complex forms a semipermeable paracellular “seal” between epithelial cells (González-Marsical et al. 2003). The passive movement of solutes between compartments of the body is dictated by the permeability properties of the TJ complex, and in aquatic vertebrates, the permeability characteristics of epithelia that come into direct contact with surrounding water (e.g. gills) play an important role in regulating solute movement between the internal and external environments (Kelly and Wood 2001, 2002a, b, 2008; Bagherie-Lachidan et al. 2008; Chasiotis and Kelly 2008).

Occludin was the first integral TJ protein to be isolated and identified from vertebrate epithelia (Furuse et al. 1993). It is a tetraspan protein with three cytoplasmic domains ranging from 10 to 254 aa in length, and two extracellular loops of equal size (i.e. 44 and 45 aa) (González-Marsical et al. 2003). Studies examining the physiological role of occludin in the TJ complex indicate that it contributes significantly to epithelial integrity, and substantial evidence suggests that occludin is a major determinant in the regula-

Helen Chasiotis and Jennifer C. Effendi contributed equally to this work.

Communicated by H. V. Carey.

H. Chasiotis (✉) · J. C. Effendi · S. P. Kelly
Department of Biology, York University,
4700 Keele Street, Toronto, ON M3J 1P3, Canada
e-mail: helench@yorku.ca

S. P. Kelly
e-mail: spk@yorku.ca

tion of barrier properties in vertebrate epithelia (for review, see Feldman et al. 2005). For example, the overexpression or disruption of occludin in epithelial cell lines (such as MDCK or A6 kidney cells) has been demonstrated to cause elevations or reductions in transepithelial resistance (TER) (Balda et al. 1996; McCarthy et al. 1996; Wong and Gumbiner 1997). Furthermore, where occludin disruption causes a reduction in TER, increased permeability to paracellular marker molecules (e.g. [^{14}C]inulin, [^3H]mannitol, etc.) also occurs (Wong and Gumbiner 1997).

The effect of environmental salinity on the permeability of ionoregulatory epithelia is well documented in fishes (for review, see Marshall and Grosell 2005). Most notable are the changes that occur when euryhaline fishes move from freshwater (FW) to seawater (SW). Gill and intestinal epithelia generally become “leakier” to assist salt and water movement into the body (i.e. across the intestinal epithelium) and subsequent ion elimination from the body (i.e. across the gill). In the kidney, discrete regions of the nephron also alter in response to SW acclimation, where “electrically tight” diluting segments that are designed to retain ions and eliminate water in hypo-osmotic surroundings exhibit varying levels of structural or functional degeneration in SW (Nishimura and Fan 2003). Therefore, alterations in epithelial permeability upon SW entry contribute to an overall net water gain and thus prevent dehydration. Goldfish are not capable of acclimating to a SW environment but are capable of gradually acclimating from FW to ion-poor FW (Cuthbert and Maetz 1972; Kelly and Peter 2006). In this regard, alterations that occur in the endocrine system (e.g. elevated pituitary prolactin expression) and extracellular fluids (e.g. lowered serum osmolality) of goldfish acclimated from regular FW to ion-poor water (IPW) are analogous to the physiological changes that take place when euryhaline fishes move from SW to FW (Kelly and Peter 2006).

In a recent study, we examined the localization of occludin in the osmoregulatory tissues of goldfish (Chasiotis and Kelly 2008). Occludin was found in the gill epithelium, intestine and discrete regions of the goldfish nephron (i.e. distal tubule and collecting duct) (Chasiotis and Kelly 2008). Furthermore, when we subjected goldfish to varying periods of food deprivation to perturb the active and passive transport properties of osmoregulatory epithelia (also see Chasiotis and Kelly 2008), occludin expression altered in a tissue-specific manner in association with time-dependent variations in hydromineral status. These observations point to a potential role for occludin in the regulation of salt and water balance in fishes. However, by altering the hydromineral status of fishes through limiting (or withdrawing) access to food, the consequences of negative energy status may have also directly affected the function of TJ proteins. Therefore, it would be of further interest to

examine the response of occludin to environmental change directly and in particular, alterations in environmental ion levels.

In the current studies, we hypothesized that goldfish would tolerate abrupt exposure to IPW. Under the assumption that goldfish would tolerate abrupt exposure to IPW, our objectives were to investigate systemic endpoints of hydromineral balance and gill occludin expression during the time course of exposure. We hypothesized that occludin expression would alter in an adaptive manner in response to ion-poor conditions. To further investigate our contention that occludin would be involved in the acclimation of goldfish to IPW, we examined alterations in hydromineral endpoints as well as occludin expression in gill, renal and intestinal tissues in goldfish acclimated to IPW for longer time periods (i.e. up to 4 weeks). To the best of our knowledge, these are the first experiments to investigate the response of TJ proteins to ion-poor conditions in an aquatic vertebrate.

Materials and methods

Experimental animals and culture conditions

Common variety goldfish (*Carassius auratus*, 6–11 g) were purchased from a local supplier and held in 600-L opaque plastic aquaria supplied with regular flow-through dechlorinated FW. The composition of dechlorinated FW (in μM) was as follows: [Na^+], 590; [Cl^-], 920; [Ca^{++}], 760; [K^+], 43; pH 7.35. Water temperature was maintained at 15–16°C and photoperiod was 12 h light: 12 h dark. Fish were held in these conditions for at least 2 weeks. During this settling period, fish were fed ad libitum once daily with commercial koi and goldfish pellets (Martin Profishnet, Elmira, ON, Canada).

Abrupt exposure of goldfish to IPW

Two weeks prior to experimentation, goldfish were transferred into 65-L opaque glass aquaria ($n = 15/\text{tank}$) supplied with flow-through dechlorinated FW and maintained under culture conditions as described above (see “Experimental animals and culture conditions”). Feeding was terminated 48 h prior to the introduction of IPW and goldfish remained unfed throughout the duration of the experiment, (i.e. for 120 h post-IPW introduction). The composition of IPW (in μM) was as follows: [Na^+], 20; [Cl^-], 40; [Ca^{++}], 2; [K^+], 0.4; pH 6.5. Without disturbing the fish, IPW was introduced into experimental tanks via inlet pipes and was allowed to overflow until ion-poor conditions were achieved (approximately 30 min). At this point, timing began and fish were held in IPW for 1, 3, 6, 12, 24 and 120 h. At each des-

ignated time point, samples were collected from up to 10 fish held in each tank (for details, see “Blood and tissue sampling”). To confirm that none of the aforementioned treatments were “lethal,” fish remaining in each tank were then reacquainted to regular FW (by switching inlet pipe water back to dechlorinated FW). Identical control experiments were run simultaneously, with control fish being sampled at the same time points. For control experiments, regular dechlorinated FW was used instead of IPW.

Long-term acclimation of goldfish to IPW

Stock goldfish were transferred into 200-L opaque plastic aquaria and held in culture conditions identical to those described above (see “Experimental animals and culture conditions”). After a 2-week settling period, goldfish were introduced to IPW abruptly as previously described (see “Abrupt exposure of goldfish to IPW”); however, this time, fish were fed throughout the acclimation process and daily thereafter. Goldfish were held in these conditions for 14 and 28 days prior to sampling.

Blood and tissue sampling

Fish were rapidly net-captured and anesthetized in 0.5 g/L tricaine methanesulfonate (MS-222; Syndel Laboratories Ltd, Canada). Blood was drawn from caudal vessels using a 1-mL syringe/25-gauge needle by multiple individuals to reduce sampling time. Blood was allowed to clot at 4°C for 30 min and was centrifuged at 10,000 rpm for 10 min to collect serum. Following blood collection, fish were killed by spinal transection and select tissues were collected for further analysis. For initial studies conducted on fish rapidly exposed to IPW (and monitored for up to 120 h), gill tissue was collected from either side of the head for measurement of enzyme activity and occludin protein expression, respectively. A full flank of epaxial white muscle (i.e. dorsal to the lateral line) was also collected. Tissues collected for experiments that examined the long-term response of fish to ion-poor conditions (i.e. 14 and 28 days) were as follows: gill and white muscle as already described, as well as kidney and a standardized region of the gastrointestinal tract (see Chasiotis and Kelly 2008). All tissues were quick-frozen in liquid nitrogen immediately upon collection and stored at –80°C until further analysis.

Serum analysis, muscle moisture content and Na⁺–K⁺–ATPase activity

Serum osmolality was determined using a Model 5500 Wescor vapor pressure osmometer (Wescor Inc., Logan, UT, USA). Serum Na⁺ was measured, after appropriate dilution, by atomic absorption spectrometry using an

AAAnalyst PerkinElmer spectrometer (PerkinElmer Life and Analytical Sciences, ON, Canada). Serum Cl⁻ was determined using the colorimetric assay described by Zall et al. (1956), and serum glucose was measured using PGO Enzymes according to the manufacturer’s instructions (Sigma-Aldrich Canada Ltd, Oakville, ON, Canada). Gill, kidney and intestinal Na⁺–K⁺–ATPase activity was determined using the methodology of McCormick (1993) with modifications as described by Chasiotis and Kelly (2008).

Western blot analysis

Occludin protein expression was examined by Western blot analysis according to methodology previously reported by Chasiotis and Kelly (2008). Briefly, tissues were homogenized in ice-cold homogenization buffer (200 mM sucrose, 1 mM EDTA, 1 mM PMSF, 1 mM DTT in 0.7% NaCl) containing protease inhibitor cocktail (1:200; Sigma-Aldrich Canada Ltd) using a PRO250 homogenizer (PRO Scientific Inc., Oxford, CT, USA). Homogenates were centrifuged (3,200g at 4°C) and supernatants were collected. In preparation for SDS-PAGE, samples (75 µg of protein each) were boiled at 100°C in 6× sample buffer (360 mM Tris–HCl, 30% glycerol, 12% SDS, 600 mM DTT, 0.03% bromophenol blue) and separated along 12% acrylamide gels. Following electrophoresis, resolved protein was transferred on to Hybond-P polyvinylidene difluoride (PVDF) membrane using a TE semidry transfer unit (GE Healthcare Bio-Sciences Inc., Baie d’Urfé, QC, Canada). Membranes were washed, blocked for 1 h in 5% non-fat dry skim milk powder in TBS-T (5% skim milk, 10 mM Tris, 150 mM NaCl, 0.05% Tween-20, pH 7.4), incubated overnight at 4°C with rabbit polyclonal antioccludin antibody (Zymed Laboratories Inc.), and then washed again prior to incubation with horseradish peroxidase (HRP)-conjugated goat antirabbit antibody (Bio-Rad Laboratories Inc., Mississauga, ON, Canada) for 1 h at room temperature. The rabbit polyclonal antioccludin antibody is directed against the C-terminal region of the human occludin protein, and its use in goldfish has previously been validated (see Chasiotis and Kelly 2008). Protein bands were visualized using an Enhanced Chemiluminescence Plus Western blotting system (GE Healthcare Bio-Sciences Inc., Baie d’Urfé, QC, Canada). After examining occludin expression, membranes were stripped and reprobed with mouse monoclonal anti-β-actin antibody (Sigma-Aldrich Canada Ltd) and HRP-conjugated goat antimouse antibody (Bio-Rad Laboratories Inc.), respectively, as an internal loading control. Occludin and β-actin expression was quantified using Labworks Image Acquisition and Analysis software (UVP BioImaging Systems and Analysis Systems, Upland, CA, USA). Occludin is expressed as a normalized value relative to β-actin as an internal control.

Statistical analysis

All data are expressed as mean values \pm SEM (n), where n equals the number of fish in a treatment group. To examine for significant differences between treatments, a two-way analysis of variance (ANOVA) was run followed by a Student–Newman–Keuls multiple comparison test. For clarity, only significant differences between FW and IPW groups are shown on 0–120 h graphics (see Table 1 for additional information). A fiducial limit of $P \leq 0.05$ was used throughout. All statistical analyses were performed using SigmaStat 3.1 (Systat Software Inc., USA).

Results

Abrupt exposure to IPW

No experimental goldfish died over the 120-h period following abrupt IPW introduction. After sampling at each time point, a subset of fish that were abruptly exposed to IPW were reintroduced to regular FW to confirm that the abrupt IPW exposure had no deleterious effect on the continued survival of fish. In these animals, no mortality or abnormal behavior was observed for up to 2 weeks following the experiments.

Goldfish abruptly introduced to IPW exhibited a rapid and sustained reduction in serum osmolality (Fig. 1a). Serum $[\text{Na}^+]$ initially appeared to increase (i.e. at 1 h) but then reduced over the first 24 h of exposure to IPW (Fig. 1b). Serum $[\text{Cl}^-]$ did not significantly alter until 24 h after introducing fish to IPW (Fig. 1c, Table 1). After 120 h in IPW, serum osmolality, $[\text{Na}^+]$ and $[\text{Cl}^-]$ exhibited further reductions relative to control fish as well as to fish exposed to IPW for up to 24 h (Fig. 1a–c, Table 1). Blood glucose levels elevated in goldfish approximately 3 h after abrupt exposure to IPW (Table 2). For the remainder of the 120-h experiment, blood glucose levels were higher in fish exposed to IPW. Muscle moisture was stable over the duration of the experiment but did significantly differ between groups after 120-h exposure to IPW (Fig. 1d).

In the gills of goldfish abruptly exposed to IPW, Na^+/K^+ -ATPase activity appeared to rapidly decline and, with the exception of the activity measured at 6 h, remained lower than the activity recorded for fish held in regular FW for the entire 120 h duration of the experiment (Fig. 2a). In contrast, gill occludin expression significantly increased 1 h after introduction of fish to IPW (Fig. 2b). Thereafter, gill occludin expression returned to levels that did not significantly differ from control fish for the remainder of the 120-h experimental period (Fig. 2b).

Long-term acclimation of goldfish to IPW

Goldfish were able to acclimate to IPW for up to 28 days without mortality or exhibiting any signs of abnormal behavior.

Serum endpoints and muscle moisture content

Serum osmolality, $[\text{Na}^+]$ and $[\text{Cl}^-]$ were all significantly lower after 14 days acclimation to IPW (Fig. 3a–c). After 28 days, serum osmolality remained lower in IPW fish than in FW fish (Fig. 3a), and serum $[\text{Cl}^-]$ declined further relative to levels measured in fish acclimated to IPW for 14 days (Fig. 3c). In contrast, serum $[\text{Na}^+]$ in fish acclimated to IPW for 28 days was not found to be significantly different from fish held in regular FW (Fig. 3b). Serum glucose levels were elevated in fish acclimated to IPW after both 14 and 28 days, and glucose levels in IPW fish after 28 days were significantly higher than those measured in fish acclimated to IPW for 14 days (Table 2). Muscle moisture did not significantly differ between any fish groups after longer periods of acclimation to IPW (Fig. 3d).

Gill, kidney and intestine Na^+/K^+ -ATPase activity and occludin expression

Gill Na^+/K^+ -ATPase activity was significantly elevated in goldfish acclimated to IPW for 14 days. However, after 28 days in IPW, gill Na^+/K^+ -ATPase activity declined to levels that were not significantly different from those found

Table 1 Summary of statistics for abrupt exposure of goldfish (from FW to IPW) generated by two-way ANOVAs of 0–120 h time course data

Variable	Parameter measured					
	Osmolality	Na^+	Cl^-	Glucose	Muscle moisture	Na^+/K^+ -ATPase activity ^a
Water	$P < 0.001$	$P < 0.001$	$P < 0.001$	$P < 0.001$	$P < 0.01$	$P < 0.001$
Time	$P < 0.001$	$P < 0.001$	$P < 0.001$	$P < 0.001$	NS	$P < 0.001$
Water \times time	$P < 0.001$	$P < 0.001$	$P < 0.001$	$P < 0.001$	$P < 0.001$	NS

Osmolality, Na^+ , Cl^- and muscle moisture data were obtained from Fig. 1; glucose data were obtained from Table 2

^a Gill Na^+/K^+ -ATPase activity, see Fig. 2

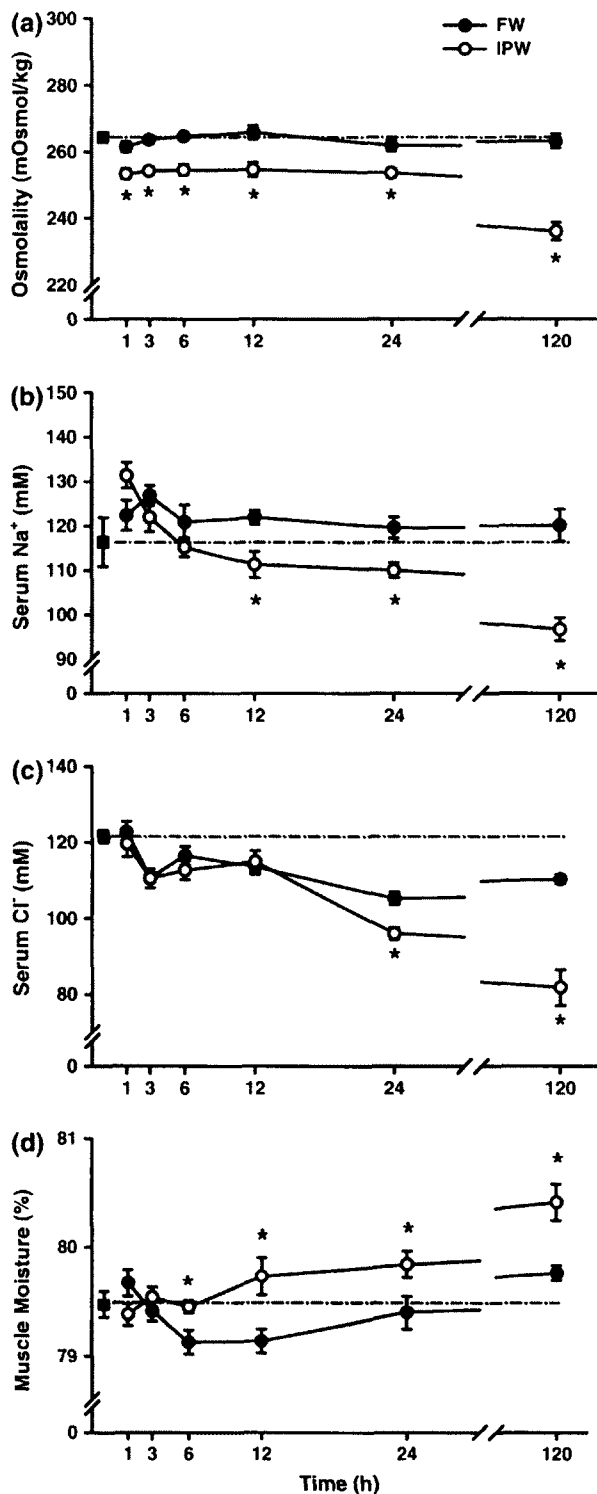


Fig. 1 Effect of abrupt exposure to ion-poor water (IPW) on (a) serum osmolality, (b) serum Na⁺, (c) serum Cl⁻ and (d) muscle moisture content of goldfish. Data are expressed as mean values ± SEM (n = 10). Control fish were exposed to regular freshwater (FW). An asterisk indicates significant difference (P < 0.05) between mean values from FW and IPW fish at the same time point. Further statistical details can be seen in Table 1

in control fish (Fig. 4a). During the same time period, gill occludin expression in the gills of fish acclimated to IPW was markedly elevated relative to occludin expression found in fish held in regular FW (Fig. 4b).

In the kidney of fish acclimated to IPW, Na⁺-K⁺-ATPase activity was elevated relative to fish held in FW at both time points examined but only significant at 28 days (Fig. 5a). After 28 days in IPW surroundings, kidney Na⁺-K⁺-ATPase activity was significantly greater than that after 14 days. Similarly, kidney occludin expression was elevated after 28 days acclimation to IPW conditions (Fig. 5b). However, when fish were held in IPW for 14 days, no significant difference was observed in renal occludin expression relative to fish held in FW (Fig. 5b).

In the intestine of goldfish, Na⁺-K⁺-ATPase activity was elevated after 28 days in IPW but not after 14 days (Fig. 6a). In contrast, intestinal occludin expression was significantly lower in fish held in IPW for 14 days relative to fish held in FW, and after 28 days, no significant difference in intestinal occludin expression was observed between groups (Fig. 6b).

Discussion

Overview

In the current study, the abrupt exposure of goldfish to ion-poor surroundings did not result in any mortality. We can therefore accept our first hypothesis that goldfish are capable of tolerating abrupt exposure to IPW. Over the course of the 120-h experiment, goldfish generally exhibited either a transient response or relatively rapid and sustained alteration in circulating electrolytes and glucose, ionomotive enzyme activity and TJ protein abundance upon exposure to IPW. Most notably, branchial occludin expression quickly altered following exposure to IPW. Furthermore, robust, tissue-specific alterations in occludin expression were observed in goldfish acclimated to IPW for 14 and 28 days. It is our contention that these alterations are adaptive and fit with current models of ion transport across the osmoregulatory epithelia of FW fishes. Therefore, we can also accept our second hypothesis that occludin expression will alter in an adaptive manner in response to ion-poor conditions.

Abrupt exposure of goldfish to IPW

The ability of fishes to tolerate rapid alterations in the ionic composition of their surroundings is well documented (e.g. Leray et al. 1981; Jacob and Taylor 1983; Usher et al. 1991; Mancera et al. 1993; Kelly and Woo 1999). However, the majority of studies that examine this phenomenon

Table 2 Serum glucose levels (mg/100 ml) in goldfish abruptly exposed to IPW or acclimated to IPW for 14- and 28-day periods

	Time (h)						Time (days)	
	1	3	6	12	24	120	14	28
FW	38.4 ± 4.0	44.1 ± 6.6	38.7 ± 5.2	52.4 ± 6.4	44.3 ± 5.4	40.6 ± 2.6	34.9 ± 3.2	39.5 ± 2.6
IPW	47.5 ± 2.5	79.3 ± 8.2*	60.4 ± 6.6*	68.3 ± 7.0	70.9 ± 3.2*	135.1 ± 5.6*	77.0 ± 8.1*	101.0 ± 9.7***

All data are expressed as mean values ± SEM ($n = 7\text{--}10/\text{group}$)

Control fish were held in regular FW

* Significant difference ($P \leq 0.05$) between FW and IPW at a specific time period

** Significant difference ($P \leq 0.05$) between IPW groups held for 14 and 28 days

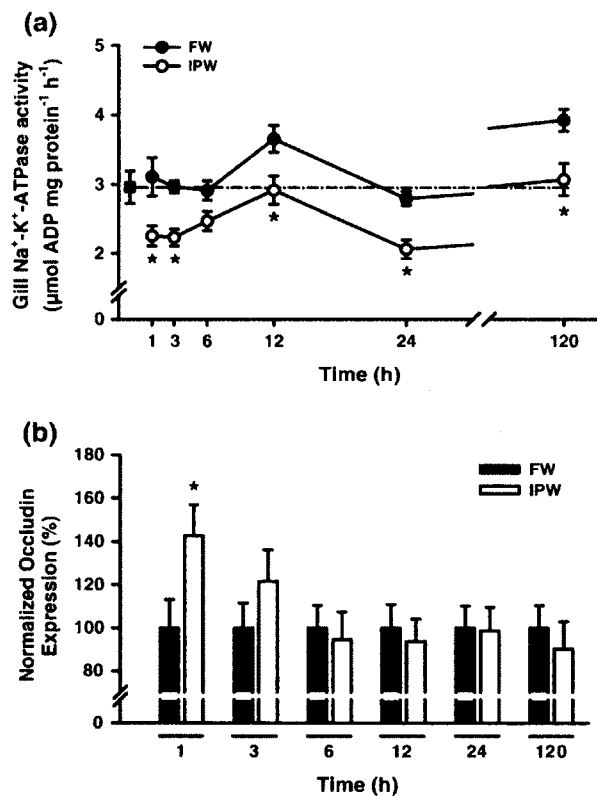
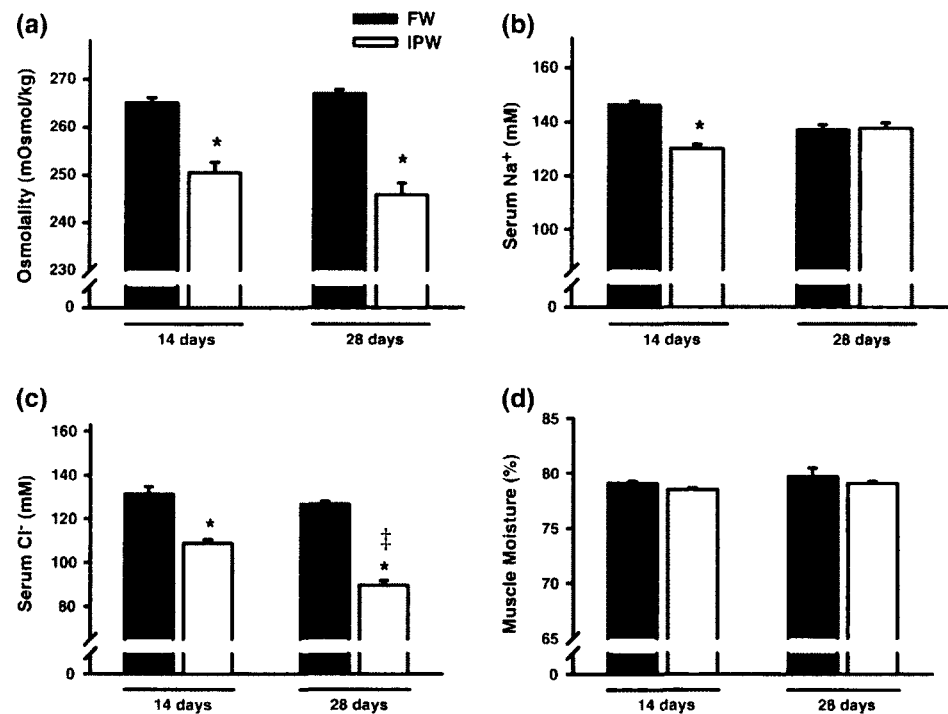


Fig. 2 Effect of abrupt exposure to ion-poor water (IPW) on gill (a) $\text{Na}^+\text{-K}^+\text{-ATPase}$ activity and (b) occludin expression. Data are expressed as mean values ± SEM ($n = 10$). Control fish were exposed to regular freshwater (FW). An asterisk indicates significant difference ($P \leq 0.05$) between FW and IPW at the same time point. For $\text{Na}^+\text{-K}^+\text{-ATPase}$ activity, further statistical details can be seen in Table 1. At each time point in IPW, gill occludin is expressed relative to control fish in FW

transfer fishes between FW and SW (or vice versa). In the current study, we abruptly exposed FW fish to IPW and observed physiological responses that generally appeared to mirror those exhibited by euryhaline fishes during challenges of a more typical nature, i.e., lowered serum osmolality and circulating ion levels as well as increased

substrate mobilization in the form of elevated glucose levels following transfer from a hyperosmotic (e.g. SW) to a hypoosmotic (e.g. FW) environment. However, it should be emphasized that in the current study, goldfish are being abruptly exposed to an environment that will amplify the external to internal osmotic/ionic gradient (i.e. FW to more “dilute” FW), and not reverse it as would be the case if SW fish were exposed to FW. This, taken together with the “stenohaline” nature of goldfish, may explain some of the differences that appear to occur in the physiological response of this species when compared to the response of other typical euryhaline fishes. For example, despite a rapid reduction in serum osmolality in response to IPW exposure, there does not appear to be a time-dependent postexposure recovery in this parameter (see Fig. 1a). A similar phenomenon occurs for serum glucose levels (see Table 2). Therefore, the prominent acute and recovery phase typically found in the hydromineral endpoints of euryhaline fishes after rapid exposure from one salinity to another (e.g. Kelly and Woo 1999) does not appear to manifest in the serum endpoints measured in this species under these conditions. While it could be argued that goldfish were not given enough time to recover, data from fish acclimated to IPW for 14 and 28 days would seem to suggest otherwise. In fact, the only variable measured in the abrupt exposure experiment that altered transiently and appeared to “recover” was gill occludin expression (see Fig. 2b). In the branchial epithelium, occludin expression increased sharply in response to IPW exposure and then eventually decreased back to control levels for the remainder of the 120-h experiment. These observations suggest that occludin may aid in the immediate modulation of gill epithelial barrier properties in response to an abrupt change in environmental ion concentrations; however, further studies will be required to decipher which TJ proteins play a prominent role after this immediate response. Regardless, the role of occludin appears to be a biphasic one as a substantial elevation in expression is once again observed after longer periods of acclimation to IPW (see Fig. 4b and discussion below).

Fig. 3 The effect of 14 and 28 days acclimation to ion-poor water (IPW) on (a) serum osmolality, (b) serum Na⁺, (c) serum Cl⁻ and (d) muscle moisture content in goldfish. Data are expressed as mean values ± SEM (*n* = 7). An asterisk indicates significant difference (*P* ≤ 0.05) between FW and IPW at the same time point. A double dagger (‡) indicates significant difference (*P* ≤ 0.05) between 14 and 28 days acclimation within an environment



Long-term acclimation of goldfish to IPW

Following exposure to IPW for longer time periods (i.e. 14 and 28 days), goldfish continued to exhibit lowered serum osmolality, [Cl⁻] and [Na⁺] (the latter at 14 days at least) (see Fig. 3a–c), as well as elevated glucose (see Table 2) with no fish mortality or observable abnormal behavior. Furthermore, muscle moisture content, a general index of hydration status, was not significantly different between fish held in FW and IPW at either 14 or 28 days (see Fig. 3d). Combined, these data indicate that goldfish can establish new steady-state conditions in IPW that are not deleterious to fish health. However, elevated glucose levels point to a potential increase in the energetic expenditure of maintaining salt and water balance in IPW. Since elevated glucose levels may also reflect an increase in circulating stress hormones (e.g. glucocorticoids such as cortisol), it seems possible that continuous culture in IPW could eventually result in the manifestation of pathophysiological problems normally associated with chronic stress (e.g. poor growth) (Mommsen et al 1999).

Tissue occludin and Na⁺–K⁺–ATPase activity after 14 days in IPW

In gill tissue, Na⁺–K⁺–ATPase activity and occludin expression were both elevated after 14 days in IPW (see Fig. 4). An increase in both of these variables would suggest that ion transport across the transcellular route (presumably in the inward direction) is increased, while solute movement through the paracellular route (i.e. in the outward direction)

is reduced. In a tissue that comes into direct contact with the surrounding environment, such as the gill, this would make adaptive sense as it would enhance ion acquisition from the surroundings whilst limiting obligatory ion loss. In a previous study where goldfish were acclimated to deionized water for 21 days, Na⁺ influx was seen to double relative to control FW fish, while Na⁺ efflux exhibited a more than sixfold decrease (Cuthbert and Maetz 1972). Our data are consistent with these observations and would suggest that alterations in ionomotive enzyme activity (e.g. Na⁺–K⁺–ATPase) as well as TJ protein expression (e.g. occludin) seem likely to contribute to this strategy of maintaining salt and water balance. In addition, recent in vitro studies have demonstrated that the TER measured across FW gill epithelia “externally” exposed to IPW is significantly greater than the TER across epithelia bathed with regular FW on the apical surface (Kelly and Wood 2008). Combined, these observations strongly suggest that, in IPW, TJ proteins reduce the paracellular permeability of the gill epithelium, and this would be adaptive in minimizing obligatory ion loss to the surroundings.

In contrast to the response of goldfish gill tissue following 14 days of IPW acclimation, alterations in Na⁺–K⁺–ATPase activity and occludin expression in renal tissue were less obvious (see Fig. 5). Although this may initially seem to suggest that the renal system does not play an “enhanced” role when goldfish are acclimated to IPW, such a conclusion can be rejected based on the alterations that occur in the renal system after 28 days in IPW (see discussion below). Therefore, it appears that in goldfish, the development of an “enhanced” role for the kidney is likely

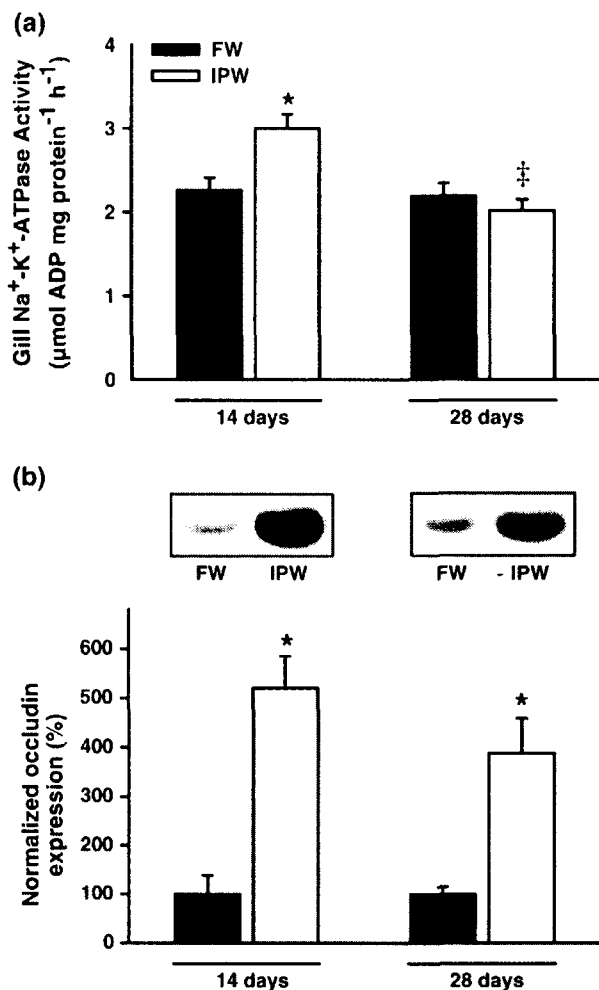


Fig. 4 The effect of 14 and 28 days acclimation to ion-poor water (IPW) on gill (a) $\text{Na}^+\text{-K}^+\text{-ATPase}$ activity and (b) occludin expression. *Insets* show representative Western blot analyses. Data are expressed as mean values \pm SEM ($n = 7$). Control fish were held in regular freshwater (FW). An *asterisk* indicates significant difference ($P \leq 0.05$) between FW and IPW at the same time point. A *double dagger* (‡) indicates significant difference ($P \leq 0.05$) between 14 and 28 days acclimation within an environment

governed by time spent in IPW, and that after 14 days, goldfish may not be fully acclimated to IPW surroundings (i.e., further changes are yet to occur).

The physiological consequences of alterations in occludin expression in the goldfish intestine after 14 days acclimation to IPW are not clear-cut (see Fig. 6). This is due to a paucity of information on the regulation of TJ proteins in the intestinal epithelia of aquatic vertebrates as well as (to the best of our knowledge) an absence of studies that have examined the role of this tissue in ionoregulatory homeostasis of fishes acclimated to IPW conditions. Nevertheless, it seems likely that a limited ability to acquire ions from the surrounding water will result in salts derived from dietary sources playing an increasingly important role in replenish-

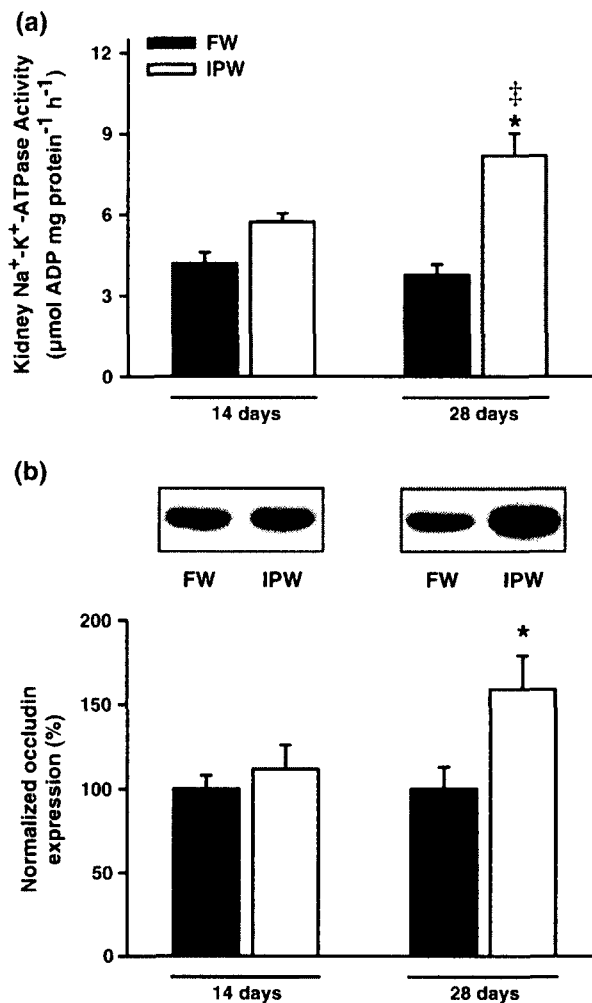


Fig. 5 The effect of 14 and 28 days acclimation to ion-poor water (IPW) on kidney (a) $\text{Na}^+\text{-K}^+\text{-ATPase}$ activity and (b) occludin expression. *Insets* show representative Western blot analyses. Data are expressed as mean values \pm SEM ($n = 7$). Control fish were held in regular freshwater (FW). An *asterisk* indicates significant difference ($P \leq 0.05$) between FW and IPW at the same time point. A *double dagger* (‡) indicates significant difference ($P \leq 0.05$) between 14 and 28 days acclimation within an environment

ing the supply of ions to IPW fish (for review, see Marshall and Grosell 2005), and an increase in intestinal permeability would likely facilitate ion absorption from the chyme of feeding goldfish. Indeed, it has been recently suggested by Scott et al. (2006) that ion absorption from chyme is critical to ionoregulatory homeostasis of euryhaline killifish transferred from brackish water to FW. Furthermore, Scott et al. (2006) observed that alterations in ion movement (uptake) across the gut were generally not coupled with alterations in transcellular transport mechanisms, leading to the suggestion that alternate mechanisms are likely responsible for enhanced ion uptake. Modulated epithelial permeability may contribute to these alternate mechanisms. Indeed, the interesting parallel between killifish held in FW and gold-

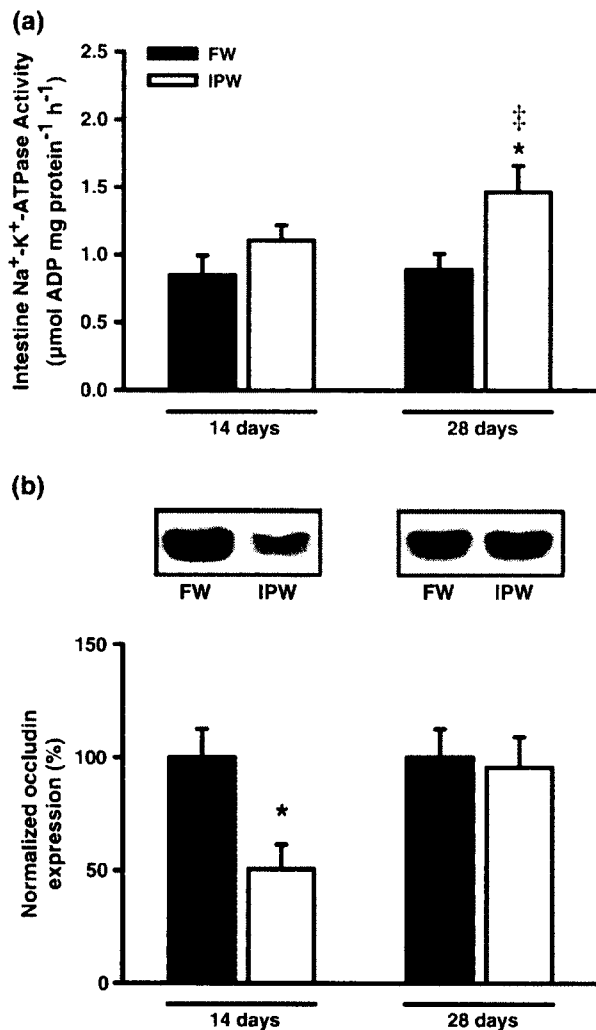


Fig. 6 The effect of 14 and 28 days acclimation to ion-poor water (IPW) on intestine (a) $\text{Na}^+\text{-K}^+\text{-ATPase}$ activity and (b) occludin expression. *Insets* show representative Western blot analyses. Data are expressed as mean values \pm SEM ($n = 7$). Control fish were held in regular freshwater (FW). An *asterisk* indicates significant difference ($P \leq 0.05$) between FW and IPW at the same time point. A *double dagger* (\ddagger) indicates significant difference ($P \leq 0.05$) between 14 and 28 days acclimation within an environment

fish held in IPW relates to the observations of Wood and Laurent (2003), which indicate that feeding is essential to maintain killifish health in FW environments. Correspondingly, we also observed that goldfish exposed to IPW and deprived of access to food began to exhibit abnormal behavior (e.g. disequilibrium) after $\sim 10\text{--}12$ days exposure (Effendi and Kelly, unpublished observations).

Tissue occludin and $\text{Na}^+\text{-K}^+\text{-ATPase}$ activity after 28 days in IPW

The status of both gill and kidney tissue in goldfish acclimated to IPW for 28 days alters relative to observations

made after 14 days. In the branchial epithelium, occludin expression remained markedly elevated relative to fish held in regular FW, most likely continuing to function by enhancing gill barrier properties. In contrast, $\text{Na}^+\text{-K}^+\text{-ATPase}$ activity in the gill declined at 28 days and was no longer found to significantly differ from the activity recorded in FW fish (see Fig. 4a). To compensate for this potential reduction in ion acquisition by the gill, the kidney appeared to be reorganized for a more central role in ion reabsorption after 28 days in IPW (i.e. kidney $\text{Na}^+\text{-K}^+\text{-ATPase}$ activity increased almost threefold, see Fig. 5a). In goldfish kidney, $\text{Na}^+\text{-K}^+\text{-ATPase}$ is particularly abundant in the distal tubule and (to a lesser extent) in the collecting duct of the nephron (Chasiotis and Kelly 2008). Within these segments (in particular the early distal tubule), $\text{Na}^+\text{-K}^+\text{-ATPase}$ generates a Na^+ gradient that permits the operation of luminal facing $\text{Na}^+\text{-K}^+\text{-2Cl}^-$ cotransporters and $\text{Na}^+\text{-H}^+$ exchangers, resulting in Na^+ and Cl^- uptake from luminal filtrate (Dantzler 2003; Nishimura and Fan 2003). In association with abundant $\text{Na}^+\text{-K}^+\text{-ATPase}$, the distal tubules and collecting ducts are the only regions of the goldfish nephron that appear to express occludin (Chasiotis and Kelly 2008), which in FW fishes in general are the electrically “tight” and relatively water-impermeable diluting segments of the kidney (Dantzler 2003; Nishimura and Fan 2003). Therefore, the observed increase in kidney occludin expression that occurs in conjunction with an elevation in kidney $\text{Na}^+\text{-K}^+\text{-ATPase}$ activity after 28 days in IPW (see Fig. 5) would likely decrease the permeability of the diluting segments of the nephron to enhance ion reabsorption and retention with little water accompaniment. These observations are consistent with the differences found in renal TJ protein expression between euryhaline fish acclimated to either FW or SW (Bagherie-Lachidan et al. 2008).

Following 28 days in IPW, occludin expression in the goldfish intestine was no longer significantly different between FW and IPW fish; however, $\text{Na}^+\text{-K}^+\text{-ATPase}$ activity was now elevated in fish held in IPW relative to those held in FW (see Fig. 6). These data suggest that, as opposed to strategies suggested previously (see above discussion), goldfish may eventually begin to rely more on the active transport of ions across the intestinal epithelium from dietary sources rather than the facilitation of passive movement. Clearly, this area will require further study.

Perspectives

The current studies demonstrate the plasticity of goldfish within the context of an extreme FW environment (i.e. ion-poor FW). In this regard, goldfish appear to be a suitable model species for studying rapid as well as long-term alterations in the physiological processes associated with main-

taining salt and water balance in ion-poor surroundings. In the gill epithelium, the integral TJ protein occludin exhibited rapid transient alterations as well as robust long-term changes, while alterations in the primary ionomotive enzyme of fish gills, $\text{Na}^+ - \text{K}^+ - \text{ATPase}$, seemed relatively moderate by comparison. In future studies, it will be interesting to examine the response of other TJ proteins (e.g. claudins), particularly right after IPW exposure when occludin expression declines. Recent studies have shown that gill claudin mRNA expression (e.g. claudin 30) alters at least 24 h after SW to FW transfer in euryhaline tilapia (Tipsmark et al. 2008). Furthermore, it is well established from *in vitro* studies that gill epithelial permeability responds rapidly to changes in the ionic concentration of surrounding water as well as to endocrine factors (e.g., cortisol, prolactin, etc.) that mediate biochemical reorganization of ionoregulatory epithelia in response to salinity change (e.g. Perry and Laurent 1989; Kelly and Wood 2001; Kelly and Wood 2002a, b). These same endocrine factors have also been demonstrated to improve epithelial integrity in normal FW as well as IPW (Kelly and Wood 2001, 2002a, 2008). It will be interesting to further examine the interplay of these endocrine factors with the molecular components that regulate the permeability of the TJ complex.

Acknowledgments This work was supported by NSERC Discovery Grants and CFI New Opportunities Funds to SPK. All procedures conformed to the guidelines of the Canadian Council for Animal Care.

References

- Bagherie-Lachidan M, Wright SI, Kelly SP (2008) Claudin-3 tight junction proteins in *Tetraodon nigroviridis*: cloning, tissue specific expression and a role in hydromineral balance. *Am J Physiol Regul Integr Comp Physiol* 294:R1638–R1647
- Balda MS, Whitney JA, Flores C, González S, Cerejido M, Matter K (1996) Functional dissociation of paracellular permeability and transepithelial electrical resistance and disruption of the apical-basolateral intramembrane diffusion barrier by expression of a mutant tight junction membrane protein. *J Cell Biol* 134:1031–1049
- Chasiotis H, Kelly SP (2008) Occludin immunolocalization and protein expression in goldfish. *J Exp Biol* 50:656–658
- Cuthbert AW, Maetz J (1972) The effects of calcium and magnesium on sodium fluxes through gills of *Carassius auratus*, L. *J Physiol* 221:633–643
- Dantzer WH (2003) Regulation of renal proximal and distal tubule transport: sodium, chloride and organic anions. *Comp Biochem Physiol A* 136:453–478
- Feldman GJ, Mullin JM, Ryan MP (2005) Occludin: structure, function and regulation. *Adv Drug Deliv Rev* 57:883–917
- Furuse M, Hirase T, Itoh M, Nagafuchi A, Yonemura S, Tsukita S, Tsukita S (1993) Occludin: a novel integral membrane protein localizing at tight junctions. *J Cell Biol* 123:1777–1788
- González-Marsical L, Betanzos A, Nava P, Jaramillo BE (2003) Tight junction proteins. *Prog Biophys Mol Biol* 81:1–44
- Jacob WF, Taylor MH (1983) The time course of seawater acclimation in *Fundulus heteroclitus* L. *J Exp Zool* 228:33–39
- Kelly SP, Peter RE (2006) Prolactin-releasing peptide, food intake and hydromineral balance in goldfish. *Am J Physiol Regul Integr Comp Physiol* 291:R1474–R1481
- Kelly SP, Woo NYS (1999) The response of seabream following abrupt hyposmotic exposure. *J Fish Biol* 55:732–750
- Kelly SP, Wood CM (2001) Effect of cortisol on the physiology of cultured pavement cell epithelia from freshwater trout gills. *Am J Physiol Regul Integr Comp Physiol* 281:R811–R820
- Kelly SP, Wood CM (2002a) Cultured gill epithelia from freshwater tilapia (*Oreochromis niloticus*): effect of cortisol and homologous serum supplements from stressed and unstressed fish. *J Membr Biol* 190:29–42
- Kelly SP, Wood CM (2002b) Prolactin effects on cultured pavement cell epithelia and pavement cell plus mitochondria-rich cell epithelia from freshwater rainbow trout gills. *Gen Comp Endocrinol* 128:44–56
- Kelly SP, Wood CM (2008) Cortisol stimulates calcium transport across cultured gill epithelia from freshwater rainbow trout. *In Vitro Cell Dev Biol Anim* 44:96–104
- Leray C, Colin DA, Florentz A (1981) Time course of osmotic adaptation and gill energetics of rainbow trout (*Salmo gairdneri* R.) following abrupt changes in external salinity. *J Comp Physiol* 144:175–181
- Mancera JM, Perez-Figares JM, Fernandez-Llebrez P (1993) Osmoregulatory responses to abrupt salinity changes in the euryhaline gilthead sea bream (*Sparus aurata* L.). *Comp Biochem Physiol* 106A:245–250
- Marshall WS, Grosell M (2005) Ion transport, osmoregulation, and acid-base balance. In: Evans DH, Claiborne JB (eds) *The physiology of fishes*, 3rd edn. Taylor and Francis Group, Boca Raton, pp 177–210
- McCarthy KM, Skare IB, Stankewich MC, Furuse M, Tsukita S, Rogers RA, Lynch RD, Schneeberger EE (1996) Occludin is a functional component of the tight junction. *J Cell Sci* 109:2287–2298
- McCormick SD (1993) Methods for nonlethal gill biopsy and measurement of Na^+ , K^+ -ATPase activity. *Can J Fish Aquat Sci* 50:656–658
- Mommsen TP, Vijayan MM, Moon TW (1999) Cortisol in teleosts: dynamics, mechanisms of action, and metabolic regulation. *Rev Fish Biol Fish* 9:211–268
- Nishimura H, Fan Z (2003) Regulation of water movement across vertebrate renal tubules. *Comp Biochem Physiol* 136A:479–498
- Perry SF, Laurent P (1989) Adaptational responses of rainbow trout to lowered external NaCl concentration—contribution of the branchial chloride cell. *J Exp Biol* 147:147–168
- Scott GR, Schulte PM, Wood CM (2006) Plasticity of osmoregulatory function in the killifish intestine: drinking rates, salt and water transport, and gene expression after freshwater transfer. *J Exp Biol* 209:4040–4050
- Tipsmark CK, Baltzegar DA, Ozden O, Grubb BJ, Borski RJ (2008) Salinity regulates claudin mRNA and protein expression in the teleost gill. *Am J Physiol Regul Integr Comp Physiol* 294:R1004–R1014
- Usher ML, Talbot C, Eddy FB (1991) Effects of transfer to seawater on growth and feeding in Atlantic salmon smolts (*Salmo salar* L.). *Aquaculture* 94:309–326
- Wong V, Gumbiner BM (1997) A synthetic peptide corresponding to the extracellular domain of occludin perturbs the tight junction permeability barrier. *J Cell Biol* 136:399–409
- Wood CM, Laurent P (2003) Na^+ versus Cl^- transport in the intact killifish after rapid salinity transfer. *Biochim Biophys Acta* 1618:106–119
- Zall DM, Fisher D, Garner MD (1956) Photometric determination of chlorides in water. *Anal Chem* 28:1665–1678

**ELSEVIER LICENSE
TERMS AND CONDITIONS**

Sep 20, 2011

This is a License Agreement between Helen Chasiotis ("You") and Elsevier ("Elsevier") provided by Copyright Clearance Center ("CCC"). The license consists of your order details, the terms and conditions provided by Elsevier, and the payment terms and conditions.

All payments must be made in full to CCC. For payment instructions, please see information listed at the bottom of this form.

Supplier	Elsevier Limited The Boulevard, Langford Lane Kidlington, Oxford, OX5 1GB, UK
Registered Company Number	1982084
Customer name	Helen Chasiotis
Customer address	York University Toronto, ON M3J 1P3
License number	2753371090566
License date	Sep 20, 2011
Licensed content publisher	Elsevier
Licensed content publication	Molecular and Cellular Endocrinology
Licensed content title	Cortisol reduces paracellular permeability and increases occludin abundance in cultured trout gill epithelia
Licensed content author	Helen Chasiotis, Chris M. Wood, Scott P. Kelly
Licensed content date	29 July 2010
Licensed content volume number	323
Licensed content issue number	2
Number of pages	7
Start Page	232
End Page	238
Type of Use	reuse in a thesis/dissertation
Intended publisher of new work	other
Portion	full article
Format	both print and electronic
Are you the author of this Elsevier article?	Yes
Will you be translating?	No

Order reference number

Title of your thesis/dissertation The role of occludin tight junction protein in freshwater teleost fish osmoregulation

Expected completion date Oct 2011

Estimated size (number of pages) 350

Elsevier VAT number GB 494 6272 12

Permissions price 0.00 USD

VAT/Local Sales Tax 0.0 USD / 0.0 GBP

Total 0.00 USD

Terms and Conditions

INTRODUCTION

1. The publisher for this copyrighted material is Elsevier. By clicking "accept" in connection with completing this licensing transaction, you agree that the following terms and conditions apply to this transaction (along with the Billing and Payment terms and conditions established by Copyright Clearance Center, Inc. ("CCC"), at the time that you opened your Rightslink account and that are available at any time at <http://myaccount.copyright.com>).

GENERAL TERMS

2. Elsevier hereby grants you permission to reproduce the aforementioned material subject to the terms and conditions indicated.

3. Acknowledgement: If any part of the material to be used (for example, figures) has appeared in our publication with credit or acknowledgement to another source, permission must also be sought from that source. If such permission is not obtained then that material may not be included in your publication/copies. Suitable acknowledgement to the source must be made, either as a footnote or in a reference list at the end of your publication, as follows:

“Reprinted from Publication title, Vol /edition number, Author(s), Title of article / title of chapter, Pages No., Copyright (Year), with permission from Elsevier [OR APPLICABLE SOCIETY COPYRIGHT OWNER].” Also Lancet special credit - “Reprinted from The Lancet, Vol. number, Author(s), Title of article, Pages No., Copyright (Year), with permission from Elsevier.”

4. Reproduction of this material is confined to the purpose and/or media for which permission is hereby given.

5. Altering/Modifying Material: Not Permitted. However figures and illustrations may be altered/adapted minimally to serve your work. Any other abbreviations, additions, deletions and/or any other alterations shall be made only with prior written authorization of Elsevier Ltd. (Please contact Elsevier at permissions@elsevier.com)

6. If the permission fee for the requested use of our material is waived in this instance,



Cortisol reduces paracellular permeability and increases occludin abundance in cultured trout gill epithelia

Helen Chasiotis^a, Chris M. Wood^b, Scott P. Kelly^{a,*}

^a Department of Biology, York University, 4700 Keele Street, Toronto, ON, Canada M3J 1P3

^b Department of Biology, McMaster University, Hamilton, ON, Canada L8S 4K1

ARTICLE INFO

Article history:

Received 29 December 2009

Accepted 22 February 2010

Keywords:

Osmoregulation
ion transport
Tight junction
Pavement cells
Transepithelial resistance
Polyethylene glycol

ABSTRACT

A role for the tight junction (TJ) protein occludin in the regulation of gill paracellular permeability was investigated using primary cultured “reconstructed” freshwater (FW) rainbow trout gill epithelia composed solely of pavement cells. Cortisol treatment reduced epithelial permeability characteristics, measured as changes in transepithelial resistance (TER) and paracellular [³H]PEG-4000 flux. Cortisol also reduced net Na⁺ flux rates when epithelia were exposed to apical FW. cDNA encoding for the TJ protein occludin was cloned from rainbow trout and found to be particularly abundant in gill tissue. In cultured gill preparations, occludin immunolocalized to the TJ complex and transcript abundance dose-dependently increased in response to cortisol treatment in association with reduced paracellular permeability. Occludin protein abundance also increased in response to cortisol treatment. However, occludin mRNA levels did not change in response to apical FW exposure, and [³H]PEG-4000 permeability did not decrease. These data support a role for occludin in the endocrine regulation of paracellular permeability across gill epithelia of fishes.

© 2010 Elsevier Ireland Ltd. All rights reserved.

1. Introduction

The tight junction (TJ) complex plays an important role in the regulation of epithelial permeability in vertebrates. It is composed of a number of transmembrane and cortical proteins and the presence, as well as abundance, of different TJ proteins appears to be a key element in TJ heterogeneity between and within tissues. Occludin is a tetraspan transmembrane TJ protein that is broadly expressed in vertebrate epithelia (Feldman et al., 2005). Since the initial discovery of occludin (Furuse et al., 1993), numerous studies have suggested an important role for this TJ protein in the regulation of epithelial permeability (Feldman et al., 2005). More specifically, an increase in occludin abundance is most often associated with reductions in paracellular permeability across diverse epithelia and endothelia (Feldman et al., 2005). However, the majority of work conducted on the physiological function of occludin in vertebrate epithelia has been accomplished using mammalian models. Recently it has been proposed that occludin may contribute to the regulation of epithelial permeability in aquatic vertebrates under conditions of altered hydromineral status (Chasiotis and Kelly, 2008, 2009; Chasiotis et al., 2009). In this regard, occludin has been found to be abundant in epithelia that

regulate salt and water balance in fishes, such as the gill, kidney and gastrointestinal (GI) tract (Chasiotis and Kelly, 2008; Chasiotis et al., 2009). In the freshwater (FW) goldfish kidney, a spatially distinct distribution pattern of occludin can be observed along the nephron (Chasiotis and Kelly, 2008). The “tight” distal tubules and collecting ducts of the nephron exhibit robust occludin immunoreactivity (occludin-ir), while the “leakier” proximal regions of the nephron exhibit little or no occludin-ir. Furthermore, in the gill tissue of goldfish, occludin protein abundance significantly increased when fish were acclimated to ion-poor water (Chasiotis et al., 2009). This has been proposed to contribute to a reduction in the permeability of the paracellular pathway across the gill (Chasiotis et al., 2009) and is consistent with the observations of Cuthbert and Maetz (1972) who reported that the gill epithelium of goldfish exposed to ion-poor conditions exhibits a considerable reduction in outwardly directed ion movement. This presumably results in a beneficial reduction in passive ion loss in an environment where limitations are set on active ion acquisition.

Despite the above observations, and to the best of our knowledge, there are no studies that have related alterations in the specific machinery of the TJ complex in fishes with measured changes in epithelial permeability. Primary cultured gill epithelial models that allow for the “reconstruction” of FW gill epithelia *in vitro* present an appropriate tool for such studies (see Wood and Pärt, 1997; Fletcher et al., 2000; Kelly et al., 2000; Kelly and Wood, 2002). These models exhibit passive transport and perme-

* Corresponding author. Tel.: +1 416 736 2100x77830; fax: +1 416 736 5698.
E-mail address: spk@yorku.ca (S.P. Kelly).

ability characteristics that closely mimic the *in vivo* characteristics of the FW gill epithelium (Wood and Pärt, 1997; Fletcher et al., 2000; Kelly et al., 2000; Kelly and Wood, 2002). Furthermore, corticosteroid (cortisol) treatment of cultured gill epithelia results in a distinct epithelial tightening effect which is driven at least in part by reduced paracellular permeability properties (Kelly and Wood, 2001, 2002). This sensitivity to cortisol provides a simple means by which to manipulate transepithelial as well as paracellular permeability characteristics and these observations in fishes are in accord with the tightening effects of corticosteroids on other vertebrate epithelia and endothelia (Zettl et al., 1992; Stelwagen et al., 1999; Antonetti et al., 2002; Förster et al., 2005).

Based on this knowledge, the objectives of the current study were to examine cortisol-induced alterations in the permeability characteristics of a cultured gill epithelium prepared from FW rainbow trout and relate alterations in paracellular permeability to modifications in occludin abundance. We hypothesized that if occludin is involved in regulating the barrier properties of gill epithelia in fishes, occludin abundance should increase in association with reductions in paracellular permeability.

2. Materials and methods

2.1. Cultured rainbow trout gill epithelia

The preparation and culture of gill epithelia from FW rainbow trout was carried out in order to produce preparations composed of gill pavement cells only. Methods have been detailed by Kelly et al. (2000) and were originally developed by Wood and Pärt (1997). Briefly, cultured epithelia were prepared using stock rainbow trout (200–450 g) held in flow-through dechlorinated tap water (approximate composition in mmol l^{-1} : $[\text{Na}^+] = 0.55\text{--}0.59$, $[\text{Cl}^-] = 0.70\text{--}0.92$, $[\text{Ca}^{2+}] = 0.76\text{--}0.90$, $[\text{K}^+] = 0.04\text{--}0.05$, pH range 7.4–8.0) at 10–12 °C. Cells were initially cultured in 25 cm^2 flasks in Leibovitz's L-15 media supplemented with 2 mmol l^{-1} glutamine and 6% foetal bovine serum (L15). At confluence (~4–5 days), cells were harvested and seeded into cell culture inserts (0.9 cm^2 growth area, 0.4 μm pore size, 1.6×10^6 pores/ cm^2 pore density; Falcon BD, Mississauga, ON, Canada). Culture inserts were housed in companion cell culture plates (Falcon BD) and after cell seeding (at a density of 700,000 cells/culture insert), epithelia were allowed to develop a stable transepithelial resistance (TER) (over ~5 days) with L15 culture media present on both apical and basolateral surfaces of the preparation (i.e. symmetrical culture conditions). The treatment of epithelia with cortisol was conducted according to methods previously outlined by Kelly and Wood (2001). Two physiologically relevant doses of cortisol were selected (50 and 500 ng/ml) based on the aforementioned study as well as observations made by Kelly and Wood (2002). Cortisol was added to culture media in flasks 24 h after first seeding and when epithelia were cultured in inserts, cortisol was added to the basolateral media only. Therefore, epithelia cultured in flasks and subsequently in inserts were exposed to cortisol for a total of 9–10 days. In a separate set of experiments which were conducted in order to determine whether alterations in occludin transcript abundance translated into alterations in occludin protein abundance, only flask-cultured epithelia were used to harvest tissue. The rationale for this was that inserts did not provide enough protein for Western blot analysis after conducting the extraction protocol used in these studies (see Section 2.6). Therefore, in these experiments cultured epithelial cells were exposed to a single dose of cortisol (500 ng/ml) for 5 days. This period of time and dose of cortisol is sufficient to elicit a significant increase in TER and accompanying decrease in $[\text{H}]$ PEG-4000 permeability (see Section 2.2) in cultured epithelia (data not shown). Finally, in experiments where FW was added to the apical side of cultured preparations (i.e. asymmetrical culture conditions), temperature-equilibrated sterile dechlorinated FW (composition as detailed above) was used.

2.2. Electrophysiological, $[\text{H}]$ PEG-4000 and net Na^+ flux measurements

Measurements of TER were conducted using chopstick electrodes (STX-2) fitted to a custom-modified voltohmmeter (World Precision Instruments, Sarasota, FL, USA). TER was recorded every 24 h after seeding cells onto culture inserts to monitor epithelial development. Under asymmetrical conditions, TER was monitored at 3 h intervals. All measurements of TER are reported as background-corrected values taking into account the resistance measured across a “vacant” culture insert containing appropriate solutions.

Paracellular permeability across cultured epithelia was examined using the paracellular permeability marker, $[\text{H}]$ polyethylene glycol (molecular mass 4000 Da; ‘PEG-4000’; NEN-Dupont, Mississauga, ON, Canada) according to previously detailed methods and calculations (Kelly and Wood, 2001). $[\text{H}]$ PEG-4000 (1 μCi) was added to the basolateral compartment of culture preparations and its appearance in the apical compartment monitored as a function of time and epithelial surface area. Net Na^+ flux rates from basolateral to apical compartments under asym-

metrical culture conditions were measured and calculated according to methods detailed by Kelly and Wood (2001).

2.3. Cloning and qRT-PCR analysis of rainbow trout occludin cDNA

Total RNA was isolated from trout gill tissue using TRIzol® Reagent (Invitrogen Canada Inc., Burlington, ON, Canada), according to manufacturer's instructions. Gill RNA was then treated with DNase I (Amplification Grade; Invitrogen Canada Inc.) and first-strand cDNA was synthesized using SuperScript™ III Reverse Transcriptase and oligo(dT)_{12–18} primers (Invitrogen Canada Inc.).

Using a ClustalX multiple sequence alignment of occludin coding sequences from 9 different species (human [NM_002538]; mouse [NM_008756]; rat [NM_031329]; cow [NM_001082433]; dog [NM_001003195]; platypus [XM_001510548]; opossum [XM_001380557]; frog [NM_001088474]; zebrafish [NM_212832]), degenerate primers were designed based on highly conserved regions. A partial rainbow trout cDNA fragment was amplified by reverse transcriptase PCR (RT-PCR) using occludin degenerate primers under the following reaction conditions: 1 cycle of denaturation (95 °C, 4 min), 40 cycles of denaturation (95 °C, 30 s), annealing (53 °C, 30 s) and extension (72 °C, 30 s), respectively, final single extension cycle (72 °C, 5 min) (0.2 μM dNTP, 2 μM forward and reverse primers, 1 × Taq DNA polymerase buffer, 1.5 mM MgCl_2 and 1 U Taq DNA polymerase) (Invitrogen Canada Inc.). Gel electrophoresis (1% agarose for ~90 min at 5 V/cm) verified a PCR product at the predicted amplicon size of ~796 bp. The DNA fragment was excised from the gel and purified using a QIAquick Gel Extraction Kit (QIAGEN Inc., Mississauga, ON, Canada). The purified amplicon was sequenced in the York University Core Molecular Biology and DNA Sequencing Facility (Department of Biology, York University, Toronto, ON, Canada). A partial coding sequence (CDS) of trout occludin was confirmed using a Basic Local Alignment Search Tool (BLAST) search.

To obtain the complete rainbow trout occludin CDS, both 5'- and 3'-rapid amplification of cDNA ends (RACE) PCR was performed using a SMART™ RACE cDNA Amplification Kit (Clontech Laboratories Inc., Mountain View, CA, USA) as per manufacturer's instructions. RACE-PCR products were resolved by electrophoresis, purified and sequenced as described above in order to complete the trout occludin CDS, GenBank accession number GQ476574.

2.4. Occludin expression profile and qRT-PCR analysis of occludin mRNA abundance in rainbow trout tissues

Quantitative real-time PCR (qRT-PCR) was used to examine occludin mRNA distribution and abundance in discrete rainbow trout tissues, as well as occludin transcript abundance in cultured epithelia from flasks and cell culture inserts. For expression profile studies, total RNA was extracted from the following tissues: brain, eye, gill, bulbus arteriosus, atrium, ventricle, esophagus, anterior and posterior stomach, pyloric ceca, anterior intestine, middle intestine and posterior intestine, liver, gallbladder, spleen, swimbladder, kidney, muscle, adipose tissue and blood. The extraction of RNA and synthesis of cDNA from all tissues was conducted as outlined in the previous section. Primers for trout occludin (forward: 5' CAGCCAGTTCCTCCAGTAG 3' and reverse: 5' GCTCATCCAGCTCTCTGCC 3', predicted amplicon size ~340 bp) were designed using the CDS generated by 5'- and 3'-RACE-PCR described above. β -Actin was used as an internal control (forward: 5' GGACTTTGAGCAGGAGATGG 3' and reverse: 5' GACGGAGTATTTACGCTCTGG 3', predicted amplicon size ~354 bp). β -Actin primers were designed based on GenBank accession number AF157514.

qRT-PCR analysis of occludin and β -actin was conducted using SYBR Green I Supermix (Bio-Rad Laboratories Ltd., Mississauga, ON, Canada) and a Chromo4™ Detection System (CFB-3240, Bio-Rad Laboratories Canada Ltd.) under the following conditions: 1 cycle denaturation (95 °C, 4 min) followed by 40 cycles of denaturation (95 °C, 30 s), annealing (58 °C, 30 s) and extension (72 °C, 30 s), respectively. To ensure that no primer-dimers or other non-specific products were synthesized during reactions, a melting curve analysis was carried out after each qRT-PCR run.

2.5. Immunolocalization of rainbow trout occludin

Trout gill epithelia cultured in inserts were allowed to develop a stable TER under symmetrical culture conditions. Epithelia were briefly rinsed with phosphate-buffered saline (PBS, pH 7.7) and fixed for 20 min at room temperature (RT) with 3% paraformaldehyde. Fixed epithelia were then permeabilized with ice-cold methanol for 5 min at –20 °C, washed with 0.01% Triton X-100 in PBS for 10 min and blocked for 1 h at RT with antibody dilution buffer (ADB; 10% goat serum, 3% BSA and 0.05% Triton X-100 in PBS). Epithelia were incubated overnight at RT with a custom-synthesized polyclonal antibody raised in rabbit against a synthetic peptide (CHIKKMGVGDYDRRA) corresponding to a 14-amino acid region of rainbow trout occludin (1:100 dilution in ADB; New England Peptide, LLC, Gardner, MA, USA). For a negative control, epithelia were also incubated overnight with ADB lacking primary antibody. Epithelia were then washed with PBS and incubated for 1 h at RT with TRITC-labeled goat anti-rabbit antibody (1:500 in ADB; Jackson ImmunoResearch Laboratories Inc., West Grove, PA, USA). After a final wash with PBS, epithelia were excised from the insert housings using a scalpel and mounted on glass microscopy slides with Molecular Probes Prolong Antifade (Invitrogen Canada

Inc.) containing $5 \mu\text{g ml}^{-1}$ DAPI (Sigma–Aldrich Canada Ltd., Oakville, ON, Canada). Fluorescence images were captured using a Reichert Polyvar microscope (Reichert Microscope Services, Depew, NY, USA) and an Olympus DP70 camera (Olympus Canada, Markham, ON, Canada). Adobe Photoshop CS2 software was used for contrast and brightness adjustment of entire images (Adobe Systems Canada, Toronto, ON, Canada).

2.6. Western blotting and protein quantification of rainbow trout occludin

Trout gill epithelia cultured in flasks were briefly rinsed with ice-cold PBS, scraped using a plastic cell scraper into a lysis buffer (10 mmol l^{-1} Tris–HCl, pH 7.5, 1 mmol l^{-1} EDTA, 0.1 mmol l^{-1} NaCl, 1 mmol l^{-1} PMSF) containing 1:200 protease inhibitor cocktail (Sigma–Aldrich Canada Ltd.) and then homogenized by repeatedly passing through a 26G needle. Homogenates were centrifuged at $20,000 \times g$ for 25 min at 4 °C to remove cell debris and the resultant supernatant was collected. To separate cytosolic and membrane protein fractions, supernatant was further centrifuged at $54,000 \times g$ for 90 min at 4 °C and the remaining pellet (membrane fraction) was resuspended in a solubilizing buffer (50 mmol l^{-1} Tris–HCl, pH 7.5, 1 mmol l^{-1} EDTA, 1% Triton-X-100, 0.5% SDS, 1 mmol l^{-1} PMSF) containing 1:200 protease inhibitor cocktail. Pellet protein concentrations were determined using the Bradford assay (Sigma–Aldrich Canada Ltd.) according to the manufacturer's guidelines. Samples ($2 \mu\text{g}$) were boiled at 100 °C in 6X sample buffer (360 mmol l^{-1} Tris–HCl, 30% glycerol, 12% SDS, 600 mmol l^{-1} DTT, 0.03% Bromophenol Blue) and subjected to SDS-PAGE on 12% acrylamide gels followed by semi-dry transfer to polyvinylidene difluoride (PVDF) membranes for 2 h. Membranes were blocked for 1 h at RT in blocking solution (Tris-buffered saline (TBS; 10 mmol l^{-1} Tris, 150 mmol l^{-1} NaCl, 0.05% Tween-20, pH 7.4) containing 5% nonfat dry skim milk powder), incubated overnight at 4 °C with the custom rabbit polyclonal anti-trout occludin antibody described above (1:1000 dilution in blocking solution), washed with TBS, incubated for 1 h at RT with horseradish peroxidase (HRP)-conjugated goat anti-rabbit antibody (Bio-Rad Laboratories Canada Ltd.; 1:5000 in blocking solution), and then washed once more prior to antigen reactivity detection using an Enhanced Chemiluminescence Plus Western blotting system (GE Healthcare Bio-Sciences Inc., Baie d'Urfé, QC, Canada).

After occludin detection, membranes were stripped and incubated with mouse monoclonal anti-actin antibody (JLA20; Developmental Studies Hybridoma Bank, Iowa City, IA, USA; 1:500 in blocking solution) and HRP-conjugated goat anti-mouse antibody (Bio-Rad Laboratories Canada Ltd.; 1:5000 in blocking solution), respectively as an internal loading control. The abundance of occludin and actin were quantified using a Molecular Imager Gel Doc XR+ System and Quantity One 1D analysis software (Bio-Rad Laboratories Canada Ltd.). Occludin is expressed as a normalized value relative to actin.

2.7. Statistical analysis

All data are expressed as mean values \pm SEM (n), where n represents the number of filter inserts, except in Fig. 2, where n represents the number of fish sampled, and Fig. 5 where n represents the number of cell culture flasks. Significant differences ($P \leq 0.05$) between groups were determined using either a two-way or one-way analysis of variance as appropriate followed by a Student–Newman–Keuls test (Sigmastat Software; Systat Software Inc., San Jose, CA, USA).

3. Results

3.1. Cultured gill epithelia and effects of cortisol on TER, $[^3\text{H}]\text{PEG-4000}$ and net Na^+ flux

Under asymmetrical culture conditions (L15 apical/L15 basolateral), untreated cultured trout gill epithelia preparations (i.e. 0 ng/ml cortisol added) exhibited a mean TER of $\sim 2900 \Omega\text{cm}^2$ (Fig. 1a). The addition of cortisol to culture media (50 or 500 ng/ml) dose-dependently elevated TER (Fig. 1a). In accord with cortisol-induced elevations in TER, cortisol treatment of cultured gill preparations dose-dependently reduced the movement (efflux) of the paracellular permeability marker PEG-4000 (Fig. 1b).

When exposed to asymmetrical culture conditions (FW apical/L15 basolateral), dose-dependent effects of cortisol on TER and $[^3\text{H}]\text{PEG-4000}$ permeability were also observed (Fig. 1a and b). However, FW addition to the apical side of preparations significantly elevated TER in both the control and 50 ng/ml treated preparations relative to measurements under symmetrical conditions (Fig. 1a). In 500 ng/ml treated preparations, no additional significant increase in TER was observed (Fig. 1a). In association with changes in TER, $[^3\text{H}]\text{PEG-4000}$ flux significantly increased in control and 50 ng/ml cortisol-treated epithelia under asymmetrical

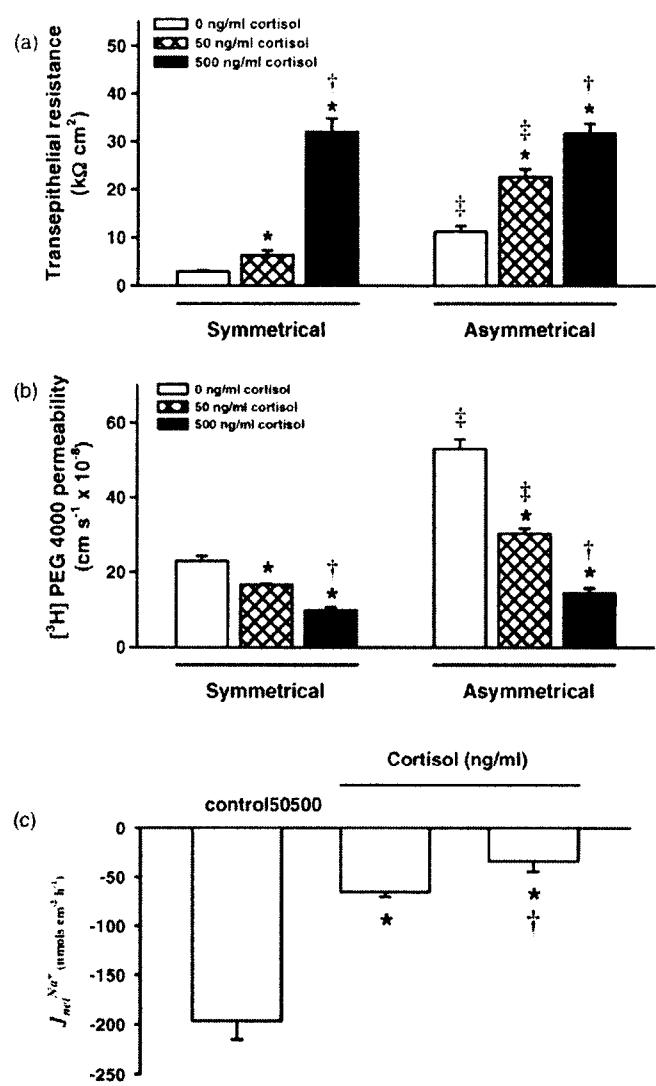


Fig. 1. Effect of cortisol on (a) transepithelial resistance (TER), (b) $[^3\text{H}]\text{PEG-4000}$ permeability and (c) net Na^+ flux rates across cultured rainbow trout gill epithelia. TER and $[^3\text{H}]\text{PEG-4000}$ permeability were measured under both symmetrical (L15 apical/L15 basolateral) and asymmetrical (FW apical/L15 basolateral) culture conditions while net Na^+ flux rates were measured under asymmetrical culture conditions only. Data are expressed as mean values \pm SEM ($n = 4-6$). *Significant difference ($P \leq 0.05$) from control treatment (0 ng/ml cortisol); †Significant difference ($P \leq 0.05$) between symmetrical and asymmetrical culture conditions.

culture conditions (Fig. 1b) but no significant increase in $[^3\text{H}]\text{PEG-4000}$ flux was observed in epithelia treated with 500 ng/ml cortisol. Under asymmetrical culture conditions, cortisol dose-dependently reduced the efflux rates (basolateral to apical movement) of Na^+ (Fig. 1c).

3.2. Cloning of trout occludin cDNA, tissue expression profile and immunolocalization

Sequencing and analysis of the 1500 bp CDS of rainbow trout occludin revealed an open reading frame for a 500-amino acid protein that exhibited 46–48% amino acid sequence identity with mammalian occludin (i.e. human, mouse, rat, cow, dog, platypus and opossum), $\sim 50\%$ identity with frog occludin and $\sim 63\%$ identity with zebrafish occludin. Using qRT-PCR analysis, occludin tran-

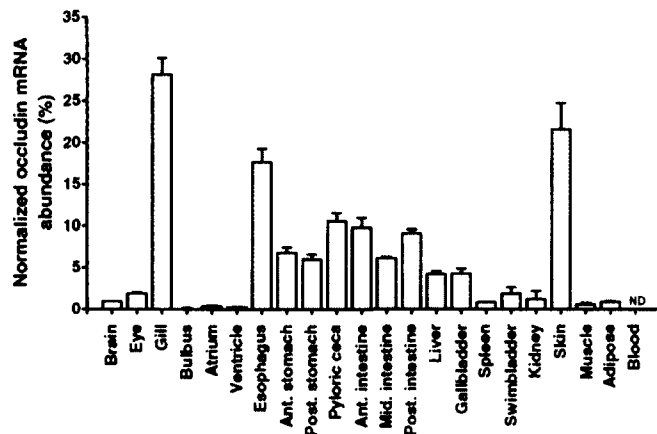


Fig. 2. qRT-PCR generated occludin expression profile for discrete rainbow trout tissues. Occludin mRNA abundance was normalized with β -actin and the abundance of occludin in each tissue was expressed relative to the brain assigned a value of 1.0. Data are expressed as mean values \pm SEM ($n=4$). Amplicon size was 340 bp and 354 bp for occludin and β -actin, respectively.

script was found to be broadly distributed in rainbow trout tissues (Fig. 2). Occludin mRNA was particularly abundant in gill tissue as well as some other tissues involved either directly or indirectly in the regulation of salt and water balance (e.g. skin and GI tract). Occludin was absent in red blood cells (a non-epithelial tissue). Immunocytochemical analysis of cultured preparations revealed occludin-ir along the cultured pavement cell periphery at the location of the TJ (Fig. 3a). A negative control exhibited no occludin-ir (Fig. 3b). Western blot analysis of cultured gill tissues using the custom-synthesized rainbow trout occludin antibody revealed a single immunoreactive band that resolved at ~ 70 kDa (Fig. 3c).

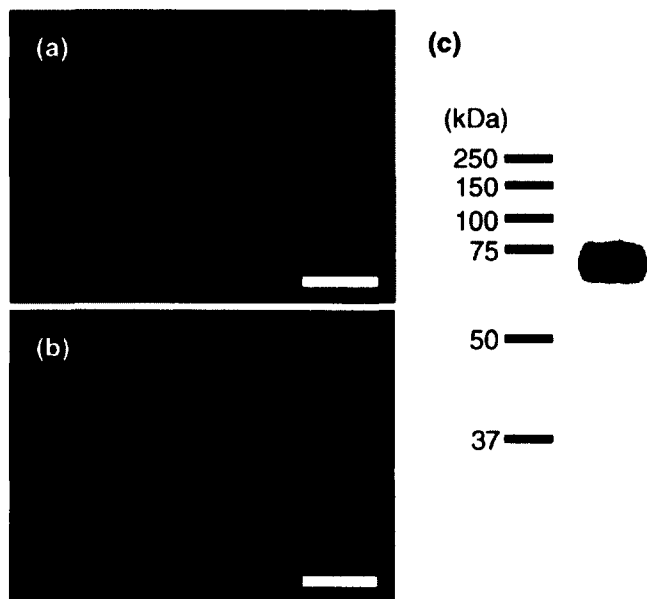


Fig. 3. (a) Immunolocalization of occludin (red) in cultured trout gill epithelia under symmetrical (L15 apical/L15 basolateral) culture conditions using a custom-synthesized rabbit polyclonal antibody raised against a synthetic region of trout occludin. Negative control (primary antibody omitted) is shown in (b). (c) Representative Western blot using the same custom-synthesized occludin antibody used for immunolocalization. A single occludin-immunoreactive band resolved at ~ 70 kDa. In panels (a) and (b), nuclei were stained with DAPI (blue) and each scale bar = 20 μ m.

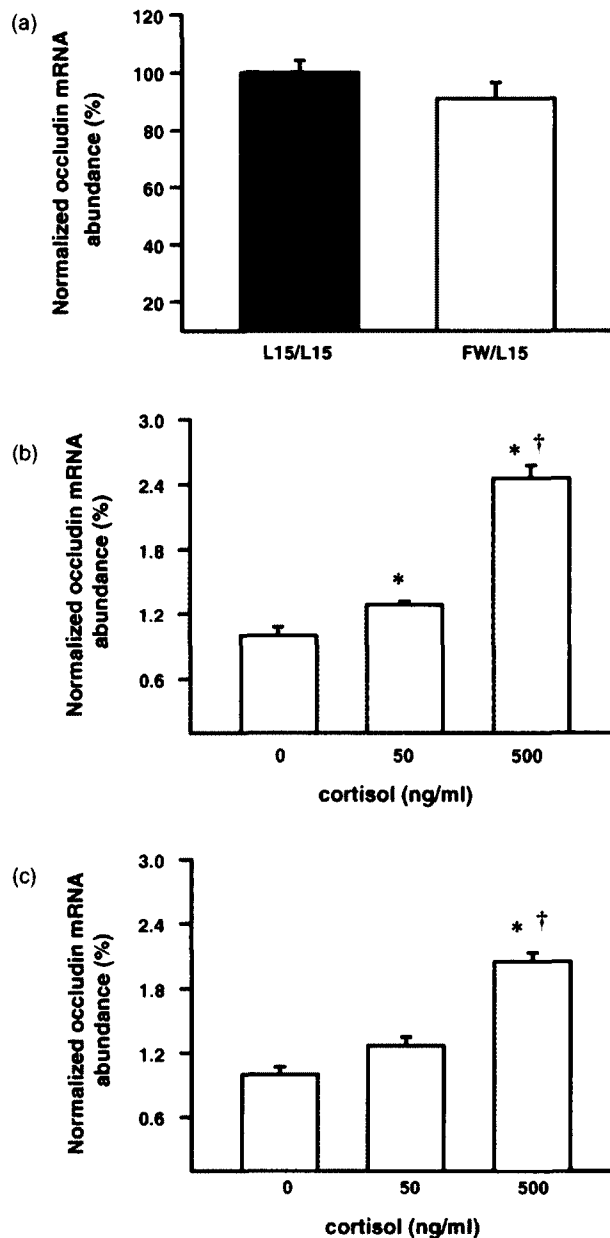


Fig. 4. Occludin mRNA abundance in response to (a) 12 h apical FW exposure and cortisol addition to media under (b) symmetrical (L15 apical/L15 basolateral) and (c) asymmetrical (FW apical/L15 basolateral) culture conditions. Data are expressed as mean values \pm SEM ($n=4-6$). In (a) β -actin normalized occludin mRNA abundance for epithelia exposed to apical FW (asymmetrical) is expressed relative to symmetrical culture conditions assigned a value of 1.0. In (b) and (c) β -actin normalized occludin mRNA abundance for cortisol-treated epithelia are expressed relative to untreated (0 ng/ml cortisol) epithelia assigned a value of 1.0. *Significant difference ($P \leq 0.05$) from control treatment (0 ng/ml cortisol); †significant difference between cortisol doses (50 versus 500 ng/ml cortisol).

3.3. Effects of culture conditions and cortisol on occludin abundance

In epithelia cultured on inserts, no significant differences in occludin mRNA abundance were observed between preparations held under symmetrical or asymmetrical culture conditions (Fig. 4a). In contrast, cortisol treatment significantly elevated occludin mRNA abundance in both 50 and 500 ng/ml treated epithelia in cell culture inserts under symmetrical conditions (Fig. 4b) and in 500 ng/ml treated preparations under asymmetrical culture conditions (Fig. 4c). No alterations in β -actin abundance were seen in any of these treatments (symmetrical versus asym-

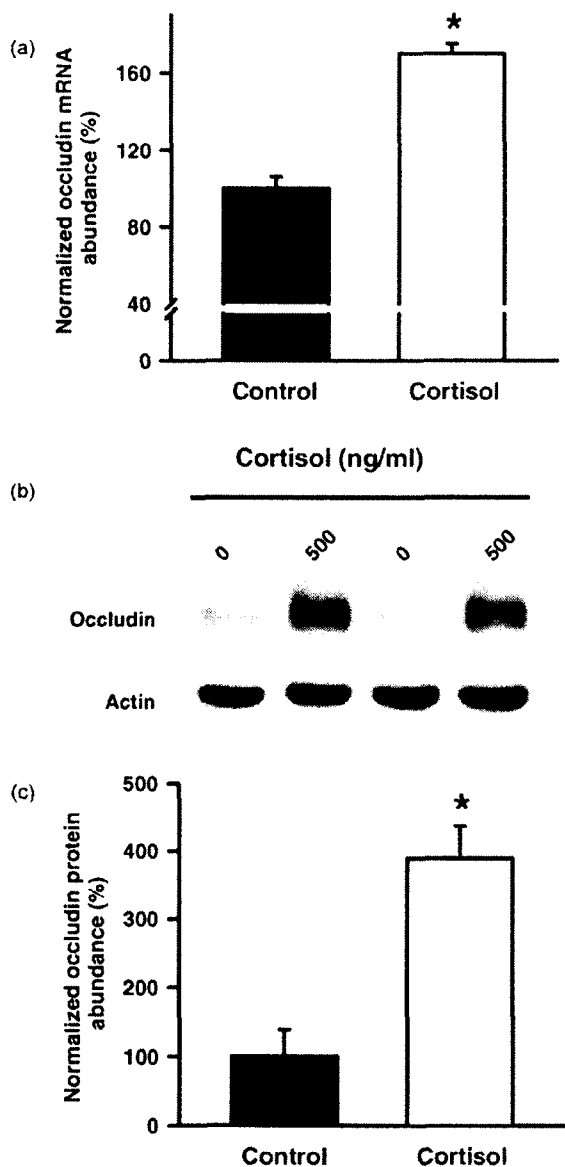


Fig. 5. Effect of cortisol (500 ng/ml) on occludin abundance in flask-cultured rainbow trout pavement cell epithelia. Alterations in occludin (a) mRNA and (b and c) protein abundance are shown. In (a) occludin mRNA abundance in cortisol-treated epithelia is normalized with β -actin and expressed relative to untreated (0 ng/ml cortisol) epithelia assigned a value of 1.0. (b) shows a representative Western blot where both occludin and actin immunoreactivity can be observed and (c) presents occludin protein abundance normalized to actin and expressed relative to untreated (0 ng/ml cortisol) epithelia assigned a value of 1.0. In (a) and (c), data are expressed as mean values \pm SEM ($n=4-6$). *Significant difference ($P \leq 0.05$) from untreated controls.

metrical, $P=0.78$; control versus cortisol-treated inserts under symmetrical conditions, $P=0.13$; control versus cortisol-treated inserts under asymmetrical conditions, $P=0.18$).

In flask-cultured epithelia exposed to 500 ng/ml cortisol for 5 days and subsequently harvested for either mRNA or protein analysis, cortisol significantly elevated both transcript and protein abundance (Fig. 5). For these studies, actin was also used to normalize both mRNA and protein abundance. Again, no significant alterations in actin levels were observed as a result of cortisol treatment (mRNA, cortisol versus control $P=0.19$; protein, cortisol versus control $P=0.76$).

4. Discussion

4.1. Cultured gill epithelia and effects of cortisol on TER, [^3H]PEG-4000 and net Na^+ flux

The electrophysiological and permeability characteristics of untreated (0 ng/ml cortisol added) cultured trout pavement cell epithelia in symmetrical culture conditions were typical for these preparations (see Fig. 1 and Kelly et al., 2000), and cortisol treatment dose-dependently elevated TER in accord with previous reports (see Kelly and Wood, 2001). Since TER is a function of both transcellular and paracellular permeability, dose-dependent reductions in the efflux rates of the paracellular permeability marker PEG-4000 in cortisol-treated epithelia (see Fig. 1b) demonstrated that elevated TER measurements were driven at least in part by reductions in the permeability of the paracellular pathway. Under asymmetrical culture conditions, epithelia exhibited a qualitatively similar response to cortisol treatment (Fig. 1a and b). However, exposure of epithelia to apical FW caused a significant elevation in TER across control and 50 ng/ml treated preparations. In epithelia cultured in the presence of a high cortisol dose (i.e. 500 ng/ml), no further increase in TER was observed. In control epithelia, and epithelia treated with 50 ng/ml cortisol, elevated TER in response to apical FW addition occurs in conjunction with a paradoxical increase in paracellular permeability. This is usual for cultured trout gill epithelia and suggests that elevated TER under asymmetrical conditions in these preparations predominantly reflects decreased transcellular permeability, while paracellular permeability may actually increase upon acute FW exposure (Wood et al., 1998). Treatment with higher doses of cortisol appears to dampen this phenomenon, most likely by causing a reduction in both transcellular and paracellular conductance prior to FW exposure. When epithelia are exposed to apical FW, cortisol caused a dose-dependent reduction in the efflux rates (basolateral to apical movement) of Na^+ . This has previously been hypothesized to reflect a beneficial reduction in passive ion loss across the gill surface of FW fishes under "stressed" conditions where cortisol would be naturally elevated in the circulatory system of a FW fish (see Kelly and Wood, 2001).

4.2. Cloning of trout occludin cDNA, tissue expression profile and immunolocalization

qRT-PCR analysis of occludin in discrete tissues of rainbow trout revealed a broad expression pattern. This is in accord with widespread distribution of occludin in other vertebrates (e.g. Furuse et al., 1993; Saitou et al., 1997; Feldman et al., 2005; Chasiotis and Kelly, 2009). In epithelia that are directly exposed to the external environment (such as the gill and skin), as well as other tissues involved in the regulation of salt and water balance in fishes, occludin was particularly abundant. Similar observations have been reported regarding occludin expression patterns in the goldfish (Chasiotis and Kelly, 2008). Occludin was also observed to immunolocalize to the periphery of cultured trout pavement cells, where TJs maintain epithelial integrity and contribute to the regulated separation of fluid compartments. This observation is in line with reports of occludin immunolocalization in numerous other vertebrate epithelia (e.g. Saitou et al., 1997; González-Mariscal et al., 2000; Ridyard et al., 2007; Chasiotis and Kelly, 2008; Chasiotis and Kelly, 2009). In goldfish gills, occludin has been reported to immunolocalize between epithelial cells in a similar manner. However, occludin has also been found to immunolocalize to the capillary endothelium (Chasiotis and Kelly, 2008). Since the cultured preparations are composed entirely of gill epithelial pavement cells, this model allows us to evaluate the effects of cortisol

on paracellular permeability properties and TJ protein mRNA abundance in gill epithelial cells only and negates any contribution from capillary endothelia.

4.3. Effects of culture conditions and cortisol on occludin abundance

In the absence of cortisol, exposure of cultured gill epithelia to asymmetrical culture conditions (i.e. apical FW) resulted in a significant increase in TER. However, occludin mRNA abundance did not significantly alter in response to asymmetrical culture conditions (see Fig. 4a). In this regard, elevated TER is not driven by a reduction in the permeability of the paracellular pathway as [³H]PEG-4000 flux did not decrease in conjunction with an increase in TER (see Fig. 1 and discussion above). Therefore it is not unexpected that occludin mRNA levels did not increase. In contrast, it is noteworthy that occludin mRNA levels did not significantly decrease in association with an increase in PEG-4000 flux across cultured preparations. Despite these observations, cortisol treatment did significantly elevate occludin mRNA and protein abundance in association with both an increase in TER and decrease in PEG-4000 flux. This would suggest that the endocrine system, and more specifically corticosteroids, play an important role in regulating occludin abundance in the fish gill epithelium. In line with these observations, corticosteroid treatment of mouse mammary epithelia has been reported to result in both a decrease in paracellular permeability and increase in occludin abundance (Stelwagen et al., 1999). Furthermore, capillary endothelia of the blood–brain–barrier (BBB) as well as the blood–retinal barrier also exhibit a similar response (Antonetti et al., 2002; Förster et al., 2005). Correspondingly, it was recently shown that glucocorticoids directly up-regulate occludin expression via activated glucocorticoid receptor binding to a glucocorticoid response element within the human occludin gene promoter (Harke et al., 2008). Given that cortisol-induced alterations in the paracellular permeability of gill epithelial preparations can be almost entirely blocked using the glucocorticoid receptor antagonist RU486 (Kelly and Wood, 2002) it is plausible that a similar mechanism may also be in place in the gill epithelial tissue of fishes.

5. Conclusion

The response of occludin to corticosteroid treatment in gill epithelial tissue is qualitatively similar to reports of corticosteroid-induced occludin upregulation in the epithelia and endothelia of other vertebrates. Therefore this report highlights a conservation of fundamental alterations in the molecular machinery of the TJ complex in response to hormone treatment across vertebrate groups. While the current study strongly supports a role for occludin in regulating the barrier properties of osmoregulatory tissue such as the gill, within the confines of this study the endocrine regulation of this process appears to surpass any response to environmental change alone (i.e. no alteration in occludin mRNA abundance after switching apical culture conditions from L15 to FW). However, under natural conditions, a fish rapidly transitioning from saline conditions to FW would typically respond by elevating circulating cortisol levels (e.g. Scott et al., 2006). A key question to address in future studies with respect to the endocrine regulation of occludin and the role that this TJ protein plays in regulating epithelial permeability in tissues such as the gill will be to determine how alterations such as those described in the current study fit into the broader scheme of endocrine-mediated alterations in the molecular machinery of the TJ complex. For example, using a primary culture system similar to the cultured trout gill preparations used in this study, Bui et al. (2010) have recently demonstrated that

mRNA encoding for 9 of 12 salinity-responsive claudin TJ proteins in puffer fish (*Tetraodon nigroviridis*) are found in cultured pavement cell epithelia and differentially respond to physiologically relevant doses of cortisol *in vitro*. Furthermore, Tipsmark et al. (2009) have also reported alterations in claudin mRNA abundance in cortisol-treated gill explants from salmon, albeit at doses higher than used here. These observations, together with the present findings, provide momentum for further study.

Acknowledgements

This work was supported by NSERC Discovery Grants to SPK and CMW as well as an NSERC Discovery Accelerator Supplement, Canadian Foundation for Innovation new opportunities grant, Ontario Early Researcher Award, and a Petro Canada Young Innovator Award to SPK. CMW is supported by the Canada Research Chair Program. The mouse monoclonal anti-actin antibody (JLA20) developed by Jim Jung-Ching Lin was obtained from the Developmental Studies Hybridoma Bank developed under the auspices of the NICHD and maintained by The University of Iowa, Department of Biology, Iowa City, IA 52242.

References

- Antonetti, D.A., Wolpert, E.B., DeMaio, L., Harhaj, N.S., Scaduto Jr., R.C., 2002. Hydrocortisone decreases retinal endothelial cell water and solute flux coincident with increased content and decreased phosphorylation of occludin. *J. Neurochem.* 80, 667–677.
- Bui, P., Bagherie-Lachidan, M., Kelly, S.P., 2010. Cortisol differentially alters claudin isoform mRNA abundance in a cultured gill epithelium from puffer fish (*Tetraodon nigroviridis*). *Mol. Cell. Endocrinol.* 317, 120–126.
- Chasiotis, H., Kelly, S.P., 2008. Occludin immunolocalization and protein expression in goldfish. *J. Exp. Biol.* 211, 1524–1594.
- Chasiotis, H., Kelly, S.P., 2009. Occludin and hydromineral balance in *Xenopus laevis*. *J. Exp. Biol.* 212, 287–296.
- Chasiotis, H., Effendi, J., Kelly, S.P., 2009. Occludin expression in epithelia of goldfish acclimated to ion poor water. *J. Comp. Physiol. B* 179, 145–154.
- Cuthbert, A.W., Maetz, J., 1972. The effects of calcium and magnesium on sodium fluxes through gills of *Carassius auratus*. *L. J. Physiol.* 221, 633–643.
- Feldman, G.J., Mullin, J.M., Ryan, M.P., 2005. Occludin: structure, function and regulation. *Adv. Drug Deliv. Rev.* 57, 883–917.
- Fletcher, M., Kelly, S.P., Pärt, P., O'Donnell, M., Wood, C.M., 2000. Transport properties of cultured branchial epithelia from freshwater rainbow trout: a novel preparation with mitochondria-rich cells. *J. Exp. Biol.* 203, 1523–1537.
- Förster, C., Silwedel, C., Golenhofen, N., Burek, M., Kietz, S., Mankertz, J., Drenckhahn, D., 2005. Occludin as direct target for glucocorticoid-induced improvement of blood–brain barrier properties in a murine *in vitro* system. *J. Physiol.* 565, 475–486.
- Furuse, M., Hirase, T., Itoh, M., Nagafuchi, A., Yonemura, S., Tsukita, S., 1993. Occludin: a novel integral membrane protein localizing at tight junctions. *J. Cell Biol.* 123, 1777–1788.
- González-Mariscal, L., Namorado, M.C., Martín, D., Luna, J., Alarcon, L., Islas, S., Valencia, L., Muriel, P., Ponce, L., Reyes, J.L., 2000. Tight junction proteins ZO-1, ZO-2, and occludin along isolated renal tubules. *Kidney Int.* 57, 2386–2402.
- Harke, H., Leers, J., Kietz, S., Drenckhahn, D., Förster, C., 2008. Glucocorticoids regulate the human occludin gene through a single imperfect palindromic glucocorticoid response element. *Mol. Cell. Endocrinol.* 295, 39–47.
- Kelly, S.P., Fletcher, M., Pärt, P., Wood, C.M., 2000. Procedures for the preparation and culture of “reconstructed” rainbow trout branchial epithelia. *Methods Cell. Sci.* 22, 153–163.
- Kelly, S.P., Wood, C.M., 2001. Effect of cortisol on the physiology of cultured pavement cell epithelia from freshwater trout gills. *Am. J. Physiol. Regul. Integr. Comp. Physiol.* 281, R811–R820.
- Kelly, S.P., Wood, C.M., 2002. Cultured gill epithelia from freshwater tilapia (*Oreochromis niloticus*): effect of cortisol and homologous serum supplements from stressed and unstressed fish. *J. Membr. Biol.* 190 (2002), 29–42.
- Ridyard, A.E., Brown, J.K., Rhind, S.M., Else, R.W., Simpson, J.W., Miller, H.R.P., 2007. Apical junction complex protein expression in the canine colon: differential expression of claudin-2 in the colonic mucosa in dogs with idiopathic colitis. *J. Histochem. Cytochem.* 55, 1049–1058.
- Saitou, M., Ando-Akatsuka, Y., Itoh, M., Furuse, M., Inazawa, J., Fujimoto, K., Tsukita, S., 1997. Mammalian occludin in epithelial cells: its expression and subcellular distribution. *Eur. J. Cell Biol.* 73, 222–231.
- Scott, G.R., Schulte, P.M., Wood, C.M., 2006. Plasticity of osmoregulatory function in the killifish intestine: drinking rates, salt and water transport, and gene expression after freshwater transfer. *J. Exp. Biol.* 209, 4040–4050.
- Stelwagen, K., McFadden, H.A., Demmer, J., 1999. Prolactin, alone or in combination with glucocorticoids, enhances tight junction formation and expression of the

- tight junction protein occludin in mammary cells. *Mol. Cell. Endocrinol.* 156, 55–61.
- Tipsmark, C.K., Jorgensen, C., Brande-Lavridsen, N., Engelund, M., Olesen, J.H., Madsen, S.S., 2009. Effects of cortisol, growth hormone and prolactin on gill claudin expression in Atlantic salmon. *Gen. Comp. Endocrinol.* 163 (3), 270–277.
- Wood, C.M., Pärt, P., 1997. Cultured branchial epithelia from freshwater fish gills. *J. Exp. Biol.* 200, 1047–1059.
- Wood, C.M., Gilmour, K.M., Pärt, P., 1998. Passive and active transport properties of a gill model, the cultured branchial epithelium of the freshwater rainbow trout (*Oncorhynchus mykiss*). *Comp. Biochem. Physiol.* 119A, 87–96.
- Zettl, K.S., Sjaastad, M.D., Riskin, P.M., Parry, G., Machen, T.E., Firestone, G.L., 1992. Glucocorticoid formation of tight junctions in mouse mammary epithelial cells *in vitro*. *Proc. Natl. Acad. Sci. U.S.A.* 89, 9069–9073.

**SPRINGER LICENSE
TERMS AND CONDITIONS**

Sep 20, 2011

This is a License Agreement between Helen Chasiotis ("You") and Springer ("Springer") provided by Copyright Clearance Center ("CCC"). The license consists of your order details, the terms and conditions provided by Springer, and the payment terms and conditions.

All payments must be made in full to CCC. For payment instructions, please see information listed at the bottom of this form.

License Number	2753370935617
License date	Sep 20, 2011
Licensed content publisher	Springer
Licensed content publication	Journal of Comparative Physiology B
Licensed content title	Permeability properties and occludin expression in a primary cultured model gill epithelium from the stenohaline freshwater goldfish
Licensed content author	Helen Chasiotis
Licensed content date	Jan 1, 2010
Volume number	181
Issue number	4
Type of Use	Thesis/Dissertation
Portion	Full text
Number of copies	1
Author of this Springer article	Yes and you are the sole author of the new work
Order reference number	
Title of your thesis / dissertation	The role of occludin tight junction protein in freshwater teleost fish osmoregulation
Expected completion date	Oct 2011
Estimated size(pages)	350
Total	0.00 USD

Terms and Conditions

Introduction

The publisher for this copyrighted material is Springer Science + Business Media. By clicking "accept" in connection with completing this licensing transaction, you agree that the following terms and conditions apply to this transaction (along with the Billing and Payment terms and conditions established by Copyright Clearance Center, Inc. ("CCC"), at the time that you opened your Rightslink account and that are available at any time at <http://myaccount.copyright.com>).

Limited License

Permeability properties and occludin expression in a primary cultured model gill epithelium from the stenohaline freshwater goldfish

Helen Chasiotis · Scott P. Kelly

Received: 13 August 2010 / Revised: 20 October 2010 / Accepted: 2 November 2010 / Published online: 18 November 2010
© Springer-Verlag 2010

Abstract Techniques for the primary culture of fish gill epithelia on permeable supports have provided ‘reconstructed’ gill models appropriate for the study of gill permeability characteristics *in vitro*. Models developed thus far have been derived from euryhaline fish species that can tolerate a wide range of environmental salinity. This study reports on procedures for the primary culture of a model gill epithelium derived from goldfish, a stenohaline freshwater (FW) fish that cannot tolerate high environmental salt concentrations. The reconstructed goldfish gill epithelium was cultured on permeable filter inserts and using electron microscopy and immunocytochemical techniques, was determined to be composed exclusively of gill pavement cells. When cultured under symmetrical conditions (i.e. with culture medium bathing both apical and basolateral surfaces), epithelial preparations generated appreciable transepithelial resistance (TER) (e.g. $1,150 \pm 46 \Omega\text{cm}^2$) within 36–42 h post-seeding in inserts. When apical medium was replaced with FW (asymmetrical conditions to mimic conditions that occur *in vivo*), epithelia exhibited increased TER and elevated paracellular permeability. Changes in permeability occurred in association with altered occludin-immunoreactive band position by western blot and no change in occludin mRNA abundance. We contend that the goldfish gill model will provide a useful *in vitro* tool for examining the molecular components of a stenohaline fish gill epithelium that participate in the regulation of gill permeability. The model will allow

molecular observations to be made together with assessment of changing physiological properties that relate to permeability. Together, this will allow further insight into mechanisms that regulate gill permeability in fishes.

Keywords Pavement cells · Transepithelial resistance · Paracellular permeability · Tight junction · Occludin

Introduction

The fish gill is a complex multifunctional tissue (reviewed by Evans et al. 2005). As a consequence, determining the permeability characteristics of the fish gill epithelium *in vivo* is technically challenging. Typically, the permeability properties of an epithelium can be established using electrophysiological endpoints such as transepithelial resistance (TER). In addition, epithelial paracellular permeability can be examined by quantifying the movement of radiolabelled paracellular permeability markers (e.g. [^3H]PEG-4000, [^3H]mannitol, [^3H]inulin) across an epithelium. The complex architecture of the fish gill, however, hinders the use of electrophysiological techniques *in vivo* and systemically administered paracellular permeability tracers can move across other epithelial tissues such as the skin or kidney. Moreover, the gill epithelium is heterogeneous and overlays an extensive vasculature. Therefore, alterations in the molecular components of the fish gill epithelium that contribute to changes in permeability can be experimentally difficult to isolate.

Techniques for the ‘reconstruction’ of gill epithelia on permeable filter supports have allowed for some of the above-mentioned challenges to be addressed (reviewed by Wood et al. 2002). A ‘reconstructed’ model gill epithelium

Communicated by H.V. Carey.

H. Chasiotis · S. P. Kelly (✉)
Department of Biology, York University, 4700 Keele Street,
Toronto, ON M3J 1P3, Canada
e-mail: spk@yorku.ca

is formed by isolated gill epithelial cells that are cultured on permeable filters at the base of culture inserts (see Kelly et al. 2000; Wood et al. 2002). These primary cultured gill epithelia are not architecturally complex. Composed of a simple flat epithelium separating an apical and basolateral compartment, reconstructed gill preparations permit the electrophysiological measurement of transepithelial permeability as well as the determination of paracellular permeability using radiotracers. Additionally, primary cultured gill epithelia have been shown to exhibit permeability characteristics that faithfully mimic those observed in vivo (see Wood et al. 2002). Furthermore, depending on the techniques used to generate a primary cultured gill preparation, these epithelia can be composed of gill pavement cells (PVCs) only or both PVCs and mitochondria-rich cells (MRCs; see Wood and Pärt 1997; Fletcher et al. 2000; Kelly et al. 2000). In this regard, cultured gill preparations not only provide a useful model for the physiological examination of gill permeability, but also a practical tool for (1) the investigation of molecular components in the fish gill epithelium that contribute to the regulation of gill permeability (see Chasiotis et al. 2010) and (2) the examination of cell specific alterations in these components (see Bui et al. 2010).

To date, methods have been developed and described for the primary culture of gill epithelia from sea bass (Avella and Ehrenfeld 1997), rainbow trout (Wood and Pärt 1997; Fletcher et al. 2000), tilapia (Kelly and Wood 2002), and puffer fish (Bui et al. 2010). Although recent studies have started to utilize cultured gill preparations for the examination of factors that regulate gill permeability (see Bui et al. 2010; Chasiotis et al. 2010), all cultured preparations developed thus far are derived from euryhaline fish species (i.e. species that can tolerate a wide range of environmental salinity). To the best of our knowledge, there are currently no primary cultured model gill epithelia derived from a stenohaline species of fish (i.e. species that can tolerate only a narrow range of environmental salinity). We contend that to gain broader insight into the importance of factors that regulate epithelial permeability in fishes, it will not only be beneficial to examine euryhaline species, but also stenohaline fishes. In this regard, we have recently reported that when hydromineral status is challenged in the stenohaline goldfish, the abundance of occludin, a key tight junction (TJ) protein in vertebrate epithelia, significantly alters in tissues such as the gill (Chasiotis and Kelly 2008; Chasiotis et al. 2009). Therefore, in the present study, our objectives were to (1) develop a method for the primary culture of a model gill epithelium from goldfish, a stenohaline freshwater (FW) fish that cannot tolerate high environmental salt concentrations, and (2) utilize the in vitro model to expand our understanding of molecular mechanisms (e.g. alterations in occludin) that may

contribute to changes in the permeability of the goldfish gill epithelium.

Materials and methods

Animals

Goldfish (*Carassius auratus*, 20–40 g) were obtained from a local supplier (Aleongs International, Mississauga, ON, Canada) and held at $25 \pm 1^\circ\text{C}$ in 200-L opaque polyethylene tanks supplied with flow-through dechlorinated FW (approximate composition in mM: $[\text{Na}^+]$ 0.59, $[\text{Cl}^-]$ 0.92, $[\text{Ca}^{2+}]$ 0.76, $[\text{K}^+]$ 0.43, pH 7.35. Fish were fed ad libitum once daily with commercial koi and goldfish pellets (Martin Profishent, Elmira, ON, Canada) and held in these conditions for at least 3 weeks prior to use.

Preparation of a primary cultured goldfish gill epithelium

Methods for gill cell isolation and culture were conducted in a laminar flow hood using sterile techniques and were based on the procedures developed by Wood and Pärt (1997) for trout gill epithelia as described in detail by Kelly et al. (2000). However, procedures for the isolation and culture of gill cells from goldfish, as outlined in the following section, involve modifications in gill tissue trypsination time, cell seeding density, the use of collagen to enhance cell attachment in flasks, culture time in flasks as well as an increase in cell culture incubation temperature. More specifically, goldfish gill arches were collected and rinsed with phosphate-buffered saline (PBS, pH 7.7) at room temperature (RT). Branchial tissue was carefully removed from gill cartilage, cut into smaller pieces and washed (3×10 min) in ice-cold PBS containing 200 IU/mL penicillin, 200 $\mu\text{g}/\text{mL}$ streptomycin, 275 $\mu\text{g}/\text{mL}$ gentamicin and 2.5 $\mu\text{g}/\text{mL}$ fungizone. Gill cells were then isolated from gill filaments using three consecutive cycles of tryptic digestion (10 min each at 4°C ; 0.05% trypsin in PBS with 5.5 mM EDTA). At the end of each 10 min tryptic digestion, gill tissue was mechanically agitated by repetitively drawing the trypsin solution plus tissue up and down with a sterile plastic transfer pipette. Following mechanical agitation, the tissue slurry was placed on a 100 μm cell strainer so that isolated cells could filter through into ice-cold PBS containing 10% fetal bovine serum (FBS). The resulting gill cell suspension was subsequently centrifuged (10 min at $500 \times g$, 4°C) to form a pellet which was resuspended in ice-cold PBS containing 2.5% FBS. The resuspended cells were then centrifuged again (10 min at $500 \times g$, 4°C) and gently resuspended in Leibovitz's L-15 culture medium supplemented with 2 mM L-glutamine and

6% FBS (L15, pH 7.6–7.65). At this stage, antibiotics (100 IU/mL penicillin, 100 µg/mL streptomycin, and 50 µg/mL gentamicin) were also present in the L15 media. Gill cells were counted using a hemocytometer and seeded into culture flasks (BD Falcon™; BD Biosciences, Mississauga, ON, Canada) at a density of $0.24\text{--}0.28 \times 10^6$ cells/cm². To enhance the cell attachment, culture flasks were pre-coated with collagen (10 µg/cm² type I, rat tail; Sigma-Aldrich Canada Ltd., Oakville, ON, Canada). After 24 h incubation at 27°C in an air atmosphere, media was aspirated from flasks to remove non-adherent material, and temperature-equilibrated L15 plus antibiotics was added. After a further 24 h in culture, flasks were gently rinsed with ice-cold PBS and subjected to four consecutive rounds of tryptic digestion (1 min each at RT). After each 1 min trypsinization, ice-cold PBS was added to flasks which were then gently agitated to facilitate cell detachment. The resulting suspensions were poured into PBS containing FBS (10%). Cells were pelleted by centrifugation (8 min at $500 \times g$, 4°C), gently resuspended in L15 (minus antibiotics) and seeded onto permeable polyethylene terephthalate (PET) filters (0.9 cm² growth area; 0.4 µm pore size; 1.6×10^6 pore/cm² pore density) at the base of culture inserts (BD Falcon™) at a density of 0.7×10^6 cells/insert. Inserts were held in 12-well companion plates (BD Falcon™). Initially, inserts (apical side) and companion wells (basolateral side) contained 1 mL of L15 each. After incubation for a further 20–22 h, media was carefully aspirated from inserts and wells, and 1.5 and 2 mL of temperature-equilibrated L15 was added to apical and basolateral sides, respectively, (symmetrical conditions; L15/L15). Epithelia were held under symmetrical culture conditions until a stable transepithelial resistance (TER; see “Transepithelial resistance and [³H]PEG-4000 flux measurements”) developed. When the effects of asymmetrical (FW/L15) conditions were tested, temperature-equilibrated sterile dechlorinated FW was added to the apical side of the insert after several careful rinses to ensure removal of residual medium. The FW was sterilized by passing through a 0.2 µm filter (VWR International, Mississauga, ON, Canada) and was the same composition as the original holding water detailed previously.

Microscopy

Phase contrast microscopy

Gill epithelia cultured in flasks and inserts were routinely examined by phase contrast microscopy using a Leica inverted microscope. Phase contrast images were captured using a Leica DFC 420 camera and Leica Imaging Suite software (Leica Microsystems Inc., Richmond Hill, ON, Canada). Adobe Photoshop CS2 software was used for

contrast and brightness adjustment of entire images (Adobe Systems Canada, Toronto, ON, Canada).

Scanning and transmission electron microscopy

Goldfish gill arches and inserts containing cultured goldfish gill epithelia were briefly rinsed with PBS and fixed in 2.5–3.5% glutaraldehyde in phosphate buffer (0.1 M, pH 7.2) at 4°C for 4 h. Following fixation, tissues were washed with phosphate buffer (2 × 10 min, RT) and post-fixed with 1% osmium tetroxide in phosphate buffer (2 h at RT). For scanning electron microscopy (SEM) studies, filaments and epithelia were dehydrated in a graded acetone series (30–100%), dried with tetramethylsilane and mounted on aluminum stubs using double-sided non-conductive tape. Mounted tissues were then sputter coated (Hummer VI Au/Pd 40/60; Anatech USA, Orange, MA, USA) and examined using a Hitachi S-520 scanning electron microscope (Hitachi High-Technologies Canada, Inc., Toronto, ON, Canada). SEM images were captured using Quartz PCI Version 6 image capture system (Quartz Imaging Corporation, Vancouver, BC, Canada).

For transmission electron microscopy (TEM) studies, epithelia were dehydrated in a graded ethanol series (50–100%) and embedded in Spurr's resin. Thin sections (50 nm) were cut using an ultramicrotome, mounted on copper grids, stained with 2% uranyl acetate (20 min at 60°C) and Reynold's lead citrate (at RT), respectively, and examined using a Philips EM 201 transmission electron microscope (Philips, Eindhoven, NB, Netherlands). For both SEM and TEM images, Adobe Photoshop CS2 software was used for contrast and brightness adjustment of entire images (Adobe Systems Canada).

Immunocytochemistry and immunohistochemistry

Goldfish gill epithelia cultured in inserts were briefly rinsed with PBS and fixed with 3% paraformaldehyde (20 min at RT). To examine for the presence of MRCs, several randomly selected inserts were pre-stained with the mitochondria specific dye, Mitotracker[®] Deep Red FM (100 nM in L15 for 45 min, 27°C; Invitrogen Canada Inc., Burlington, ON, Canada) prior to fixation. Fixed epithelia were then permeabilized with ice-cold methanol (5 min at –20°C), washed with 0.01% Triton X-100 in PBS (10 min at RT) and blocked with antibody dilution buffer (ADB; 10% goat serum, 3% BSA and 0.05% Triton X-100 in PBS; 1 h at RT). Epithelia were subsequently incubated overnight at RT with a rabbit polyclonal anti-occludin antibody (1:100 dilution in ADB; Zymed Laboratories, Inc., South San Francisco, CA, USA) and mouse monoclonal anti-Na⁺/K⁺-ATPase α-subunit (NKA) antibody (α5, 1:10 in ADB; Developmental Studies Hybridoma Bank, Iowa City,

IA, USA). As negative controls, several inserts were also incubated overnight with ADB alone (primary antibodies omitted). After washing with PBS (3 × 5 min at RT), epithelia were incubated (1 h at RT) with TRITC-labeled goat-anti-rabbit and FITC-labeled goat anti-mouse antibodies (1:500 in ADB each; Jackson ImmunoResearch Laboratories Inc., West Grove, PA, USA). Epithelia were washed with PBS once more (3 × 5 min at RT) and then filters were excised from insert housings and mounted on slides with Molecular Probes ProLong Antifade (Invitrogen Canada Inc.) containing 5 µg/mL DAPI. Mitotracker® staining was examined using a Nikon Eclipse Ti inverted microscope (Nikon Instruments Inc., Melville, NY, USA). Occludin and NKA immunolocalization were examined using a Reichert Polyvar microscope (Reichert Microscope Services, Depew, NY, USA) and an Olympus DP70 camera (Olympus Canada, Markham, ON, Canada). Immunohistochemical analysis of NKA in goldfish gill tissue was conducted according to the procedures outlined by Chasiotis and Kelly (2008). Adobe Photoshop CS2 software was used for contrast and brightness adjustment of entire images (Adobe Systems Canada).

Transepithelial resistance and [³H]PEG-4000 flux measurements

TER was measured using chopstick electrodes (STX-2) connected to an EVOM epithelial voltohmmeter (World Precision Instruments, Sarasota, FL, USA). All TER measurements are expressed as Ωcm² and background-corrected for TER measured across blank inserts bathed in appropriate solutions. Paracellular permeability across cultured epithelia was determined using the paracellular marker, [³H] polyethylene glycol (molecular mass 4000 Da; PEG-4000; PerkinElmer, Woodbridge, ON, Canada) according to the methods and calculations previously outlined by Wood et al. (1998). Briefly, [³H]PEG-4000 flux from the basolateral to apical compartment was monitored at appropriate time intervals after the addition of 1 µCi of [³H]PEG-4000 to basolateral culture medium. All flux measurements are expressed as a function of time and epithelial surface area.

Cloning of goldfish occludin cDNA

Total RNA was isolated from goldfish gill tissue using TRIzol® Reagent (Invitrogen Canada Inc.) according to the manufacturer's instructions. Gill RNA was then treated with DNase I (Amplification Grade; Invitrogen Canada Inc.) and first-strand cDNA was synthesized using SuperScript™ III Reverse Transcriptase and Oligo(dT)_{12–18} primers (Invitrogen Canada Inc.). Based on highly

conserved regions of zebrafish (NM_212832) and rainbow trout (NM_001190446) occludin coding sequences (as determined by a ClustalX multiple sequence alignment), degenerate primers were designed and used to amplify a partial goldfish occludin cDNA fragment by reverse transcriptase PCR (RT-PCR). The following reaction conditions were utilized: 1 cycle of denaturation (95°C, 4 min), 40 cycles of denaturation (95°C, 30 s), annealing (53°C, 30 s) and extension (72°C, 30 s), respectively, final single extension cycle (72°C, 5 min) (0.2 µM dNTP, 2 µM forward and reverse primers, 1× Taq DNA polymerase buffer, 1.5 mM MgCl₂ and 1 IU Taq DNA polymerase) (Invitrogen Canada Inc.). Gel electrophoresis (1% agarose) verified a PCR product at the predicted amplicon size. The putative occludin fragment was then excised, purified using a QIAquick Gel Extraction Kit (QIAGEN Inc., Mississauga, ON, Canada) and sequenced in the York University Core Molecular Biology and DNA Sequencing Facility (Department of Biology, York University, ON, Canada). A partial coding sequence (CDS) of goldfish occludin was confirmed using a Basic Local Alignment Search Tool (BLAST) search. To obtain the complete goldfish occludin CDS, both 5'- and 3'-rapid amplification of cDNA ends (RACE) PCR was subsequently performed using a SMART™ RACE cDNA Amplification Kit (Clontech Laboratories Inc., Mountain View, CA, USA) according to the manufacturer's instructions. The GenBank accession number for goldfish occludin is HQ110086.

Quantitative real-time PCR analysis

Quantitative real-time PCR (qRT-PCR) was used to examine occludin mRNA distribution and abundance in discrete goldfish tissues, as well as occludin mRNA transcript abundance in cultured goldfish gill epithelia. For expression profile studies, total RNA was extracted from the following goldfish tissues: brain, eye, heart, gill, gastrointestinal (GI) tract, liver, gallbladder, spleen, swimbladder, kidney, skin, muscle, fat, and blood. Because the goldfish GI tract is not separated into morphologically distinct regions, the total length of the GI tract was measured and then dissected into eight equal segments. These segments were numbered as GI 1–GI 8 (anterior-most segment to posterior-most segment). RNA extraction and cDNA synthesis from all goldfish tissues and cultured gill epithelia were conducted as outlined above (see “Cloning of goldfish occludin cDNA”). Primers for goldfish occludin (forward: 5' CAACAGCACAACTACGACAAACC 3' and reverse: 5' CCACTTCAGCCAGACGCTTG 3', amplicon size ~356 bp) were designed based on the complete goldfish CDS. β-actin was used as an internal control and

β -actin primers (forward: 5' CTACGAGGGTTATGC TCTTC 3' and reverse: 5' ATTGAGTTGAAGGTG GTCTC 3', amplicon size ~351 bp) were designed based on GenBank accession number AB039726. qRT-PCR analysis of occludin and β -actin was conducted using SYBR Green I Supermix (Bio-Rad Laboratories Canada Ltd., Mississauga, ON, Canada) and a Chromo4™ Detection System (CFB-3240; Bio-Rad Laboratories Canada Ltd.) under the following conditions: 1 cycle denaturation (95°C, 4 min) followed by 40 cycles of denaturation (95°C, 30 s), annealing (60°C for occludin or 51°C for β -actin, 30 s) and extension (72°C, 30 s), respectively. Samples were run in duplicate and to ensure that a single PCR product was synthesized during reactions, a melting curve was carried out after each qRT-PCR run. For all qRT-PCR analyses, occludin mRNA abundance was normalized to β -actin abundance. For the occludin expression profile, occludin mRNA abundance in goldfish tissues was expressed relative to GI 1 which was assigned a value of 100. For epithelia exposed to asymmetrical culture conditions (12 and 24 h) as well as epithelia held under symmetrical control conditions at 24 h, occludin mRNA data are expressed relative to occludin abundance in symmetrical culture conditions at 12 h which was assigned a value of 100.

Western blotting

Cultured goldfish gill epithelia were processed in ice-cold lysis buffer (50 mM Tris-HCl, pH 7.5, 150 mM NaCl, 1% sodium deoxycholate, 1% Triton X-100, 0.1% SDS, 1 mM DTT, 1 mM EDTA, 1 mM PMSF) containing 1:200 protease inhibitor cocktail (Sigma-Aldrich Canada Ltd.) by repeatedly passing through a 26G needle. Homogenates were then centrifuged (20 min at 20,000×g, 4°C). Following centrifugation, the supernatants were collected and protein concentration was determined using the Bradford assay (Sigma-Aldrich Canada Ltd.). Western blot analysis of occludin and β -actin was conducted according to procedures outlined by Chasiotis and Kelly (2008) using 10 μ g of protein from each insert sampled, a 1:1,000 dilution of a rabbit polyclonal anti-occludin antibody (Zymed Laboratories, Inc.) and a 1:20,000 dilution of mouse monoclonal anti- β -actin antibody (Sigma-Aldrich Canada Ltd.). Occludin and β -actin abundance was quantified using a Molecular Imager Gel Doc XR+ System and Quantity One 1D analysis software (Bio-Rad Laboratories Canada Ltd.). Occludin protein abundance is expressed as a normalized value relative to β -actin abundance. Occludin protein abundance in epithelia exposed to FW/L15 conditions is expressed relative to occludin protein abundance in epithelia held under symmetrical control conditions which was assigned a value of 100.

Statistical analysis

All data are expressed as mean values \pm SEM (n), where n represents the number of inserts, except in Fig. 4, where n represents the number of fish sampled. A one-way or two-way analysis of variance (ANOVA) followed by a Student–Newman–Keuls test was used to determine significant differences ($P \leq 0.05$) between the groups. When appropriate, a Student's t test was also used. All statistical analyses were conducted using SigmaStat 3.5 Software (Systat Software Inc., San Jose, CA, USA).

Results

Characterization of primary cultured goldfish gill epithelia

General epithelial morphology

When enzymatically isolated gill cells were seeded into uncoated cell culture flasks, cell attachment was rare and those cells that did attach did not proliferate (i.e. detached within 2–3 days in culture). Pre-coating flasks with collagen enhanced cell attachment and survival (see Fig. 1a, b). Cell seeding densities of $0.24\text{--}0.28 \times 10^6$ cells/cm² yielded flasks that were ~50–70% confluent after 24 h (Fig. 1a). A further 24 h in culture resulted in flasks that were ~85–100% confluent (Fig. 1b). During culture in flasks, most cells exhibit an irregular and elongated morphology, however, colonies of cells with a more rounded appearance were also observed. When harvested from collagen-coated flasks, gill cells readily attach to the surface of PET filters in culture inserts and achieve 100% confluence within 6–8 h. Approximately 36–42 h after seeding gill cells in inserts, preparations exhibit a typical epithelial morphology. More specifically, cultured cells take on a flattened polygonal morphology with well-defined intercellular junctions (see Fig. 1c, d). When viewed at higher magnification, the apical surfaces of cultured gill cells exhibit occasional microvilli and prominent microridges (Fig. 1e, f, h). These structures are characteristic of goldfish gill PVCs as seen in vivo (Fig. 1g). MRC apical openings observed in vivo by SEM were not observed in cultured gill epithelia in vitro (Fig. 1e, g).

TEM sections demonstrated that cultured goldfish epithelia were typically composed of 1–2 (occasionally 3) overlapping cell layers (e.g. Fig. 1h). Furthermore, epithelia exhibited TJs between cells on the apical surface cell layer, desmosomes near the apical surface as well as between cell layers, few mitochondria and abundant rough endoplasmic reticulum (Fig. 1h, i).

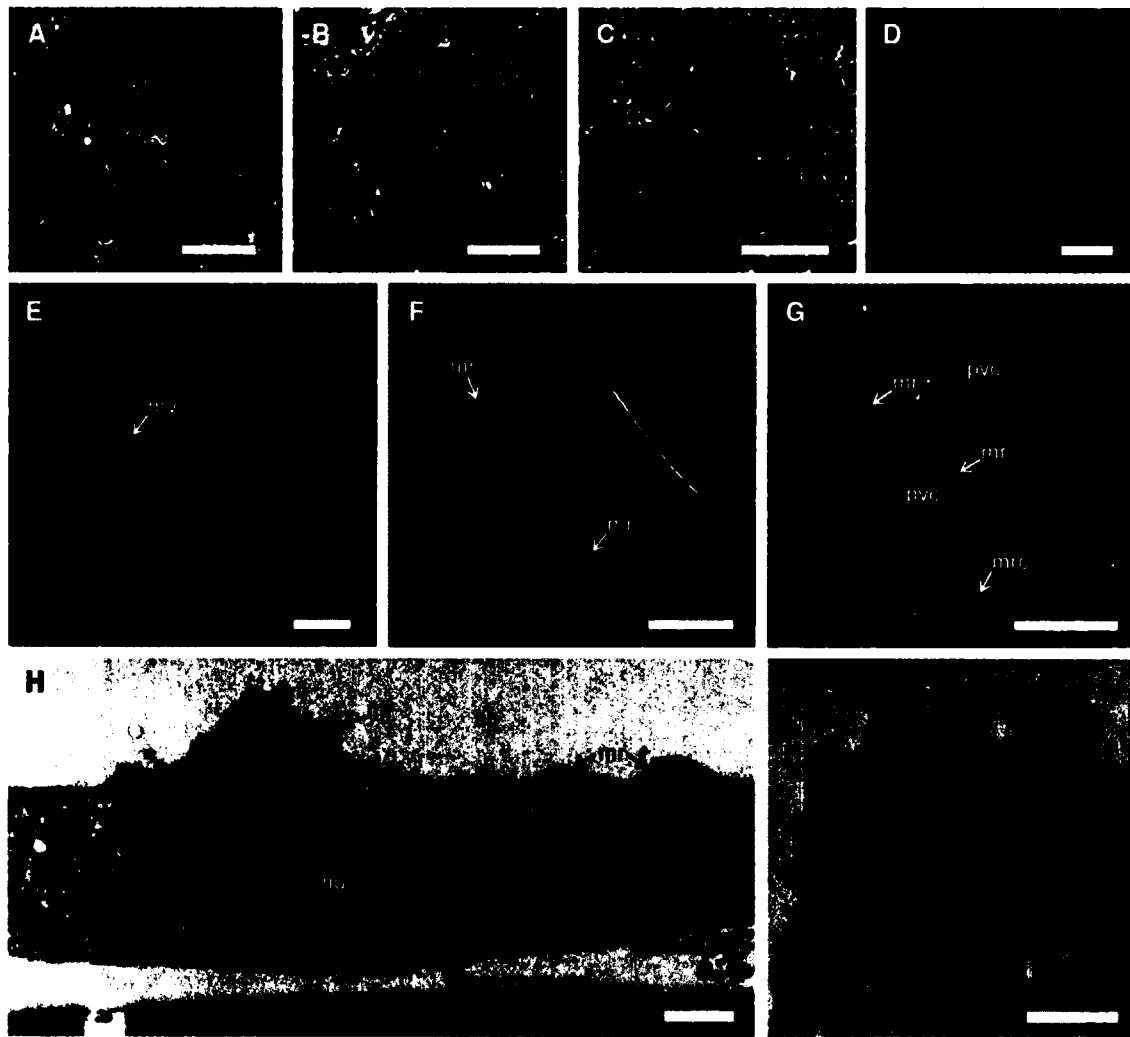


Fig. 1 Phase contrast micrographs of cultured goldfish gill cells at **a** 24 h post-seeding in flasks, **b** 48 h post-seeding in flasks, and **c**, **d** 48 h post-seeding in culture inserts under symmetrical (L15/L15) conditions. Scanning electron microscopy (SEM) images of the apical surfaces of **(e, f)** a cultured goldfish gill epithelium at 48 h post-seeding in inserts under L15/L15 conditions, and **g** a goldfish gill filament. **h, i** Transmission electron microscopy (TEM) images of a

cultured goldfish gill epithelium at 48 h post-seeding in culture inserts under L15/L15 conditions. *mv* microvilli, *mr* microridge, *pvc* pavement cell, *mrc* mitochondria-rich cell, *ap* apical surface, *tj* tight junction, *nu* nucleus, *pet* polyethylene terephthalate filter, *ds* desmosome, *rer* rough endoplasmic reticulum. Scale bars **a,b,c** 100 μm, **d** 20 μm, **e,f,g** 10 μm, **h** 1 μm, **i** 500 nm

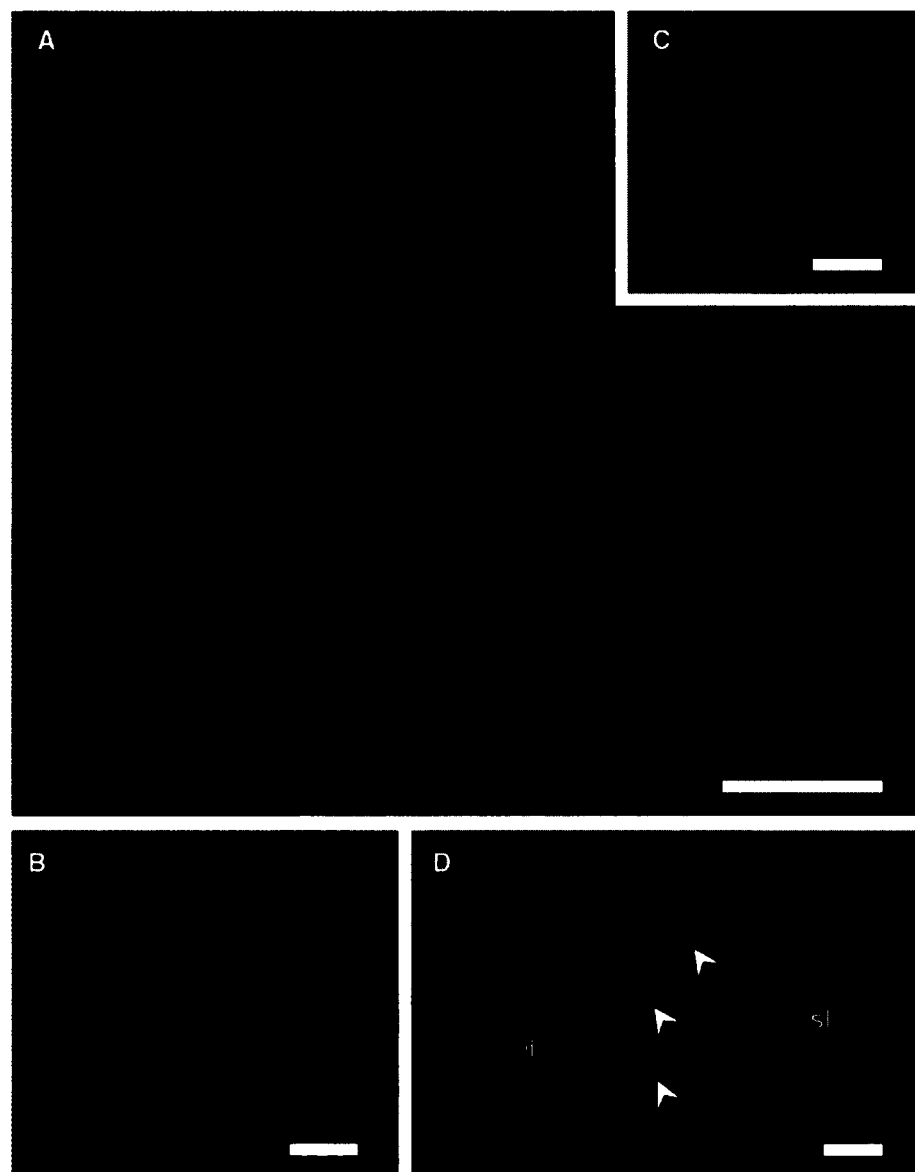
Immunocytological analysis

Occludin immunostaining was observed at intercellular junctions along the borders of adjacent cultured gill cells (Fig. 2a). NKA immunostaining was absent in cultured gill preparations (Fig. 2b). Occludin immunostaining was absent in negative control preparations (i.e. primary antibody omitted) (Fig. 2c). As a positive control, robust NKA immunoreactivity could be observed in putative MRCs in vivo (Fig. 2d). Consistent with TEM images, live and fixed cultured goldfish gill epithelia pre-treated with Mitotracker[®] showed no appreciable mitochondrial staining (data not shown).

Transepithelial resistance

Goldfish gill epithelia cultured under symmetrical (L15/L15) conditions exhibit a sigmoidal increase in TER over time (Fig. 3a). TER typically plateaus 36–42 h after seeding cells in inserts and this corresponds with the appearance of a more distinct epithelial-like morphology with well-defined intercellular junctions (see “General epithelial morphology”; Fig. 1c, d). The plateau in TER that cultured goldfish gill epithelia exhibit has proven to be quite consistent between fish. Based on 331 inserts generated from 41 goldfish, TER stabilizes at $1,150 \pm 46 \Omega\text{cm}^2$ ($n = 41$) and these levels are maintained for at least 30 h

Fig. 2 Immunolocalization of **a** occludin (red) and **b** Na^+/K^+ -ATPase (NKA, green) in a cultured goldfish gill epithelium at 48 h post-seeding in a culture insert under symmetrical (L15/L15) conditions. Note that no NKA immunostaining is observed in cultured goldfish gill epithelia. A negative control for occludin immunoreactivity (primary antibody omitted) is shown in (c). Putative mitochondria-rich cell localization (arrowheads) via NKA immunostaining in goldfish gill tissue is also shown in (d). *il* interlamellar region of a primary gill filament, *sl* secondary lamellae. Scale bars 20 μm



(data not shown). Goldfish gill epithelia were also tolerant of asymmetrical (FW/L15) conditions. Abrupt apical FW exposure resulted in a significant increase in TER (to more than sevenfold pre-exposure values) within 0.5 h. TER then decreased sharply after 1 h (to \sim fourfold initial values) and remained stable for at least another 2 h (Fig. 3b). Upon restoration of symmetrical conditions, TER significantly dropped below pre-exposure values, but then steadily (after 1 h) recovered to pre-exposure values where it remained stable for at least a further 2 h (Fig. 3b).

Cloning of goldfish occludin cDNA and occludin mRNA tissue expression profile

Cloning and sequence analysis of the 1,503-bp protein coding region for goldfish occludin revealed an open

reading frame for a 500-amino acid protein with a molecular weight of \sim 56 kDa. Goldfish occludin exhibited \sim 89% amino acid sequence similarity (identical matches plus mismatches with similar amino acids) with zebrafish occludin (GenBank accession number NP_997997), \sim 75% similarity with rainbow trout occludin (NP_001177375) and 58–61% similarity with mammalian occludin (i.e. human [NP_002529], mouse [NP_032782], rat [NP_112619], dog [NP_001003195], pig [NP_001157119] and cow [NP_001075902]). Using qRT-PCR to measure transcript abundance, occludin mRNA was found to be widely expressed in discrete goldfish tissues (Fig. 4). Transcript abundance was highest in the gill, followed by the gallbladder, kidney, and skin. Transcript was absent from the heart, spleen, muscle and blood (Fig. 4).

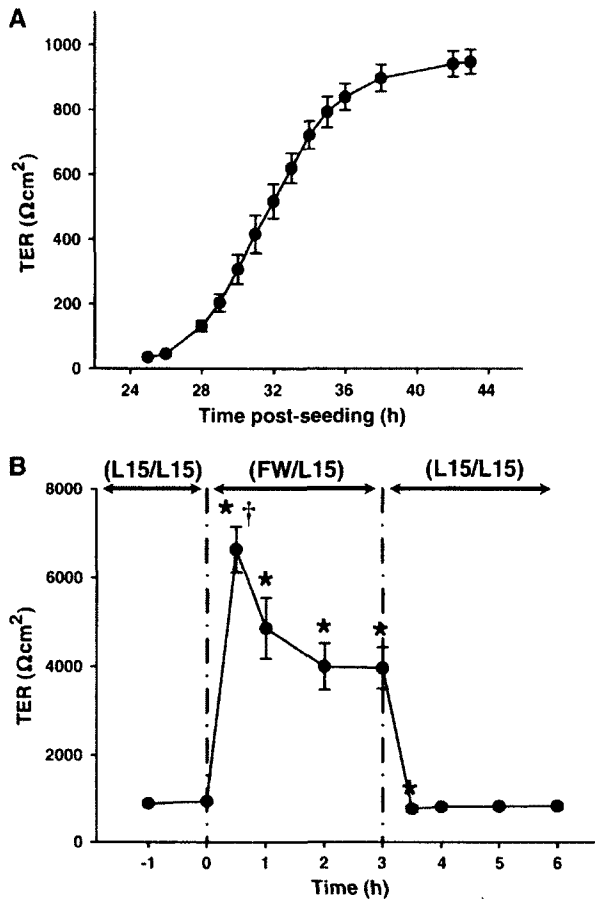


Fig. 3 **a** Changes in transepithelial resistance (TER) of cultured goldfish gill epithelia post-seeding in culture inserts. Epithelia were cultured under symmetrical (L15/L15) conditions. **b** The effect of short-term (3 h) asymmetrical (FW/L15) conditions and subsequent recovery under L15/L15 on the TER of goldfish gill epithelia cultured in inserts. Data are expressed as mean values \pm SEM ($n = 6$). *Significant difference ($P \leq 0.05$) from pre-FW exposure values; †significant difference ($P \leq 0.05$) from all other FW exposure values

Effects of 24 h exposure to asymmetrical culture conditions on cultured gill epithelia

TER and [³H]PEG-4000 flux

When exposed to asymmetrical culture conditions (i.e. FW apical/L15 basolateral) for a period of 24 h, TER initially exhibited a rapid and significant increase that was relatively stable for the first few hours of the exposure period (Fig. 5a). These were consistent with changes in TER previously observed during short-term exposure to asymmetrical culture conditions (see “Transepithelial resistance”). Following this early response, TER remained significantly elevated throughout the entire course of the 24-h asymmetrical experiment (Fig. 5a). However,

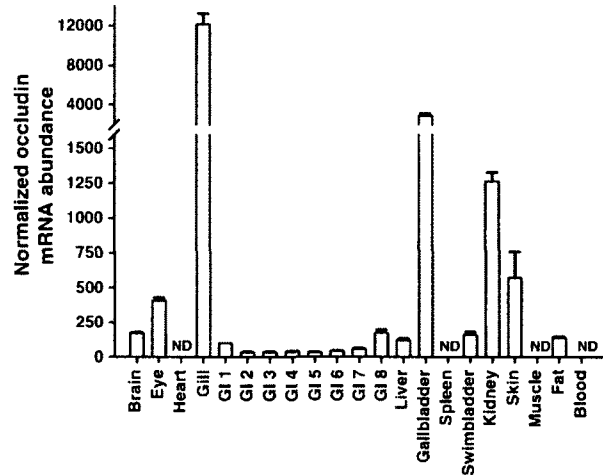


Fig. 4 Occludin mRNA expression profile for discrete goldfish tissues as generated by qRT-PCR. Occludin mRNA abundance was normalized to β -actin abundance. Occludin mRNA abundance in each goldfish tissue was expressed relative to GI 1 which was assigned a value of 100. Data are expressed as mean values \pm SEM ($n = 3-4$). ND not detected

although TER remained significantly elevated relative to L15/L15 preparations throughout the duration of the experiment, TER exhibited a gradual decline that was greater during the 3–12 h post-FW exposure period ($\sim 32\%$ reduction) than during the 12–24 h post-FW exposure period ($\sim 14\%$ decline) (Fig. 5a).

[³H]PEG-4000 permeability significantly elevated in response to asymmetrical culture conditions. [³H]PEG-4000 flux exhibited an ~ 27 and $\sim 48\%$ increase relative to control epithelia during the 6–12 h and 18–24 h flux periods, respectively (Fig. 5b). Cultured epithelia were routinely examined by phase contrast microscopy throughout the 24-h asymmetrical experiment and no signs of significant morphological change or epithelial deterioration were observed. Within a treatment group (i.e. L15/L15 or FW/L15), TER across epithelia 24 h following the start of the experiment was moderately but significantly lower than TER measurements recorded at 12 h (Fig. 6a).

Occludin mRNA and protein abundance

The introduction of asymmetrical (FW/L15) conditions had no significant effect on occludin mRNA abundance in cultured goldfish gill epithelia relative to control L15/L15 preparations (Fig. 6b). Transcript abundance, however, was significantly altered over time regardless of culture conditions. Samples (both symmetrical and asymmetrical) collected at the 24-h time point exhibited significantly lower levels of occludin mRNA when compared to samples

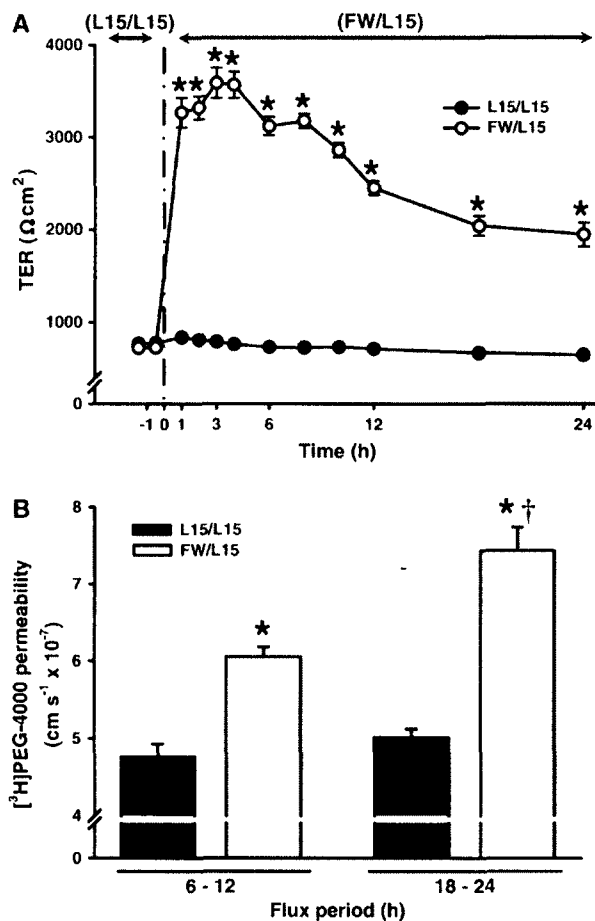


Fig. 5 Effect of long-term (24 h) asymmetrical (FW/L15) conditions on **a** transepithelial resistance (TER) and **b** [^3H]PEG-4000 permeability across goldfish gill epithelia cultured in inserts. [^3H]PEG-4000 fluxes were conducted over 6 h periods between 6–12 and 18–24 h post-FW exposure. Data are expressed as mean values \pm SEM ($n = 6$ –12). *Significant difference ($P \leq 0.05$) between L15/L15 and FW/L15 groups at the same time point or within the same flux period; †significant difference ($P \leq 0.05$) from the FW/L15 group within the 6–12 h flux period

collected at 12 h (Fig. 6b). Neither asymmetrical conditions nor time significantly altered ($P > 0.05$) β -actin mRNA abundance. Conversely, protein abundance of the 68 kDa occludin form was marginally but significantly elevated by 24-h apical FW exposure relative to control L15/L15 preparations (Fig. 6c). By western blot analysis, both L15/L15 and FW/L15 cultured gill epithelia expressed the dominant 68 kDa form of occludin, however, FW/L15 cultured epithelia also exhibited three additional occludin-immunoreactive bands which resolved at ~ 60 , 56 and 35 kDa, respectively (Fig. 6d). β -actin protein resolved at ~ 42 kDa and its abundance was not significantly altered ($P > 0.05$) by apical FW exposure (Fig. 6e).

Discussion

General characterization of primary cultured goldfish gill epithelia

Cultured goldfish gill epithelia appear to be composed exclusively of PVCs. More specifically, electron microscopy demonstrated that cultured goldfish gill preparations comprise cells which exhibit morphological characteristics typical of PVCs. These cells are polygonal, squamous, and possess apical surface microridges identical to those observed in goldfish gill PVCs in vivo (Fig. 1e–h). The cells also possess few mitochondria and abundant rough endoplasmic reticulum. In addition to these morphological observations, immunocytochemistry results indicated that cultured goldfish gill epithelia did not possess any cells exhibiting robust NKA-immunoreactivity or Mitotracker[®] staining. Both NKA-immunoreactivity and staining with a mitochondrial dye such as Mitotracker[®] are reliable markers of MRC presence in fish gill epithelia (see Fig. 2d; Chasiotis and Kelly 2008; Mitrovic and Perry 2009). The observations made of goldfish epithelia in this study are consistent with the morphological characteristics of other cultured PVC epithelia generated from species such as the sea bass (Avella and Ehrenfeld 1997), rainbow trout (Wood and Pärt 1997) and tilapia (Kelly and Wood 2002). It remains to be determined whether isolated goldfish gill cells can be used to generate double seeded insert (DSI) epithelia containing MRCs (see Fletcher et al. 2000). In this regard, preliminary attempts to generate single direct seeded inserts (SDSI; see Wood et al. 2003) using freshly isolated goldfish gills cells were not successful.

Approximately 24 h after seeding cells in inserts, and over a period of ~ 14 h (i.e. ~ 24 –38 h post-seeding; see Fig. 3a), goldfish gill epithelia exhibit a sigmoidal increase in TER. The development of a sigmoidal TER curve is characteristic of many epithelia in culture including PVC epithelial preparations from rainbow trout (Wood and Pärt 1997; Kelly et al. 2000) and tilapia (Kelly and Wood 2002). However, in trout and tilapia preparations, the development of a stable plateau in TER usually takes days rather than hours (see Wood and Pärt 1997; Kelly et al. 2000; Kelly and Wood 2002). This observed difference in time taken to develop a stable plateau in TER (i.e. ~ 36 –42 h for goldfish versus 5–7 days for rainbow trout and tilapia preparations) is consistent with the general observation that development rates exhibited by cultured goldfish gill preparations were much faster than those demonstrated by cultured rainbow trout and tilapia gill models. For example, cultured goldfish gill cells were ready to be harvested and seeded into inserts following 2 days of culture in flasks (Fig. 1a, b) versus 4–5 days flask culture for cultured rainbow trout and tilapia gill cells

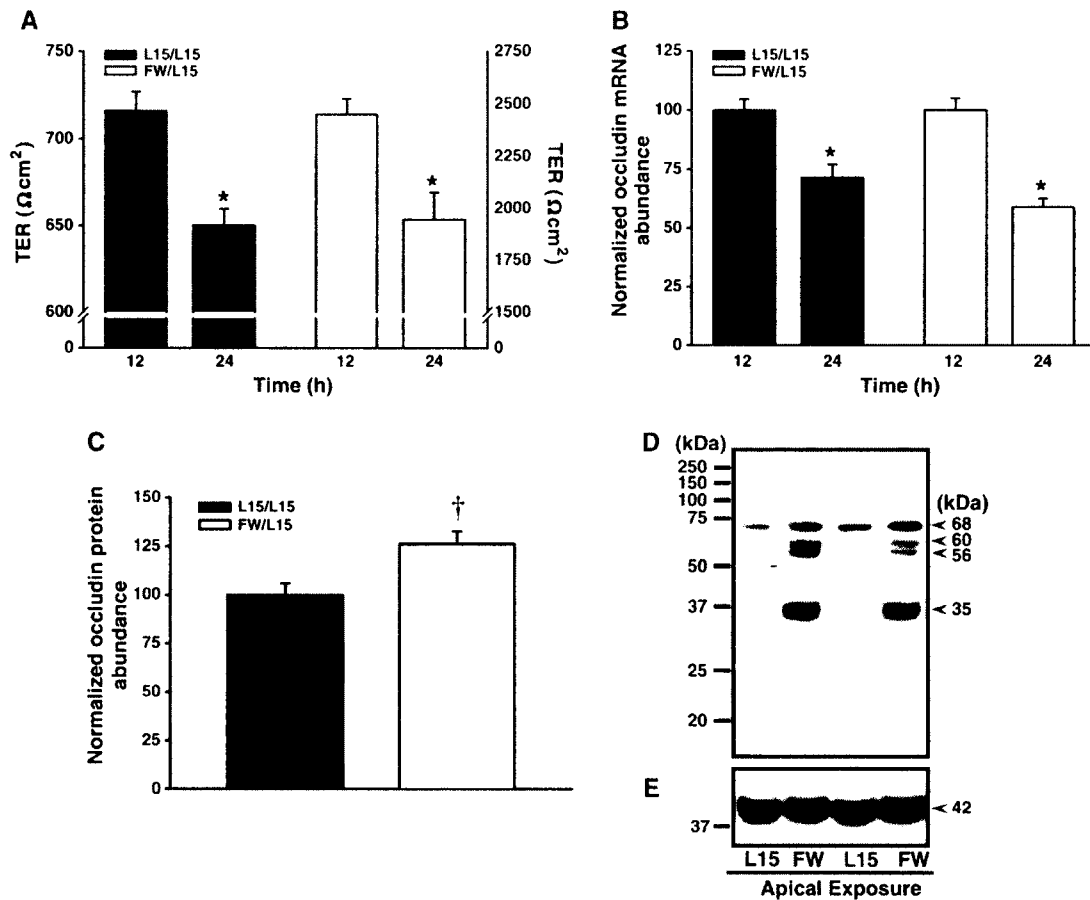


Fig. 6 Effect of long-term asymmetrical (FW/L15) culture conditions on **a** TER, **b** occludin mRNA abundance and **c** occludin protein abundance in primary cultured goldfish gill epithelia. Representative western blots of **d** occludin and **e** β -actin from cultured goldfish gill epithelia exposed to L15/L15 or FW/L15 conditions are shown. Note that occludin-immunoreactive bands resolve at \sim 60, 56 and 35 kDa in the FW/L15 cultured epithelia in addition to the dominant \sim 68 kDa form expressed by L15/L15 cultured epithelia. Plate **(c)** illustrates the quantification of the 68 kDa form of occludin shown in **(d)**. mRNA samples were collected at 12 and 24 h, and

protein samples were collected 24 h post-FW exposure. Occludin mRNA or protein abundance was normalized to β -actin mRNA or protein abundance, respectively. All occludin mRNA data are expressed relative to occludin mRNA abundance in epithelia held under L15/L15 conditions at 12 h which was assigned a value of 100. Data are expressed as mean values \pm SEM ($n = 6-8$). *Significant difference ($P \leq 0.05$) from the 12 h sampling point within the same treatment group (L15/L15 or FW/L15); †significant difference ($P \leq 0.05$) from the L15/L15 group

(Kelly et al. 2000; Kelly and Wood 2002). However, goldfish preparations maintain a stable TER for less time after plateau (usually \sim 30 h; data not shown) than rainbow trout preparations (several days; Wood and Pärt 1997; Kelly and Wood 2001). Therefore, although the accelerated development of cultured goldfish gill epithelia can save a considerable amount of time when compared to other in vitro FW fish gill models, the optimal experimental time window for conducting analyses may be shortened. The differences observed in the development of epithelia and duration of culture could be species specific but may also be influenced by factors such as difference in culture incubation temperature (e.g. 18–20°C for trout and tilapia versus 27°C for goldfish). However, primary cultured gill epithelia generated from euryhaline puffer fish (*Tetraodon*

nigroviridis) are also incubated at 27°C and develop a stable TER following 5–7 days in culture (Bui and Kelly, unpublished observations). Therefore, despite temperature differences, cultured puffer fish gill epithelia develop in a manner similar to cultured rainbow trout and tilapia preparations. This strongly supports the idea that species specific differences could play an important role in the physiological diversity of cultured gill epithelia.

Irrespective of time taken to develop, the sigmoidal TER curve can be attributed to the gradual formation of TJs between cells which limit the paracellular electrical conductance across an epithelium (Cerejido et al. 1981). In this regard, a positive linear relationship between [³H]PEG-4000 flux (a measurement of paracellular permeability and thus TJ 'tightness') and epithelial

conductance (inverse of TER) across cultured rainbow trout preparations has previously been demonstrated by Wood et al. (1998). TER across cultured goldfish gill epithelia stabilizes at $\sim 1,150 \Omega\text{cm}^2$ and this value falls within the range of stable resistance measurements reported for other gill PVC epithelial preparations derived from fish held in FW such as rainbow trout (1,000–5,000 Ωcm^2 , Kelly et al. 2000) and tilapia (1,000–3,000 Ωcm^2 , Kelly and Wood 2002). In addition, a value of $\sim 1,150 \Omega\text{cm}^2$ in the current study is also very similar to the TER across a PVC-rich opercular epithelium isolated from FW brook trout (i.e. $\sim 1,170 \Omega\text{cm}^2$) as reported by Marshall (1985). It is also of interest to note that in cultured goldfish epithelia, an increase and plateau in TER occurs in conjunction with the appearance of well-defined intercellular junctions between cultured cells (Fig. 1c, d, h, i). This provides a convenient tool for visually monitoring the development of cultured goldfish gill epithelia (i.e. a morphological indicator of TER development and electrophysiological integrity) and also provides further support for a correlation between TJ assembly and TER development as discussed previously.

Goldfish occludin mRNA distribution and protein immunolocalization

Occludin is a transmembrane TJ protein that contributes significantly to TJ barrier function and thus the permeability of the paracellular pathway across an epithelium (for review see Feldman et al. 2005). Occludin mRNA is widely expressed in goldfish tissues and is particularly abundant in the gill as well as other tissues involved in the maintenance of hydromineral balance (i.e. kidney and skin; see Fig. 4). Broad occludin distribution and high levels of mRNA in gill tissue have also recently been described in rainbow trout (Chasiotis et al. 2010) and the widespread presence of occludin has additionally been demonstrated in other non-aquatic vertebrate species (Saitou et al. 1997; Feldman et al. 2005). With regard to gill tissue, a recent study has reported that occludin immunolocalizes to areas of cell-to-cell contact (presumably PVCs-PVCs and PVCs-MRCs) in the gill epithelium of the goldfish (Chasiotis and Kelly 2008). Therefore, observations in the current study that reveal occludin immunostaining restricted quite distinctly to intercellular junctions along the borders of adjacent polygonal PVCs in a cultured goldfish gill model confirm that occludin does indeed localize between goldfish gill PVCs at least. This pattern of localization in vitro is consistent with observations of occludin immunostaining in various vertebrate epithelial cell lines (e.g. McCarthy et al. 1996; Wong and Gumbiner 1997; Finamore et al. 2008; Benedicto et al. 2009; Vermeer et al. 2009). Furthermore, these observations are also consistent with a

recent report on occludin immunolocalization between PVCs in a cultured trout gill epithelium (Chasiotis et al. 2010). However, a particular advantage of the cultured goldfish gill model pertains to the observations of Chasiotis and Kelly (2008) who report that in addition to localizing to the gill epithelium, occludin also localizes to the goldfish gill capillary endothelium. In the currently described culture preparation, there is no capillary endothelium. Therefore, alterations in molecular factors that may play a role in the regulation of gill permeability, such as occludin, can be examined in the absence of any contribution from the vasculature.

In contrast to the abundance of occludin mRNA in osmoregulatory tissues such as the gill and kidney, occludin mRNA abundance was relatively low along the GI tract of goldfish (see Fig. 4). However, TER measurements across the goldfish intestine suggest that this is not a tight epithelium (i.e. $\sim 24 \Omega\text{cm}^2$; Siegenbeek van Heukelom et al. 1982). Therefore, low levels of occludin transcript may be expected.

Effects of asymmetrical conditions

Measurements of epithelial permeability

Conditions that occur in vivo were mimicked in vitro by introducing FW to the apical side of the cultured goldfish gill epithelium. Exposure to apical FW resulted in a sharp increase in TER (Figs. 3b, 5a). This type of response to apical FW exposure has previously been noted in other cultured gill epithelia (Wood and Pärt 1997; Kelly and Wood 2002), as well as opercular epithelia isolated from a FW fish (Marshall 1985). In cultured trout gill epithelia, elevated TER in response to apical FW exposure appears to predominantly reflect decreased transcellular permeability since it occurs in conjunction with a paradoxical increase in paracellular permeability (i.e. increased [^3H]PEG-4000 flux; see Wood et al. 1998). This is not the case in cultured tilapia gill epithelia which exhibit both an increase in TER and decrease in [^3H]PEG-4000 upon apical FW exposure (Kelly and Wood 2002). Consistent with the response of cultured trout gill epithelia, cultured goldfish gill preparations exhibit an increase in [^3H]PEG-4000 flux when FW is present on the apical side of the epithelium (Fig. 5b). Therefore, it seems likely that elevated TER in goldfish gill epithelia also primarily reflects changes in transcellular permeability since the paracellular pathway becomes 'leakier' to [^3H]PEG-4000 movement.

TER across goldfish gill preparations exhibited a gradual decline during prolonged apical FW exposure and this has also been observed in cultured rainbow trout and tilapia gill epithelia (Fig. 5a; Kelly and Wood 2001, 2002). Taking into account that [^3H]PEG-4000 flux elevates even

further during long-term (24 h) asymmetrical culture (Fig. 5b), it is possible that the increasingly 'leaky' paracellular barrier properties of the preparation may contribute to the gradual decline in TER, although to what extent remains unclear.

Occludin mRNA and protein abundance

Recent studies have reported that occludin abundance alters in the gill tissue of goldfish under conditions where hydromineral status is challenged (Chasiotis and Kelly 2008; Chasiotis et al. 2009). However, alterations in occludin abundance have yet to be reported in conjunction with measured changes in epithelial permeability in goldfish. Therefore, to gain insight into the potential contribution of occludin to alterations in cultured goldfish gill permeability characteristics, occludin abundance was examined following the introduction of asymmetrical culture conditions (see Fig. 6). Exposure to asymmetrical culture conditions for 12 or 24 h had no significant effect on occludin mRNA abundance relative to control preparations held under symmetrical conditions (Fig. 6b). This occurred despite a significant increase in paracellular permeability (Fig. 5b). These observations are consistent with unaltered occludin mRNA levels in cultured rainbow trout gill epithelia exposed to asymmetrical culture conditions which also exhibited an increase in paracellular permeability (Chasiotis et al. 2010). Of interest, however, was a significant decline in occludin mRNA abundance in both symmetrical and asymmetrical epithelia 24 h following the start of the experiment (see Fig. 6b). This data correspond with reductions in TER between the 12 and 24-h time-points (Fig. 6a), and in the case of epithelia held under asymmetrical conditions, a reduction in occludin mRNA abundance also corresponds with an increase in paracellular permeability (see Figs. 5b, 6b). Although there is no significant difference in [³H]PEG-4000 flux between symmetrical epithelia at the 6–12 versus 18–24 h time points, it should be remembered that mRNA data are generated from tissue collected at the end of the flux period (i.e. at 12 or 24 h) and in this particular case, transcript abundance may not represent the entire 6 h flux period. Therefore, in cultured goldfish epithelia, occludin mRNA does not decline in association with an apical FW exposure-mediated increase in paracellular permeability, however, over time in culture, occludin mRNA does change in a manner that reflects changes in permeability. This temporal change most likely reflects the general decline in TER that can be observed in cultured epithelial preparations as the culture time progresses after TER plateau.

Despite no observable difference in transcript abundance upon exposure to asymmetrical culture conditions, western blot analysis was used to examine if any alterations

in protein abundance could be detected at 24 h. A slight but significant increase in occludin protein abundance was observed (i.e. 100 vs. 120; Fig. 6c) despite an absence of change at the transcript level. The physiological significance of this modest change is not clear and since it is not coupled with changes in mRNA, it could reflect differences in protein degradation rates. However, of far more interest were the changes observed in occludin-immunoreactive band position that took place under asymmetrical conditions. More specifically, under symmetrical culture conditions, occludin resolved as a 68 kDa band that was identical to the occludin-immunoreactive band found in the goldfish gill in vivo (see Chasiotis and Kelly 2008). However, under asymmetrical culture conditions, goldfish gill preparations were found to possess both the dominant 68 kDa (high molecular weight; HMW) form of occludin as well as three additional low molecular weight (LMW) occludin-immunoreactive bands at ~60, 56 and 35 kDa, respectively (Fig. 6d). Since apical FW exposure did not significantly alter occludin mRNA abundance in cultured goldfish gill epithelia (Fig. 6b), it is likely that the observed 60 and 56 kDa LMW immunoreactive bands reflect post-translational modifications of existing occludin protein. In this regard, multiple differentially phosphorylated forms of occludin, ranging from ~50–82 kDa have previously been detected by western blot in a variety of vertebrate epithelia, which upon treatment with phosphatases converge to LMW forms, thereby demonstrating that HMW forms of occludin are in fact hyperphosphorylated LMW forms (Sakakibara et al. 1997; Wong 1997; Feldman et al. 2005; Zeng et al. 2004). Furthermore, a growing body of research seems to indicate that occludin phosphorylation status may regulate TJ complex assembly and disassembly (reviewed by Rao 2009), whereby hyperphosphorylated HMW forms of occludin are recruited into TJ complexes to 'tighten' TJs, while dephosphorylation of occludin disrupts TJs by relocalizing resultant LMW forms out of the complex (Wong 1997). This general trend was clearly demonstrated in a human cervical epithelial cell line where estrogen-mediated reductions in TER closely correlated with a decrease in HMW occludin and simultaneous increase in LMW occludin in a time- and dose-dependent manner, and in the absence of a change in occludin mRNA abundance (Zeng et al. 2004). Therefore, the additional 60 and 56 kDa LMW forms of occludin and observed increase in [³H]PEG-4000 flux during the asymmetrical culture of goldfish gill epithelia (Figs. 5b, 6d) may involve a disruption in TJ integrity by occludin dephosphorylation. The significance of the 35 kDa LMW form of occludin (Fig. 6d) with respect to TJ barrier function is currently unclear, as its appearance cannot be attributed to dephosphorylation. But it should be noted that similar occludin-immunoreactive bands (i.e. 30–35 kDa) have previously been reported in other

epithelia (e.g. Wu et al. 2000; Minagar et al. 2003) and likely reflect protein degradation or some other uncharacterized post-translational modification.

Conclusion

To conclude, methodology for the primary culture of a goldfish gill epithelium composed exclusively of PVCs is described. Epithelia generate an appreciable TER under symmetrical culture conditions and tolerate exposure to FW. The physiological response of the cultured goldfish gill epithelium to asymmetrical culture conditions was qualitatively similar to responses previously reported for rainbow trout PVC cultures (Wood and Pärt 1997), and in this regard, no differences based on stenohalinity versus euryhalinity were obvious. In future studies, it will be interesting to examine if stenohaline versus euryhaline distinctions will become apparent when osmoregulatory hormones are introduced to cultured goldfish gill epithelial preparations. For example, it has recently been reported that occludin mRNA and protein abundance increase in response to cortisol treatment in the cultured gill epithelia from a euryhaline fish (i.e. rainbow trout, Chasiotis et al. 2010). Whether epithelia derived from a stenohaline fish, such as the goldfish, respond in a similar manner has yet to be determined. In addition, it will also be of interest to examine other proteins involved in the regulation of permeability in vertebrate epithelia such as the claudin family or cortical proteins such as ZO-1. This provides momentum for further study.

Acknowledgments This work was supported by an NSERC Discovery Grant, NSERC Discovery Accelerator Supplement, Canadian Foundation for Innovation New Opportunities Grant and a Petro Canada Young Innovator Award to SPK. HC was supported by an Ontario Graduate Scholarship. The monoclonal antibody developed by D.M. Fambrough ($\alpha 5$) was obtained from the Developmental Studies Hybridoma Bank developed under the auspices of the NICHD and maintained by The University of Iowa, Department of Biological Sciences, Iowa City, IA, 52242, USA. All procedures conformed to the guidelines of the Canadian Council of Animal Care. We also extend our thanks to Karen Rethoret for her technical assistance with the electron microscopy.

References

- Avella M, Ehrenfeld J (1997) Fish gill respiratory cells in culture: a new model for Cl^- secreting epithelia. *J Membr Biol* 156: 87–97
- Benedicto I, Molina-Jiménez F, Bartosch B, Cosset FL, Lavillette D, Prieto J, Moreno-Otero R, Valenzuela-Fernández A, Aldabe R, López-Cabrera M, Majano PL (2009) The tight junction-associated protein occludin is required for a postbinding step in hepatitis C virus entry and infection. *J Virol* 83:8012–8020
- Bui P, Bagherie-Lachidan M, Kelly SP (2010) Cortisol differentially alters claudin isoforms in cultured puffer fish gill epithelia. *Mol Cell Endocrinol* 317:120–126
- Cerejido M, Meza I, Martínez-Palomo A (1981) Occluding junctions in cultured epithelial monolayers. *Am J Physiol* 240:C96–C102
- Chasiotis H, Kelly SP (2008) Occludin immunolocalization and protein expression in goldfish. *J Exp Biol* 211:1524–1534
- Chasiotis H, Effendi J, Kelly SP (2009) Occludin expression in goldfish held in ion-poor water. *J Comp Physiol B* 179:145–154
- Chasiotis H, Wood CM, Kelly SP (2010) Cortisol reduces paracellular permeability and increases occludin abundance in cultured trout gill epithelia. *Mol Cell Endocrinol* 323:232–238
- Evans DH, Piermarini PM, Choe KP (2005) The multifunctional fish gill: dominant site of gas exchange, osmoregulation, acid-base regulation, and excretion of nitrogenous waste. *Physiol Rev* 85:97–177
- Feldman GJ, Mullin JM, Ryan MP (2005) Occludin: structure, function and regulation. *Adv Drug Deliv Rev* 57:883–917
- Finamore A, Massimi M, Conti Devirgiliis L, Mengheri E (2008) Zinc deficiency induces membrane barrier damage and increases neutrophil transmigration in Caco-2 cells. *J Nutr* 138:1664–1670
- Fletcher M, Kelly SP, Pärt P, O'Donnell MJ, Wood CM (2000) Transport properties of cultured branchial epithelia from freshwater rainbow trout: a novel preparation with mitochondria-rich cells. *J Exp Biol* 203:1523–1537
- Kelly SP, Wood CM (2001) Effect of cortisol on the physiology of cultured pavement cell epithelia from freshwater trout gills. *Am J Physiol Integr Comp Physiol* 281:R811–R820
- Kelly SP, Wood CM (2002) Cultured gill epithelia from freshwater tilapia (*Oreochromis niloticus*): effect of cortisol and homologous serum supplements from stressed and unstressed fish. *J Membr Biol* 190:29–42
- Kelly SP, Fletcher M, Pärt P, Wood CM (2000) Procedures for the preparation and culture of 'reconstructed' rainbow trout branchial epithelia. *Methods Cell Sci* 22:153–163
- Marshall WS (1985) Paracellular ion transport in trout opercular epithelium models osmoregulatory effects of acid precipitation. *Can J Zool* 63:1816–1822
- McCarthy KM, Skare IB, Stankewich MC, Furuse M, Tsukita S, Rogers RA, Lynch RD, Schneeberger EE (1996) Occludin is a functional component of the tight junction. *J Cell Sci* 109:2287–2298
- Minagar A, Ostanin D, Long AC, Jennings M, Kelley RE, Sasaki M, Alexander JS (2003) Serum from patients with multiple sclerosis downregulates occludin and VE-cadherin expression in cultured endothelial cells. *Mult Scler* 9:235–238
- Mitrovic D, Perry SF (2009) The effects of thermally induced gill remodeling on ionocyte distribution and branchial chloride fluxes in goldfish (*Carassius auratus*). *J Exp Biol* 212:843–852
- Rao R (2009) Occludin phosphorylation in regulation of epithelial tight junctions. *Ann N Y Acad Sci* 1165:62–68
- Saitou M, Ando-Akatsuka Y, Itoh M, Furuse M, Inazawa J, Fujimoto K, Tsukita S (1997) Mammalian occludin in epithelial cells: its expression and subcellular distribution. *Eur J Cell Biol* 73:222–231
- Sakakibara A, Furuse M, Saitou M, Ando-Akatsuka Y, Tsukita S (1997) Possible involvement of phosphorylation of occludin in tight junction formation. *J Cell Biol* 137:1393–1401
- Siegenbeek van Heukelom J, van den Ham MD, Dekker K (1982) The modulation by glucose transport of the electrical responses to hypertonic solutions of the goldfish intestinal epithelium. *Pflügers Arch* 395:65–70
- Vermeer PD, Denker J, Estin M, Moninger TO, Keshavjee S, Karp P, Kline JN, Zabner J (2009) MMP6 modulates tight junction integrity and cell viability in human airway epithelia. *Am J Physiol Lung Cell Mol Physiol* 296:L751–L762
- Wong V (1997) Phosphorylation of occludin correlates with occludin localization and function at the tight junction. *Am J Physiol Cell Physiol* 273:C1859–C1867

- Wong V, Gumbiner BM (1997) A synthetic peptide corresponding to the extracellular domain of occludin perturbs the tight junction permeability barrier. *J Cell Biol* 136:399–409
- Wood CM, Pärt P (1997) Cultured branchial epithelia from freshwater fish gills. *J Exp Biol* 200:1047–1059
- Wood CM, Gilmour KM, Pärt P (1998) Passive and active transport properties of a gill model, the cultured branchial epithelium of the freshwater rainbow trout (*Oncorhynchus mykiss*). *Comp Biochem Physiol A Mol Integr Physiol* 119:87–96
- Wood CM, Kelly SP, Zhou B, Fletcher M, O'Donnell M, Eletti B, Pärt P (2002) Cultured gill epithelia as models for the freshwater fish gill. *Biochim Biophys Acta* 1566:72–83
- Wood CM, Eletti B, Pärt P (2003) New methods for the primary culture of gill epithelia from freshwater rainbow trout. *Fish Physiol Biochem* 26:329–344
- Wu Z, Nybom P, Magnusson KE (2000) Distinct effects of *Vibrio cholera* haemagglutinin/protease on the structure and localization of the tight junction-associated proteins occludin and ZO-1. *Cell Microbiol* 2:11–17
- Zeng R, Li X, Gorodeski GI (2004) Estrogen abrogates transcervical tight junctional resistance by acceleration of occludin modulation. *J Clin Endocrinol Metab* 89:5145–5155

**ELSEVIER LICENSE
TERMS AND CONDITIONS**

Sep 20, 2011

This is a License Agreement between Helen Chasiotis ("You") and Elsevier ("Elsevier") provided by Copyright Clearance Center ("CCC"). The license consists of your order details, the terms and conditions provided by Elsevier, and the payment terms and conditions.

All payments must be made in full to CCC. For payment instructions, please see information listed at the bottom of this form.

Supplier	Elsevier Limited The Boulevard, Langford Lane Kidlington, Oxford, OX5 1GB, UK
Registered Company Number	1982084 -
Customer name	Helen Chasiotis
Customer address	York University Toronto, ON M3J 1P3
License number	2753370407834
License date	Sep 20, 2011
Licensed content publisher	Elsevier
Licensed content publication	General and Comparative Endocrinology
Licensed content title	Effect of cortisol on permeability and tight junction protein transcript abundance in primary cultured gill epithelia from stenohaline goldfish and euryhaline trout
Licensed content author	Helen Chasiotis, Scott P. Kelly
Licensed content date	1 July 2011
Licensed content volume number	172
Licensed content issue number	3
Number of pages	11
Start Page	494
End Page	504
Type of Use	reuse in a thesis/dissertation
Portion	full article
Format	both print and electronic
Are you the author of this Elsevier article?	Yes
Will you be translating?	No
Order reference number	

Title of your thesis/dissertation	The role of occludin tight junction protein in freshwater teleost fish osmoregulation
Expected completion date	Oct 2011
Estimated size (number of pages)	350
Elsevier VAT number	GB 494 6272 12
Permissions price	0.00 USD
VAT/Local Sales Tax	0.0 USD / 0.0 GBP
Total	0.00 USD
Terms and Conditions	

INTRODUCTION

1. The publisher for this copyrighted material is Elsevier. By clicking "accept" in connection with completing this licensing transaction, you agree that the following terms and conditions apply to this transaction (along with the Billing and Payment terms and conditions established by Copyright Clearance Center, Inc. ("CCC"), at the time that you opened your Rightslink account and that are available at any time at <http://myaccount.copyright.com>).

GENERAL TERMS

2. Elsevier hereby grants you permission to reproduce the aforementioned material subject to the terms and conditions indicated.

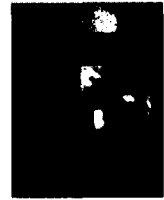
3. Acknowledgement: If any part of the material to be used (for example, figures) has appeared in our publication with credit or acknowledgement to another source, permission must also be sought from that source. If such permission is not obtained then that material may not be included in your publication/copies. Suitable acknowledgement to the source must be made, either as a footnote or in a reference list at the end of your publication, as follows:

“Reprinted from Publication title, Vol /edition number, Author(s), Title of article / title of chapter, Pages No., Copyright (Year), with permission from Elsevier [OR APPLICABLE SOCIETY COPYRIGHT OWNER].” Also Lancet special credit - “Reprinted from The Lancet, Vol. number, Author(s), Title of article, Pages No., Copyright (Year), with permission from Elsevier.”

4. Reproduction of this material is confined to the purpose and/or media for which permission is hereby given.

5. Altering/Modifying Material: Not Permitted. However figures and illustrations may be altered/adapted minimally to serve your work. Any other abbreviations, additions, deletions and/or any other alterations shall be made only with prior written authorization of Elsevier Ltd. (Please contact Elsevier at permissions@elsevier.com)

6. If the permission fee for the requested use of our material is waived in this instance, please be advised that your future requests for Elsevier materials may attract a fee.



Effect of cortisol on permeability and tight junction protein transcript abundance in primary cultured gill epithelia from stenohaline goldfish and euryhaline trout

Helen Chasiotis*, Scott P. Kelly

Department of Biology, York University, Toronto, Ontario, Canada M3J 1P3

ARTICLE INFO

Article history:

Received 14 January 2011

Revised 13 April 2011

Accepted 19 April 2011

Available online 28 April 2011

Keywords:

Pavement cells

Transepithelial resistance

Paracellular permeability

Occludin

Claudin

ZO-1

ABSTRACT

Primary cultured gill epithelia from goldfish and rainbow trout were used to investigate a role for cortisol in the regulation of paracellular permeability and tight junction (TJ) protein transcript abundance in representative stenohaline versus euryhaline freshwater (FW) fish gills. Glucocorticoid and mineralocorticoid receptors are expressed in cultured goldfish gill preparations and cortisol treatment (100, 500 and 1000 ng/mL) dose-dependently elevated transepithelial resistance (TER) and reduced paracellular [³H]PEG-4000 flux across cultured goldfish gill epithelia. Despite these dose-dependent 'tightening' effects of cortisol, the response of goldfish TJ protein transcripts (i.e. occludin, claudin b, c, d, e, h, 7, 8d and 12, and ZO-1) were surprisingly small, with only claudin c and h, and ZO-1 transcript levels significantly decreasing at a dose of 1000 ng/mL. Extending the duration of cortisol exposure from 24 to 48 or 96 h (at 500 ng/mL) did little to alter this phenomenon. By comparison, exposing primary cultured trout gill epithelia (i.e. a euryhaline fish gill model) to 500 ng/mL cortisol resulted in a qualitatively similar, but quantitatively stronger epithelial 'tightening' response. Furthermore, transcript abundance of orthologous trout TJ proteins (i.e. occludin, and claudin 30, 28b, 3a, 7, 8d and 12) significantly elevated as would be expected in a 'tighter' epithelium. Taken together, data suggest a conservative role for cortisol in the endocrine regulation of paracellular permeability across the goldfish gill that may relate to stenohalinity.

© 2011 Elsevier Inc. All rights reserved.

1. Introduction

Cortisol is the main corticosteroid in fishes, functioning as both a glucocorticoid and mineralocorticoid hormone (reviewed by [35]). Although cortisol is involved in the stress response, growth and reproduction, this remarkably versatile hormone also has a well-established role in the endocrine control of osmoregulation [35,33]. In this regard, cortisol appears to possess a dual function, as it has long been associated with salt secretion across the gills of fishes under hyperosmotic conditions (i.e. seawater, SW) and has more recently been linked to ion uptake across the gill epithelium in a hypoosmotic setting (i.e. freshwater, FW) [14,33]. These observations have been generated largely by studies that have focused on the role of cortisol in altering elements of the transcellular transport pathway in gill tissue [14]. However, there is also evidence to suggest that cortisol may play an important role in regulating the physiological properties of the paracellular pathway in gill epithelia [7,23,24] and that tight junction (TJ) proteins may be integrally involved in this endocrine mediated event [4,7,43].

TJs comprise transmembrane and cytoplasmic protein networks encircling the apical-most domain of vertebrate epithelial cells and form a semi-permeable seal that limits the movement of water and solutes across the paracellular pathway. While transmembrane TJ proteins, such as occludin and claudins, form the physical paracellular barrier that selectively restricts the passage of ions and solutes between epithelial cells, the cytoplasmic adaptor or 'scaffolding' TJ proteins, such as ZO-1, tether occludin and claudins to actin filaments within the cytoskeleton. This link between the 'sealing' transmembrane TJ proteins and the actin cytoskeleton allows signals from the external environment to be transmitted to the inside of the cell in order to influence transcriptional pathways that regulate TJ permeability and thus the 'tightness' or 'leakiness' of the epithelium (reviewed by [19]).

Corticosteroids have a well documented ability to alter the permeability characteristics of cultured vertebrate epithelia and endothelia (e.g. [17,41,48]), including the gill epithelia of euryhaline fishes such as the rainbow trout [23] and tilapia [24]. These latter observations are in line with a growing body of evidence that suggests an important role for TJ proteins in the regulation and maintenance of hydromineral balance in fishes, particularly during conditions of altered environmental salinity. In this regard, significant changes in occludin and claudin transcript and/or protein abundance in the teleost gill have been demonstrated following

* Corresponding author. Address: Department of Biology, York University, 4700 Keele Street, Toronto, Ontario, Canada M3J 1P3. Fax: +1 416 736 5698.
E-mail address: helench@yorku.ca (H. Chasiotis).

acclimation to ion-poor water [6,13], SW [2,3,13,42] as well as hypersaline SW [2]. However, the majority of the aforementioned studies and all *in vitro* studies that have examined the effects of cortisol on gill permeability have been conducted using either euryhaline fishes or gill epithelial models derived from euryhaline fishes. To the best of our knowledge, no studies have examined the effects of cortisol on the permeability characteristics and TJ components of a stenohaline FW fish gill, or compared these with a euryhaline fish gill.

Therefore, the first objective of the present study was to utilize a recently developed cultured gill epithelium derived from the goldfish (see [8]) to investigate a role for cortisol in the endocrine regulation of gill permeability in a representative stenohaline FW fish. A second objective was to compare results obtained in the goldfish gill model to those observed in a cultured euryhaline fish gill epithelium derived from rainbow trout (see [22]). Since corticosteroid-induced alterations in the permeability characteristics of vertebrate epithelia have been linked to alterations in the transcriptional and post-translational abundance of TJ proteins (e.g. [7,16,17,41]), a third objective was to identify and examine the transcript abundance of select TJ proteins in goldfish and rainbow trout gill preparations that are associated with changes in epithelial permeability in other vertebrates. Where possible, these TJ components were selected on the basis that they have already been associated with changes in the hydromineral status of fishes, such as occludin (see [5–7]), claudin h (which is a claudin 3a ortholog; see [2,4,13]), claudin 8d (see [3,4,13]), and claudin b and e (orthologs of claudin 30 and 28b, respectively; see [42,43]). It is our view that in order to gain broader insight into the various mechanisms that regulate gill permeability in fishes, it is important to consider the physiology and molecular components of a stenohaline model in addition to the traditional euryhaline archetype.

2. Materials and methods

2.1. Animals

Goldfish (*Carassius auratus*, 18–30 g) and rainbow trout (*Oncorhynchus mykiss*, ~125 g) were obtained from local suppliers (Aleongs International, Mississauga, ON, Canada; Humber Springs Trout Club and Hatchery, Orangeville, ON, Canada) and held in either 200-L (goldfish) or 600-L (trout) opaque polyethylene tanks. Tanks were supplied with flow-through dechlorinated FW (approximate composition in mM: [Na⁺] 0.59, [Cl⁻] 0.92, [Ca²⁺] 0.76, [K⁺] 0.43, pH 7.35) at 25 ± 1 °C for goldfish and 10 ± 2 °C for rainbow trout. All fish were held under the above described conditions for at least 3 weeks prior to use and fed *ad libitum* once daily with commercial pellets (Martin Profishment, Elmira, ON, Canada).

2.2. Preparation of cultured gill epithelia

Procedures for goldfish gill cell isolation and the culture of goldfish gill epithelia (composed of pavement cells only) were conducted according to previously described methods (see [8]). Methods for rainbow trout gill cell isolation and the preparation of rainbow trout gill epithelia (composed of pavement cells only) were conducted according to procedures originally developed by [45] and described in detail by [22]. In brief, isolated goldfish or rainbow trout gill cells were initially cultured in flasks with Leibovitz's L-15 culture medium supplemented with 2 mM L-glutamine (L15) and 6% fetal bovine serum (FBS). At confluence (~2 days for goldfish; ~4–5 days for rainbow trout), cells were harvested from flasks by trypsinization and seeded into cell culture inserts (polyethylene terephthalate filters, 0.9 cm² growth area, 0.4 µm pore size, 1.6 × 10⁶ pore/cm² pore density; BD Falcon™, BD Biosciences,

Mississauga, ON, Canada). Epithelia were allowed to develop under symmetrical culture conditions (i.e. with FBS-supplemented L15 culture medium bathing both apical and basolateral surfaces of the epithelial preparations) and were maintained in an air atmosphere at either 27 or 18 °C for cultured goldfish and rainbow trout gill epithelia, respectively. All experimental procedures conformed to the guidelines of the Canadian Council on Animal Care and were approved by the York University Animal Care Committee.

2.3. Transepithelial resistance (TER) and [³H]PEG-4000 flux measurements

Measurements of TER were conducted using chopstick electrodes (STX-2) connected to a custom-modified EVOM epithelial voltohmmeter (World Precision Instruments, Sarasota, FL, USA). All TER measurements are expressed as kΩ cm² and background-corrected for TER measured across 'vacant' culture inserts containing appropriate media. Paracellular permeability across cultured epithelia was determined using the paracellular marker, [³H] polyethylene glycol (molecular mass 4000 Da; PEG-4000; PerkinElmer, Woodbridge, ON, Canada) according to previously described methods and calculations [46]. Briefly, the appearance of [³H]PEG-4000 in the apical compartment was monitored as a function of time and epithelial surface area after the addition of 1 µCi of [³H]PEG-4000 to basolateral culture media.

2.4. Cortisol treatment

Single-use aliquots of a stock cortisol solution were prepared by dissolving cortisol (hydrocortisone 21-hemisuccinate sodium salt; Sigma-Aldrich Canada Ltd., Oakville, ON, Canada) in sterile phosphate-buffered saline (PBS; pH 7.7). Aliquots were stored at –30 °C until use. Cortisol treatment of cultured goldfish and rainbow trout gill epithelia commenced at ~24 h after seeding cells in culture inserts when TER measurements were ~100–200 Ω cm² above background levels (see Section 2.3). Inserts were randomly assigned to either a control group or a cortisol-treated group. In the cortisol-treated group, basolateral culture media were supplemented with an appropriate amount of thawed stock cortisol in order to achieve the desired concentration of hormone. Control media contained no cortisol supplement.

2.4.1. Series 1

To investigate the dose-dependent effects of cortisol on cultured goldfish gill epithelia, basolateral media were supplemented with three concentrations of cortisol (100, 500 and 1000 ng/mL), the lower two of which are within the physiological range for goldfish [37]. Once control and hormone-treated preparations developed a stable plateau in TER (~21 h after the addition of cortisol), [³H]PEG-4000 permeability was measured over a 3 h flux period and then epithelia were collected for RNA extraction (see Section 2.5). Therefore, in these experiments, epithelia were treated with cortisol for a total of 24 h.

2.4.2. Series 2

To examine the time-course effects of cortisol on cultured goldfish gill epithelia, basolateral media were supplemented with 500 ng/mL cortisol, and control and cortisol-treated preparations were collected for RNA extraction at 48 and 96 h after the addition of cortisol. To confirm that cortisol was having the desired effect, the TER across epithelia was monitored periodically throughout the incubation period. A single dose of 500 ng/mL cortisol was used in this series based on physiological relevance and on observations made in *series 1*. Control and cortisol-supplemented media were renewed once at 48 h for epithelia collected at 96 h.

2.4.3. Series 3

In a side-by-side comparison of the effects of cortisol on cultured goldfish and rainbow trout gill epithelia, respectively, basolateral media of goldfish and rainbow trout preparations were supplemented with 500 ng/mL cortisol. This cortisol concentration was selected based on observations made in series 1 and series 2, the results of previous *in vitro* studies conducted in cultured rainbow trout gill epithelia [7,23], and the physiological relevance of this cortisol dose as it pertains to both goldfish and rainbow trout [37]. When control and cortisol-treated preparations exhibited a plateau in TER, [³H]PEG-4000 permeability was determined, following which epithelia were collected for RNA extraction. The period of cortisol exposure was 24 h for goldfish gill epithelia and ~96 h for rainbow trout gill epithelia.

2.5. RNA extraction and cDNA synthesis

Total RNA was isolated from goldfish gill tissue and cultured goldfish and rainbow trout gill epithelia using TRIzol[®] Reagent (Invitrogen Canada, Inc., Burlington, ON, Canada) according to manufacturer's instructions. Extracted RNA was treated with DNase I (Amplification Grade; Invitrogen Canada, Inc.) and then first-strand cDNA was synthesized using SuperScript[™] III Reverse Transcriptase and Oligo(dT)₁₂₋₁₈ primers (Invitrogen Canada, Inc.).

2.6. Cloning of goldfish corticosteroid receptor, claudin and ZO-1 cDNA

Using ClustalX multiple sequence alignments [28] of known coding sequences for corticosteroid receptors, claudins and ZO-1 from various species, degenerate primers were designed based on highly conserved regions. For example, degenerate primers for corticosteroid receptors were designed based on highly conserved regions identified within the aligned coding sequences for zebrafish, common carp and rainbow trout glucocorticoid receptor 1 (GR1), glucocorticoid receptor 2 (GR2) and mineralocorticoid receptor (MR) orthologs (see Table 1 for ortholog Accession Nos.). For claudin b, c, d, e, h, 7 and 12 degenerate primer design, coding sequences for appropriate *Takifugu* (= *Fugu*) *rubripes* and zebrafish claudin orthologs, as defined by [9,30], were aligned (see Table 2 for ortholog Accession Nos.). For claudin 8d degenerate primer design, coding sequences for *Fugu* and rainbow trout claudin 8d orthologs were aligned (see Table 2 for ortholog Accession Nos.). Finally, for ZO-1 (=tight junction protein-1; TJP1) degenerate primer design, coding sequences for mouse (NM_009386), rat (NM_001106266), human (NM_003257), dog (NM_001003140), chicken (XM_413773) and zebrafish (XM_001922655) ZO-1 orthologs were aligned. Degenerate primers were used in reverse transcriptase PCR (RT-PCR) to amplify partial goldfish corticosteroid receptor, claudin or ZO-1 cDNA fragments from a goldfish gill cDNA template. The following RT-PCR reaction conditions were utilized: 1 cycle of denaturation (95 °C, 4 min), 40 cycles of dena-

turation (95 °C, 30 s), annealing (53–62 °C, 30 s) and extension (72 °C, 30 s), respectively, final single extension cycle (72 °C, 5 min). Gel electrophoresis (1% agarose stained with ethidium bromide) verified PCR products at predicted amplicon sizes. Putative cDNA fragments were then excised, purified using a QIAquick Gel Extraction Kit (QIAGEN, Inc., Mississauga, ON, Canada) and sequenced in the York University Core Molecular Biology and DNA Sequencing Facility (Department of Biology, York University, ON, Canada). Partial goldfish GR1, GR2, MR, claudin b, c, d, e, h, 7, 8d and 12, and ZO-1 sequences were confirmed using a BLAST search [1] and submitted to GenBank (Accession Nos. are shown in Tables 1 and 2).

2.7. Identification of rainbow trout claudins

Full-length and partial coding sequences for rainbow trout claudin 3a, 7, 8d, 12 and 30 were assembled from overlapping rainbow trout EST sequences using ClustalX multiple sequence alignments. Rainbow trout EST sequences were identified by submitting known *Fugu* and/or Atlantic salmon claudin coding sequences (see Table 3 for ortholog Accession Nos.) to a BLAST search against a rainbow trout EST database available at the NCBI (www.ncbi.nlm.nih.gov). Assembled sequences for rainbow trout claudins were submitted to the Third Party Annotation (TPA) database (Accession Nos. are shown in Table 3).

2.8. RT-PCR of goldfish corticosteroid receptors

Expression of goldfish corticosteroid receptor mRNA in goldfish gill tissue and cultured goldfish gill epithelia was examined by routine RT-PCR under reaction conditions described above (see Section 2.6) using gene-specific primer sets for goldfish corticosteroid receptors (see Table 1). Primers were designed based on the partial coding sequences determined above (see Section 2.6). The sequence identities of RT-PCR products were confirmed by sequence analysis (Department of Biology, York University) to verify that the gene-specific primer sets were targeting the correct genes. β-actin mRNA abundance was used as a loading control and was amplified using primers previously reported by [8]. Resulting RT-PCR amplicons were resolved by gel electrophoresis (1% agarose stained with ethidium bromide), and images were captured using a Molecular Imager Gel Doc XR + System and Quantity One 1D analysis software (Bio-Rad Laboratories Canada Ltd., Mississauga, ON, Canada).

2.9. Quantitative real-time PCR analysis

TJ protein mRNA abundance in goldfish gill tissue and cultured goldfish and rainbow trout gill epithelia was examined by quantitative real-time PCR analysis (qRT-PCR). Based on the coding sequences determined above (see Sections 2.6 and 2.7), gene-

Table 1
Primer sequences and corresponding fish orthologs for goldfish corticosteroid receptors.

Goldfish gene (Accession No.)	Primer sequence (5' → 3')	Amplicon size (bp)	Fish ortholog (Accession No.)
GR1 (HQ656017)	FOR: GATGCCGATTACAGGCTCATTC REV: CTCCTTACTACTGCTGGTAGG	368	zf nr3c1 (NM_001020711) crp GR1a (AJ879149) rt GR (NM_001124730)
GR2 (HQ656018)	FOR: TTACAGCAACAGCCAGTC REV: CCACCAATCAAGGAGTCTG	351	zf GRβ (EF436285) crp GR2 (AM183668) rt GR2 (NM_001124482)
MR (HQ656019)	FOR: AGGTGAGCCAGGAGTTTGTC REV: TGGTCGCTGATTATTTCCAC	340	zf nr3c2 (NM_001100403) crp MR (AJ783704) rt MRa (AY495584)

GR1, glucocorticoid receptor 1; GR2, glucocorticoid receptor 2; MR, mineralocorticoid receptor; zf, zebrafish; crp, carp; rt, rainbow trout.

Table 2
Primer sequences and corresponding fish orthologs for goldfish claudins and ZO-1.

Goldfish gene (Accession No.)	Primer sequence (5' → 3')	Amplicon size (bp)	Fish ortholog (Accession No.)
claudin b (HQ656008)	FOR: GTGCCCTCACCATCATTTCC REV: GCTCTCTTCTGTGCTTGGTTC	237	zf claudin b (AF359426) fu claudin 30d (AY554376)
claudin c (HQ656009)	FOR: CATTGTGGGTGCTCTAGCG REV: CAATACGACTTTGCCGTGG	335	zf claudin c (AF359432) fu claudin 3d (AY554368)
claudin d (HQ656010)	FOR: AATCCTCGTGACCTTCTTGG REV: CCAGCCGATGAACAGAC	244	zf claudin d (BC078260) fu claudin 29a (AY554372)
claudin e (HQ656011)	FOR: TCTGTGGATGACCTGTGTGG REV: CCCTGACGATGGTGTAGTTG	289	zf claudin e (AF359425) fu claudin 28b (AY554375)
claudin h (HQ656012)	FOR: ACCTTCAGGCTTCCAGAGC REV: CAGCGCAAACCTATGTAG	285	zf claudin h (BC053223) fu claudin 3a (AY554377)
claudin 7 (HQ656013)	FOR: GCAAGGTGTACGACTCCATC REV: TGTGTTGACTGGTGTGAAGG	281	zf claudin 7 (BC066408) fu claudin 7b (AY554347)
claudin 8d (HQ656014)	FOR: GAGGGACTGTGGATGAAGTGC REV: GACACGGGAATAATGGTGGTC	272	fu claudin 8d (AY554390) rt claudin 8d (BK007966)
claudin 12 (HQ656015)	FOR: TTTCCAGCTTGCTCTTCTG REV: GCTAAGATCAGACCACCAGCAC	280	zf claudin 12 (BC075744) fu claudin 12 (AY554346)
ZO-1 (HQ656016)	FOR: CTGGCTGGAGAAATGATGTG REV: CCACCACTCTGAACCTCTCC	330	zf TJP1 (XM_001922655)

zf, zebrafish; fu, *Fugu*; rt, rainbow trout.**Table 3**
Primer sequences and corresponding fish orthologs for trout claudins.

Trout gene (Accession No.)	Primer sequence (5' → 3')	Amplicon size (bp)	Fish ortholog (Accession No.)
claudin 3a (BK007964)	FOR: TGGATCATTGCCATCGTGC REV: GCCTCGTCTCAATACAGTTGG	285	fu claudin 3a (AY554377) sl claudin 3a (BK006381)
claudin 7 (BK007965)	FOR: CGTCTGCTGATTTGGATCTC REV: CAAACGTACTCTTGTCTGCTG	261	fu claudin 7b (AY554347) sl claudin 7 (BK006387)
claudin 8d (BK007966)	FOR: GCAGTGTAAGGTGTACGACTCTCTG REV: CACGAGGAACAGGCATC	200	fu claudin 8d (AY554390)
claudin 12 (BK007967)	FOR: CTTTCATCATCGCTTCTATCTC REV: GAGCCAAACAGTAGCCAGTAG	255	fu claudin 12 (AY554346) sl claudin 12 (NM_001140081)
claudin 30 (BK007968)	FOR: CGGGGAGAACATAATCACAG REV: GGGATGAGACAGGATGC	297	sl claudin 30 (BK006405)

fu, *Fugu*; sl, Atlantic salmon.

specific primer sets for goldfish claudins and ZO-1 (see Table 2) and rainbow trout claudins (see Table 3) were designed for use in qRT-PCR. The sequence identities of amplicons generated using gene-specific primer sets were confirmed by sequence analysis (Department of Biology, York University). Goldfish and rainbow trout occludin mRNA were also amplified using primers previously reported by [8] and [7], respectively. Primers for rainbow trout claudin 28b (forward: 5'CTTTCATCGGAGCCAACATC3' and reverse: 5'CAGACAGGGACCAGAACCAG3', amplicon size ~310 bp) were designed based on GenBank Accession No. EU921670. qRT-PCR analysis of TJ protein mRNA was conducted using SYBR Green I Supermix (Bio-Rad Laboratories Canada Ltd.) and a Chromo4™ Detection System (CFB-3240; Bio-Rad Laboratories Canada Ltd.) under the following reaction conditions: 1 cycle denaturation (95 °C, 4 min) followed by 40 cycles of denaturation (95 °C, 30 s), annealing (51–61 °C, 30 s) and extension (72 °C, 30 s), respectively. A standard curve was constructed for each TJ gene examined in order to optimize the template cDNA concentration used and to ensure that the threshold cycle for each gene occurred within an acceptable range. A melting curve was also carried out after each qRT-PCR run to ensure that a single product was synthesized during reactions. For all qRT-PCR analyses, TJ protein mRNA abundance was normalized to β -actin transcript abundance after

verifying that β -actin did not alter in response to experimental conditions. Goldfish and rainbow trout β -actin mRNA was amplified using primers previously described by [8] and [7], respectively.

2.10. Statistical analysis

All data are expressed as mean values \pm SEM (n), where n represents the number of inserts, except in Fig. 2B, where n represents the number of fish sampled. A one-way or two-way analysis of variance (ANOVA) followed by a Student–Newman–Keuls test was used to determine significant differences ($P < 0.05$) between groups. When appropriate, a Student's t -test was also used. All statistical analyses were conducted using SigmaStat 3.5 software (Sy-stat Software, Inc., San Jose, CA, USA).

3. Results

3.1. Corticosteroid receptor mRNA expression and dose-dependent effects of cortisol on permeability in cultured goldfish gill epithelia

Using degenerate primers, partial coding sequences for goldfish corticosteroid receptors (GR1, GR2 and MR) were cloned. Translated

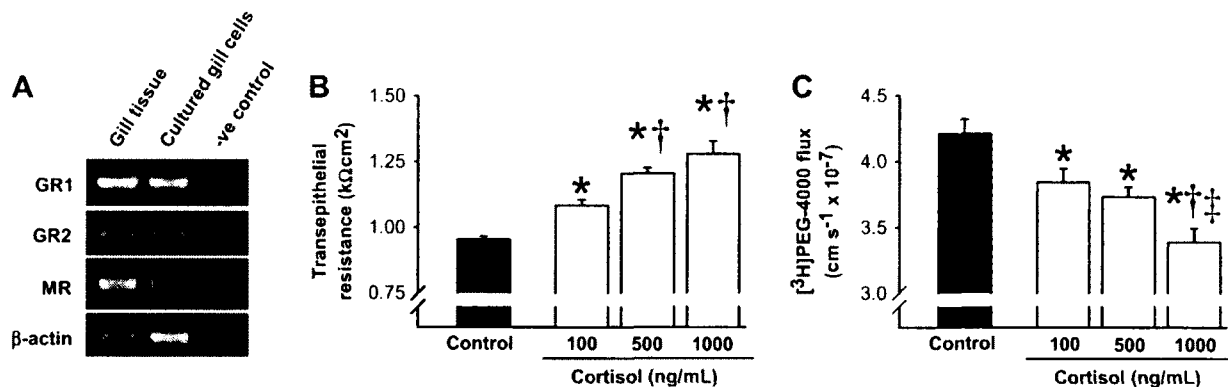


Fig. 1. (A) Corticosteroid receptor mRNA expression in goldfish gill tissue and cultured goldfish gill cells by routine RT-PCR and gel electrophoresis. β -actin mRNA was used as a loading control. Dose-dependent effects of 24 h cortisol treatment on (B) transepithelial resistance and (C) [³H]PEG-4000 flux across cultured goldfish gill epithelia. Data are expressed as means \pm SEM ($n = 8-11$). * Significant difference ($P < 0.05$) from the untreated control (0 ng/mL) group. † Significant difference ($P < 0.05$) from the 100 ng/mL cortisol group. ‡ Significant difference ($P < 0.05$) from the 500 ng/mL cortisol group. GR1, glucocorticoid receptor 1; GR2, glucocorticoid receptor 2; MR, mineralocorticoid receptor.

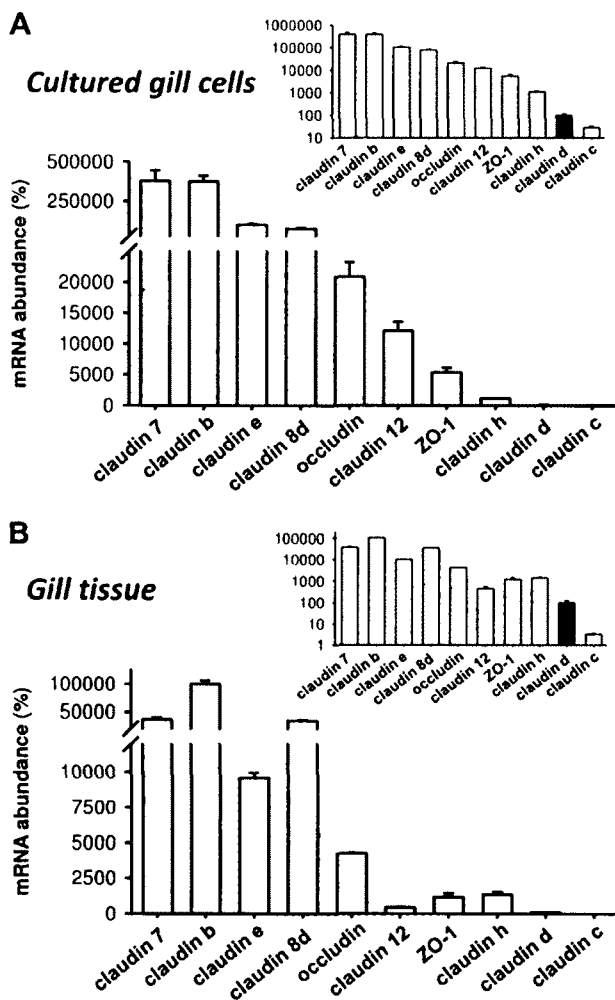


Fig. 2. Goldfish occludin, claudin and ZO-1 mRNA abundance in (A) cultured gill cells and (B) gill tissue by qRT-PCR analysis. Inset graphs show data re-expressed on a semi-logarithmic scale. Transcript abundance was normalized to β -actin mRNA abundance, and mRNA abundance for each gene examined was expressed relative to claudin d transcript abundance (indicated by the solid bar) which was assigned a value of 100%. In (A) and (B), transcripts for TJ proteins are shown in descending order of abundance (left to right) as found in the primary cultured goldfish gill epithelium. Data are expressed as means \pm SEM (A, $n = 6$; B, $n = 3-4$).

goldfish GR1, GR2 and MR fragments shared $\sim 99\%$ amino acid sequence similarity (identical matches plus mismatches with similar amino acids) with aligned regions of corresponding carp, zebrafish and trout corticosteroid receptor orthologs (see Table 1 for ortholog Accession Nos.). Using RT-PCR and gel electrophoresis, cultured gill cells were examined for the presence of goldfish GR1, GR2 and MR expression. As a positive control, corticosteroid receptor mRNA in goldfish gill tissue was also evaluated. Transcript for all three goldfish corticosteroid receptors were found to be present in both goldfish gill tissue and cultured gill cells (Fig 1A).

To examine the dose-dependent effects of cortisol on the permeability characteristics of cultured goldfish gill epithelia, basolateral media were supplemented with 100, 500 and 1000 ng/mL of cortisol. Following 24 h of cortisol treatment, all three tested doses significantly elevated TER when compared to untreated control preparations (Fig. 1B). All tested cortisol doses also significantly reduced [³H]PEG-4000 flux across cultured goldfish gill preparations (Fig. 1C). [³H]PEG-4000 permeability appeared to decrease in a stepwise manner with increasing cortisol concentration, however flux across 500 ng/mL cortisol-treated preparations was not significantly different ($P > 0.05$) from 100 ng/mL cortisol-treated epithelia (Fig. 1C).

3.2. TJ protein mRNA expression in cultured goldfish gill epithelia and goldfish gill tissue

Using degenerate primers, partial coding sequences for goldfish claudins and ZO-1 were cloned. Translated goldfish claudin fragments exhibited $\sim 94-99\%$ and $\sim 84-92\%$ amino acid sequence similarity with aligned regions of corresponding zebrafish and *Fugu* claudin orthologs, respectively (see Table 2 for ortholog Accession Nos.). Goldfish claudins were therefore designated a single letter or number based on the nomenclature of the zebrafish claudin family originally described by [26], except for goldfish claudin 8d which was named according to *Fugu* terminology (outlined by [30]) since a zebrafish ortholog for claudin 8d has yet to be identified. The translated goldfish ZO-1 fragment exhibited 100% and 97–98% amino acid sequence similarity with aligned regions of zebrafish and mammalian (e.g. mouse, rat, human, dog) ZO-1 orthologs, respectively.

Because all TJ protein genes were expressed in gill tissue and the cultured gill epithelium, the relative abundance of TJ protein mRNA was compared within each tissue to examine whether tissue-specific levels of TJ protein mRNA in the *in vitro* preparation

matched native gill tissue (see Fig. 2). In broad terms, the relative abundance of TJ protein mRNA in each tissue matched well. For example, claudin 7, b, e and 8d mRNA were the most abundant in both tissues and claudin d and c were the least abundant. However, subtle differences were also notable. Claudin b for example, was the most abundant transcript in gill tissue, but in cultured gill epithelia, both claudin b and claudin 7 were the most abundant (Fig. 2).

3.3. Dose-dependent effects of cortisol on TJ protein mRNA abundance in cultured goldfish gill epithelia

In series 1 experiments, cultured goldfish gill epithelia were treated with 100, 500 and 1000 ng/mL of cortisol for 24 h to examine the dose-dependent effects of the hormone on TJ protein mRNA abundance. Occludin and claudin b, d, e, 7, 8d and 12 did not significantly alter in response to cortisol treatment ($P > 0.05$) (Fig. 3A,B,D,E,G,H,I). Cortisol doses of 500 and 1000 ng/mL however significantly reduced claudin c mRNA abundance by ~28% and 44%, respectively when compared to untreated control epithelia (Fig. 3C). Similarly, treatment with 1000 ng/mL cortisol significantly reduced claudin h and ZO-1 transcript abundance by ~42% and 39%, respectively (Fig. 3F and J). β -actin mRNA abundance was not significantly altered by cortisol treatment ($P = 0.994$).

3.4. Time-course effects of cortisol on permeability and TJ protein mRNA abundance in cultured goldfish gill epithelia

In series 2 experiments, cultured goldfish gill epithelia were treated with 500 ng/mL of cortisol for 48 and 96 h to examine the response of epithelia to prolonged cortisol exposure. TER was significantly elevated after 48 and 96 h of cortisol treatment when compared to untreated control preparations within the same time group (Fig. 4A). Over time, TER within the control group significantly decreased, however TER within the cortisol-treated group remained unchanged ($P > 0.05$; Fig. 4A). Neither cortisol treatment nor time significantly altered claudin b, d, e and 8d transcript abundance ($P > 0.05$; data not shown). Claudin 7 mRNA abundance however, was significantly decreased over time but was not dependent on cortisol treatment as there was no statistically significant interaction between hormone treatment and time ($P > 0.05$; data not shown). Although occludin, claudin h and 12, and ZO-1 transcript abundance remained unchanged ($P > 0.05$) relative to control preparations after 48 h cortisol treatment, mRNA expression levels were significantly reduced by cortisol following 96 h (Fig. 4B,D,E,F). Occludin, claudin 12 and ZO-1 mRNA expression were also significantly reduced after 96 h cortisol treatment relative to cortisol-treated epithelia at 48 h (Fig. 4B,E,F). Furthermore, control epithelia collected at 96 h exhibited significantly lower levels of claudin 12 mRNA when compared to control preparations collected at 48 h (Fig. 4E). Finally, cortisol supplementation reduced claudin c mRNA abundance following both 48 h ($P < 0.05$) and 96 h ($P = 0.139$), however this was only significant following 48 h (Fig. 4C). Neither cortisol treatment nor time significantly altered ($P > 0.05$) β -actin mRNA abundance.

3.5. Comparative effects of cortisol on permeability and TJ protein mRNA abundance in cultured goldfish and rainbow trout gill epithelia

To compare changes in TJ protein mRNA abundance in cultured goldfish and rainbow trout gill epithelia, several trout claudin orthologs were identified using a BLAST search to compare known *Fugu* and/or Atlantic salmon sequences to a rainbow trout EST database. Translated rainbow trout claudin 3a, 7, 12 and 30 fragments exhibited ~85–99% and 99–100% amino acid sequence sim-

ilarity with aligned regions of corresponding *Fugu* and Atlantic salmon orthologs, respectively (see Table 3 for ortholog Accession Nos.), and were therefore named according to previously reported Atlantic salmon claudin nomenclature (see [42]). Since an Atlantic salmon claudin 8d ortholog has yet to be identified, rainbow trout claudin 8d was named after *Fugu* claudin 8d (see [30]) which shares ~89% amino acid sequence similarity with aligned regions of the trout ortholog. Taken together, this allowed a comparison of seven TJ orthologs. Specifically, rainbow trout occludin, claudin 30, 28b, 3a, 7, 8d and 12 genes are orthologs of goldfish occludin, claudin b, e, h, 7, 8d and 12 genes, respectively.

In series 3 experiments, cultured goldfish and rainbow trout gill epithelia were supplemented with a single dose of 500 ng/mL cortisol. When compared to control preparations, cortisol treatment significantly elevated TER by ~35% and 530% in cultured goldfish and rainbow trout gill epithelia, respectively (Fig. 5A and C). Cortisol also significantly reduced [^3H]PEG-4000 flux by ~22% and 42% in cultured goldfish and rainbow trout gill epithelia, respectively (Fig. 5B and D). Transcripts encoding for goldfish TJ proteins were unaltered ($P > 0.05$) by cortisol treatment, except for claudin e mRNA abundance, which exhibited a marginal but significant increase in response to cortisol (Fig. 5E). In contrast, cortisol treatment significantly elevated the transcript abundance of all rainbow trout TJ orthologs examined. In both cultured goldfish and rainbow trout gill epithelia, β -actin mRNA abundance was not significantly altered ($P = 0.478$ and 0.6806, respectively) by cortisol treatment.

4. Discussion

4.1. Overview

During SW acclimation of euryhaline fishes, circulating cortisol levels have been shown to rapidly elevate (e.g. [10,32]). Under these circumstances, elevated cortisol levels help to increase salinity tolerance by stimulating active ion extrusion mechanisms in the gill (e.g. [14,21]). The ability of fishes to acclimate to ion-poor surroundings has also been linked to elevated cortisol levels [36]. In studies conducted on euryhaline rainbow trout, hypercortisolemia was proposed to enhance acclimation to ion-poor surroundings by enlarging gill mitochondria-rich cells and enhancing ion uptake [36]. However a decrease in ion efflux rate was also reported to occur (see [36]), an observation that is consistent with the ability of cortisol to reduce ion efflux rates and increase the abundance of the TJ protein occludin in cultured gill epithelia derived from FW rainbow trout [7,23]. In contrast, the goldfish is a stenohaline FW fish that cannot survive in SW [27]. However, when gradually acclimated to elevated salinity, it has been reported that goldfish can survive indefinitely in half-strength SW [27]. Interestingly, goldfish serum cortisol levels have also been shown to significantly elevate when acclimated to a tolerable saline environment [39]. Furthermore, goldfish are able to acclimate to ion-poor surroundings (e.g. [6]). Serum cortisol levels have not been described in goldfish during ion-poor water exposure however increased ion influx and reductions in ion efflux across the gills have been observed [11]. Correspondingly, occludin TJ protein abundance is markedly elevated in the gills of goldfish when acclimated to ion-poor water [6]. Therefore, the literature appears to indicate that cortisol may be a common link between the ionoregulatory response of euryhaline and stenohaline species to altered environmental salinity. However, the current set of studies does not entirely support this view. In contrast, the modest (or absent) response of cultured goldfish gill epithelia to cortisol treatment seems to suggest that cortisol may play a less important role in controlling salt and water balance in goldfish and introduces the

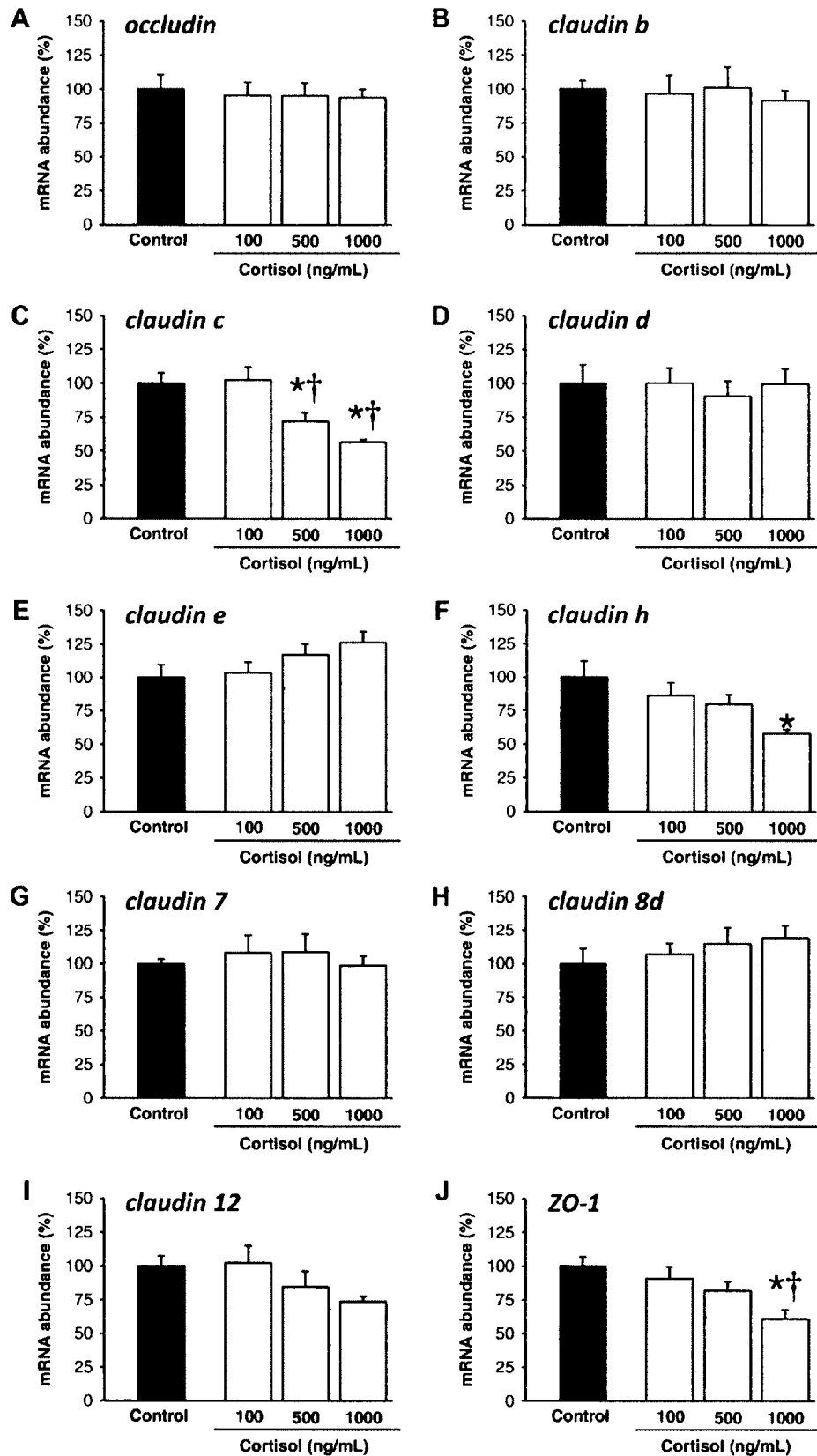


Fig. 3. Dose-dependent effects of 24 h cortisol treatment on (A) occludin, (B) claudin b, (C) claudin c, (D) claudin d, (E) claudin e, (F) claudin h, (G) claudin 7, (H) claudin 8d, (I) claudin 12 and (J) ZO-1 mRNA abundance in cultured goldfish gill epithelia. Occludin, claudin and ZO-1 transcript abundance were normalized to β -actin mRNA abundance. Data are expressed as means \pm SEM ($n = 5-6$). * Significant difference ($P < 0.05$) from the untreated control (0 ng/mL) group. † Significant difference ($P < 0.05$) from the 100 ng/mL cortisol group.

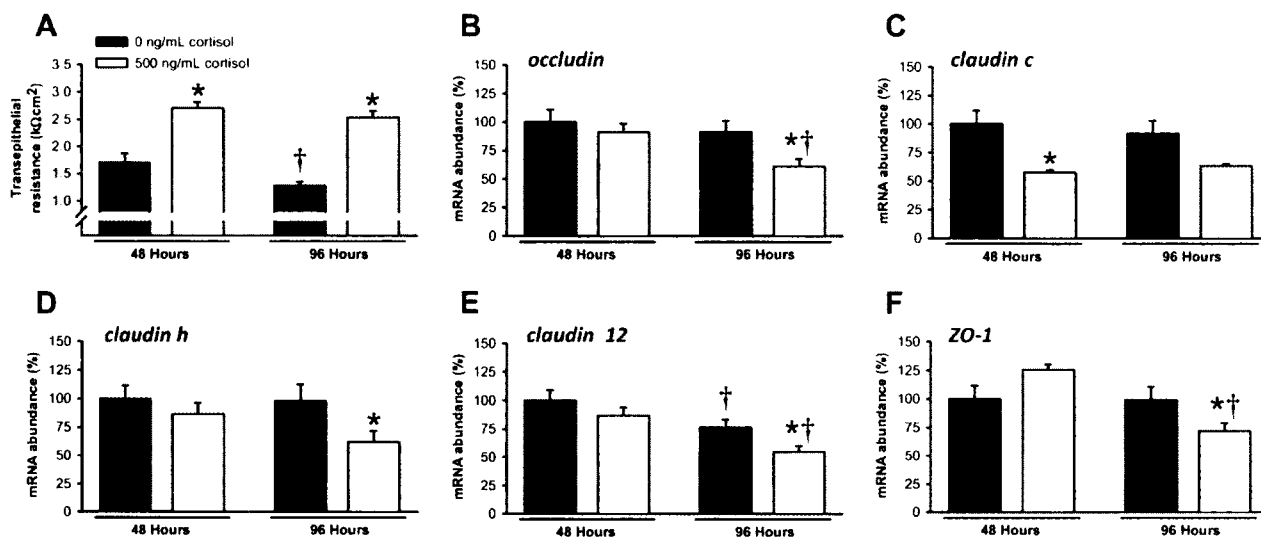


Fig. 4. Time-course effects of 48 and 96 h cortisol treatment on (A) transepithelial resistance and (B) occludin, (C) claudin c, (D) claudin h, (E) claudin 12 and (F) ZO-1 mRNA abundance in cultured goldfish gill epithelia. Occludin, claudin and ZO-1 transcript abundance were normalized to β -actin mRNA abundance, and mRNA data were expressed relative to transcript abundance for control (0 ng/mL cortisol) epithelia collected at 48 h which were assigned a value of 100%. Data are expressed as means \pm SEM ($n = 5-6$). * Significant difference ($P < 0.05$) between control and cortisol groups within the same time period (e.g. control versus cortisol at 48 h). † Significant difference ($P < 0.05$) between time periods within a treatment group (e.g. control at 48 h versus control at 96 h).

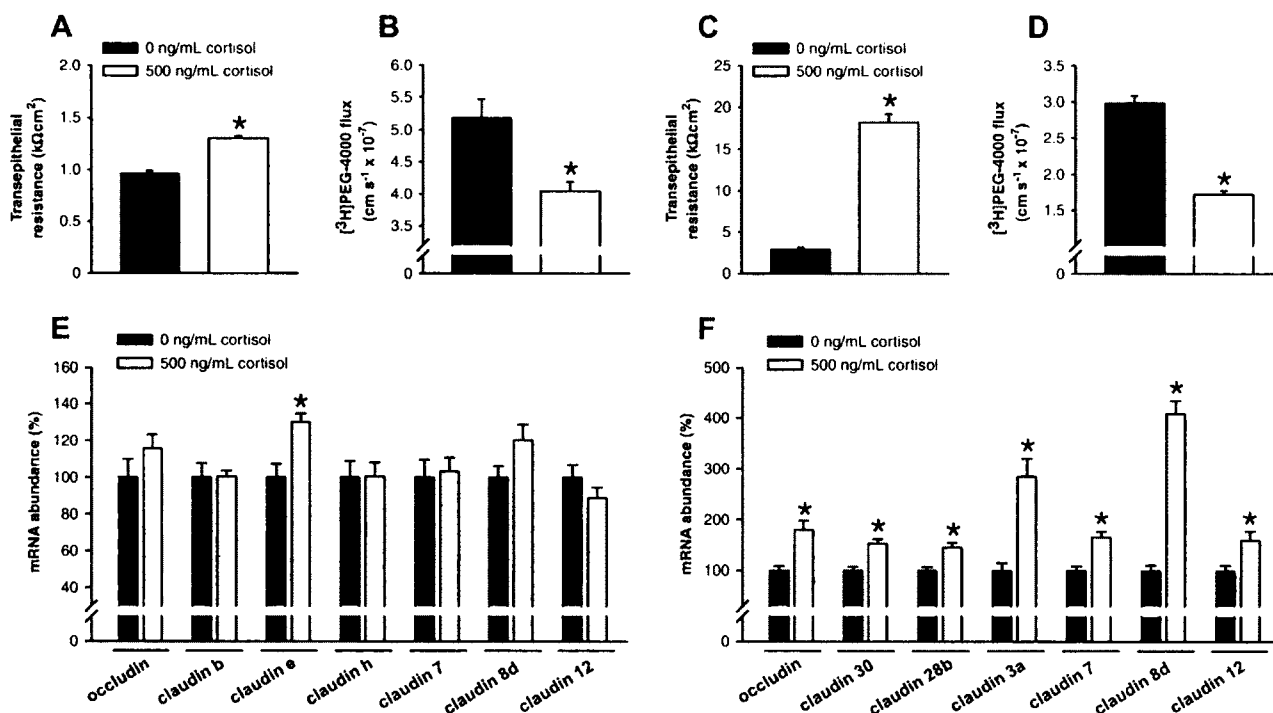


Fig. 5. Comparative effects of cortisol on (A, C) transepithelial resistance, (B, D) [³H]PEG-4000 flux and (E, F) TJ protein mRNA abundance in cultured (A, B, E) goldfish and (C, D, F) rainbow trout gill epithelia. Note: goldfish occludin, claudin b, e, h, 7, 8d and 12 genes are orthologs of rainbow trout occludin, claudin 30, 28b, 3a, 7, 8d and 12 genes, respectively. Goldfish and rainbow trout occludin and claudin transcript abundance were normalized to β -actin mRNA abundance. Data are expressed as means \pm SEM ($n = 5-8$). * Significant difference ($P < 0.05$) from the untreated control (0 ng/mL) group.

idea that the stenohaline nature of goldfish may be related to this phenomenon.

4.2. Dose-dependent effects of cortisol on permeability

Cultured goldfish gill epithelia are composed exclusively of pavement cells, therefore goldfish corticosteroid receptors were

cloned to establish their presence in cultured preparations. Transcripts for all three goldfish corticosteroid receptors (GR1, GR2 and MR) examined were found in goldfish gill tissue and cultured gill epithelia (Fig. 1A). In view of this, it seemed reasonable to conclude that cultured goldfish gill epithelia would be capable of mounting a response to cortisol treatment. Therefore three cortisol concentrations were tested, using doses (100, 500 and 1000 ng/mL)

that were selected based on the reported physiological range for plasma cortisol in goldfish and other cyprinids subjected to various stressors (e.g. noise stress, air exposure) [12,37,40].

Cortisol treatment elicited a distinct epithelial 'tightening' effect by significantly elevating TER and reducing [^3H]PEG-4000 flux across cultured goldfish gill epithelia in a dose-dependent manner (Figs. 1B and C). This 'tightening' of cultured goldfish gill preparations is in accordance with observed glucocorticoid-mediated reductions in permeability across other cultured vertebrate epithelia and endothelia [17,41,48], including primary cultured fish gill models derived from rainbow trout and tilapia [23,24]. However, although the effect of cortisol on cultured goldfish gill preparations was qualitatively similar to those observed in cultured trout gill epithelia (see [23]), the response of trout preparations to cortisol treatment was quantitatively different. For example, when compared to untreated controls, cortisol concentrations of 100 and 1000 ng/mL elevated TER measurements by ~13% and 34%, respectively in cultured goldfish gill epithelia (Fig. 1B) versus ~475% and 1900%, respectively in cultured trout preparations [23]. Similarly, cortisol doses of 100 and 1000 ng/mL reduced paracellular [^3H]PEG-4000 flux by ~10% and 20%, respectively in cultured goldfish gill epithelia (Fig. 1C) versus ~40% and 68%, respectively in cultured trout preparations [23]. In terms of the corticosteroid regulation of epithelial permeability, this provides unique insight into species-specific differences that could relate to the environmental physiology of these organisms (i.e. euryhaline versus stenohaline).

4.3. Expression patterns of TJ protein transcripts in a cultured goldfish gill epithelium and goldfish gill tissue

A comparison of occludin, claudins and ZO-1 within gill tissue indicated that transcript abundance of the TJ proteins claudin b, e, 7, 8d and occludin were considerably greater than claudin c, d, 3a and 12, and ZO-1 (Fig. 2B). With the exception of a few subtle differences, the same pattern of abundance was present in the primary cultured goldfish gill model (see Fig. 2A). Therefore, although the TJ mRNA abundance profile in the *in vitro* model was largely the same as native gill tissue, it is likely that the few observed differences relate to the cultured gill epithelium being composed of pavement cells only whereas in gill tissue there would be TJs between other cell types (e.g. pavement cells with mitochondria-rich cells and/or junctions between cells of the capillary endothelium).

4.4. Dose-dependent and time-course effects of cortisol on TJ protein mRNA abundance

Of the ten goldfish TJ genes evaluated in *series 1* experiments, only three TJ protein transcripts, claudin c and h, and ZO-1, were significantly altered by 24 h cortisol exposure (Fig. 3C,F,J). Furthermore, only claudin c mRNA abundance was significantly altered by a physiologically relevant dose of cortisol (i.e. 500 ng/mL) (Fig. 3C). It is interesting that transcript abundance of goldfish claudin c and h genes decreased as they are orthologs of claudin 3d and 3a genes, respectively within the claudin 3 family of TJ protein genes in puffer fish, as well as orthologs of the single claudin 3 gene in mammals. Several lines of evidence in both fish [2,13] and mammals [25,31,34] strongly support a role for claudin 3 orthologs as barrier-forming or 'tightening' TJ proteins. However, contrary to this strongly supported function, cultured puffer fish gill epithelia have also been reported to exhibit a significant reduction in claudin 3a (and no change in claudin 3d) transcript abundance in response to cortisol treatment [4]. In addition to the aforementioned claudins, the observed reduction in ZO-1 mRNA abundance also conflicts with a previous study that reported glucocorticoid

treatment of mouse mammary epithelia to significantly augment ZO-1 protein levels in association with elevated TER [38].

Despite unchanged expression or the paradoxically observed decrease in transcript abundance of barrier-forming TJ genes, the paracellular barrier across cultured goldfish gill epithelia was significantly enhanced by cortisol treatment (Fig. 1C). It is possible that the observed reductions in paracellular [^3H]PEG-4000 flux were due to non-genomic actions, such as alterations in TJ protein turnover rates, recruitment of existing TJ proteins from the cytosolic pool to the TJ complex, or TJ assembly and disassembly by rapid phosphorylation or dephosphorylation of TJ proteins. To address the possibility that the duration of cortisol treatment was not long enough to elicit a genomic response, in *series 2* experiments the cortisol treatment period was extended to 48 and 96 h. In this experimental set, a single dose of 500 ng/mL cortisol was used as this was the only physiologically relevant dose that significantly altered TJ protein mRNA abundance in *series 1* experiments (Fig. 3). In addition, this dose and these exposure times are similar to those reported to elicit alterations in the transcript abundance of TJ proteins in cultured gill epithelia derived from euryhaline fishes (i.e. 44 h at 500 ng/mL, *Tetraodon nigroviridis* (see [4]); ~96 h at 500 ng/mL, *O. mykiss*, this study, see Section 4.5). Within the same time group (i.e. 48 or 96 h), TER was significantly elevated by cortisol treatment relative to untreated controls (Fig. 4A). Therefore prolonged cortisol treatment significantly 'tightened' goldfish gill preparations as was seen following 24 h exposure. However, and also consistent with *series 1* experiments, minimal alterations in TJ protein mRNA abundance were elicited. At 48 h, only claudin c mRNA was significantly altered in response to cortisol while the abundance of transcripts encoding for occludin, claudin b, d, e, h, 7, 8d and 12, and ZO-1 did not change (Fig. 4). Following 96 h exposure to cortisol, claudin b, d, e, 7 and 8d transcript abundance continued to be unaffected by cortisol, but significant reductions in occludin, claudin h and 12, and ZO-1 mRNA were observed. Therefore, although some additional changes in TJ protein mRNA abundance were observed after a longer duration of cortisol exposure, these alterations were contrary to what may have been expected (i.e. decreased mRNA rather than increased) based on the physiological characteristics of the cortisol-treated preparations at 96 h (i.e. elevated TER) and our understanding of the barrier-enhancing roles these TJ proteins play in other epithelia ([2,13,34,44]; see discussion above).

4.5. Comparative effects of cortisol on permeability and TJ protein mRNA abundance in cultured goldfish and rainbow trout gill epithelia

Despite its epithelial 'tightening' effect, cortisol treatment elicited limited alterations in TJ protein mRNA abundance in goldfish gill preparations in *series 1* and *series 2* experiments. Furthermore, in instances when TJ protein transcript levels were altered (either by high concentrations of cortisol or prolonged cortisol treatment), these were decreased rather than increased as would be anticipated to match the observed reductions in epithelial permeability and the understood functions of orthologous mammalian and fish TJ proteins (e.g. [2,13,34]); see discussion in Section 4.4). It seems reasonable to assume that the molecular TJ components that contribute to alterations in the paracellular permeability properties of the cultured goldfish epithelium still require identification. However, it is also of interest to consider the possibility that species-specific differences could be a factor in the somewhat unusual observations from *series 1* and *2* experiments, and that these could relate to the stenohaline nature of goldfish. Indeed, the literature already supports this idea to some extent as occludin transcript and protein abundance have been reported to increase in cultured trout gill epithelia treated with cortisol (see [7]) and mRNA encoding for a number of claudin isoforms have been reported to alter in

response to cortisol treatment in a cultured puffer fish gill epithelium (see [4]). Therefore, to explore this idea further, series 3 experiments sought to use a comparable system derived from a euryhaline fish (the rainbow trout) to conduct a side-by-side comparison of cortisol-mediated alterations in orthologous TJ protein transcripts. These studies were conducted using comparable doses of cortisol (i.e. 500 ng/mL), and although the time-frame for cortisol exposure was different (i.e. 24 h for goldfish versus ~96 h for trout, as is necessitated by the differences in epithelium development between the two preparations, (see [8]), series 2 experiments indicated that time did little to further alter the effects of cortisol on goldfish gill preparations.

As previously noted, a single physiologically relevant dose of cortisol significantly elevated TER measurements and reduced [³H]PEG-4000 flux across cultured gill epithelia derived from both goldfish and rainbow trout (Fig. 5A–D; [7,23]). This 'tightening' effect, however, was much more pronounced in trout gill preparations, where elevations in TER were almost 15-fold higher and reductions in [³H]PEG-4000 flux were 2-fold lower than those observed across goldfish gill preparations (Fig. 5A–D).

In accordance with the results of series 1, cortisol treatment did not significantly alter TJ protein transcript abundance in goldfish gill preparations, except for claudin e mRNA, which was marginally elevated (Fig. 5E). An equivalent dose of cortisol, however significantly elevated all orthologous trout TJ protein transcripts examined (Fig. 5F). Up-regulated occludin mRNA expression in the rainbow trout gill model in response to cortisol treatment confirms earlier results reported by [7] and is in agreement with a barrier-forming role for occludin [6,15]. Furthermore, the cortisol-mediated elevation in claudin 30 mRNA abundance is consistent with the observations of [43] where claudin 30 transcript abundance was significantly increased in whole gill tissue from Atlantic salmon following *in vitro* incubation with cortisol. These observations are also in line with a role for claudin 30 as a 'tightening' TJ protein, as claudin 30 mRNA abundance was significantly reduced in the Atlantic salmon gill following SW acclimation [42]. Rainbow trout claudin 28b mRNA abundance significantly increased in the present study and interestingly, orthologous goldfish claudin e mRNA was also increased in response to cortisol treatment (Fig. 5E and F). Goldfish claudin e was the only goldfish TJ gene examined in the present study that exhibited a significant elevation following cortisol treatment (Fig. 5E) and (although not significant) also appeared to be elevated in response to cortisol in a dose-dependent manner in series 1 experiments (Fig. 3E). Claudin 28b mRNA abundance in the Atlantic salmon gill has been reported to transiently decrease during the early stages of SW acclimation [42], therefore it is possible that rainbow trout claudin 28b and orthologous goldfish claudin e proteins may contribute to the TJ barrier. Cortisol treatment significantly elevated rainbow trout claudin 3a mRNA abundance in accordance with a well-supported barrier role for orthologous mammalian and fish claudin 3 ([2,13,34]; see discussion in Section 4.4), and out of the seven rainbow trout TJ genes examined in this study, claudin 8d exhibited the greatest increase in mRNA abundance in response to cortisol treatment (i.e. an ~310% elevation relative to untreated controls; Fig. 5F). A large body of research suggests a barrier-forming role for mammalian claudin 8 [18,25,29,31,47] and in fishes a similar barrier role for claudin 8 isoforms has also been proposed to exist [3,13]. Claudin 7 is a peculiar TJ protein as siRNA knockdown studies have demonstrated that it can form a barrier to the paracellular movement of Na⁺ ions or facilitate the permeability of Cl⁻ ions by formation of Cl⁻-selective paracellular pores [20]. In the present study, rainbow trout claudin 7 transcript abundance was significantly elevated in response to cortisol (Fig. 5F), and correspondingly it has previously been demonstrated that cortisol treatment significantly reduces both net Na⁺ and Cl⁻ flux across cultured rainbow trout gill pre-

parations in a dose-dependent manner [7,23]. Therefore, it seems likely that rainbow trout claudin 7 may function as a barrier to Na⁺ permeability. Taken together, the response of rainbow trout TJ protein orthologs appears to be very much in line with the physiological changes that occur in response to cortisol (i.e. epithelial 'tightening'). In addition, the changes in trout transcript abundance that take place fit well with what we currently know about the physiological role of these TJ components in fishes and other vertebrates. Therefore, it would seem that the conservative response in goldfish preparations at the physiological and molecular level represents a species-specific phenomenon that could be linked to differences between how a stenohaline and euryhaline fish may respond to the osmoregulatory actions of cortisol.

5. Conclusions

In the present study, data clearly support a role for cortisol in the endocrine regulation of paracellular permeability across the euryhaline rainbow trout gill, as cortisol treatment elicited significant alterations in several genes encoding for TJ proteins. Whether a similar role for cortisol in the stenohaline goldfish gill exists however is far less evident. Although cortisol treatment significantly reduced the epithelial permeability of cultured goldfish gill epithelia in a manner that was qualitatively similar to trout preparations, quantitatively these modifications in permeability were very different from those exhibited by the trout model. Furthermore, alterations in goldfish TJ components in response to cortisol were either entirely absent or did not correlate with the observed changes in epithelial permeability and our current understanding of the specific functions of the TJ proteins examined. In this regard, we introduce the notion that perhaps, at least in goldfish, stenohalinity is in part a consequence of a reduced capacity to limit diffusional salt influx by altering requisite TJ components as a result of an inability to adequately respond to cortisol during SW acclimation. Clearly more work is required, including the complete enumeration and analysis of goldfish TJ proteins (particularly members of the claudin family), an examination of the effects of other osmoregulatory hormones (e.g. prolactin, growth hormone) on epithelial permeability, as well as similar comparison studies in other stenohaline and euryhaline species. Furthermore, future studies examining the effects of cortisol on a cultured stenohaline gill epithelium composed of both pavement and mitochondria-rich cells may also be revealing.

Acknowledgments

This work was supported by a NSERC Discovery Grant, NSERC Discovery Accelerator Supplement and Canadian Foundation for Innovation New Opportunities Grant to S.P.K. H.C. was supported by an Ontario Graduate Scholarship.

References

- [1] S.F. Altschul, T.L. Madden, A.A. Schäffer, J. Zhang, Z. Zhang, W. Miller, D.J. Lipman, Gapped BLAST and PSI-BLAST: a new generation of protein database search programs, *Nucleic Acids Res.* 25 (1997) 3389–3402.
- [2] M. Bagherie-Lachidan, S.I. Wright, S.P. Kelly, Claudin-3 tight junction proteins in *Tetraodon nigroviridis*: cloning, tissue specific expression and a role in hydromineral balance, *Am. J. Physiol. Integr. Comp. Physiol.* 294 (2008) R1638–R1647.
- [3] M. Bagherie-Lachidan, S.I. Wright, S.P. Kelly, Claudin-8 and -27 tight junction proteins in puffer fish *Tetraodon nigroviridis* acclimated to freshwater and seawater, *J. Comp. Physiol. B* 179 (2009) 419–431.
- [4] P. Bui, M. Bagherie-Lachidan, S.P. Kelly, Cortisol differentially alters claudin isoforms in cultured puffer fish gill epithelia, *Mol. Cell. Endocrinol.* 317 (2010) 120–126.
- [5] H. Chasiotis, S.P. Kelly, Occludin immunolocalization and protein expression in goldfish, *J. Exp. Biol.* 211 (2008) 1524–1534.

- [6] H. Chasiotis, J. Effendi, S.P. Kelly, Occludin expression in goldfish held in ion-poor water, *J. Comp. Physiol. B* 179 (2009) 145–154.
- [7] H. Chasiotis, C.M. Wood, S.P. Kelly, Cortisol reduces paracellular permeability and increases occludin abundance in cultured trout gill epithelia, *Mol. Cell. Endocrinol.* 323 (2010) 232–238.
- [8] H. Chasiotis, S.P. Kelly, Permeability properties and occludin expression in a primary cultured model gill epithelium from the stenohaline freshwater goldfish, *J. Comp. Physiol. B* 181 (2011) 487–500.
- [9] E.S. Clelland, S.P. Kelly, Tight junction proteins in zebrafish ovarian follicles: stage specific mRNA abundance and response to 17 β -estradiol, human chorionic gonadotropin, and maturation inducing hormone, *Gen. Comp. Endocrinol.* 168 (2010) 388–400.
- [10] P.M. Craig, H. Al-Timimi, N.J. Bernier, Differential increase in forebrain and caudal neurosecretory system corticotrophin-releasing factor and urotensin I gene expression associated with seawater transfer in rainbow trout, *Endocrinology* 146 (2005) 3851–3860.
- [11] A.W. Cuthbert, J. Maetz, The effects of calcium and magnesium on sodium fluxes through gills of *Carassius auratus* L., *J. Physiol.* 221 (1972) 633–643.
- [12] M. Dror, M.S. Sinyakov, E. Okun, M. Dym, B. Sredni, R.R. Avtalion, Experimental handling stress as infection-facilitating factor for the goldfish ulcerative disease, *Vet. Immunol. Immunopathol.* 109 (2006) 279–287.
- [13] N.M. Duffy, P. Bui, M. Bagherie-Lachidan, S.P. Kelly, Epithelial remodeling and claudin mRNA abundance in the gill and kidney of puffer fish (*Tetraodon bioellatus*) acclimated to altered environmental ion levels, *J. Comp. Physiol. B* 181 (2011) 219–238.
- [14] D.H. Evans, P.M. Piermarini, K.P. Choe, The multifunctional fish gill: dominant site of gas exchange, osmoregulation, acid-base regulation, and excretion of nitrogenous waste, *Physiol. Rev.* 85 (2005) 97–177.
- [15] G.J. Feldman, J.M. Mullin, M.P. Ryan, Occludin: structure, function and regulation, *Adv. Drug Deliv. Rev.* 57 (2005) 883–917.
- [16] E.A. Felinski, A.E. Cox, B.E. Phillips, D.A. Antonetti, Glucocorticoids induce transactivation of tight junction genes occludin and claudin-5 in retinal endothelial cells via a novel cis-element, *Exp. Eye Res.* 86 (2008) 867–878.
- [17] C. Förster, M. Burek, I.A. Romero, B. Weksler, P.O. Couraud, D. Drenckhahn, Differential effects of hydrocortisone and TNF α on tight junction proteins in an *in vitro* model of the human blood–brain barrier, *J. Physiol.* 586 (2008) 1937–1949.
- [18] H. Fujita, H. Chiba, H. Yokozaki, N. Sakai, K. Sugimoto, T. Wada, T. Kojima, T. Yamashita, N. Sawada, Differential expression and subcellular localization of claudin-7, 8, 12, 13 and -15 along the mouse intestine, *J. Histochem. Cytochem.* 54 (2006) 933–944.
- [19] L. González-Mariscal, A. Betanzos, P. Nava, B.E. Jaramillo, Tight junction proteins, *Prog. Biophys. Mol. Biol.* 81 (2003) 1–44.
- [20] J. Hou, A.S. Gomes, D.L. Paul, D.A. Goodenough, Study of claudin function by RNA interference, *J. Biol. Chem.* 281 (2006) 36117–36123.
- [21] W.F. Jacob, M.H. Taylor, The time course of seawater acclimation in *Fundulus heteroclitus* L., *J. Exp. Zool.* 228 (1983) 33–39.
- [22] S.P. Kelly, M. Fletcher, P. Pärt, C.M. Wood, Procedures for the preparation and culture of 'reconstructed' rainbow trout branchial epithelia, *Methods Cell. Sci.* 22 (2000) 153–163.
- [23] S.P. Kelly, C.M. Wood, Effect of cortisol on the physiology of cultured pavement cell epithelia from freshwater trout gills, *Am. J. Physiol. Regul. Integr. Comp. Physiol.* 281 (2001) R811–R820.
- [24] S.P. Kelly, C.M. Wood, Cultured gill epithelia from freshwater tilapia (*Oreochromis niloticus*): effect of cortisol and homologous serum supplements from stressed and unstressed fish, *J. Membr. Biol.* 190 (2002) 29–42.
- [25] Y. Kiuchi-Saishin, S. Gotoh, M. Furuse, A. Takasuga, Y. Tano, S. Tsukita, Differential expression patterns of claudins tight junction membrane proteins in mouse nephron segments, *J. Am. Soc. Nephrol.* 13 (2002) 875–886.
- [26] R. Kollmar, S.K. Nakamura, J.A. Kappler, A.J. Hudspeth, Expression and phylogeny of claudins in vertebrate primordia, *Proc. Natl. Acad. Sci. USA* 98 (2001) 10196–10201.
- [27] B. Lahlou, I.W. Henderson, W.H. Sawyer, Sodium exchanges in goldfish (*Carassius auratus* L.) adapted to a hypertonic saline solution, *Comp. Biochem. Physiol.* 28 (1969) 1427–1433.
- [28] M.A. Larkin, G. Blackshields, N.P. Brown, R. Chenna, P.A. McGettigan, H. McWilliam, F. Valentin, I.M. Wallace, A. Wilm, R. Lopez, J.D. Thompson, T.J. Gibson, D.G. Higgins, Clustal W and Clustal X version 2.0, *Bioinformatics* 23 (2007) 2947–2948.
- [29] W.Y. Li, C.L. Huey, A.S. Yu, Expression of claudin-7 and -8 along the mouse nephron, *Am. J. Physiol. Renal Physiol.* 286 (2004) F1063–1071.
- [30] Y.H. Loh, A. Christoffels, S. Brenner, W. Hunziker, B. Venkatesh, Extensive expansion of the claudin gene family in the teleost fish *Fugu rubripes*, *Genome Res.* 14 (2004) 1248–1257.
- [31] A.G. Markov, A. Veshnyakova, M. Fromm, M. Amasheh, S. Amasheh, Segmental expression of claudin proteins correlates with tight junction barrier properties in rat intestine, *J. Comp. Physiol. B* 180 (2010) 591–598.
- [32] W.S. Marshall, T.R. Emberley, T.D. Singer, S.E. Bryson, S.D. McCormick, Time course of salinity adaptation in a strongly euryhaline estuarine teleost, *Fundulus heteroclitus*: a multivariable approach, *J. Exp. Biol.* 202 (1999) 1535–1544.
- [33] S.D. McCormick, Endocrine control of osmoregulation in teleost fish, *Amer. Zool.* 41 (2001) 781–794.
- [34] S. Milatz, S.M. Krug, R. Rosenthal, D. Günzel, D. Müller, J.D. Schulzke, S. Amasheh, M. Fromm, Claudin-3 acts as a sealing component of the tight junction for ions of either charge and uncharged solutes, *Biochim. Biophys. Acta.* 1798 (2010) 2048–2057.
- [35] T.P. Mommsen, M.M. Vijayan, T.W. Moon, Cortisol in teleosts: dynamics, mechanisms of action, and metabolic regulation, *Rev. Fish Biol. Fisher.* 9 (1999) 211–268.
- [36] S.F. Perry, P. Laurent, Adaptational responses of rainbow trout to lowered external NaCl concentration: contribution of the branchial chloride cell, *J. Exp. Biol.* 147 (1989) 147–168.
- [37] T.G. Pottinger, A multivariate comparison of the stress response in three salmonid and three cyprinid species: evidence for inter-family differences, *J. Fish Biol.* 76 (2010) 601–621.
- [38] K.L. Singer, B.R. Stevenson, P.L. Woo, G.L. Firestone, Relationship of serine/threonine phosphorylation/dephosphorylation signaling to glucocorticoid regulation of tight junction permeability and ZO-1 distribution in non-transformed mammary epithelial cells, *J. Biol. Chem.* 269 (1994) 16108–16115.
- [39] J.A. Singley, W. Chavin, The adrenocortical–hypophyseal response to saline stress in the goldfish *Carassius auratus* L., *Comp. Biochem. Physiol. A Comp. Physiol.* 51 (1975) 749–756.
- [40] M.E. Smith, A.S. Kane, A.N. Popper, Noise-induced stress response and hearing loss in goldfish (*Carassius auratus*), *J. Exp. Biol.* 207 (2004) 427–435.
- [41] K. Stelwagen, H.A. McFadden, J. Demmer, Prolactin alone or in combination with glucocorticoids enhances tight junction formation and expression of the tight junction protein occludin in mammary cells, *Mol. Cell. Endocrinol.* 156 (1999) 55–61.
- [42] C.K. Tipsmark, P. Kiilerich, T.O. Nilsen, L.O.E. Ebbesson, S.O. Stefansson, S.S. Madsen, Branchial expression patterns of claudin isoforms in Atlantic salmon during seawater acclimation and smoltification, *Am. J. Physiol. Regul. Integr. Comp. Physiol.* 294 (2008) R1563–R1574.
- [43] C.K. Tipsmark, C. Jorgensen, N. Brande-Lavridsen, M. Englund, J.H. Olesen, S.S. Madsen, Effects of cortisol, growth hormone and prolactin on gill claudin expression in Atlantic salmon, *Gen. Comp. Endocrinol.* 163 (2009) 270–277.
- [44] C.M. Van Itallie, A.S. Fanning, A. Bridges, J.M. Anderson, ZO-1 stabilizes the tight junction solute barrier through coupling to the perijunctional cytoskeleton, *Mol. Biol. Cell* 20 (2009) 3930–3940.
- [45] C.M. Wood, P. Pärt, Cultured branchial epithelia from freshwater fish gills, *J. Exp. Biol.* 200 (1997) 1047–1059.
- [46] C.M. Wood, K.M. Gilmour, P. Pärt, Passive and active transport properties of a gill model the cultured branchial epithelium of the freshwater rainbow trout (*Oncorhynchus mykiss*), *Comp. Biochem. Physiol. A Mol. Integr. Physiol.* 119 (1998) 87–96.
- [47] A.S. Yu, A.H. Enck, W.I. Lencer, E.E. Schneeberger, Claudin-8 expression in Madin–Darby canine kidney cells augments the paracellular barrier to cation permeation, *J. Biol. Chem.* 278 (2003) 17350–17359.
- [48] K.S. Zettl, M.D. Sjaastad, P.M. Riskin, G. Parry, T.E. Machen, G.L. Firestone, Glucocorticoid-induced formation of tight junctions in mouse mammary epithelial cells *in vitro*, *Proc. Natl. Acad. Sci. USA* 89 (1992) 9069–9073.